

6th Study Conference on BALTEX



14 - 18 June 2010

Międzyzdroje, Island of Wolin, Poland

Conference Proceedings

Editors: Marcus Reckermann
and Hans-Jörg Isemer

Partners

BONUS
Baltic Organisations Network
for Funding Science EEIG



HELCOM
Baltic Marine Environment
Protection Commission



NEESPI
Northern Eurasia Earth Science
Partnership Initiative



LOICZ
Land-Ocean Interactions
in the Coastal Zone



BALTEX is a Regional Hydroclimate Project in the context of the Coordinated Energy and Water Cycle Observations Project (CEOP) within GEWEX (Global Water and Energy Cycle Experiment) and WCRP (World Climate Research Programme).



Sponsors

**Institute of Oceanology
Polish Academy of Science
Sopot, Poland**



**Swedish Meteorological and
Hydrological Institute
Norrköping, Sweden**



**NEESPI
Northern Eurasia Earth Science
Partnership Initiative**



**Gesellschaft zur Förderung des
GKSS Forschungszentrums e.V.
Geesthacht, Germany**



**GKSS Research Centre Geesthacht
Germany**



Organisers

**Institute of Oceanology
Polish Academy of Science
Sopot, Poland**



University of Szczecin, Poland



**Polish Academy of Sciences
Research Centre of Agriculture
and Forest Environment
Poznań, Poland**



**West Pomeranian University of Technology
Szczecin, Poland**



**GKSS Research Centre Geesthacht
Germany**



Scientific Conference Committee:

Joakim Langner, Sweden (Chair)
Andris Andrusaitis, Latvia
Mikko Alestalo, Finland
Berit Arheimer, Sweden
Franz Berger, Germany
Ryhor Chekan, Belarus
Jüri Elken, Estonia
Pavel Groisman (NEESPI), USA
Sven-Erik Gryning, Denmark
Daniela Jacob, Germany
Hermann Kaartokallio, Finland
Sirje Keevallik, Estonia
Kaisa Kononen (BONUS EEIG), Finland
Hartwig Kremer (LOICZ), Germany
Zbigniew W. Kundzewicz, Poland
Maria Lamaanen (HELCOM), Finland
Michael Lautenschlager, Germany
Andreas Lehmann, Germany
Philippe Lucas-Picher, Denmark
Anders Omstedt, Sweden
Janusz Pempkowiak, Poland
Dan Rosbjerg, Denmark
Bernd Schneider, Germany
Benjamin Smith, Sweden
Tapani Stipa, Finland
Hans von Storch, Germany
Valery Vuglinsky, Russia

Organising Committee:

Janusz Pempkowiak, Poland (Chair)
Jan Harff, Poland
Hans-Jörg Isemer, Germany
Zbigniew W. Kundzewicz, Poland
Jan Piechura, Poland
Mikołaj Protasowicki, Poland
Marcus Reckermann, Germany
Andrzej Witkowski, Poland

Preface

BALTEX has evolved from a programme describing the physical aspects of the Earth system to an integrative, truly interdisciplinary programme, encompassing many aspects of environmental research related to climate change in the Baltic Sea drainage basin. This is demonstrated by the thematic foci of the submitted contributions to this 6th Study Conference on BALTEX: Almost 2/3 of the contributions are addressing regional climate change research and adaptation options, as well as biogeochemical cycles in the Earth system. The target region is the Baltic Sea and its drainage basin, but papers on other regions were accepted as well. The research objectives of many contributions cover several disciplines, again underlining the interdisciplinary nature of the conference.

The conference sessions reflect the BALTEX objectives and goals:

- Session 1: Climate variability and change in the past and future
- Session 2a: Water and energy cycles in the regional Earth system
- Session 2b: Biogeochemical cycles in the regional Earth system
- Session 3: Hydrological modelling, water management and extreme hydrological events
- Session 4: Regional adaptation to climate change

The conference is envisaged as a communication platform for the research community, water and environmental resources managers, policy makers and other stakeholders. It is organised in cooperation with several relevant international research programmes and organisations: NEESPI, HELCOM, BONUS and LOICZ. NEESPI, the Northern Eurasian Earth Science Partnership Initiative is a sister programme of BALTEX in the context of the Coordinated Energy and Water Cycle Observations Project (CEOP) of GEWEX, the Global Energy and Water Cycle Experiment, asking similar scientific questions and having a regional interest in the northern Baltic Sea basin. HELCOM, the intergovernmental Helsinki Commission, is currently working to implement the “Baltic Sea Action Plan” which is an overarching strategy for the restoration of the marine environment of the Baltic Sea. BONUS, the Baltic Organisations Network for Funding Science, plays a prominent role in defining and focussing research themes in the Baltic Sea basin. Results from many BONUS+ funded projects are presented at the Conference. Finally, the global goals of LOICZ (Land-Ocean Interactions in the Coastal Zone) and the regional goals of BALTEX are similar in several aspects, making both programmes natural partners.

Poland, the host country of this conference, is the predominant riparian state in the southern Baltic Sea basin. The conference is taking place on Wolin, the only Polish island in the Baltic Sea. Thereby, the tradition to have BALTEX Study Conferences on Baltic Sea islands and in different countries is kept up.

This proceedings volume contains the extended abstracts accepted for presentation at the conference, sorted alphabetically within each Conference session. No distinction was made between oral and poster presentations; they are deliberately treated equally in this volume.

The conference is jointly organized by the Institute of Oceanology in Sopot, the University of Szczecin, the Research Centre of Agriculture and Forest Environment, Poznań, and the West Pomeranian University of Technology, Szczecin (all Poland), and the International BALTEX Secretariat at GKSS Research Centre, Geesthacht, Germany. We would like to thank Silke Köppen, Regina Terlecka and Anna Ciosmak for invaluable support in the preparation of the conference.

June 2010

Marcus Reckermann and Hans-Jörg Isemer

Editors

Contents

Poland, a Baltic country: Climate, waters, people Zbigniew Kundzewicz and Rajmund Przybylak	1
BONUS-169: Future perspectives for environmental research for the Baltic Sea region Kaisa Kononen and Andris Andrusaitis	2
NEESPI current status and its objectives within north-western Eurasia Pavel Groisman	3
 <u>TOPIC 1: Climate variability and change in the past and future</u>	
ECOSUPPORT (Advanced tool for scenarios of the Baltic Sea ECOSystem to SUPPORT decision making): Project approach and selected results Helèn C. Andersson and the ECOSUPPORT consortium	5
Detection and attribution of an anthropogenic effect on temperature and precipitation changes in the Baltic Sea catchment Jonas Bhend and H. von Storch	7
Impact of recent changes of snow cover and climate on river runoff in the Baltic Sea basin of the East European plain Ala Bildziuh, L. Trafimova, I. Danilovich and R. Chekan	9
Precipitation changes in the Russian sector of the Baltic Sea basin after accounting for comprehensive biases in their measurements Esfir G. Bogdanova, B. Iljin, S-Y. Gavrilova and P. Groisman	10
Changes in snow cover characteristics over northwestern Russia Olga Bulygina, P. Groisman and V. Razuvaev	11
Analysis of the water balance and wind climate over the Baltic Sea drainage basin using dynamically downscaled climate simulations Björn Carlsson, I. Sjöström, A. Rutgersson and A. Omstedt	12
Long term water level and surface temperature changes in the lagoons of the South and East Baltic Inga Dailidienė, H. Baudler and B. Chubarenko	14
Evaluating the combined effects of nutrient load reduction and climate scenarios for the Baltic Sea catchment Chantal Donnelly, J. Strömqvist, J. Dahné and B. Arheimer	15
Climate variability and change detected from Baltic Sea level data since 1774: An overview Martin Ekman	17

The response of the Baltic Sea to climate variability Klaus Getzlaff, A. Lehmann and J. Harlaß	18
What do we know about sea-level change in the Baltic Sea? Birgit Hünicke	20
Changes in wind directions in Estonia during 1966-2008 and their relationship with large-scale atmospheric circulation Jaak Jaagus	22
Climate change in the Baltic Sea area in an ensemble of regional climate model simulations Erik Kjellström, G. Nikulin and L. Bärring	24
Environmental changes in the Pomeranian Bay in the Holocene, based on diatomological and geochemical studies Robert Kostecki and B. Janczak-Kostecka	26
Categorical temperature data as indicators of warming in Poland Zbigniew Kundzewicz and H. Lorenc.....	27
Detailed assessment of climate variability of the Baltic Sea area for the period 1958-2009 Andreas Lehmann, K. Getzlaff and J. Harlass	28
Long term trend and decadal variability of the hydrological cycle in the Baltic Sea region as modelled by the ENSEMBLES regional climate models Philip Lorenz, K. Meraner and D. Jacob.....	30
High resolution reanalysis for the Baltic Sea region during 1965-2005 Andres Luhamaa, K. Kimmel, A. Männik and R. Rõõm.....	31
Long-term changes in frequency and duration of southern cyclones influencing climate variability in Estonia Kaupo Mändla, M. Sepp and J. Jaagus	33
Transient scenario simulations for the Baltic Sea for 1961-2099 HE Markus Meier and ECOSUPPORT collaborators.....	35
Impact of climate change on biogeochemical fluxes of nitrogen and phosphorus in the Gulf of Riga Bärbel Müller-Karulis, J. Sennikovs, A.Valainis and J. Aigars.....	37
Uncertainties in the projected climate changes of wind extremes over the Baltic region Grigory Nikulin, E. Kjellström and C. Jones	38
Impact of climate change on the water balance of a mesoscale catchment of the Western Bug Thomas Pluntke, K. Barfus, K. Schwärzel, C. Burmeister and C. Bernhofer.....	39

Comparison of the sea surface temperatures and sea ice concentration from ERA-Interim and BSH

Thomas Raub, T. Cesko, K. Getzlaff, A. Lehmann and D. Jacob 42

Estimating the impact of potential climate change in the 21st century on the Baltic Sea ecosystem

Vladimir Rybachenko, L. Karlin, I. Neelov, T. Eremina, O. Savchuk, R. Vankevich and A. Isaev 44

On regime shift in the general atmospheric circulation over the Baltic Sea region in winter

Mait Sepp 46

Changes in some elements of the water cycle in the Baltic Sea areas of the former Soviet Union

Nina Speranskaya 48

Interference of climate change, geosphere and anthroposphere – A new focus of the Szczecin science community

Andrzej Witkowski, J. Batóg, R. K. Borówka, K. Furmańczyk, J. Harff, M. Kowalewski, P. Krajewski, R. Marks, S. Musielak, M. Rębkowski and H. von Storch 49

Holocene coastal morphogenesis at the southern Baltic Sea: An interplay of climate forcing and the geological environment – A case study of the Darss-Zingst Peninsula

Wenyang Zhang, J. Harff, R. Schneider and E. Zorita 50

Is the Baltic sea-level change accelerating?

Eduardo Zorita and B. Hünicke 52

TOPIC 2: Water, energy and biogeochemical cycles in the regional Earth system

Topic 2a. Water and energy cycles

Current status of the BALTEX in-situ reference sites in CEOP

Frank Beyrich, C. Heret, U. Rummel, F. Bosveld, E. Kyrö and R. Kivi 55

Wave conditions along the Latvian coast of the Baltic Proper derived from visual wave observations

Anita Draveniece 57

Spatial variability of thermohaline and dynamical parameters during wind-driven coastal upwelling in the south-eastern Baltic Sea

Mariy Golenko and N. Golenko 58

Combining MODIS and SAR images in research of water dynamics in the south-eastern Baltic Sea

Evgenia Gurova and A. Ivanov 59

Modelling of ice cover of the Baltic Sea

M. Janecki, J. Jakacki, L. Dzierzbicka-Głowacka and R. Osinski 61

Assessment of precipitation conditions in the Polish zone of the southern Baltic coastland Eliza Kalbarczyk and R. Kalbarczyk	63
Wind parameters in the centre of the Gulf of Finland from measurements and HIRLAM outputs Sirje Keevallik.....	65
An advanced weather radar network for the Baltic Sea Region – BALTRAD Daniel Michelson	67
Impact of aerosol optical properties on climate change processes. The Baltic case study A. Ponczkowska, P. Makuch, J. Kowalczyk, T. Zielinski, T. Petelski, J. Piskozub, A. Smirnov, B. Holben, J. Pasnicki and K. Zielinski.....	69
A reliability study of wave climate modelling in the Baltic Sea Andrus Räämet and T. Soomere	71
Energy and water budget over the BALTEX domain from a suite of atmospheric regional climate models (present and future) Burkhardt Rockel	73
Introducing air-sea interaction processes in numerical models Anna Rutgeresson, Ø. Sætra, A. Semedo, B. Carlsson, R. Kumar and Ø. Breivik	74
New dataset of highly resolved atmospheric forcing fields for 1850-2009 Frederik Schenk and E. Zorita.....	76
A study of ASCAT wind measurements near the coastal region of Estonia Jekaterina Služenikina and A. Männik.....	78
Sensitivity of the CCLM to changing land use in Eastern Europe Dennis Söhl, D. Pavlik and C. Bernhofer	80
Large scale skill in regional climate modelling and the lateral boundary condition scheme: 32-day ensemble experiments Katarina Veljovic, B. Rajković and F. Mesinger	82
Air-sea interaction model for momentum and mass in the presence of wind waves Christoph Zülicke.....	84
Mesoscale patterns of wind and precipitation due to inertia-gravity waves in model simulations and observational networks Christoph Zülicke.....	86
 <i>Topic 2b. Biogeochemical cycles</i>	
Atmospheric deposition of particulate nitrogen, sulphur and benzo(a)pyrene into the Baltic Sea between 1995 and 2005 considering the influence of ship emissions Armin Aulinger, V. Matthias and M. Quante	89

Depositions of acidifying and neutralising compounds over the Baltic Sea drainage basin between 1960 and 2006 Björn Carlsson and A. Rutgersson	91
Development of the marine planktonic copepod <i>Acartia spp</i> in the southern Baltic Sea Lidia Dzierzbicka-Glowacka, I.M. Żmijewska, J. Jakacki, A. Lemieszek and S. Mudrak.....	93
Quality assessment of state-of-the-art coupled physical-biogeochemical models for the Baltic Sea Kari Eilola, B.G. Gustafson, R. Hordoir, A. Höglund, I. Kuznetsov, H.E.M Meier, T. Neumann and O.P. Savchuk.....	95
Can observational pH data confirm the predicted acidification of Baltic Sea surface water? Anders Grimvall, A. Omstedt and M. Pertillä.....	97
Variability of the marine boundary layer parameters over the Baltic Sea sub-basins in HIRLAM parameterizations since 1993 and their impact on the nitrogen deposition Marke Hongisto.....	99
Impact of climate change on the distribution of phytoplankton biomass in the Baltic Sea J. Jakacki, L. Dzierzbicka-Glowacka and M. Janecki.....	100
The distribution of phytoplankton biomass in the Baltic Sea simulated by a three-dimensional model Maciej Janecki, L. Dzierzbicka-Glowacka and J. Jakacki	101
Carbon budget of the Baltic Sea Karol Kuliński and J. Pempkowiak.....	102
Determination of carbon return flux from the Baltic bottom sediments Karol Kuliński, A. Szczepańska and J. Pempkowiak	103
Impact of climate change on the development of <i>Temora longicornis</i> in the southern Baltic Sea Anna Lemieszek, L. Dzierzbicka-Glowacka and I.M. Żmijewska	104
Modelling the egg production of <i>Temora longicornis</i> Anna Lemieszek, L. Dzierzbicka-Glowacka and I. M. Żmijewska	106
Particulate organic carbon in the southern Baltic Sea Anna Maciejewska, L. Dzierzbicka-Głowacka, K. Kuliński and J. Pempkowiak.....	107
Dissolved organic phosphorus in the Baltic Sea: Temporal and spatial variations Monika Nausch, G. Nausch, D. Setzkorn, B. Sadkowiak and A. Welz.....	108
Factors influencing the acid-base (pH) balance in the Baltic Sea: A sensitivity analysis Anders Omstedt, M. Edman, L. Anderson and H. Laudon	109

Importance of the Szczecin Lagoon for the Odra River mouth area in the light of geochemical studies in the Polish part of the basin Andrzej Osadczuk, A. Skowronek, A. Witkowski and Ł. Maciąg	110
Database of published nitrogen concentrations in air and precipitation around the Baltic Sea 1850-1960 Tuija Ruoho-Airola, M. Parviainen and V. Tarvainen.....	111
Do the ratio of pigments and carbon content in main groups of algal classes depend on trophicity? Preliminary results Mirosława Ostrowska, J. Stoń-Egiert, M. Łotocka and R. Majchrowski	113
Response of Polish rivers (Vistula, Oder) to reduced pressure from point sources and agriculture during the transition period (1988-2008) Marianna Pastuszak and K. Pawlikowski	115
Use of a spatially-irregular simulation model to study nitrogen and phosphorus transformation processes and dynamics of dissolved oxygen in the ecosystem of the Neva Bay, Gulf of Finland K.A. Podgorny	118
Ecological and hydrological field studies in southern Karelia within the easternmost part of the Baltic Sea Basin: The Onego/Ladoga lakes system Tatiana Sazonova, V. Bolondinsky and V. Pridacha	120
Phosphate release at the sediment surface during anoxic conditions: Myths, mysteries and facts Bernd Schneider	122
Simulating dissolved organic carbon in the Baltic Sea catchment area Guy Schurgers, P. Miller, C.-M. Mörth, T. Wällstedt, A. Yurova and B. Smith.....	123
Long term changes in phytoplankton pigments characteristics in Southern Baltic region Joanna Stoń-Egiert	124
Towards a comprehensive biogeochemical model of the Baltic Sea Letizia Tedesco, T. Stipa, A. Westerlund and A. Nummelin.....	126
Modelling nutrient balance for the Western Bug catchment under global change and data scarce conditions Tatyana Terekhanova, B. Helm and J. Tränckner.....	128
Simulation of nutrient transport from different depths during an upwelling event in the Gulf of Finland Germo Väli, V. Zhurbas, J. Laanemets and J. Elken	130
A methodological approach for the assessment of the ecological status of urban water bodies (Saint-Petersburg as a case study) Valery Vuglinsky, T. Gronskaya and N. Lemeshko	132

Modelling biogeochemical fluxes in the Vistula Lagoon Mariusz Zalewski, Z. Witek and M. Wielgat-Rychert	133
---	-----

 **TOPIC 3: Hydrological modelling, water management and extreme hydrological events**

Using multi-year circulation simulations to identify areas of reduced risk for marine transport. Application to the Gulf of Finland Oleg Andrejev, A. Sokolov, T. Soomere, K. Myrberg and B. Viikmäe	135
Frequencies of spring floods in the Belarus part of the Baltic Sea basin according to the atmospheric circulation Irina Danilovich and R. Chekan	137
Towards a quantification of areas of high and low risk of pollution in the Gulf of Finland, with the application to ecologically sensitive areas Nicole Delpeche, T. Soomere and B. Viikmäe	138
Spatio-temporal changes in thunderstorm frequency in Estonia Sven-Erik Enno	140
Integrated Water Resource Management for the Western Bug catchment as a multi-scale - multi-objective approach Björn Helm, T. Terekhanova and F. Blumensaat	142
Extreme storm surge events in the Pomeranian Bay and their impact on water levels in the Lower Odra River Halina Kowalewska-Kalkowska	144
Drought analysis of the Mediterranean region using the z-score Aleksandra Kržič and I. Tošić	145
Drought analysis of the Mediterranean region according to the A2 scenario using the Standard Precipitation Index Aleksandra Kržič and I. Tošić, B. Rajković and V. Djurdjević	146
Identifying high risk areas of pollution in the western Baltic Sea Andreas Lehmann, H-H. Hinrichsen and K. Getzlaff	148
Circulation of groundwater below a rippled sea bed Stanisław R. Massel	150
Tsunami waves in coastal zones due to an asteroid impact Stanisław R. Massel	152
Baltic inflows – Extreme oceanographic events Jan Piechura and R. Osiński	154
Temporal variability of extreme precipitation in Estonia 1961-2008 Kalev Päädam and P. Post	155

Recent dynamics and prediction of heavy precipitation events in Lithuania Egidijus Rimkus, J. Kažys and A. Bukantis.....	156
Submarine groundwater discharge to the Gulf of Gdańsk Beata Szymczycha, L. Kotwicki and J. Pempkowiak	158
Utilizing lagrangian trajectories for reducing environmental risks Bert Viikmäe, T. Soomere, N. Delpeche, H.E.M. Meier and K. Döös	159
Changes of mean and peak river runoff in Belarus during the 20th century Alexander Volchek, J. Stefanenko, S. Parfomuk, V. Luksha, A. Volchek, O Natarova and T. Shelest	161
Droughts in Poland, recent variability and future predictions Joanna Wibig.....	163
Physical characteristics of extreme storm surges and falls on the Polish coast Bernard Wiśniewski and T. Wolski	165
Hydrological modelling of the lake flow using “Hydrograph” model Sergey Zhuravlev and Y. Vinogradov.....	166
 <u>TOPIC 4: Regional adaptation to climate change</u>	
A northern European perspective on adaptation to climate change Sten Bergström.....	167
The perceptions of Baltic Sea region climate scientists pertaining to climate change in the Baltic Sea region: Results of the survey SurBACC 2010 Dennis Bray.....	169
Meteorologically possible potato yields for Estonia, derived from climate change scenarios Triin Saue and J. Kadaja	171
Connections between the atmospheric circulation type and the modelled potato crop yield in Estonia Mait Sepp and T. Saue	173
Climate services – Concepts and examples Hans von Storch and I. Meinke	175
Warm season degree-days in south-western Belarus and their dynamics Alexander Volchek, O. Meshik and V. Luksha	176
“Ecohydrological dams” for compensation of climate change and reduction of fluxes nutrients and pollutants from the river basins to Baltic Sea Maciej Zalewski	178

Design practice for urban drainage, incorporating climate change impacts

Qianqian Zhou, K. Arnbjerg-Nielsen, P.-S. Mikkelsen, K. Halsnæs and S. Balslev Nielsen.. 180

Author Index

- Aigars, J. 37
Anderson, L. 109
Andersson, H. 5
Andrejev, O. 135
Arheimer, B. 15
Arnbjerg-Nielsen, K. 180
Aulinger, A. 89
Bärring, L. 24
Balslev Nielsen, S. 180
Barfus, K. 40
Batóg, J. 49
Baudler, H. 14
Bergström, S. 167
Bernhofer, C. 40, 80
Beyrich, F. 55
Bhend, J. 7
Bildziuh, A. 9
Blumensaat, F. 142
Bogdanova, E. G. 10
Bolondinsky, V. 120
Borówka, R. K. 26, 49
Bosveld, F. 55
Bray, D. 169
Breivik, Ø. 74
Bukantis, A. 156
Bulygina, O. 11
Burmeister, C. 40
Carlsson, B. 12, 74, 91
Cesko, T. 42
Chekan, R. 9, 137
Chubarenko, B. 14
Dahné, J. 15
Dailidienė, I. 14
Danilovich, I. 9, 137
Delpeche, N. 138, 159
Djurdjević, V. 146
Döös, K. 159
Donnelly, C. 15
Draveniece, A. 57
Dzierzbicka-Głowacka, L.
..... 61, 93, 100, 101, 104, 106
Edman, M. 109
Eilola, K. 95
Ekman, M. 17
Elken, J. 130
Enno, S.-E. 140
Eremina, T. 44
Furmańczyk, K. 49
Gavrilova, S. Y. 10
Getzlaff, K. 18, 28, 42, 148
Golenko, M. 58
Golenko, N. 58
Grimvall, A. 97
Groisman, P. Y. 3, 10, 11
Gronskaya, T. 132
Gurova, E. 59
Gustafson, B. G. 95
Halsnæs, K. 180
Harff, J. 49, 50
Harlaß, J. 18, 28
Helm, B. 128, 142
Heret, C. 55
Hinrichsen, H.-H. 148
Höglund, A. 95
Holben, B. 69
Hongisto, M. 99
Hordoir, R. 95
Hünicke, B. 20, 52
Iljin, B. M. 10
Isaev, A. 44
Ivanov, A. 59
Jaagus, J. 22, 33
Jacob, D. 30, 42
Jakacki, J. 61, 93, 100, 101
Janczak-Kostecka, B. 26
Janecki, M. 61, 100, 101
Jones, C. 38
Kadaja, J. 171
Kalbarczyk, E. 63
Kalbarczyk, R. 63
Karlin, L. 44
Kažys, J. 156
Keevallik, S. 65
Kimmel, K. 31
Kivi, R. 55
Kjellström, E. 24, 38
Kononen, K. 2
Kostecki, R. 26
Kotwicki, L. 158
Kowalczyk, J. 69
Kowalewska-Kalkowska, H. 144
Kowalewski, M. 49
Krajewski, P. 49
Kržič, A. 145, 146
Kuliński, K. 102, 103, 107
Kumar, R. 74

Kundzewicz, Z.....	1, 27	Pavlik, D.	80
Kuznetsov, I.....	95	Pawlikowski, K.	115
Kyrö, E.	55	Pempkowiak, J. ...	102, 103, 107, 158
Laanemets, J.	130	Perttilä, M.	97
Laudon, H.	109	Petelski, T.	69
Lehmann, A.	18, 28, 42, 148	Piechura, J.	154
Lemeshko, N.....	132	Piskozub, J.	69
Lemieszek, A.....	93, 104, 106	Pluntke, T.....	40
Lorenc, H.....	27	Podgornyj, K. A.	118
Lorenz, P.....	30	Ponczkowska, A.....	69
Łotocka, M.	113	Post, P.	69
Luhamaa, A.	31	Pridacha, V.....	120
Luksha, V.	161, 176	Przybylak, R.....	1
Maciąg, Ł.....	110	Quante, M.	89
Maciejewska, A.	107	Räämet, A.	71
Mändla, K.....	33	Rajković, B.	82, 146
Männik, A.....	31, 78	Raub, T.....	42
Majchrowski, R.	113	Razuvaev, V.....	11
Makuch, P.....	69	Rębkowski, M.	49
Marks, R.	49	Rimkus, E.....	156
Massel, S.....	150, 152	Rockel, B.....	38, 73
Matthias, V.	89	Rõõm, R.	31
Meier, H. E. M.....	35, 95, 159	Rummel, U.....	55
Meinke, I.....	175	Ruoho-Airola, T.....	111
Meraner, K.....	30	Rutgersson, A.....	12, 74, 91
Meshik, O.	176	Ryabchenko, V.....	44
Mesinger, F.....	82	Sadkowiak, B.	108
Michelson, D.	67	Sætra, Ø.....	74
Mikkelsen, P. S.....	180	Saue, T.	171, 173
Miller, P.....	123	Savchuk, O. P.....	44, 95
Mörth, C.-M.....	123	Sazonova, T.....	120
Mudrak, S.	93	Schenk, F.....	76
Müller-Karulis, B.	37	Schneider, B.....	122
Musielak, S.	49	Schneider, R.....	50
Myrberg, K.	135	Schurgers, G.....	123
Nausch, G.	108	Schwärzel, K.	40
Nausch, M.....	108	Semedo, A.	74
Natarova, O.....	161	Seņņikovs, J.	37
Neelov, I.	44	Sepp, M.	33, 46, 173
Neumann, T.	95	Setzkorn, D.	108
Nikulin, G.....	24, 38	Shelest, T.....	161
Nummelin, A.	126	Sjöström, I.....	12
Omstedt, A.....	12, 97, 109	Skowronek, A.	110
Osadczyk, A.	110	Služenikina, J.	78
Osinski, R.	61, 154	Smirnov, A.	69
Ostrowska, M.	113	Smith, B.	123
Päadam, K.....	155	Söhl, D.	80
Parfomuk, S.	161	Sokolov, A.	135
Parviainen, M.	111	Soomere, T.....	71, 135, 138, 159
Pasnicki, J.....	69	Speranskaya, N. A.....	48
Pastuszek, M.....	115	Stefanenko, J.	161

Stipa, T.	126
Stoń-Egiert, J.	113, 124
Strömqvist, J.	15
Szczepańska, A.	103
Szymczycha, B.	158
Tarvainen, V.	111
Tedesco, L.	126
Terekhanova, T.	128, 142
Tošić, I.	145, 146
Tränckner, J.	128
Trafimova, L.	9
Väli, G.	130
Valainis, A.	37
Vankevich, R.	44
Veljovic, K.	82
Viikmäe, B.	135, 138, 159
Vinogradov, Y.	166
Volchek, Alexander 161,176	
Volchek, Anastasiya.	161
Von Storch, H.	7, 49, 175
Vuglinsky, V.	132
Wällstedt, T.	123
Welz, Ä.	108
Westerlund, A.	126
Wibig, J.	163
Wielgat-Rychert, M.	133
Wiśniewski, B.	165
Witek, Z.	133
Witkowski, A.	49
Wolski, T.	165
Yurova, A.	123
Zalewski, Maciej 178	
Zalewski, Mariusz.	133
Zhang, W.	50
Zhou, Q.	180
Zhuravlev, S.	166
Zhurbas, V.	130
Zielinski, K.	69
Zielinski, T.	69
Żmijewska, I. M. 93, 104, 106	
Zorita, E.	50, 52, 76
Zülicke, C.	84, 86

Abstracts

Poland, a Baltic country: Climate, waters, people

Zbigniew W. Kundzewicz^{1,2} and Rajmund Przybylak³

¹ Institute for Agricultural and Forest Environment, Polish Academy of Sciences, Bukowska 19, 60-809, Poznań, Poland (kundzewicz@yahoo.com; zkundze@man.poznan.pl)

² Potsdam Institute for Climate Impact Research, Telegrafenberg, 14 412 Potsdam, Germany (zbyszek@pik-potsdam.de)

³ Department of Climatology, Nicolaus Copernicus University, Torun, Poland (rp11@umk.pl)

The aim of the present contribution, foreseen for oral presentation during the opening session of the Sixth Study Conference on BALTEX in Międzyzdroje, Island of Wolin, Poland, is to offer general information on Poland, its climate, waters, and people, in a nutshell. The material will be prepared and delivered by Polish scientists. Such a contribution, relevant to the international BALTEX Project, could be of interest to many international participants in the BALTEX Conference who have not been to Poland frequently, and, in particular, to those who will now be visiting Poland for the first time.

Brief and general information on the complex climate of Poland, driven by several influences, will be given. The climate of Poland can be described as moderate, in transition between oceanic and continental. Besides geographical location (main determinant of incoming solar radiation), it is influenced markedly by air masses coming from all directions – maritime and continental, arctic and tropical. Important factor driving the climate of Poland are also oceanic currents. A brief discussion on the evidence of climate change (overwhelming warming and more complicated changes in precipitation) and projections for the future will be offered. A broader historical background will be based on the illustrative material from the monograph by Przybylak et al. (2010).

Nearly the entire territory of Poland belongs to the Baltic Sea Basin and most of the country's area is divided into two large river basins – of the River Vistula and of the River Odra (the latter river being shared with two other countries – Czech Republic and Germany). There are also several smaller coastal rivers flowing into the Baltic Sea and numerous lakes, in particular in the North of the country. Among three basic water-related problems: having too much, too little and too polluted water, all three have manifested themselves in Poland. The abundance of water, leading to destructive floods, has been occurring in Poland from time to time (most recent, and record-holding, flood events occurred in 1997). Having too little water occurs more frequently (e.g., summer droughts of 1992, 2003, 2006, 2008), while water pollution, the heritage of decades of inadequate wastewater management, has been ubiquitous and has manifested itself in the inadequate water quality in rivers and water bodies (Krysanova et al. 2006). However, a considerable improvement of water quality has been achieved and further developments are expected, related to the implementation of the EU Water Framework Directive (Hattermann and Kundzewicz 2010).

Finally, information on the people of Poland will be given in a nutshell. This part of the presentation will contain a few glimpses on the complex history of the country. It will review a few interlinkages between the states sharing the Baltic Sea basin.

References

- Hattermann, F. F., and Kundzewicz, Z. W. (Eds) (2010) Water Framework Directive: Model supported Implementation. A Water Manager's Guide. IWA Publishing, London, 268pp.
- Krysanova, V., Kundzewicz, Z. W., Pińskwar, I., Habeck, A., Hattermann, F. (2006) Regional socio-economic and environmental changes and their impacts on water resources on example of Odra and Elbe basins. *Water Resour. Management* 20(4):607-641.
- Przybylak, R., Brazdil, R., Majorowicz, J., Kejna, M. (Eds) (2010) *The Polish Climate in the European Context: An Historical Overview*. Springer, 535pp.

BONUS-169: Future perspectives for environmental research for the Baltic Sea region

Kaisa Kononen and Andris Andrusaitis

Baltic Organisations Network for Funding Science EEIG (kaisa.kononen@bonuseeig.fi)

The importance of excellence in marine research and technology has been highlighted in several contexts as a cornerstone for the success of the integrated European Maritime Policy. The message to the science community has been the request to develop scientific bases for Ecosystem Based Management (EBM) or in other words the Ecosystem Approach to Management (EAM).

The challenge is by no means trivial, since it involves¹

- Research linking human and ecosystem sciences;
- Methodological research to evaluate the effectiveness of terrestrial management strategies and tools when applied to marine ecosystems and to clarify the nature of any necessary adaptations;
- Research to build the capacity for assessing impacts of human activities, singly or in combination, on marine ecosystems and to partition effects of different anthropogenic and natural stressors on these ecosystems.

The Joint Baltic Sea Research Programme - BONUS-169, aims at responding to the challenge by fostering policy driven, excellence based research on the Baltic Sea System. The programme Outline² defines four principles as a foundation for the development of the Strategic Research Agenda for the years 2012-2016:

The Research Agenda must be developed with scientific thinking and be receptive to emerging research needs. From this conclusion arises the most important principle of the Strategic Research Agenda: A dynamic approach to be followed. The second principle involves the inclusion of both marine and coastal aspects in order to fully encompass the ecosystem of the Baltic Sea and its coasts – the Baltic Sea System. The third principle recognizes the importance of knowledge on the influences and inputs to the Baltic Sea System from the catchment. Finally, the fourth principle concerns the strengthening of stakeholder participation.

BONUS-169 is currently starting the process of definition of the themes and research issues for its Strategic Research Agenda and the coming calls for proposals. Following the already agreed Outline the main themes will be:

- 1: The sea-coast-catchment continuum
- 2: The changing ecosystem
- 3: Sustainable coastal and marine goods and services
- 4: Chemical condition of the Baltic Sea System

5: Research, policy and management in the Baltic Sea System

[6: New innovations in monitoring, observation and data management]³

Proposals for sub-themes and research issues are currently enquired from research professionals in academia and sector research institutes, government officers and experts in all relevant spheres: agriculture, fisheries, transportation and energetics, environment, regional development and spatial planning, local governments, tourism and recreation, as well as industries having a stake. The Poll for proposals will be open until August 16th, 2010 at www.bonusportal.org.

Funding for this programme is secured – after almost seven years' of preparation there is now a trilateral consensus, and soon the formal decisions between the European Council, European Parliament and the Commission about ca. 100 million EUR funding for research to be carried out during 2012-2016. The first call for proposals is scheduled for late 2011.

¹ ESF Marine Board, Working Group on Science Dimensions of Ecosystem Approach to Management of Biotic Ocean Resources

² BONUS Publications No. 11: Outline of the BONUS-169 Joint Baltic Sea Research Programme

³ This Theme has not been formally adopted by the time of writing this abstract

NEESPI current status and its objectives within north-western Eurasia

Pavel Ya. Groisman

University Corp. for Atmospheric Research at the NOAA National Climatic Data Center, Asheville, North Carolina, USA
(pasha.groisman@noaa.gov)

1. Background

The Northern Eurasia Earth Science Partnership Initiative, NEESPI, *strives to understand how the land ecosystems and continental water dynamics in Northern Eurasia interact with and alter the climatic system, biosphere, atmosphere, and hydrosphere of the Earth.* Not a single national agency can afford a near-continent-wide research framework offered by the NEESPI community, but together they can. Regional climate change, methane emissions from the Arctic shelf seas, carbon cycle monitoring across the boreal zone of Eurasia, regional climatic, hydrological, cryospheric, and environmental modeling, land use and socio-economic studies, and the feedbacks to the Global Earth System of rapidly changing conditions on the subcontinent are the topics of numerous NEESPI studies. The last one, involving the consequences for the Global Earth System of the changes over Northern Eurasia, is a major reason for international involvement in the NEESPI domain studies. Currently, NEESPI is widely recognized and endorsed by several Earth System Science Partnership (ESSP) programmes and projects. In particular, in 2006, NEESPI has been endorsed by IGBP as the IGBP External Project.



Figure 1. NEESPI study area is loosely defined as the region between 15°E in the west, the Pacific Coast in the east, 40°N in the south, and the Arctic Ocean coastal zone in the north. Territory of the Former Soviet Union, Eastern Europe, Fennoscandia, Mongolia, and north China are all included in this area. Northwestern Eurasia is outlined in this map borrowed from Groisman et al. (2009).

2. NEESPI activities

Since 2004, NEESPI participants have been able to seed several waves of research proposals to international and national funding agencies and institutions and also contribute to the International Polar Year. In the year 2009, 130 individually funded projects in the United States, Russian Federation, China, European Union, Japan, and Canada have been working to address the NEESPI Science Plan objectives (more than 560 scientists from more than

200 institutions of 30 countries). Gradually, a new focus of the NEESP initiative has emerged: the build up a suite of regional climatic, hydrological, environmental, and land use models well linked to global change models that can be used for comprehensive projections of environmental and climatic changes within Northern Eurasia.

NEESPI organizes several meetings and workshops per year. In the last year, two open sessions at the AGU Annual Meeting and the EGU Annual Assembly and four Specialty and/or Regional NEESPI Workshops were convened. Two of these workshops (in Krasnoyarsk, Russia and Bishkek, Kyrgyzstan) were accompanied by the Early Career Scientists Schools. The Workshop results were broadly disseminated electronically via the NEESPI web site (<http://neespi.org/meetings/>). During the past 3 years, more than 350 papers and books were published (the total number of peer-reviewed publications exceeds 500). NEESPI compendium peer-reviewed publications include: the NEESPI Science Plan (Available at <http://neespi.org/science/>); 1st Special NEESPI issue (13 papers; April 2007) in *Global and Planetary Change*; 2nd Special NEESPI issue in *Environ. Res. Lett.* (15 papers; <http://www.iop.org/EJ/toc/1748-9326/2/4>; December 2007); the book "Regional Aspects of Climate-Terrestrial-Hydrologic Interactions in Non-boreal Eastern Europe" (2009); an overview NEESPI paper in *Bull. Amer. Meteorol. Soc.* (Groisman et al. 2009); the 3rd Special NEESPI Issue in *Environ. Res. Lett.* (as of February 15, 2010, 30 papers were published on line at <http://www.iop.org/EJ/toc/1748-9326/4/4> or accepted and 8 manuscripts remained in the review process). Two books devoted to the boreal and tundra zones of Eurasia are scheduled to be published in early 2010.

3. NEESPI science questions in northwestern Eurasia

We anticipate the most significant environmental changes along the borders of the ecosystems (e.g. taiga–tundra, taiga–broad-leaf forest, -forest –steppe etc). Therefore, during the development of the NEESPI Science Plan (<http://neespi.org/science/>), the NEESPI domain was partitioned by the ecosystems instead of the watersheds. Priorities in surface energy and water cycle studies in the NEESPI studies were set according to two criteria. First, attention must be paid to the processes that directly feed back to the global Earth system. This justifies the interest of the international community in environmental changes in Northern Eurasia. Secondly, the processes of major societal importance must be addressed. They may or may not affect the Global Earth System, but for the region's population, they are of pivotal importance. These include extreme weather events, water supply, and impacts on agriculture and air and water quality. In northwestern Eurasia (especially in the densely populated Baltic Sea Basin), the processes (and therefore, their studies) prevail that are more responsive to the second criterion.

The Baltic Sea basin occupies a large part of the northwestern part of the NEESPI domain (Figure 1). Observed contemporary changes in the Atlantic Sector of

Eurasia are characterized by very high variability ($\sigma = 0.7^{\circ}\text{C}$), especially during the past 50 years (Figure 2). These changes (while dramatic themselves) caused shifts in several environmentally important thresholds of the seasonal cycle that affect the regional water cycle and ecosystems, as well as societal well-being. They include changes in the duration of periods with snow cover and the growing season and increases in maximum snow depth and snow water equivalent over European Russia north of 55°N . The stability of the winter season is also affected being much more frequently interrupted by thaws. In the warm season, the species composition and agriculture practices that are controlled by changes in growing degree-days and water availability (cf. Bulygina et al. 2007, 2009, 2010; Groisman et al. 2003, 2007; Groisman and Reissell 2010; Gutman and Reissell 2010; Oltchev et al. 2009, Sazonova and Oltchev 2010; and accompanied presentations of Bulygina et al. and Speranskaya, at this conference).

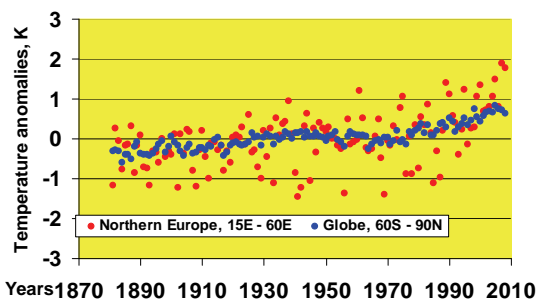


Figure 2. Annual surface air temperature anomalies ($^{\circ}\text{C}$), area averaged over the globe and Northern Eurasia north of 40°N within the 15°E to 60°E latitudinal band for the 1881–2008 period. Rates of increase of annual temperature for the “globe” (60°S to 90°N) and Northern Eurasia are $0.86^{\circ}\text{C}/128\text{ yr}$ and $1.13^{\circ}\text{C}/128\text{ yr}$ respectively. Data source: Archive of Lugina et al. (2007, updated).

4. The presentation

An overview of the ongoing NEESPI projects in the Northwestern sector of the NEESPI domain (Figure 1) will be presented at the Conference.

References

- Bulygina, O.N., V.N. Razuvaev, N.N. Korshunova and P. Ya. Groisman (2007) Climate variations and changes in the climate extreme events in Russia. *Environ. Res. Lett.* 2, 045020 (7 pp) doi:10.1088/1748-9326/2/4/045020.
- Bulygina O N, Razuvaev V N and Korshunova N. N 2009a Changes in snow cover over Northern Eurasia in the last decades *Environ. Res. Lett.* 4 045026 (6pp) doi: 10.1088/1748-9326/4/4/045026
- Bulygina, O.N., P.Ya. Groisman, V.N. Razuvaev, and V.F. Radionov (2010) Snow cover basal ice crust changes over Northern Eurasia since 1966, *Environ.Res. Lett.*, 4, in review.
- Groisman, P.Ya., and 27 Co-Authors (2009) The Northern Eurasia Earth Science Partnership: An Example of Science Applied To Societal Needs. *Bull. Amer. Meteorol. Soc.*, 90, 671-688.
- Groisman P.Ya. and S.V. Ivanov, eds. (2009) *Regional Aspects of Climate-Terrestrial-Hydrologic Interactions in Non-boreal Eastern Europe*. Springer, Amsterdam, The Netherlands, 251 pp.
- Groisman, P.Ya. and A.J. Soja, (2009) Ongoing climatic change in Northern Eurasia: Justification for expedient research. *Environ.Res. Lett.*, 4, doi:10.1088/1748-9326/4/4/045002 (7 pp.).
- Groisman, P.Ya. and A. Reissell, eds. (2010) Proceedings of the Northern Eurasia Earth Science Partnership Initiative (NEESPI) Regional Science Team Meeting devoted to the High Latitudes, 2-6 June, Helsinki, Finland. *iLEAPS Science Report Series No 1*, University of Helsinki Press, Helsinki, Finland ~ 100 pp.[Available also at <http://www.iLEAPS.org>].
- Groisman, P.Ya., B.G. Sherstyukov, V.N. Razuvaev, R.W. Knight, J.G. Enloe, N.S. Stroumentova, P. H. Whitfield, E. Førland, I. Hannsen-Bauer, H. Tuomenvirta, H. Aleksandersson, A. V. Mescherskaya, and T.R. Karl (2007) Potential forest fire danger over Northern Eurasia: Changes during the 20th century. *Global and Planetary Change*, 56, issue 3-4, 371-386.
- Gutman G. and A. Reissell, eds. (2010) *Arctic land cover and land use in a changing climate: Focus on Eurasia*. Springer, Amsterdam, The Netherlands, in press
- Lugina K M, Groisman P Ya, Vinnikov K Ya, Koknaeva V V and Speranskaya N A 2007 Monthly surface air temperature time series area-averaged over the 30-degree latitudinal belts of the globe, 1881-2007 Trends: A Compendium of Data on Global Change Carbon Dioxide Information Analysis Center Oak Ridge National Laboratory U.S. Department of Energy Oak Ridge Tennessee USA [Available at: <http://cdiac.ornl.gov/trends/temp/lugina/lugina.html>].
- Oltchev, A, E. Novenko, O. Desherevskaya, K. Krasnorutskaya, and J. Kurbatova (2009) Effects of climatic changes on carbon dioxide and water vapor fluxes in boreal forest ecosystems of European part of Russia. *Environ. Res. Lett.* 4 (2009) 045007 (8pp) doi:10.1088/1748-9326/4/4/045007
- Sazonova T.A. and A.V. Oltchev (2010) The response of coniferous trees to industrial pollution in northwest Russia *Environ. Res. Lett.*, in review.
- Vygodskaya N N, Groisman P Ya, Tchebakova N M, Kurbatova J A, Panfyorov O, Parfenova E I and Sogachev A F (2007) Ecosystems and climate interactions in the boreal zone of Northern Eurasia *Environ. Res. Lett.* 2 045033 doi:10.1088/1748-9326/2/4/045033

ECOSUPPORT (Advanced tool for scenarios of the Baltic Sea ECOSystem to SUPPORT decision making): Project approach and selected results

The ECOSUPPORT Consortium^{1,2,3,4,5,6,7,8,9,10,11}

¹ Swedish Meteorological and Hydrological Institute (SMHI), Research Department, Sweden (Helen.Andersson@smhi.se)

² Baltic Nest Institute, Resilience Centre, Stockholm University, Sweden

³ Atlantic Branch of P.P Shirshov Institute of Oceanology, Russian Academy of Sciences, Russia

⁴ Tjärnö Marine Biological Laboratory, Gothenburg University, Sweden

⁵ National Institute for Aquatic Resources (DTU-Aqua), Technical University of Denmark and Department of Marine Ecology, University of Aarhus, Denmark

⁶ Baltic Sea Research Institute Warnemünde, Germany

⁷ Institute of Oceanology, Polish Academy of Sciences, Poland

⁸ Marine Systems Institute, Tallinn University of Technology, Estonia

⁹ Finnish Meteorological Institute, Finland

¹⁰ GKSS Research Centre Geesthacht, Institute for Coastal Research, Germany

¹¹ Centre for Climate Science and Policy Research, Linköping University, Sweden

1. Abstract

The response of the marine ecosystem during the 21st century depends on several, partly competing drivers, like expected reduced phosphorus and nitrogen loads, increased water temperatures, and reduced salinities. Thus, presently discussed targets for nutrient load reductions that may be sufficient to improve the ecological status in present climate might fail under future climate conditions. The proposed project ECOSUPPORT combines the assessments of various drivers to promote an ecosystem approach to the management of human activities. The main aim of ECOSUPPORT is to provide a multi-model system tool to support decision makers. To meet the aim, extensive efforts have been put into producing reliable forcing data sets that can be used for validation, hindcast and future projections of marine biogeochemistry and food web models of the Baltic Sea. Transient GCM runs of future climate, using IPCC's latest scenarios, have been downscaled to the Baltic region. Quality assessment and performance inter comparison of three state-of-the-art coupled physical-biogeochemical models have been performed, as well as further development of existing food-web models for the Baltic Sea that will be used to study future interplay between forcing factors from climate and human activity.

2. Introduction

To confidently assess the combined effects of changing human activities and a changing climate on the state of the Baltic Sea one needs reliable predictive tools. To rely on the models' capacity to simulate a changing climate one must first ensure their capacity to simulate past and present states. Comparing observed and simulated past climate variability (i.e. quantification of model uncertainties) and analyzing causes of observed variations will add to scenario reliability. Comparing results between structurally different physical-biogeochemical models will also aid to understand model behaviour at key marine processes and model sensitivity to the forcing fields. The state-of-the-art models will then be used to perform simulations of the marine ecosystem for 1850-2100, forced by reconstructions of past climate and by various future greenhouse gas emission and air- and river-borne nutrient load scenarios (ranging from a pessimistic *business-as-usual* to the *most optimistic case*). By analyzing the projections of the future Baltic Sea ecosystem with a probabilistic approach accounting for uncertainties caused by biases of regional and global climate models (RCMs and GCMs), lack of process description in the ecosystem

models, unknown greenhouse gas emissions and nutrient loadings, and natural variability, the impacts of climate change on the marine biota, biodiversity and fish populations (with focus on cod, sprat and herring) can be assessed. This offers a tool to support decision makers and stakeholders and will help to raise wider public awareness in these issues. Local-scale impacts of changing climate on coastal areas will focus on the Gulf of Finland, Vistula Lagoon, and the Polish coastal waters.



Figure 1. The ECOSUPPORT logo.

3. Models

To calculate future climate of the Baltic Sea region under different scenarios dynamical downscaling with a high-resolution coupled atmosphere-ice-ocean-land surface model (the Rossby Centre Atmosphere Ocean model, RCAO (SMHI)) with lateral boundary data from four transient GCM runs have been applied. To calculate future river flow and river-borne nutrient loadings the new hydrological SMHI model HYPE is used. It simulates a range of hydrological variables including phosphorus and nitrogen in soils, rivers and lakes. The physical-biogeochemical state of the Baltic Sea is assessed by three state-of-the-art coupled models: BALTSEM (BNI), ERGOM (IOW), and RCO-SCOBI (SMHI). The models have been used to calculate changing concentrations of nitrate, ammonium, phosphate, diatoms, flagellates, cyanobacteria, zooplankton, detritus, and oxygen in the Baltic Sea. They are structurally different in that ERGOM and RCO-SCOBI are 3D circulation models with uniform high horizontal resolution while BALTSEM resolves the Baltic Sea spatially in 13 sub-basins.

Development of several types of fish-climate models are in progress: statistical single- and multispecies models (DTU Aqua), bioclimatic envelope models (GU) and food-web models using Ecopath/Ecosim (BNI), in order to evaluate the impact of climate and fisheries.

4. Results

Historical airborne load to the Baltic Sea have been reviewed and the relevant concentration and deposition data have been transformed into electronic form. The data cover the period from 1860 to 1970. Nutrient loads from atmospheric, point and river sources have also been compiled by BNI for the period 1902-2006 and results from the HYPE watershed model estimates river and point loads from 1960 to present. Daily sea-level pressure (SLP) is physically closely connected with wind, precipitation, and short wave radiation. The daily SLP data set from the EMULATE project have been used to reconstruct those daily fields. Realistic RCAO hindcast runs have been performed at 25 and 50 km resolution and the control period gives at hand that the high resolution version gives generally more realistic surface winds, while e.g. temperature fields are well produced in both runs. Scenario runs have been carried out in both 25 km and 50 km atmospheric configuration, driven by ECHAM/5MPI-OM and HADCM3.

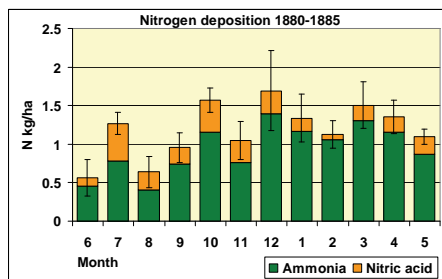


Figure 2. Seasonal variation in atmospheric nitrogen load at an agricultural research area near Copenhagen, Denmark.

Model experiments have been performed in order to reveal more information about the dynamics of organic matter, nitrogen, phosphorus, oxygen and cyanobacteria in the Baltic Sea (Eilola 2009, Eilola et al. 2009). Work has also been performed on quality assessment and model inter-comparison between the coupled physical-biogeochemical models. Results from hindcast simulations were compared with observations for the period 1970-2005 and it was found that all three investigated models are able to reproduce the observed variability of biogeochemical cycles well. Uncertainties are primarily related to differences in the bio-available fractions of nutrient loadings from land and parameterizations of key processes like sediment fluxes that are presently not well known (Eilola et al. 2010).

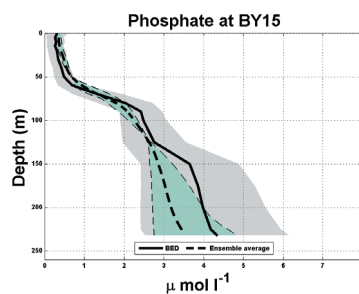


Figure 3. Average (1970-2005) phosphate concentration at BY15. The black solid line and the grey shaded area indicate the mean value and ± 1 standard deviation of BED data. The black dashed line and the blue shaded area indicate the mean and spread of the models ERGOM, RCO-SCOB1 and BALTSEM.

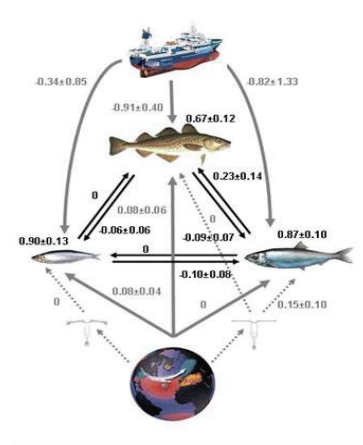


Figure 4. Food-web interactions are influenced by the combined effects of climate and fisheries.

The food-web models are developed to address the combined consequences of management and climate change and may serve as a tool for decision making for fisheries. Cod recruitment is vulnerable to climate related decline in salinity resulting from both direct and indirect effects (i.e. through species interactions). A stochastic foodweb model driven by regional climate scenarios was used to produce quantitative forecasts of cod dynamics. It was demonstrated how exploitation has to be adjusted in order to reduce risks of future stock collapse under different climate scenarios (Lindgren et al. 2009).

ECOSUPPORT results from first year is summarized in the annual report (www.baltex-research.eu/ecosupport/results.html).

References

- Eilola, K., (2009) On the dynamics of organic nutrients, nitrogen and phosphorus, in the Baltic Sea. Rapport Oceanografi No.99, SMHI, Norrköping, Sweden, 16 pp.
- Eilola, K., H.E.M. Meier, and E. Almroth, (2009) On the dynamics of oxygen, phosphorus and cyanobacteria in the Baltic Sea; a model study. *J. Marine Systems*, 75, 163-184.
- Eilola, K., B. G. Gustafson, R. Hordoir, A. Höglund, I. Kuznetsov, H. E. M. Meier, T. Neumann, O. P. Savchuk, (2010) Quality assessment of state-of-the-art coupled physical-biogeochemical models in hind cast simulations 1970-2005, Rapport Oceanografi No.101, SMHI, Norrköping, Sweden.
- Lindgren, M., C. Möllmann, A. Nielsen, K. Brander, B. R. MacKenzie, and N. C. Stenseth. (2010) Ecological forecasting under climate change - the case of Baltic cod. *Proc. Roy. Soc. Lond. B* (in review).

Detection and attribution of an anthropogenic effect on temperature and precipitation changes in the Baltic Sea catchment

Jonas Bhend¹ and Hans von Storch^{2,3}

¹ Institute for Atmospheric and Climate Science, ETH Zürich, Switzerland (jonas.bhend@gmx.ch)

² Institute for Coastal Research, GKSS Research Centre, Geesthacht, Germany

³ Meteorological Institute, University of Hamburg, Germany

1. Introduction

Extensive evidence of a large-scale anthropogenic climate change has been collected during the last decades. In contrast, regional-scale climate change is less well understood. Therefore, this study aims at contributing to the discussion of an observable human influence on changes in near-surface temperature and precipitation in the Baltic Sea catchment using a formal detection and attribution analysis. Climate change detection and attribution is a signal in noise problem. We try to decompose the observed change into the responses to external forcing mechanisms, the signals, and internal variability, the noise. Detection of an external influence is reached, if we can falsify the null-hypothesis that the observed change is due to internal variability alone with a given probability of error. Attribution of the observed change to a single forcing mechanism or a combination of forcing mechanisms is less straightforward. First, we have to show that the response to the proposed forcing mechanism is consistent with the observed change. Second, we have to be able to rule out all other (physically plausible) forcing mechanisms as causes of the observed change.

2. Observed change and simulated signals

We use gridded land station data to describe the observed change in the Baltic Sea catchment. The observed temperature change is expressed in anomalies of 5-yearly averages of seasonal, area-average temperature from 1953 to 2007 according to the CRUTEM3v dataset (Jones and Moberg 2003) as shown in the left column of Figure 1. The observed change in precipitation is derived from the GPCC v4 reanalysis product (Schneider *et al.* 2008, right column of Figure 1). The precipitation change is expressed in relative anomalies, thereby correcting – to first order – for observation errors such as wind-induced undercatch and evaporation losses. We use all four seasons combined in the analysis.

The climate change signals are derived from model simulations with global atmosphere-ocean general circulation models (AOGCMs) from the WCRP CMIP3 database (Meehl *et al.* 2007). We use the simulations with observed or reconstructed temporally varying forcings for the 20th century and extend these into the 21st century with simulations driven by emissions according to the SRES A1B emission scenario. The simulations are split in two subsets: 34 (29 for precipitation) simulations of 11 (10) models are driven with varying anthropogenic (at least greenhouse gases and sulfate aerosols) and natural (solar and volcanic) forcings in the 20th century. The multi-model ensemble mean of these simulations is used to estimate the ALL signal (thin solid lines in Figure 1). 20 simulations from 12 models are driven with anthropogenic forcings only in the 20th century. These are used to derive the ANT signal (crosses in Figure 1). Furthermore we use the pooled control runs from the 23 (22) models to estimate internal variability (not shown).

Additional analyses reveal that dynamical downscaling has only a minor effect on the representation of the response to anthropogenic forcing in area-average quantities in the Baltic Sea catchment (not shown). We note, however, that there are significant systematic model biases in the representation of the mean climate in this region likely due to misrepresented small-scale processes such as snow cover/snow melt and convective precipitation. Furthermore, we stress that the variability in area-average precipitation is underestimated in all the models analyzed. As a first-order correction, we inflate the variability in the models to better match the observations. Nonetheless, we recommend interpreting detection and attribution results for precipitation with caution.

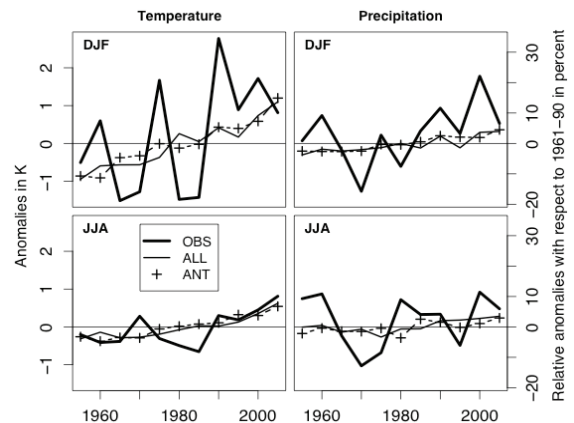


Figure 1. Time series of observed area-average temperature anomalies according to CRUTEM3v (left column, solid thick lines) and relative precipitation anomalies according to GPCC v4 (right column, solid thick lines) along with the climate change signals as derived from the simulations in the CMIP3 multi-model ensemble with anthropogenic forcing only (crosses) and anthropogenic and natural forcing (thin black lines)

3. Total least squares regression

We compare the observed and simulated temperature and precipitation changes using total least squares regression, a variant of optimal fingerprinting, as introduced by Allen and Stott (2003). We assume that the temporal evolution of the signal is known, but the scaling is uncertain. The regression model (equation 1) accounts for contamination of the observed change (y) and of the estimated signal (x) with noise from internal variability (v_x and v respectively).

$$y = a(x + v_x) - v \quad (1)$$

We assume that the internal variability in the observations and the models have both the same covariance structure, the magnitude of the noise contamination in the signal (v_x)

compared to the noise in the observations (v), however, is reduced by the square root of the number of ensemble members used to estimate the signal.

In the linear regression framework, the detection and attribution problem can be expressed as follows: Detection of an external influence is achieved if the null-hypothesis $a = 0$ (i.e. the observed change is due to internal variability v alone) can be falsified. The proposed signal x is consistent with the observed change y if the best-fit scaling a is not significantly different from 1 (see Figure 2).

4. Results and discussion

We find a detectable external signal in seasonal temperature anomalies from 1953 to 2007 (Figure 2). Both the anthropogenic and the all-forcings signals are detected with 10% risk of error (i.e. zero scaling on these signals is inconsistent with the data). The best-fit scalings for the anthropogenic and all-forcings signals are very similar and close to unit scaling, indicating that either of the proposed responses is a plausible explanation for the observed change. From the small difference in scaling on the anthropogenic and all-forcings response follows, that the response to natural forcings is rather weak and unimportant in explaining the observed change or not well-known. This is further confirmed by using an estimate of the natural signal in the single-signal detection analysis. Unit scaling on the natural signal is inconsistent with the observations.

The natural signal, however, is computed as the difference between the all-forcings and anthropogenic signals. Therefore, the natural signal reflects not only differences in forcing mechanisms between the all-forcings and anthropogenic signals, but also the different set of models used to derive the former two signals. Additional analyses with model simulations driven by natural forcings only confirm that natural forcing alone is no plausible explanation for the observed temperature change in the Baltic Sea catchment (not shown).

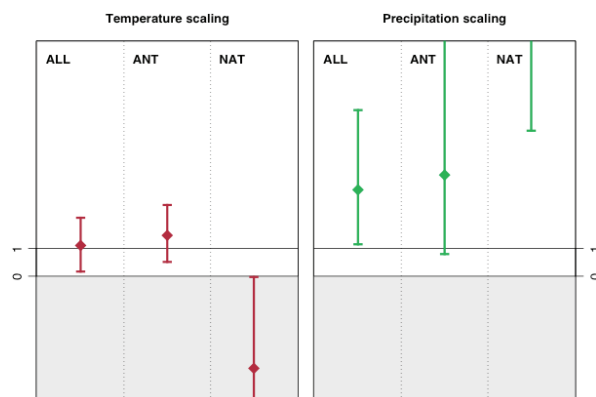


Figure 2. Scaling factors and corresponding confidence intervals of a single-signal detection analysis with time series of 5-yearly averages of seasonal area-average temperature and precipitation anomalies from 1953 to 2007. The signals are derived from simulations of the CMIP3 ensemble with all forcings (left), anthropogenic forcings (middle), and the difference between all and anthropogenic forcing signals (NAT, rightmost column). The diamonds indicate the best-fit scaling on the signals, vertical lines denote the 90% confidence interval about the best-fit scaling.

In contrast to temperature, detection results for seasonal precipitation in the Baltic Sea catchment are less consistent.

Even though we detect external influences in the observed changes from 1953 to 2007 for all three different signals, we have to amplify the signals considerably to best fit the observations (Figure 2). As for temperature, the best-fit scalings on the anthropogenic and all-forcings signals are similar, thus indicating that the natural response as derived from the CMIP3 ensemble is unimportant in explaining the observed change in precipitation.

In contrast to temperature, the observed change in area-average precipitation is considerably stronger than simulated in AOGCMs. If we use signals from individual models, we have to amplify the anthropogenic and all-forcings signals by factors of three to ten to best fit the observations (not shown), the natural signals have to be amplified even more. This misrepresentation of observed precipitation changes in present-day climate models is a well-known fact (Zhang et al. 2007, Bhend and von Storch 2008) and the limited skill in simulating changes in sea-level pressure and sea-surface temperature over Europe and the North Atlantic have been identified as possible causes (G. J. van Oldenborgh, pers. comm.).

5. Conclusions

We are able to detect an external influence on the observed temperature changes in the Baltic Sea catchment. Furthermore, the simulated response to anthropogenic forcing is consistent with the observed warming, the response to natural forcing is inconsistent. Attribution of the observed change to anthropogenic forcing requires the exclusion of all other plausible causes. Potentially important forcing mechanisms at the regional scale such as land-use changes and the indirect effects of aerosols, however, are not yet included in the models. Therefore, we are not able to formally attribute the observed change to anthropogenic forcing. Instead, we conclude that anthropogenic forcing is the dominant influence on the observed warming in the Baltic Sea catchment.

We are also able to detect an external influence on the observed precipitation changes. The simulated response to anthropogenic and natural forcings, however, is considerably (and in most cases also significantly) weaker than the observed change. We conclude that according to changes in area-average precipitation, neither the simulated response to combined anthropogenic and natural forcing, nor to anthropogenic or natural forcing alone provide plausible explanations for the observed change.

References

- Allen, M. R. and Stott, P. A. (2003). Estimating signal amplitudes in optimal fingerprinting, Part I: Theory. *Climate Dynamics*, Vol. 21, No. 5-6, pp. 477–491.
- Bhend, J. and von Storch, H. (2008). Consistency of observed winter precipitation trends in northern Europe with regional climate change projections. *Climate Dynamics*, Vol. 31, No. 1, pp. 17–28.
- Jones, P. D. and Moberg, A. (2003). Hemispheric and large-scale surface air temperature variations: An extensive revision and an update to 2001. *Journal of Climate*, Vol. 16 No. 2, pp. 206–223.
- Meehl, G. A. et al. (2007). The WCRP CMIP3 multimodel dataset - a new era in climate change research. *Bulletin of the American Meteorological Society*, Vol. 88, pp. 1383–1394.
- Zhang, X. et al. (2007). Detection of human influence on twentieth-century precipitation trends. *Nature*, Vol. 448, pp. 461–465.

Impact of recent changes of snow cover and climate on river runoff in the Baltic Sea basin of the East European plain

Ala Bildziuh, Liudmila Trafimova, Irina Danilovich and Ryhor Chekan

Republican Hydrometeorological Centre, Minsk, Republic of Belarus

1. The space-time analysis of the parameters defining formation of river runoff of the Baltic Sea basin of the East European plain

Characteristics of water runoff at 19 hydrological posts, data on air temperature, precipitation and snow cover at 20 meteorological stations have been used for the analysis of the role of modern changes of snow cover and climate information of river runoff of the rivers of the Baltic Sea within Belarus.

Formation of river runoff at the annual and seasonal time scales has a close dependence on precipitation. However, formation of the snow-melt flood (or peak) is defined not only by precipitation, but also by the temperature condition during the winter season. The river runoff and the maximum discharge for the snow-melt flood are defined by the snow water equivalent amount before the beginning of the snow-melt. Water equivalent of snow has an inverse relationship to air temperature for a winter season.

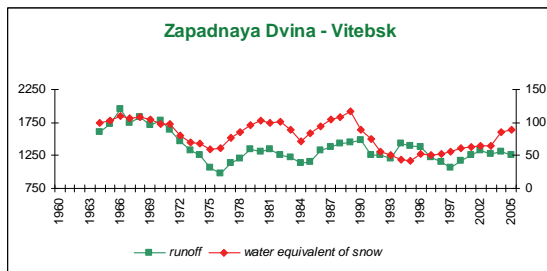


Figure 1 Runoff during the snow-melt peak (flood) and snow water equivalent prior to the snow-melt.

2. Estimation of long-term changes of river runoff dependence on changes of meteorological parameters

With the increase of precipitation during global warming since 1989 over the river basin of Zapadnaya Dvina and some rivers of the Neman basin (Neman, Viliya, Naroch, Oshmianka), a marked increase in annual river runoff has been observed. During the same period, for the majority of the rivers of the Neman basin and in the basin of Western Bug, a reduction of annual river runoff associated with reduction of precipitation has been observed.

With the increase in the seasonal sums of precipitation in the period of global warming, a reduction in the maximum water equivalent of snow is observed. It is connected with snowmelt during the more frequent periods of thaw.

Changes of all kinds of meteorological and climatic characteristics correspond to changes of characteristics of river runoff. By predicting meteorological parameters, we can predict the snow-melt flood that depends upon them.

3. Classification of dependence of river runoff on from the meteorological circulation characterized by the Wangengeim-Girs types of atmospheric circulation in the northern extratropics.

A detailed description of the Wangengeim-Girs types of the atmospheric circulation (W, E, and M) in the northern extratropics is provided in Girs (1974). Our analysis of the runoff behavior in the Belarus territory associated with the prevalence during the cold season of three major types of atmospheric circulation according to the Wangengeim-Girs classification: western (W), eastern (E), and meridional (M) types shows:

The western circulation type (W) over Belarus is characterized by an increased runoff during the winter season and lowered runoff during the snow-melt peak streamflow, and by earlier dates of the snow-melt peak compared to its long-term average dates.

The eastern circulation type (E) is characterized by a reduced runoff during the winter season and increased runoff during the snow-melt and by later dates of the snow-melt peak than its long-term average dates.

The prevalence of the meridional circulation type (M) is characterized by an insignificant runoff decrease during the winter season, increased runoff of the snow-melt peak, and later dates of the snow-melt peak.

Providing that projections of the form of circulation of the atmosphere for a specific period are available, it is possible to predict the river runoff and expected values of the seasonal runoff in the Republic of Belarus.

References

- Bildziuh A. and L. Trafimova (2009) Research of change of a hydrological mode of the rivers of the Republic of Belarus 1988-2007, Theses of reports. Scientific conference «175 years of the Hydrometeorological service of Russia - scientific problems and ways of their decision» (in Russian).
- Danilovich I., P. Lopuh, and L. Trafimova (2009) Scenarios of formation of the river runoff of Belarus in a of the snow-melt flood for 2010-2050, *The Bulletin of the Byelorussian State University*, **3**, No 2., pp. 85-87 (in Russian, abstract in English).
- Danilovich I. (2007) Influence of atmospheric circulation on a drain of the rivers of Belarus during winter and spring seasons, *Natural resources*, **8**, No 1., pp. 39-46.
- Girs A.A. (1974) *Macrocirculation method of the long-term meteorological forecast*. Leningrad, Hydrometeoizdat, 488 pp. (in Russian)

Precipitation changes in the Russian sector of the Baltic Sea basin after accounting for comprehensive biases in their measurements

Esfir G. Bogdanova¹, Boris M. Iljin¹, Svetlana Yu. Gavrilova¹ and Pavel Ya. Groisman²

¹ Voeikov Main Geophysical Observatory, St. Petersburg, Russia (esfir.bogdanova@gmail.com)

² NOAA National Climatic Data Center, Asheville, North Carolina, USA (pasha.groisman@noaa.gov)

We shall present the results of our analyses of the time series of precipitation characteristics that have been corrected according to the modern comprehensive bias correction routine (Bogdanova et al. 2002a, b). Corrections were made for daily totals for the period from 1936 to 2006 for the stations within the Baltic Sea Basin over the former USSR territory (for the Baltic States, analyses end in 1991). Changes in annual totals and the seasonal cycle of precipitation (its solid, frozen, and mixed fraction separately) during the past 70 years will be discussed. Furthermore, the differences of the rates of precipitation change (trends) will be presented, when using bias-corrected time series rather than the raw precipitation measurements. These differences will be discussed and caveats for their use will be explained.

References

- Bogdanova, E.G., Ilyin, B.M., and Dragomilova, I.V. (2002a) Application of a comprehensive bias correction model to precipitation measured at Russian North Pole drifting stations. *J. Hydrometeorol.*, **3**, 700-713.
- Bogdanova, E.G., V.S. Golubev, B.M. Ilyin, and Dragomilova I.V. (2002b) A new model for bias correction of precipitation measurements, and its application to polar regions of Russia. *Russian Meteorol. and Hydrol.*, No.10, 68-94
- Groisman P. Ya., Rankova E. Ya. (2001) Precipitation trends over the Russian permafrost-free zone: removing the artifacts of pre-processing. *International Journal of Climatology*, **21**, 657–678
- NOAA National Climatic Data Center (2005) Daily and Sub-daily Precipitation for the Former USSR. DSI-9813, description available at <http://www1.ncdc.noaa.gov/pub/data/documentlibrary/tdoc/td9813.pdf>

Changes in snow cover characteristics over north-western Russia

Olga Bulygina¹, Pavel Groisman², and Vyacheslav Razuvaev¹

¹ Russian Institute for Hydrometeorological Information, Obninsk, Russia (bulygina@meteo.ru)

² UCAR at National Climatic Data Center, Asheville, North Carolina, United States (pasha.groisman@noaa.gov)

1. Introduction

During the past 128 years (since 1881), the annual surface air temperature in Northern Eurasia has increased by 1.5°C and in the winter season by 3°C. Nearby to the north in the Arctic Ocean, the late summer sea ice extent decreased by 40% exposing a near-infinite source of water vapor for the dry Arctic atmosphere in early cold season months. Both large-scale processes, global warming and the Arctic sea ice retreat, substantially affected snow cover characteristics over northwestern Russia. This presentation will describe the contemporary changes of these characteristics since 1966.

2. Data

In addition to a standard suite of synoptic snow observations (snow depth, snow type, state of the ground at the meteorological site and its surroundings), we used in our study the national snow survey data set archived at the Russian Institute for Hydrometeorological Information.

This dataset has routine snow surveys run throughout the cold season each 10 days (during the intense snowmelt, each 5 days) at all meteorological stations of the former USSR, thereafter, in Russia since 1966. Prior to 1966 snow surveys are also available but the methodology of observations has substantially changed during that year. Therefore, this analysis includes only data of 201 Russian stations within the northwestern part of Russia (i.e., European Russia north of 55°N) from 1966 to 2009 that have a minimal number of missing observations. Surveys run separately along all types of environment typical for the site for 1 to 2 km, describing the current snow cover properties such as snow density, depth, water equivalent, and characteristics of snow and ice crust.

3. Results

During the past several decades, the following changes in snow cover characteristics over European Russia north of 55°N have been observed: (a) in autumn the dates of the onset of snow cover have not changed noticeably despite the strong temperature increase in this season; (b) in late spring, snow cover extent has decreased, retreating by 1 to 2 weeks earlier during the past 40 years; (c) in the cold season maximum snow depth and snow water equivalent (SWE) at open areas have increased (Figure 1) but in the

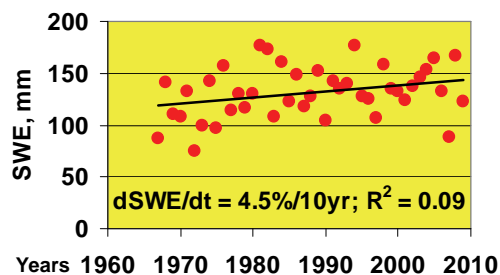


Figure 1. Maximum snow water equivalent changes over the northwestern quadrant of the Great Russian Plain during the 1967-2009 period at the “field” snow courses (Archive of Bulygina et al. 2010).

westernmost areas (e.g., within the Russian Sector of the Baltic Sea Basin) maximum snow depth decreased (Bulygina et al. 2009), and (d) days with winter thaw became more frequent (the last statement is also true for Fennoscandia; Figure 2). The snowmelt process over European Russia north of 55°N can be lengthy (on average 45 days) but even the first such melt initiates a process of snow metamorphosis on its surface changing snow albedo and generating snow crust as well as on its bottom generating basal ice crust layer. Once formed, the crusts will not disappear until complete snowmelt and have numerous modes of impact on the wild life and the winter crop yield. Our study reveals substantial changes in the basal ice crust characteristics that have practical importance for the major agricultural regions of Russia including the northwestern part of European Russia. In this region, the entire process of the spring snowmelt has become shorter in duration and (taking into account a parallel rise in the maximum snow depth and SWE) more intense.

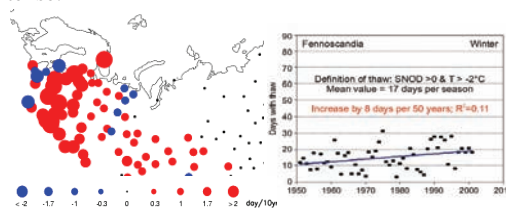


Figure 2. Changes in the days with winter thaw during the 1950-2000 period. Left: Linear trend estimates in the winter number of days with thaw (days/10yr; Groisman et al. 2003). Right: As on left, but regional time series for Fennoscandia (Groisman et al. 2009).

References

- Bulygina O N, Razuvaev V N and Korshunova N N (2009) Changes in snow cover over Northern Eurasia in the last decades *Environ. Res. Lett.* **4** 045026 (6pp) doi: [10.1088/1748-9326/4/4/045026](https://doi.org/10.1088/1748-9326/4/4/045026)
- Bulygina, O.N., P.Ya. Groisman, V.N. Razuvaev, and V.F. Radionov (2010) Snow cover basal ice crust changes over Northern Eurasia since 1966, *Environ.Res. Lett.*, **4**, in review.
- Groisman, P.Ya., B. Sun, R. S. Vose, J. H. Lawrimore, P. H. Whitfield, E. Førland, I. Hanssen-Bauer, M. C. Serreze, V. N. Razuvaev, and G. V. Alekseev (2003) Contemporary climate changes in high latitudes of the Northern Hemisphere: Daily time resolution. In: Proceedings of the 14th AMS Symposium on Global Change and Climate Variations, CD ROM with Proc. of the Annual Meeting of the Amer. Meteorol. Soc., Long Beach, California, 9-13 February, 2003, 10 pp.
- Groisman, P.Ya., Gutman, G., and Reissell A. (2010) Introduction: climate and land-cover changes in the Arctic In: Gutman G. and A. Reissell (eds.) *Arctic land cover and land use in a changing climate: Focus on Eurasia*. Springer, Amsterdam, The Netherlands, in press.

Analysis of the water balance and wind climate over the Baltic Sea drainage basin using dynamically downscaled climate simulations

Björn Carlsson¹, Ida Sjöström¹, Anna Rutgersson¹ and Anders Omstedt²

¹ Department of Earth Sciences, Uppsala University, Sweden (Bjorn.Carlsson@met.uu.se)

² Earth Sciences Centre, University of Gothenburg, Sweden

1. Introduction

The Baltic-C project (<http://www.baltex-research.eu/baltic-c/index.html>) is aiming at closing the carbon budget and to predict the future biochemical and acid-base state of the Baltic Sea drainage basin in a holistic approach. In this system of models, the Baltic Sea model PROBE-Baltic (Omstedt and Axell 2003), the run-off model CSIM (Mörth et al. 2007) and the vegetation model LPJ-GUESS (Smith et al. 2001) atmospheric forcing describing present and future climate is required. Several global coupled atmospheric-ocean climate model are dynamically downscaled at the, Rossby Centre at the Swedish Meteorological and Hydrological Institute (SMHI), this data will serve as atmospheric forcing to the carbon cycle model system. In the present investigation the relevant parameters from the model run outputs are analysed over the Baltic Sea drainage basin. For present climate they are compared to the ERA-40 re-analysis data. For future climate three types of analysis are done: Variation between the different global models, between the emission scenarios and internal variation.

2. Models

The climate data were retrieved from the Rossby Centre at SMHI where a climate change ensemble for the European area (Kjellström et al. 2008) was done within the ENSEMBLES project (Hewitt and Griggs, 2004, <http://www.ensembles-eu.org/>). Coupled global atmospheric and oceanographic climate models were dynamically downscaled to a $0.44^\circ \times 0.44^\circ$ (c. 50×50 km) grid using the regional atmospheric climate model RCA3 (Kjellström et al. 2005). The following models were chosen for the present study: ECHAM5/OPYC3 (scenarios A1B, A2, B1), HadCM3 (scenario A1B) and CCSM3 (scenario A1B) The ECHAM5/MPI-OM model (Roeckner et al. 2006; Jungclaus et al. 2006) is developed at Max-Planck Institute (MPI) in Hamburg, Germany. ECHAM5 is the atmospheric part and MPI-OM (MPI Ocean Model) the ocean part. HadCM3 model (Gordon et al., 2000) is developed at the Hadley Centre at the UK Met Office. The CCSM (Community Climate System Model) (Collins et al. 2006) is developed at NCAR, US. The ERA40 global re-analysis data (Uppala et al. 2005) was also downscaled with RCA3 to compare the models with present climate.

The present set of model runs makes it possible to do make three different types of analysis:

Model variation: A1B (3 models)

Scenario variation: ECHAM5 (3 scenarios).

Internal variation: ECHAM5 A1B (3 different initializations)

3. Present climate

The scenarios are evaluated against the present climate (1961–2005) by comparing the yearly averages and seasonal cycles for 2-m temperature and humidity, geostrophic and 10-m wind, and total cloudiness with the ERA-40 data. In figure 1 the annual mean 2-m temperature in 5 different basin of the Baltic Sea are shown for 5 different global

model runs including 3 different initializations of the ECHAM5 model. The difference between the models are generally large (1–2°C). In comparison to ERA40 the models underestimates the temperature in all basins except in Kattegat and Bothnian Bay. The internal variation of ECHAM5 is almost as large as the spread between the different models.

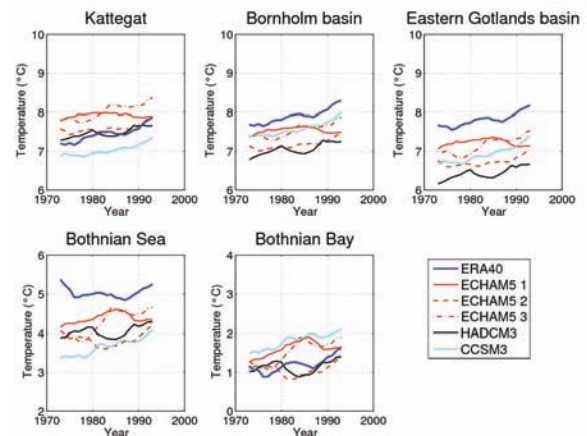


Figure 1. 2-meter temperature from different model runs in relation to ERA-40 during the control period. A 25-year running mean is applied.

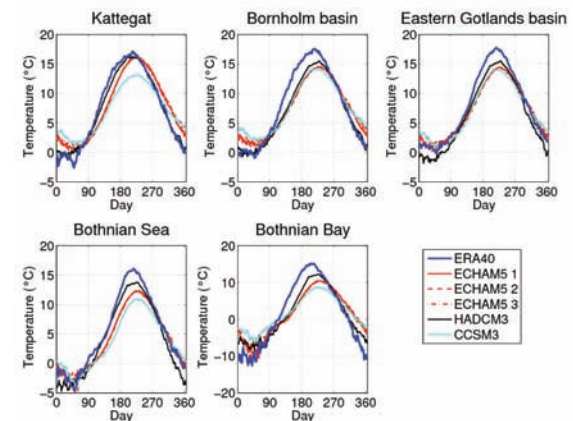


Figure 2. Seasonal mean cycle for 2-m temperature from different model runs in relation to ERA-40 during the control period.

Figure 2 shows the mean seasonal cycle of 2-m temperature in 5 different basins of the Baltic Sea during the control period. The general result is that the model runs underestimate the seasonal variability, with too mild winters and too cold summers.

Similar analyses will be discussed for the other parameters and also over land areas. For wind, the distribution of

wind events will be presented as well. Also, the water balance, P–E, will be analysed and presented.

4. Future climate

Similar analyses as for the present climate will be presented for the future climate. In figure 3 the 2-m temperature in 5 different basins of the Baltic Sea are shown for 5 different runs including 3 different scenarios of the ECHAM5 model. The emission scenario A1B is common for the three models. All runs show an obvious trend towards higher temperatures. But a striking feature is that the variations among the models are of the same order as the variations among the scenarios in the ECHAM5 runs.

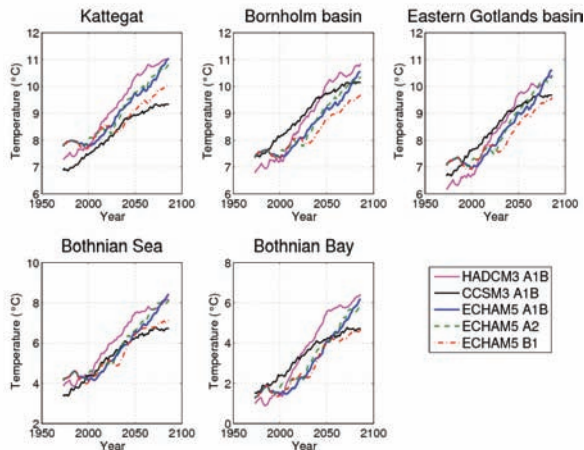


Figure 3. 2-meter temperature from different model runs in relation in future climate. A 25-year running mean is applied.

References

- Collins, W.D., et al. (2006) The Community Climate System Model Version 3 (CCSM3), *J. Clim.*, 19, 2122–2143.
- Gordon, C., et al. (2000) The simulation of SST, sea ice extent and ocean heat transports in a version of the Hadley Centre coupled model without flux adjustments, *Clim. Dyn.*, 16, 147–168.
- Hewitt, C.D., and D.J. Griggs (2004) Ensemble-based predictions of climate changes and their impacts, *EOS, Transactions AGU*, 85, doi:10.1029/2004EO520005, 2004.
- Jungclaus, J.H., et al. (2006) Ocean Circulation and Tropical Variability in the Coupled Model ECHAM5/MPI-OM, *J. Clim.*, 19, 3952–3972.
- Kjellström, E., et al. (2005) A 140-year simulation of European climate with the new version of the Rossby Centre regional atmospheric climate model (RCA3), *Reports Meteorology and Climatology*, 108, SMHI, SE-60176 Norrköping, Sweden, 54pp.
- Kjellström, E., U. Hansson, C. Jones, G. Nikulin, G. Strandberg, and Anders Ullerstig (2009) Changes in wintertime temperature climate as deduced from an ensemble of regional climate change simulations for Europe, *Rosby Centre Newsletter*, May 2009, SMHI, SE-60176 Norrköping, Sweden
- Mörth, M., et al. (2007) Modeling Riverine Nutrient Transport to the Baltic Sea: A Large-scale Approach, *Ambio*, 36, pp. 124–133
- Nakicenovic, N., et al. (2000) Emission scenarios, A Special Report of Working Group III of the Intergovernmental

- Panel on Climate Change. Cambridge University Press, 599pp.
- Omstedt, A. L. Axell (2003) Modeling the variations of salinity and temperature in the large gulfs of the Baltic Sea. *Continental Shelf Research*, 23, pp. 265–294.
- Roeckner, E., et al. (2006) Sensitivity of Simulated Climate to Horizontal and Vertical Resolution in the ECHAM5 Atmospheric Model, *J. Clim.*, 19, 3771–3791.
- Rutgersson, A., M. Norman, and G. Åström (2009) Atmospheric CO₂ variation over the Baltic Sea and the impact on air–sea exchange, *Bor. Env. Res.*, 14, 238–249.
- Smith B., I.C. Prentice, M.T. Sykes (2001) Representation of vegetation dynamics in the modeling of terrestrial ecosystems: comparing two contrasting approaches within European climate space, *Global Ecology and Biogeography*, 10, 621–637.
- Uppala, S.M., et al. (2005) The ERA-40 Re-analysis, *Q. J. Roy. Met. Soc.*, 131, 2961–3012.

Long term water level and surface temperature changes in the lagoons of the southern and eastern Baltic Sea

Inga Dailidienė¹, Henning Baudler², Boris Chubarenko³

¹ Klaipėda University, Geophysical Sciences Department, Lithuania (inga.dailidienne@ku.lt)

² Universität Rostock, Mathematisch-Naturwissenschaftliche Fakultät, Institut für Biowissenschaften (IFBI), Germany

³ Atlantic Branch of P.P.Shirhov Institute of Oceanology of Russian Academy of Sciences, Russia

1. Introduction

The global average rate of water level rise is estimated to $1.7 \pm 0.5 \text{ mm yr}^{-1}$ in the 20th century (Bates et al. 2008). Christiansen et al. (2001) estimated the eustatic sea level rise in the North Sea to 1.3 mm year^{-1} during the last century. The same order of average mean water level rise rate ($1.5 \pm 0.5 \text{ mm year}^{-1}$) was estimated for the Finnish coast of the Baltic Sea by Johansson et al. (2004). The observed rise in sea-level is also recorded at many Baltic Sea countries tide gauge stations at the end of the 20th century (Kalas 1993, Stigge 1993, Fenger et al. 2001, Ekman 2003, Kahma 2003, Suursaar et al. 2006). For Germany, an average sea level rise for the North Sea was $1.88 - 1.95 \text{ mm year}^{-1}$, and $1.14 \text{ mm year}^{-1}$ for the Baltic Sea, for the period of 1965-2001 (Jensen and Mudersbach 2007).

The global sea surface temperature is approximately 1°C higher now than 140 years ago, and this is one of the primary physical impacts of climate change (Coppini et al. 2007). The same source says that the sea surface temperature (SST) in European seas is increasing more rapidly than in the global oceans. For instance, in the period 1982-2006, the SST in the North Sea, Baltic Sea and Mediterranean Sea increased five, six and three times faster than the global average SST ($0.01^\circ\text{C yr}^{-1}$), respectively. The water level rises following the temperature, but the rate is slightly different: 12.3 (19.5) and 15 (18.8) cm per 100 years for the island and continental shore, respectively, in the North Sea, and 9.2 (11.4) cm per 100 years for the Baltic Sea for the whole period of 1843-2001 and its sub-period of 1965-2001, respectively (Jensen and Mudersbach 2007).

The aim of the paper is to compare tendencies of sea level and temperature rise for three Baltic coastal lagoons – the Darss-Zingst Bodden chain, the Vistula Lagoon, and the Curonian Lagoon during the period starting from 60th.

2. Water level and sea surface data considered.

The data at the Curonian Lagoon are from five tide gauges: one tide gauge is located in the Klaipėda Strait (lagoon inlet), four tide gauges are near the coast of the Curonian Lagoon, and one at the mouth of the River Nemunas. The monitoring data of water level and water temperature are presented by the Center of Marine Research, which belongs to the Ministry of Environment of the Republic of Lithuania. The data of water level and sea surface temperature at the Vistula Lagoon was taken from the open literature sources. These data represents two tide gauges: one is located in the Baltiysk Strait (lagoon inlet), and second one is located in Kaliningrad (8 km upstream from the Pregel River mouth in the western corner of the lagoon).

Data for the Darss-Zingst Bodden Chain was taken from measurements points Althagen, Zingst and Barth (within the lagoon) and for Barhöft and Zingst Sea Bridge for the lagoon inlet and sea coast respectively.

The increase in water level (mm per year) at various stations is evaluated using linear regression, which expresses

unidirectional tendency of water level rise in respect of time. The linear regression analysis was performed on the annual and monthly mean water level data for the period from 1961 till 2005. The information on regression representability is provided by coefficient of determination, R^2 , which gives the square of the correlation coefficient. The water level data were also used to calculate probability distributions for different time periods. We used the correlations analysis to study relations between different time series. Student t-test was used a significance test.

Graphs and trends of water level changes are made according to monthly and yearly means of water level, which are calculated using hourly (Klaipėda, Nida, Uostadvaris stations) and 1--3 times per day water level data (all stations in the Darss-Zingst Bodden Chain and Vistula Lagoons). The resolution of the measurement data is 1 cm.

Linear regressions for monthly and annual mean water level variations during the 1961--2004 period show positive trend in level magnitude for three studied lagoons, but, rates are differ significantly: maximal rate is for the Curonian Lagoon ($2-4 \text{ mm year}^{-1}$) and minimal for the Darss-Zingst Bodden Chain Lagoon (approximately 1 mm year^{-1}).

Rate is varied through years. The highest rate for the Curonian Lagoon was observed during 1980-1990 (approximately 10 mm year^{-1}), while in Darss-Zingst Bodden Chain it was observed for 1990-2005 and had two times less magnitude (5 mm year^{-1}).

The positive linear trend for monthly and yearly averaged data observed for all three lagoons is a result of an increase of minimal and maximal levels, in more extent for the sake of maximum levels, accompanied by an increase of the range of level variations.

Characteristic variations of monthly mean level is similar for all three lagoons – 40-80 cm.

Long-term average values (10-year average and more) of the water level increase towards the inner part of a lagoon. General conclusion is that sea level and temperature rise is evident for all three coastal Baltic lagoons, as well as others global tendencies in climate change, but each area has so specific hydrographic conditions, that these tendencies exhibit itself in different way in time and magnitudes.

Evaluating the combined effects of nutrient load reduction and climate scenarios for the Baltic Sea catchment

Chantal Donnelly, Johan Strömqvist, Joel Dahné and Berit Arheimer

Swedish Meteorological and Hydrological Institute, Norrköping, Sweden (Chantal.donnelly@smhi.se)

Eutrophication is one of the most serious and hardest to mitigate challenges facing the Baltic Sea and via its effects including algal blooms, dead-sea beds and reductions in fish stocks is detrimental to the future economic prosperity of the Baltic Sea Region (HELCOM 2007). For this reason, the Helsinki Commission (HELCOM) commissioned the preparation of the Baltic Sea Action Plan (BSAP), a programme to restore good ecological status of the Baltic Marine Environment by 2021. HELCOM is a governing body including all countries along the Baltic Sea Coast, which works to coordinate, supervise, and make policy to protect and improve the marine environment of the Baltic Sea.

A Baltic Sea Action Plan was approved in 2007 by the countries surrounding the Baltic Sea to improve the ecological status of this sea. An important part of this plan is reduction of nutrient inflows from the Baltic Sea basin into the sea (HELCOM 2007). Required nutrient reductions have been apportioned to the countries within the basin and these countries are now planning the remedial measures required to meet the plan's requirements.

An important factor that remains to be considered, however, is how well the planned nutrient reductions improve nutrient inflows into the Baltic Sea in a changed future climate. Nutrient inflows from land to sea are a result of point-source emissions from industry and urban sources, atmospheric deposition, erosion, subsurface, leaching from soil, diffusion from river and lake sediments and biochemical processes in the freshwater system. With the exception of the point-source emissions, these factors are temperature and precipitation dependent and are therefore affected by changes in climate. Scenarios that have been modelled to assess future nutrient reduction measures have thus far not taken into account potential climate change.

A number of studies have investigated the effect of future climate change assuming similar future anthropogenic nutrient inputs. In summary it can be said that such studies show large variations in results and show even contradictory conclusions between catchments, for example, Cruise et al. (1999), Bouraoui et al. (2002), Kallio et al. (1997), and Varanou et al. (2002). Such conclusions are of course related to regional differences in both climate and the climate change pattern as well as local site specific conditions; however, Rosberg and Arheimer (2007) also concluded that such climate studies depend on a number of interacting assumptions and uncertainties as well as the climate change scenario modeled. These varied results indicate the need for processed based modeling of how a number of climate change scenarios may affect the hydrology and nutrient processes within the Baltic Sea catchment.

A high resolution, process based hydrological and nutrient flux model was set up for the entire Baltic Sea catchment area using the HYPE (Hydrological Predictions for the Environment) model (Lindström et al. in press). The HYPE model introduces the ability to model detailed hydrological processes at high resolution simultaneously and homogeneously across many river basins. When using a modelling tool to assess water resources and their quality for a basin entailing several political entities, it is an advantage

that the methods and data used are homogenous across such political boundaries.

Readily available, regional and global databases were used to set up the model inputs including topography, precipitation, temperature, land use, soil-type, and nutrients from atmospheric, agricultural, industrial and urban wastewater sources, over the entire model domain. Daily river runoff data from the BALTEX and GRDC databases was used to calibrate and validate the parameters describing runoff processes, while monthly and seasonal data from the European Environment Agency's WISE database were used to calibrate and validate the water quality parameters in the model. Figures 1 and 2 show the total phosphorous and nitrogen concentrations, respectively, for each subbasin in the model domain, as well as a comparison of modeled volumes of phosphorus and nitrogen at major river outlets.

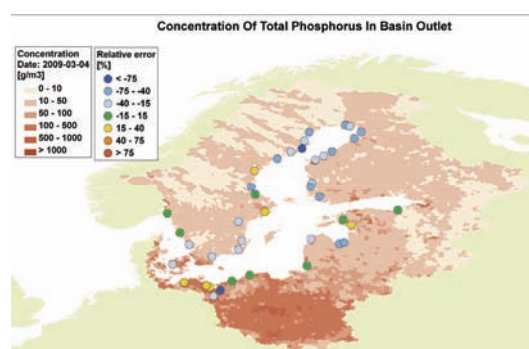


Figure 1. Total phosphorus concentrations in each subbasin and relative error of total phosphorus load at major river outlets

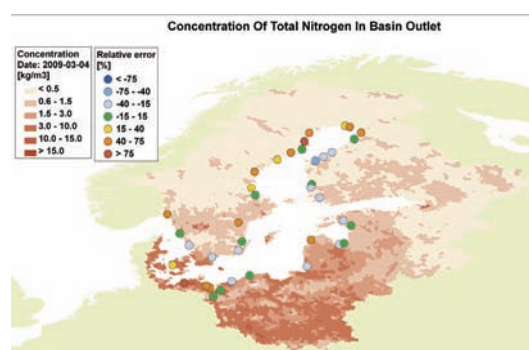


Figure 2. Total nitrogen concentrations in each subbasin and relative error of total nitrogen load at major river outlets

The model application is able to reproduce measured daily flow variations and magnitude in both large and small waterways across the model domain, and measured seasonal variation and overall magnitude of nutrient fluxes to the Baltic Sea. Total yearly volumes of discharge, total nitrogen and total phosphorus also compare well to

published figures for total fluxes to the Baltic Sea (HELCOM 2008). The validated model is used as a tool to examine the effects of different climate and remedial measure scenarios for both the land regions of the model domain, and influxes to the Baltic Sea. Generally, results show a lessened effect of the remedial scenarios tested for future climate scenarios at the end of this century.

References

- Bourroui, F., Galbiati, L. and Bidoglio, G. (2002) Climate change impact on nutrient loads in the Yorkshire Ouse catchment (UK). *Hydrol. Earth System Sci.* **6**, 197–209.
- HELCOM (2007) Towards a Baltic Sea unaffected by Eutrophication. Helsinki. <http://www.helcom.fi/>. 2010-01-13
- HELCOM (2008) PLC-Group. The Data Consultant SYKE. Waterborne loads of nitrogens and phosphorus to the Baltic Sea in 2006. HELCOM Indicator Fact Sheets 2008. Online. [Jan 2010], http://www.helcom.fi/environment2/ifs/en_GB/cover/.
- Cruise, J. F., Limaye, A. S. and Al-Abed, N. (1999) Assessment of impacts of climate change on water quality in the southeastern United States. *J. Am. Water Resour. Assoc.* **35**, 1539–1550
- Kallio, K., Rekolainen, S., Ekholm, P., Granlund, K., Laine, Y., Johnsson, H. and Hoffman, M. (1997) Impacts of climatic change on agricultural nutrient losses in Finland. *Boreal Environ. Res.* **2**, 33–52.
- Lindström, G., Pers, C., Rosberg, J., Strömqvist, J. and Arheimer, B. In Press. Development and test of the HYPE (Hydrological Predictions for the Environment) model - A water quality model for different spatial scales. Accepted for publication in *Hydrology Research*.
- Rosberg, J. and Arheimer, B. 2007. Modelling climate change impact on phosphorus load in Swedish rivers. In: *Water Quality and Sediment Behaviour of the Future: Predictions for the 21st Century*, IAHS Publ.314:90-97.
- Varanou, E., Gkouvatsou, E., Baltas, E. and Mimikou, M. (2002) Quantity and quality integrated catchment modeling under climate change with use of soil and water assessment tool model. *J. Hydrol. Engng.* (May/June), 228–244.

Climate variability and change detected from Baltic Sea level data since 1774: An overview

Martin Ekman

Summer Institute for Historical Geophysics, Haraldsby, Åland Islands (martin.ekman@ha.ax)

1. Introduction

The Baltic Sea has the world's longest series of sea level observations, that of Stockholm commencing in 1774. It also has a large number of other long sea level series, including that of Swinemünde/Świnoujście dating back to 1811. Moreover, Stockholm happens to be an ideally situated station for studying long-term sea level changes, short-term changes being almost non-existent there because of its closeness to the nodal line of the Baltic.

The changes on various time scales of the level of the Baltic Sea as measured since 1774 contain a wealth of information about the Earth and its changes. We will here concentrate on climate variability and climate changes.

2. Baltic sea level and melting glaciers

Analysing the extremely long series of annual means of the Stockholm sea level, one finds a change in the rate of the apparent postglacial land uplift. The uplift rate during the 1900s is 1.0 mm/yr smaller than during the 1700s and most of the 1800s. This change is statistically significant at the 99.9 % level.

Comparisons with other studies of Baltic Sea level data show that this figure is very close to the climatic sea level rise during the 1900s. Consequently, the climatic sea level rise during the 1700s and most of the 1800s was close to 0.0 mm/yr.

These results are in good accordance with the sparse knowledge from the lengths of glaciers. They have been more or less constant during the 1700s and most of the 1800s, followed by a quite abrupt decrease due to melting in the 1900s.

3. Baltic sea level and changes in atmospheric circulation pattern

Analysing the monthly means of the Stockholm sea level series reveals a considerable variability in the deviations of winter mean sea level from normal sea level. This winter sea level deviation varies between + 40 cm and - 37 cm; the phenomenon may be called the inter-winter sea level oscillation. It is caused by persistent winter winds over northern Europe transporting Atlantic water into or out of the Baltic, westerly winds causing a high winter level in the Baltic and easterly winds a low winter level. Consequently a high level will correspond to a warm winter with only little ice in the Baltic, and a low level to a cold winter with much ice. Thus, the Stockholm sea level series may be said to reflect the winter climate over northern Europe back to 1774.

Since the Stockholm sea level is related to the atmospheric circulation pattern over northern Europe it is also related to the air pressure distribution. In particular, the Stockholm sea level series can be used for calculating the winter south-north air pressure difference across the North Sea back to 1774.

Now, a further analysis reveals that the inter-winter sea level variability was larger during the early decades (1774 – 1840), smaller during the central 100 years (1841 – 1940), and again larger during the late decades (1941 – 2000). The

decrease in the inter-winter sea level oscillation from the early to the central period is statistically significant at the 99 % level, the increase from the central period to the late one is also statistically significant at the 99 % level. Both these changes reveal systematic changes in the winter atmospheric circulation pattern over northern Europe since 1774.

4. Baltic sea level and change in storm frequency

As mentioned, Stockholm is situated at the nodal line of the Baltic Sea and only has long-term sea level variations. Świnoujście (formerly Swinemünde) on the other hand, situated at the southern end of the Baltic Sea, clearly has short-term variations superimposed on the long-term ones. Based on the long-term variations at Stockholm, the long-term variations at Świnoujście can be eliminated, leaving the short-term variations at Świnoujście to be investigated separately.

The winter means of the short-term sea level effect shows a variability reflecting the frequency of winter storms (and gales) since 1825. Analysing this variability shows that it was larger during the 1800s and smaller during the 1900s. The decrease in the variability of the short-term sea level effect is statistically significant at the 99.9 % level. This reveals a systematic decrease in the storm (and gale) activity during winters over the Baltic Sea from the 1800s to the 1900s.

5. Conclusion

The extremely long sea level series of the Baltic Sea contain valuable information on climate variability and climate changes. These things and also other topics related to the Baltic Sea level are thoroughly treated in a recently issued book by Ekman (2009). This book will be for sale at the BALTEX conference.

References

- Ekman, M (2009) The changing level of the Baltic Sea during 300 years: A clue to understanding the Earth. Summer Institute for Historical Geophysics, Åland Islands, 155 pp.

The response of the Baltic Sea to climate variability

Klaus Getzlaff, Andreas Lehmann and Jan Harlaß

Leibniz Institute of Marine Sciences at University of Kiel (kgetzlaff@ifm-geomar.de)

1. Introduction

A detailed assessment of climate variability of the Baltic Sea area for the period 1958-2009 (Lehmann et al. submitted) revealed that the recent changes in the warming trend are associated with changes in the large-scale atmospheric circulation over the North Atlantic. Furthermore, number and pathways of deep cyclones (<980 hPa) changed considerably (Figure 1) in parallel with the eastward shift of the NAO centres of action. For the Baltic area there exists a seasonal shift of strong wind events from autumn to winter and early spring (Figure 2).

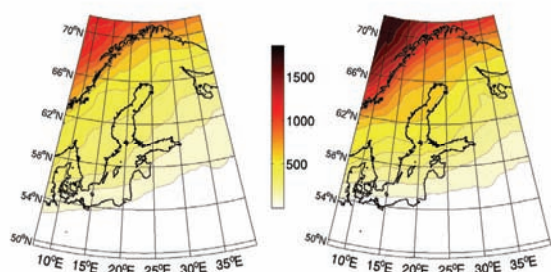


Figure 1: Number of deep (<980 hPa) winter (DJFM) cyclones for two periods 1970-1988 (left) and 1989-2007 (right), calculated from SMHI meteorological data base. The total number of cyclones in the second period is about 1.5 times larger compared to the first one.

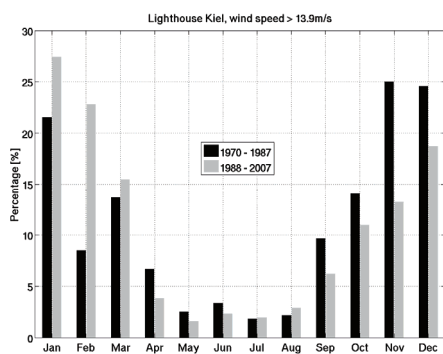


Figure 2: Percentage of days with wind speeds higher than 13.9 ms^{-1} (>bft 7) for all months, two periods 1970-1987 (black) and 1988-2007 (gray) at the position Lighthouse Kiel, in Kiel bight, interpolated from the gridded SMHI meteorological data base.

As climate, to a large extent, controls patterns of water circulation and biophysical aspects relevant for biological production, such as the vertical distribution of temperature and salinity, alterations in climate may severely impact the trophic structure and functioning of

marine food webs. Since the mid 1980s an acceleration of climate warming has occurred, which agrees remarkably well with a regime shift in the pelagic food webs (Hinrichsen et al. 2007). To answer which are the processes linking changes in the marine environment and climate variability, it is essential to investigate all components of the climate system. Here, we focus on the link between changes/shifts in the atmospheric conditions and their impact on the general circulation of the Baltic Sea.

2. Data and methods

We performed a detailed analysis of about 2 decades periods before and after the regime shift. We used atmospheric data from the SMHI meteorological data base ($1 \times 1^\circ$, 3 hours, 1970-2008) together with ICES Oceanographic data, IFM-GEOMAR atmospheric and oceanographic measurements (1987-2008) and BSH SSTs (1990-2008). Additionally, the PSMSL tide gauge records maintained by POL were used to correlate with changes in the local atmospheric field and with results from numerical model simulations for the period 1970-2008.

3. Results

In addition to the thoroughly analysed and reported changes in surface air temperature and SST (e. g. Chen and Hellström 1999, Siegel et al. 2006, Hinrichsen et al. 2007), we observed changes in prevailing winds for the periods 1970-1988 and 1989-2007. There exists a decrease in frequency of wind from westerly directions during autumn (SON) and an increase of westerly winds during winter (DJF). The shift in wind directions is associated with a decrease of strong wind events during autumn and a corresponding increase in winter (Figure 2). In accordance with these changes for the two periods are changes in the de-trended anomalies of sea level data taken from tide gauges along the coast of the Baltic Sea (Figure 3).

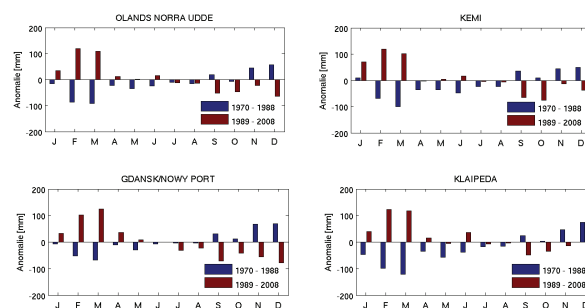


Figure 3: De-trended sea level anomalies for all months calculated for the periods 1970-1988 (blue) and 1989-2008 (red) at Olands Norra Udde (top left), Kemi (top right), Gdansk (bottom left) and Klaipeda (bottom).

There exists an increase in the monthly mean sea level during late winter (DJFM) in the second period (1989-2008), whereas a decrease in monthly mean sea level exists in autumn (SON). This suggests that a prevailing westerly wind situation, as commonly observed in winter, causes a “blocking” of Baltic Sea water outflow and/or an increase of inflow events. These results confirm findings of recent studies, such as Lehmann and Hinrichsen (2001) or Johansson et al. (2004), that used historical sea level time series to demonstrate the key role played by winter climate, especially that of wind forcing. Lehmann and Hinrichsen (2001) showed that a change of the local atmospheric index (Baltic Sea Index) to positive phases results in a decrease of outflow accompanied by an increase in mean sea level due to the freshwater surplus. Consequently, a change to more frequent and more pronounced winter NAO⁺ pattern could thus change patterns of the general circulation in the Baltic Sea as shown exemplarily for two winter averages, representing a NAO⁻ pattern and a NAO⁺ pattern, taken from numerical model simulations (Figure 4).

References

- Chen D, Hellström C: The influence of the North Atlantic Oscillation on the regional temperature variability in Sweden: spatial and temporal variations. *Tellus* 51A, 505–516, 1999
- Hinrichsen H-H, Lehmann A, Petereit C, Schmidt J: Correlation analysis of Baltic Sea winter water mass formation and its impact on secondary and tertiary production. *Oceanologia*, 49, 381-395, 2007
- Johansson M, Kahma KK, Boman H, Launiainen J: Scenarios for sea level on the Finnish coast. *Boreal Env Res*, 9, 153-166, 2004
- Lehmann A, Hinrichsen H-H: The Importance of Water Storage Variations for Water Balance Studies of the Baltic Sea. *Phys Chem Earth*, 26, 383-389, 2001
- Lehmann A, Getzlaff K, Harlaß J: Detailed assessment of climate variability of the Baltic Sea area for the period 1958-2009. *Clim Res* (submitted)
- Siegel H, Gerth M, Tschersich G. Sea surface temperature development of the Baltic Sea in the period 1990-2004. *Oceanologia*, 48, 119-131, 2006

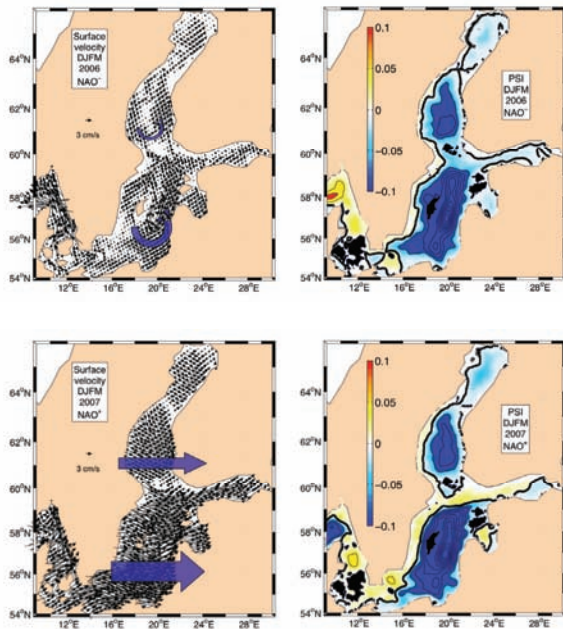


Figure 4: Showcase of a possible change in preferred surface circulation according to shifts in the wind regime. Here shown is the seasonal winter (DJFM) mean surface circulation (left column) and barotropic streamfunction (right column) from model output for year 2006 (NAO⁻ pattern, top panel) and year 2007 (NAO⁺ pattern, bottom panel).

What do we know about sea-level change in the Baltic Sea?

Birgit Hünicke

Institute for Coastal Research, GKSS Research Centre, Max-Planck-Str.1, 21502 Geesthacht, Germany.
(birgit.huenicke@gkss.de)

1. Background

Sea-level change is becoming an issue of increasing importance, especially in the context of anthropogenic global climate change. In addition, it is also closely linked to studies of solid earth processes and geodetic science. The possible impact of sea-level rise on the coast (see Figure 1) and the associated costs for coastal protection is of great interest to governmental bodies and the public.

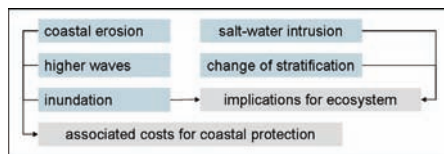


Figure 1. Possible impacts of sea-level rise.

The understanding of sea-level rise and variability on a global scale is nowadays the focus of many research studies worldwide and was one of the key topics of the IPCC Fourth Assessment Report (AR4). However, sea-level changes are not uniform over the globe. Considerable regional variations that may be caused by regional and local-scale processes are not captured in the global averaging of sea level.

2. Understanding global sea level change

The two main reasons for sea-level rise are thermal expansion of ocean waters and the increase in the ocean mass from land-based sources of ice (Figure 2).

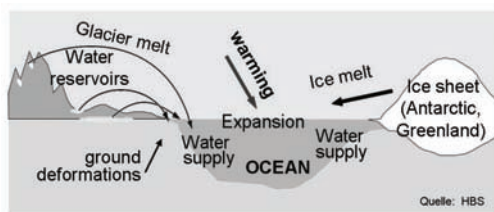


Figure 2. Main factors causes sea-level rise.

Both factors are significantly affected by global warming. For the 20th century, tide gauge measurements show an increase in mean global sea-level rise of around 1.7 mm/year, whereas satellite-altimeter observations since 1993 report values in the range of 3.1 ± 0.4 mm/year (Church et al. 2008).

Climate projections of the IPCC AR4 (2007) under different scenarios of atmospheric greenhouse concentrations foresee an estimated rise of 18-59 cm for the end of the 21st century. About 3/4th of this increase will be mainly caused by thermal expansion of the oceanic water volume. However, the effect of increasing ice sheet discharge (melting, but also flow) is still highly uncertain. We can expect that sea-level will continue to rise with at least the same rates as seen in the 20th century, but higher rates are more likely.

3. What effects Baltic Sea-level Change?

The changes in mean Baltic Sea level can be seen as the sum of global, regional and local effects. Regional effects include a) thermo- and halosteric effects (which can reach, according to Skovgaard Madsen (2009), similar magnitudes at basin-scale) b) general changes in wind, surface pressure and ocean currents and c) gravitational effects, whereas land uplift and wind effects, increasing freshwater input and higher increase in temperatures than open ocean can account for local effects.

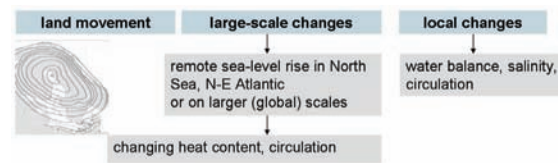


Figure 3. Main factors affecting long-term Baltic Sea level.

Land Movement: The Baltic Sea is a region strongly influenced by the effect of the glacial isostatic adjustment (GIA) with the Earth crust in the Northern Baltic rising at roughly 9 mm/year (resulting in a negative trend in sea-level) and in parts of the Southern Baltic sinking at about 1 mm/year (resulting in a slight positive trend) (e.g. Rosentau et al. 2007) However, these values are based on local observations of long-term relative sea-level trends, presenting the position of sea-level with respect to land and therefore include both: the signal related to vertical crustal movements and the absolute sea-level change. On timescales up to 200 years, the trend caused by post-glacial land-movement can be assumed to be approximately linear. Currently, new geodetic techniques such as GPS are applied to measure the rates of vertical movements (e.g. ongoing research projects in Denmark and Germany) and allow for comparison with results of GIA models and corrections out of geological data.

Climate influence: Baltic Sea level variations at inter-annual to decadal timescales are generally believed to be caused essentially by variations in the North Atlantic Oscillation (NAO) index. The NAO influences sea level not just through the influence on zonal winds, but also through direct pressure and steric effects. However, the correlation between individual Baltic Sea level stations and the 20th century winter NAO index is heterogeneous in space and in time. Although the NAO is the dominant SLP large-scale pattern of the North Atlantic, it explains (on average) only 32% of the total variability of sea level at inter-annual timescales (Kauker & Meier 2003). Thus, the estimation of the full amount of variability which can be explained by the atmospheric circulation has to consider the whole SLP field of the North Atlantic –West European region. Especially for the south-western Baltic coast, other atmospheric forcing factors seem to be more relevant. Statistical analyses (e.g. Hünicke et al. 2008) found a relation between long-term Baltic Sea level variations and precipitation changes for Southern Baltic Sea level

records. As on timescales larger than 1 month, the Baltic Sea acts like an open basin (Samuelsson and Stigebrandt 1996), this relation cannot be explained by the direct volume effect, but possibly due to changes in water density due to changed salinity.

4. Tide gauge records

The understanding of climatic future trends of sea level on regional scales presumes the understanding of the decadal variability in the observational period. Thus, long time-series of sea level are required. Fortunately, the Baltic Sea Area is one of the most investigated sea-level sites of the world. Many of the available sea-level time-series can be obtained through the webpage of the Permanent Service for Mean Sea level (PSMSL)¹. In addition, historical sea-level time-series are available due to different sources, e.g. via publications for Stockholm (1774-2000; Ekman 2003) Kronstadt (1816-1999; Bogdanov et al. 2000) and Travemünde (since 1826; Jenssen and Töppe 1986), but also from national institutions. Interestingly, significant differences seem to exist in the datasets, depending on the data source (Dimke and Fröhle 2009).

5. Satellite altimetry

Since 1993, high-quality satellite-altimeter observations of sea levels allow for more accurate estimates of globally averaged and regional sea-level change (Cazenave et al. 2008), although the satellite data of coastal areas is still not applicable without special treatment. For the open ocean the trend in Baltic Sea level rise is found to be very likely higher than the global mean, but also higher than the North Sea trend (Skovgaard Madsen 2009).

6. Is Baltic Sea level rise accelerating?

At global scales, acceleration in sea-level rise has already been detected in the 20th century (Merrifield and Merrifield 2009), while other studies do not detect a significant change (Holgate 2007). For regional planning agencies more important than the global number is, however, the change in the rate at regional scales. According to the BACC report, the eustatic increase of sea level was found to accelerate at many Baltic Sea tide gauge stations at the end of the 20th century (e.g. Ekman 2003; Johansson et al. 2004; Suursaar and Kullas 2006). Also the recent Sea level Report by SMHI, which put together sea-level information from 23 Swedish gauges, quotes an acceleration in the average sea-level rise of about 3cm/century since 1980 (average rate 1886-1980: 1.5 mm/year). However, according to engineers, in sea-level observations of the southwestern Baltic coastline (e.g. record Warnemünde) no significant acceleration is evident. The question arises if the different findings can be attributed to different methods used to identify the changes in the sea-level time-series.

7. Summary

An overview of the available knowledge about mean sea-level variability and change in the Baltic Sea Region is presented, as regional sea-level rise appears more and more to be a major issue with high relevance for stakeholders and planning authorities, but also the public in large. A number of new studies about mean sea-level change have been published since the conclusion of the BACC report (2006). Thus, the presented work tries to provide an overview of the state-of-the art of Baltic sea-level research outlining not just regional information, but also looking from the global

perspective. As sea-level change is a wide range topic, the focus will be placed on answering selected questions of high relevance, such as: What drives global sea-level change in general and what specifically affects Baltic Sea level change? Are satellite-altimeter observations currently useful for the study of Baltic Sea level variability? Are there new efforts being made in the development of advanced geodetic techniques for measuring vertical land movement at tide gauges? Which sea-level data is available for the Baltic Sea Community and which of the data has been quality controlled by peer-reviewed scientific studies? Which studies about Baltic sea-level projections exist up-to-date, as they are a priority for coastal engineers and planning authorities (Hünicke and von Storch 2009). What is known? What is very likely? What is still uncertain? How convinced is the BALTEX community that the Baltic is experiencing a) more gradual impacts of sea-level rise due to climatic change and b) a sea-level rise that poses a very serious threat to the Baltic Sea? (Bray and von Storch 2009).

References

- BACC Author Team. Assessment of Climate Change for the Baltic Sea, Springer, Berlin, Heidelberg, 2008.
- Bray, D and H von Storch, An introspective look at BACC: SURBACC2009, BALTEX Newsletter 13, 2009.
- Bogdanov et al., Mean monthly series of sea level observations (1777-1993) at the Kronstadt gauge, Reports of the Finnish Geodetic Institute 2000: 1, 34pp, 2000.
- Cazenave, A, et al., Present-day sea level rise: A synthesis. *Comptes Rendus Geosciences* 340(11), 761-770, 2008.
- Church J, et al., Understanding global sea levels: past, present and future, *Sustain Sci* 3 (1), 9-22, 2008.
- Dimke, S and F Fröhle, Measured sea level rise at the Baltic Sea coast of Mecklenburg -Vorpommern and implications for the design of coastal structures, Proceedings of the International Conference on Climate Change, 25-28 May 2009, University of Szczecin, Poland, ISSN 1681-6471.2009.
- Ekman, M, The world's longest sea level series and a winter oscillation index for Northern Europe 1774-2000, *Small Publ Hist Geophys* 12, 30pp, 2003.
- Holgate, SJ, On the decadal rates of sea-level change during the 20th century, *Geophys Res Lett* 34, L01602, 2007.
- Hünicke, B and H von Storch, What is known about sea-level change in the Baltic Sea? BALTEX Newsletter 13, 2009.
- Hünicke B, et al., Regional differences in winter sea-level variations in the Baltic Sea for the past 200 years, *Tellus* 60A, 384-393, 2008.
- Jensen, J and A Töppe, Composition and Evaluation of Original Records of the Gauge at Travemünde/ Baltic Sea since 1826. (in german). *Deutsche Gewässerkundliche Mitteilungen DGM* 30, 4, 99-107, 1986.
- Johansson M, et al., Scenarios for sea level on the Finnish coast. *Boreal Env Res* 9:153-166, 2004.
- Kauker, F and MHB Meier, Modeling decadal variability of the Baltic Sea: 1. Reconstructing atmospheric surface data for the period 1902-1998. *J Geophys Res* 108 (C8), 2003.
- Merrifield MA and ST Merrifield, An anomalous recent acceleration of global sea level rise, *J Climate* 22, 2009.
- Rosentau et al., Relative Sea level change in the Baltic Sea since the Littorina Transgression, *Z geol Wiss* 35, 3-16, 2007.
- Samuelsson, M & A, Stigebrandt, Main characteristics of the long-term sea level variability in the Baltic Sea, *Tellus* 48A, 673-683, 1996.
- Suursaar, Ü and T Kullas, Influence of wind climate changes and the mean sea level and current regime in the coastal waters of west Estonia, *Baltic Sea, Oceanologia* 48 (3), 361-383, 2006.
- Skovgaard Madsen, K, Recent and future climatic changes in temperature, salinity, and sea level of the North Sea and the Baltic Sea, PhD Thesis, Planet and Geophysics, Niels Bohr Institute, University of Copenhagen, 2009.

¹ <http://www.pol.ac.uk/psmsl/>

Changes in wind directions in Estonia during 1966-2008 and their relationship with large-scale atmospheric circulation

Jaak Jaagus

Department of Geography, University of Tartu, Estonia (jaak.jaagus@ut.ee)

1. Introduction

Atmospheric circulation is an essential climatic component, which determines general weather conditions, especially air temperature. In studies of climate change, main attention has been paid to large-scale circulation patterns. Few studies have been made on changes in near surface winds. First attempts to assess changes in the frequencies of wind directions were made in Estonia, (Kull 2005; Keevallik 2008; Jaagus 2009), where an increase in SW winds was detected.

The main objectives of this study are to analyse long-term changes in the percentages of different wind directions in homogeneous time series from 14 stations of Estonia, and relationships between the indices of large-scale atmospheric circulation and near-surface wind directions.

2. Material and methods

Frequencies of wind directions, measured by eight main sectors at 14 stations in Estonia, were used for the analysis. The stations were chosen following the criteria of data homogeneity and continuity. Measuring sites were not significantly changed at these stations.

The starting year 1966 was chosen because since that time, eight observations per day at 3, 6, 9 and 12 GMT were introduced. Three changes of instrument occurred during the observation period of 1966-2008. Wild's type wind vanes were used during the first decade, automatic anemorhumbometers were used since November 1976, and automatic weather stations were used since September 2003. It can be assumed that the changing of instruments had no effect on the records of wind direction. At the same time, the exactness of the wind direction measurements improved significantly. All the records of different exactness are calculated so that the frequencies of eight main wind directions are fully comparable during the whole study period (Jaagus 2009).

Using the Lilliefors and Shapiro-Wilk tests, it was determined that the data on the frequencies of wind duration were normally distributed. Therefore, a linear regression analysis was applied for the trend analysis. Slopes of time series and changes by trend were calculated separately for different wind directions for different months and seasons. Seasons were defined by three months as usual, i.e. spring (MAM), summer (JJA), autumn (SON) and winter (DJF).

Long-term changes are presented in the form of wind roses where two lines indicate mean wind roses, i.e. the percentage distributions of different wind directions in case of the first (1966) and the last year (2008) of the observation period according to the linear trend. The larger the difference between the two wind roses, the larger was the change.

The large-scale atmospheric circulation is characterized by various circulation indices – the Arctic Oscillation Index (AO) and five teleconnection indices obtained from the NOAA CPC (<http://www.cpc.noaa.gov/products/>), and four different NAO indices presented at the Jim Hurrell's web page (<http://www.cgd.ucar.edu/cas/jhurrell/indices.html>). Relationships between the frequencies of wind directions in

Estonia and the large-scale atmospheric circulation indices were analysed using correlation coefficients.

3. Changes in wind roses in Estonia

Rather significant changes were detected in wind roses at different meteorological stations in Estonia during 1966-2008. Generally, the main tendencies in the frequencies of wind directions are presented on Figure 1. The part of the easterly, north-easterly and south-easterly winds has decreased and the percentage of the westerly, south-westerly and north-westerly winds has increased.

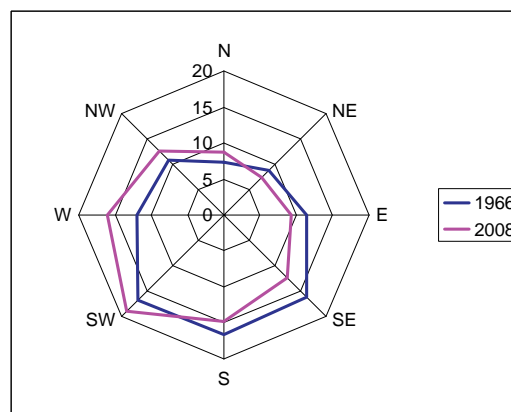


Figure 1. Annual wind roses in Türi calculated for the years 1966 and 2008 according to linear trends.

The most significant changes have occurred during the winter season. Few changes were detected in summer and autumn. Wind roses have changed much in some months (January, February, March, May, June) while they have been nearly unchanged during the other months (April, July, October, November, December).

The highest increase in the frequency of SW winds, by 12 %, was observed on the western coast of the west Estonian archipelago (Figure 2) and the highest decrease in the frequency of SE winds, by 15 %, on the west Estonian mainland (Figure 3).

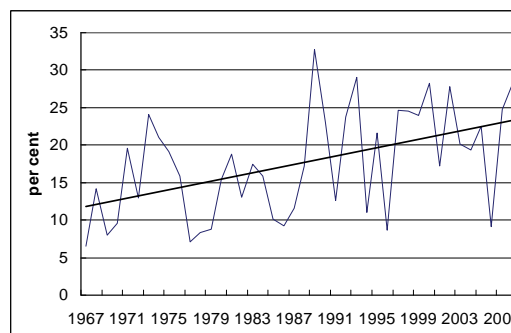


Figure 2. Frequency of SW winds at the Sõrve station during the winters 1966/67-2007/08 and its linear trend.

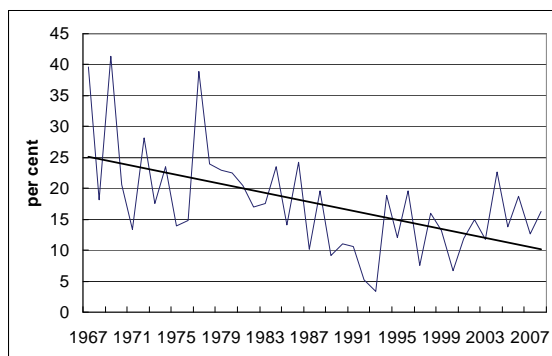


Figure 3. Frequency of south-easterly winds at the Nigula station during the winters 1966/67-2007/08 and its linear trend.

In case of the winter wind roses, a dramatic decrease was observed in the frequencies of south-easterlies and easterlies, and an increase in the frequency of south-westerlies. The greatest changes occurred in the western coast of Estonia. (Figure 4). The prevailing wind direction has likely turned from the south-east to the south-west.

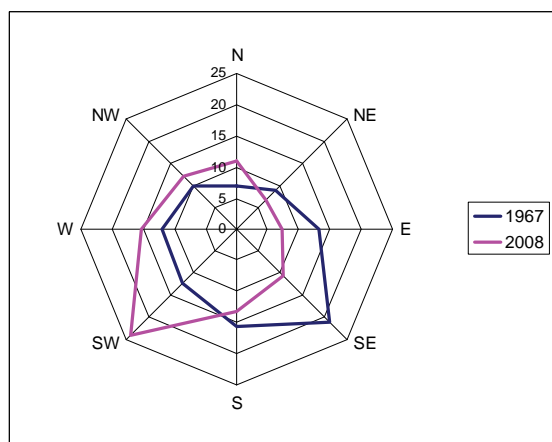


Figure 4. Winter wind roses in Vilsandi calculated for 1966/67 and 2007/08 according to linear trends.

4. Relationships between changes in wind direction and in parameters of large-scale atmospheric circulation

It is natural that wind directions near the surface are determined by the character of large-scale atmospheric circulation. But these relationships are not similar during the year and at different stations. Local conditions play an important role also in the formation of wind climate.

The majority of the circulation indices used reflect the intensity of zonal circulation and only two of them (SCA, EAWR) represent mostly meridional circulation. As a rule, the AO index and the NAO indices are highly positively correlated with the frequencies of south-westerly and westerly winds, and negatively correlated with the frequencies of easterly and north-easterly winds.

The highest correlations are typical for the winter season, when the absolute values of correlation coefficients between the AO and NAO indices, and the frequencies of SW, W, E and NE winds are 0.5-0.7. Other wind directions are not related to the AO and NAO indices. It should be mentioned that the NAO indices, calculated by the use of the SLP data at single stations, have a much lower correlation with the frequencies of wind directions in Estonia in comparison with

the NAO indices, calculated using the SLP data from much wider territories.

Higher correlation coefficients are found for the coastal stations where local wind obstacles do not disturb the wind field as much as in the hinterland. The highest correlation coefficient 0,80 was observed between the frequency of winter SW wind direction in Vilsandi and the winter NAO index presented by Li and Wang (2003).

The Scandinavia teleconnection pattern (SCA) represents the synoptic situation when a high pressure system is located over northern Scandinavia. The SCA index is positively correlated with the frequencies of easterly (throughout a year), north-easterly (during the warm period) and south-easterly winds (during the cold period). Correlation coefficients lie between 0.4-0.6. A significantly negative correlation with the SCA index revealed in case of SW, W and in some months also NW winds. The East Atlantic/West Russia teleconnection pattern (EAWR) is related to a high over the British Isles and a low in the southern Russia. The EAWR index has a positive correlation with the frequency of westerly and north-westerly winds, mostly in winter and also in autumn, and a negative correlation with the frequency of southerly and south-easterly winds.

5. Discussion and conclusions

The results of this analysis are consistent and lie in a good concordance with other knowledge indicating climate changes in Estonia (Jaagus 2006). Air temperature has increased mostly in winter and spring. Correspondingly, the percentage of the wind directions (SE, E, NE), which transport colder air into Estonia in winter, has significantly decreased, while the part of these winds (SW, W) that bring warmer air has increased considerably. Changes in the proportions of these winds clearly cause temperature changes. Large-scale atmospheric circulation indices are densely correlated with the frequencies of wind directions. It is logical that the indices indicating zonal circulation are positively related to the frequency of W and SW winds and negatively to NE and E winds. Higher correlation between circulation and wind direction is observed during the cold period of a year. During this time, circulation is the most important factor determining weather conditions in Estonia. In the warm half-year, the effect of large-scale atmospheric circulation on weather becomes weaker and local factors prevail.

References

- Jaagus, J. (2006) Climatic changes in Estonia during the second half of the 20th century in relationship with changes in large-scale atmospheric circulation, *Theoretical and Applied Climatology*, 83, 77-88
- Jaagus, J. (2009) Long-term changes in frequencies of wind directions on the western coast of Estonia, Publications, Institute of Ecology, Tallinn University, 11, 11-24 (in Estonian, summary in English)
- Keevallik, S. (2008) Wind speed and velocity at three Estonian coastal stations 1969-1992, *Estonian Journal of Engineering*, 14, 209-219
- Kull, A. (2005) Relationship between inter-annual variation of wind direction and wind speed, *Publicationes Instituti Geographici Universitatis Tartuensis*, 97, 62-70
- Li, J., Wang, J.X.P. (2003) A new North Atlantic oscillation index and its variability, *Advances in Atmospheric Sciences*, 20, 661-676

Climate change in the Baltic Sea area in an ensemble of regional climate model simulations

Erik Kjellström, Grigory Nikulin and Lars Bärring

Swedish Meteorological and Hydrological Institute, Norrköping, Sweden (erik.kjellstrom@smhi.se)

1. Introduction

Uncertainties in future climate change are related to external forcing, model formulation and natural variability. A way to handle these uncertainties is to perform several simulations constituting an ensemble. Previous attempts to do this on the regional scale in the European projects PRUDENCE (e.g. Déqué et al. 2007) and ENSEMBLES (Sanchez-Gomez et al. 2008) have limitations in that only a few global climate models (GCMs) have been used to provide lateral boundary conditions (PRUDENCE) or that only one emission scenario has been considered (ENSEMBLES). At the Rossby Centre, a regional ensemble has been created that makes use of a number of GCMs, several emission scenarios, and in some case several simulations differing only in initial conditions in the GCM (Kjellström et al. 2010). The objective of this study is to assess future climate change in the Baltic Sea area based on this ensemble of in total 16 climate change simulations for the time period 1961-2100. Uncertainties are discussed by presenting the spread between them.

2. The RCA3 ensemble

We use the regional climate model RCA3 (Samuelsson et al. 2010) to dynamically downscale several experiments with different GCMs. RCA3 has been set up at a domain covering most of Europe at 0.44° horizontal resolution (c. 50km). Table 1 summarizes the experiments in terms of GCM, emission scenario (Nakićenović et al. 2000) and initial conditions (see also Kjellström et al. 2010).

Table 1. RCA3 simulations used here. The HadCM3 boundary conditions are from a perturbed physics ensemble in which “ref” denotes the reference version, “low”/“high” represents model versions that have a low and high climate sensitivity respectively. Simulations in italics constitute a mini-ensemble of six A1B simulations with different GCMs.

No	GCM (Institute, country)	SRES Emission scenario
1	<i>Arpège (CNRM, France)</i>	<i>A1B</i>
2	<i>BCM (NERSC, Norway)</i>	<i>A1B</i>
3		A2
4	CCSM3 (NCAR, USA)	<i>A1B</i>
5		B2
6		A2
7	ECHAM4 (MPI-met, Germany)	B2
8		A2
9		A1B-r1
10	ECHAM5 (MPI-met, Germany)	A1B-r2
11		<i>A1B-r3</i>
12		B1
13		<i>A1B-ref</i>
14	HadCM3 (Hadley Centre, UK)	A1B-low
15		A1B-high
16	<i>IPSL-CM4 (IPSL, France)</i>	<i>A1B</i>

In addition to the climate change experiments we also present results from a simulation with boundary conditions from the reanalysis product ERA40 (Uppala et al. 2005). This simulation is used for model evaluation. Results for the time period 1961-1990 from all simulations are compared to the gridded observational data set E-OBS from the ENSEMBLES project (Haylock et al. 2008).

3. The recent past climate

Given perfect boundary conditions RCA3 have been shown to reproduce many aspects of the recent past climate. For the Baltic Sea region the main biases are seen in the wintertime temperature climate with an overestimate of up to 3-4°C in the northeast (Figure 1) and in summertime when precipitation is overestimated (not shown) with up to locally 100% (Samuelsson et al. 2010). The deviations from observational data are partly related to model deficiencies but also to representativity problems (models and observations are not always comparable) and uncertainties in the observational data sets that sometimes differ from each other (e.g. Lind and Kjellström 2009).

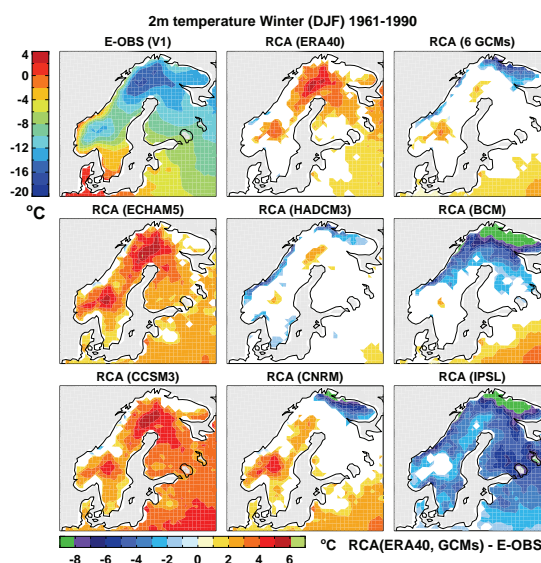


Figure 1. (top, left) Winter (DJF) mean T_{2m} (colour, °C, E-OBS) and MSLP (hPa, ERA40) and biases of T_{2m} and MSLP estimated from the RCA3 simulations driven by (top, middle) the ERA40 reanalysis, (middle and bottom rows) six different GCMs, (top, right) their ensemble mean and with respect to the E-OBS and ERA40 (1961-1990). Only differences significant at the 5% significance level are shown.

For most of the GCM-driven simulations it is clear that the biases are larger than in the ERA40-driven simulation (Figure 1). In Kjellström et al. (2010) it is shown that these larger biases can to a large degree be explained by errors in the large-scale atmospheric circulation as simulated by the GCMs.

4. Simulated climate change

The ensemble shows a statistically significant warming of the European continent in the future. This warming is most pronounced in the northeast during winter. For the Baltic Sea the simulations show a warming of 3.5-6.5°C by the end of the century (2071-2100) compared to the recent past climate in winter and even more locally in surrounding land areas (not shown). For precipitation a general increase is simulated in the north, including the Baltic Sea area and most so in winter. In summer changes in the southern part of the region are uncertain not only in size but also in sign as some simulations indicate decreases (not shown). Changes in the wind climate are uncertain and relatively small in most of the model domain. The main changes include generally decreasing mean wind speed in much of the model domain except for northern ocean areas during winter (Figure 2) for which many (but not all) simulations show increased wind speed with up to 10-15% corresponding to about 1 m/s.

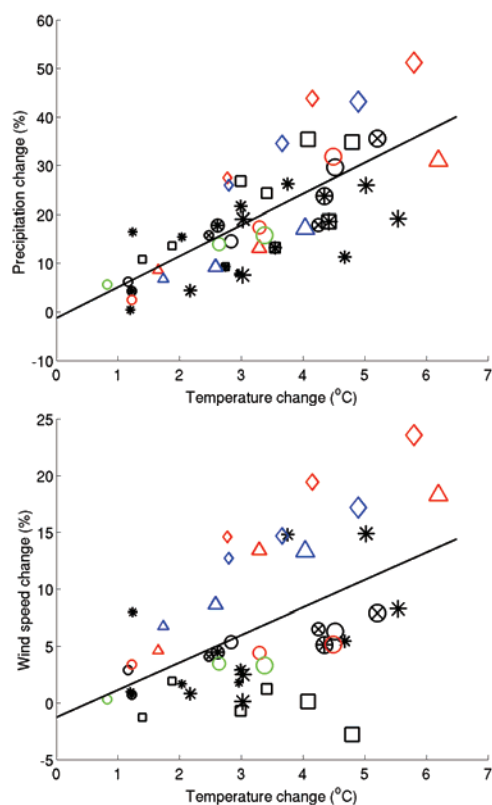


Figure 2. Wintertime (DJF) change in (upper panel) precipitation (%) and (lower panel) 10m wind speed versus T_{2m} (°C) over the Baltic Sea. Small symbols represent 2011-2040, medium 2041-2070 and large 2071-2100. Colors indicate emission scenarios (A2-red, A1B-black, B2-blue, B1-green). (*) denote the six-member A1B-ensemble, (o) represent RCA3(ECHAM5, in case of A1B all three simulations; r1, r2 and r3), (□) RCA3(HadCM3, ref, low and high), (◇) RCA3(ECHAM4) and (Δ) RCA3(CCSM3).

5. Summary and conclusions

The spread in the results are largely dependent on the choice of GCMs and differences in how they simulate the large-scale circulation. Emission scenarios are important for the total spread in temperature and precipitation of the ensemble in the last decades of the century while at earlier periods it is

not the dominating source of uncertainty. For wind speed the differences due to emission scenarios are smaller also at the end of the century. The ensemble also shows that natural variability is an important source of uncertainty for the next few decades. Sometimes this uncertainty dominates over the spread due to model formulation (and thereby climate sensitivity).

6. Acknowledgements

Part of the simulations and subsequent analysis work has been funded by the European ENSEMBLES (GOCE-CT-2003-505539) project, the Nordic Climate and Energy Systems (CES) project and the Swedish Mistra-SWECIA programme funded by Mistra (the Foundation for Strategic Environmental Research). The model simulations were made on the climate computing resource Tornado funded with a grant from the Knut and Alice Wallenberg foundation. The institutes providing the global model data used as boundary conditions are kindly acknowledged. We are grateful for the E-OBS dataset from the EU-FP6 project ENSEMBLES (<http://www.ensembles-eu.org>) and the data providers in the ECA&D project (<http://eca.knmi.nl>).

References

- Déqué, M., et al., 2007. An intercomparison of regional climate simulations for Europe: assessing uncertainties in model projections. *Climatic Change*, 81, 53-70.
- Haylock, M.R., et al. 2008: A European daily high-resolution gridded dataset of surface temperature and precipitation. *J. Geophys. Res (Atmospheres)*, 113, D20119, doi:10.1029/2008JD10201
- Kjellström, E., et al., 2005. A 140-year simulation of European climate with the new version of the Rossby Centre regional atmospheric climate model (RCA3). *Reports Meteorology and Climatology*, 108, SMHI, SE-60176 Norrköping, Sweden, 54 pp.
- Kjellström, E., Boberg, F., Castro, M., Christensen, J.H., Nikulin, G., and Sanchez, E., 2010. Enhancing confidence in climate change projections; evaluation of daily and monthly statistics of temperature and precipitation in the ENSEMBLES regional models. Manuscript submitted to *Climate Research*.
- Lind, P. and Kjellström, E. 2009: Water budget in the Baltic Sea drainage basin: Evaluation of simulated fluxes in a regional climate model. *Boreal Env. Res.* 14: 56-67.
- Nakićenović, N., et al., 2000. Emission scenarios. A Special Report of Working Group III of the Intergovernmental Panel on Climate Change. Cambridge University Press, 599 pp.
- Samuelsson, P., Jones, C., Willén, U., Ullerstig, A., Gollvik, S., Hansson, U., Kjellström, E., Nikulin, G., Wyser, K., 2010. The Rossby Centre Regional Climate Model RCA3: Model description and performance. Manuscript submitted to *Tellus*.
- Sanchez-Gomez E., et al., 2008: Ability of an ensemble of regional climate models to reproduce weather regimes over Europe-Atlantic during the period 1961-2000, *Clim. Dyn.*, 10.1007/s00382-008-0502-7.

Environmental changes in the Pomeranian Bay in the Holocene, based on diatomological and geochemical studies

Robert Kostecki and Beata Janczak-Kostecka

Department of Quaternary Geology and Paleogeography, Adam Mickiewicz University, Poznań, Poland
(kostecki@amu.edu.pl)

1. Introduction

Previous studies indicate that the Pomeranian Bay was created in the Holocene as a result of a marine incursion into the hinterland. After deglaciation from the beginning of the Holocene to the Atlantic period, the contemporary bay was land. During the Baltic Ice Lake period, the water table rose to about 10 m, creating a lagoon south of the Odra Bank (Lampe 2005). The main goals of this study were to determine the characteristic and rate of the Late Atlantic incursion and to ascertain how important the coastal Pre-Littorina lagoons and lake basins were in the development of the Baltic Sea incursion.

2. Materials and methods

We examined six sediment cores taken from Pomeranian Bay by the Institute for Baltic Sea Research in Warnemünde aboard the research vessel FS "A. v. Humboldt". The cores were obtained from the western part of Pomeranian Bay at 3.5-9 km from the east and north coast of Rugia. Cores 246040 and 246040 were collected at 16 m b.s.l., and core 246060 was drilled below 20 m b.s.l. Cores 233230 were collected at 28.7 m b.s.l., 233240 at 29,5 m b.s.l. and 233250 at 30.7 m b.s.l.

Geochemical analyses included determination of loss of ignition, terrigenous silica, biogenic silica, sodium, potassium, magnesium, calcium, iron, and manganese.

Samples for diatom analyses were prepared according to the standard method described by Battarbee (1986). Determination of taxonomy and ecological grouping were performed according to Krammer and Lange-Bertalot (1991a, 1991b) and Witkowski et al. (2000).

3. Results and discussion

Based on geochemical and diatomological analyses, the cores could be divided into three different environmental zones. The lowest zone M1 is related with the lacustrine environment, the zone in middle part of core M2 is related to a transition period from freshwater to marine environment. The highest zone M3 developed in saline marine conditions. The lowest zone (M1) consisted of sandy and clayey silt of an olive gray colour. This zone contained an abundant diatom flora that was dominated by freshwater species and lowest values of ratio Mg/Ca. The next zone (M2) mainly consisted of olive black peat gyttja at the bottom and olive grey mud. It is transition layer, diatom assemblages rapidly switched from freshwater to marine-brackish water, while magnesium and calcium reached highest values in the entire core. The ratio of Mg/Ca gradually changed into higher values then in zone M1.

The upper zone (M3) consisted mainly of olive gray mud. Sediments of this zone was characterized by dominating marine diatom species and highest values of ratio magnesium to calcium in entire core. The rapid change of the diatom assemblages from freshwater species to marine species and the increasing level of ratio magnesium to calcium in the sediment deposited at the beginning of the

Littorina period confirms that the transgression occurred rapidly.

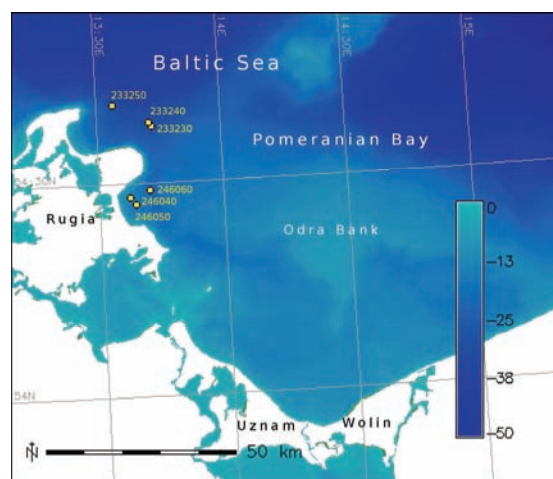


Figure 1. Location of coring site on the Pomeranian Bay.

Saline waters rapidly flooded the land after the disruption of the sand barrier that once existed on the contemporary Odra Bank. Such an event could have taken place during extremely strong surges (Borówka et al. 2005). The Littorina transgression drastically changed the environment of the entire south Baltic coast. Marine diatom assemblages almost completely replaced freshwater communities. We suggest that this could have happened in the Pomeranian Bay area rapidly within a short period during the Late-Atlantic period.

References

- Battarbee R. W. 1986. Diatom analysis. In: Berglund B. E. (ed.) Handbook of Holocene paleoecology and paleohydrology. London, John Wiley and Sons. Ltd., pp. 527–570.
- Borówka R.K., Osadczuk A., Witkowski A., Wawrzyniak-Wydrowska B., Duda T. (2005) Late Glacial and Holocene depositional sequences in the eastern part of the Szczecin Lagoon (Great Lagoon) basin – NW Poland. Quaternary International 130, pp. 87–96.
- Krammer K., Lange-Bertalot H. 1991a. Bacillariophyceae 3, Centrales, Fragilariaceae, Eunotiaceae. In: Ettl H., Gerloff J., Heynig H., Mollenhauer D. (eds.). Süßwasserflora von Mitteleuropa 2. Fischer, Stuttgart. T 3, pp. 1–577.
- Krammer K., Lange-Bertalot H. 1991b. Bacillariophyceae 4, Achnanthaceae. In: Ettl H., Gärtner G., Gerloff J., Heynig H., Mollenhauer D. (eds.). Süßwasserflora von Mitteleuropa 2. Fischer, Stuttgart T 4, pp. 1–437.
- Lampe R. (2005) Lateglacial and Holocene water-level variations along the NE German Baltic Sea coast: review and new results. Quaternary International 133-134, pp. 121–136.
- Witkowski A., Lange-Bertalot H., Metzeltin D. 2000. Diatom Flora of Marine Coasts. I. Iconographia Diatomologica 7:1–925.

Categorical temperature data as indicators of warming in Poland

Zbigniew W. Kundzewicz^{1,2} and Halina Lorenc³

¹ Institute for Agricultural and Forest Environment, Polish Academy of Sciences, Bukowska 19, 60-809 Poznań, Poland (kundzewicz@yahoo.com; zkundze@man.poznan.pl)

² Potsdam Institute for Climate Impact Research, Telegrafenberg, 14 412 Potsdam, Germany (zbyszek@pik-potsdam.de)

³ Institute of Meteorology and Water Management, Warsaw, Poland (halina.lorenc@imgw.pl)

Temperature variability and change are of major and general interest due to important consequences. It is now evident from observations of global mean air temperature that global warming is unequivocal. Examination of the global data shows that among the 15 warmest calendar years in the global instrumental observation record (available since 1850) there are 14 years from the time interval of the last 15 years (1995-2009). It is of considerable interest to compare this large-scale finding to the national, regional, and local temperature records.

The present contribution makes use of openly accessible (public domain) categorical (qualitative) information on monthly and annual air temperature (thermal classification of months and years), based on station data from Poland, available from January 1971 until the month preceding the current date. The high rise in the mean temperature of twelve consecutive months (July 2006 – June 2007) was first noted during visual inspection of Polish categorical data. Examination of anomalies in the mean twelve-month temperature, being a brand new element in the global warming debate gave new evidence of a strong warming at local, national, continental, and hemispheric scales.

The present contribution contains the analysis of changes in mean temperature, based on seasonal and monthly categorical data from seven stations distributed over the territory of Poland that provides a persuading evidence of warming. A visual and explanatory inspection of categorical temperature data from Poland (presented as coloured cells in a mosaic) helps to sense the particularities of the temperature changes in recent decades. Over the last decades, the ratio of the number of seasons colder than the long-term “norm” to the number of seasons warmer than the “norm” has decreased dramatically. There is an increasing frequency of occurrence of months and seasons warmer than the „normal” temperature range and decreasing frequency of occurrence of months and seasons colder than the „normal” temperature range. For instance, over a consecutive period of 42 months (April 2006 – September 2009), not a single month was colder than the „normal” range (interpreted as a long-term monthly temperature mean plus/minus half standard deviation). However, October 2009 was slightly cold and January 2010 was very cold, in fact coldest since 24 years.

Detailed assessment of climate variability of the Baltic Sea area for the period 1958-2009

Andreas Lehmann, Klaus Getzlaff and Jan Harlaß

Leibniz Institute of Marine Sciences at University of Kiel, Germany (alehmann@ifm-geomar.de)

1. Introduction

The warming trend for the entire globe (1850-2005) is 0.04°C per decade. A specific warming period started around 1980 and continues at least until 2005, with a temperature increase of about 0.17°C per decade. This trend is equally well evident for many areas on the globe, especially on the northern hemisphere in observations and climate simulation. For the Baltic Sea catchment, which lies between maritime temperate and continental sub-Arctic climate zones, an even stronger warming of about 0.4°C per decade appeared since 1980. From 1960 to 1980 the annual mean air temperature for the Baltic Sea catchment was closely or slightly below the long-term mean with respect to the period 1871-2004, between 1965-1975 the temperature was slightly above the mean. With the beginning of the 1980s, the annual mean temperature increased by about 1°C until 2004. A similar warming trend could be observed for the sea surface temperature (SST) of the Baltic Sea (Siegel et al. 2006; MacKenzie and Schiedek 2007). Even the annual mean water temperatures averaged spatially and vertically for the deep basins of the Baltic Sea show similar trends (Hinrichsen et al. 2007).

We provide a detailed analysis of the climate variability and associated changes in the Baltic Sea area for the period 1958-2009, in which the recent acceleration of the climate warming happened. The focus of this work is on assessment of climate change and not on the attribution either by human activity or natural variability.

Of course the period is too short to discriminate between changes related to climate change and decadal variability. The main questions we like to answer by this work are: Can we detect similar changes, as those seen in the mean air temperature, in other atmospheric variables? Are these changes related to changes in the large-scale atmospheric circulation?

2. Data and methodology

The detailed analysis of the climate variability is based on NCEP/NCAR reanalysis, hereafter NNR, data (Kalnay et al. 1996) provided by the NOAA/OAR/ESRL PSD, Boulder, Colorado, USA (available at <http://www.esrl.noaa.gov/psd>) covering the Northern Hemisphere for the period 1948-2009. However, NNR data are only poorly resolved ($2.5^{\circ}\times 2.5^{\circ}$, 6 hours) for the Baltic Sea area. Thus, the approach here is to use additionally atmospheric data from the Swedish Meteorological and Hydrological Institute (SMHI) meteorological data base ($1^{\circ}\times 1^{\circ}$, 3 hours, 1970-2008, L. Mueller, pers. comm.) together with IFM-GEOMAR atmospheric measurements (1997-2008), BSH (Federal Maritime and Hydrographic Agency, Hamburg, Germany) SSTs (1990-2008) and the long-term record (1891-2009) of surface air temperature at Hamburg-Fuhlsbüttel, Germany (hereafter HT for Hamburg timeseries) provided by German Weather Service, DWD (available at <http://www.dwd.de>, station code 10147).

Besides linear regression and correlation, we used wavelet analysis. To analyze large-scale atmospheric sea level pressure (SLP) patterns, especially the NAO which contributes largely to the climate variability of northern Europe, EOF (or principal component) analysis has been performed. EOFs have been calculated for the period 1958-2008 using 20 years time windows, each overlapping by 10 years (P1: 1958-1977, P2: 1968-1987, P3: 1978-1997, P4: 1988-2007).

3. Large-scale atmospheric variability

EOF analysis was applied to winter (DJFM) monthly mean SLP anomalies from NNR data (1958-2007), for time windows of 20 years each overlapping by 10 years (Figure 1). The first EOF is well separated from subsequent modes thus representing a robust pattern which can be associated with the NAO. The four periods demonstrate a change in the NAO-pattern manifested by an eastward shift of the centers of action. A shift of the NAO centers of action between the periods P1 and P3 has been described previously by Hilmer and Jung (2000). Our extended EOF analysis confirms the persistent eastward shift during P4, which results in an increased influence of the NAO on northern Europe.

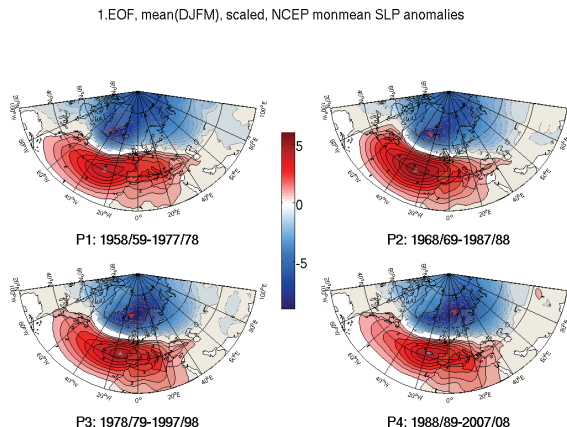


Figure 1. First EOF of winter (DJFM) averaged monthly mean North Atlantic SLP anomalies (hPa) from the NCEP/NCAR reanalysis data for periods of 20 years, each overlapping 10 years. Triangles in red and gray represent the position of the centers of action. Explained variances of first EOF (second EOF) in chronological order: 44.9% (15%), 47% (14%), 52.8% (13%), 47.8%. (16.6%). Contour interval is 0.5 hPa.

4. Regional atmospheric variability

From the NNR SLP data, changes in number and pathways of deep cyclones have been determined for the same 20-year periods (P1-P4) as have been used for determination of the EOFs (Figure 1). We simply counted the occurrence of deep (< 980 hPa) cyclones at each grid point in a 6-hourly interval. With a horizontal resolution of 2.5° of the SLP data multiple counting of deep cyclones at one location is possible which increased the number of

deep cyclone occurrences. Figure 2 shows the changes of the number of deep cyclones for winter (DJFM) counted for each 20-year period P1-P4, respectively. Taking P1 as reference period, the occurrence of deep cyclones over the North Atlantic region increased continuously in comparison with P2-P4.

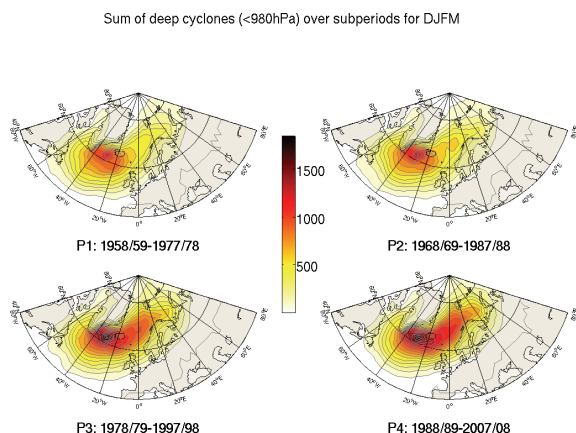


Figure 2. Total number of deep (<980 hPa) cyclones counted during periods P1-P4, based on NCEP/NCAR reanalysis 4 times daily SLP data (DJFM). Unit is number of deep cyclones, with an increment of 100.

Figure 3 shows the percentage of days with wind speeds higher than 13.9 m/s (> 7 bft) for the periods 1970-1987 and 1988-2008. There exists a shift of strong wind events from autumn to winter and early spring. Furthermore, the frequency distribution of wind directions (Figure 4) highlights a decrease of south-westerly winds in autumn (SON) accompanied by an increase of easterly winds. Whereas, during winter (DJF) the number of westerly wind events increased while at the same time easterly wind situations decreased.

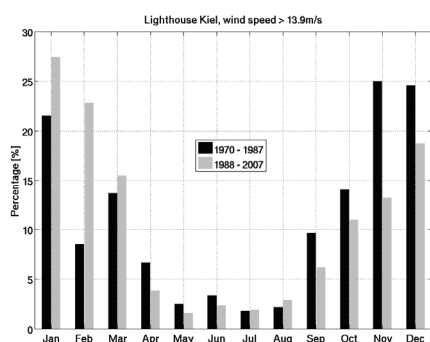


Figure 3. Percentage of days with wind speeds higher than 13.9 m/s (>bft 7) for all months, two periods 1970-1987 (black) and 1988-2007 (gray) at the position Lighthouse Kiel, in Kiel bight, Germany.

The trend in precipitation for the period (1979-2008) shows less rain in the central and northern areas (2-4 mm/year) and an increase in the southern part (2-4 mm/year). Because trends for the seasonal contributions were not significant within the 95% confidence level, we considered the difference in precipitation dividing the period to equal parts (1979-1993 and 1994-2008) and restricted the analysis to be only qualitative (Figure 5).

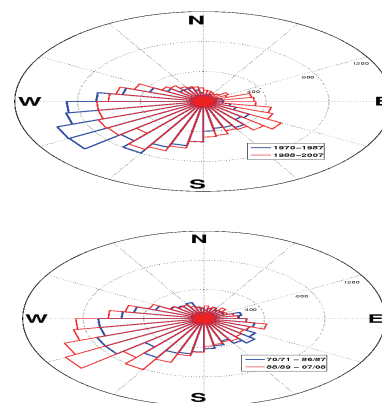


Figure 4. Frequency distribution of wind direction of two periods 1970-1987 (blue) and 1988-2007 (red) at the position Lighthouse Kiel, in Kiel Bight, based on SMHI meteorological data. Shown is the seasonal autumn (SON; left) and winter (DJF; right).

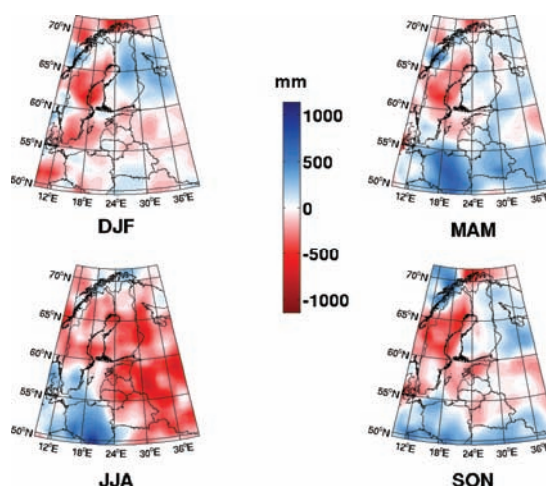


Figure 5. Seasonal differences of precipitation [mm] between two periods of equal length: 1979-1993 and 1994-2008 based on SMHI meteorological data base.

Generally, winter (DJF) contributed with less rain over most parts of the Baltic Sea, except the north-eastern area. Spring (MAM) contributed with more rain in the southern part and less rain for the northern Baltic Sea including most parts of Sweden. Summer (JJA) showed more rain in the south-west and less in the north-east, and autumn (SON) contributed with less rain over the northern Baltic Sea including Sweden and more rain in the south-western part of the Baltic area, respectively.

References

- Hilmer M, Jung T (2000) Evidence for a recent change in the link between the North Atlantic Oscillation and Arctic sea ice export. *Geophysical Research Letters*, 27:989-992.
- Hinrichsen H-H, Lehmann A, Peterit C, Schmidt, J (2007) Correlation analysis of Baltic Sea winter water mass formation and its impact on secondary and tertiary production. *Oceanologia*, 49:381-395.
- Kalnay et al. (1996) The NCEP/NCAR 40-year reanalysis project. *Bull. Amer. Meteor. Soc.*, 77:437-470.
- MacKenzie BR, Schiedek D (2007) Daily ocean monitoring since the 1860s shows record of warming northern European seas. *Global Change Biology* 13(7):1335-1347.
- Siegel H, Gerth M, Tschersich G (2006) Sea surface temperature development of the Baltic Sea in the period 1990-2004. *Oceanologia*, 48:119-131.

Long term trend and decadal variability of the hydrological cycle in the Baltic Sea region as modeled by the ENSEMBLES regional climate models

Philip Lorenz¹, Katharina Meraner² and Daniela Jacob²

¹Freie Universität Berlin, Institute of Meteorology, Berlin, Germany (Philip.Lorenz@fu-berlin.de)

²Max Planck Institute for Meteorology, Hamburg, Germany

1. Introduction

A main focus of BALTEX is the investigation of the water and energy cycles of the Baltic Sea region. Jacob and Lorenz (2009) performed an analysis of future trends and variability of the hydrological cycle within the Baltic Sea region as modeled by the Max Planck Institute's Regional Climate Model (RCM) REMO for different IPCC SRES emission scenarios.

As a continuation the study has been extended to the multi-model RCM projection ensemble produced within the ENSEMBLES EU FP6 project (<http://www.ensembles-eu.org>).

2. ENSEMBLES RCM experiments

Within ENSEMBLES, several European institutions used their RCMs to carry out validation as well as transient climate change projections under the IPCC SRES A1B scenario for whole Europe at 25 km horizontal resolution. The validation experiments (1961-2000) were driven by the ERA40 re-analysis data. The transient climate change projections (1950-2050; partly until 2100) were driven by several coupled atmosphere-ocean general circulation

models (GCM). The experimental RCM-GCM matrix is shown in Table 1.

3. Analysis of the decadal variability in the hydrological cycle

For the analysis of the decadal variability of the hydrological cycle, decadal area sums of precipitation, evaporation and runoff have been calculated for the land part fraction of the Baltic Sea catchment area and for the area of the Baltic Sea itself (except for runoff) for all RCM simulations listed in Table 1 and for the respective simulations of their driving GCMs. An analysis of the decadal variability and long-term trends for several budget quantities of the hydrological cycle for the Baltic Sea region will be presented.

References

Jacob D., Lorenz P. (2009) Future trends and variability of the hydrological cycle in different IPCC SRES emission scenarios – a case study for the Baltic Sea region, Boreal Environmental Research, Vol. 14, pp. 100-113

Table 1: Matrix of the ENSEMBLES RCM simulations and their driving GCMs

GCM RCM	ERA40	METO-HC, Std	METO- HC,Low	METO- HC,High	MPIMET	IPSL	CNRM	NERSC	CGCM3	Total
METO-HC <i>HadRM</i>	1961- 2002	1950-2100	1950-2100*	1950-2100*	1950-2100					4
MPIMET <i>REMO</i>	1961- 2002				1950-2100	1950- 2050*				2
CNRM <i>ALADIN</i>	1961- 2002						1950- 2050			1
DMI <i>HIRHAM</i>	1961- 2002				1950- 2100*		1950- 2100	1950- 2100*		3
ETH <i>CLM</i>	1961- 2002	1950-2100								1
KNMI <i>RACMO</i>	1961- 2002				1950-2100					1
ICTP <i>RegCM</i>	1961- 2002				1950-2100					1
SMHI <i>RCA3</i>	1961- 2002		1950-2100*		1950- 2100*			1950- 2100		3
UCLM <i>PROMES</i>	1961- 2002		1950-2050							1
C4I <i>RCA3</i>	1961- 2002			1950-2100*	1950- 2050*					2
GKSS <i>CLM</i>	1961- 2002					1950- 2050*				1
Met.No <i>HIRHAM</i>	1961- 2002							1950- 2050*		1
CHMI <i>ALADIN</i>	1961- 2002						1950- 2050*			1
OURANOS* <i>CRCM</i>	1961- 2002								1950- 2050*	1
EC* <i>GEMLAM</i>	1961- 2002									
VMGO* <i>VMGO</i>		1950-2050*								1
Total		3	3	2	7	2	3	3	1	24

High resolution reanalysis for the Baltic Sea region during 1965-2005

Andres Luhamaa^{1,2}, Kaarel Kimmel¹, Aarne Männik^{1,2} and Rein Rõõm¹

¹ Laboratory of Atmospheric Physics, Institute of Physics, University of Tartu, Estonia (andres.luhamaa@ut.ee)

² Estonian Meteorological and Hydrological Institute, Estonia

1. Introduction

Reliable data are the basis of any climatological study. While regular meteorological observations provide high-quality information, they are irregular in space and time and sparse in many parts of the world. Since the development of modern numerical weather prediction models, atmospheric data assimilation has been among the most reliable and used methods for determining the realistic states of the atmosphere, by combining different types of observations and best knowledge about atmospheric physics. As numerical weather prediction models have improved over the years, it is possible to use them for analysing the past data. Bengtsson and Shukla (1988) and Trenberth and Olson (1988) proposed reanalysis of archived meteorological observations, to create internally consistent, long term multivariate datasets of the Earth's climate system. A well known and successful example of such a reanalysis is the ERA40 global reanalysis (Uppala et al 2005).

As the Baltic Sea region has a rather variable landscape with mountains, many lakes and islands together with undulating coastlines, the ERA40 is not well suited for analysing local meteorological conditions due to its coarse resolution. The current article gives a short overview of the regional reanalysis project BaltAn65+.

2. Experiment description

The state of the art numerical weather prediction model HIRLAM (version 7.1.4, www.hirlam.org) is applied for the Baltic Sea region (Figure 1) over the time period 1965-2005 to produce high-resolution meteorological database with a 6-hour interval. For the data assimilation, the 3DVAR scheme is used and 6-hour hindcasts from previous cycles are used as background fields. Standard surface observations and meteorological soundings together with ship and buoy measurements from the WMO network are used as input data for the data assimilation system. For boundary fields, the ERA40 reanalysis data are used. Horizontal resolution is 11 km and 60-layers are used in vertical.

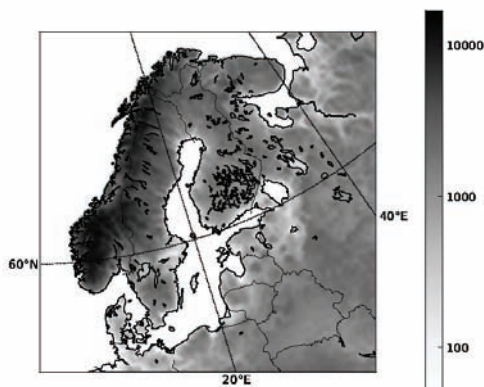


Figure 1. Modelling domain of BaltAn65+, surface geopotential.

The modelling domain, shown in Figure 1, is chosen in a way to best suit the needs of the Baltic Sea region. BaltAn65+ could be illustrated as a regional refinement of the global reanalysis like ERA40.

The Baltic Sea area has a good observation network compared to most parts of the world. The average number of surface measurements used in data assimilation is 300-400, and radiosonde measurements between 20-30 at 00' UTC and 12' UTC, but significantly lower at other times.

While the purpose of the current paper is not a thorough analysis of all the available data in a new database, a simple seasonal 2m temperature trend calculation is provided for illustrative purpose. The highest temperature trend using linear regression is found during winter months, being 0.56 °C/decade, Figure 2 and lowest trend for autumn months, 0.1 °C/decade.

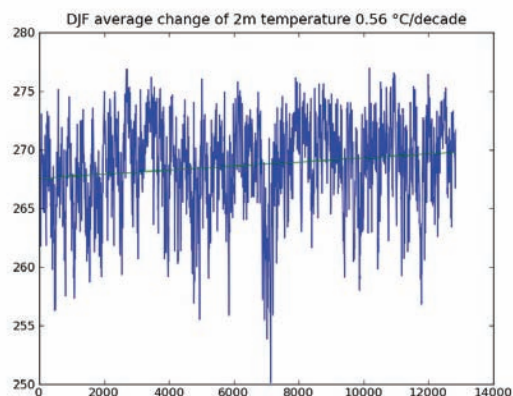


Figure 2. Wintertime 2m temperature trend over the 1965-2005 period.

3. Conclusion

Current project hopes to provide the best possible synthesis of available meteorological observations put together by the high quality meteorological model. The reanalysis data will be useful for examining the variability of climatic processes and gives additional source of information for those who observe trends and changes in local climates. The data will be accessible for all interested parties via the web page of Estonian Meteorological and Hydrological Institute, www.emhi.ee.

References

- Bengtsson L. and Shukla J. 1988. Integration of space and in situ observations to study global climate change. *Bull. Am. Meteorol. Soc.* 69: 1130–1143
- Trenberth K. E. and Olson J. G. 1988. An evaluation and intercomparison of global analyses from NMC and ECMWF. *Bull. Am. Meteorol. Soc.* 69: 1047–1057
- Uppala S.M., Kallberg P.W., Simmons A.J., Andrae U.A., Da Costa Bechtold V., Fiorino M., Gibson J.K., Haseler J., Hernandez A., Kelly G.A., Li X., Onogi K., Saarinen S., Sokka N., Allan R.P., Andersson E., Arpe K., Balmaseda M. A., Beljaars A.C.M., Van de Berg L., Bidlot J., Bormann N., Caires S., Chevallier F., Dethof H., Dragosavac M., Fisher M., Fuentes M., Hagemann S., Holm E., Hoskins B.J., Isaksen I., Janssen P.A.E.M., Jenne R., McNally A.P., Mahfouf J.-F., Morcrette J.-J., Rayner N.A., Saunders R.W., Simon P., Sterl A., Trenberth K.E., Untch A., Vasiljevic D., Viterbo P. and Woolen J. 2005. The ERA-40 re-analysis. *Quarterly journal of the Royal Meteorological Society* 131: 2961-3012

Long-term changes in frequency and duration of southern cyclones influencing climate variability in Estonia

Kaupo Mändla, Mait Sepp and Jaak Jaagus

Department of Geography, University of Tartu, Estonia (kaupo85@ut.ee)

1. Introduction

Estonia is located in a climatic transition zone characterised by very high cyclonic activity and alternation of different air masses. Therefore, weather conditions vary much from day to day and year to year.

Cyclonic activity affects weather in this region throughout a year. Most of the cyclones having an effect on Estonian weather come from the west, south-west and north-west, caused by dominant westerlies. The number of cyclones forming on the sub-tropic latitudes over the Mediterranean, Black and Caspian Seas and moving generally northwards is much smaller. They are called southern cyclones.

Southern cyclones cause large contrasts in air temperature that could reach up to 15°C between the warm and cold air masses. Heavy thunderstorms, wind gusts and even strong destructive tornadoes have been observed in their frontal zones. The most extreme precipitation events in Estonia have been concurred with southern cyclones (Mätlik and Post 2008). Although significant changes have been observed in the large-scale atmospheric circulation in this region, possible changes in parameters of southern cyclones have not been studied yet.

The objective of this study is to analyse long-term changes in the frequency and duration of southern cyclones, and their effects on precipitation and air temperature changes in Estonia.

2. Material and methods

We used the database of cyclones compiled by Gulev et al. (2001), using the SLP data with a 6-hour time lag derived from the NCEP/NCAR re-analysis for the period 1948-2004. We defined southern cyclones as cyclones that have formed south of 47°N and east of the 0° meridian. The limits were chosen so that the formation region of a southern cyclone was located over the Mediterranean, Black and Caspian Sea regions.

In the present study, we found from the database of cyclones all such southern cyclones that should, supposedly, have an effect on the weather in Estonia. The criterion of 1000 km distance between the centres of a cyclone and Estonia was used to select the cyclones affecting weather in Estonia. The point with coordinates 58.75°N and 25.5°E was used as the central point of Estonia. The 1000 km distance corresponds to the average radius of cyclones at mid latitudes.

For describing the inter-annual variability, the cyclones are divided by seasons: winter (DJF), spring (MAM), summer (JJA) and autumn (SON). In order to determine cyclones during the turn of a month, they are added to the month of their formation.

The southern cyclones are also divided into four classes according to their trajectories: A) moving from the south to the north and passing Estonia from the eastern side; B) moving from the south to the north and passing Estonia from the western side (border between these classes is 25°E); C) moving from the west to the east south of Estonia and D) moving from the east to the west south of Estonia (Figure 1). Daily precipitation and daily mean air temperature data from the Türi meteorological station were used in studying the

effect of southern cyclones on weather changes in Estonia. The station is located close to the geographical centre of Estonia.

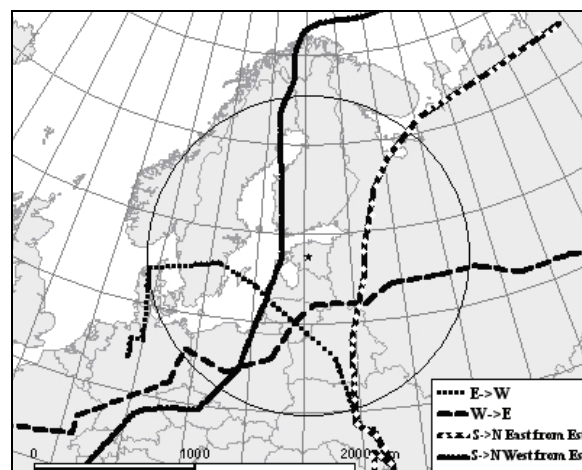


Figure 1. The 1000 km-radius circle with its centre at 58.75°N and 25.5°E, and the typical trajectories of the four classes of southern cyclones: A) S->N west of Estonia (occurred in the circle at 19.08-20.08.1948); B) S->N east of Estonia (15.08-16.08.1951); C) W->E (20.06-21.06.1957); D) E->W (09.12-10.12.1972).

Daily precipitation data were summed up for the period when a southern cyclone was located inside the 1000 km-circle. The cyclones with the total precipitation of above 10, 5, 2 and 0 mm were counted. Two methods were used for analysing the effect of southern cyclones on temperature. The first calculates temperature changes between the three-day mean temperatures before and after the cyclone is located within the 1000 km-circle. The second method calculates the temperature change between the first and last day when the cyclone located within the 1000 km-circle.

Linear regression analysis was used for detecting trends. The trends were considered statistically significant on the $p < 0.05$ level. Pierson correlation coefficients were used for relationships analysis.

3. Results and discussion

760 southern cyclones had an effect on Estonia during 1948-2004, giving the mean of 13.3 cyclones per year. This is about 10-13 per cent of all cyclones that affect weather conditions in Estonia. The largest number of southern cyclones has been observed in summer (total number 235). Almost the same amount was detected in spring (226). The number of southern cyclones was much smaller in autumn and in winter.

The numbers of cyclones in the trajectory classes were the following: A – 203; B – 415; C – 91 and D – 52. The frequency of the class B was the highest in every season with the maximum in spring. The class A was the most frequent in summer. The two other trajectory classes of southern cyclones were much less common (Figure 2).

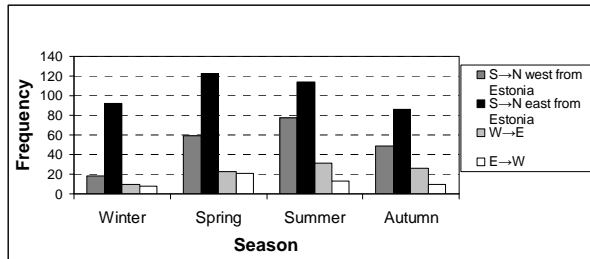


Figure 2. Frequency of the four trajectory classes of southern cyclones in different seasons during 1948-2004.

The total number of southern cyclones shows a decreasing trend by 3.5 cyclones for the whole period (Figure 3), but the trend is statistically not significant. The only significant decrease (by ca 2 cyclones) was detected for the frequency of the class C. This trend appears in summer and winter seasons only. Other trajectory classes of southern cyclones had no significant trends in their frequency.

The decreasing trend in the frequency of southern cyclones detected in this study resembles the decreasing of southern cyclones over Central Europe (Sepp 2005). A number of studies have drawn conclusions that confirm a general decrease in the frequency of cyclones in mid-latitudes (30-60°N) during the second half of the 20th century (Held 1993, Lambert 1996, Sickmüller et al. 2000, McCabe et al, 2001, Serreze et al. 1997, Gulev et al. 2001).

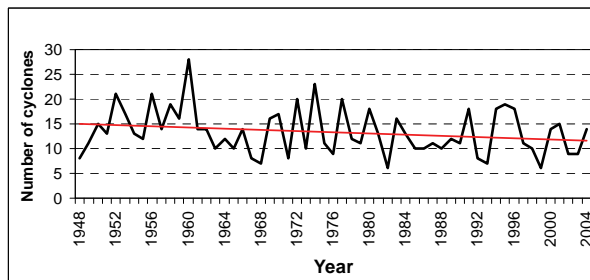


Figure 3. Time-series of the total number of southern cyclones during 1948-2004.

In the average, southern cyclones spent about one third (30.2%) of their lifetime within the 1000 km-circle and had an effect on weather conditions in Estonia. The mean duration of their stay within the circle was 33.5 hours. According to a linear trend, it has decreased insignificantly (by 1.8 hours) during 1948-2004. Thereby, the duration of the cyclones in the class C has increased by 25.1 hours. The duration of the cyclones in the class D in summer has decreased by 31 hours and in the class A in autumn by 14.9 hours. All the mentioned changes are statistically significant. All southern cyclones caused fairly 0.2°C temperature increase during the period 1951-2004 (1. method). This number has positively changed during the study period, approximately by 0.37°C. A similar but also statistically insignificant change was obtained using the second method. It was assumed that the southern cyclones of the class A bring warmer air into Estonia and those of the class B cause cooling. This was proven only in case of the 2nd method. Cyclones of the class C were related to a decrease in temperature and those of the class D caused an increase in temperature, but these changes were not statistically significant.

Generally, the effect of southern cyclones on air temperature change in Estonia was not as large as expected. However, clear temperature changes were found in single cases. For

example, the southern cyclone of the trajectory class A, passing Estonia from the west (in 23.-24.04.1980), caused a temperature rise by 11.5°C while a southern cyclone of the trajectory class B, passing Estonia from the east (01.-03.02.2001), caused a cooling by 12.3°C. Obviously, most of the southern cyclones did not have as clear effect on air temperature as we had expected. Also, the two methods used might not be the best ones for the estimation of the effect of southern cyclones on temperature.

During the 45 year-period (1960-2004), all days that were affected by a southern cyclone had a mean precipitation of 2.2 mm per 24 hours. This number increased by 0.6 mm during the study period, which is a statistically significant change.

Almost a quarter of all southern cyclones did not bring precipitation at the Türi station. Probably, they passed Estonia from too far. Approximately a half of all southern cyclones caused a moderate precipitation over 2 mm per 24 hours, about one third of them brought heavy precipitation of over 5 mm per 24 hours and slightly less than 15% induced an extreme rainfall over 10 mm per 24 hours. These precipitation quantities caused by southern cyclones show no trends.

References

- Gulev, S.K., Zolina, O., Grigoriev, S. (2001) Extratropical cyclone variability in the Northern Hemisphere winter from the NCEP/NCAR reanalysis data, *Climate Dynamics*, 17, 795-809
- Held, I.M. (1993) Large-scale dynamics and global warming, *Bull. Amer. Meteor. Soc.*, 74, 228-241
- Lambert, S.L. (1996) Intense extratropical Northern Hemisphere winter cyclone events: 1899-1991, *J. Geophys. Res.*, 101, 319-325
- McCabe, G.J., Clark, M.P., Serreze, M.C. (2001) Trends in northern hemisphere surface cyclone frequency and intensity, *J. Climate*, 14, 2763-2768
- Mätlik, O., Post, P. (2008) Synoptic weather types that have caused heavy precipitation in Estonia in the period 1961-2005, *Estonian Journal of Engineering*, 14, 195-208
- Sickmüller, M., Blender, R., Fraedrich, K. (2000) Observed winter cyclone tracks in the northern hemisphere in re-analysed ECMWF data, *Q. J. R. Meteorol.Soc.*, 126, 591-620
- Sepp, M. (2005) Influence of atmospheric circulation on environmental variables in Estonia, *Dissert. Geogr. Univ. Tartuensis*, 25
- Serreze, M.C., Carse, F., Barry, R.G., Rogers, J.C. (1997) Icelandic low cyclone activity: climatological features, linkages with the NAO, and relationships with the recent changes in the northern hemisphere circulation, *J. Climate*, 10, 453-464

Transient scenario simulations for the Baltic Sea for 1961-2099

H. E. M. Meier and ECOSUPPORT co-workers

Swedish Meteorological and Hydrological Institute, Sweden (markus.meier@smhi.se)
www.baltex-research.eu/ecosupport

1. Abstract

Within the ECOSUPPORT project (Advanced modeling tool for scenarios of the Baltic Sea ECOSystem to SUPPORT decision making) a dynamical downscaling approach is applied to calculate future climate of the Baltic Sea using a high-resolution coupled atmosphere-ice-ocean-land surface regional climate model (RCM) with lateral boundary data from global climate models (GCMs). An ensemble of regional scenario simulations is performed to assess the uncertainty related to the natural variability, unknown future greenhouse gas emissions, unknown future nutrient loads to the sea, and biases of the RCM and GCMs. In difference to earlier studies addressing selected time slices (see BALTEX Assessment of climate change for the Baltic Sea basin, BACC), the new scenario simulations are transient simulations covering the whole period 1961-2099. In addition, improved versions of the GCMs used for the latest IPCC assessment are utilized. Results from the first available scenario simulations will be presented and discussed. For the control period 1961-2007 the model results are validated with available observations and compared with hindcast simulations that are able to reproduce the history of climate variability by applying data from the global re-analysis ERA-40 at the lateral boundaries of the RCM. We found that both hindcast and control simulations are of high quality. However, the projections of future climate at the end of the 21st century differ considerably depending on the driving GCM used. For the near future the uncertainties of the projected ocean physics related to the natural variability are largest whereas at the end of the century the uncertainties due to unknown greenhouse gas emissions are getting more important.

2. Introduction

Within ECOSUPPORT, the combined effects of changing climate and changing nutrient loads on the Baltic Sea ecosystem are investigated. Using a coupled atmosphere-ice-ocean regional climate model (RCM), models for the atmospheric (MATCH) and land surface chemistry (HYPE), three marine biogeochemical models (RCO-SCOBI, BALTSEM, ERGOM) and several food web models for the Baltic Sea ecosystem (e.g. EwE, BEM, see Figure 1), transient simulations driven by two GCMs (ECHAM5, HadCM3) and two greenhouse gas emission scenarios for 1961-2099 are investigated. These scenario simulations are novel because transient model runs were performed, instead of selected time slices as in BACC (2008). Thus, restricting assumptions on the changes of the high frequency variability were not necessary. Further, new model versions of the GCMs and the RCM were utilized. For instance, both the RCM and the coupled physical-biogeochemical model RCO-SCOBI (Meier and Kauker 2003, Eilola et al. 2009) have higher horizontal resolutions compared to earlier studies. The horizontal resolution of RCAO amounts to 25 instead of 50 km causing improved wind speed simulations. RCO-SCOBI is used with a horizontal resolution of 3.6km and 83 vertical levels (earlier 10.8 km and 41 levels) causing more realistic simulations of salt water inflow dynamics. Novel is also the usage of a multi-model ensemble to

estimate uncertainties due to the lacking knowledge of some biogeochemical processes. Finally, marine food web models that include higher trophic levels (from zooplankton upwards to fish and seals) will be used within ECOSUPPORT to estimate the impact of changing climate on the marine ecosystem.

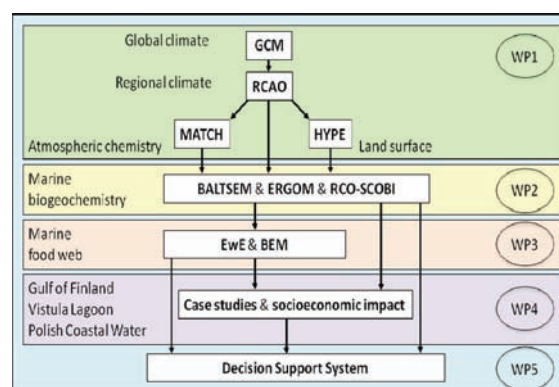


Figure 1. Model hierarchy in the ECOSUPPORT project and work package (WP) structure (see <http://www.baltex-research.eu/ecosupport>). The schematic is highly simplified neglecting complex interactions (e.g. fish predation pressure on zooplankton, changing society/policy will affect climate and nutrient load scenarios).

In this study mainly results from work packages 1 and 2 of ECOSUPPORT are presented. The marine biogeochemical models are used to calculate changing concentrations of nitrate, ammonium, phosphate, diatoms, flagellates, cyanobacteria, zooplankton, detritus, and oxygen in the Baltic Sea.

3. Results

Mean seasonal cycles of important parameters like 2 m air temperature are well simulated by the RCM when lateral boundary data from the two selected GCMs are used (Figure 2). We found that a horizontal resolution of the atmospheric model of at least 25 km is needed to simulate 10m wind fields over the Baltic Sea sufficiently well. However, modelled wind speed extremes are still underestimated compared to observations. The impact of the horizontal resolution on the 2 m air temperature is minor (Figure 2). In ECHAM5 driven simulations the 2 m air temperature over the Baltic during summer is improved when the fully coupled RCAO model is used instead of the standalone atmospheric RCA model (Figure 2). In winter the climate of northern Europe is significantly controlled by the large-scale circulation and the added value of the coupled RCAO is minor.

We found that all three investigated biogeochemical models are able to reproduce the observed variability of biogeochemical cycles (Eilola et al. 2010). Uncertainties were primarily related to differences in the bioavailable

fractions of nutrient loadings from land and parameterizations of key processes like sediment fluxes that are presently not well known.

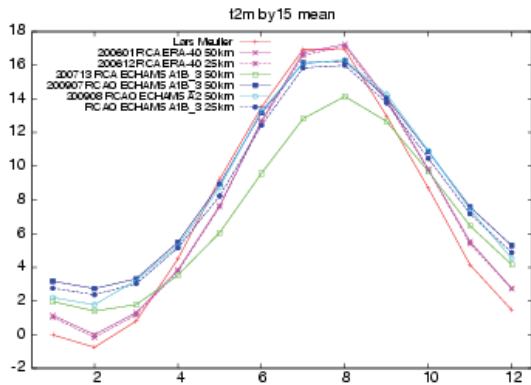


Figure 2. Monthly mean 2m air temperature (in °C) at Gotland Deep (BY15) in the central Baltic proper for 1980-2006: gridded observations (red, solid line with plus signs), RCA-ERA40 50km (pink, solid line with crosses), RCA-ERA40 25km (pink, dashed line with crosses), RCA-ECHAM5/A1B_3 50km (green, solid line with open squares), RCAO-ECHAM5/A1B_3 50km (blue, solid line with filled squares), RCAO-ECHAM5/A2 50km (light blue, solid line with open squares), and RCAO-ECHAM5/A1B_3 25km (blue, dashed line with open circles).

As the saturation concentration of oxygen in warmer water is lower, in future climate the oxygen concentrations in coastal waters will be reduced (Figure 3). Consequently, also in the deepwater oxygen concentrations should decrease assuming that nutrient loads from land will only alter according to volume flow changes. However, in both GCM driven simulations there are also small bottom areas, e.g. at the slopes of the Gulf of Finland, northern Baltic proper, Bothnian Sea and Bothnian Bay, with improved oxygen concentrations caused by reduced stability (Figure 3). In the present study, this and other impacts of changing climate on the marine biogeochemistry will be discussed in detail and compared with earlier results from BACC (2008). The projections of the future marine environment performed within ECOSUPPORT are of key relevance for several Swedish and international projects, e.g. the projects AMBER (<http://www.io-warnemuende.de/amber.html>) and INFLOW (<http://projects.gtk.fi/inflow/index.html>) within the BONUS+ program (<http://www.bonusportal.org>).

References

- BACC author team, 2008: Assessment of Climate Change for the Baltic Sea Basin Series. [Regional Climate Studies](#), Springer, 474 pp.
- Eilola, K., Meier, H.E.M. and Almroth, E., 2009: On the dynamics of oxygen, phosphorus and cyanobacteria in the Baltic Sea; A model study. *Journal of Marine Systems*, 75: 163-184.
- Eilola, K., B. G. Gustafson, R. Hordoir, A. Höglund, I. Kuznetsov, H. E. M. Meier, T. Neumann and O. P. Savchuk, 2010: Quality assessment of state-of-the-art coupled physical-biogeochemical models in hind cast simulations 1970-2005. Rapport Oceanografi No.101, SMHI, Norrköping, Sweden.
- Meier, H.E.M., and F. Kauker, 2003: Modeling decadal variability of the Baltic Sea: 2. Role of freshwater inflow

and large-scale atmospheric circulation for salinity. *J. Geophys. Res.*, 108(C11), 3368.

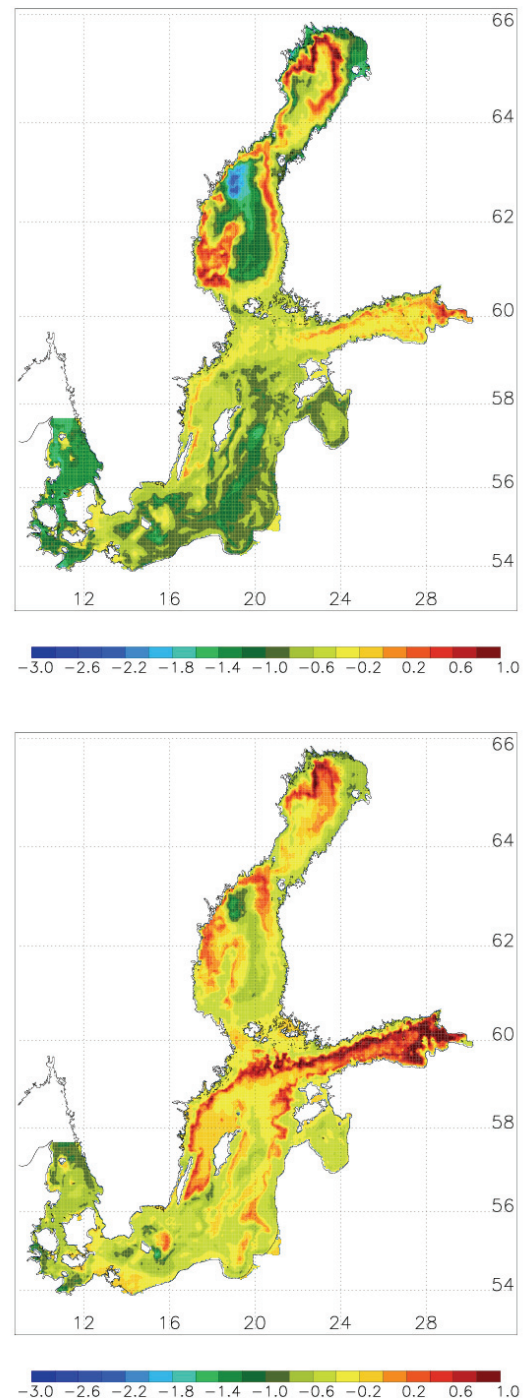


Figure 3. Summer (June, July, August) mean bottom oxygen changes (in ml/l) between the future scenario time slice (2060-2089) and the control period (1970-1999) driven with RCAO-HadCM3/ A1B (upper panel) and RCAO-ECHAM5/A1B (lower panel). For the depicted results concentrations of nutrient and phosphorus loads from land are assumed to be unchanged.

Impact of climate change on biogeochemical fluxes of nitrogen and phosphorus in the Gulf of Riga

Bärbel Müller-Karulis¹, Juris Seņņikovs², Aigars Valainis², Juris Aigars¹

¹ Latvian Institute of Aquatic Ecology, Riga, Latvia (Barbel.Muller-Karulis@lhei.lv)

² Laboratory for Mathematical Modelling of Environmental and Technological Processes, Faculty of Physics and Mathematics, University of Latvia, Riga, Latvia

1. Modeling approach

We used a 1D physical model to simulate the effect of climate change on water temperature and vertical mixing in the Gulf of Riga and forced a biogeochemical box model with its output to simulate secondary effects on phytoplankton, nitrogen, phosphorus and dissolved oxygen dynamics in the Gulf. The physical model used is the General Ocean Turbulence Model (Umlauf et al. 2007), with vertical turbulent fluxes parameterized according to Cheng (2002). The biogeochemical model is a box model based on Savchuk (2002), which divides the water column into a pelagic and a demersal box. It includes all major biogeochemical fluxes of nitrogen and phosphorus, specifically their assimilation by phytoplankton, pelagic regeneration, sedimentation and subsequent remineralization, sequestering and burial in bottom sediments. Depending on bottom water oxygen concentrations, remineralized nitrogen is denitrified or returned to the water column. All biogeochemical reactions in the model are coupled to stoichiometrically equivalent oxygen fluxes. Both physical and biogeochemical models were carefully calibrated against long-term monitoring data.

2. Climate change scenarios

Output from a regional climate model (RCAO high res., driving data HadAM3H) collected by the PRUDENCE project was used to generate control (CTL, 1961-1990) and future forcing to the physical model according to the IPCC A2 emission scenario (A2, 2070-2100). Extra downscaling by bias correction via histogram equalization (Seņņikovs and Bethers 2009) was applied to relative humidity and air temperature, while the original regional climate model output was used for sea level pressure, cloudiness, wind speed and direction. As a result of the downscaling, the vertical temperature distribution in the Gulf of Riga modeled during the control period corresponded well to observed values.

3. Water temperature and stratification

Compared to the control run, the physical model forced with the downscaled A2 regional climate model output predicted the annual average temperature in the Gulf to increase by 3 °C at the surface and 1.5 °C at the bottom. The A2 Gulf of Riga was ice free in all simulation output years. As a consequence of the warming, the water column stratified earlier, stratification lasted longer and the density gradient at the pycnocline was more pronounced. Therefore, the residual turbulent water exchange between the pelagic and demersal water layers of the Gulf of Riga that governs the exchange of nutrients and oxygen during the stratified period, was reduced in the A2 scenario.

4. Oxygen conditions

Oxygen concentrations in the bottom water are presently often at the anoxic threshold before the breakup of stratification in the Gulf. Our model simulations predict

warming to decrease the demersal oxygen conditions in the Gulf. This is caused by diminished oxygen solubility in the warmer surface waters, reduced transport through the pycnocline due to the stronger and longer stratification, and increased consumption by degrading organic matter.

5. Phytoplankton and primary production

Because stratification governs the light climate experienced by phytoplankton, earlier pycnocline formation together with the absence of ice cover translates to an earlier and more vigorous spring bloom in the A2 model scenario. Despite the increased stratification and thus reduced water exchange between pelagic and demersal layer, also during the rest of the growth season phytoplankton biomass and primary production in the A2 scenario is larger than in the control run. This is caused by the warmer water temperatures which in turn increase the rates of nitrogen and phosphorus regeneration.

6. Denitrification

The intensity of denitrification governs the nitrogen budget of the Gulf of Riga and the magnitude of its further export to the Baltic Proper. Corresponding to the average depth and oxygen conditions assumed for the demersal water layer in the Gulf, our biogeochemical model predicts denitrification to increase in the A2 climate scenario. However, oxygen conditions in the deeper parts of the Gulf will be significantly lower than the modeled demersal layer averages. Observations and experimental results indicate, that under these conditions, denitrification rates decrease and the impact of climate change on biogeochemical fluxes might be less linear than predicted by our box model.

Acknowledgments

This study was supported by the Latvian national research programme KALME, the EU FP6 project SPICOSA.

References

- Cheng, Y., Canuto, V.M., Howard, A.M. 2002. An improved model for the turbulent PBL, *J. Atmos. Sci.*, 59, 1550–1565, 2002.
- Savchuk, O. 2002. Nutrient biogeochemical cycles in the Gulf of Riga: scaling up field studies with a mathematical model. *J. Mar. Syst.* 32: 253-280.
- Seņņikovs, J., Bethers, U. Statistical downscaling method of regional climate model results for hydrological modeling. 18th World IMACS/MODSIM Congress, Cairns, Australia, 13-17 July 2009, <http://mssanz.org.au/modsim09>
- Umlauf, L., Burchard, H., Bolding, K. 2007. GOTM. Sourcecode and Test Case Documentation Version 4.0. <http://www.gotm.net/pages/documentation/manual/pdf/a4.pdf>, 346 p.

Uncertainties in the projected climate changes of wind extremes over the Baltic region

Grigory Nikulin, Erik Kjellström and Colin Jones

Swedish Meteorological and Hydrological Institute, Norrköping, Sweden (grigory.nikulin@smhi.se)

1. Introduction

The projected climate changes in temperature and precipitation extremes are, in general, in agreement among different regional climate models (RCM) over Europe. For wind extremes RCM studies show a general tendency to stronger and more frequent extreme winds in the end of the century but there are very large discrepancies in magnitude, frequency and spatial patterns of the change among models which critically depend on how the driving global climate models (GCMs) simulate future changes in the large-scale circulation over the North Atlantic/European domain (Leckebusch et al. 2006, Beniston et al 2007, Rockel and Woth 2007). In this study, applying two ensembles of regional climate simulations over the Baltic region, we examine uncertainties in projected climate changes of wind extreme related to driving GCMs and to natural variability.

2. Data and methods

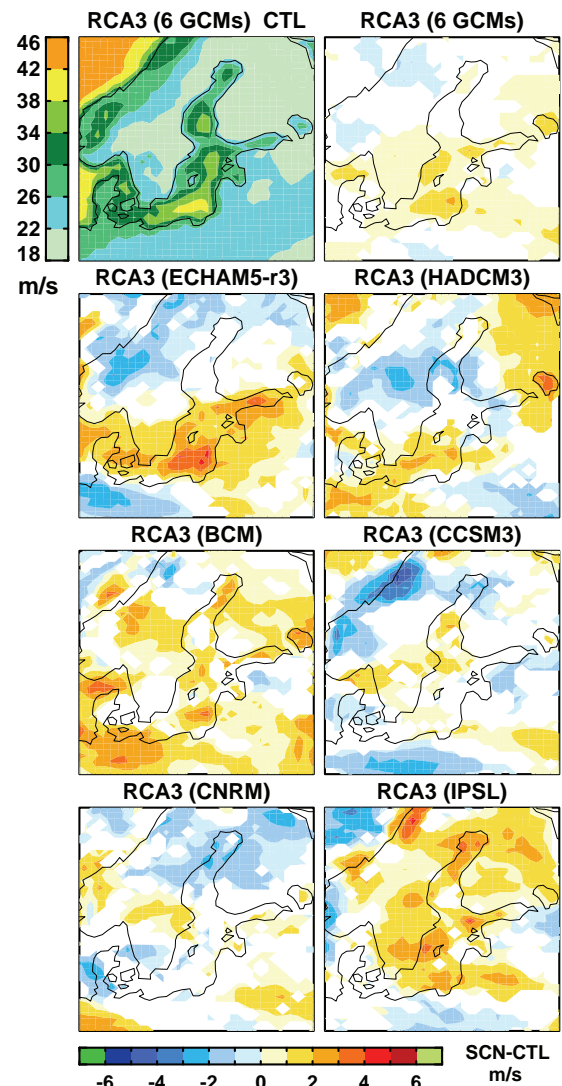
The downscaling of GCM simulations is performed with the Rossby Center Regional Climate Model (RCA3) at 50 km resolution and under the SRES-A1B emission scenario. The first ensemble which samples uncertainties related to driving GCMs consists of six simulations driven by different GCMs (ECHAM5, HadCM3, CCSM3, BCM, IPSL and CNRM). The second ensemble is formed from three simulations driven by ECHAM5 that are only different in initial conditions hence sampling uncertainties related to natural variability.

The wind extremes are expressed in terms of 20-year return values of annual maximum of daily maximum gust wind ($W_{\max,20}$). The 20-year return value is defined as the magnitude of an extreme event which occurs once in a 20-year period.

3. Results

The ensemble mean $W_{\max,20}$ for the CTL period and for both ensembles ranges from 18 to 46 m s^{-1} showing the same spatial pattern that is basically defined by the land and sea distribution (Figures 1 and 2). At the same time $W_{\max,20}$ among the individual simulations can locally differ by 10 m s^{-1} and more (not shown). The projected changes in $W_{\max,20}$ in the SCN period show a wide spread among the six simulations driven by different GCMs (Figure 1): the individual changes vary from -6 to 6 m s^{-1} in different runs without any coherent pattern. The ensemble mean shows a significant strengthening of wind extremes in southern Scandinavia (1 m s^{-1}) with several maxima (2 m s^{-1}) over the Baltic Sea. Five of six simulations presented in Fig. 1 more or less agree in the strengthening of wind extremes over different parts of the Baltic Sea. At the same time we note that regional details of the ensemble mean changes in wind extremes are sensitive to the number of simulations in the ensemble.

There is also a spread in the projected changes in $W_{\max,20}$ among three simulations driven by the same GCM - ECHAM5 and different only in initial conditions (Figure 2). For example RCA3(ECHAM5-r1) shows an significant



increase over Denmark and no changes over southern Sweden and a substantial part of the Baltic Sea while two

Figure 1. (top, left) The ensemble mean of the 20-year return levels of annual maximum wind gust for 1961-1990 (SCN) [m s^{-1}] and the projected changes in the return levels for six individual simulations and their ensemble mean for 2071-2100 (SCN). Only the changes significant at the 10% significance level are shown.

other simulations project an increase in extreme wind over this region. However, again, local details, like location of maximum change, are different between these two members of the second ensemble. The ensemble average of the three ECHAM5 driven runs reveals a combination of three simulations resulting in a strengthening of wind extremes with similar magnitude (2-3 m s^{-1}) over the south part of Scandinavia and the Baltic Sea.

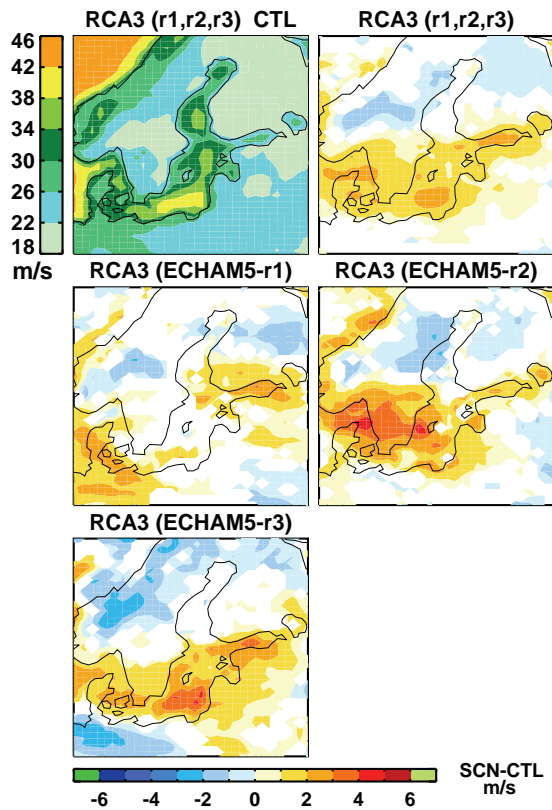


Figure 2. (top, left) The ensemble mean of the 20-year return levels of annual maximum wind gust for 1961-1990 (SCN) [m s^{-1}] and the projected changes in the return levels for three individual simulations different only in initial conditions and their ensemble mean for 2071-2100 (SCN). Only the changes significant at the 10% significance level are shown.

4. Summary

The projected future climate changes in wind extremes over the Baltic region show a strong dependence of regional simulations on driving GCMs but in most simulations and respectively in the ensemble mean a tendency to an increase in wind extremes approximately south of 60°N and some decrease north of it can be identified. In addition to uncertainties related to driving GCMs, uncertainties related to natural variability can also play an important role in local projections of wind extremes. Possible future projections based on the same ECHAM5 GCM with different initial conditions differ in spatial patterns and local details. These differences depend on the simulated large-scale circulations over the Atlantic region in individual members of the ECHAM5 family. Since we do not know what phase of the large-scale circulation over the Atlantic region will dominate in 2071-2100 all these projections are equally likely.

Acknowledgements

Part of the simulations and subsequent analysis work has been funded by the European ENSEMBLES (GOCE-CT-2003-505539) project, the Nordic Climate and Energy Systems (CES) project and the Swedish Mistra-SWECIA programme funded by Mistra (the Foundation for Strategic Environmental Research). The model simulations were made on the climate computing resource Tornado funded

with a grant from the Knut and Alice Wallenberg foundation. The institutes providing the global model data used as boundary conditions are kindly acknowledged.

References

- Leckebusch, G. C., Koffi, B., Ulbrich, U., Pinto, J., Spanghel, T. and Zacharias, S. 2006. Analysis of frequency and intensity of winter storm events in Europe on synoptic and regional scales from a multi-model perspective. *Clim. Res.* **31**, 59-74.
- Beniston, M., Stephenson, D. B., Christensen, O. B., Ferro, C. A. T., Frei, C., Goyette, S., Halsnaes, K., Holt, T., Jylhä, K., Koffi, B., Palutikof, J., Schöll, R., Semmler, T. and Woth, K. 2007. Future extreme events in European climate: an exploration of regional climate model projections. *Clim. Change* **81**, 71-95, doi:10.1007/s10584-006-9226-z.
- Rockel, B. and Woth, K. 2007. Extremes of near surface wind speed over Europe and their future changes as estimated from an ensemble of RCM simulations. *Clim. Change* **81**, 267-280.

Impact of climate change on the water balance of a mesoscale catchment of the Western Bug

Thomas Pluntke¹, Klemens Barfus¹, Kai Schwärzel², Cornelia Burmeister³ and Christian Bernhofer¹

¹ Institute of Hydrology and Meteorology, Technische Universität Dresden, Germany (Thomas.Pluntke@tu-dresden.de)

² Institute of Soil Science and Site Ecology, Technische Universität Dresden, Germany

³ Chair of Environmental Development and Risk Management, Technische Universität Dresden, Germany

1. Introduction

The investigations take place within the project “International Water Alliance Saxony” (IWAS, <http://www.iwas-sachsen.ufz.de/>). The focus is to solve water management problems in five regions of the world, namely Ukraine, Mongolia, Brazil, Vietnam and Oman. The reasons why we deal with the river Western Bug in Ukraine, are the poor river water quality, the insufficient and bad water infrastructure and its location at the border of the European Union. Pollution loads from punctual and diffuse sources are high, because of insufficient water treatment and formerly intensive agriculture. The main aims of the subproject are: system analysis and modelling, evaluation of the current state, development of model-based future scenarios and management options for the catchment.

Our work focuses on the determination of the past, current and future water balance of the investigated catchment Western Bug/Kamianka Buzka. It is a prerequisite to determine the matter balance of the catchment. Climatological trends were identified using data of climatological stations. Land-use information was derived from satellite images and pedological conditions from a map of the scale 1:200.000. Uncertainties of the input data are high. To account for future climate scenarios we plan to use the results of the Global Climate Model (GCM) ECHAM5 for the period 2051-2080.

2. Investigation area, data and methods

The Western Bug is a tributary of the river Vistula. It originates in Galicia (north of the Carpathian Mountains) at an altitude of 345m. We investigate the catchment of Kamianka Buzka (2560 km²), because runoff measurements exist.

We applied the model SWAT (<http://swatmodel.tamu.edu/>), abbreviation of Soil and Water Assessment Tool. It is a public domain river basin scale model developed to quantify water and matter fluxes and the impact of land management practices in large, complex watersheds. Daily values of precipitation, global radiation, wind speed, relative humidity and minimum and maximum temperature are needed as meteorological input. Land use and soil data as well as a digital elevation model DEM are used to define hydrological response units and to parameterise them.

Daily meteorological data were downloaded from the internet databases ECA&D and NOAA (<http://eca.knmi.nl/>, <http://www.ncdc.noaa.gov>). A further source of meteorological data was the Rostotsky Landscape Geophysical Station in Briuchovychi, near Lviv. The density of climatological stations is low in comparison to e.g. Germany (e.g. for precipitation 50 times less). Missing values were added applying multiple regression with neighbouring stations. Homogeneity was tested using the Alexandersson test (Alexandersson, 1986) and if necessary data were homogenised.

Daily runoff data of the gauges Sasiv and Kamianka Buzka were checked on homogeneity.

Trends of meteorological parameters of the period 1951-2000 were calculated and checked on significance using the MANN-KENDALL-test (Franke et al., 2004).

Future climate time series were used from the GCM ECHAM5/MPIOM considering the emission scenario SRES-A1B.

A soil map in the scale of 1:200.000 was available for the Oblast Lviv. Soils were aggregated to eight soil associations and soil and hydraulic parameters (texture, water content at field capacity and at wilting point, porosity, bulk density and saturated hydraulic conductivity) were derived using local expert knowledge. Land-use for the climatic reference period was derived from the satellite Landsat-TM5, (7 bands, resolution 30 m, image from August 1989). Data were classified according to the CORINE Land Cover classification scheme (http://www.corine.dfd.dlr.de/intro_en.html), a European approach for recording land cover and land use. Up to now 7 classes were detected, namely: water (0.1%), grassland and agriculture (47.9%), deciduous forest (5.6%), coniferous forest (15.1%), bare ground (28.5%), peat cutting (0.6%) and artificial surface (2.1%).

3. First Results

Exemplarily the trends of precipitation and temperature at the station Lviv are shown in Table 1. The mean yearly temperature increased about 0.41 °C within 50 years, a value that is comparable to the low mountain ranges of Saxony, Germany. Warming took place in spring and winter, whereas in summer and autumn temperatures decreased. Yearly precipitation values had a slight positive trend. In spring and autumn trends were positive, whereas in summer and winter trends were negative about the same amount. Only the trend of spring temperature was significant at the 5% significance level.

Table 1. Trends of precipitation and temperature at the meteorological station Lviv (49.817 N; 23.57 E) of the period 1951-2000. (significance level: * <0.1, ** <0.05)

	Spring	Summer	Autumn	Winter	Year
Temperature (°C)	1.44**	-0.24	-0.39	1.48	0.41
Precipitation (mm)	31.36	-37.07	33.79	-21.85	5.21

According to simulation results of a multi-model ensemble of GCM (Van der Linden and Mitchell., 2009) the temperature will raise until the end of the 21st century about 3°C and precipitation will increase about 3% in Western Ukraine (Table 2). Lower precipitation amounts are simulated for the summer and higher for the winter. From this figures one can expect shifts in the seasonal water balance. Especially critical are the warmer and dryer summer that can result in water stress for plants.

Table 2. Projected changes in seasonal mean surface temperature and precipitation for the period 1971-2100 in comparison to 1961-1990 (SRES A1B) for western Ukraine.

	Spring	Summer	Autumn	Winter	Year
Temperature (°C)	+2.5	+3	+3	+4	+3
Precipitation (%)	+6	-15	+5	+15	+3

Water balance was modelled for the period 1963-1993. Areal precipitation is around 700 mm. Together with the modelled evapotranspiration it had a slight decreasing tendency in the simulated period (Figure 1). Evapotranspiration should theoretically be positively correlated to precipitation, radiation, wind and temperature. Therefore decreasing evapotranspiration rates can not be explained by observed temperature (increasing trend), not by radiation (no trend) and not by wind speed (positive trend). Precipitation is the factor with most influence on evapotranspiration in the region. On average 70% of the precipitation is utilised by evapotranspiration.

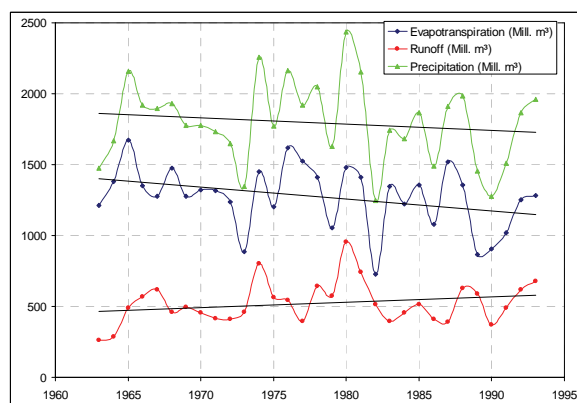


Figure 1. Areal precipitation, runoff and evapotranspiration of the catchment Western Bug/ Kamianka Buzka.

Up to now we did not model the future water budget of the catchment. Until the conference presentation results will exist.

The uncertainties of data used for modelling were high. The low density of meteorological stations does not guarantee an adequate input, especially of precipitation and radiation. Also soil information was limited. Heterogeneity and variability of soils in the region could not be reproduced adequately using the soil map 1:200.000. No details of the plant cover, like root depth or LAI, were known. Therefore we applied default datasets for the vegetation.

4. Outlook

On major aspect for future work is the improvement of input data quality. Soil data can be improved using a soil map in the scale 1:10.000. Parameters have to be estimated on the basis of the existing map metadata and of measurements that took and will take place in the next months.

SWAT uses as climatological input the station that is closest to the centre of area of the hydrological response unit. Because station density is low, an approach will be tested to regionalise the climatological elements (using secondary information as e.g. DEM). The aim is to improve areal estimates of the climatic variables.

Land-use was considered as static for the modelling period. Classification of further satellite images and examination of

past topographic maps will allow a more dynamic approach. Currently images for the time steps 2000 (Landsat-7 ETM) and 2009 (SPOT-5 resp. RapidEye) are analysed for change detection. To specify the land-cover data regarding their interference with the regional climate and water balance, a more comprehensive land-use model is under preparation. The time horizon of future climate change needs also the consideration of land-use change. Thus land-use scenarios are planned for the ongoing work. Consistency of both climate change and land-use change will be ensured by a common methodology for scenario planning (Luther and Schanze, 2009).

Within the scope of this work we considered only one possible climate scenario of one GCM. We intent to expand our simulation using other scenarios. Furthermore, the results of the regional climate model CCLM of the western Ukraine that is set up at the Technische Universität Dresden can be used in a few months to simulated climate changes in more detail.

References

- Alexandersson H (1986) A homogeneity test applied to precipitation data, *Journal of Climatology*, 6, pp. 661-675
- Franke J, Goldberg V, Eichelmann U, Freydank E, Bernhofer C (2004) Statistical Analysis of Regional Climate Trends in Saxony, Germany, *Climate Research* 27, pp.145-150
- Luther J, Schanze J (2009) Exploring and evaluating futures of riverine flood risk systems - the example of the Elbe River. In: Samuels P et al. (eds.) *Flood Risk Management - Research and Practice*. Taylor & Francis, London, pp. 1753-1763
- Van der Linden P and Mitchell JFB (eds) (2009) *ENSEMBLES: Climate change and its impacts: Summary of research and results from the ENSEMBLES project*. Met Office Hadley Centre, UK, 160 pp.

Comparison of the sea surface temperatures and sea ice concentration from ERA-Interim and BSH

Thomas Raub¹, Thomas Cesko², Klaus Getzlaff², Andreas Lehmann² and Daniela Jacob¹

¹ Max Planck Institute for Meteorology, Hamburg, Germany (thomas.raub@zmaw.de)

² Leibniz Institute of Marine Science (IFM-GEOMAR), Kiel, Germany

1. Introduction

Reanalysis data play an important role for regional climate models. They are used as boundary conditions to force regional atmospheric and oceanic models with a higher spatial resolution. The results can be compared with other observations to validate the performance of the model.

The sea surface temperatures (SST) and the sea ice concentrations (SIC) are the lower boundary conditions for an atmospheric model over water surfaces and determine the fluxes of sensible and latent heat between the atmosphere and the ocean.

We have compared the sea surface temperatures and the sea ice concentrations from the ERA-Interim Reanalysis of the Baltic Sea with data from the German Federal Maritime and Hydrographic Agency Hamburg (BSH) for the period from 1990 to 2008.

2. Description of the data sets and method of comparison

The lower boundary conditions of ERA-Interim are taken from the ERA-40 project until 2001 and the operational data from the ECMWF afterward. A detailed description can be found in Fiorino (2004). The SST's are based on two different global data sets from NCEP. For the period until June 2001 the weekly NCEP 2DVAR data with a resolution of 1° is used. This data set is a reanalysis of observations from the Advanced Very High Resolution Radiometer (AVHRR) of the National Oceanic and Atmospheric Administration (NOAA) weather satellites and in-situ observations from buoys and ships. The 2D variational analysis also includes a climatology. From July 2001 on the SST's are based on the daily NCEP optimal interpolation analysis (OISSTv2) with a resolution of 0.5° that uses a different bias correction algorithm as described in Thiébaux et al. (2003).

The data set from the BSH is also a product derived from the AVHRR satellite measurements, without any additional observations. The data are available as weekly means at a resolution of 1.2 km.

We performed a bilinear interpolation of the ERA-Interim data to the BSH grid and compared the monthly means of the two data sets.

3. Results and discussion

The comparison exhibits quite large differences between the SST's of ERA-Interim and BSH. The mean differences for the four seasons are shown in figure 1. Due to the coarse resolution of ERA-Interim the largest deviations are situated close to the coast. However, we also found significant differences over the whole basin.

The seasonal cycle of the ERA-Interim SST's is on the average weaker than that of the temperatures of the BSH as can be seen in figure 2.

From about 2002 on we found a better agreement between the two data sets. This can be explained by the change from the NCEP 2DVAR data set to OISSTv2.

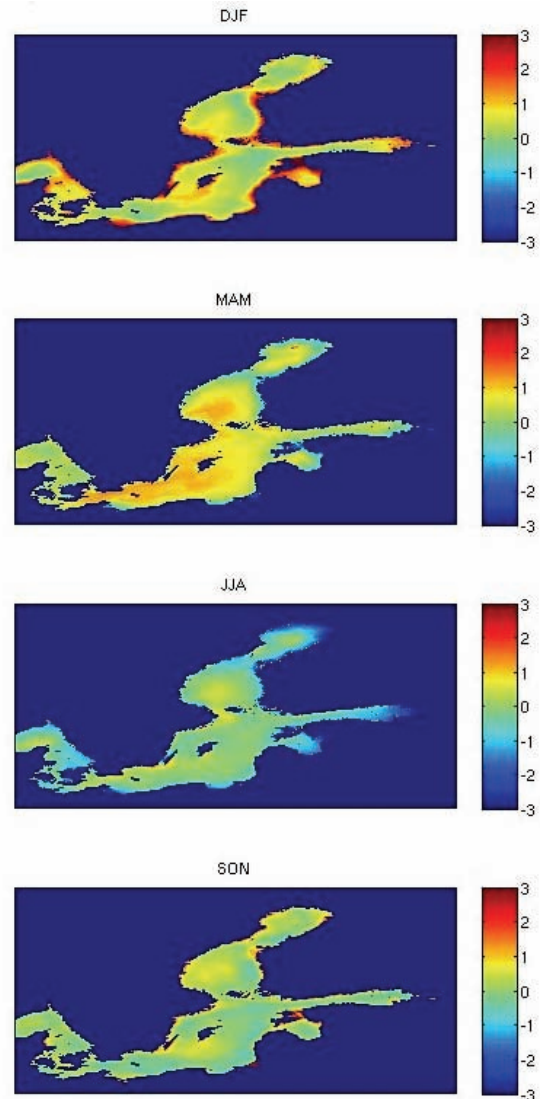


Figure 1. Differences of the SST's of the Baltic Sea from ERA-Interim and BSH for the years 1990 until 2008 for the four seasons.

We will also present a comparison of the sea-ice concentrations.

4. Conclusion

Our study has shown that the lower boundary conditions from global reanalysis data do not necessarily represent the local features when they are used as forcing of regional climate models. The reasons are the usually relatively coarse resolution and also the algorithms used to preprocess the input data, which may not be suitable for the smaller scales.

For ERA-Interim we found that the SST's of the Baltic Sea differ quite strongly from a data set of the BSH, at

least for the period until 2001. One cannot expect very realistic results when the forcing is used for uncoupled regional climate simulations in the Baltic region, especially for the SIC due to the generally too warm SST's in winter.

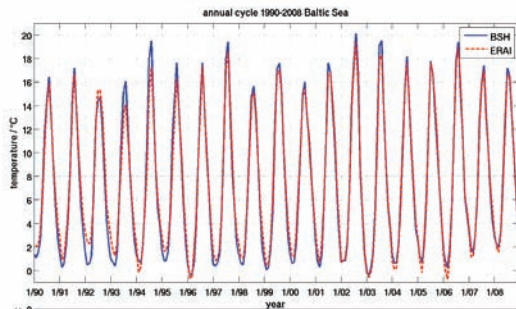


Figure 2. Time averaged monthly means of the sea surface temperatures of the Baltic Sea

References

- Fiorino, M. (2004), A Multi-decadal daily sea surface temperature and sea ice concentration data set for the ECMWF ERA-40 Reanalysis. ERA-40 Project Report Series No. 12, ECMWF.
- Grumbine, R.W., (1996), Automated passive microwave sea-ice concentration analysis at NCEP, NOAA NCEP Tech Note 120, 13 pp
- Lehmann, A., Tschersich, G. (2006), Trends in sea surface temperature of the Baltic Sea since 1990, BALTEX Newsletter, No. 9, pp. 7-9.
- Siegel, H., Gerth, M., Tschersich, G. (2006), Sea surface temperature development of the Baltic Sea in the period 1990-2004, *Oceanologia*, 48, pp. 119-131.
- Thiébaux, J., Rogers, E., Wang, W., Katz, B. (2003), A new high-resolution blended real-time global sea surface temperature analysis, *Bulletin of the American Meteorological Society*, vol. 84, Issue 5, pp. 645-656.

Estimating the impact of potential climate change in the 21st century on the Baltic Sea ecosystem

V. Ryabchenko¹, L. Karlin², I. Neelov¹, T. Eremina², O. Savchuk³, R. Vankevich² and A. Isaev²

¹ St.Petersburg Branch, P.P. Shirshov Institute of Oceanology, Russia (vladimir_ryabchenko@VR5841.spb.edu)

² Russian State Hydrometeorological University, St.Petersburg, Russia

³ Baltic Nest Institute, Resilience Centre, Stockholm University, Sweden

1. Introduction

The purpose of this study is to estimate the changes in the basic non-biotic and biotic components of the Baltic Sea ecosystem in the coming 100 years which are due to scenarios of climate change in the 21st century. The estimation is based upon a recent version of St. Petersburg Baltic Eutrophication Model (SPBEM) and scenarios of climate change for the Baltic Sea region.

2. The coupled hydrodynamic-ecosystem model

SPBEM includes the 3D hydrodynamic ocean-sea ice module of Neelov et al. (2003) and the biogeochemical cycles (BGC) module of Savchuk (2002). The BGC module describes nutrient cycling in the coupled pelagic and sediment sub-systems and contains 12 pelagic (zooplankton, diatoms, cyanobacteria, flagellates, nitrogen, phosphorus and silica detritus, ammonium, nitrite + nitrate, phosphate, silicate and dissolved oxygen) and 3 sediment (benthic nitrogen, phosphorus and silica) state variables. The current model version has a horizontal resolution of 2 nm, and 78 levels of thickness of 2m in the upper 30-meters and of 6m below.

3. Set-up of simulations

Climate changes in the Baltic Sea region (53-68° N, 8-32° E) in 2001-2099 were estimated as slices of global forecasts for the region. The forecasts were obtained using general atmosphere-ocean circulation models which participated in the climate model inter-comparison project CMIP3. These regional slices of global model solutions were obtained for runs performed in accordance with scenario A2 (maximal CO₂ emission) and scenario B1 (minimal CO₂ emission). Here we consider the results of a run with the SPBEM using the forecast of atmospheric meteorological forcing of model ECHAM5/MPI-OM for scenario A2 which demonstrates the maximal near-surface air temperature increase in the Baltic Sea region. Initial distributions of physical and biogeochemical fields in the Baltic Sea were constructed from the data available in the Baltic Environmental Database (<http://data.ecology.su.se/Models/bed>) for 3 wintertime months (January – March) of 3 consecutive years (1998-2001). Riverine discharges and nutrient land loads were prescribed as mean monthly values obtained by averaging throughout the period of 1996-2000. They remained the same during the whole period considered.

4. Results

According to results, the water temperature in the Baltic Sea will increase in the 21st century in such way that the clearly expressed thermal stratification of the sea - excluding only a thin seasonal thermocline - will disappear after 2045 and an intensive heating of the whole water column will start. The low temperatures below the thermocline in the Bornholm Deep and Gotland Deep where the cold North Sea water

occasionally penetrates in will exist longer than in other parts of the sea. By the end of the 21st century, the sea surface temperature growth in the central Baltic Sea will be about 2 °C in the Bornholm Deep and almost 3 °C in the Gotland Deep regions (Fig.1). The changes in salinity of the Baltic Sea will be small so that the vertical salinity stratification will be practically the same during the whole century.

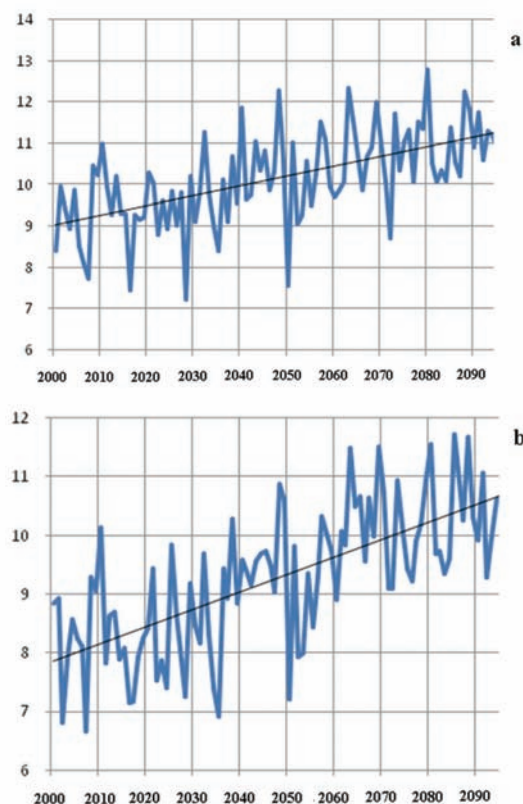


Figure 1. Mean annual water temperature (°C) at the sea surface over the Bornholm Deep(a) and Gotland Deep (b) in 2001-2099.

The future changes in dissolved oxygen, phosphate and nitrate show that there is an alternation of stagnation periods (when hypoxic conditions, increased phosphate concentration and lowered nitrate concentrations are typical) and ventilation periods (when - as a result of the advective transport of cold North Sea water - near-bottom oxygen and nitrite concentration increase and phosphate concentration decreases).

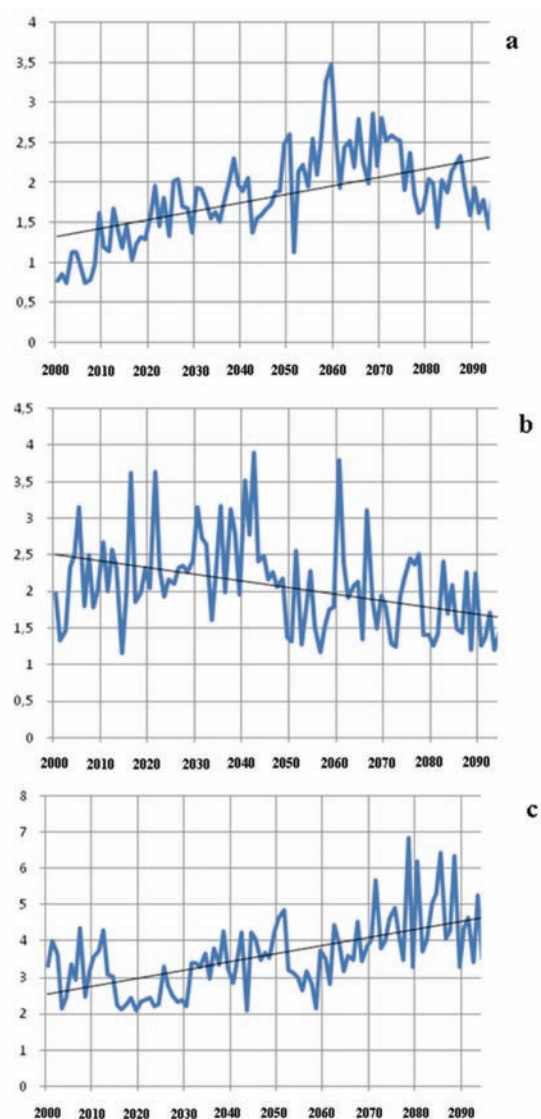


Figure 2. Mean annual, area-averaged primary production ($\text{gN}\cdot\text{m}^{-2}\cdot\text{y}^{-1}$) of blue-green algae (a), diatoms (b) and flagellates (c) in the euphotic layer of the Baltic Sea in 2001-2099.

According to model results, the longest stagnation period (about 8 years) will be after 2050. Different algae will respond in different ways to temperature increase in the upper (euphotic) sea layer. The primary production of flagellates will grow during the whole century (Fig.2c); the growth of production of green-blue algae in the first half of the 21st century will be changed by its lowering in the second half of this century (Fig. 2a). The production of diatoms (Fig. 2b) will drop, which could be explained by the increase in water temperature limiting the growth of spring cryophile diatoms.

References

- Neelov I.A., T.A. Eremina, A.V. Isaev, V.A. Ryabchenko, O.P. Savchuk, Vankevich R.E. 2003. A simulation of the Gulf of Finland ecosystem with 3-D model. Proceedings Estonian Academy of Science. Biology. Ecology 52: 347-359.

Savchuk O.P. 2002. Nutrient biogeochemical cycles in the Gulf of Riga: scaling up field studies with a mathematical model. *J. Mar. Syst.* 32: 253-280.

On regime shift in the general atmospheric circulation over the Baltic Sea region in winter

Mait Sepp

Department of Geography, University of Tartu, Estonia (mait.sepp@ut.ee)

1. Introduction

There are several methods for analyzing the effects of climatic changes on general atmospheric circulation. One of the possibilities is to study the periodic changes in the atmospheric processes. By the tradition of the synoptic climatology boards, the cyclic changes in the frequency of circulation types are of paramount importance. In Leningrad, Vangengeim and later Girs developed their long term forecast methods on the so-called epochs, during which certain circulation types would dominate for a decade (Girs 1971). In determining the epochs, the critical question is when one epoch or its stage ends and another one begins. According to Vangengeim and Girs (Girs 1971), such changes take place quite rapidly – the frequency of one circulation type (or group of circulation types) increases, while the frequency of others (e.g. meridional circulation types) decreases. A rapid change or a shift in regime follows.

The aim of the present research is to study whether the possible regime shifts are also visible in the atmospheric circulation classifications of the catalogue 1.2 of COST 733. It also studies when and in which classifications and directions these changes have taken place in connection with which circulation types. The present study concentrates on possible changes in winter, as climate change over the Baltic Sea Region is most prominent in cold season.

2. Data and methods

The analyzed data were about the 73 circulation classification type frequencies for the Baltic Sea region (domain 05 by COST 733), given in catalogue 1.2 of COST 733 (Huth et al. 2008). The appearance of different types (altogether 1370 circulation types) in winter (DJF) was studied. Classifications presented in the catalogue are generated using SLP data obtained from ERA40. Accordingly, the analysed period is 1958-2002.

For determining the regime shift, the software developed by S. N. Rodionov from the Washington University, was used (Rodionov 2004, Rodionov and Overland 2005). The method is based on the sequential application of the Student's t-test. The developed macro is very user-friendly. The researcher can select the cut of length – the length of the period that undergoes the t-test and that is drawn over the study time-series to find the place where a statistically reliable shift is taking place. To harmonize the effect of extreme values, their weight can be decreased by selecting Huber's Weight Parameter. In addition, this tool allows the detection of red noise by three different methods and to perform the pre-whitening of time series. The shifts can be studied in either mean or variance values.

In the first stage of the data analysis, the different possibilities of the method and the effects of the selected variables on the data analysis were acquainted with according to the suggestions of (Rodionov 2004, Rodionov & Overland 2005). It was discovered that the most rational course of action was to select the software's default settings: to analyze the shifts in mean values, whereas the target significance level was 0.1, the cut-off length was 10, and the

Huber's weight parameter was 1. The effect of red noise was not analyzed and the pre-whitening was not performed.

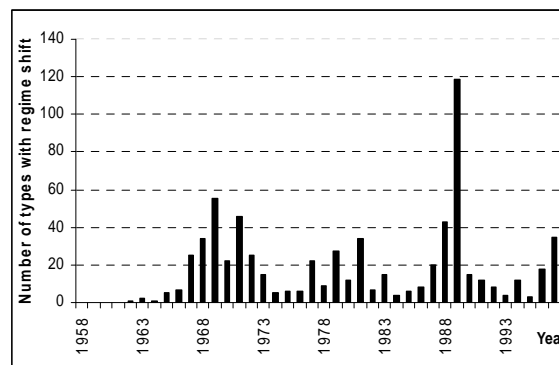


Figure 1. The number of circulation types in which significant regime shifts in frequency have occurred in the winter. Years 1998-2002 are excluded.

3. Results

The analysis of the individual circulation type winter sums shows that most regime shifts took place between the years 1998-2002. These changes are probably artificial and those should be regarded as a distinctive feature of the method that has also been noted by Rodionov. But if we were to leave the data of the four final years aside, most regime shifts in circulation type time series occurred in 1989, as shown on Figure 1. The second relatively highest peak occurred in 1969 but hereinafter the 1989 year is studied in details.

There were 119 such circulation types that have a regime shift in 1989, 59 of which had a negative and 60 had a positive shift. In only 9 classifications (HBGWL, HBGWT, OGWL, PERRET, TPCA07, TPCAC09, TPCAV, WLKC28, and WLKC733) no such shifts occurred.

Next, the question was studied whether the types with positive (negative) shifts were comparable. To do that, the time series with positive (negative) shifts were made to correlate with each other. This showed that in general, the correlation of the type frequencies were positive and very strong (at the level of the statistical significance of $p < 0.01$), which gives reason to assume that these types illustrate similar processes.

Based on the composite plots of MSLP of the circulation types' by COST 733 catalogue, we can conclude that for the regime shift in 1989, there was a decrease in the frequency of three types of circulation: a) those that have a high pressure area in the northern or north-eastern part of the domain; b) those that have a high pressure area in the eastern part of the domain and/or a low pressure area in the western part of the domain; c) those that have a low pressure area in the central part of the domain.

If the types that belong to the first class prevail, there are anticyclonic conditions in the Baltic Sea region. In the winter season, this means radiative cooling and the inflow of cold air masses from the east or south-east.

The decrease in southern inflow means that there is a lower frequency of the types that carry strong snowfalls in the winter.

Those circulation types that have a low pressure area in the central or northern part of the domain, can be related to the cyclones that move from west to east in the southern part of the domain and that also bring along strong snowfalls in the Baltic Sea region.

In the case of the types with a positive shift, it is also visible that almost all those types are related to a western flow. The types are somewhat different according to where the relative centre of the low pressure area lies – is it due east or west. In the case of some types in the type chart, there dominates a strong high pressure area in the southern or south-western part of the domain, but in the Baltic Sea region, the western flow prevails. This, however, means an inflow of relatively warmer air masses from the ocean in winter.

4. Conclusions

A clear regime shift in the frequency of circulation types in the winter occurred in 1989. Due to the fact that the climatic changes in the Baltic Sea region are most clearly visible in the winter, it was more thoroughly studied which circulation types changed over the regime shift of 1989. During the analysis, it was found that the shift (either positive or negative) had been undergone by the similar types of different classification. Thus, the types related to very cold winters have decreased – these are the types that bring along anticyclonic conditions in the Baltic Sea region with the inflow of cold air from the east or south-east, and the types that bring along heavy snowfall. There has been a positive shift in the types that in winter bring along relatively warmer air masses from above the ocean.

References

- Girs, A.A. (1971) *Mnogoletnije kolebanija atmosfernoj cirkuljacii i dolgosročnyje gidrometeorologičeskije prognozy*. Gidrometeoizdat, Leningrad. (Interannual variations of atmospheric circulation and long-term hydrometeorological forecasts)
- Huth, R., Beck, C., Philipp, A., Demuzere, M., Ustrnul, Z., Cahynová, M., Kyselý, J. and Tveito, O. E. (2008), *Classifications of Atmospheric Circulation Patterns. Recent Advances and Applications*. *Annals of the New York Academy of Sciences*, 1146, pp105-152
- Rodionov, S.N. (2004) A sequential algorithm for testing climate regime shifts. *Geophysical Research Letters*, Vol. 31, L09204, Doi:10.1029/2004gl019448.
- Rodionov, S. and Overland, J. E. (2005): Application of a sequential regime shift detection method to the Bering Sea ecosystem, *ICES J. Mar. Sci.*, Vol. 62, pp. 328–332.

Changes in some elements of the water cycle in the Baltic Sea areas of the former Soviet Union

Nina A. Speranskaya¹

¹ State Hydrological Institute, St. Petersburg, Russia (speran@mail.rcom.ru)

1. Introduction and data

Soil moisture and evaporation are the most important elements of the land water cycle. Soil moisture characterizes water amount that accumulates within the active (1 meter) soil layer, and pan evaporation can be accepted as potential evaporation value. Pan evaporation and soil moisture observations in the USSR began in the middle of 1950s. From 1990s the number of stations was significantly reduced, and at present data from only 14 stations with soil moisture observations and 15 stations with pan evaporations can be used for analysis. Additionally, data from 86 stations with precipitation were used for the present analysis of visible evaporation.

2. Soil moisture

Within the study region, a soil moisture increase is observed during the whole growing period (May-August) and in autumn (September-November) from the 1950s to 2000 (2001). Moreover, changes during autumn are most evident, while in spring (April-May) systematic changes are negligibly small.

3. Evaporation

Systematic changes in pan and visible evaporation from the 1950s to 2008 within the study region are very small. Only in the southeast of the region some moistening of the territory is noted.

References

- Golubev, V.S., Lawrimore, J., Groisman, P.Ya., Speranskaya, N.A., Zhuravin, S.A., Menne, M.J., Peterson, T.C., and Malone, R.W. (2001) Evaporation changes over the contiguous United States and the former USSR: A reassessment *Geophys. Res. Lett.*, **28**, 2665-2668.
- Speranskaya, N.A. (2009) Soil moisture changes in non-boreal European Russia: In situ data, pp.151-160. In: Groisman P.Ya. and S.V. Ivanov, eds. (2009) *Regional Aspects of Climate-Terrestrial-Hydrologic Interactions in Non-boreal Eastern Europe*. Springer, Amsterdam, The Netherlands, 251 pp.
- Speranskaya, N.A. (2010) Soil moisture changes in the Russian Federation: in situ data. *Environ. Res. Lett.*, **4**, No.4, in review.

Interference of climate change, geosphere and anthroposphere – A new focus of the Szczecin science community

Andrzej Witkowski^{1*}, Jacek Batóg¹, Ryszard K. Borówka¹, Kazimierz Furmańczyk¹,
Jan Harff¹, Maciej Kowalewski¹, Przemysław Krajewski¹, Roman Marks¹, Stanisław
Musielak¹, Marian Rębkowski¹, Hans von Storch²

¹ University of Szczecin, Poland (Witkowsk@univ.szczecin.pl)

² GKSS Research Centre Geesthacht, Germany

It is widely accepted that spatial downscaling of global processes to the regional scale is needed to understand the general climate system through the functioning of its regional components. For this understanding, key areas play a crucial role as zones of transition for high gradients of measurable meteorological, geological and socioeconomic parameters. The southern Baltic area can be regarded a key region in this sense as it covers the border between two major tectonic units – the Eastern and the Western European platform; it serves as transit areas for air masses driven by the deep pressure systems of the Northern Atlantic from the West and the Eurasian high pressures systems from the East. It also represents an important ecological gradient of the southern Baltic Sea coast as a transition from terrestrial to marine ecosystems. In terms of socioeconomics, the area is mainly characterized by gradients between eastern and western Europe, historically and still in the recent development. To answer the complex questions of climate dynamics of the southern Baltic basin, interdisciplinary and international research networks are required. The location of Szczecin at the German/Polish border and in the centre of the historical region of Pomerania qualifies the site from the logistical and cultural point of view to host a cross-bordering European centre of sciences. As a first step in order to establish this centre in 2009, the University of Szczecin hosted an international conference on “Climate Change – the socio-economic response in the southern Baltic region” (Witkowski et al. 2009). During that conference, scientists from countries around the Baltic Sea reported about significant correlations between changing climate and the natural and socioeconomic systems under investigation. In order to explain this correlation by cause-effect relations, a more intensive interdisciplinary cooperation between geoscientists, archaeologist, sociologists, economists and climate researchers is needed. As a direct result of the conference in Szczecin, a group of scientists established an interdisciplinary research group at the University, dealing with cause-effect relation of the dynamics of climate, terrestrial and marine ecosystems and socio-economic systems. It is planned to develop with regular interdisciplinary seminars the scientific environment for the establishment of an inter-institutional climate research centre focusing on three main topics:

- Marine, terrestrial and paleo-climate change,
- Climate related coastal dynamics,
- Climate and anthroposphere.

In the first stage, the institutes will collaborate based on a joint research program using existing resources. Secondly, personal and technical resources shall be upgraded by national and international funding in order to guarantee outstanding results in terms of innovative concepts and high qualitative experimental and

monitoring data. The interdisciplinary exchange of ideas, concepts and data will be realized by a program that networks projects and disciplinary units in a matrix-like structure. Modelling procedures will serve for the space/time assignment of research results. The competence for the application of modern climate model concepts has to be developed at Szczecin.

International co-operation shall help to develop this competence. The cooperation with related research groups within the Baltic area and beyond is one of the prerequisites of a successful establishment of the research centre at Szczecin. On the local level, the centre shall cooperate with local authorities and agencies in order to get spin-offs results for the direct practical use.

Reference

- Witkowski, A., Harff, J., Isemer, H.-J. (eds.) (2009): International Conference on Climate Change – The socio-economic response in the southern Baltic region. University of Szczecin, Poland, 25-28 May 2009 – Conference Proceedings - Int. BALTEX Secr. Publ. No. 42, 140 p.

Holocene coastal morphogenesis at the southern Baltic Sea: An interplay of climate forcing and the geological environment – A case study of the Darss-Zingst Peninsula

Wenyan Zhang¹, Jan Harff², Ralf Schneider³ and Eduardo Zorita⁴

¹ Center for Coastal Ocean Science and Technology Research, Zhongshan University, Guangzhou, China (wzhang@ipp.mpg.de)

² University of Szczecin, Poland / Leibniz-Institute for Baltic Sea Research, Warnemuende, Germany

³ Institute of Physics, Ernst-Moritz-Arndt University, Greifswald, Germany

⁴ GKSS Research Centre, Geesthacht, Germany

1. Introduction

A modeling methodology for simulation of centennial-to-millennial-scale (long-term hereafter) morphological evolution of the wave-dominated coastal environment in the southern Baltic Sea is developed. The methodology consists of two main components: (1) an analysis of the key processes driving the morphological evolution of the study area based on statistical analysis of wind data and sensitivity studies and (2) a multi-scale high-resolution process-based model.

The methodology is used to hindcast the Holocene evolution of the Darss-Zingst peninsula as well as to project its future based on different climate scenarios. The Darss-Zingst peninsula at the southern Baltic Sea is a typical wave-dominated barrier island system which includes an outer barrier island and an inner lagoon. The formation of the Darss-Zingst peninsula is traced back to the Littorina Transgression onset about 8000 cal. y BP. It originated from several discrete islands, has been reshaped by littoral currents, wind-induced waves and aeolian transport during the last 8000 years, and evolved into a complex barrier island system as today. Thus it may serve as an example to study the coastal evolution under long-term climate change.

2. Wind analysis

Boundary input conditions for a long-term morphodynamic model such as time series of tides, winds, waves and mass fluxes are not possible to be specified at a centennial or millennial time span due to the lack of measurement. Representative input conditions, which are extracted from the measured time series by means of statistical analysis, provide an effective way for the solution of the input problem for the long-term model (de Vriend et al. 1993). The representative input conditions should be able to reflect the spectrum of the real natural conditions and produce similar results to the reality.

A successful example for applying the representative wind series to a simulation of the centennial morphological evolution of the Darss-Zingst peninsula is given in Zhang et al. (submitted a, b). High-resolution hindcasted wind series covering the southern Baltic Sea for a 50 years' period (1958-2007, provided by Weisse, GKSS-Research Centre Geesthacht) were analyzed to generate the representative time series for the model to hindcast the morphological evolution of the Darss-Zingst peninsula from 1696 to 2000. Based on the validated modeling methodology on a centennial-scale simulation, the daily-averaged paleo-wind data covering the Baltic Sea from 7000 cal. y BP to 2000 AD is analyzed to generate the representative wind series for the model to simulate the Holocene morphological evolution of the Darss-Zingst peninsula. The paleo-wind data set is derived from a hindcast of the ECHO-G model in which the global climate change from 7000 cal. y BP to present was

simulated (Huenicke et al. submitted). The last 7000 years are divided into 7 periods, each with a millennium. Statistical analysis of the paleo-wind data indicates a high similarity in every millennium interval except trends for increasing wind speed in the summer season and a decreasing trend of the easterly wind components. Representative wind series are generated for the 7 periods, respectively. Four seasonal wind classes (Figure 1), each with a predominant distribution of wind direction and speed, are derived from statistical analysis for each representative series. The Weibull distribution function is used to analyze the wind strength of each class. The Weibull distributed random number generator is used to generate the representative wind series based on the Weibull parameters of each class. Trend terms of the wind speeds within each series are analyzed by linear best-fit functions of the centennial Weibull parameters. Auto-correlation coefficients are calculated to obtain the cyclical terms of the wind series. Extreme value theory is applied to calculate the return periods of storms. The generated wind series (including the representative storms) are further calibrated by sensitivity studies.

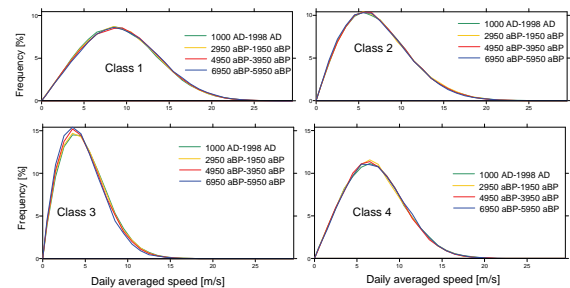


Figure 1. Weibull distributions of the wind speeds for different periods.

3. A multi-scale process-based model

A multi-scale process-based model is constructed for simulation of long-term morphological evolution of the wave-dominated coastal environment. The process-based model is structured into 9 main modules. The 2DH current module, the wave module, the bottom boundary layer module, the sediment transport module, the aeolian sand transport module, the cliff erosion module and the nearshore storm module are real-time calculation modules which aim at solving the short-term processes. A bathymetry update module and a long-term control function set, in which the 'reduction' concepts and technique for morphological update acceleration are implemented, are integrated to extrapolate the effects of short-term processes to a longer-term scale. The 9 modules are nested, with output from one serving as input

for another. Three coupled grid systems are designed to incorporate all important processes relevant to coastal morphological evolution and calculation of these processes at their corresponding scales (Zhang et al. submitted c).

4. Model application

Based on a reconstructed Digital Elevation Model for 8000 cal. yr BP (courtesy of M. Naumann, Hannover and M. Meyer, Rostock), a sea level curve (Lampe 2008), the neotectonic pattern based on a study of Rosentau et al. (2007) and Harff and Meyer (in press), and the representative paleo-wind series, the formation and evolution of the Darss-Zingst peninsula during the last 7000 years is hindcasted by the model. A series of sensitivity runs are carried out to study the influence of different parameterizations of boundary conditions on the long-term morphological evolution of the Darss-Zingst peninsula and to tune the boundary input such as wind series and rate of sea level change in a reasonable range. Selected results obtained from the model are shown in Figure 2. Although the differences between the simulation results and the paleo-coastlines have to be taken into account, the general formation and evolution process of the Darss-Zingst peninsula is reflected in the model results.

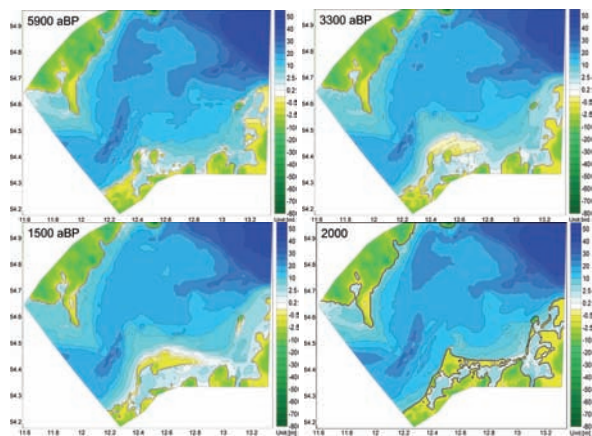


Figure 2. Simulated morphological evolution of the Darss-Zingst peninsula (5900 cal. y BP, 3300 cal. y BP, 1500 cal. y BP) and – for comparison – the recent Digital Elevation Model for 2000 AD.

5. Result analysis

Simulation results indicate that the millennial-scale morphological evolution of the barrier island system is a combination of long-term effects of climate change, tectonic movement, wave dynamics and aeolian transport. The sea level has reached a stable level with minor fluctuations of a few meters since about 6000 cal. y BP. The rate of sea level change is generally between -1 mm/yr and 1 mm/yr in the southern Baltic Sea in the last 4000 years (Lampe 2005), which is in the same magnitude as neotectonic movements in this area (Harff and Meyer, in press). Along with the moderately changing sea level and neotectonic conditions, other processes such as climate change, hydrodynamics and sediment transport have become increasingly important for the coastline evolution. The formation of the barrier island starts from the development of the sand spit at the tip of the discrete islands due to abundant sediment supply transported by the dominant westerly wind-induced longshore currents. The aeolian transport plays a key role in directing the development of the new barrier and maintaining the land by redistributing the sands on the land and building the sand

dunes which help to protect the barrier from the erosion of wind storms. Several critical factors such as substrate gradient, sediment supply and control nodes for the formation and evolution of the barrier island are also revealed. The formation of the barrier island needs to fulfill two important conditions: a mild substrate gradient and sufficient sediment supply. The relatively high-altitude parts of the island such as cliffs and dunes act as nodes controlling the direction of the barrier growth. The formation of the headland is an effect of balance between the dominated westerly winds and the strong easterly wind storms. Model results also indicate that the rates of Holocene coastline change are relatively low compared to recent rates. This implies the accelerated sea level rise as an important climate factor influencing the coastline evolution in the recent centuries and the future.

References

- de Vriend, H.J., Copabianco, M., Chesher, T., De Swart, H.E., Latteux, B., Stive, M.J.F. (1993 a) Long term modelling of coastal Morphology, *Coastal Eng.*, 21, 225-269
- Harff, J., Meyer, M. (in press) Changing Holocene coastal zones of the Baltic Sea – a modelling approach. In: Harff, J., Lüth, F. (Eds.) (in press), *Sinking Coasts–Geosphere, Ecosphere and Anthroposphere of the Holocene Southern Baltic Sea*. Berichte der Romische Germanischen Kommission (RGK)
- Huenicke, B., Zorita, E., Haeseler, S. (submitted) Holocene climate simulations for the Baltic Sea region – application for sea level and verification of proxy data. Berichte der Romische Germanischen Kommission (RGK)
- Lampe, R. (2005) Lateglacial and Holocene water-level variations along the NE German Baltic Sea coast: review and new results. *Quaternary International*, 133-134, p. 121-136
- Rosentau, A., Meyer, M., Harff, J., Djetchich, R., Richter, A. (2007) Relative Sea Level Change in the Baltic Sea since the Littorina Transgression, *Z. geol.Wiss.*, vol. 35, no. 1/2, p. 3-16
- Zhang, W.Y., Harff, J., Schneider, R., Wu, C.Y. (submitted a) A multi-scale centennial morphodynamic model for the southern Baltic coast, *Journal of Coastal Research*
- Zhang, W.Y., Harff, J., Schneider, R., Wu, C.Y. (submitted b) Statistical analysis of wind data in the southern Baltic Sea and influence of different climate scenarios on the coastline change, *Climate Research*
- Zhang, W.Y., Harff, J., Schneider, R., Wu, C.Y. (submitted c) Development of a modeling methodology for simulation of long-term morphological evolution of the southern Baltic coast, *Ocean Dynamics*

Is the Baltic sea-level change accelerating?

Eduardo Zorita and Birgit Hünicke

Institute for Coastal Research, GKSS Research Centre, Max-Planck-Str.1, 21502 Geesthacht, Germany.
(eduardo.zorita@gkss.de)

1. Background

As a consequence of increasing concentrations of greenhouse gases in the atmosphere, the global rate of sea-level rise is expected to accelerate in the future. Some studies indicate that this acceleration has already been detected in the 20th century record of global sea-level rise (Merrifield and Merrifield, 2009) while others do not detect a significant change (Holgate 2007). For regional planning agencies more important than the global number is, however, the change in the rate at regional scales.

The Baltic Sea is a region strongly influenced by isostatic rebound from the last deglaciation, with the Earth crust in the Northern Baltic rising at roughly 10 mm/year and in parts of the Southern Baltic sinking at about 1 mm/year (Ekman 1996, Rosentau et al. 2007). Time series of sea-level measured by coastal gauges thus display strong linear trends due to isostasy. The values of these trends form the basis for sea-level rise projections related to coastal protection, with a rough estimate of possible sea-level rise caused by climate change added to the isostatic trends.

In this contribution we analyse long Baltic sea-level time series with the aim to identify accelerations indicative of a climatic contribution to Baltic Sea-level rise and thus help refine the estimations of Baltic Sea level rise in the future.

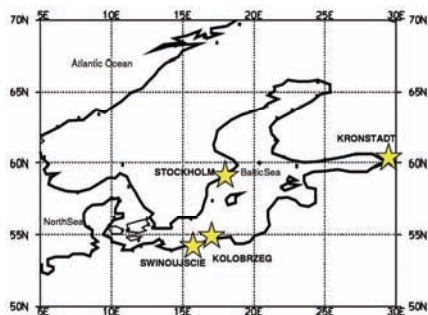


Figure 1. Sketch of the Baltic Sea, showing the location of the sea-level gauges used in this study.

2. Data

Following Hünicke et al. (2008) annual means of four of the longest time series of sea level records (up to 200 years long) from stations situated in the central, eastern and southern Baltic Coast have been examined: Swinoujscie (Permanent Service for Mean Sea level [PSMSL]¹), Kolobrzeg (PSMSL; before 1951 provided by TU Dresden), Stockholm (Ekman 2003) and Kronstadt (Bogdanov et al., 2000).

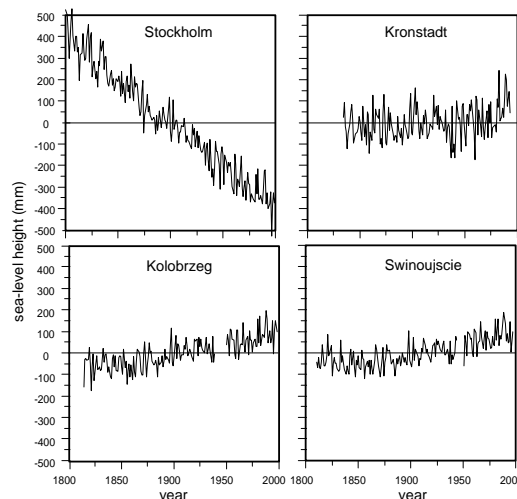


Figure 2. Sea level time-series.

In addition, satellite data from the Topex-Poseidon and Jason missions covering about the last three decades have been also included in the analysis. As these records have a monthly resolution, possible differences in the seasonal rates of sea-level change have been also considered.

3. Methods

Different statistical methods have been applied to identify changes in the rate of change. One method is based on the estimation of multidecadal linear trends, followed by the estimation of temporal changes in these trends. Another method attempts to fit the sea-level records to a linear and a quadratic, instead of only linear, trend over the whole observed period. As the possible acceleration signal is small, and the overall linear trend is heavily contaminated by the influence of isostatic adjustment, great care has to be put on the estimation of uncertainty ranges.

Furthermore, spatial discrepancies in the estimated accelerations should be explained by the presence of additional climate factors, such as the North Atlantic Oscillation in the winter season, which is spatially heterogeneous.

4. Preliminary results

Preliminary results indicate that, although the present rates of sea-level rise are not unprecedented and the maximum rates were observed at the turn of the 19th century, the 200-year long records are best explained if a small acceleration of the rate is allowed for.

¹ <http://www.pol.ac.uk/psmsl/>

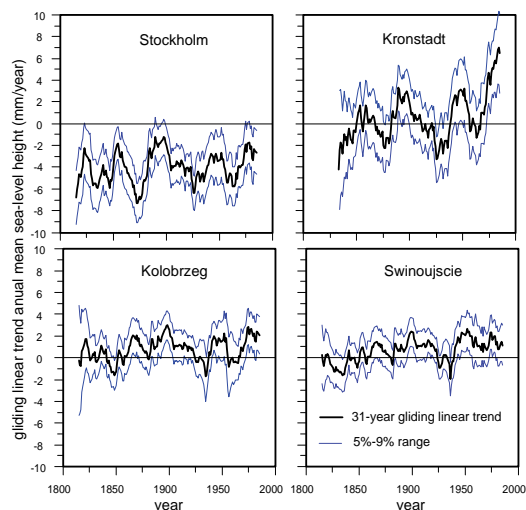


Figure 3. Gliding linear trends of selected sea-level records, estimated by linear fit in moving 31-year windows, together with the 5% and 9% uncertainty range. The abscissa of each data point indicates the centre of the 31-year window.

5. Summary and conclusions

Several studies have attempted to identify a possible acceleration of the global sea-level rise in the 20th century. The impacts of sea-level rise on the coast in the future will, however, occur at regional scales. Coastal engineers and planning authorities require projections of future sea-level rise at these local and regional scales (Hünicke and Storch 2009).

In this study we analyze long mean Baltic sea-level records with the aim of identifying changes in the rate of sea-level change. The analysis is based on the estimation of gliding linear trends through the records and its comparison with simultaneous trends derived from reconstructions of global sea-level (Holgate 2007, Jevrejeva et al. 2006) for the 19th and 20th century and with satellite data for the last few decades.

Future sea-level rise in the Baltic will be determined by several factors, some of them still poorly known, such as the dynamics of polar ice sheets. Many planning agencies assume a continuation of the present broadly linear trends, allowing for an additional 'climate contribution'. The estimation of an acceleration rate can contribute to improve these pragmatic estimations.

References

- Bogdanov et al., Mean monthly series of sea level observations (1777-1993) at the Kronstadt gauge, *Reports of the Finnish Geodetic Institute* 2000: 1, 34pp, 2000.
- Ekman, M, The world's longest sea level series and a winter oscillation index for Northern Europe 1774-2000, *Small Publ Hist Geophys* 12, 30pp, 2003.
- Ekman, M, A consistent map of the postglacial uplift of Fennoscandia, *Terra Nova* 8, 158-165, 1996.
- Holgate, SJ, On the decadal rates of sea-level change during the 20th century, *Geophys Res Lett* 34, L01602, 2007.
- Hünicke, B and H von Storch, What is known about sea-level change in the Baltic Sea? *BALTEX Newsletter* No. 13. International BALTEX Secretariat, GKSS, Geesthacht, Germany.

Hünicke B, J. Luterbacher, A. Pauling and E. Zorita, Regional differences in winter sea-level variations in the Baltic Sea for the past 200 years, *Tellus* 60A, 384-393, 2008.

Jevrejeva, S, A Grinsted, JC Moore and S Holgate. Nonlinear trends and multiyear cycles in sea level records. *J Geophys Res* 111, C09012, 2006.

Merryfield MA and ST Merrifield, An anomalous recent acceleration of global sea level rise, *J. Climate* 22, 5772-5781, 2009.

Rosentau et al., Relative Sea level change in the Baltic Sea since the Littorina Transgression, *Z geol Wiss* 35, 3-16, 2007.

Current status of the BALTEX in-situ reference sites in CEOP

Frank Beyrich¹⁾, Claudia Heret¹⁾, Udo Rummel¹⁾, Fred Bosveld²⁾, Esko Kyrö³⁾, and Rigel Kivi³⁾

¹⁾ German Meteorological Service (DWD), Meteorological Observatory Lindenberg / Richard-Aßmann-Observatory, Lindenberg, Germany. (frank.beyrich@dwd.de)

²⁾ Royal Netherlands Meteorological Institute (KNMI), De Bilt, The Netherlands

³⁾ Finnish Meteorological Institute (FMI), Sodankylä Observatory, Sodankylä, Finland

1. Introduction

The Coordinated Energy and Water Cycle Observations Project (CEOP) has been developed and implemented within the Global Energy and Water Cycle Experiment (GEWEX) of the World Climate Research Programme (WCRP) with the fundamental aim to establish an integrated global observing system for the water cycle which responds to both scientific and social needs of the human society. The CEOP implementation strategy includes both science studies on a number of topics relevant to understand the global energy and water cycle (e.g., monsoon studies, cold region process studies, semi-arid studies) and the collection, central archiving, and synergetic management of

- data from experimental and operational satellites (e.g., NOAA-AVHRR, TRMM, LandSat, Terra, Aqua, EnviSat, ADEOS-II),
- model output products from leading numerical weather prediction and climate modelling centres around the world, and
- comprehensive land surface / atmosphere data sets collected at about 50 world-wide distributed reference sites.

The Regional Hydroclimate Projects (RHPs) within GEWEX, such as BALTEX, are an essential element of CEOP.

2. BALTEX reference sites for CEOP

BALTEX has nominated three observatory sites to act as in-situ reference sites from its member states, namely Sodankylä (Finland), Cabauw (The Netherlands), and Lindenberg (Germany). These sites represent different major climate and vegetation zones in the BALTEX study domain Table 1, Figure 1).

	Sodankylä	Cabauw	Lindenberg
Location	67.4°N, 26.6°E	52.0°N, 4.9°E	52.2°N, 14.1°E
Elevation	179 m	-1 m	73 m
Climate	sub-arctic	temperate, dominating marine influence	temperate, transition from marine to continental influence
Vegetation	boreal forest	mainly grassland	mixed farmland / forest

Data sets are submitted from the in-situ reference sites to the CEOP Central Data Archive (CDA), which is managed by the Earth Observing Laboratory (EOL) of the National Center for Atmospheric Research (NCAR) (see <http://www.eol.ucar.edu/projects/ceop/dm/>). They include

- standard surface meteorology data,
- soil temperature and soil moisture profiles,

- the full set of energy flux data describing the radiation and energy budget at the Earth's surface,
- tower profiles of basic atmospheric state variables, and
- high-resolution radiosonde data characterising the status of the whole atmospheric column at the sites.

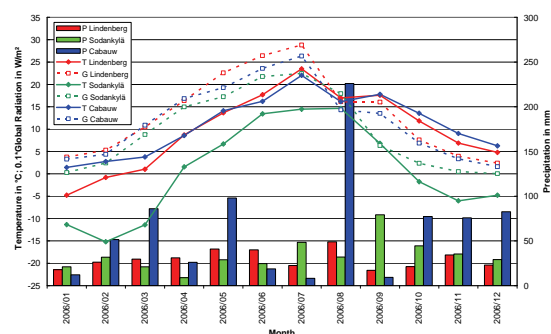


Figure 1. Monthly mean values of temperature (T) and global radiation (G) and monthly precipitation sums for the European CEOP reference sites during the year 2006.

All data are quality-controlled according to procedures implemented at the institutions of the data providers, and they are available in a common data format. Information on measurement details, on the data quality control procedures, and on specific characteristics of the data is available from the site documentation material that is updated regularly with the delivery of a new data set (e.g., Beyrich and Adam 2007).

Upon request, additional data could be made available from the European reference sites such as profiles of mean atmospheric state variables measured with ground-based remote sensing systems (e.g. wind profiler, microwave radiometer profiler), cloud parameters (from ceilometer or cloud radar measurements) or additional radiation and aerosol parameters (UV radiation, aerosol optical depth). These data are not part of the CEOP data sets, they are not available for each of the sites, and the formats have not been harmonized.

The reference site data are collected at the CDA, starting with measurements from October 2002. The intention is to provide a full decadal data set on land surface – atmosphere interaction processes for each site. An updated report on the current status of data availability from the BALTEX reference sites will be given at the conference.

The managers of the European reference sites have discussed issues related to their participation in CEOP including data quality control procedures at a common meeting in 2008 (Beyrich 2008).

3. A data example

The data sets available allow for studies of the interannual variability of energy and water cycle variables. An

example is shown in Figure 2. It reveals remarkable differences in the mean sensible heat flux between the grassland and pine tree surfaces. There is also a strong seasonal and inter-annual variability which has to be basically attributed to soil moisture availability.

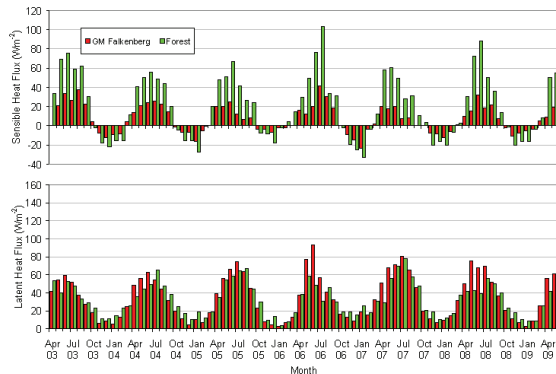


Figure 2. Monthly mean sensible and latent heat fluxes for the Lindenberg-Falkenberg and Lindenberg-Forest stations during the period Apr 2003 – May 2009.

4. Use of CEOP reference site data for monitoring NWP model output

At their meeting in 2008, the European CEOP reference site managers agreed to set up a near-real time data exchange of selected data from their observatory sites for use in monitoring the output of the operational NWP models run at the participating Weather Services. This exchange has been established in the meantime, and corresponding plots of selected model output parameters versus their measured values are routinely created. An example is shown in Figure 3.

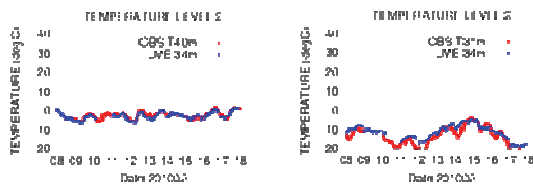


Figure 3. Routine monitoring of the DWDs COSMO-EU model output for temperature at the 2nd model level (31m) at Cabauw and Sodankylä during the period Feb 08-17, 2010.

5. Use of CEOP reference site data for parameterization studies

The comprehensive data sets from the CEOP reference sites might be used also for detailed case studies on the performance of different parameterizations describing the surface – atmosphere interaction in NWP and climate models. Figure 4 illustrates a winter time situation when air temperatures down to -20°C were observed at Lindenberg-Falkenberg over snow.

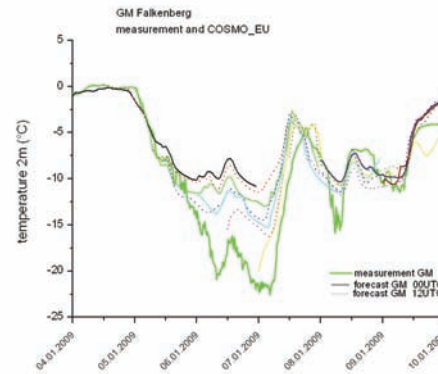


Figure 4. Measured and predicted (by the COSMO-EU model) 2m-temperatures at the Lindenberg-Falkenberg site during a winter episode from Jan 04, 2009 till Jan 10, 2009.

The temperature forecast in the NWP models did not properly resolve these low values. This could be attributed to three main causes:

- albedo of snow is prescribed as 0.7 which is too small for fresh-fallen snow resulting in a higher absorption of shortwave radiative energy at the surface,
- vertical turbulent mixing in the lower atmospheric boundary layer is too strong, and
- the heat transfer across the snow and into the soil is too strong, as well.

References

- Beyrich, F. (2008) BALTEX Reference Site Managers Discussed Further Contribution to CEOP. BALTEX-Newsletter 11, 7
- Beyrich, F., Adam, W. (2007) Site and Data Report for the Lindenberg Reference Site in CEOP - Phase I. Berichte des Deutschen Wetterdienstes 230, 55pp.

Wave conditions along the Latvian coast of the Baltic Proper derived from visual wave observations

Anita Draveniece

Latvian Academy of Sciences, Akademijas laukums 1, Riga LV 1050, Latvia (int@lza.lv)

1. Introduction

A number of studies discuss the wave activity along the north-eastern and southern part of the Baltic Proper. Although the wave activity is the major hydrodynamic factor affecting Latvia's coast, so far the wave data collected along the Latvian coastline have rarely been analyzed. The last two decades have brought warmer winters to the Baltic Sea region, higher mean and extreme sea levels. More frequent high wind events likely intensify coastal processes and wave analysis could give valuable insights into factors affecting these processes. Moreover, the wave energy could be effectively harnessed as a renewable energy source. In this regard, Kalnins et.al. (2008) analysed wave and wind observation data (2003-2007) collected at Ventspils and regarded the wave potential as sufficient for wave energy converter technology.

This study is the first attempt to establish the basic features of seasonal and inter-annual variations of wave and wind conditions based on three time series of wind measurements and visual wave observation data along the Latvian coast of the Baltic Proper. Furthermore, the relationship between the maximum wave height and air mass advection and /or passage of atmospheric fronts was examined.

2. Observation sites and data

The wave observations along the Latvian coastline started in the middle of the 20th century. The visually observed data is the only available source of wave properties because of the absence of instrumental measurements. Although such data has several disadvantages, Soomere and Zaitseva (2007) have shown that visually collected data represent relatively well the general features of the open sea wave fields.

This study used the data collected at the observation sites Liepaja, Pavilosta and Ventspils, which are located along the eastern coast of the open Baltic Sea from Liepaja to Ventspils (a total length of ca 120 km). These observation sites are open to a large part of the dominant winds, being best exposed to north-westerly winds, but are sheltered from waves when easterly winds are blowing. The waves were observed only during daylight hours and therefore from March until the first half of October three observations could be made, but during the winter months the short duration of daylight allowed only two observations. The water depth at the wave observation points ranges from 3 m at Ventspils to 6-7 m at Pavilosta.

The observation data are now kept at the data fund of Latvian Environment, Geology and Hydrometeorology Center in Riga. Only a small fraction of the wave data has been digitized (starting from 2002).

This study covers the years 1990-2004 and all necessary data needed to be digitized. The created digital data set contains information about wave direction, the maximum and the mean wave height, the wave period and wind speed. For the time series of this length, it was not considered reasonable to extract temporal changes in the wave activity. The data of daily air mass advection and front passage, as identified by Draveniece (2007), were used to examine factors that likely influence wind and wave activity.

3. Seasonal variation, extremes and annual mean wave heights

During the analyzed period of 15 years, the character of seasonal variations in wave activity was similar in all locations. Throughout the year, the monthly mean wave heights were the highest in Liepaja and the lowest in Pavilosta. Apparently, various factors as configuration of the coastline and more specific coastal features, like long shoal at Akmenrags (Stone Cape) to the south of Pavilosta, exert influence upon the spatial differences.

The wave activity was most intense from October through March, when vigorous westerly circulation establishes over mid-latitudes and the cyclones are very active. In exceptional cases, as in November 1993, when under the influence of the western edge of the high pressure system continental and transformed maritime air masses were brought into Latvia, the weather was cold, no atmospheric fronts crossed the territory, the monthly wave height was untypical for this season, namely 0.36 m in Liepaja and even lower in other two locations. The curves of monthly average wind data followed the same pattern as wave heights and, as expected, in virtual absence of tides in the Baltic Sea, demonstrated direct wind speed-wave height relationship.

In general, the performed analysis showed a moderate wave activity along the Latvian coast of the Baltic Proper, namely the annual mean wave height in Liepaja was 0.8 m and slightly less in Ventspils and Pavilosta. Some years showed considerably weak wave activity with the annual mean wave height as low as 0.6 m. The typical wave periods were 3-4 s, but the highest waves reached 3,5 – 4 m.

4. Preliminary results

A good correlation was found between mean monthly wave heights and inflow of maritime (subarctic and arctic) air masses over the coastal area of Latvia, as well as passage of atmospheric fronts.

Further examination of historical wave data and extension of the digitized wave data set may shed more light on the spatial and temporal patterns of changes in the wave conditions at the eastern coast of the Baltic Proper.

References

- Draveniece A. (2007) Oceanic and continental air masses in Latvia (in Latvian), *Latvian Vegetation (Latvijas Veģetācija)*, 14, 135 p.
- Kalnins L., Avotins A., Greivulis J. (2008) Wave energy conversion potential of the Baltic Sea (in Latvian), *Proceedings of Riga Technical University, Energetics and Electrotechnics.*, pp. 213-222
- Soomere T., Zaitseva I. (2007) Estimates of wave climate in the northern Baltic Proper derived from visual wave observations at Vilsandi, *Proceedings of Estonian Academy of Sciences*, 13, pp. 48-64

Spatial variability of thermohaline and dynamical parameters during wind-driven coastal upwelling in the south-eastern Baltic Sea

Mariy Golenko¹ and Nikolay Golenko¹

¹ Atlantic Branch of Oceanology Institute, RAN, Kaliningrad, Russia

A modeling study of the wind-driven coastal upwelling circulation and thermohaline fields in the South-East Baltic Sea is presented. One of the aims of this study is to provide a detailed description of the three-dimensional sea-shelf circulation off the Kaliningrad region. We also aim to determine where the upwelled water originates from wind-driven upwelling.

The Princeton Ocean Model (POM: Blumberg and Mellor 1987) is configured for the South-East Baltic Sea with open semi-boundary layer conditions.

At the first step, the model has been adjusted to the region under investigation, so it reproduced the features of the upwelling thermohaline structure measured in October 2005 near the Curonian Spit. On the base of field data and simulations it was revealed that space inhomogeneity of the temperature field, along-shore and cross-shore currents, and current vorticity depend on the bottom relief and the coastline configuration.

It was picked out the area where onshore return flow during upwelling is concentrated. In the case of the classic scenario of upwelling the water entrainment from the open sea into the coastal area is in the near slope area with the horizontal scale of 10 km (in the thermocline the horizontal scale may reach ~ 30 km). This intermediate onshore return flow is determined by horizontal advection.

A non-dimensional parameter is proposed, which allows determining the following regimes of upwelling: 1) the upwelling core outcrops at a distance offshore; 2) the upwelling core is adjoined to shore; 3) the upwelling core does not outcrop.

Combining MODIS and SAR images in research of water dynamics in the south-eastern Baltic Sea

Evgenia Gurova.^{1,3} and Andrei Ivanov²

¹ Atlantic Branch of P.P. Shirshov Institute of Oceanology, Russian Academy of Sciences, Kaliningrad, Russia (jessica_geo@mail.ru)

² P.P. Shirshov Institute of Oceanology, Russian Academy of Sciences, Moscow, Russia

³ Applied Research Center, Institute of Aerial Geodesy, Kaunas, Lithuania

1. Introduction

Use of different remote sensing data for marine research covers a variety of scientific tasks as well as practical applications. Both the complexity of hydrodynamics and the heterogeneity of water properties in the Baltic Sea allows using satellite data for research of water dynamics. In the South-Eastern Baltic Sea, sandy coasts and river run-off increase the turbidity and color of coastal waters, and change other water properties such as temperature, salinity etc. Algae blooms also can be used for identification of water dynamics features. All these factors form different signatures in optical, thermal and synthetic aperture radar (SAR) remote sensing data, but all of them have limitations: Optical data require a sun illumination; cloudiness affects the results of passive remote sensing (optical and infrared bands), wind and sea state influence on SAR images. In this study a combined use of optical, thermal and SAR is applied to study water dynamics features in the South-Eastern Baltic Sea, mostly in the coastal zones. The main idea of the study is to show, first, how all these three types of images reflect the same circulation features in the sea in different regional conditions, and, second, to get additional information about current pattern and boundaries of dynamical features by combining MODIS and SAR data.

2. Data and method

We, in the frameworks of multi-sensor approach (see, e.g. Rud and Gade (1999)), selected imagery of ten days in 2006, when quasi-synchronous optical, sea surface temperature (SST) (MODIS) and SAR (Envisat) data were available. They are Kd_488_Lee, nLw_551 and SST products of MODIS and Wide Swath Mode SAR images of Envisat. All satellite scenes were acquired over the same area within two to six hours. For analysis, overlapping of SAR scenes with SST and optical images were performed, as well as transecting of images for analysis and visualization.

Wind records from the weather stations in Batiysk, Hel and the D6 offshore platform were used to evaluate wind conditions. Information about algae/cyanobacteria blooms in the Baltic Sea was available from the annually Report on the Conditions of the Coastal and Offshore Waters of the Baltic Proper (www.ab.lst.se).

3. Results and discussion

Upwelling zones, river outflows in the sea, near-shore and open sea eddies were the main objects of interest in this study.

Upwelling usually can be identified in SST images acquired in cloud-free conditions as areas with lower temperature of water, and sometimes can be also visible in optical data in areas of turbid/blooming coastal waters (Figures 3,4,5). Lower SST decreases the wind stress, that, in turn, reduces the sea surface roughness. This delineates the boundaries of upwelling zones and visualizes the movement and water mass patterns and can be imaged by SAR. Combining them with information about temperature variability and optical data provides more detailed information about the process.

At wind speed 2-4 m/s SAR data show very informative results and good correlation with SST data for all the cases investigated, and also with optical data in the areas of turbid waters, river waters inflows and even during the Cyanobacteria blooms, which can completely change the sea surface roughness (Naumenko et al. 1994). Such correlation allows using SAR data not only as additional source of information, but also instead of SST/optical data when they are not available due to cloudiness which is a typical problem of remote sensing of the Baltic Sea.

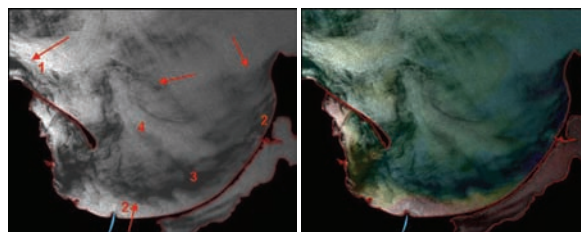


Figure 1. SAR (left) and overlapping SST with SAR (right) image of Gdansk Bay on 10.05.2006.

The SAR image in Figure 1 shows a complex picture of hydrodynamics with alternation of cold and warm water areas. Here, the important source of warm water is the Vistula River with its mouth at the south of Gdansk Bay. Its waters produce a significant contrast with marine waters in fields of temperature, salinity as well as optical properties. Depending on wind these warm colored waters can move to the north and north-west (Figure 3) or spread for a long distance along the Vistula Spit to north-east direction (Figures 1,2), if they are not quickly mixed with marine waters due to strong wind or currents.

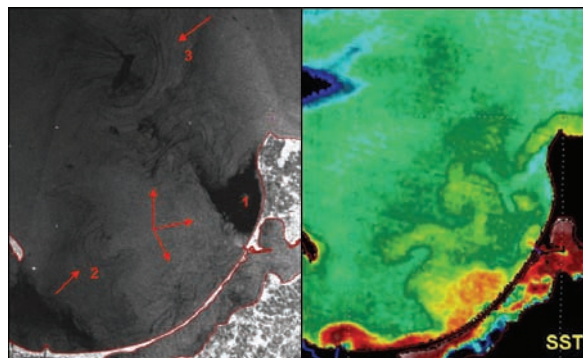


Figure 2. SAR (left) and SST (right) images of the Gdansk Bay. 07.06.2006.

In Figure 1 two upwelling zones can be identified: the one close to Hel Peninsula is small (denoted by “1” in Figure 1), while another large one starts near Cape Taran on the right upper part of the scene and ends close to the Vistula mouth (“2” in fig. 1), where warm river waters spreading along the Vistula Spit separate it from the coast (“3” in

Figure 1). It was caused probably by a quick change of winds from E-NE direction during the five preceding days - which produced upwelling along the Vistula Spit and west off Sambian Peninsula - to NW direction, moving the Vistula River' waters along the coast. In the central part of Gdansk Bay another elongated area of warmer water is visible, it also has a higher turbidity comparing to the surroundings. It can be as well former Vistula waters, which spread along the Vistula Spit, and then moved from the coast by processes related to the upwelling.

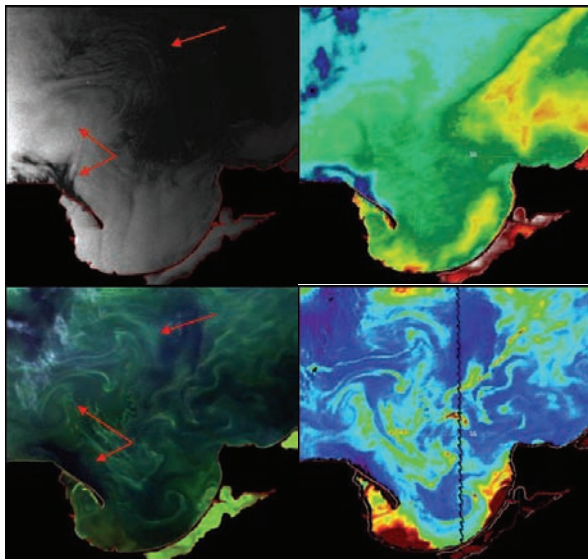


Figure 3. From top left to bottom right: SAR and MODIS (SST, RGB-143 and Kd_488_Lee accordingly) images of South-Eastern Baltic on 03.07.2006.

Another example of clearly identified upwelling near Sambian Peninsula is shown in Figure 2. On the SST image we can see very warm Vistula waters, spread along the Vistula Spit, but its pattern on SAR image is not so clearly visible as colder water area.

In the periods of Cyanobacteria blooms the scum floating on the sea surface may change the sea surface roughness and, thus, produce signatures in optical and SAR images (Figures 3,4,5) (Rud and Gade (1999)). In such periods upwelling form the areas of clean water from surfacing scum, with narrow (in SST field) upwelling boundary areas. On the SAR image, surrounding waters look quite homogeneous with high roughness – contrary to the very heterogeneous optical images. As an exception here the eddies (Figures 2, 3) and eddy pairs (Figure 4) are very well seen in SAR and optical images, also during the Cyanobacteria bloom period (Figures 3,4).

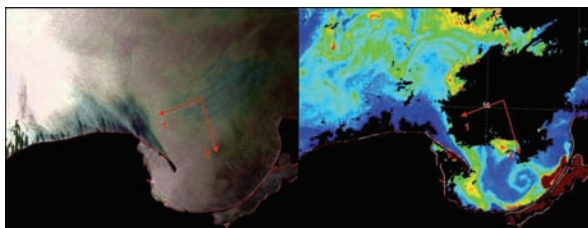


Figure 4. Overlapping of the SAR image with MODIS SST (left) and MODIS Kd_488_Lee (right) image of South-Eastern Baltic on 06.07.2006.

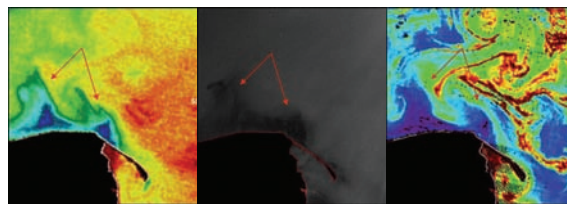


Figure 5. MODIS SST (left), SAR (center) and Kd_488_Lee (right) images of the Hel upwelling area on 11.07.2010.

Upwelling on the SAR image presented on Figure 4 looks very interesting with an interchange of strips, which seems to be strips of high and low sea surface roughness. It can be also caused by heterogeneous concentration and redistribution of floating algae at the surface during the upwelling, moving the surface water from the coast (S-SE wind at time of SAR image acquisition). But no single dark, low backscatter area is visible on this image. This upwelling has been observed during quite a long period – Figures 3, 4 and 5 show the same event on 3, 6 and 11 July 2006.

4. Conclusions

Combining of active and passive remote sensing data in studies on water dynamics in the South-Eastern Baltic Sea provides additional information for characterization and understanding of the processes involved. Correlation between them depends on nature of the oceanographic process and physical conditions on the water interface. In a case of non-blooming sea (Cyanobacteria blooms) temperature difference may produce quite strong signatures in SAR images. Blooms significantly decrease the visibility of many phenomena, except the upwelling zones, which remain clearly visible. Other phenomena causing pronounced signatures, even during the blooms, are eddies and eddy pairs, which form significant contrasts in sea surface roughness. However, optical images seem to be more informative during the Cyanobacteria blooms, when floating scum forms a variety of signatures in convergent/divergent zones, as well as up- and downwelling areas. Finally, the results of the analysis show that a multi-sensor approach is an important source of information on water dynamics in the upper layer of the Baltic Sea.

SAR images have been collected in the frameworks of the ESA AO project C1P.3424. This work has been supported by the Russian Foundation for Basic Research, grant № 09-05-90744-mob_st.

References

- Aneer G., Löfgren S. (2007) Algal bloom - some questions and answers. County Administrative Board of Stockholm.
- Espedal H.A. (2001) Oil spill and its look-alikes in ERS SAR imagery, *Earth Observation and Remote Sensing*, 16. pp. 813-825.
- Jackson Ch., Apel J. (Eds.) (2004) SAR Marine User's Manual. NOAA.
- Naumenko M.A., Beletsky D.V., Rummyantsev V.B., Etkin V.S., Litovchenko K.Ts., Smirnov A.V. (1994) Investigations of the hydrobiological situation in Lake Onega using joint spaceborne radar, airborne and in situ measurements, *Int. J. Rem. Sens.*, V. 15. № 10. pp. 2039-2049.
- Rud O., Gade M. (1999) Monitoring algae blooms in the Baltic Sea: A multi-sensor approach. *Proc. IGARSS-1999*, V. 2, pp. 1211-1213.

Modeling of ice cover of the Baltic Sea

M. Janecki, J. Jakacki, L. Dzierzbicka-Glowacka and R. Osinski

Institute of Oceanology, Polish Academy of Sciences, Sopot, Poland (jjakacki@iopan.gda.pl)

1. Abstract

A coupled ice-ocean model has been used to analyze ice cover of the Baltic Sea. The model consists of the Parallel Ocean Program (POP) and the Community Ice Code (CICE). Both models are from Los Alamos National Laboratory (LANL) and were coupled by the authors. The model was forced by ECMWF atmospheric data (ERA 40 reanalysis). A 40-years hindcast scenario calculation was performed. Anomalies of ice extension, ice thickness and ice area of the whole Baltic Sea are presented.

2. Model description

The ocean model is based on Los Alamos National Laboratory (LANL) Parallel Ocean Program (POP, Smith and Gent, 2004), evolved from the Semtner (1974) global ocean model with added free surface formulation (Killworth et al., 1991). It is a z-level coordinates, general circulation ocean model that solves the 3-dimensional primitive equations for stratified fluid using the hydrostatic and Boussinesq approximations. Numerically the model computes spatial derivatives in the spherical coordinates using finite difference technique. The placement of model variables in the horizontal direction is Arakawa B-grid (Arakawa and Lamb, 1977). A barotropic equation is solved using preconditioned conjugate gradient solver (PCG), a centered differencing scheme is used for the advection scheme. A biharmonic operator has been chosen as a horizontal mixing parameterization and a simple Richardson function to cover vertical mixing. We also use the equation of state introduced by McDougall, Wright, Jackett and Feistel (2003)

The ocean model is coupled through the “flux coupler” with the sea ice model (Community Ice Code – CICE model). CICE uses an elastic-viscous-plastic ice rheology (Hunke and Dukowicz 1997).

The Los Alamos CICE model is the result of an effort to develop a computationally efficient sea ice component for a fully coupled atmosphere-ice-ocean-land global climate model. It was designed to be compatible with the POP for use on massively parallel computers. CICE has several interacting components: a thermodynamic model that computes local growth rates of snow and ice due to vertical conductive, radiative and turbulent fluxes, along with snowfall; a model of ice dynamics, which predicts the velocity field of the ice pack based on a model of the material strength of the ice; a transport model that describes advection of the ice area concentration, ice volumes and other state variables; and a ridging parameterization that transfers ice among thickness categories based on energetic balances and rates of strain. The CICE includes also multiple thickness categories and the ice thickness distribution evolves in time. The model is called IOPAS-POPCICE.

3. Model configuration.

The IOPAS-POPCICE model is configured at two horizontal resolutions of about 9-km (model A) and 2-km (model B), ($1/12^\circ$ and $1/48^\circ$ respectively). The model bathymetry is

represented on 21 vertical levels and the thickness of the first three surface layers was chosen to be 5 meters. The bottom topography is based on Seifert et al. (2001) for the Baltic Sea and ETOPO5 (<http://www.ngdc.noaa.gov/mgg/global/etopo5.HTML>, NOAA 1988) for the Kattegat and the North Sea. The bathymetry data were interpolated to the model grid using kriging method and it is presented in figure 1. The initial state of the ocean model was prepared using temperature and salinity climatologically data (Jansen et al., 1999). The coupled model is forced using realistic daily-averaged forty-years reanalysis data derived from European Centre for Medium-range Weather Forecast (ECMWF, ERA-40). The ocean surface level (5m thick) is restored based on monthly timescale to the monthly average T and S climatology, as a correction term to the explicitly calculated fluxes and overlying atmosphere or sea ice. The restoring was set to 30 days at the surface and to 10 days at the domain boundary.

4. Examples of results

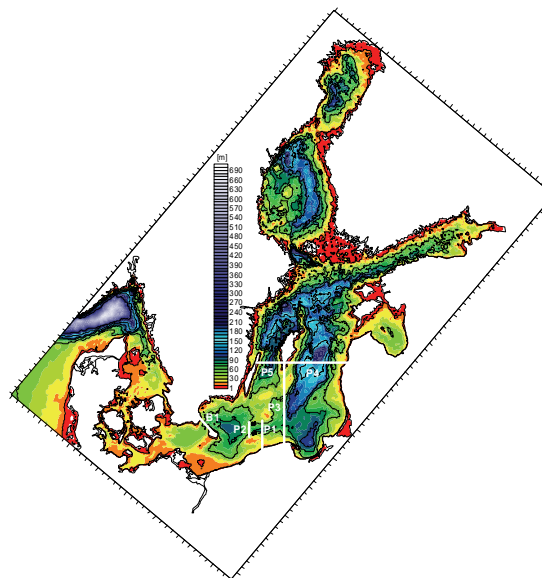


Figure 1. Bottom topography and the IOPAS-POPCICE model domain.

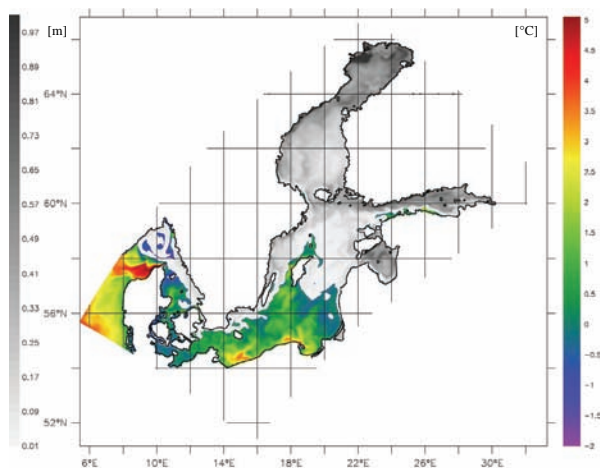


Figure 2. Sea surface temperature [C] (colors) and ice distribution [m] (gray scale) during a severe winter (22 of February 1966). Model B.

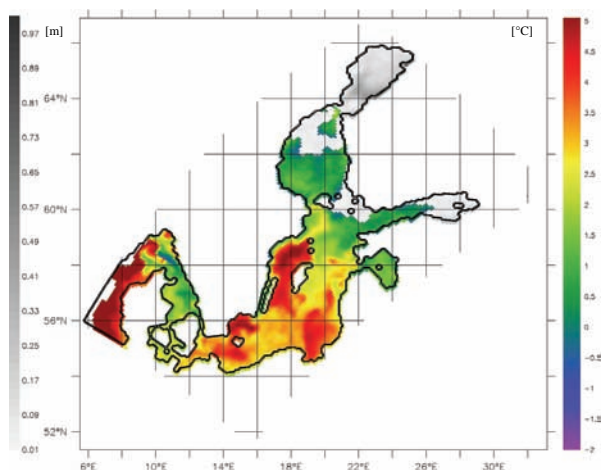


Figure 3. Sea surface temperature [C] (colors) and ice distribution [m] (gray scale) during a mild winter (17 of February 1975). Model A.

5. References

- Arakawa, A., V.R. Lamb, 1977. Computational design of the basic dynamic processes of the UCLA general circulation model. *Methods Comput. Phys.*, 17, 173–265.
- McDougall, T.J., D.R. Jackett, D.G. Wright, R. Feistel, 2003. Accurate and Computationally Efficient Algorithms for Potential Temperature and Density of Seawater. *J. Atmos. Oceanic Technol.*, 20, 730–741.
- Hunke, E. C. and J. K. Dukowicz, 1997. An elastic-viscoplastic model for sea ice dynamics. *J. Phys. Oceanogr.*, 27, 1849–1867.
- Jansen, F., C. Schrum, J.O. Backhaus, 1999. A climatological data set of temperature and salinity for the Baltic Sea and the North Sea. *Dt.hydrogr. Z.*, Supplement 9, 245 pp.
- Seifert, T., F. Tauber, B. Kayser, 2001. A high resolution spherical grid topography of the Baltic Sea – 2nd edition. Baltic Sea Science Congress, Stockholm 25-29. November 2001, Poster #147.

Smith, R., P. Gent, 2004. Reference manual for the Parallel Ocean Program (POP). Los Alamos National Lab., New Mexico, 75 pp.

Semprner, A.J., 1974. A general circulation model for the World Ocean. UCLA Dept. of Meteorology Tech.Rep., No.8, 99pp.

Killworth, P.D., D. Stainforth, D.J. Webb, S.M. Paterson, 1991. The development of a free-surface Bryan-Cox-Semprner ocean model. *J. Phys. Oceanogr.*, 21, 1333-1348.

Assessment of precipitation conditions in the Polish zone of the southern Baltic coastland

Eliza Kalbarczyk and Robert Kalbarczyk

Department of Meteorology and Climatology, West Pomeranian University of Technology, Szczecin, Poland
(Eliza.Kalbarczyk@zut.edu.pl)

1. Introduction

The South-Baltic Coastland is among the regions of Poland with highly diverse precipitation conditions, both spatially and temporally (Czarnecka et al. 2004). Average multi-annual precipitation totals oscillate from below 550 mm in the western part of the described region to above 700 mm in its central part (Kozmiński and Michalska 2004). In particular years both extremely wet and extremely dry periods are recorded and it is difficult to forecast frequency, intensity and area of drought (Kalbarczyk and Kalbarczyk 2006).

The goal of the work was to assess precipitation conditions in the Polish zone of the South-Baltic Coastland taking into consideration multi-annual variability.

2. Material and Methods

Meteorological data from 6 stations of the Institute of Meteorology and Water Management (IMGW) situated in the Polish zone of the South-Baltic Coastland (Figure 1) covering seasonal and yearly atmospheric precipitation totals in the years 1965-2004 constituted the material for the research.



No	Station	Hs	Φ N	Λ E
1	Świnoujście	7	53°55'	14°14'
2	Koszalin	32	54°12'	16°09'
3	Ustka	6	54°35'	16°52'
4	Łębork	38	54°33'	17°45'
5	Gdańsk	13	54°23'	18°36'
6	Elbląg	40	54°10'	19°26'

Figure 1. Location of meteorological stations considered in the research

Precipitation was classified on the basis of the standardised precipitation index (SPI), calculated according to the formula:

$$SPI = \frac{f(P) - \mu}{\sigma}, \text{ where:}$$

$f(P)$ – transformed sum of precipitation; μ – mean value of normalised sequence of precipitation; σ – standard deviation of normalised sequence of precipitation. A precipitation sequence undergoes normalisation using a transforming function $f(P)$, prior to standardisation (Bąk and Łabędzki 2002, Łabędzki 2006). Classification of periods was conducted on the basis of SPI values: $SPI \leq -2.0$ – extremely dry; $-1.99 \leq SPI \leq -1.50$ – very dry, $-1.49 \leq SPI \leq -0.50$ – moderately dry; $-0.49 \leq SPI \leq 0.49$ – normal; $0.49 \leq SPI \leq 1.49$ – moderately wet; $1.5 \leq SPI \leq 1.99$ – very wet; $SPI \geq 2.0$ – extremely wet. The SPI enables comparisons between sites of diverse climatic conditions and also periods of different duration (Łabędzki 2006). Statistical calculations, including a trend of the SPI, were carried out with the use of the program Statistica 8.0.

3. Results

The amount of average yearly precipitation totals in the zone of the Polish South-Baltic Coastland is diverse. On average, the lowest precipitation is recorded in the vicinity of the Pomeranian Bay and the Bay of Gdańsk where it amounts to about 540 and 560 mm, and the highest precipitation is observed in the Koszalin Coastland, including Koszalin, where they amount to record-breaking values of 740 mm. Spatial diversity of precipitation is very similar to distribution of the degree of cloudiness in this area (Kalbarczyk 2004, Kozmiński and Michalska 2004). Around a third of the yearly precipitation total occurs in summer months: From June to August the coast receives between 170 mm of precipitation in Świnoujście to 240 mm in Koszalin. Only in Ustka, higher precipitation than in summer, by about 40 mm, occurs in autumn. The lowest precipitation totals, from 16 to 22% of the yearly total, occur in winter – in the vicinity of the Pomeranian Bay and the Bay of Gdańsk or in spring – in the remaining regions. In Koszalin, however, spring and winter precipitation totals differ only by 0.5 mm. Like in summer and the whole year, the lowest precipitation in winter and spring occurs in the vicinity of the Pomeranian Bay and the Bay of Gdańsk and the highest precipitation in Koszalin. In the multi-annual period at particular meteorological stations the lowest yearly precipitation totals, ranging from 56% of the average yearly totals in Elbląg to 71% in Świnoujście, were recorded in the years 1969, 1975, 1982 and 1989. The highest totals, ranging from 138% of the multi-annual total in Koszalin to 149% in Ustka occurred in 1970 and 1981.

On the basis of the value of the SPI in the forty-year period 1965-2004, years of diverse precipitation conditions were identified – from extremely dry, through very dry, moderately dry and normal to moderately wet, very wet and extremely wet. In the examined years average conditions occurred most often, in 45% of cases, in Ustka and least often, in 30% of cases, in Łębork. Among the remaining cases, years of a various degree of wetness slightly outnumbered dry years (in Elbląg, Koszalin and Świnoujście) or occurred equally often (in Gdańsk, Łębork and Ustka). After normal years in terms

of precipitation conditions, the second most frequent group was years moderately deviating from the norm; moderately dry years constituted 17% in Elbląg to 30% of cases in Lębork, moderately wet years occurred with frequency of from 17% in Ustka to 27% in Elbląg. At three stations moderately dry years occurred slightly more frequently than moderately wet ones, at two stations the situation was the reverse and at one station they occurred with equal frequency. Overall frequency of the occurrence of moderately dry or moderately wet years amounted to from 37% in Ustka to 55% in Świnoujście. Cases of very dry and very wet years occurred several times less frequently, with frequency of 2-7% for very dry years and 2-10% for very wet years. Extremely dry years occurred once in 40 years or did not occur at all; extremely wet years did not occur in Elbląg and Koszalin, once in 40 years they were recorded in Gdańsk and Lębork, two times in 40 years – in Świnoujście and three times in 40 years – in Ustka. With regard to particular seasons the highest frequency of normal seasons occurred mainly in winter (in Elbląg, Koszalin and Lębork), but also in spring (in Elbląg and Ustka), in summer (in Świnoujście) and in autumn (in Gdańsk). Seasons of various drought intensity most often occurred in spring, from 25 to 37% of cases, least frequently in winter, from 17 to 32%. The highest frequency of seasons with above-normal precipitation was recorded also in spring and at particular stations there occurred high diversity of frequency, from 22% in Ustka to 42% in Lębork; the lowest frequency of wet seasons took place in winter, from 20% in Lębork to 35% in Ustka. Moderately dry seasons most frequently occurred in autumn and spring and least frequently in winter; in the case of moderately wet seasons the highest frequency was observed in spring and summer and the lowest in autumn and winter. In total, at all the stations moderately wet seasons occurred 15% more often than moderately dry seasons. Very dry conditions at the majority of stations most often occurred in summer (15 times), in Lębork in autumn, in Ustka also in spring and least frequently in winter (5 times). On the other hand, it is hard to notice regularity in the occurrence of extremely dry conditions – in Świnoujście and Ustka they occurred with the same frequency in all seasons, in Elbląg most often in spring, in Koszalin – in spring and autumn (Figure 2), in Lębork – in summer and winter, in Gdańsk – in winter.

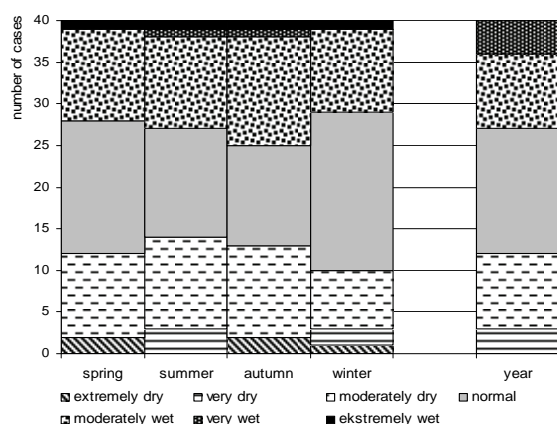


Figure 2. Number of cases with periods of various precipitation conditions in Koszalin in the years 1965-2004

Taking into account all seasons, they occurred slightly more often in winter (9 times, most frequently) and spring than in autumn and summer (6 times, least frequently). Very wet conditions at the majority of stations most often occurred in autumn (16 times), in Koszalin and Świnoujście additionally

in summer and in Lębork only in summer; they occurred least frequently in spring and winter (6 times in each). In comparison with very dry seasons (in total 34), very wet seasons occurred 20 per cent more often. Occurrence of extremely wet seasons, like extremely dry ones, is marked by lack of distinct regularities; taking into account all seasons, they occurred more often in spring (6 times) and winter than in summer and autumn (2 times), in comparison with extremely dry seasons almost two times less frequently. At the majority of stations, considering both years and seasons, no distinct, statistically confirmed tendencies of changes in the amount of precipitation in the years 1965-2004 were noted. The only significant trend, a negative one, was statistically confirmed for the yearly precipitation total in Gdańsk.

4. Conclusions

The most diverse season of the year in terms of precipitation conditions is spring and the least diverse – winter. In the Polish zone of the South-Baltic Coastland one can observe the prevalence of frequency of moderately wet and very wet seasons; it is higher by 15 and 20% respectively, compared to moderately dry and very dry seasons. On the other hand, during half of the seasons extremely dry conditions occur more often than extremely wet conditions. Years of average precipitation conditions constitute from 30 to 45% of years, years of a various degree of wetness occur as frequently as dry years or slightly more often. At the majority of stations, both considering years and seasons, no distinct, statistically confirmed tendencies of changes in the amount of precipitation in the years 1965-2004 were observed.

5. References

- Bąk B., Łabędzki L. (2002) Assessing drought severity with the relative precipitation index (RPI) and the standardized precipitation index (SPI), *J. Water Land Develop.*, 6, pp. 89-105
- Czarnecka M., Koźmiński C., Michalska B., Kalbarczyk E., Kalbarczyk R. (2004) Warunki wilgotnościowe powietrza i gleby na Pomorzu. Monografie – Współczesne problemy inżynierii środowiska. III – Bilanse wodne ekosystemów rolniczych. Wyd. AR Wrocław, 38(503), pp. 27-45
- How to work out a drought mitigation strategy. An ICID Guide(1998). DVWK Guidelines, 309, pp. 29
- Kalbarczyk E. (2004) Time and spatial structure of the state of the sky in Pomerania. *Przegl. Nauk. Inżynieria i Kształtowanie Środowiska*, 1(28), pp. 174-183(in Polish)
- Kalbarczyk E., Kalbarczyk R. (2006) Identification of atmospheric drought periods in north-west Poland over 1965-2004. *EJPAU*, www.ejpau.media.pl/volume9/issue4
- Koźmiński C., Michalska B. (eds), Atlas of climatic resources and hazards in Pomerania (2004), AR w Szczecinie, pp. 69
- Łabędzki L. (2006) Susze rolnicze. Zarys problematyki oraz metody monitorowania i klasyfikacji. *Woda - Środowisko - Obszary Wiejskie Rozpr. nauk. i monograf.*, 17, pp. 107

Wind parameters in the centre of the Gulf of Finland from measurements and HIRLAM outputs

Sirje Keevallik

Marine Systems Institute at Tallinn University of Technology, Akadeemia tee 21, 12618 Tallinn, Estonia (sirje.keevallik@gmail.com)

1. Wind regime on the Gulf of Finland

The wind regime of the Gulf of Finland is very specific. Basically, it is formed as a superposition of globally dominating southwest and north winds, and local winds blowing along the axis of the gulf (Soomere and Keevallik 2003). Therefore, getting adequate estimations of open-sea wind properties is not a simple task. One possibility is to extrapolate lighthouse measurements to a wider region around it. The other possibility is to rely on some model outputs. In this paper a comparison is carried out between HIRLAM 6.4.0 wind outputs and measurements at two lighthouses – Kalbådagrund and Tallinnamadal. The aim of the paper is definitely not to validate one data set against another assuming that one of them is more reliable than the other.

2. Data

Wind speed and direction were recorded during the period of April 2007 – March 2008. Averages of wind speed and direction over 10 minutes before the synoptic observation times (00, 03, 06, 09, 12, 15, 18, 21 GMT) were recorded by means of Väisälä automatic weather stations. From this data set observations at 00, 06, 12 and 18 GMT were chosen for comparison.

Kalbådagrund (59°59'N, 25°36'E) is a lighthouse near the northern coast of the Gulf of Finland, about 20 km from the archipelago. The wind is measured at the height of 32 m above mean sea level.

The lighthouse of Tallinnamadal (59°43'N, 24°44'E) is situated about 20 km from the Estonian islands Naissaar and Aegna. The wind is measured at 36 m above the sea level.

3. HIRLAM outputs

HIRLAM version 6.4.0 with minor modifications is run in the Estonian Meteorological and Hydrological Institute (see Keevallik et al. 2010 for details).

The 54h forecasts together with 3DVAR analyses are produced four times a day at main synoptic hours. Wind data were drawn from the lowest model level that is located approximately 30 m above the ground. Horizontally bilinear interpolation of wind components to the measurement point was performed when data for a specific point was gathered. A transformation of the wind direction from HIRLAM rotated coordinate system to the geographical coordinate system was performed.

In the current paper, the 3DVAR analysis data were used to simulate marine winds as a hindcasting problem.

4. Comparison of air-flow components

To compare the HIRLAM outputs with measurements at lighthouses, mean deviation (bias) and root mean square deviation (RMSD) were calculated. Table 1 shows these characteristics for air flow. A bias is positive when HIRLAM values are larger than the measured values.

Table 1. Comparison of HIRLAM 3DVAR analysis and lighthouse measurements for wind velocity components: u is zonal and v is meridional air-flow component

	Bias (m/s)		RMSD (m/s)	
	u	v	u	v
Tallinnamadal	0.53	0.08	3.00	3.09
Kalbådagrund	0.12	1.26	2.86	3.61

It can be noticed that HIRLAM approximates the zonal component better at Kalbådagrund and the meridional component at Tallinnamadal.

The mean deviation of the meridional component at Tallinnamadal is negligible, but there seems to be problems at Kalbådagrund. Here, the annual average of the measured meridional component is 0.65 m/s and the bias is nearly twice larger

5. Comparison of wind speed and direction data

For a better understanding, wind speed and direction are treated separately.

Table 2. Comparison of HIRLAM 3DVAR analysis with measured wind parameters

	Speed (m/s)		Direction (°)	
	Bias	RMSD	Bias	RMSD
Tallinnamadal	-1.22	2.77	2.5	36.0°
Kalbådagrund	-0.30	2.02	-23.8	37.9°

Negative bias of wind speed in Table 2 shows that HIRLAM underestimates wind speed, especially at Tallinnamadal. Here also the RMSD is somewhat larger than at Kalbådagrund.

Assuming that the probability distribution of wind direction is Gaussian, one can say that approximately 70% of HIRLAM values are expected to be within a sector of 70° around the measured value. The bias of wind direction is negligible at Tallinnamadal, but large and negative at Kalbådagrund. Negative wind direction bias means that HIRLAM wind direction is turned counter-clockwise in relation to the measured wind direction.

Next $\pm 22.5^\circ$ sectors were separated around each of the eight rhumbs and average differences between HIRLAM outputs and measured wind parameters were calculated in the boundaries of the respective sector. Sectors were chosen from the measured data set, so that the numbers in Table 3 show the bias of HIRLAM estimates for winds that are measured in the respective sector.

According to Table 3, HIRLAM underestimation of the wind speed at Tallinnamadal is the largest for N and S winds (that blow across the gulf) and the smallest for E and NW winds (that blow along the gulf). At Kalbådagrund the bias of the wind speed is slightly positive for SW and W winds.

HIRLAM underestimation of the wind direction at Kalbådagrund is the largest for N and NW winds, reaching

values of more than 30°. At Tallinnamadal, the difference between HIRLAM and measured wind direction is uniformly small.

Table 3. Average differences between HIRLAM 3DVAR analysis and measured values within $\pm 22.5^\circ$ sectors around principal rhumbs that are determined from measured data

	Wind speed, m/s		Wind direction, °	
	Tallinna-madal	Kalbåda-grund	Tallinna-madal	Kalbåda-grund
NE	-1.0	-0.8	4	-28
E	-0.8	-1.2	5	-15
SE	-1.4	-0.9	2	-19
S	-1.5	-0.5	-1	-17
SW	-1.2	0.2	0	-19
W	-1.2	0.5	6	-26
NW	-0.9	-0.2	1	-32
N	-1.7	-0.9	5	-36

The picture is somewhat different when we separate the sectors around principal rhumbs from HIRLAM files. Such information is interesting for modellers who have only NWP outputs at their disposal. Table 4 shows expected average differences between HIRLAM data and measured values for such situation. The modeller could expect that wind speed at Kalbådagrund is well (within ± 0.6 m/s) modelled for S, SW, W and NW winds (that are the most frequent). Wind speed estimations show the largest bias at Tallinnamadal for E and N winds (more than -2 m/s). Wind direction is well approximated at Tallinnamadal and uniformly biased at Kalbådagrund.

Table 4. Average differences between HIRLAM 3DVAR analysis and measured values within $\pm 22.5^\circ$ sectors around principal rhumbs that are determined from HIRLAM files.

	Wind speed, m/s		Wind direction, °	
	Tallinna-madal	Kalbåda-grund	Tallinna-madal	Kalbåda-grund
NE	-1.7	-1.0	3	-27
E	-2.2	-1.5	0	-24
SE	-1.6	-0.8	6	-23
S	-0.8	-0.1	10	-20
SW	-0.7	0.6	2	-22
W	-0.9	0.1	-6	-29
NW	-1.5	-0.6	7	-22
N	-2.1	-1.1	-2	-26

6. Conclusions

Wind parameters measured at two lighthouses in the Gulf of Finland are compared with HIRLAM 6.4.0 outputs for the period of April 2007 – March 2008 with the aim to detect discrepancies between these data sets that are widely used by marine modellers.

It is shown that HIRLAM approximates well wind speed at Kalbådagrund, but underestimates it at Tallinnamadal by more than 1 m/s.

HIRLAM outputs coincide well with the wind direction measurements at Tallinnamadal. At Kalbådagrund HIRLAM wind direction is turned counter-clockwise in relation to the measured wind direction by more than 20°. Evidently HIRLAM overestimates the sea surface roughness, as the angle between geostrophic flow and actual balanced air flow increases with the roughness of the underlying surface.

Analysis of directional distributions of wind speed and direction biases shows that the results depend on the choice of the initial data set. In practice, a modeller has only HIRLAM data at his/her disposal. If he/she separates sectors around principal rhumbs from HIRLAM data, he/she could expect that HIRLAM approximates well speed of the winds blowing from south, southwest and west. For other directions, HIRLAM underestimates the wind speed. This underestimation is especially large at Tallinnamadal for north and east winds. HIRLAM underestimates the wind direction at Kalbådagrund by 20-30° in all sectors. At Tallinnamadal the difference between HIRLAM and measured wind direction is less than 10°.

Acknowledgements

The author is grateful to Dr Tarmo Kõuts (Marine Systems Institute at TUT) and Estonian Maritime Administration for the wind data at Tallinnamadal. The Kalbådagrund wind data were drawn from the files of Finnish Meteorological Institute. Special thanks to Mr Juhan Hinnov who provided the author with HIRLAM outputs. This research is supported by Estonian Ministry of Education and Science (SF0140017s08).

References

- Soomere, T., Keevallik, S. (2003) Directional and extreme wind properties in the Gulf of Finland. Proc. Estonian Academy of Sci. Engineering, 9, 2, 73-90
- Keevallik, S., Männik, A., Hinnov, J. (2010) Comparison of HIRLAM wind data with measurements at Estonian coastal meteorological stations. Estonian Journal of Earth Sciences, 59, 1.

An advanced weather radar network for the Baltic Sea Region - BALTRAD

Daniel Michelson

Swedish Meteorological and Hydrological Institute, Norrköping, Sweden (daniel.michelson@smhi.se)

1. Introduction

International weather radar networking is a topic that has been addressed in Europe in different ways throughout the last few decades: in COST actions, EUMETNET, and through regional networks. International networking is a prerequisite for achieving the greatest cost-effectiveness in radar hardware investments in Europe, with its great diversity of countries, physical environments, and hazardous weather conditions. Despite this, however, exchange of radar data is still largely performed bilaterally using primitive mechanisms. Real radar networking is uncommon and mostly limited to domestic solutions. The prototype European composite at EUMETNET OPERA's Pilot Data Hub is a welcome step towards a true European weather radar network, yet much work remains before this goal is achieved. The BALTRAD project was officially underway on 1 February 2009, and it will continue until 31 January 2012. The source of funding is the European Union's regional programme INTERREG IV B, the Baltic Sea Region (BSR). The project's budget is 2.1 M€, and the allocated amount of work, expressed in full-time equivalent, is around 27 years. In addition, we have significant resources as external services, travel, and investments in the form of computer servers.

2. Objective and partnership

The objective of BALTRAD is to create an advanced weather radar network for the BSR, as a durable and sustainable element of regional infrastructure. The Partnership comprises the following government organizations:

- Swedish Meteorological and Hydrological Institute (SMHI, Lead Partner)
- Finnish Meteorological Institute (FMI)
- Institute of Meteorology and Water Management (IMGW), Poland
- Latvian Environment, Geology and Meteorology Centre (LEGMC)
- Danish Meteorological Institute (DMI)
- Republican Hydrometeorological Center (RHMC), Belarus
- Radiation and Nuclear Safety Authority (STUK), Finland
- Estonian Meteorological and Hydrological Institute (EMHI)

We have also associated organizations in Denmark (Ålborg University), Latvia (LGS, the aeronavigation service provider), and Poland (Silesian Voivodship Office) who will be contributing in various ways.

3. Heritage and concept

BALTRAD represents the first dedicated international weather radar networking project funded by the European Union. However, the concept we're following has already been proven once before, with the establishment of the NORDRAD network involving the radars from Norway, Finland and Sweden, around 20 years ago. The original NORDRAD technology has become outdated and it is time

to follow a new paradigm. In doing so, we hope to create the following:

- exchange of polar data among all members of the partnership
- a weather radar data exchange framework fully compliant and preferably integrated with the WMO Information System (WIS)
- a common production framework containing harmonized algorithms, including those employing dual-polarization data
- consistent end-to-end management of quality information
- a software system which is available according to Open Source principles.

The goal is to achieve cutting-edge distributed radar networking, ie. a network where data is exchanged on equal terms and where each institute processes the data according to its local needs. In achieving this, we hope to establish a community-based critical mass that will be sustained and enlarged after the completion of the project.

It is worth emphasizing that the collaboration in the BALEX Working Group on Radar has also contributed significant critical mass and experience, and it is collaborations like this that has given the BALTRAD project and its partnership credibility.

4. Project content

The project is organized into the following work packages, which are limited to a maximum of seven by the BSR.

1. **Management and Administration.** This is a mandatory work package run by SMHI.
2. **Communications.** This is also a mandatory work package dedicated to both internal and external communications. It is the responsibility of FMI.
3. **Core network.** This work, led by IMGW, is dedicated to creating the real-time networking functionality. We foresee that it will be based on secure HTTP-based mechanisms with subscription services. Our long-term goal is that we contribute such mechanisms for weather radar to WIS for Europe.
4. **Data catalogue.** This work involves managing all data to be exchanged and processed. EMHI leads this work, which will focus on creating a database for all metadata and systematic methods for storing data files.
5. **Production framework.** FMI leads this work, which deals with developing, collecting, and harmonizing numerous algorithms for improving the quality of data and creating products from them such as composites directly from polar volume data. Products based on dual-polarization moments will be included in this

work, as several of the operational radars in the region are dual-pol, and more are on the way. The production framework itself will likely be RPC-based, where algorithms may be implemented using any of the C/C++, Java, and Python programming languages.

6. **Deployment.** This involves integrating the outputs of work packages 3-5 into a real-time system suitable for operational deployment. SMHI leads this task. Regular releases will be installed at all Partners, and they will be evaluated within the project using dedicated teams in e.g. LEGMC and the RHMC.
7. **Pilots.** This work, led by IMGW, serves to make the BALTRAD system and its radar-based information available to test pilots, to collect the pilots' feedback to integrate new and improved software and products. A case log will be prepared containing cases relevant to air traffic, flash flooding, urban hydrology, and radiation accident scenarios. In this way we will demonstrate the value achieved in a true end-to-end radar network.

However, we should clarify that there are no resources in BALTRAD for procuring new radars. Notwithstanding this constraint, BALTRAD will create software converters that will harmonize all polar data from all radars in the network to a common format: HDF5 following the official European standard defined in OPERA. BALTRAD software will be available for free according to EU regulations, in our case the Lesser Gnu General Public License.

In summary, BALTRAD will deliver freely-available, community-developed software which we hope will spread "organically" throughout Europe, enabling the advanced networking of weather radar data in a harmonized way. A harmonized set of production algorithms will also be included, and we encourage the community to contribute their algorithms too. An important outcome is the ability to provide end users with high-quality radar-based information that will facilitate their daily decision-making activities.

Impact of aerosol optical properties on climate change processes. The Baltic case study

A. Ponczkowska¹, P. Makuch¹, J. Kowalczyk¹, T. Zielinski¹, T. Petelski¹, J. Piskozub¹,
A. Smirnov², B. Holben², J. Pasnicki³ and K. Zielinski⁴,

¹ Institute of Oceanology, Polish Academy of Sciences, Sopot, Poland (ponczesa@iopan.gda.pl)

² NASA/Goddard Space Flight Center, USA

³ Gdansk Polytechnic, Gdansk, Poland

⁴ Junior High School No. 3, Sopot, Poland

1. Introduction

The characterization of aerosols involves the specification of not only their spatial and temporal distributions but also their multi-component composition, particle size distribution and physical properties as.. Due to their light attenuation and scattering properties, aerosols influence radiance measured by satellite for ocean color remote sensing.

Studies of marine aerosol production and transport are important for many earth sciences such as cloud physics, atmospheric optics, environmental pollution studies, and interaction between ocean and atmosphere. This is one of the reasons for the increasing number of research programs dealing with marine aerosols (Zielinski 2004).

Sea salt aerosols are one of the most abundant components of atmospheric aerosols, and thus they exert a strong influence on radiation, cloud formation, meteorology and chemistry of the marine atmosphere. An accurate understanding and description of these mechanisms is crucial to modeling climate and climate change (Smirnov et al. 2009).

However, on the global scale, a major unknown of the spatial aerosol distribution is the vertical distribution. Transport in the planetary boundary layer and the free troposphere can be decoupled, resulting in different chemical composition, and thus aerosol optical properties in different layers. Lidar measurements give detailed information on occurrence, extent and development of aerosol structures (Li et al. 1996, Markowicz et al. 2008).

This work reports results of measurements performed in the lower troposphere during several measurement sessions in the Baltic Sea area (2000-2009).

2. Measurement and instrument description

The experimental setup includes lidars, ceilometers, sunphotometers and laser particle counters. The measurements were made both on shore and onboard the r/v *Oceania*. The full meteorological coverage was obtained from the in-situ measurements, coastal meteorological stations and from the BADC or calculated from HYSPLIT.

Measurements of Aerosol Optical Depth (AOD) were performed with hand-held Microtops II sun photometers and the Ozone Monitor. These instruments facilitated investigations of AOD at different wavelengths and were used at all locations (Table 1).

Single measurement "shots" were acquired over about 1 minute periods (in which measurements were made at all wavelengths, 10 second per channel: 340, 380, 440, 500, 675 nm) every 20 minutes. During the measurements the photographic documentation was made by using a CCD camera equipped with a wide-angle lens that was pointed on the solar target. The photos were used during further quality analyses.

Table 1. Technical parameters of Microtops II sun photometers used during the studies.

	340 ± 0.3 nm, 2 nm FWHM
	380 ± 0.4 nm, 4 nm FWHM
Optical channels	440 ± 1.5 nm, 10 nm FWHM
	500 ± 1.5 nm, 10 nm FWHM
	675 ± 1.5 nm, 10 nm FWHM
Resolution	0.01 W m ⁻²
Dynamic range	>300000
Viewing angle	2.5°
Precision	1-2%
Non linearity	max. 0.002%

3. Results

It was discovered that the near-water layer in the coastal areas is significantly different from that over the open seas, both in terms of structure and physical properties. The aerosol composition and concentrations are usually uniform over the open ocean. In coastal areas, the composition can change over short periods of time, and the real aerosol concentrations depend on many factors, concerned with different particle origins.

Aerosols measured in the marine boundary layer can be divided into three groups: marine, a mixture of marine and continental, and continental. The aerosol type depends on the history of air masses, wind speed and direction.

Both horizontal and vertical aerosol concentrations and size distributions vary significantly seasonally and over short periods of time. The results show a significant increase in aerosol concentration with continental air masses. However, the marine aerosol concentrations above the surf zones can be even two fold higher than those over the open ocean. Those results were among the first once ever published (deLeeuw et al., 2000).

Depending on aerosol origin, different light refraction indices must be applied for calculations of particle optical properties. For marine aerosols, the light refraction index is the same as for the water in the area, while the continental aerosols must be regarded as absorbing particles.

The aerosol particles in the marine boundary layer significantly influence the light extinction in the visible and infrared ranges. The difference between the extinction coefficients at the sea level and at the altitude of 30 m a.s.l. can reach a magnitude of up to two orders. Also the Angström coefficients show a significant variability, both in short-term and seasonally.

The coastal area of the southern Baltic Sea should be divided into two regions, which can be called, “eastern” and “western”. In the area east of 17°30' E (e.g. Lubiatowo, Cetniewo, Jastarnia) it is possible to detect typically marine aerosols with onshore winds. In the areas west of 17°30' E (e.g. Darłowo, Kołobrzeg, Międzyzdroje) it is very difficult to detect marine aerosols, even with onshore winds. This area is constantly under the act of continental air masses (Scandinavia), which transport large amounts of continental aerosols.

4. Conclusions

Direct and indirect radiative effects of aerosol particles have been identified as key uncertainties for the prediction of the future global climate. Hence, the following issues are necessary to be addressed:

1. A validation of satellite and lidar based data regarding the aerosol physical properties and aerosol optical thickness,
2. The determination of the spatial and temporal variability of aerosol properties.

Acknowledgements

This research was partly done within the scope of the Polish National Grant MACS/AERONET/59/2007. Starting in 2007, the studies were also done within the framework of the MAN: A maritime component of AERONET.

References

- Zielinski, T. (2004). Studies of aerosol physical properties in coastal areas, *Aerosol Sci.&Tech.*, No. 38, 513-524
- Li, X.H., Moring, Savoie, D., Voss, K., Prospero, M. (1996). Dominance of mineral dust in aerosol light-scattering in the North Atlantic trade winds. *Nature* 380, 416-419
- Smirnov, A. B. Holben, I. Slutsker, D. Giles, C. McClain, T. Eck, S. Sakerin, A. Macke, P. Croot, G. Zibordi, P. Quinn, J. Sciare, S. Kinne, M. Harvey, T. Smyth, S. Piketh, T. Zielinski, A. Proshutinsky, J. Goes, N. Nelson, P. Larouche, V. Radionov, P. Goloub, K. Krishna Moorthy, R. Matarrese, E. Robertson, F. Jourdin (2009). Maritime Aerosol Network (MAN) as a component of AERONET, *Journal of Geophysical Research-Atmospheres*, Vol. 114, D06204, doi: 10.1029/2008JD011257
- Markowicz, K.M.; Flatau, P.J.; Kardas, A.E.; Remiszewska, J.; Stelmazczyk, K.; Woeste, L (2008). Ceilometer retrieval of the boundary layer vertical aerosol extinction structure. *J. Atmos. Oceanic Technol* Vol. 25, 928-944
- Leeuw de G., Neele F., Hill M., Smith M., Vignati E., (2000). Production of sea spray aerosol in the surf zone, *Journal of Geophys. Res.*, 105, D24, 29397-29409.

A reliability study of wave climate modelling in the Baltic Sea

Andrus Räämet^{1,2} and Tarmo Soomere^{2,1}

¹ Department of Mechanics, Tallinn University of Technology, Estonia (andrus.raamet@ttu.ee)

² Institute of Cybernetics at Tallinn University of Technology, Estonia

1. Introduction

One of the key issues in surface wave hindcast is the proper choice of the wind information. This is especially important in the Baltic Sea basin. Here, wind data even from sites that are known to predominantly represent the properties of open sea winds, still reveal a major mismatch when compared to measured or visually observed wave data (Broman et al. 2006, Soomere 2008). This mismatch is also present in reproductions of wave fields with the use of one-point fetch-based wave models (Räämet et al. 2009). In particular, long-term variability of wave fields in the northern Baltic Proper (NBP, Figure 1) is weakly correlated to the variations of the average wind speed measured at the Island of Utö.



Figure 1. Location scheme of the wave and wind measurement sites.

The annual mean wave height increased from the mid-1980s until the middle of the 1990s at Vilsandi (according to visual observations, Soomere and Zaitseva 2007) and Almagrundet (where wave properties were measured with the use of an upward-directed echosounder, Broman et al. 2006). After that, wave activity rapidly decreased (Figure 2). At the same time, the wind speed measured at Utö continued to increase. This mismatch has led to the question about the reliability and drivers of the wave climate changes.

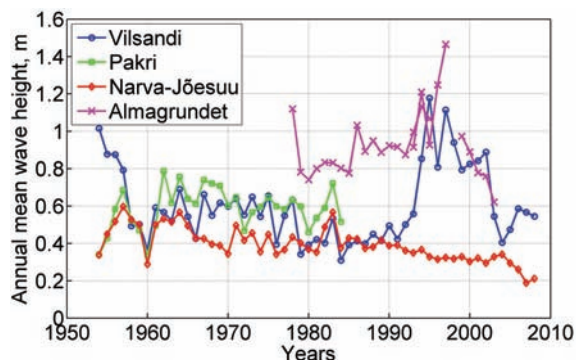


Figure 2. Long-term variations of wave heights at Vilsandi, Pakri, Narva-Jõesuu and Almagrundet (Zaitseva-Pärnaste et al. 2010).

Moreover, since the beginning of the wave observations, wave heights have behaved similarly at all Estonian coastal observation sites over about thirty years. This coherence and in-phase manner of interannual variations are completely

lost in the mid-1980s. Later on, both wave height trends and details of interannual variations of the wave intensity are different at Vilsandi and at Narva-Jõesuu (Figure 2).

Another important feature of wave conditions since the mid-1990s is the apparent increase in the number of extreme wave conditions on the background of the overall decrease in mean wave heights in the northern Baltic Sea. Extremely rough seas occurred in December 1999 and the legendary storm in January 2005 caused the all-time highest significant wave height $H_S \approx 9.5$ m (Soomere et al. 2008). These events have raised a number of questions: whether coastal processes in the Baltic Sea have become more intense compared to the situation a few decades ago or not; (ii) whether the trends for average and extreme wave heights are different, etc.

A recently completed hindcast of the entire Baltic Sea wave fields for 38 years (1970–2007) makes an attempt to shed light to the above questions (Räämet and Soomere 2010). It also revealed considerable mismatches between certain characteristics of measured and modelled waves. They may stem from a variety of factors. In this note we present an overview of a sensitivity study of the results of this initiative with respect to the wind forcing.

2. The wave model

Wave properties were computed with the third-generation spectral wave model WAM (Komen et al. 1994). The bathymetry was based on data prepared by Seifert et al. (2001). The calculation was done over a regular rectangular grid (239×208 points; 11545 sea points) with a resolution about 3×3 nautical miles (grid increment for latitude 3' and for longitude 6'). The grid extends from 09°36' to 30°18' E and from 53°57' to 65°51' N. At each sea point, 1008 components of 2D spectrum (24 equally spaced directions with the angular resolution of 15° and 42 frequencies ranging from 0.042 Hz to about 2 Hz) were computed. The extended frequency range up to 2 Hz was used to ensure realistic wave growth rates in low wind conditions after calm situations (Soomere 2005). In general, the WAM model gives good results in the Baltic Sea if the model information is appropriate and the wind information is correct.

3. Wind and wave data

The WAM model was forced with three versions of wind fields for the whole Baltic Sea. For the long-term hindcast, the near-surface wind at 10 m level was constructed from the geostrophic wind database prepared by the Swedish Meteorological and Hydrological Institute (SMHI). The geostrophic wind speed was multiplied by 0.6 and the wind direction was turned counter-clockwise by 15° (Bumke and Hasse 1989). The wind grid resolution and time step were 1×1° and 3 hours. This forcing led to a good reproduction of statistics and the seasonal course of waves, to a less satisfactory representation of the time series of wave properties, and to quite large mismatches in the course of measured and modelled annual mean wave heights (Räämet and Soomere 2010).

In order to locate the source of the described deviations, we used two alternative wind databases. MESAN wind (Häggmark et al. 2000) developed by the SMHI presents hourly gridded wind information since October 1996. It accounts for local wind variations in rough landscapes and coastal areas to some extent. The grid resolution and time step were 22×22 km and 3 hours, respectively. Owing to the short temporal coverage, this data was not suitable for climatological studies.

The wave properties were also calculated over several windy weeks in 2001 and 2005 with the use of recently reanalysed wind fields developed by the European Centre for Medium-Range Weather Forecasts (ECMWF). The resolution of this data was $0.25 \times 0.25^\circ$ and the wind input time step for the WAM model was 1 hour.

The overall course of the significant wave heights simulated with the use of these winds match well each other but none of the forcings led to clearly better reproduction of measured wave properties (Figures 3 and 4). A typical feature of all model runs is that several storms are almost perfectly reproduced while for others all the models almost totally fail. The largest mismatch occurred during certain extreme wave events. For example, all the models underpredicted by two to three meters the extreme wave events on 7/9.01.2005.

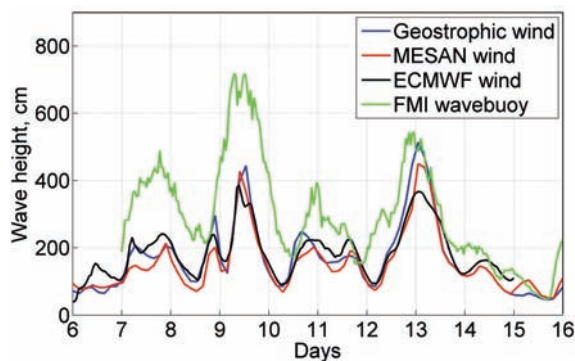


Figure 3. Measured and modelled wave heights in January 2005 in the northern Baltic Proper (cf. Soomere et al. 2008).

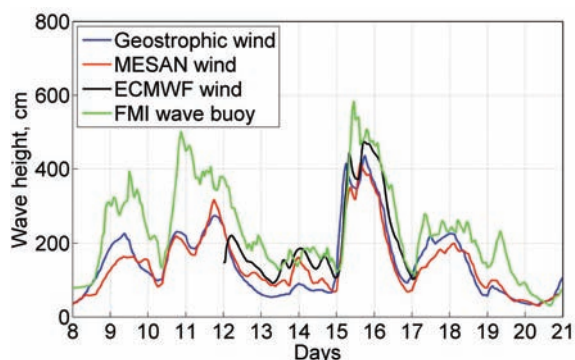


Figure 4. Measured and modelled wave heights in November 2001 in the northern Baltic Proper.

4. Conclusions

It is well known that wind fields reconstructed from atmospheric models frequently underestimate the open sea wind speeds. It is therefore, not unexpected that runs based on the high-quality ECMWF wind fields result in a certain underestimation of the wave properties. Therefore an alternative source of wind information is necessary in order to reproduce the temporal course of wave fields in particular storms. This conjecture has been highlighted, for example,

by studies in the Mediterranean over decades ago (L. Cavaleri, personal communication). A first-order solution would be, for example, the use of altimeter data and, if possible, scatterometer data.

Another interesting feature in Figures 3 and 4 is that the highly sophisticated ECMWF model consistently leads to results that insignificantly differ from those obtained with the use of the simplest adjustment of the geostrophic wind. Therefore, although geostrophic wind suffers from shortcomings for semi-enclosed sea areas, its use for long-term wave hindcast properties seems to be a very reasonable, if not the best, way to account for realistic wind fields in the Baltic Sea today. There are, of course clear limitations in its use. For example, one can trust general statistics and selected trends but generally not the hindcast time series or instantaneous values.

The ECMWF winds were kindly presented by Luciana Bertotti and Luigi Cavaleri for the reconstruction of wave fields in extreme wave storms in the Baltic Sea basin.

References

- Broman, B., Hammarklint, T., Rannat, K., Soomere, T., Valdmann, A. (2006) Trends and extremes of wave fields in the north-eastern part of the Baltic Proper, *Oceanologia*, Vol. 48, Special Issue, pp. 165–184.
- Bumke, K., Hasse, L. (1989) An analysis scheme for determination of true surface winds at sea from ship synoptic wind and pressure observations, *Boundary-Layer Meteorology*, Vol. 47, pp. 295–308.
- Häggmark, L., Ivarsson, K.-I., Gollvik, S., Olofsson, P.-O. (2000) MESAN, an operational mesoscale analysis system, *Tellus*, Vol. 52A, pp. 2–20.
- Komen, G. J., Cavaleri, L., Donelan, M., Hasselmann, K., Hasselmann, S., Janssen, P. A. E. M. (1994) *Dynamics and Modelling of Ocean Waves*, Cambridge University Press.
- Räämet, A., Soomere, T. (2010) The wave climate and its seasonal variability in the northeastern Baltic Sea, *Estonian Journal of Earth Sciences*, Vol. 59, in press.
- Räämet, A., Suursaar, Ü., Kullas, T., Soomere, T. (2009) Reconsidering uncertainties of wave conditions in the coastal areas of the northern Baltic Sea, *Journal of Coastal Research*, Special Issue 56, Vol. 1, pp. 257–261.
- Seifert, T., Tauber, F., Kayser, B. (2001) A high resolution spherical grid topography of the Baltic Sea, 2nd edition, *Baltic Sea Science Congress*, Stockholm 25–29 November 2001, Poster 147.
- Soomere, T. (2005) Wind wave statistics in Tallinn Bay, *Boreal Environment Research*, Vol. 10, pp. 103–118.
- Soomere, T. (2008) Extremes and decadal variations of the northern Baltic Sea wave conditions, in Pelinovsky, E., Kharif, Ch., Eds., *Extreme Ocean Waves*, Springer, pp. 139–157.
- Soomere, T., Zaitseva, I. (2007) Estimates of wave climate in the northern Baltic Proper derived from visual wave observations at Vilsandi, *Proceedings of Estonian Academy of Sciences. Engineering*, Vol. 13, pp. 48–64.
- Soomere, T., Behrens, A., Tuomi, L., Nielsen, J.W. (2008) Wave conditions in the Baltic Proper and in the Gulf of Finland during windstorm Gudrun, *Natural Hazards and Earth System Sciences*, Vol. 8, pp. 37–46.
- Zaitseva-Pärnaste, I., Soomere, T., Räämet, A. (2010) Seasonal and long-term variations of wave conditions in Estonian coastal waters, *Boreal Environment Research*, submitted.

Energy and water budget over the BALTEX domain from a suite of atmospheric regional climate models (present and future)

Burkhardt Rockel

Institute for Coastal Research, GKSS Research Centre, Geesthacht, Germany (rockel@me.com)

1. Introduction

One of the main aims of BALTEX is the quantitative description of the energy and water cycle over the Baltic Sea catchment area. One can try to achieve this by observations or/and model simulations. In the present study the main focus is on model simulations.

2. Data bases

In the European Union funded project ENSEMBLES (<http://ensembles-eu.metoffice.com/>) the major European institutes in regional climate modeling attended and even from Canada and Russia institutes joint voluntarily, i.e. non-funded. These institutes provide results from a variety of regional climate simulations for the period 1950-2050 and some even 1950-2100. The simulations were performed with a few exceptions for the scenario A1B and a horizontal grid mesh size of 25km. Driving data were taken from different global climate models. A total number of twenty GCM-RCM combinations are considered in the present study. I used the monthly mean results provided in the ENSEMBLES RCM data archive at the DMI (Danish Meteorological Institute).

3. Theory

The four water and energy budget equations described by Roads et al. (2002, 2003) are adopted in this study. A short overview with illustrations and definitions of the terms can also be found in the internet at <http://www.usask.ca/geography/MAGS/WEBS/html/3.html>

1. The atmospheric water budget:

$$\frac{\partial Q}{\partial t} = E - P + MC + RESQ$$

2. The surface water budget

$$\frac{\partial W}{\partial t} = P - E - N + RESW$$

3. The atmospheric energy budget

$$C_p \frac{\partial \{T\}}{\partial t} = QR + LP + SH + HC + REST$$

4. The surface energy budget

$$C_p \frac{\partial \{T_s\}}{\partial t} = QRS - LE - SH + RESG$$

4. Results

As examples (additional results will be presented on the conference) the future change in P-E (precipitation - evaporation) and the surface energy budget QRS-LE-SH is given in Figures 1 and 2 over the Baltic Sea catchment area, respectively. The box plots show the spread of the model mean daily values for three thirty year periods of the present (or better: near past) (1971-2000), near future (2021-2050)

and the end of this century (2071-2100). For comparison the results from hindcast simulations are also plotted. In the hindcast simulations RCMs were driven with ERA40 reanalysis. Even though the P-E values show an increase of the model mean in future the spread of the results from the models is very large.

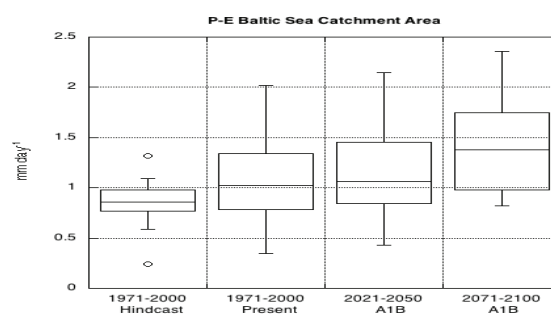


Figure 1. Daily mean P-E from an ensemble of RCM simulations over the Baltic Sea Catchment area for three thirty year periods.

The model mean of the surface energy budget (Figure 2) decreases slightly from present to the near future and increases towards the end of this century.

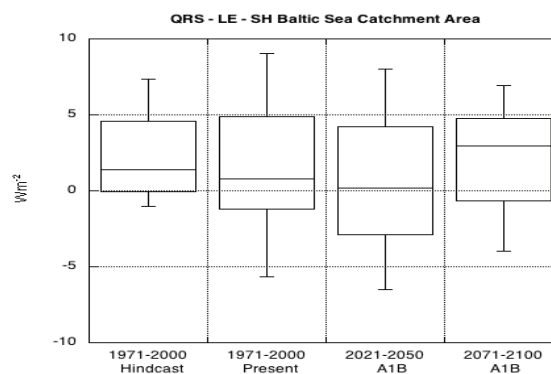


Figure 2. Mean surface energy budget from an ensemble of RCM simulations over the Baltic Sea Catchment area for three thirty year periods.

References

- Roads, J., M. Kanamitsu, R. Stewart (2002) CSE Water and Energy Budgets in the NCEP-DOE Reanalysis II, *J. Hydrometeorol.*, 3, 227-248
- Roads, J., R. Lawford, E. Bainto, E. Berbery, S. Chen, B. Fekete, K. Gallo, A. Grundstein, W. Higgins, M. Kanamitsu, W. Krajewski, V. Lakshmi, D. Leathers, D. Lettenmaier, L. Luo, E. Maurer, T. Meyers, D. Miller, K. Mitchell, T. Mote, R. Pinker, T. Reichler, D. Robinson, A. Robock, J. Smith, G. Srinivasan, K. Verdin, K. Vinnikov, T. Vonder Haar, C. Vösömarty, S. Williams, E. Yarosh, (2003) GCIP water and energy budget synthesis (WEBS), *J. Geophys. Res.*, Vol. 108, No. D16, 8609, doi:10.1029/2002JD002583, pp. 39

Introducing air-sea interaction processes in numerical models

Anna Rutgersson¹, Øyvind Sætra², Alvaro Semedo^{1,3}, Björn Carlsson¹, Rajesh Kumar¹ and Øyvind Brevik²

¹ Department of Earth Sciences, Meteorology, Uppsala University, Sweden (anna.rutgersson@met.uu.se)

² Norwegian Meteorological Institute, Oslo, Norway

³Riso-DTU National Laboratory for Sustainable Energy Technical University of Denmark, Roskilde, Denmark

1. Introduction

The globe surface is to 70% covered by water and a substantial part of most global as well as regional models cover partly ocean areas. Thus it is of great importance that processes over sea and air-sea interaction are included in atmosphere- and ocean-climate, as well as prediction models. What makes the ocean different from land areas is the fact that the surface roughness changes as a result of the forcing (in terms of waves), and also that sea surface temperature changes as a result of the forcing (due to mixing in the ocean). Ocean areas are to a much less extent driven by the diurnal cycle, being of great importance over land. The importance of sea surface temperature changes and waves introduces the need for atmospheric models coupled to the ocean as well as wave models for a correct surface description. It is, however, not enough to introduce coupled model systems. The important air-sea interaction processes need a correct description and the model components need to be consistent. In this study, the coupled atmosphere-wave model RCA-WAM (Rutgersson et al. 2009) is used to analyse the importance of introducing surface waves in a regional climate model and the sensitivity to resolution as well as to other factors. Using a coupled wave-atmosphere model introduces the possibility to improve a number of air-sea interaction processes, such as introducing a wave dependent roughness length, but also to take into account precipitation effects on wave growth.

2. Models

2.1 RCA

The atmosphere model RCA is developed at SMHI (Swedish Meteorological and Hydrological Institute) and its domain covers Europe (see Figure 1). It is a hydrostatic model, with terrain-following coordinates and the calculations are semi-Lagrangian, semi-implicit and with 30-min time step. The horizontal resolution is c. 50 km and resolved in the vertical by 24 levels between 90 m above the surface and 10 hPa. For the present study no present or future climate model is used for the boundary forcing to the RCA but reanalysis data from ERA40 (Uppala et al. 2005). The ECMWF (European Centre for Medium range Weather Forecasts) reanalysis uses all available observations integrated into a 3D model to give the best possible gridded data base on atmospheric parameters. The purpose of using reanalysis data is to evaluate the model system and investigate the impact on the atmosphere as well as on the wave field in using a coupled system. For more details on the model, see Jones et al. (2004).

2.2 Wave model - WAM

The wave model WAM is a state-of-the-art third generation wave model designed for ocean wave modelling (WAMDI, 1988; Komen et al. 1994). The WAM model is based on the spectral energy balance equation, which describes the evolution of the wave spectrum as the sum of the local wind input, wave dissipation, nonlinear wave-wave interaction

and the propagation of waves from non-local sources. The wave transport equation is explicitly solved without prior imposed restrictions on the shape of the wave spectrum. Wind speed at 10 meters from the atmospheric model is used as input to the model. When having a limited domain as in the present study, information of propagating waves should also be introduced at the boundaries. This is, however, not included in this study. For the semi-enclosed basins (Baltic Sea and Mediterranean) this has minimal direct impact on the wave field. Also for the North Sea, the direct impact of swell propagating across the boundaries is very limited since the majority of swell is expected to be transported from the western boundary of the domain. For the Atlantic basin the impact can, however, be substantial. The expected impact on the results is an underestimation of the swell part of the wave spectra, especially in the outer part of the modelling domain.

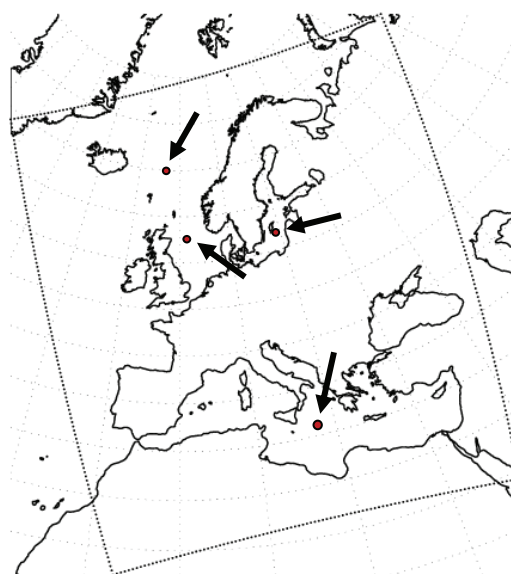


Figure 1. Model domain and the four regions being particularly investigated.

3. Results

Introducing a wave dependent surface roughness and the strong reduction found during swell (Figure 2) gave relatively large impact on the model simulation. The direct effect is a reduced mean surface roughness, a slight increase in wind speed and wave height and a reduction of surface heat fluxes. Also secondary effects can be seen such as a reduction and a redistribution of precipitation. Figure 3 shows the mean difference between a reference run (C1), a run when growing waves are introduced (C2)

and a run when both growing waves and swell are introduced (C3).

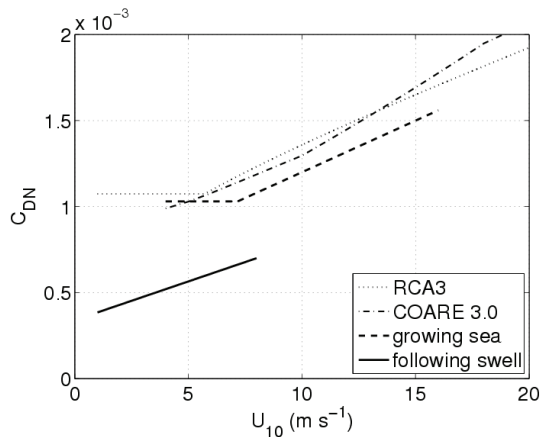


Figure 2. Drag coefficient for growing sea (dotted line show expression used in the original version of the RCA3 model, dashed-dotted line show the commonly used COARE algorithm (Fairall et al., 2003) and dashed line the expression developed in (Carlsson et al., 2009) and swell (solid line, expression developed in Carlsson et al., 2009).

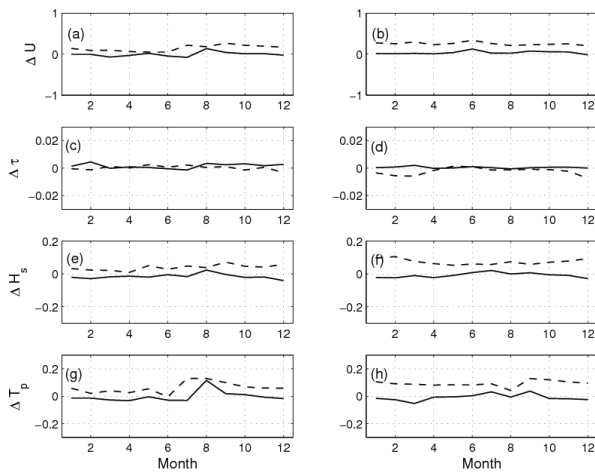


Figure 3. Mean monthly difference between simulation C1 and C2 and C3 respectively (C2-C1 solid and C3 – C1 dashed) for wind speed at 10 m (a and b), surface stress (c and d), significant wave height (e and f) and peak wave period (g and h). Left panel (a, c, e and g) shows the Baltic Sea area and right panel (b, d, f and h) the Mediterranean area.

Additional air-sea interaction processes are shown to have a great importance, such as the near-neutral regime, which increases the sensible and latent heat fluxes under near neutral stratification and also the height of the boundary layer, which alters the non-dimensional gradients and thus the applicability of Monin-Obukhov similarity theory over the sea.

References

- Carlsson B., A. Rutgersson and A. Smedman: Investigated the effect of including wave effects in the process oriented model PROBE-Baltic. *Bor. Env Res.*, 14, 3-17, 2009.
- Fairall C. W., E. F. Bradley, J. E. Hare, A. A. Grachev and J. B. Edson, Bulk Parameterization of Air-Sea Fluxes: Updates and Verification for the COARE Algorithm, *J. Climate*, Vol. 16, 571-591, 2003.
- Jones, C. G., Willén, U., Ullerstig, A. and Hansson, U. The Rossby Centre Regional Atmospheric Climate Model Part I: Model Climatology and Performance for the Present Climate over Europe. *Ambio* 33:4-5, 199-210.
- Komen, G. J., Cavaleri, L., Donelan, M., Hasselmann, K., Hasselmann, S. and P. A. E. M. Janssen, 1994, "Dynamics and Modelling of Ocean Waves", Cambridge University Press, 532 p.
- Rutgersson, A. Ø. Sætra, A. Semedo and B. Carlsson, Impact of surface waves in a Regional Climate Model. Submitted.
- Uppala et al. The ERA-40 Re-analysis, Q.J. Roy. Meteorol. Soc., 131, 2961-3012. 2005
- WAMDI Group, 1988. "The WAM Model - A Third Generation Ocean Wave Prediction Model," *J. Phys. Oceanogr.* 18, 1775-1810.

New dataset of highly resolved atmospheric forcing fields for 1850-2009

Frederik Schenk and Eduardo Zorita

Institute for Coastal Research, GKSS Research Centre, Geesthacht, Germany (frederik.schenk@gkss.de)

1. Introduction

For the detection and attribution of changes in the ocean-climate system of the Baltic Sea, long, homogeneous and spatiotemporal highly resolved data sets are needed. Besides their possible use as forcing fields of regional climate and biochemical ocean models, these data sets are important for a better estimation of model uncertainties on a high resolution level.

Resulting from the relatively shallow and complex basin of the Baltic Sea, the marine ecosystem is highly sensitive to changes also on short timescales. Most prominently, the occurrence of extreme events like storms can have a high impact on oxygen and salinity exchange with the North Sea. In order to attribute short-term variability and extremes, highly resolved daily atmospheric forcing fields for Northern Europe are reconstructed from long historical station measurements for 1850-2009 with a horizontal resolution of $0.25^\circ \times 0.25^\circ$.

2. The Analog-Method

Underestimating the variability by more than a factor of two, linear regression techniques are not useful if the variability of the reconstruction is of great importance (von Storch et al. 2004). In order to obtain a comparably good variance in the reconstruction, we use the analog-method as a simple non-linear upscaling method of station data to related atmospheric fields. The large-scale atmospheric circulation fields (predictand) are taken from a pool of atmospheric fields from a regional climate model. The best fitting atmospheric fields to the given variables from station measurements (predictor) are found by searching the smallest Euclidian distance between the vector field of the analogs and the vector field of the provided station data for each time step.

3. Data

As predictor for the analog-method, time series for SLP and T2m of 23 stations are used. Daily SLP data from 1850 is mainly taken from the EMULATE project (Mean Sea Level Pressure data set, EMSLP) (Ansell et al. 2006), updated till 2009 with data provided by the European Climate Assessment & Dataset (ECA&D) project (Klein Tank et al. 2002). As not all stations are contributing anymore to ECA&D, many station updates were kindly made available by the SMHI, FMI and the University of Jena, Germany.

In addition to daily SLP, monthly T2m station data is used as predictor for the T2m field reconstruction. This data is taken from Jones & Moberg (2003), updated by WMO.

For the predictands (analogs), daily atmospheric fields of SLP, wind, T2m, precipitation, rel. humidity and total cloud cover are used from a simulation of the Swedish Rossby Centre regional Atmosphere-Ocean model (RCAO) for 1957-2007. The simulation was interpolated from rotated grid to a regular grid and from a horizontal resolution of 0.5° to 0.25° . The model domain spans from 70.5° N and from 5° W to 36.75° E (see Figure 1).

4. Settings

In a first step, the analog-method is tested using the RCAO model as a surrogate climate. Spanning from 1958 to 2007, 25 years of the simulation are used crosswise for calibration and validation. Different numbers of grid points are used as synthetic stations (predictors) providing daily SLP (or T2m) information to find the best fitting atmospheric fields for SLP, U-/V-wind, precipitation, rel. humidity, total cloud cover and T2m.

The tests already show very good reconstruction skills for SLP and wind using only four to ten equally distributed grids/stations, if daily SLP is used as predictor. Due to the weak physical link between SLP and T2m, only T2m as predictor yields good skills for the reconstruction of T2m fields. Precipitation, cloud cover and humidity are showing low but significantly higher skills than their climatological mean on daily scale but good skills when comparing their monthly means.

As the analog of a given day in one month could also occur in the next surrounding months, the sample size for finding an analog is set to two months around the month of the searched day. This significantly improves the reconstruction skills with exception of T2m. Here, the analog is only searched in one month.

5. Results

In a second step, the calibration and validation is now repeated like before with real station data for 25 years, respectively. The general reconstruction skills are close to the testing results within the model environment.

The most important variables on daily scale, SLP and wind, show very good skills in winter (Figure 1 for January) and good skills in summer (fig. 2 for June). Lower skills in summer in the east and southeast part of the domain are caused climatically by the generally low wind speed off the sea and technically by partly missing data in this region.

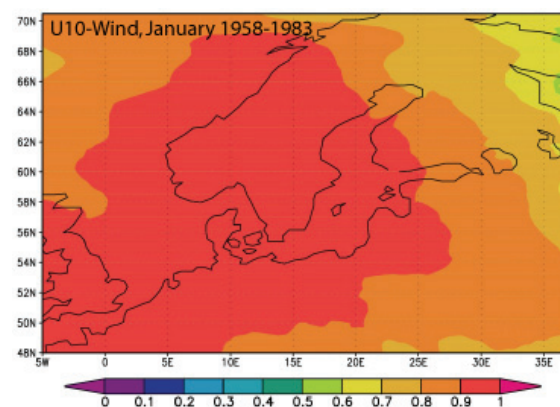


Figure 1. Field correlation of the reconstructed U-wind field with the original RCAO fields for January over the validation period of 1958-1983 (calibration 1984-2007).

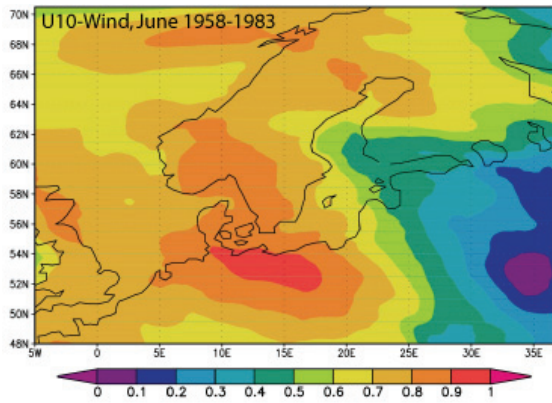


Figure 2. Field correlation of the reconstructed U-wind field with the original RCAO fields for June over the validation period of 1958-1983 (calibration 1984-2007).

In a third step, the analog-method is now applied for the reconstruction from 1850 to 2009 using 1958-2007 as calibration period. The reconstruction skills for the calibration period are shown for January in the Taylor-diagram in Figure 3. In addition to the mean cross-correlation of the reconstructed and the original field, the Taylor radius shows the standardized deviations which are calculated as the variance of the reconstruction divided by the variance of the reference fields from RCAO. For daily scale, the analog-method always leads to a ratio around one (blue dots). For monthly means, the variance of the reconstruction generally decreases while the correlation increases (red dots). Note, that only SLP and wind are important on daily scale while the other variables are needed on monthly to seasonal resolution.

As SLP is a too weak predictor for T2m also on monthly scale (Figure 3, blue dot Nr. 2), T2m is additionally reconstructed using monthly T2m data. The reconstructed monthly T2m fields are then interpolated on daily values and added on the daily anomalies of T2m reconstructed by daily SLP. While the skill for daily values is only slightly increasing (Figure 3, green dot), the monthly skill is now very good (Figure 3, orange dot) due to the added information from T2m predictor.

6. Discussion

The analog-method as a simple non-linear upscaling technique from daily station data is an excellent method to reconstruct daily SLP and wind with correlations up to 0.9. Although the physical link between SLP, humidity, cloud cover, and T2m is weak, these reconstructions are still showing better skills than their climatological mean on the daily scale.

However, these variables are more important on a monthly to seasonal scale. Here, their skills highly recommend also the use of the analog-method. This is also the case for precipitation which shows good daily skills in winter and generally good skills on monthly and seasonal scale.

Using the analog-method, T2m reconstructions generally need T2m as predictor because very similar SLP patterns are leading to very different T2m fields i.e. in spring and autumn. In addition, T2m is also influenced by other effects (e.g. SST, solar activity etc.) than SLP which also makes the analog-method blind for climate change signals in T2m when SLP is used as predictor.

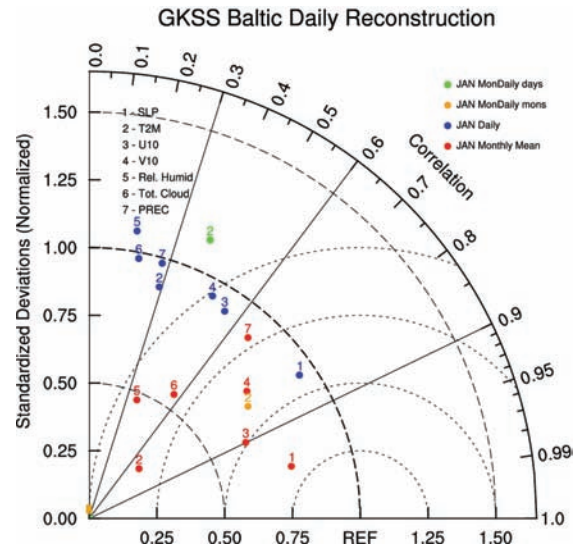


Figure 3. Taylor-diagram for the reconstruction skills of January over the calibration period 1958-2007 on daily and monthly scale.

References

- Ansell, T. J. et al. (2006): Daily mean sea level pressure reconstructions for the European - North Atlantic region for the period 1850-2003, *Journal of Climate*, Vol. 19, No. 12, pp 2717-2742.
- Jones, PD and A. Moberg (2003): Hemispheric and large-scale surface air temperature variations: An extensive revision and an update to 2001. *J. Climate*, Vol. 16, pp. 206-223.
- Klein Tank, A.M.G. et al., (2002): Daily dataset of 20th-century surface air temperature and precipitation series for the European Climate Assessment. *Int. J. Climatol.*, Vol. 22, pp. 1441-1453.
- Storch, H. v. and A. Omstedt (2008): Assessment of Climate Change for the Baltic Sea Basin. (BACC-Report)
- Storch, H. v., Zorita, E., Jones, J.M., Dimitriev, Y., González-Rouco, F. and S.F.B. Tett (2004): Reconstruction Past Climate from Noisy Data. *Science*, Vol. 306, No. 5696, pp. 679-682.
- Zorita, E. & H. von Storch (1999): The Analog Method as a simple statistical Downscaling Technique: Comparison with more complicated Methods, *Journal of Climate*, Vol. 12, No. 8, pp. 2474-2489.

A study of ASCAT wind measurements near the coastal region of Estonia

Jekaterina Služenikina¹ and Aarne Männik²

¹ Tallinn University of Technology, Estonian Meteorological and Hydrological Institute, Tallinn, Estonia (katjas@emhi.ee)

² University of Tartu, Estonian Meteorological and Hydrological Institute, Tallinn, Estonia.

1. Introduction

The Advanced Scatterometer (ASCAT) on Meteorological Operational (MetOp) satellite is a C-band radar whose primary function is to determine the wind field at the ocean surface (Figa-Saldaña et al. 2002). Wind scatterometers are instruments that are used to infer data on wind speed and direction from radar measurements of the sea surface. They rely for their operation on the fact that winds moving over the sea influence the radar backscattering properties of its surface in a manner that is related to wind speed and wind direction (Gelsthorpe et al. 2000).

The ASCAT wind product provides the wind speed and direction measurements at 10 m above sea surface. Data are provided on swath grid resolution of 25 km with grid spacing of 12.5 km and 50 km resolution with grid spacing of 25 km across and along swath, each spanning is 550 km wide on both sides of nadir track. ASCAT data are processed jointly by the EUMETSAT Advanced Retransmission Service (EARS) ground system and the Koninkrijk Nederlands Meteorologisch Instituut (KNMI). The processed ASCAT level 2 product is distributed to the users by EUMETSAT and Ocean and Sea Ice Satellite Application Facility (OSI SAF).

The ASCAT mission has been primarily designed to provide global ocean wind vectors operationally. The main application foreseen is the assimilation of those winds into numerical weather prediction (NWP) models. Furthermore, its dense coverage makes the winds useful for direct use by operational weather forecasters when performing the necessary real-time interpretation of NWP model results to elaborate a forecast (Figa-Saldaña et al. 2002).

The Estonian Meteorological Hydrological Institute (EMHI) is interested in the quality measurements of wind speed and direction over the Baltic Sea and is looking for ASCAT as a possible solution for operational monitoring of sea winds. The representativity of coastal wind measurements for the open sea should be evaluated as well.

2. The HIRLAM Model

HIRLAM (Unden et al. 2002) is a High Resolution Limited Area Model which generates operational numerical weather forecasts in the Estonian Meteorological and Hydrological Institute. HIRLAM version 7.1.2 calculates the weather forecasts in two modelling areas. The bigger ETA_II modelling area has a horizontal resolution 11.1 km and an experimental ETB_II modelling area with resolution 3.3 km. The boundary fields for the HIRLAM model are provided by the European Centre for Medium-Range Weather Forecasting (ECMWF) model, and HIRLAM has 60 vertical layers. The fields of ETA_II model are provided four times a day with forecasting start-point at 00, 06, 12 and 18 UTC with calculation of the forecasts every 3-hour time-step until 54 hours.

In the given research the ETA_II modelling area forecasts were used. Figure 1 shows the ETA_II and ETB_II modelling areas, as used in HIRLAM.

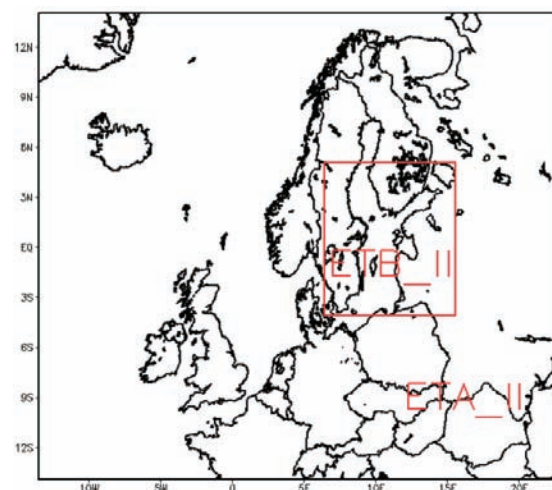


Figure 1. HIRLAM ETA_II and ETB_II modelling areas.

3. Study method

In the present study, the EARS ASCAT 12.5 km wind speed and the wind direction were used during the period of 01.10 – 04.12.2009. ASCAT wind observations were compared with the coastal wind observations at eleven automatic ground stations in Estonia. The ground station 10 m high wind measurements were implemented with a 1-hour interval. For the comparison of the ASCAT and the coastal ground station measurements, the wind product data were filtered geographically and the comparison was provided in the given area of interest: latitude 56°-61°, longitude 20°-28°. The time of ASCAT data measurements was compared with the time of automatic observations and the closest to ASCAT measurements 1-hour mean wind speed and direction were used. In the present study, the automatic wind measurements closest to the MetOp measurements were used. In addition, the closest HIRLAM wind and mean sea level pressure forecast data was coincidentally added. As a result, all three data types were compared between each other. Unfortunately, sea buoy or ship measurements were not available for the study but it would be really advantageous to extend the study in this respect.

4. Preliminary results

In general, the wind directions of ASCAT, HIRLAM and coastal stations in the present study showed similar results. The visual comparison of wind direction and wind speed showed quite good coincidence between the ASCAT measurements and HIRLAM forecasts (Figure 2).

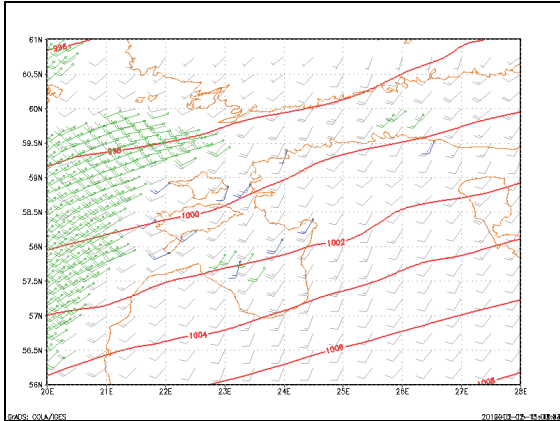


Figure 2. The winds of ASCAT, HIRLAM and coastal stations of Estonia. (ASCAT wind measurements 28.11.2009 at 17:52 UTC). The green wind barbs (m/s) represent ASCAT wind, blue coloured wind barbs (m/s) are the coastal station winds. On the figure the mean sea level pressure (red contours, hPa), the wind speed and direction (grey wind barbs, m/s) is the HIRLAM model 6-hour forecast.

In addition, the study results showed (Figure 3) that the coastal ground stations measure in some cases weaker winds than the ASCAT and the measurements are direction specific due to the friction of mainland.

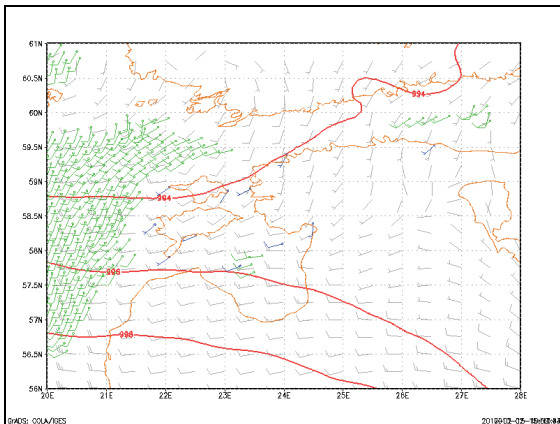


Figure 3. The winds of ASCAT, HIRLAM and coastal stations of Estonia. (ASCAT wind measurements 19.11.2009 at 19:19 UTC).

Preliminary results show the ASCAT winds have a good potential to be used in the operational tracking of the weather over Baltic Sea during a stormy conditions. However, the study has to be extended to find a quantitative estimation of the difference between the numerical model and the ASCAT observations.

References

- Figa-Saldaña, J., J.J.W. Wilson, E. Attema, R. Gelsthorpe, M.R. Drinkwater en A. Stoffelen, (2002) The advanced scatterometer (ASCAT) on the meteorological operational (MetOp) platform: A follow on for the European wind scatterometers Can. Jour. Remote Sensing, 2002, 28, 3, 404-412.

- Gelsthorpe, R.V., Schied, E., and Wilson, J.J.W. (2000) ASCAT-MetOp's advanced scatterometer. ESA Bulletin 102. Available at <http://esapub.esrin.esa.it/bulletin/bullet102_.htm>.
- Undén P., Rontu L., Järvinen H., Lynch P., Calvo J., Cats G., Cuxart J., Eerola K., Fortelius C., Garcia-Moya J.A., Jones C., Lenderink G., McDonald A., McGrath R., Navascues, B., Nielsen N.W., Ødegaard V., Rodrigues E., Rummukainen M., Rööm R., Sattler K., Sass B.H., Savijärvi H., Schreur B.W., Sigg R., The H., Tijn, A. (2002) HIRLAM-5 scientific documentation. <Available at member institutes or online at <http://hirlam.org>>.

Sensitivity of the CCLM to changing land use in Eastern Europe

D. Söhl, D. Pavlik and C. Bernhofer

Chair of Meteorology, Technische Universität, Dresden, Germany (dennis.soehl@tu-dresden.de)

1. Introduction

In the framework of the BMBF research project “International Water Research Alliance Saxony” (IWAS) the answers to typical water problems in five regions of the world should be revealed via an “Integrated Water Resource Management” (IWRM) approach. One of these five regions is the Western Bug River Basin (Figure 1), representing a small subbasin of the Baltic Sea and its catchment area. For this subdomain, regional climate simulations with the dynamical regional climate model CCLM (Doms et al. 2002), are performed by the Chair of Meteorology at the Technische Universität Dresden (TUD). For the dynamical downscaling from a driving model with ca. 200km resolution to a 7km-grid, the model chain consists on a double-nesting approach with an intermediate downscaling step to 50km. The model setup for an ERA40-driven control run from 1961 to 1990 is evaluated with 2m temperature and precipitation reference data from the CRU and the GPCC, respectively.

2. Main goal

To construct a realistic driving-scenario for these regional climate projections, together with the atmospheric driving data, possible changes in land use and their effects to atmospheric variables have to be considered. The construction of realistic regional land use scenarios is a complex problem. Therefore this study should clarify, if the sensitivity of the CCLM to expected land use changes justifies such considerable effort in the context of omnipresent model uncertainties.

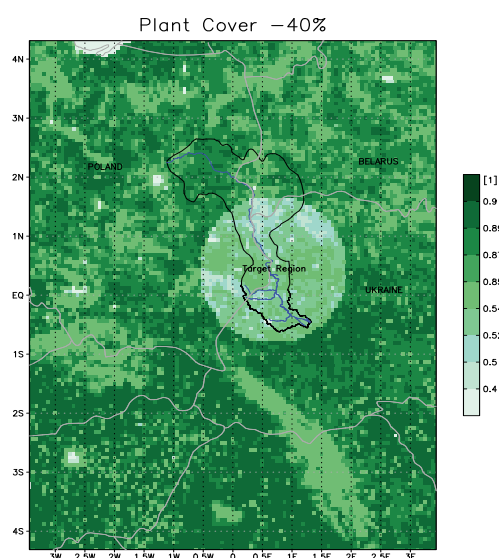


Figure 1. Western Bug River Basin; Plant cover variation in the test area to -40%. (circular region).

3. Research plan

For this sensitivity studies the external surface parameters plant cover (PLCOV), leaf area index (LAI), and total forest cover (FOR), consisting on the two parts evergreen and deciduous forest cover, are selected from the external model parameter fields. Inside a circular area with 280km diameter covering the target region, these three parameter fields are varied to investigate effects on the model variables. The parameter variation ranges from +20% to -20% and -40% see, Figure 1. Although this range extends to quite unrealistic land use changes it gives a first idea of the models sensitivity. To save computing time, each of these nine model runs have been limited to two years, 1960 for spin up and 1961 for comparison with the reference run.

4. Results

As important output variables for further water balance studies, the effects on total precipitation (tot_prec), 2m-temperature (t_2m), and absolute 10m-wind speed (wind_speed_10m) are evaluated for the year 1961. Figure 2 shows the monthly mean 2m-temperature differences from the a model run with -40% plant cover in the test region (Figure 2) compared to the reference run for June.

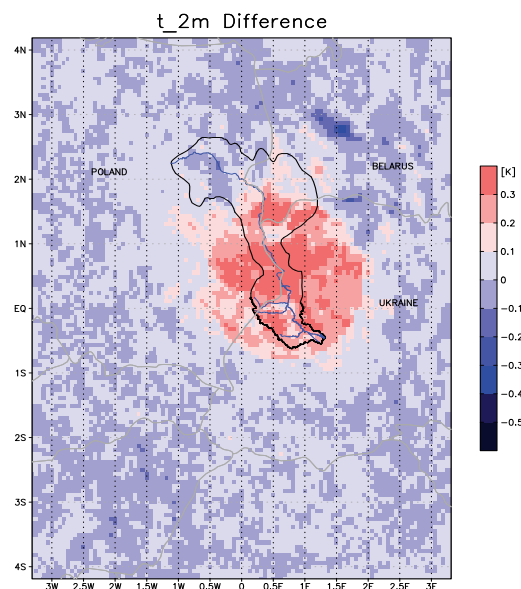


Figure 2. 2m-temperature differences resulting from plant cover change to -40% in the target region.

It shows a warm bias up to 0.3 K in the area corresponding to 40% less plant cover. Figure 3 shows the annual cycles of the variables for 1961, averaged over the test region, and their variations related to changed external parameters. The strongest effects are visible during the vegetation period.

5. Conclusions

The effects on the 2m and 10m levels might be explained due to direct impacts of physics, whereas the structure of total precipitation differences shows a more chaotic behavior which might be linked to the complex model dynamics.

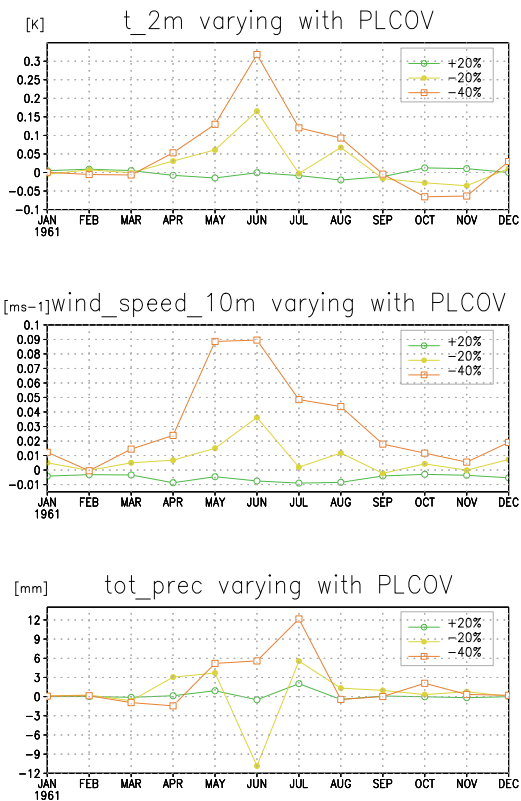


Figure 3. Monthly mean annual cycles of evaluated variables for 1961 and three variations of plant cover. The variables differences to the reference run are averaged over the test area (Figure 1 and 2).

6. Outline

A statistical analysis of the deviation from the reference run should give information about the sensitivity of the CCLM. It must be clarified whether the model results correspond to the theoretically expected tendencies. Finally the effects of land use scenarios have to be compared to model uncertainties.

References

- G. Doms, U. Schättler (2002) A Description of the Nonhydrostatic Regional Model LM

Large scale skill in regional climate modeling and the lateral boundary condition scheme: 32-day ensemble experiments

Katarina Veljovic¹, Borivoj Rajkovic¹ and Fedor Mesinger²

¹ Institute of Meteorology, Faculty of Physics, Univ. Belgrade, Serbia (katarina@ff.bg.ac.rs)

² ESSIC, Univ. Maryland, College Park, Maryland, and Serbian Academy of Sciences and Arts, Belgrade, Serbia

1. Summary

The main question we address is whether a regional climate model (RCM), with no large scale nudging, can maintain the large scale skill of the driver global model supplying its lateral boundary condition (LBC). More ambitiously, can an RCM even improve on the large scales of the driver model? Another issue we address is that of the RCM's lateral boundary condition scheme: is the almost universally used but somewhat costly relaxation scheme necessary for a desirable RCM performance?

We address this by running the Eta model in two versions differing in the lateral boundary scheme used. One of these is the traditional relaxation scheme and the other is the Eta model scheme in which information is used at the outermost boundary only and not all variables are prescribed at the outflow boundary. The skills of these two RCM forecasts are compared against each other and also against that of their driver. Global data dynamically downscaled to address these issues is an ECMWF 32-day ensemble forecast. A novel verification method is used in the manner of precipitation verifications in that forecast spatial wind speed distribution is verified against analyses by calculating bias adjusted (or, corrected) equitable threat score (ETSa) and bias score for wind speeds greater than a chosen threshold. In this way, focusing on the forecast position of high wind speed values in the upper troposphere, verification of large scale features we suggest can be done in a manner that is physically more direct than verifications via spectral decomposition often used as RCM verification method.

Our results show the Eta RCM skill in forecasting large scales with no interior nudging to be just about the same as that of the driver model. As to the LBC impact no disadvantage compared to relaxation was seen from using the Eta LBC scheme, in spite of its requiring information from the outermost RCM boundary only.

2. Background

In spite of this considerable maturity of the field, there are issues on which there is little agreement in the RCM user community. The one which we shall address here is that of the desirable, or attainable, "added value" of the RCM simulation compared to the information present in the driver global fields used. Clearly, the extra effort of running a limited area model in order to make sense needs to achieve results which are in some ways superior to those we have; that is, they need to have "added value". Higher regional detail resulting from higher resolution is the obvious candidate. What is not obvious though is, for given resources, what resolution should we aim at? The choice of resolution is in our hands, but it is related to the size of the RCM domain we can afford to use. Thus, what size RCM domain is desirable is a related question. Common sense suggests that a domain size sufficiently large so as to accommodate regional-scale synoptic systems over the region of interest, with the lateral boundaries some distance away, is needed for the desired result. This consideration as just stated encourages the use of larger domains, e.g. larger

than the continent of Europe or perhaps North America, and maybe larger still. But for larger domains an additional issue comes in: that of "internal variability", or of the spread between members in an ensemble of simulations with the same lateral boundary conditions (LBCs) and surface forcing (e.g. Laprise et al. 2008). This should come as no surprise since the larger the RCM domain is the more freedom is there for the chaotic behavior of the atmosphere to have an impact on the results. Thus, the larger the domain is the more we should expect RCM results to differ from the driver global fields not only in regional detail but in the larger scales to the extent they can be accommodated in the domain used as well. It has however been repeatedly argued by one of us (e.g. Mesinger 2004) that in the regional weather forecasting at NCEP using the Eta model strong indications were seen that the Eta model benefited from its very large domain, and that this can only be explained by its improving on the large scales compared to those of the driver global model supplying the lateral boundary conditions. Following in the footsteps of this experience, also in the regional climate use of the Eta large domains tended to be used.

3. Methodology

We are running the regional Eta model in two versions differing in the lateral boundary scheme used. One of these schemes is the traditional relaxation scheme, and the other the Eta model scheme in which information is used at the outermost boundary only, and not all variables are prescribed at the outflow boundary. Skill of these two RCM forecasts is compared against each other and also against that of their driver global forecast.

We have run 26 32-day forecasts, driven by the ECMWF control and 25 ensemble members, and have performed verifications of both the Eta and the driver ensemble members' results against ECMWF analyses. We have run the Eta on a 12,000 x 7,580 km domain using a 31 km/45 layer resolution.

4. Results

In Figure 1 we show the bias adjusted equitable threat score (ETSa) for the chosen wind speed threshold of 45 m s⁻¹, upper panel, and bias score, lower panel, of the ECMWF control forecast (red line), and of the two Eta forecasts driven by this ECMWF control: the standard Eta (blue line) and the Eta using the relaxation LBC scheme (green line), respectively.

The bias adjusted equitable threat score (ETSa) displayed suggests that the Eta model run using the Eta LBC scheme had significantly better large scale skill than the ECMWF global model that was supplying its LBCs no less than 15 days continuously, from January 8 to 23, and the last two days of the integration time as well. From January 24 to 30, the global model shows a better ETSa than the Eta, by a similar but perhaps overall a slightly smaller margin.

As to the comparison of the blue and the green lines after

the first 10 days of integration, displaying the Eta scores using two different LBC schemes, we can see that the Eta LBC scheme run had a visibly higher ETSa during a total of about 10 days of that 22-day period, and the relaxation scheme run during a period of overall about half that long, respectively. Note that for the purposes of our two objectives the initial period of perhaps about 10 days while the Eta runs are adjusting to their different topography and the initial condition is being flushed out of the domain is not as relevant as the period afterwards, which is why we are focusing on the period we do.

Regarding the bias plot of the lower panel, the standard Eta is seen to deal visibly better than the others with the period of the intense jet stream inside the domain, during the days 17-19. But perhaps the main point worth noting is that no systematic tendency can be seen for one of the runs to maintain a continuous advantage over the others. In other words, both in this and in the upper panel plot each of the models has times of its displaying a better score than the others.

Next we present skill scores of two ensembles, global and regional in the form of one line for whole ensemble, cumulative score. Figure 2 shows cumulative scores of global ECMWF (in red lines) and regional Eta ensemble forecasts (in blue lines). In the upper panel of Fig. 2 we can see that after the initial 10-day period of the integration the ETSa of the Eta ensemble forecast for the chosen 45 m s^{-1} category is most of the time slightly better than that of its driver forecasts. One should recall that the ETS score is not credited for random skill so that in contrast to individual forecasts in the overall ensemble scores both models do exhibit some large scale skill throughout the 32-day integration period. It is worth noting that one may expect the Eta in this verification to be somewhat at a disadvantage given that the verification analysis used shares the same ECMWF forecasting model with the ensemble the Eta is compared against. This, the advantage of the Eta at some of the time such as around days 21-23 and 25-26 might not be as insignificant as it may seem looking at the plot of the upper panel of Figure 2.

References

- Laprise, R., R. de Elía, D. Caya, S. Biner, P. Lucas-Picher, E. Diaconescu, M. Leduc, A. Alexandru, and L. Separovic, 2008: Challenging some tenets of Regional Climate Modelling. – *Meteor. Atmos. Phys.*, **100**, 3-22.
- Mesinger, F., 2004: The Eta model: Design, history, performance, what lessons have we learned? In: Symposium on the 50th anniversary of operational numerical weather prediction, Univ. of Maryland, College Park, MD, 14-17 June 2004, 20 pp, Preprints CD-ROM, available from NCEP, 5200 Auth Road, Room 101, Camp Springs, MD 20746-4304 (ppt at <http://www.ncep.noaa.gov/nwp50/Presentations/>)

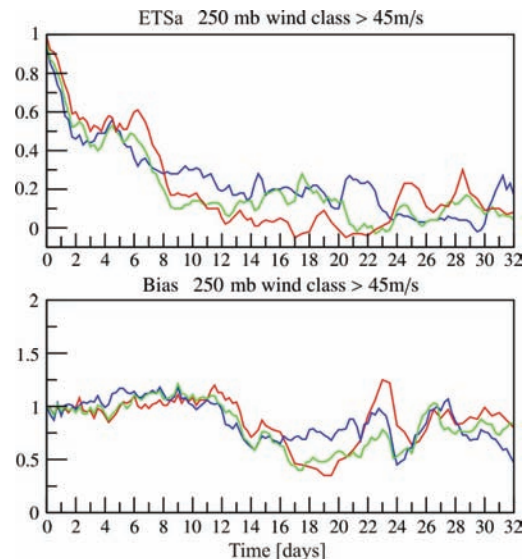


Figure 1. Bias adjusted ETS (ETSa), upper panel, and bias, lower panel, of 250 mb wind speeds $\geq 45 \text{ m s}^{-1}$, of three 32-day integrations, verified against ECMWF T799 analyses, as a function of forecast time (days). ECMWF T399 control forecast, used for the initial condition and for the LBCs of the two Eta forecasts, red line; Eta forecast using the Eta LBC scheme, blue line; and the Eta forecast using the relaxation LBC scheme, green line. See text for more detail.

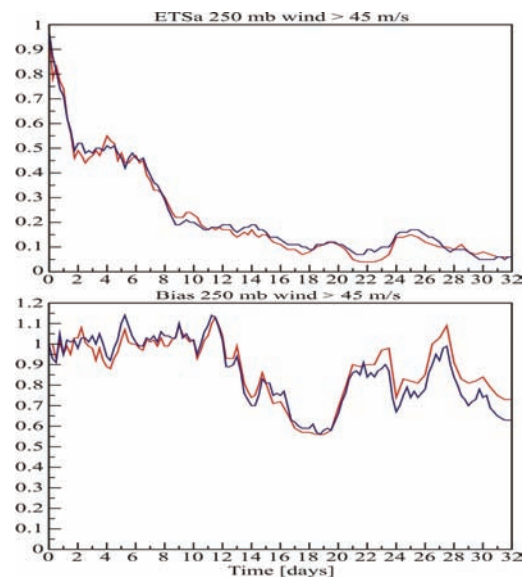


Figure 2. Bias adjusted ETS score, upper panel, and bias, lower panel, of 250 mb wind speed $\geq 45 \text{ m s}^{-1}$, of the ECMWF T399 global ensemble (control plus 25 members, red lines) used for the initial condition and for the LBCs of the 32-day Eta forecasts whose scores are shown in blue; verified against ECMWF T799 analyses, as a function of forecast time (days). Initial time is 0000 UTC 1 January 2009.

Air-sea interaction model for momentum and mass in the presence of wind waves

Christoph Zülicke

Leibniz Institute for Baltic Sea Research at Rostock University, Warnemünde, Germany.

Currently at: Leibniz Institute of Atmospheric Physics at Rostock University, Kühlungsborn, Germany (zuelicke@iap-kborn.de)

1. Introduction

The air-sea fluxes of momentum and mass are important quantities for the coupled ocean-atmosphere system. Analytical formulae are helping to understand empirical data and allowing for numerical simulations. In this paper, I aim to construct and apply an analytical air-sea interaction model (ASIM) for the transfer of momentum and mass including molecular and turbulent transport mechanisms. The impact of growing and breaking waves is included in the balance equations. This way, wave properties such as wave height and slope are reproduced together with the drag coefficient and the gas transfer velocity.

In the following the major assumptions and results are indicated for brevity. Further details are lined out in Zülicke (2010). The basic idea is, to find a simple formulation which allows for an analytic treatment and the derivation of scaling relations while basic experimental findings are readily reproduced. The task is to find profiles of dissipation, velocity and concentration for a given momentum and mass flux. The wave field should include primary (gravity) and secondary (capillary-gravity) waves.

2. Construction of the model

The balance equations for momentum, mass and turbulence are formulated as follows: The momentum flux

$$\tau = \tau_m + \tau_t + \tau_w = \rho u_*^2$$

is decomposed into a molecular, turbulent and wave-related part (indices “m”, “t” and “w”; ρ is the density and u_* the friction velocity). The drag coefficient is commonly used to relate the momentum flux to available wind speed data $Cd_{air} = \tau / (\rho_{air} \Delta u_{air}^2)$. For the mass flux

$$F_C = F_{C,m} + F_{C,t} = \rho u_* c_*$$

the wave-related advection is excluded (c_* is the friction concentration). The turbulent transport processes are specified with a K-L-closure including the turbulent dissipation rate (ε_t). Matching the turbulent bulk and molecular skin layer allows for relating the gas transfer velocity (Levich, 1962; Brutsaert, 1982)

$$K_{sea} = \frac{F_C}{\rho_{sea} \Delta c_{sea}} = 0.14 \frac{(v_{sea} \varepsilon_{v,sea})^{1/4}}{(v_{sea}/D_{sea})^{1/2}}$$

Here, the sea-side kinematic viscosity (ν), the diffusion coefficient (D) and viscous-sublayer dissipation (ε_v) are involved.

Wave properties are incorporated with specifying the saturation parameter (B_k) and the wave growth rate (γ_k). They include primary waves (characterized by the peak wave speed $c_p = \chi_p u_{*,air}$) and secondary waves (centered around the phase speed of $c_\gamma = 0.23 \text{ m s}^{-1}$). Hence, the wave-related momentum and energy flux are

$$\tau_w = \rho_{sea} \int_{k_p}^{k_v} dk \frac{B_k}{k^3} \omega_k \gamma_k$$

$$F_{e,w} = \rho_{sea} \int_{k_p}^{k_v} dk \frac{B_k}{k^3} \omega_k c_k \gamma_k$$

Here appears the wave frequency (ω_k) and phase speed (c_k); the integral extends over the wavenumbers (k) from the peak wave (k_p) to the viscous limit (k_v).

The model includes 11 independent parameters which were tuned against classical wall-flow theory and available data on significant wave height and surface slope (Toba, 1972; Wu, 1972).

3. Wind-wave interaction

The effect of growing waves is associated with a reduction of turbulent momentum flux in the air. This is modeled with the wave coupling parameter $\alpha_w = \tau_w / \tau$ which reproduced the compilation of Makin & Mastenbroek (1996). I adopt their form of the air-side balances

$$(1 - \alpha_w) u_{*,air}^2 = (v_{air} + v_{t,air}) \frac{\partial u_{air}}{\partial z}$$

$$c_{*,air} u_{*,air} = (D_{air} + D_{t,air}) \frac{\partial c_{air}}{\partial z}$$

$$\varepsilon_{t,air} = u_{*,air}^2 \frac{\partial u_{air}}{\partial z}$$

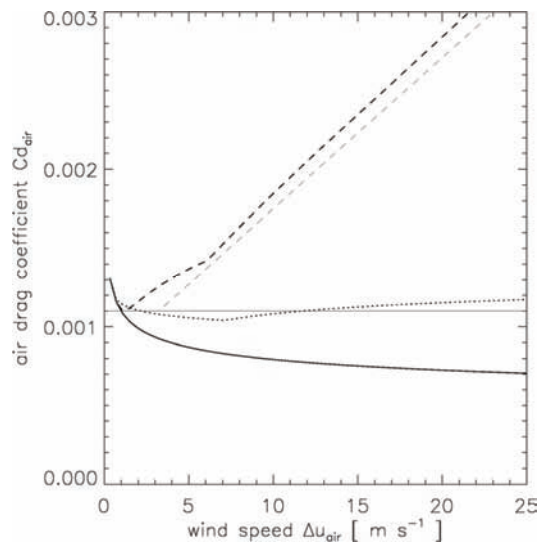


Figure 1. Wind-dependent drag coefficient for different wave ages (0: solid; 5: dashed; 25: dotted) for the analytical solution (thick) and the fit (thin).

The related drag coefficient (fig. 1) is most increased for young waves. I found a reasonable fit with

$$\overline{Cd}_{air} = \begin{cases} 1.1 \times 10^{-3} & \text{(smooth)} \\ 1.1 \times 10^{-3} + 5.6 \times 10^{-5} (0.34 \chi_p \Delta u_{air} - 5.5 \text{ m s}^{-1}) & \text{(rough)} \end{cases}$$

for the regimes of aerodynamically smooth and rough sea surfaces.

4. Wave-current interaction

The wave breaking is modeled as an injection of turbulent kinetic energy into the sea over a certain wave scale ($Z_{k,sea} = 1/(2k)$). The balance equations are oriented on Craig & Banner (1994) and read

$$u_{*,sea}^2 = (v_{sea} + v_{t,sea}) \frac{\partial u_{sea}}{\partial z_{sea}}$$

$$c_{*,sea} u_{*,sea} = (D_{sea} + D_{t,sea}) \frac{\partial c_{sea}}{\partial z_{sea}}$$

$$\epsilon_{t,sea} = u_{*,sea}^2 \frac{\partial u_{sea}}{\partial z_{sea}} - \frac{\partial F_{e,t,sea}}{\partial z_{sea}}$$

completed with the boundary condition $F_{e,t,sea}(z=0) = F_{e,w}(z=0)$. The dissipation profiles reproduced the observational findings of Terray et al. (1996) and Craig (2005). Beside these effects of primary waves at the meter scale I could also include the impact of secondary waves at the centimeter scale (Siddiqui & Loewen, 2007). The related process of microscale wave breaking increases the dissipation and, consequently, the gas transfer velocity considerably (fig. 2).

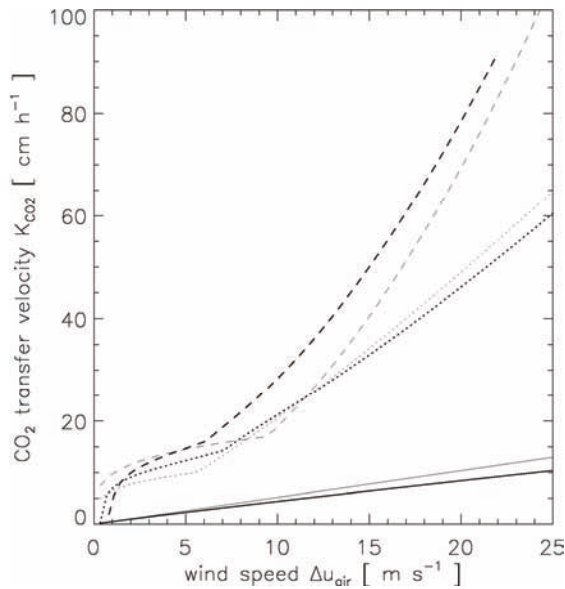


Figure 2. Wind-dependent CO₂ transfer velocity for different wave ages (0: solid; 5: dashed; 25: dotted) for the analytical solution (thick) and the limiting cases (thin).

In waveless situations a linear wind speed dependence is found. When primary waves are involved, the transfer velocity makes a jump and levels with a weaker wind speed dependence (1/4 power). It continues with a 5/4 power when secondary waves are breaking (Kitaigorodskii, 1984). For a wind speed exceeding 6 m s⁻¹, the sea surface becomes rough for the air flow, and the wind power continues even

steeper with 15/8 – nearly 2 (compare Wanninkhof et al., 2009). These limiting cases can be identified in

$$\overline{K}_{CO2} = \begin{cases} 0.52 \Delta u_{air} & \text{(waveless)} \\ 5 \frac{\Delta u_{air}^{1/4}}{\chi_p^{1/4}} & \text{(primary)} \\ 1.2 \Delta u_{air}^{5/4} & \text{(secondary \& smooth)} \\ 0.092 \Delta u_{air}^{15/8} \chi_p^{5/8} & \text{(secondary \& rough)} \end{cases}$$

Ter velocity is in cm h⁻¹ and the 10 m wind speed in m s⁻¹.

5. Summary and conclusion

The ASIM was developed to describe wind, waves and currents with a unified consistent approach. As a result, the wave-related momentum and energy flux could be connected with the drag coefficient, dissipation and gas transfer velocity. The air-side drag coefficient is mainly influenced by primary (gravity) waves, while the transfer velocity is highest when secondary (capillary-gravity) waves are involved. The inclusion of the wave age in the transfer velocity is a original achievement of this contribution.

The present model is applicable to neutral stratification and medium winds. For very calm situations, heating and cooling effects can be incorporated as has been described in Zülicke (2006). For stormy conditions, bubbles and sea spray require further model extensions.

References

- Brutsaert, W., 1982: Evaporation into the atmosphere. Reidl
- Craig, P.D., 2005: Modeling turbulence generation by breaking waves. in: Marine Turbulence. H.Z. Baumert, J. Simpson & J. Sünderman Eds. Cambridge Univ. Press: 273 – 276.
- Craig, P.D. & M.L. Banner, 1994: Modelling wave-enhanced turbulence in the ocean surface layer. J. Phys. Oceanogr. 24: 2546 – 2559.
- Kitaigorodskii, 1984: On the fluid dynamical theory for turbulent gas transfer across an air-sea interface in the presence of breaking wind-waves. J. Phys. Oceanogr. 14: 960 – 972.
- Levich, V.G., 1962: Physicochemical Hydrodynamics. Prentice-Hall Inc., London, 700 pp.
- Makin, V.K. & C. Mastenbroek, 1996: Impact of waves on air-sea exchange of sensible heat and momentum. Bound. Layer Meteorol. 79: 279 – 300.
- Siddiqui, M.H.K. & M.R. Loewen, 2007: Characteristics of the wind drift layer and microscale breaking waves. J. Fluid Mech. 573: 417 – 456.
- Terray et al., 1996: Estimates of kinetic energy dissipation under breaking waves. J. Phys. Oceanogr. 26: 792 – 807.
- Toba, Y., 1972: Local balance in the air-sea boundary processes. I. On the growth process of wind waves. J. Oceanogr. Soc. Japan 28: 109 – 121.
- Wanninkhof, R.H. et al., 2009: Advances in quantifying air-sea gas exchange and environmental forcing. Ann. Rev. Mar. Sci. 1: 213 – 244.
- Wu, J., 1972: Sea-surface slope and equilibrium wind-wave spectra. Phys. Fluids 15: 741 – 747.
- Zülicke, Ch., 2006: Air-sea fluxes including the effect of the molecular skin layer. Deep-Sea Res. Pt. II: 1220 – 1245.
- Zülicke, Ch., 2010: Air-sea fluxes of momentum and mass in the presence of wind waves. in preparation

Mesoscale patterns of wind and precipitation due to inertia-gravity waves in model simulations and observational networks

Christoph Zülicke

Leibniz Institute of Atmospheric Physics at Rostock University, Kühlungsborn, Germany (zuelicke@iap-kborn.de)

1. Introduction

The identification of mesoscale features in models and observations is a good test for the performance of both tools for regional and local weather forecasts. In this paper I present a case of wind pulsations and precipitation patterns in the Baltic Sea region which were related to inertia-gravity waves.

The meteorological situation from 17 to 19 December 1999 was characterized with a ridge over the North-East Atlantic including an upper-level jet streak at about 8 km altitude. From its exit region above the Baltic Sea inertia-gravity waves were emitted, which propagated upward and downward. They had a horizontal wavelength of ~ 220 km, a vertical wavelength of ~ 3.6 km and an intrinsic period of ~ 7.1 h. In a basic wind of 15 m s^{-1} they appear with a period of about 9.3 h at a fixed position.

The physical link of the wave properties to the wind and precipitation fields are discussed in Zülicke & Peters (2007). Here, I report on the validation exercise.

2. Compiled data sets

For following data sets were used:

MM5 (Fifth-generation mesoscale model, Pennsylvania State University / NCAR Boulder): Nested setup with $72 / 24 / 8$ km resolution covering the Northeast Atlantic / North European region centered over the Baltic Sea, up to 30 km altitude, run with full physics, using initial and boundary conditions from ECMWF Reading.

MESAN (Mesoscale Analysis System, Swedish Meteorological and Hydrological Institute, Norrköping): Merged analysis product using the High-resolution Regional Model (HIRLAM) on a hourly 22 km grid.

ELDAS (European Land Data Assimilation System, University of Vienna): Precipitation analyses of rain gauge data using ECMWF-ERA40, provided 3-hourly on a 22 km grid.

BALTRAD (BALTEX radar network, Norrköping): radar composite including rain rate estimates with 15 min and 2 km resolution.

DWDPI (international radar composites, Deutscher Wetterdienst (DWD) Offenbach): all 15 min at 4 km.

GFZGPS (GPS atmospheric sounding project, Geoforschungszentrum Potsdam): hourly estimates of integrated water vapor at six German stations.

DWDMI (MIRIAM/AFMS2 automated weather stations, DWD Offenbach): gathered 214 stations providing meteorological observations each 20 min.

3. Wind pulsations

For the Gotland Basin (56.5°N , 20.0°E), the comparison of MM5 and MESAN times series of 10 m winds showed an excellent agreement both in timing and magnitude of 5 wind pulsations labeled W1, ..., W5 (Figures 1 and 2 a).

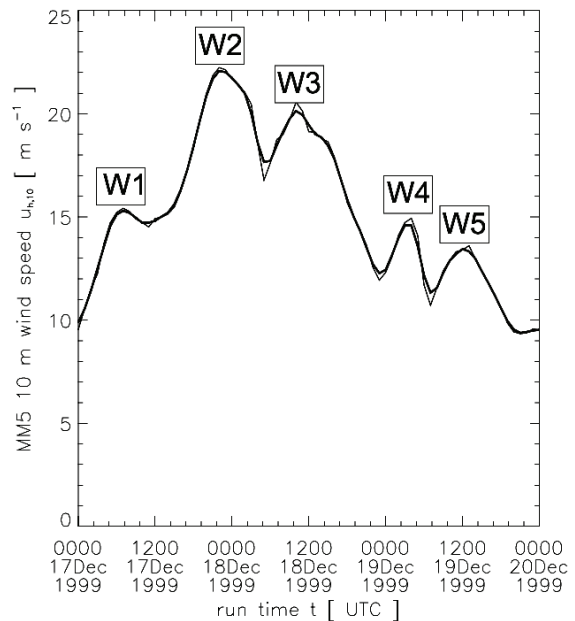


Figure 1. MM5 10 m wind speed at the Gotland Basin (56.5°N , 20.0°E)

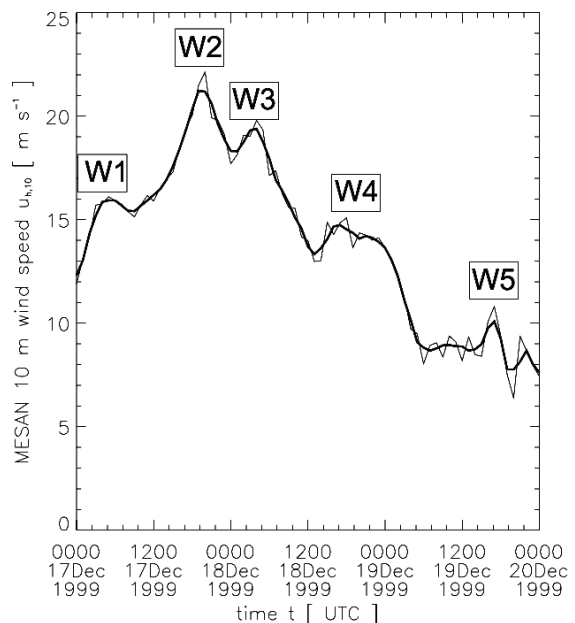


Figure 2. MESAN 10 m wind speed at the Gotland Basin.

4. Precipitation events

Figs 3 and 4 show 3-hourly precipitation in the Gotland Basin from MM5 and BALTRAD. 5 events are labeled P1, ..., P5 can be identified in both datasets, although their magnitude differs slightly.

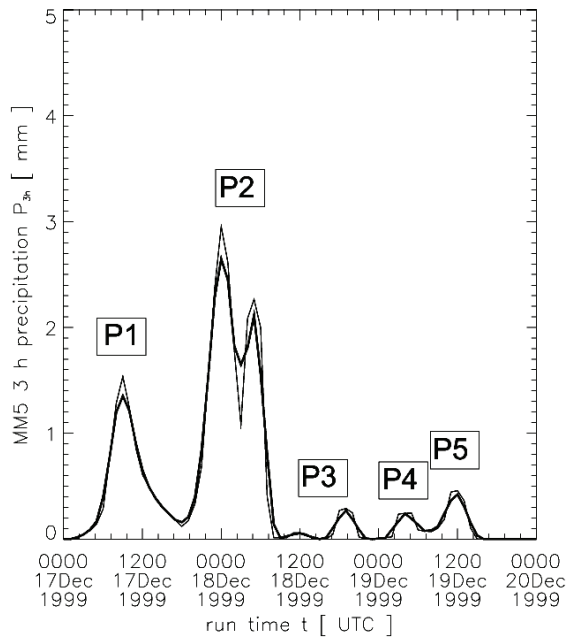


Figure 3. MM5 3-hourly precipitation at the Gotland Basin.

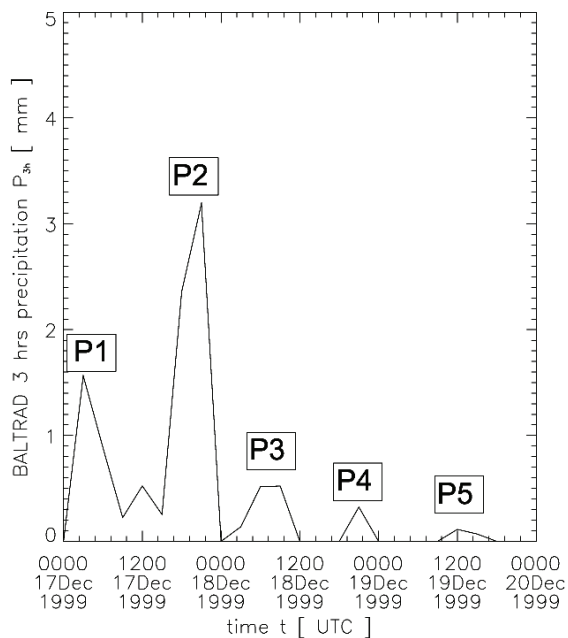


Figure 4. BALTRAD 3-hourly precipitation at the Gotland Basin.

5. Summary and conclusion

The correspondence of wind and precipitation between the MM5 model and the assimilated products like MESAN and ELDAS was convincing. The directly measured data like DWDMI, DWDPI, BALTRAD and GFZGPS contained the mesoscale structures, but differed for some cases in timing

and magnitude. It is matter of further-going studies to identify the cause of these discrepancies in terms of instrumental and environmental fluctuations.

The improvement of statistics and understanding of mesoscale dynamics represents a basic aspect of air-sea exchange and has implications on regional energy and water budget studies. Let us briefly consider the consequences of a sinusoidal wind fluctuations of 3.5 m s^{-1} on a mean wind of 15 m s^{-1} . For quantities depending quadratically on the wind, such as the momentum flux and gas transfer velocity, it would imply an enhancement of 2.6 %. Cubic wind exponents, appearing for example for the air-to-sea kinetic energy flux, an increase by 7.9 % would result. Hence, in special weather situations characterized by strong winds in lower and upper troposphere these effects of inertia-gravity waves should be taken into account.

Acknowledgements: The funding of the work through the DFG project PIGW (Precipitation and Inertia-gravity waves; contract PE 474/4-1/2) with logistic support from the DFG priority program QPF (Quantitative Precipitation Forecast, SPP 1167) is gratefully acknowledged. We are also thankful to the user support groups at DKRZ Hamburg (HLRE project 48) and NCAR Boulder for keeping MM5 running. ECMWF Reading and DWD Offenbach have kindly provided the ECANA data. Special thanks for data provision and assistance in processing goes to: K. Boqvist (SMHI Norrköping) for MESAN, J. Wickert and G. Dick (GFZ Potsdam) for GFZGPS, F. Rubel and P. Skomorowski (U Vienna) for ELDAS, D. Michelson and G. Haase (SMHI Norrköping) for BALTRAD and C. Koziar (DWD Offenbach) for DWDPI and DWDMI. Fruitful discussions with G. Schmitz and A. Gabriel (IAP Kühlungsborn), R. Feistel (IO Warnemünde), C. Nappo (NOAA Oak Ridge) and K. Bumke (IfM-GEOMAR Kiel) were very helpful.

References

Zülicke, Ch. and D. Peters, 2007: Impact of upper-level jet-generated inertia-gravity waves on surface wind and precipitation. *Atm. Chem. Phys. Disc.* 7: 15873 – 15909.

Atmospheric deposition of particulate nitrogen, sulphur and benzo(a)pyrene into the Baltic Sea between 1995 and 2005, considering the influence of ship emissions

Armin Aulinger, Volker Matthias, Markus Quante

GKSS Research Center, Max-Planck-Strasse 1, 21502 Geesthacht, Germany (armin.aulinger@gkss.de)

1. Introduction

The Baltic Sea as an interior sea, being surrounded by several industrialized regions especially at its southern border between Germany and Russia, is threatened by atmospheric deposition of pollutants in addition to inflows from rivers. Among the most harmful ones are particulate nitrogen and sulphur species as well as carcinogenic organic chemicals like benzo(a)pyrene (ATSDR, 1995). While after the political changes in Eastern Europe and the economic decline as a consequence, the emission of air pollutants appeared to decrease at the beginning of the 1990s, the emissions increased again at the end of the 1990s when the economic situation in the Eastern European countries recovered. Atmospheric transport of pollutants is very quick, and especially aerosol species are easily scavenged by cloud water and thus deposited quickly in regions with abundant precipitation. For this reason, the amount of air pollutants being directly deposited into the Baltic Sea via the atmosphere reacts immediately on changes in emissions. In addition to land based emissions, ships emissions play a major role for the air quality over the Baltic Sea. Ship emissions can have considerable impact on atmospheric concentrations of several important pollutants, especially in coastal areas (Matthias et al. 2010, Endresen et al. 2003). Corbett et al. (2007) have recently shown that ship emissions lead to an increase in ambient air concentrations of fine particles with diameter less than 2.5 μm (PM_{2.5}). The future use of low sulphur fuels could enhance air quality and possibly prevent impacts on human health and ecosystems due to ship emissions (Winebrake et al. 2009). The simulations presented here were performed with the Models-3 Community Multiscale Air Quality modelling system (CMAQ) (Byun and Ching, 1999), a state-of-the-art Eulerian chemistry transport model that has been extended by our group to treat semivolatile POPs, in particular Benzo(a)pyrene. The regular model run covers the period between 1995 and 2005. In addition, the impact of ship emissions is investigated for the years 1995, 2000 and 2005.

2. Model description

CMAQ is a 3D Eulerian regional model which is in our case configured for the European continent. The entire model domain covers Europe from the Mediterranean Sea to the North Polar Sea and from Iceland to Western Russia with a grid cell size of 54 x 54 km². The CMAQ system consists of three primary components which are devoted to meteorology, emissions, and chemical transport, respectively. The chemistry transport module is mainly designed for classical air pollutants like SO₂, NO_x, O₃, and particulate matter (PM).

At GKSS, the CMAQ systems was extended to cope with the transport of B(a)P in the gas phase and adsorbed to particles (Aulinger et al. 2007). As B(a)P is almost completely bound to particles under conditions prevailing in northern latitudes, the most important processes are particle scavenging and heterogeneous degradation.

The model is driven by meteorological fields derived from CCLM model runs that were driven by NCEP 6 hourly global reanalysis data.

3. Emissions

Land based emissions of the main pollutants were created with a top-down emissions model on the basis of the European Monitoring and Evaluation Program (EMEP) emissions inventory and the European Pollutant Emission Register (EPER). The temporal disaggregation was implemented by applying average emission profiles for each emission sector. For the spatial allocation, we used the population density (e.g. sector residential heating), street maps (sector road traffic) and geographical location of point sources.

Emission data for B(a)P are partly taken from a technical report published by Denier van der Gon et al. (2005) on emissions of B(a)P and other POPs for Europe. Emissions for years that are not contained in this report were taken from Pacyna et al (1997). Because according to Denier van der Gon (2005), more than 80% of the B(a)P emissions emanate from the sector residential heating, they were linearly correlated to the ambient air temperature where the yearly total emissions in each grid cell were kept constant. For the spatial allocation of the B(a)P emissions, the population density was used.

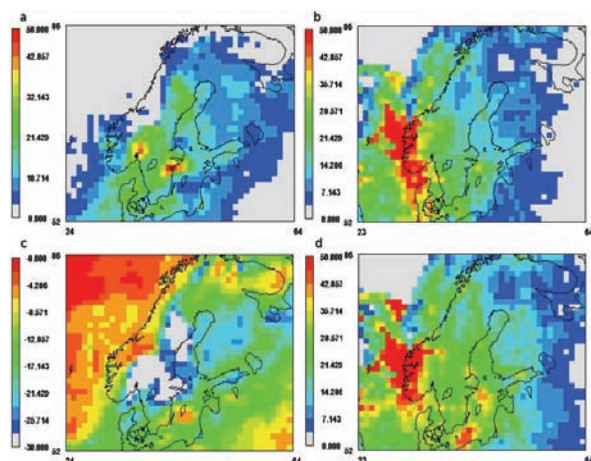
For the estimation of the ship emissions in this study, a bottom-up approach on the basis of ship movement data together with average engine loads and emission factors available in literature (Cooper and Gustafsson, 2004) is used to generate a ship emission inventory. The yearly differences in ship emissions were derived from the EMEP annual reports.

4. Model results

The influence of ship traffic is exemplified for the year 2000. The total deposition of NO₃-N in 2000 was 700 tones without considering ships and 813 tones including ships, which corresponds to a difference of 16%. For SO₄, the increase of total yearly deposition was 10%. The gaseous precursors of nitrate and sulfate – i.e. NO_x and SO₂ – are both directly emitted by ship engines. Ship engines do not only lead to increased concentrations of the species they emit, but also to an increase of secondary particle concentrations and thus to enhanced deposition fluxes of particulate species. The most important cation for anthropogenic inorganic particles is ammonium. It turned out that actually ship traffic leads also to higher ammonium depositions even if neither ammonium nor ammonia is directly emitted by ships. However, the equilibrium between ammonia (stemming from land sources) and ammonium is shifted towards ammonium if more nitrate or sulphate is present. Thus, the total deposition of NH₄-N was slightly increased by about 2%. The relative contribution of ship traffic was different in winter and summer. The amount of nitrate caused by NO_x emissions from ships is lower in winter because oxidation

of NO₂ into HNO₃ is much slower in winter compared to summer. At the same time less ammonium is in the atmosphere, which is quickly consumed by the additional sulfate. This leads to even less nitrate concentration and deposition in winter but in summer nitrate aerosol deposition might be increased by 50% (see figure).

The concentration differences between summer and winter are less pronounced for sulfate aerosol particles. Generally, the levels are comparable with somewhat higher aerosol concentrations in summer. Like NO₂, SO₂ is oxidized more efficiently in summer, leading to higher sulphate concentrations in summer. In contrast to nitrate sulphate, aerosols can also be formed in regions where no gaseous ammonia exists. This is because in presence of sulphate, ammonium nitrate aerosol particles may break up, and gaseous nitric acid and ammonium sulphate are formed.



Deposition increase in % by ships for sulphate in January (a) and July (b) and nitrate in January (c) and July (d)

The third scenario we tested was one with ship fuel containing less than 1.5% sulphur as is mandatory in the Baltic Sea since 2006. In this case the sulfate deposition decreased by 40% compared to the model run with ships that consume high sulphur fuel. On the other hand, more nitrate is formed with less sulfate present in aerosols. Due to low ammonium concentrations, this does not play a role over the open sea. However, over land, near-shore particulate nitrate depositions increase by up to 10%.

The atmospheric input of B(a)P in 2000 without ship emissions amounted to 701 kg. As already mentioned, the source sector residential heating dominates by far over traffic emissions. For this reason, the contribution ship emissions is below 1% and thus nearly negligible.

5. Conclusion

By means of numerical modeling, the transport and deposition of some important particulate pollutants over Europe was exemplified for the year 2000. Ship emissions account for a large part of the secondary inorganic aerosol formation in North Sea coastal areas. Therefore, they are capable of increasing the direct atmospheric input of sulfate and nitrate, and to a smaller extent also of ammonium. Due to the chemistry involved in forming nitrate and sulphate, the concentrations and deposition rates are higher in summer than in winter. This fact has also to be taken into account when considering possible consequences of increased inputs for ecosystems which are more active in summer. The concentrations and depositions of sulfate follow closely the emission rates, while the abundance of nitrate is very much dependent on the presence of excess ammonium. Therefore, an increase of sulfate that consumes ammonium diminishes

nitrate, and vice versa. An influence of ships on B(a)P can also be stated, but appeared to be very small.

Results for the other years will be shown in detail at the conference.

References

- Agency for Toxic Substances and Disease Registry (ATSDR), Toxicological Profile for Polycyclic Aromatic Hydrocarbons (PAHs). Public Health Service, US Department of Health and Human Services, Atlanta, GA, USA, 1995
- Aulinger, A., V. Matthias, M. Quante, 2007. Introducing a partitioning mechanism for PAHs into the Community Multiscale Air Quality modelling system and its application to simulating the transport of benzo(a)pyrene over Europe, *J. Appl. Meteorol.*, 46 (11), 1718-1730
- Byun, D., J.K.S. Ching, Science Algorithms of the EPA Models-3 Community Multiscale Air Quality Modelling System. --EPA report, EPA/600/R-99/030, Office of Research and Development, Washington DC 20406, 1999
- Cooper D.A., Gustafsson, T., 2004. Methodology for Calculating Emissions from Ship: 1. Update of Emission Factors. SMHI Swedish Metrological and Hydrological Institute. Norrköping. Sweden.
- Corbett J.J., Winebrake, J.J., Green, E.H., Kasibhatla, P., Eyring, V., Lauer, A., 2007. Mortality from Ship Emissions: A Global Assessment. *Environmental Science & Technology* 41 (24), 8512 - 8518
- Endresen Ø., Sjørgård, E., Sundet, J.K., Dalsøren, S.B., Isaksen, I.S.A., Berglen, T.F., Gravir, G., 2003. Emission from international sea transportation and environmental impact. *J. Geophys. Res.* 108 (D17), 4560
- Denier van der Gon, H.A.C., M. van het Bolscher, A.J.H. Visschedijk, P.Y.J. Zandveld, Study of the effectiveness of UNECE Persistent Organic Pollutants Protocol and cost of possible additional measures. Phase I: Estimation of emission reduction resulting from the implementation of the POP Protocol. --TNO-report. B&O-A R 2005/194. Laan van Westenenk 501, P.O. Box 342, 7300 AH Appeldoorn, The Netherlands, 2005
- Matthias, V., Bewersdorff, I., Aulinger, A., Quante, M. 2010. The Contribution of Ship Emissions to Air Pollution in the North Sea Regions. *Environmental Pollution*. ENVPOL-D-09-00693R1
- Pacyna, M.J., Breivik, K., Münch, J., Fudala, J. 2003. European Atmospheric Emissions of Selected Persistent Organic Pollutants, 1970 - 1995. *Atmospheric Environment*, 37 supplement 1, 119-131
- Winebrake, J. J., Corbett, J. J., Green, E. H., Lauer, A., Eyring, V., 2009. Mitigating the Health Impacts of Pollution from Oceangoing Shipping: An Assessment of Low-Sulfur Fuel Mandates. *Environmental Science & Technology* 43(13), 4776-4782.

Depositions of acidifying and neutralising compounds over the Baltic Sea drainage basin between 1960 and 2006

Björn Carlsson and Anna Rutgersson

Department of Earth Sciences, Meteorology, Uppsala University, Sweden (Bjorn.Carlsson@met.uu.se)

1. Introduction

The atmospheric deposition of acidifying compounds affects the pH and the chemical processes in the soil and in the ocean. Secondary effects are on the chemistry in the terrestrial water flows and the biological cycle. The sulphur and nitrogen deposition over Northern Europe has been monitored since the 1960s, but in the beginning only at a few sites. The deposition of other acidifying or neutralising compounds are less known, at least before the middle of the 1980s.

The Baltic-C project (<http://www.baltex-research.eu/baltic-c/index.html>) aims to close the carbon budget and to predict the future biochemical and acid-base state of the Baltic Sea drainage basin system in a holistic approach. In this model system the deposition of acidifying and neutralising species are derived as forcing to the Baltic Sea model PROBE-Baltic (Omstedt and Axell 2003) and the run-off model CSIM (Mörth et al. 2007).

In this study we derive the distribution of atmospheric deposition of acid-base species and pH in the precipitation with a monthly resolution for the period 1960–2006. The data used are primarily output from the European Monitoring and Evaluation Programme (EMEP) chemical transport model (oxidized sulphur/SO₄²⁻, oxidized nitrogen/NO₃⁻ and reduced nitrogen/NH₄⁺) or interpolated measurement data within the EMEP programme (base cations and chloride). When model data or measurement data were not available, the depositions were either estimated using historical emissions from the EDGAR-HYDE data set (sulphur, nitrogen and ammonia) or assumed to follow a mean seasonal cycle without a trend. The pH in precipitation was estimated using a simple model.

2. Data

The EMEP chemical transport model available on internet at <http://www.emep.int/OpenSource/index.html> has a ca. 50 x 50 km² (at 60°N) grid covering Europe. It has 20 levels and 20 min time step (chemistry subroutine order 1 min). For present purposes the dry and wet depositions of oxidized sulphur and nitrogen and reduced nitrogen (ammonia) were used. For more details of the model see Simpson et al. (2003).

The pH and deposition (wet) of chloride and base cations (Na, Mg, K, and Ca) are taken from the measurements of the EMEP co-operative programme (e.g. Hjellbrekke and Fjærraa 2007). The data are from 1977–2006, but since the observation network is very sparse until about 1990 only data from 1990 and later are used.

The emissions used for the period before EMEP data were available were taken from the gridded (1°x1°) EDGAR-HYDE data set (<http://www.mnp.nl/edgar/model/>). It contains global, spatially modelled anthropogenic emissions of NO_x, SO₂, NH₃ among others species. The years 1990, 1995, 2000 are covered by EDGAR-HYDE 3.2 (Olivier et al. 2001). An older data set lacking (EDGAR-HYDE 1.3, Van Aardenne et al. 2001) presents yearly gridded emissions each 10 years beginning in 1890.

The atmospheric CO₂ concentration is needed to calculate the pH in precipitation before 1990. CO₂ is approximated by a constructed data set from the measurements at the station “Baltic Sea” (Global Atmospheric Watch Programme, GWA) in southern Baltic Sea (Rutgersson et al. 2009).

3. Method

The deposition of oxidized sulphur and nitrogen and reduced nitrogen is taken primarily from the EMEP model, whereas the chloride and base cations, pH and precipitation were taken from the EMEP measurements. When there were missing data the depositions were estimated from the EDGAR-HYDE emission data set. For the years 1960–1989, the trends in emissions were scaled by the modelled yearly deposition for 1990 of the related species (NH₃ for NH₄). Then the mean seasonal cycle of the modelled depositions (1990–2006) was applied. In Figure 1 are shown some steps of the procedure and the resulting constructed data of deposition of oxidized sulphur. The same procedure was used for oxidized and reduced nitrogen.

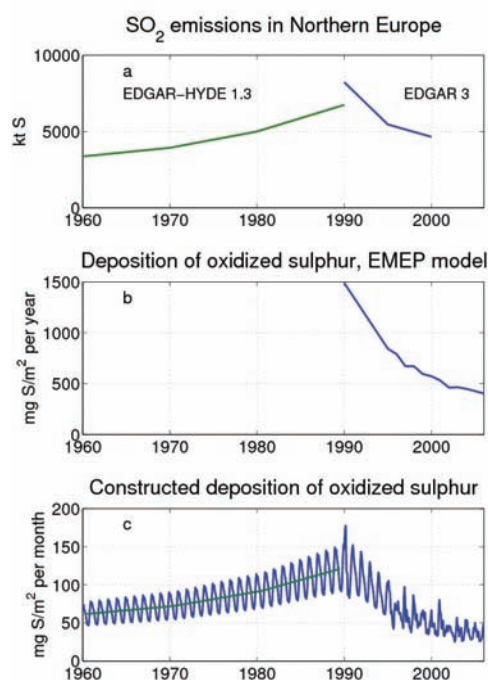


Figure 1. Some steps of the procedure to estimate the deposition of oxidized sulphur before 1990.

The data from the EMEP measurements were spatially interpolated over the Baltic Sea region. Near the boundaries of the domain a background field based on the gradient of the measurements was applied. The direction of the gradient was set west-east for sea salt ions (Na, Mg, Cl) and north-south for ions with other dominant sources

(K, Ca). For all ions except calcium no trend was assumed before 1990. The mean yearly cycle was applied on a yearly average identical to the average of the 1990–2006 period for each ion. The trend of calcium deposition was approximated using the same trend as sulphur emissions and adding a background sea salt value correlated with sodium. In Figure 2, the yearly wet deposition of base cations and chloride during 2006 are shown.

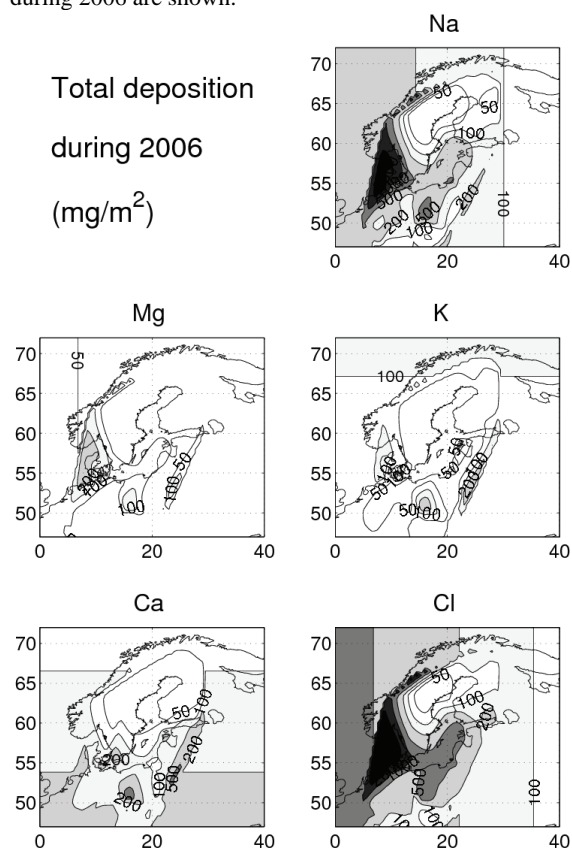


Figure 2. Interpolated fields of wet deposition of base cations and chloride.

The pH before 1990 is calculated by a simple model modified from Rodhe et al. (2002) using the spatially interpolated molar concentrations of SO_x , NO_x , NH_x , Na, K, Ca and Cl in precipitation. The approximate total molar charge concentration of protons (H^+) and bicarbonate ions (HCO_3^-) is given as a residual if assuming zero total charge. With atmospheric CO_2 as input, the equilibrium concentration of H^+ and thus pH can be calculated (Millero 1995).

4. Results

It is shown that the depositions of sulphur and nitrogen (reduced and oxidized) over the Baltic Sea drainage basin are now at approximately the same level as in the 60s or earlier. This is due to the success in the reductions of sulphur dioxide, nitrogen oxides and ammonia emissions since the 80s and 90s. However, emission of neutralising calcium particles (for instance from cement production and power generation) has also to a great extent been reduced. This has slowed down the recovery of pH in precipitation. More figures and a more thorough analysis will be presented. The focus will be on total depositions and historical trends over the drainage basin and also on the calculated pH. Further, the error sources are discussed,

including an evaluation of the interpolated measurements of sulphur and nitrogen in relation to the EMEP model output.

References

- Hjellbrekke, A.-G., A.-M. Fjæraa (2007) Data Report 2005: Acidifying and eutrophying compounds, and particulate matter, EMEP/CCC-Report 1/2007.
- Millero, F. (1995) Thermodynamics of the carbon dioxide system in the oceans, *Geochemica et Cosmochimica Acta*, 59, pp. 661–677.
- Mörth, M., et al. (2007) Modeling Riverine Nutrient Transport to the Baltic Sea: A Large-scale Approach, *Ambio*, 36, pp. 124–133.
- Olivier, J.G.J., J.J.M. Berdowski (2001) Global emissions sources and sinks. In: Berdowski, J., Guicherit, R. and B.J. Heij (eds.) "The Climate System", pp. 33–78. A.A. Balkema Publishers/Swets & Zeitlinger Publishers, Lisse, The Netherlands. ISBN 9058092550.
- Omstedt, A. L. Axell (2003) Modeling the variations of salinity and temperature in the large gulfs of the Baltic Sea, *Continental Shelf Research*, 23, pp. 265–294.
- Rodhe, H., F. Dentener, M. Schulz (2002) The global distribution of acidifying wet deposition, *Environ. Sci. Technol.*, 36, pp. 4382–4388.
- Rutgersson, A., M. Norman, G. Åström (2009) Atmospheric CO_2 variation over the Baltic Sea and the impact on air–sea exchange, *Bor. Env. Res.*, 14, pp. 238–249.
- Simpson, D., H. Fagerli, J.E. Jonson, S. Tsyro, P. Wind, J.-P. Tuovinen (2003) Transboundary Acidification, Eutrophication and Ground Level Ozone in Europe. PART 1: Unified EMEP Model Description. EMEP Status Report, 1/2003.
- Van Aardenne, J.A., F.J. Dentener, J.G.J. Olivier, C.G.M. Klein Goldewijk, J. Lelieveld (2001) A $1^\circ \times 1^\circ$ resolution dataset of historical anthropogenic trace gas emissions for the period 1890–1990. *Global Biogeochemical Cycles*, 15, 4, pp. 909–928.

Development of the marine planktonic copepod *Acartia* spp. in the southern Baltic Sea

L. Dzierzbicka-Głowacka¹, I.M. Żmijewska², J. Jakacki¹, A. Lemieszek² and S. Mudrak²

¹ Institute of Oceanology, Polish Academy of Sciences, Sopot, Poland (dzierzb@iopan.gda.pl)

² Institute of Oceanography, University of Gdansk, Gdynia, Poland

1. Abstract

This paper outlines an approach to couple a structured zooplankton population model using state variables for eggs, nauplii, five copepodite stages and adults of *Acartia* spp. with the marine ecosystem model of Baltic Sea, using four state variables. These state variables for the carbon cycle represent the functional units of phytoplankton, pelagic detritus, benthic detritus, and bulk zooplankton, which represent all zooplankton other than the structured population. This paper describes numerical simulations of the seasonal dynamics of *Acartia* spp. in the southern Baltic Sea. The annual cycle simulated for the year 2000 under realistic weather and hydrographic conditions was studied with the coupled ecosystem–zooplankton model applied to the Gdańsk Gulf (southern Baltic Sea). The main ecosystem state variables were validated against observed monthly mean values. The vertical profiles of selected state variables were compared to the physical forcing to study differences between bulk and structured zooplankton biomass. The simulated population dynamics of *Acartia* spp. and zooplankton as one biomass state variable were compared with observations in the Gdańsk Gulf. This work was carried out in support of a grant by the Polish state Committee of Scientific Research.

2. The ecosystem model structure

Recently, Dzierzbicka-Głowacka (2005b, 2006) developed a one-dimensional ecosystem upper layer model: the 1D CEM Coupled Ecosystem Model. This ecosystem model, supplemented with the population dynamics submodel for copepods and a component for pelagic detritus, was used to study the dynamics of *Pseudocalanus minutus elongatus* in the southern Baltic Sea (Dzierzbicka-Głowacka 2005a,b). The flow field and water temperature used as the inputs in the ecosystem model, were reproduced by the 3D hydrodynamical model IOPAS-POPCICE (see the EU project ECOOP IP WP10). The model was forced using daily-averaged reanalysis and operational atmospheric data (ERA-40) that were derived from the European Centre for Medium-range Weather Forecast (ECMWF). The interpolated output of the hydrodynamical model was used as the input in the ecosystem+copepod model, since in the simulated area the dynamical characteristics remain almost unchanged in a horizontal plane in comparison to vertical changes. Hence, the magnitudes of the lateral import/export are lower, and the above assumption can be made.

3. Copepod model for *Acartia* spp.

The copepod model (Dzierzbicka-Głowacka 2009a) includes here the rate of transfer from stage i to the next ($i+1$). It consists of sixteen state variables with masses W_i and numbers Z_i for each of the eight model stages, where stages are grouped into: the non feeding stages and eggs are represented by the stage – eggs-N2, the following are the naupliar stages – N3-N6, then five copepodite stages – C1, C2, C3, C4, C5 and finally the adult stage – C6. For each of

the eight model stages, mass W_i and number Z_i were calculated.

The changes in the stage-specific mean biomass, which is the algebraic sum of the products of the masses, W_i , and numbers, Z_i , of *Acartia* spp. for each of the model stages, are controlled by ingestion, egestion, metabolism, mortality, predation and transfer. Both processes, ingestion and transfer, depend on individual weights in successive stages using critical moulting masses, C_m , as described by Carlotti and Sciandra (1989).

In this study, the hypothesis that the food-saturated rate of production of egg matter is equivalent to the maximal specific growth rate of copepods was used for the calculation of the number of eggs produced by each female during one day (Dzierzbicka-Głowacka et al. 2009b).

4. Results

The vertical distributions shown in Figure 1 demonstrate the annual biomass profiles for the selected state variables representing *Acartia* spp. stage dynamics. The four state variables for eggs: N2, naupliar stage, N3-N6, copepodite stage, C1-C5 (including five copepodite stages together) and finally the adult stage, C6 are presented. First, eggs occurred at the end of March corresponding to the phytoplankton spring bloom and increasing temperatures. Several generation peaks within the stage biomass variables can be observed during the development period of *Acartia* spp. throughout the year. The development assembles in the water column – mainly in the euphotic layer, where food – a mixture of phytoplankton, microzooplankton and small pelagic detritus – is available but also extends beyond the thermocline due to ingestion of dead organic matter. The highest proportion of all the development stages is found above the thermocline. In June, a thermocline developed at a depth of 30 m; the temperature in the surface layer increased from 13 °C in June to 17 °C in July and 18.5 °C in August, before cooling started. In November, the thermocline was destroyed. During the same time, most of the total biomass of *Acartia* spp., as the sum over four state variables, non-feeding, naupliar, copepodite and adult stages, was observed.

Figure 2 presents the simulated stage biomasses, which are the algebraic sum of the products of the weights, W_i , and numbers, Z_i , of each stage, as vertical mean values and also the number of *Acartia* spp. generations in the southern Baltic Sea (Gdansk Deep) is illustrated. The simulation starts with over wintering copepodites C4 and C5 and adults. The small maxima occurring in the distribution of the eggs-N2 stage are the result of a brood by successive females causing their numbers to increase. The strong increase in an available food concentration – mainly of phytoplankton biomass, in the spring bloom begins egg production. The hatching time at 4-6 °C is 20 days. Five complete distinct generations, from eggs to adults, developed throughout the year, the first beginning in mid-March. The stage duration for the first generation is

65 days (Dzierzbicka-Glowacka et al. 2009a). During the development of the second generation (51 days), surface temperature increases from 8 to 15 °C causing accelerated growth, while a drop in food concentration causes a retard. The third generation starts in the first half of July (day 191) and takes 47 days to complete as a result of the low food concentration (ca 70 mg C m⁻³ in the upper 20 m layer) and the high surface temperature (15-18.5 °C).

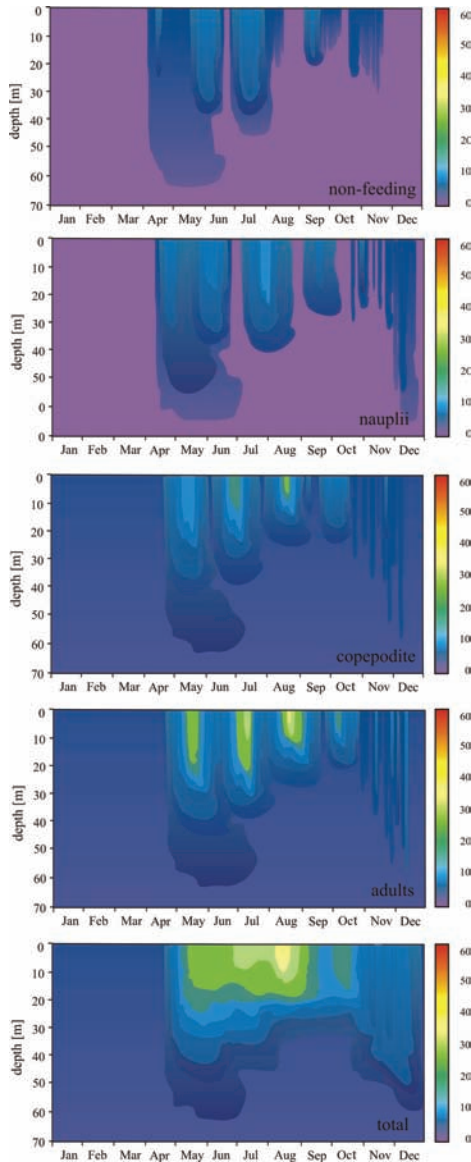


Figure 1. Simulated annual profiles of four *Acartia* spp. groups representing: biomasses of eggs, nauplii, copepodites and adults and of total biomass of *Acartia* spp. (mg C m⁻³).

The total development time for the next generation is the shortest and assumes the value of 45 days similar to that of the third generation. During the fourth generation, temperature is lower, with a mean of ca 2.5 °C, than during the previous generation but the food supply concentration is higher, mean value of $Food = 120 \text{ mg C m}^{-3}$ in the 50 m water column. This is equal to the surface value as a result of vertical mixing. Individuals of the fifth generation (day 283) are produced in the first half of October and reach adulthood at the end of the numerical simulation when there is a lack of food and a decrease in temperature. The total biomass of *Acartia* spp. is characterized by one main

biomass peak at the end of August, and two smaller peaks. The first is slightly smaller, occurring during the first half of July and the second small peak occurs in mid-October. The peak of biomass in August (ca. 15 mg C m⁻³) is mainly due to the high biomass of copepodites and adults of the third generation and the high egg production as a result of the very high numbers of adults of the previous generation. The high reproduction is a result of high temperature at this time. The smaller peaks of biomass (ca 11 mg C m⁻³ and 5 mg C m⁻³, respectively) also are mainly due to the high biomass of copepodites and adults of the 2nd and 4th generations and the high egg production of the 1st and 3rd generations, respectively. However, the nauplii biomass of successive generations influences the peaks of the total biomass at the beginning of the growth. The phytoplankton peak in September-October permits a new growth period for the 4th generation and females of this generation produce relatively small eggs to give a 5th generation in October-November.

Generally, the biomasses of total zooplankton and *Acartia* spp. biomass are in agreement with observations (see Dzierzbicka-Glowacka et al. 2010).

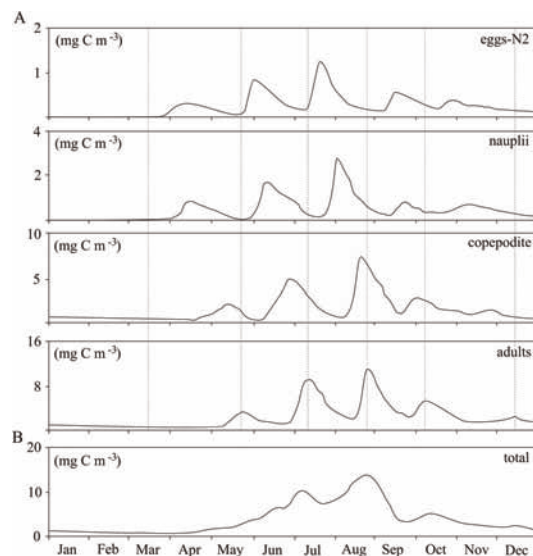


Figure 2. Simulated *Acartia* spp. generations (A) vertical mean biomasses of eggs, nauplii, copepodites and adults (mg C m⁻³), (B) total biomass as vertical mean concentrations; vertical lines indicate the durations of five generations.

References

- Dzierzbicka-Glowacka, L. (2005a) A numerical investigation of phytoplankton and *Pseudocalanus elongatus* dynamics in the spring bloom time in the Gdansk Gulf, J. Mar. Sys., 53, pp. 19–36
- Dzierzbicka-Glowacka, L. (2005b) Modelling the seasonal dynamics of marine plankton in southern Baltic Sea. Part I. A Coupled Ecosystem Model, Oceanologia, 47(4), pp. 591–619
- Dzierzbicka-Glowacka, L., Lemieszek, A., Żmijewska, I.M. (2009) Parameterization of a population model for *Acartia* spp. in the southern Baltic Sea. Part 1: Development time. Part 2: Egg production Oceanologia, 51(2), pp.165-201
- Dzierzbicka-Glowacka, L., Żmijewska, I.M., Mudrak S., Jakacki J., Lemieszek, A. (2010) Population modelling of *Acartia* spp. in a water column ecosystem model for the southern Baltic Sea, Biogeosciences (submitted)

Quality assessment of state-of-the-art coupled physical-biogeochemical models for the Baltic Sea

K. Eilola¹, B. G. Gustafson², R. Hordoir¹, A. Höglund¹, I. Kuznetsov³, H. E. M. Meier¹, T. Neumann³, O. P. Savchuk²

1. Swedish Meteorological and Hydrological Institute, Sweden

2. Baltic Nest Institute, Resilience Centre, Stockholm University, Sweden

3. Baltic Sea Research Institute Warnemünde, Germany

1. Abstract

The objectives of the project ECOSUPPORT (Advanced modeling tool for scenarios of the Baltic Sea ECOSystem to SUPPORT decision making) are to calculate the combined effects of changing climate and changing human activity (e.g. changing nutrient loads) on the Baltic Sea ecosystem (see <http://www.baltex-research.eu/ecosupport>). Three state-of-the-art coupled physical-biogeochemical models are used to calculate changing concentrations of nitrate, ammonium, phosphate, diatoms, flagellates, cyanobacteria, zooplankton, detritus, and oxygen in the Baltic Sea. This presentation summarises results of the quality assessment and model intercomparison within ECOSUPPORT. Results from hindcast simulations were compared with observations for the period 1970-2005. We found that all three investigated models are able to reproduce the observed variability of biogeochemical cycles well. Uncertainties were primarily related to differences in the bioavailable fractions of nutrient loadings from land and parameterizations of key processes like sediment fluxes that are presently not well known. Results from the ongoing evaluation of the model ensemble means as well as of the differences between individual models will be further discussed in this presentation.

2. Introduction

Within the ECOSUPPORT project a hierarchy of existing state-of-the-art sub-models of the Earth system is used. This includes the three state-of-the-art coupled physical-biogeochemical models that are used to calculate changing concentrations of nutrients and organic matter in the Baltic Sea. These are BALTSEM (Gustafsson 2003; Savchuk 2002), ERGOM (Neumann et al. 2002), and RCO-SCOBI (Swedish Coastal and Ocean Biogeochemical model, SCOBI, Eilola et al. 2009) and the Rossby Centre Ocean circulation model, RCO (Meier and Kauker 2003; Meier et al. 2003). The models are structurally different in that ERGOM and RCO-SCOBI are 3D circulation models comprising sub-basin scale processes while BALTSEM resolves the Baltic Sea spatially in 13 sub-basins.

The ERGOM, RCO-SCOBI and BALTSEM models are similar in that they handle dynamics of nitrogen, oxygen and phosphorus including the inorganic nutrients, nitrate, ammonia and phosphate (and also silicate in BALTSEM and inorganic carbon in ERGOM), and particulate organic matter consisting of phytoplankton (autotrophs), dead organic matter (detritus) and zooplankton (heterotrophs). Primary production assimilates the inorganic nutrients by three functional groups of phytoplankton, diatoms, flagellates and others, and cyanobacteria. Organic material may sink and accumulate in the model sediment as benthic nitrogen and phosphorus (and silicate in BALTSEM).

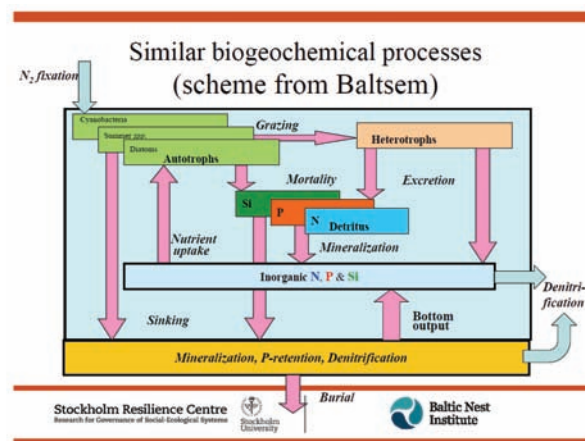


Figure 1. A highly simplified description of model components and nutrient fluxes exemplified from the BALTSEM model.

The cycling of nutrients within different compartments of the biogeochemical system is illustrated in Fig. 1. In brief, the key differences between the state-of-the-art models are described by:

- Differences in treatment of dead organic matter: one state-variable for each nutrient vs. a single variable with constant N/P ratio
- Differences in parameterizations of P sediment dynamics, in particular redox dependent P processes
- Resuspension and sediment transport: mechanistic description (from waves and currents) vs. simple parameterization
- Resolving coastal boundary and deep pits vs. large-scale horizontally integrated sub-basins
- Different vertical resolution

In addition there are other “minor” quantitative (relationships) and qualitative (numerical values of constants) differences in parameterizations of similar pelagic and sediment biogeochemical processes that have not been listed and analyzed yet.

3. Results

The figures 2 and 3 below show an example of ensemble mean results from the first assessment and model intercomparison within ECOSUPPORT that were summarized in the report by Eilola et al. (2010) (<http://www.smhi.se/sgn0106/if/biblioteket/rapporter/o.htm#2010>).

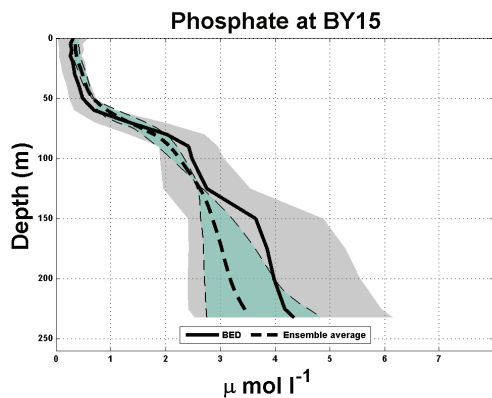


Figure 2. Average (1970-2005) phosphate ($\mu\text{mol l}^{-1}$) concentrations in the central Baltic proper (BY15). The observational data were extracted from the Baltic Environmental Database (BED). The black solid line and the grey shaded area indicate the mean value and ± 1 standard deviation of BED data. The black dashed line and the blue shaded area indicate the mean and spread of the model ensemble.

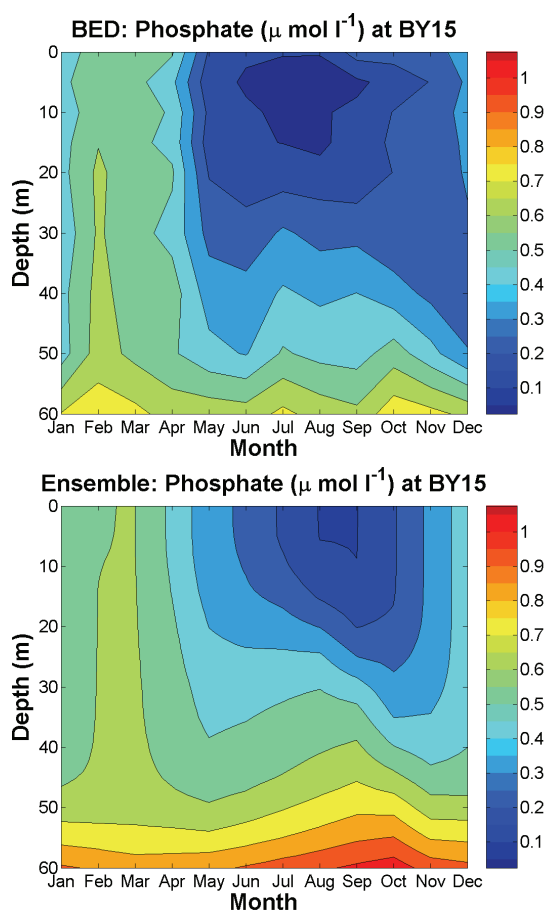


Figure 3. Annual cycle of monthly average (1970-2005) phosphate ($\mu\text{mol l}^{-1}$) concentrations at BY15. Results from BED and the ensemble average are shown in the upper and lower panels, respectively.

References

- Eilola, K., Meier, H.E.M. and Almroth, E., 2009. On the dynamics of oxygen, phosphorus and cyanobacteria in the Baltic Sea; A model study. *Journal of Marine Systems*, 75: 163-184.
- Eilola, K., B. G. Gustafson, R. Hordoir, A. Höglund, I. Kuznetsov, H. E. M. Meier, T. Neumann and O. P. Savchuk, 2010, Quality assessment of state-of-the-art coupled physical-biogeochemical models in hind cast simulations 1970-2005, Rapport Oceanografi No.101, SMHI, Norrköping, Sweden.
- Gustafsson, B.G., 2003: A time-dependent coupled-basin model of the Baltic Sea. C47, Earth Sciences Centre, Göteborg University, Göteborg, 61pp.
- Meier, H.E.M., Döscher, R. and T. Faxén, 2003, A multiprocessor coupled ice-ocean model for the Baltic Sea: Application to the salt inflow. *J. Geophys. Res.* 108(C8), 3273.
- Meier, H.E.M., and F. Kauker, 2003, Modeling decadal variability of the Baltic Sea: 2. Role of freshwater inflow and large-scale atmospheric circulation for salinity. *J. Geophys. Res.*, 108(C11), 3368.
- Neumann, T., W. Fennel, Ch. Kremp 2002: Experimental Simulations with an Ecosystem Model of the Baltic Sea: A Nutrient Load Reduction Experiment, *Global Biogeochemical Cycles* 16, No 3, 7-1 – 7-19.
- Savchuk, O. P., 2002: Nutrient biogeochemical cycles in the Gulf of Riga: scaling up field studies with a mathematical model, *Journal of Marine Systems*, 32, 253-280.

Can observational pH data confirm the predicted acidification of Baltic Sea surface water?

Anders Grimvall¹, Anders Omstedt¹ and Matti Perttilä²

¹ Swedish Institute for the Marine Environment, Gothenburg, Sweden (anders.grimvall@liu.se)

² Finnish Meteorological Institute, Helsinki, Finland

1. Introduction

Theoretical considerations show that the increasing concentration of CO₂ in the atmosphere can acidify marine environments (e.g. Zeebe and Wolf-Gladrow 2007). However, the estimated decrease in the pH of sea water is relatively small (about 0.1 units in 100 years), and the pH is strongly influenced also by marine primary production, input of freshwater, and water exchange within and between sea basins. Moreover, careless sampling and errors in measurement procedures, such as neglecting salinity effects, can decrease the reliability and comparability of the measured pH values. These factors raise the question whether the accuracy and signal-to-noise ratio in observations of pH in sea water is sufficiently high to enable precise conclusions about the predicted acidification.

Here, we focused on the dynamics of pH in the Baltic Sea, and in particular the Baltic Proper. Our study involved statistical analysis of both observational pH data and outputs from a process-based model of the carbonate system in the Baltic Sea. In addition, we compared data collected by the Swedish Meteorological and Hydrological Institute (SMHI) and the Finnish Institute for Marine Research (FIMR) at a sampling site in the Baltic Proper where the two organizations have long collected and analyzed water samples.

2. A Baltic Sea CO₂ model

Model simulations of the pH dynamics were performed using a process-oriented, coupled-basin ocean model that has been explored and validated for the Baltic Sea (Omstedt et al. 2009). This model describes the interaction between major physical, chemical and biological processes and characteristics. The physical processes include stratification, sun penetration, formation of ice, and their relationship to temperature and salinity. The chemical processes involve alkalinity, pH, dissolved inorganic carbon, oxygen, and nutrients, and the biological processes focus on the formation and decay of plankton and dissolved organic carbon.

3. Observational data

Data on pH, salinity, and alkalinity in the Baltic Sea were procured from SMHI and FIMR. Observations made at the sampling sites BY5, BY15, BY29 and BY31 in the Baltic Proper were used to assess the quality of the collected data, and a comparison of SMHI and FIMR data was undertaken for BY15 in the Gotland Deep. Further details about the sampling sites can be obtained from www.smhi.se.

4. Statistical methods

All observational data and model outputs were inspected using standard descriptive statistics, time series plots and plots of related variables. Animated scatter-plots, also called motion charts enabled detailed inspection of changes over time in scatter-plots.

Formal tests of temporal trends in monthly means were undertaken by applying multivariate Mann-Kendall tests

with corrections for serial dependence (Wahlin and Grimvall 2009).

5. Temporal trends in model outputs

Trend analysis of modelled pH values showed that there was a strongly significant overall downward trend ($p=6E-10$). Closer examination of the test statistics for individual months showed that this trend was strongly significant ($p<0.001$) for all months but May and June. When the statistical analysis was constrained to a shorter time period (1994-2008), there was still a significant downward trend ($p=0.019$), but the seasonal pattern in the trend was unclear. Moreover, our simulations revealed that elevated input of nutrients produced increased pH levels in summer and decreased levels in winter. In Figure 1, we can also notice a few low pH values in winter, and these events were found to be associated with strong winds and increased mixing.

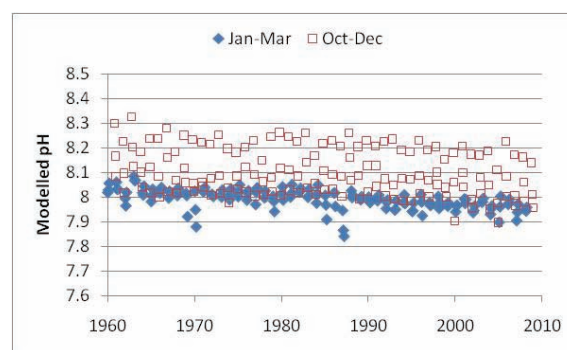


Figure 1. Time series plots of modelled mean monthly pH in surface water from the Baltic Proper.

6. Quality of observational data

In general, the observational pH data we examined had a good precision in the sense that the observed values were almost identical for samples taken at the same time at comparable depths. For example, we found that, for a majority of the sampling occasions, the range of observed pH values at depths 0-10 m was less than 0.05 units. In addition, many of the exceptionally high ranges were observed during periods of high primary production, when the actual differences between the analysed samples can be considerable.

The observational pH data were satisfactory also in the sense that there were no significant differences in the average pH values reported by SMHI and FIMR. However, scatter-plots and motion charts of pH vs salinity and alkalinity revealed a temporal variability that called for closer examination. As shown in Figure 2, the pH values reported for samples of medium to high salinity were more variable at the onset of the water quality monitoring than during the past decade. Further analysis of the pH values provided additional examples of single outliers and general level shifts that were inexplicably

synchronous at different depths. This indicated that some observations have been strongly influenced by measurement or calibration errors or variation in the handling of the collected samples.

Scatter-plots of observed vs modelled pH (Figure 3) strengthened the evidence that at least a minor fraction of the observed values had been influenced by measurement or sampling errors. However, it is important to note that the observational data represent a single sampling site whereas the model outputs are spatial averages, and this may explain considerable differences between the two types of data.

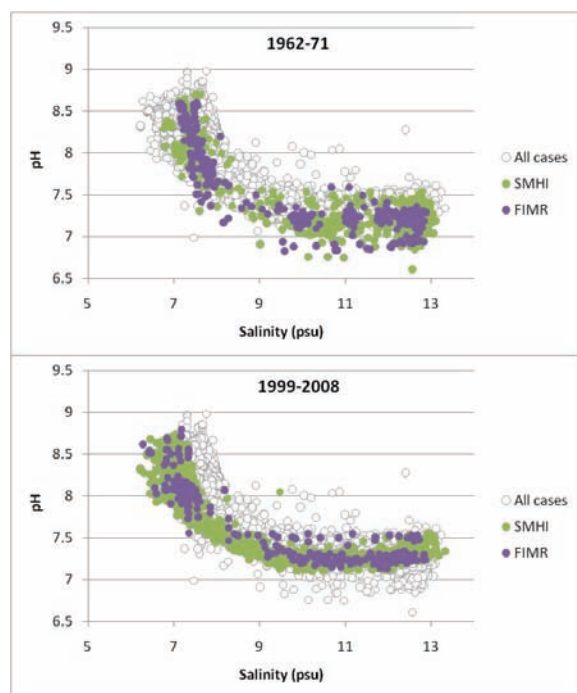


Figure 2. Observed pH and salinity at BY15 in the Baltic Proper. The open circles represent all data collected by SMHI and FIMR during the entire study period 1964-2008. Markers on the border of the plot area indicate incomplete observations.

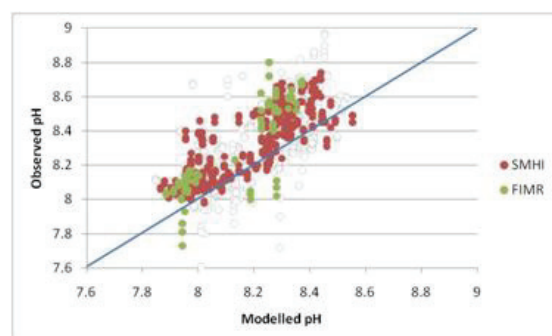


Figure 3. Observed and modelled pH at the surface of the Baltic Proper. Observational data represent mean values for samples collected at the same occasion at BY15 (depth 0-10 m). Modelled data are spatial averages for the surface of the Baltic Proper the same days as water samples were collected. Solid markers stand for data 1994-2008.

7. Temporal trends in observational data

Trend analysis of observational data from BY15 did not reveal any overall downward trend from the 1960s to the present. Neither was any significant trend detected when the

analysis was constrained to more recent data that might be of higher quality. Similar results were obtained for time series representing individual months. The temporal trend was not significant for any of the twelve months.

The temporal variability of autumn and winter data is illustrated in Figure 4. The variability of pH in spring and summer samples was substantially higher, because of the higher primary production during these months.

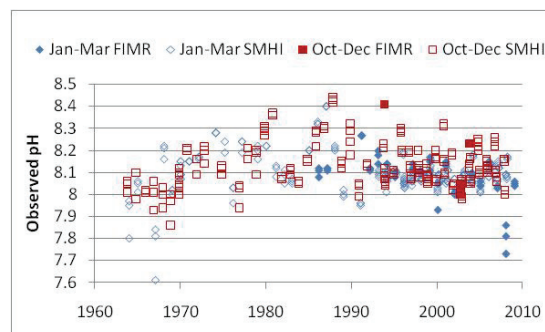


Figure 4. Time series plots of observed pH values in samples collected by SMHI and FIMR at BY15 (depth 0-10 m).

8. Discussion and conclusions

All pH data from the Baltic Proper exhibit a strong temporal variation. First, such data have a considerable seasonal and interannual variation related to natural cycles in primary production. Second, our model simulations show that vertical mixing caused by strong wind events can produce a significant variation in pH also during periods of low biological activity. In addition, observational data are point data, whereas acidification of marine environments is a large-scale spatial phenomenon. These circumstances indicate that, even if measurement errors were reduced to a minimum by standardizing the sampling and correcting for variation in salinity, there is a substantial risk that ecologically important trends in pH are concealed by the high variability of observational data. Our study also revealed some weak points of the current process-oriented model. As shown in Figure 3, the model output is biased, which indicates further research needs. Nonetheless, a monitoring strategy in which sampling programmes are designed to support modelling appears to be the most promising method to assess pH trends in sea water. A model that can describe at least part of the natural fluctuations in pH opens the possibility to adjust observational data so that temporal trends emerge more clearly. In addition, a properly validated process-oriented model is indispensable to attribute observed changes to different sources or interventions. In particular, such a model is needed to separate effects of CO₂ in the atmosphere from the influence of eutrophication on the pH of sea water.

References

- Omstedt, A., Gustafsson, E. and K., Wesslander, (2009). Modelling the uptake and release of carbon dioxide in the Baltic Sea surface water. *Continental Shelf Research* 29, 870-885. DOI: 10.1016/j.csr.2009.01.006.
- Wahlin, K. and Grimvall, A. (2009). Roadmap for assessing regional trends in groundwater quality, *Environmental Monitoring and Assessment*, DOI: 10.1007/s10661-009-0940-7.
- E. Zeebe and D. Wolf-Gladrow (2007). CO₂ in sea water: equilibrium, kinetics, isotopes. *Elsevier Oceanographic Series* 65.

Variability of the marine boundary layer parameters over the Baltic Sea sub-basins in HIRLAM parameterizations since 1993 and their impact on the nitrogen deposition

Marke Hongisto

Finnish Meteorological Institute. Erik Palmenin Aukio 1, P.O.Box 503, FI-00101 Helsinki (marke.hongisto@fmi.fi)

At the end of the 1990's, an upward trend was observed during the past several decades in the wintertime AO, indicating a strengthening of the wintertime polar vortex from sea level to the lower stratosphere (Thompson and Wallace 1998). At the end of the 2000's, it was found that the average location of upper air jet streams, a driving factor for weather in the northern hemisphere, shifted weakly (19 kilometers per decade) poleward in recent decades (Archer and Caldeira 2008). There are changes in latitude of the polar front and cyclone tracks, an increase in NH cyclone depth and radius, a decrease in cyclone number (Simmonds and Keay 2009) and changes in blocking frequency. After 2000, however, some features in general circulation have slightly changed.

The weather prediction model HIRLAM has been in operational use at the Finnish Meteorological Institute since 1990. Because the Baltic Sea (BS) is a shallow and eutrophic water area, vulnerable to any external forcing and nutrient loading, the 6th hour HIRLAM forecasts have been collected for air pollution model studies in a meteorological data base. These forecasts have been used to study variation of nitrogen deposition over the Baltic Sea with a 3D chemistry-transport model HILATAR (Hongisto 2003).

In this study, we analyse if any of the changes in large scale circulation can be detected in forecasted meteorological marine boundary (MABL) parameters, most importantly for nitrogen deposition processes since 1993 over the Baltic Sea, and their effect on nitrogen deposition to the Baltic Sea. We studied numerical time series, trends, frequency of occurrence of certain peak values in MABL variables and influence of changes in MABL parameterization schemes on parameters forecasted by HIRLAM. In addition, dependency of deposition episodes on regional weather phenomena such as storm frequency, storm track latitude and variability of precipitation are studied. We also investigate with a model – measurement inter-comparison, the difference between precipitation measurements made at the coastal EMEP air quality or coastal meteorological stations, and the HIRLAM prediction, to estimate which value should be used to get best estimates of the nitrogen wet deposition over the Baltic Sea.

References

- Archer C. and Caldeira K., 2008. GRL 35, L08803.
Hongisto 2003. <http://lib.hut.fi/Diss/2003/isbn9512264811/index.html>
Simmonds I. and Keay K, 2009. GRL 36, L19715.
Thompson D.W.J. & Wallace J.M., 1998. Geophys Res. Lett. 25(9), 1297-1300.

Impact of climate change on the distribution of phytoplankton biomass in the Baltic Sea

J. Jakacki, L. Dzierzbicka-Glowacka, and M. Janecki

Institute of Oceanology, Polish Academy of Sciences, Sopot, Poland (jjakacki@iopan.gda.pl)

1. Abstract

This work presents numerical simulations of the long-term variations of physical and biological parameters (currents, temperature, salinity, phytoplankton and nutrient) in the Baltic Sea using the 3D CEMBS1 model. The biological model was embedded in existing hydrodynamical model of the Baltic Sea. Described in project ECOOP IP WP 10.1.1 sea – ice model (POPCICE) has been used to implement biological equations for plankton system. This work was carried out in support of grant (No N N305 111636 - the Polish state Committee of Scientific Research) and the EU-cofunded project ECOOP, IP WP 10.1.3.

2. The model

The three-dimensional model is implemented for an extended Baltic Sea area, discretized on a $9 \text{ km} \times 9 \text{ km}$ grid. A maximum of 21 vertical layers is used with 5 m resolution from the surface to ~300 m depth and with progressively increasing grid steps to span a maximum depth of 459 m for the Jama Landsort. The mean water depth in the Baltic Sea is 55 m.

In this 3D model, phytoplankton is represented by one state variable and the model formulations are based on a simple total inorganic nitrogen ($\text{NO}_3 + \text{NO}_2 + \text{NH}_4$) cycle. Nutrient serves initially as a means to trigger the bloom of phytoplankton and later to limit the phytoplankton production. The model is conceptualized for a shelf sea including the shallow sea characteristic for the replenishment of the mixed layer with nutrients from the bottom. The water column dynamics are implemented in a three-dimensional frame, where phytoplankton and nutrient (nitrogen) are transported by advection and diffusion.

3. Results

The 3D CEMBS1 model was used to simulate the long-term variations of physical and biological parameters (currents, temperature, salinity, phytoplankton and nutrient) in the Baltic Sea. The calculations were carried out assuming the following three scenarios:

- 1) an increase of air temperature by 3 degrees;
- 2) Increase of air temperature by 3 degrees, increase of wind speed by 30%, increase of westerly component of wind speed by 30% and increase of short wave radiation by 20%;
- 3) Increase of air temperature by 3 degrees, increase of wind speed by 30%, increase of westerly component of wind speed by 30% but a decrease of short wave radiation by 20%.

Daily, biweekly, monthly, seasonal and annual variabilities of investigated variables were calculated for the years 2004 - 2045 (1, 2 and 3 scenarios). The starting-point of the numerical simulations was assumed to be the end of 2004. We chose ten locations within our domain to present different model variables. These stations are: Gulf of Gdańsk, Gdansk Deep, Gotland Deep, Bornholm Deep, Gulf of Finland, Gulf of Riga, Gulf of Bothnian, Bothnian Sea, Danish Straits. Examples of results for three scenarios for Gulf of Gdańsk, Gdansk Deep, Gotland Deep:

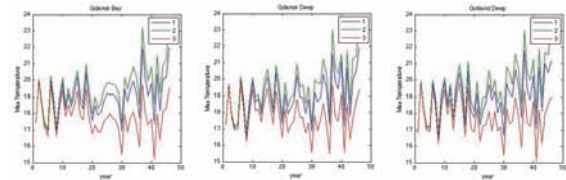


Figure 1. Maximum sea surface temperature (SST) ($^{\circ}\text{C}$) for each year at selected stations

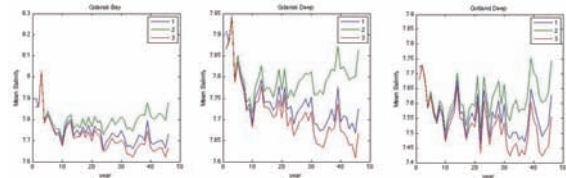


Figure 2. Annual averages of salinity for surface layer at selected stations

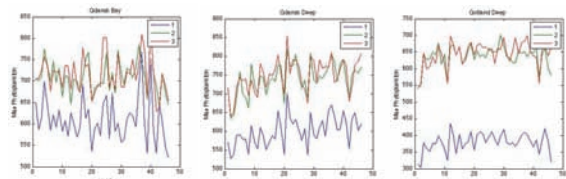


Figure 3. Annual maximum of phytoplankton biomass (mgC m^{-3}) for surface layer at selected stations.

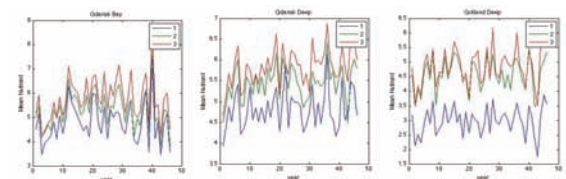


Figure 4. Annual averages of total inorganic nitrogen concentration (mmolN m^{-3}) for surface layer at selected stations.

References

- Dzierzbicka-Glowacka L., Jakacki J., Janecki M., (2010) ECOOP IP, Report on (WP 10.1.3): Quantify the monthly to decadal variability of the shelf seas-coastal physics/climate

The distribution of phytoplankton biomass in the Baltic Sea simulated by a three-dimensional model

M. Janecki, L. Dzierzbicka-Głowacka and J. Jakacki

Institute of Oceanology, Polish Academy of Sciences, Sopot, Poland (maciej.janecki@gmail.com)

1. Abstract

An integrated ecological model system has been developed that will serve as a first step towards an operational model system for the Southern Baltic area. This three-dimensional model is being developed at the Institute of Oceanology PAS, called 'Coupled Ecosystem Model of Baltic Sea, Version 1' (CEMBS1). This model has been used to estimate the annual phytoplankton biomass under circulation and solar radiation forcing conditions. The time scales of the atmosphere are governed by ERA 40 (ECMWF). The marine biogeochemical model (CEMBS1) has been coupled to the three-dimensional, time-dependent hydrodynamical model POPCICE for the Baltic Sea. The POPCICE model provides velocities, diffusion coefficients and temperature on a temporal and spatial scale that resolves the atmospherically induced variability mentioned above. The goal of our study is to construct a three-dimensional, physical-biological model to simulate the biological and chemical processes of the plankton system that are most important to quantify the annual primary production for the Baltic Sea. This work was carried out in support of grant (No N N305 111636 - the Polish state Committee of Scientific Research) and project SatBaltic.

2. The model

The three-dimensional model is implemented for an extended Baltic Sea area, discretized on a $9 \text{ km} \times 9 \text{ km}$ grid. A maximum of 21 vertical layers is used with 5m resolution from the surface to ~300 m depth and with progressively increasing grid steps to span a maximum depth of 459 m for the Jama Landsort. The mean water depth in the Baltic Sea is 55 m.

Conceptual basis

In this 3D model, phytoplankton is represented by one state variable and the model formulations are based on a simple total inorganic nitrogen ($\text{NO}_3 + \text{NO}_2 + \text{NH}_4$) cycle. Nutrients initially serve as a means to trigger the bloom of phytoplankton and later to limit the phytoplankton production. The model is conceptualized for a shelf sea including the shallow sea characteristic for the replenishment of the mixed layer with nutrients from the bottom. The water column dynamics are implemented in a three-dimensional frame, where phytoplankton and nutrients (nitrogen) are transported by advection and diffusion.

Forcing

The intention was to simulate production within a physical environment which is as realistic as possible. The actual oceanographic forcing is required for reliable simulations of the phytoplankton dynamics. The external forcing depends on meteorological data (as air density, wind stresses and wind speed, surface 2m air temperature and dew point, short and long waves radiation) and all atmospheric forces are provided by the ECMWF (ERA 40 reanalysis). The simple biological model is set up on the same grid as the hydrodynamical model POPCICE for Baltic Sea (ECOOP WP 10.1.1) and uses the daily forcing values to advect and

diffuse phytoplankton and phosphate. The biological reaction terms are not implemented within the circulation model. The primary production model is an independent transport model that uses the circulation model output, since no major effects from biology back to the physics are expected, and this makes simulations much easier to implement. Another important forcing for primary production simulations is solar radiation with its daily cycle. The total irradiance at the surface is calculated using the model by Rozwadowska and Isemer (1999) and Isemer and Rozwadowska (1999). This method was tested by Isemer and Rozwadowska (1999). The local weather conditions were made on board Voluntary Observing Ships and those data have been used to estimate climatological characteristics of the solar radiation flux at the surface of the Baltic Sea. Monthly loads are interpolated to give daily values. The nutrient contributions by the rivers are not included in this model, but the initial values for nutrients are based on SCOBI 3D-model. Phytoplankton production is limited in the model by light and total inorganic nitrogen. The phytoplankton biomass is limited by zooplankton grazing due to mesozooplankton. The zooplankton biomass is prescribed as forcing using the abundance data from the Mańkowski (1978), Ciszewski (1983) and Mudrak (2004) for the southern Baltic Sea. Using these observed biomass values and the abundances, the annual cycles of abundances were transformed to carbon biomass cycles. Trigonometric polynomial has been used to assign values at any model time and for all of the grid points.

3. Results

Daily, biweekly, monthly and seasonal variabilities (currents, temperature, salinity, phytoplankton and nutrient) of investigated variables were calculated for the year 2004. We chose ten locations within our domain to present different model variables. These stations are: Gulf of Gdańsk, Gdansk Deep, Gotland Deep, Bornholm Deep, Gulf of Finland, Gulf of Riga, Gulf of Bothnian, Bothnian Sea, Danish Straits.

References

- Dzierzbicka-Głowacka L., Jakacki J., Janecki M. (2010) ECOOP IP European COastal-shelf sea OPerational observing and forecasting system Integrated Project, Report on (WP 10.1.3): Quantify the monthly to decadal variability of the shelf seas-coastal physics/climate

Carbon budget of the Baltic Sea

Karol Kulinski and Janusz Pempkowiak

Institute of Oceanology, Polish Academy of Sciences, Sopot, Poland (kroll@iopan.gda.pl)

The last few decades in the history of mankind are characterized not only by the very rapid socio-economic transformation but also, resulting from this progress, environment degradation. The greenhouse effect is one of the most appreciable among all the symptoms. It is believed that people emit to the atmosphere approximately 10.4 Pg of carbon each year (IPCC 2007), and approximately 30-35 % of this amount is stored in the ocean (Sabine et al. 2004; Emerson and Hedges 2008). Here, shelf seas are responsible for about 20 % of all marine carbon dioxide uptake, while they constitute only 7 % of the whole sea surface (Thomas et al. 2004).

On the European shelf, the Baltic Sea seems to be particularly important with regard to CO₂ uptake. The Baltic Sea, together with the transition zone of the Danish Straits and the Kattegat, form a unique system through which transport of organic and inorganic carbon species takes place from land to the North Sea, and further to the deep Atlantic Ocean.

The Baltic Sea is a semi-enclosed shelf sea and its hydrology is well established. This distinctive features allows the evaluation of the CO₂ uptake, using the budgeting approach. However, it requires the accurate estimation of the all carbon inflows and outflows in the Baltic Sea, based on the accurate hydrological fluxes and carbon concentrations. These include: exchange with the North Sea, riverine runoff, precipitation, sedimentation and carbon return flux from the sediments, coastal point sources, and fish catching. If all these fluxes are added, assuming negative signs for the outputs and positive for the inputs, the rate of the atmosphere/water CO₂ flux results. The sign of the result will point at its direction. This approach was used to establish CO₂ flux through the atmosphere/water interface for the Baltic Sea in the period 2006-2008.

The obtained results imply very high temporal and spatial variability of carbon inputs/outputs to/from the Baltic Sea. Rivers are the major sources of both: inorganic (6.8 Tg C year⁻¹)* and organic carbon species (4.1 Tg C year⁻¹)*. When carbon export from the Baltic Sea is considered, two fundamental fluxes should be mentioned: net carbon export to the North Sea and net carbon deposition to the sediments, constituting respectively: -7.7 Tg C year⁻¹ and -2.6 Tg C year⁻¹. Since the majority of the carbon inputs and outputs balance one another only slightly, an imbalance of the Baltic Sea carbon budget was observed. This was attributed to the net CO₂ emission to the atmosphere at the level of 1.1 Tg C year⁻¹.

*based on the BALTIC-C database (financed by BONUS, Baltic Organisations Network for Funding Science EEIG).

Emerson S. R., Hedges J. I., 2008, *Chemical Oceanography and the Marine Carbon Cycle*. Cambridge University Press, Cambridge, 453 pp.

Sabine C. L., Feely R. A., Gruber N., Key R. M., Lee K., Bullister J. L., Wanninkhof R., Wong C. S., Wallace D. W. R., Tilbrook B., Millero F. J., Peng T.-H., Kozyr A., Ono T., Rios A. F., 2004, The ocean sink for anthropogenic CO₂. *Science* 305, 367-371.

Thomas H., Bozec Y., Elkalay K., de Baar H. J. W., 2004, Enhanced Open Ocean Storage of CO₂ from Shelf Sea Pumping. *Science* 304, 1005-1007.

References

IPCC, 2007, *Climate change 2007. Synthesis Report. A contribution of working groups I, II and III to the Fourth Assessment Report of the Intergovernmental Panel on Climate Change*. Cambridge University Press, Cambridge, 73 pp.

Determination of carbon return fluxes from Baltic Sea bottom sediments

Karol Kuliński, A. Szczepańska and Janusz Pempkowiak

Institute of Oceanology, Polish Academy of Sciences, Sopot, Poland (kroll@iopan.gda.pl)

1. Introduction

The carbon cycle is one of the major biogeochemical cycles that describe the flow of matter and energy in the environment. The main element of the carbon cycle is carbon dioxide. In the last century, we observed a significant increase of carbon dioxide in the atmosphere, resulting in an observed global warming. The significant increase in the temperature of the Earth causes the melting of ice caps and raising of sea levels.

It is estimated that almost 35% of carbon dioxide is absorbed by seas and oceans. Values concerning marginal seas including the Baltic are largely unknown. Major carbon fluxes in the Baltic Sea are: exchange between the Baltic Sea and the North Sea, CO₂ (carbon dioxide), air-sea flux, river run-off. Also, deposition to sediments is one of major carbon sinks in the Baltic Sea as is return carbon from sediments to sea water.

It has been proven that the deposition of carbon to the bottom sediment is one of the most important sinks of carbon in the Baltic Sea, it account for almost 23% of all the losses.

2. Modelling of carbon return flux

The carbon flux to the bottom sediments was calculated as a product of carbon concentration and sediment accumulation rates. Sediment accumulation rates were determined using the lead method and validated by the ¹³⁷Cs activity. The lead method is based on calculation of ²¹⁰Pb_{ex} (²¹⁰Pb excess). Two methods were used in determination of sediment accumulation rates: (i) CRS model (Constant Rates of Supply) which assume the variable initial concentration of ²¹⁰Pb_{ex} and sediment accumulation rate but the constant flux of ²¹⁰Pb_{ex} that reaches the sediment-water interface, and (ii) CIC model (Constant Initial Concentration) which assumes the constant initial concentration of ²¹⁰Pb_{ex}.

Carbon return flux was estimated using Fick's law of diffusion of both organic and inorganic carbon derived from the actual measurements of DIC and DOC in the pore water at surface sediments.

The lowest value of the carbon return flux was calculated for sediments from the Gotland Deep, Gulf of Finland and Gulf of Riga.

Table 1. Deposition to and return flux from sediments in selected regions of the Baltic Sea.

Area of deposition	Carbon flux to the sediments [Tg year ⁻¹]	Carbon return flux from the sediments	
		[Tg year ⁻¹]	[%]
Arcona Basin	0,064	0,033	51%
Bornholm Deep	0,764	0,249	32%
Gdansk Deep	0,729	0,232	32%
Gotland Deep	1,130	0,268	25%
Gulf of Riga	0,036	0,009	25%
Gulf of Finland	0,038	0,009	25%
Gulf of Bothnia	1,018	0,339	33%
Sum	3,779	1,139	30%

References:

- Appleby, P.G., Oldfield, F., (1978) The concentration of lead-210 dates assuming a constant rate of supply and unsupported ²¹⁰Pb to the sediment. *Cantena* 5, pp. 1-8.
- Kuliński, K., Pempkowiak, J., (2008) Dissolved organic carbon in the southern Baltic Sea: Quantification of factors affecting its distribution. *Estuarine, Coastal and Shelf Science* 78, pp. 38-44.
- Lima, A.L., Hubeny J.B., Reddy, Ch., King, J.W., Hughen, K.A., Eglinton, T., (2004) High-resolution historical records from Pettaquamscutt River basin sediments: 1. ²¹⁰Pb and varve chronologies record of ¹³⁷Cs released by the Czernobyl accident. *Geochimica and Cosmochimica Acta* 69.
- Pempkowiak, J; (1985) The input of biochemically labile and resistant organic matter to the Baltic Sea from the Vistula River. In: Degens, E. T., Kempe, S., Herrera, R. (Eds.), *Transport of Carbon and Minerals in Major World Rivers*, Pt. 3, SCOPE/UNEP Sonderband, 58, pp. 345- 350.
- Pempkowiak, J., Knapińska-Skiba, D., (1988) The determination of accumulation rates in the recent Baltic Sea sediments on the basis of Pb-210 and Cs-137 profiles. *Proceedings 16th Congressional Budget Officen* 2, pp. 824-832.
- Schneider, B., Thomas, H., Stamer, A., (1996) The carbon budget in Gotland sea surface waters: October to February. *Meereswiss. Ber.*, 19, pp. 105-113.
- Thomas, H., Pempkowiak, J., Wulff, F., Nagel, K., (2003) Autotrophy, nitrogen accumulation and nitrogen limitation in the Baltic Sea: A paradox or a buffer for eutrophication?. *Geophysical Research Letters* 30, pp. 2130-2135.
- Thomas, H., Schneider, B., (1999) The seasonal cycle of carbon dioxide in Baltic Sea surface waters. *Journal of Marine Systems* 22, pp. 53-67.

Impact of climate change on the development of *Temora longicornis* in the southern Baltic Sea

A. Lemieszek¹, L. Dzierzbicka-Głowacka² and I.M. Żmijewska¹

¹Institute of Oceanography, University of Gdansk, Gdynia, Poland (anna_lemieszek@op.pl)

²Institute of Oceanology, Polish Academy of Sciences, Sopot, Poland

1. Abstract

The present work advances the idea of establishing the combined effect of temperature and food concentration on the development of the naupliar stage and copepodid stages (C1, C2, C3, C4, C5) of *Temora longicornis*. It is important to investigate and identify the critical factors in mathematical models of pelagic communities with a high-resolution zooplankton (herbivorous copepods) module as a top-down regulator that may play a significant role in marine ecosystems. The paper presents an empirical model describing the total development time of *Temora longicornis* as a function of food concentration and temperature. Relationships were obtained between the above-mentioned parameter and temperature for the 5-20°C temperature range and food concentrations from 25 mg C m⁻³ to excess. The generation time during the seasons in upper layer of the southern Baltic Sea (Gdańsk Deep) were calculated for the years: 1965-1998 and 50 years later. The calculations were made assuming the following: 1) increase in the water temperature in the upper layer: 0.008°C per year; 2) increase in the available light: 0.2% per year; 3) nutrients concentration increase 1% per year; 4) wind speed equal to the average values for 1965-1998 period. The starting-point of the numerical simulations was assumed as average values of the investigated pelagic variables for the 1965-1998 period. 50 years later, 1.7 and 1.9 fold increases of food concentration in spring bloom were calculated as well as the postponement of the maximum food concentration. It is speculated that due to food availability increase generation time of *T. longicornis* will decrease, while growth its will increase. This work was carried out in support of grant (the Polish state Committee of Scientific Research).

2. Development time

The present analysis is based on literature data concerning material collected from the south-eastern and southern parts of the North Sea (Klein Breteler et al. 1982; Klein Breteler and Gonzalez 1986; Klein Breteler et al. 1990).

Conversion of the data for the development times D after Klein Breteler and Gonzalez (1986) to natural logarithms yielded a linear relationship between time and food concentration. This relationship was described by the equation:

$$\ln(D - D_{\min}) = aFood + b$$

hence,
$$D = e^{aFood+b} + D_{\min}$$

where $\log D_{\min} = a_1 \log T + b_1$

The coefficients a and b of the equations describing D as a function of food concentration were obtained as a function of temperature in the 5-20°C range by a third-degree polynomial. The regression equations for each of the stages N1 – N6, C1, C2, C3, C4, C5 and for the total period of growth from N1 to medium adult are given in Table III in Dzierzbicka-Głowacka et al. (2010). 93% of the values of D

computed with the equation as a function of food concentration and temperature lie within the range of the parameter D given by Klein Breteler et al. (1982). The sets of stage duration curves computed with equation (2) of *T. longicornis* for each of model stages are shown in Figure 2 Dzierzbicka-Głowacka et al. (2010).

3. Numerical simulation

In this paper, the development of individuals in the southern Baltic Sea is manifested by a change in the total stage duration (N1-C5) as a function of both temperature and food concentration. The impact of the above parameters on the generation time of *Temora longicornis* during the seasons in the upper 10 m layer in the Gdańsk Deep (southern Baltic Sea) is described by above equation. The temperature and food composition (equal to 60% of the phytoplankton biomass, 15% of the zooplankton biomass and 25% of the pelagic detritus concentration) used in this paper are mean values from the last 38 years (1965-98) (data from the 1DCM model – Dzierzbicka-Głowacka et al. 2006).

The annual cycle of the generation time as a result of the above-mentioned parameters is shown. The calculations also suggest that three complete generations of *T. longicornis* from the Gdańsk Deep can develop during a single year in the upper layer. Simulated generation times are affected mostly by temperature and to a lesser degree by food availability. But in spring bloom, the effect of food concentration on the first generation is more evident.

This paper also presents a seasonal change of D for *T. longicornis* in the southern Baltic Sea 50 years later. The study was based on a 1DCM model describing food composition (phytoplankton, zooplankton and pelagic detritus). This model was used to simulate the long-term variations of pelagic variables in the southern Baltic Sea (see ECCOP WP10 Project). The annual cycle of *Food* and contributing factors: phytoplankton (*Phyt*), zooplankton (*Zoop*), and detritus (*DetrP*), in the upper zone indicates large food concentration in spring bloom resulting from the *Phyt* bloom and generation of detritus originating from *Phyt* mortality and in summer due to increased concentrations of zooplankton. As a consequence, concentration of *Food* in the range between 310 and 330 mg m⁻³ persist between April and October with, just, a two and a three weeks long brake in May and July, respectively. The level of *Food* 50 years later is 1.7 in the spring bloom and 2.2 times larger in summer than on average in the period 1965-1998.

It is speculated that due to an increasing food availability, generation times of *T. longicornis* will decrease, ca 30 days in winter (in February/March) and ca 14 days in spring/summer, while growth will increase. The numerical simulations suggest that any increase in temperature and food (above 300 mg C m⁻³) in the summer time will affect the complete development of *T. longicornis*.

References

- Dzierzbicka-Glowacka, L., Bielecka, L. and Mudrak, S. (2006) Seasonal dynamics of *Pseudocalanus minutus elongatus* and *Acartia* spp. in the southern Baltic Sea (Gdańsk Deep) - numerical simulations, *Biogeosciences*, 3, pp. 635-650
- Dzierzbicka-Glowacka, L., Lemieszek, A. and Żmijewska, M.I. (2009) Parameterisation of a population model for *Acartia* spp. in the southern Baltic Sea. Part 1. Development time, *Oceanologia*, 51, pp. 165-184
- Dzierzbicka-Glowacka, L., Lemieszek, A. and Żmijewska, M.I. (2010) Development and growth of *Temora longicornis* - numerical simulations using a laboratory culture data, *Journal of Marine Biology* (submitted)
- Klein Breteler, W.C.M. (1980) Continuous breeding of marine pelagic copepods in the presence of heterotrophic dinoflagellates, *Mar. Ecol. Progr. Ser.*, 2, pp. 229-233
- Klein Breteler, W.C.M., Fransz, H.G. and Gonzalez, S.R. (1982) Growth and development of four calanoid copepod species under experimental and natural conditions, *Neth. J. Sea Res.*, 16, pp. 195-207
- Klein Breteler, W.C.M. and Gonzalez, S.R. (1986) Culture and development of *Temora longicornis* (Copepoda, Calanoida) cultured at different temperature and food conditions, *Mar. Ecol. Progr. Ser.*, 119, pp. 99-110
- Klein Breteler, W.C.M., Schogt, N. and Gonzalez, S.R. (1990) On the role of food quality and development of life stages, and genetic change of body size during cultivation of pelagic copepods, *J. Exp. Mar. Biol. Ecol.*, 135, 177-189

Modeling the egg production of *Temora longicornis*

A. Lemieszek¹, L. Dzierzbicka-Glowacka² and I.M. Żmijewska¹

¹Institute of Oceanography, University of Gdansk, Gdynia, Poland (anna_lemieszek@op.pl)

²Institute of Oceanology, Polish Academy of Sciences, Sopot, Poland

This paper describes the egg production of *Temora longicornis* in the changing environmental conditions in the southern Baltic Sea (Gdańsk Deep) by means of modeling. Here, we use the hypothesis that food-saturated rate of production of egg matter is equivalent to specific growth rate of copepods. The average number of eggs produced per day by one female of *Temora longicornis* as a function of growth rate, i.e. multiplying $\text{exp}g_N - 1$ from the growth rate of the naupliar stage equation by $W_{\text{female}} / W_{\text{egg}}$ is obtained. The effects of temperature and food concentration on growth rate of *Temora longicornis* for each of model stages is presented in Dzierzbicka-Glowacka et al. (2010). In this part, the egg production as a function of the above mentioned parameters is evaluated. Also, the rate of reproduction during the seasons in the upper layer at the Gdańsk Deep is determined.

To describe the potential egg production we need (i) the maximum growth rate for the naupliar stage, (ii) egg dry weight, (iii) weight of female and (vi) experimental temperature.

The mean growth rate of *T. longicornis* for three developmental stages (N1 – C1, C1 – C3 and C3 – C5) as a function of food concentration at 15°C is given by the equation (1) (see Dzierzbicka-Glowacka et al. 2010):

$$g_i = g_{\max} fte \left\{ 1 - \exp\left(\frac{-(\text{Food} - \text{Food}_o)}{k_{\text{Food}}}\right) \right\} \quad (1)$$

where g_{\max} (% of weight day^{-1}) is the maximum growth rate at 15°C and excess food, Food (mg C m^{-3}) is the food concentration, Food_o (mg C m^{-3}) is the value of Food at which $g = 0$, and k_{Food} (mg C m^{-3}) is the half saturation constant, since g_{\max}/k_{Food} for Food is slightly greater than Food_o , and fte is a function of temperature. For each stage, $\text{Food}_o = 0$ and $fte = 1$ at $T = 15^\circ\text{C}$; however, k_{Food} lies in the 90-140 mg C m^{-3} range (see Dzierzbicka-Glowacka et al. 2010). The growth rates for successive stages at 15°C were obtained according to the correction of the 'Moult Rate' method that allows use of mean weights and durations of stages (see Klein Breteler et al. 1982, Hirst et al. 2005, Dzierzbicka-Glowacka et al. 2010).

The function of g_{\max} for model nauplii stage (Figure 1) can predict food-saturated, temperature-dependent, specific production rate of egg matter by female as: $\text{ProdEgg} = \text{exp}g_{\max} - 1$ after Sekiguchi et al. (1980) and McLaren and Leonard (1995). The rate of production of egg matter, ProdEgg , obtained in this work as a function of temperature through maximum growth rate (for N3-N6), for well-fed female of *T. longicornis* increases with increasing temperature and assumes values from 0.145 to 0.332 $\mu\text{g } \mu\text{g}^{-1}\text{day}^{-1}$ at temperatures ranging from 5 to 20°C. Potential daily growth rate can be converted to the equivalent maximum number of eggs produced per day by one female, as: $\text{Egg} = W_{\text{female}} / W_{\text{egg}} \text{ProdEgg}$, assuming that W_{egg} and W_{female} are the weights of an egg and female, respectively. Equation (1), which determines the growth of *T. longicornis* (reduced by food limitation) was used to obtain the production rate of egg matter by female, as: $\text{ProdEgg} =$

$\text{exp } g_i - 1$, where $g_i = f(\text{Food}, T)$ is the growth rate for the naupliar stage – N3-N6. Hence, considering g_i for specific development stage N3-N6, ProdEgg for females of *T. longicornis* computed as a function of food concentration and temperature. The calculations demonstrate that ProdEgg becomes less dependent on food concentration than on temperature and assumes from 0.031 to 0.134 $\mu\text{g } \mu\text{g}^{-1}\text{day}^{-1}$ at 5°C, 0.072 to 0.332 $\mu\text{g } \mu\text{g}^{-1}\text{day}^{-1}$ at 15°C and 0.067 to 0.307 $\mu\text{g } \mu\text{g}^{-1}\text{day}^{-1}$ at 20°C in the 25 – 300 mg C m^{-3} food concentration range. However, successively the values of ProdEgg were used to determine the number of eggs produced per day by one female. Transformation of these data yields a relationship between the temperature and the number of eggs at selected food levels:

$$\text{Egg} = a \exp(b T) \quad (2)$$

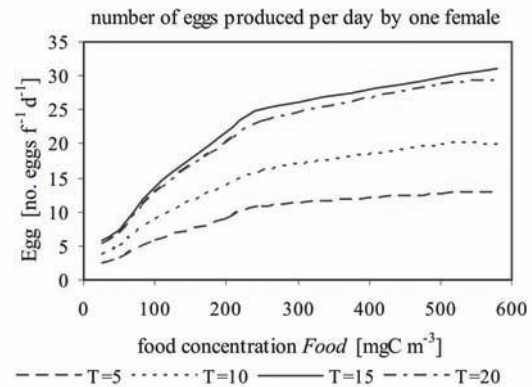


Figure 1. Relationships between the number of eggs produced per day by one female of *T. longicornis* (no. eggs day^{-1}) and food concentration (mg C m^{-3}) at different temperature T ($^\circ\text{C}$): 5, 10, 15 and 20 $^\circ\text{C}$.

However, the coefficients a and b were obtained as a function of food concentration. The regression equations are given in Figure 1.

References

- Dzierzbicka-Glowacka, L., Lemieszek, A. and Żmijewska, M.I. (2010) Development and growth of *Temora longicornis* - numerical simulations using a laboratory culture data, Journal of Marine Biology (submitted)
- Hirst, A.G., Peterson, W.T., Rothery, P. (2005) Errors in juvenile copepod growth rate estimates are widespread: problems with the Moulting Rate method, Mar. Ecol. Prog. Ser., 296, pp. 263-279
- Klein Breteler, W.C.M., Fransz, H.G., Gonzalez, S.R. (1982) Growth and development of four calanoid copepod species under experimental and natural condition, Neth. J. Sea Res., 16, pp. 195-207
- McLaren IA, Leonard A (1995) Assessing the equivalence of growth and egg production of copepods, ICES J Mar Sci 52, pp. 397-408

Particulate organic carbon in the southern Baltic Sea

A. Maciejewska, L. Dzierzbicka-Głowacka, K. Kuliński and J. Pempkowiak

Institute of Oceanology, Polish Academy of Sciences, Sopot, Poland (aninamac@iopan.gda.pl)

1. Numerical simulations and experimental data

Particulate Organic Carbon (POC) is an important component in the carbon cycle of estuarine systems. We assess the POC concentration dynamics in the Gdansk Deep, southern Baltic Sea, for 2007. Our study is based both on a 1D POC Model and the actual POC concentrations measurements. The aim is twofold: (i) validation of the simulated concentrations with actual measurements, and (ii) qualitative assessment of sources contributing to the POC pool.

Mathematically, the pelagic variables of 1D POC model are described by a second-order partial differential equations of the diffusion type with biogeochemical sources and sinks. This model consists of six coupled equations: five diffusion-type equations for phytoplankton, zooplankton, pelagic detritus and nutrients (phosphate and total inorganic nitrogen) and one ordinary differential equation for detritus at the bottom. The POC concentration is determined as the sum of phytoplankton, zooplankton and dead organic matter (pelagic detritus) concentrations, all expressed in carbon equivalents (bacteria were not simulated). The temporal changes in the phytoplankton, zooplankton biomass and pelagic detritus concentration are caused by specific relation between them in trophic zone.

Observed large fluctuations of the measured POC concentrations are attributed to its appreciable seasonal variability. The maximum concentration of POC fluctuated between 870 mg C m^{-3} (1030 mg C m^{-3} for 2008) in May and 580 mg C m^{-3} in September, coinciding with the period of both the maximum dead organic matter and the phytoplankton biomass concentrations. The results of the numerical simulations are in good agreement with the observed values. The difference between the modeled and observed POC concentrations is equal to 3 - 28 % and depend on the month for which the calculations were made, although, no time trend of the difference is observed (Figure 1). The conclusion is that the numerical simulations mimic sufficiently well POC dynamics in the Baltic.

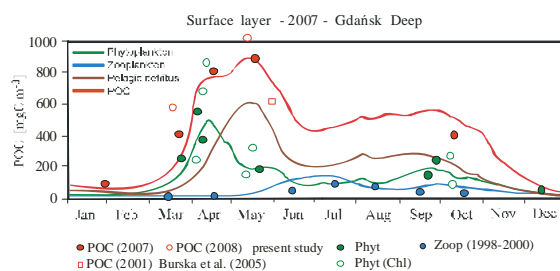


Figure 1. Modelled POC seasonality presented against background of *Phyt*, *Zoop* and *DetrP* and in situ measured POC concentrations.

2. Scenarios

The 1D POC model was then used to test the influence of nutrients and available light conditions. 1D POC model was used to simulate variations of POC in the southern Baltic Sea (Gdansk Deep, Bornholm Deep and Gotland Deep). Daily, monthly, seasonal and annual variability of POC in the upper layer were calculated for the different nutrients

concentrations, available light, water temperature and wind speed scenarios. The starting-point of the numerical simulations was assumed as average values of the investigated pelagic variables for 1965-1998 period. Two- to three-fold increases of POC concentrations in late spring were found as well as the postponement of the maximum POC concentrations. It is speculated that, due to POC increase, oxygenation of under-halocline water layer will decrease, while supply of feed should increase.

References

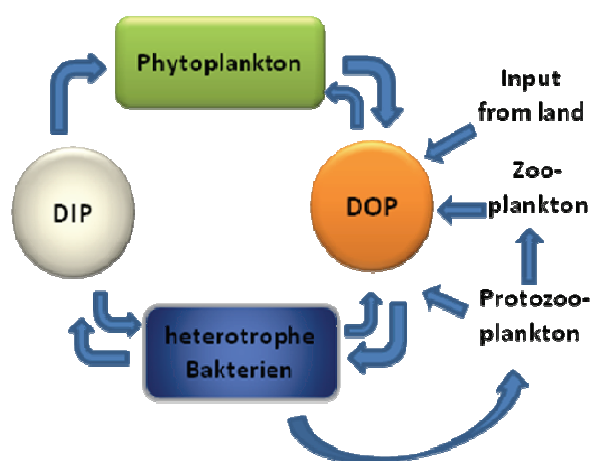
- Andersson, A., Rudehäll, Å., 1993. Proportion of plankton biomass in particulate organic carbon in the northern Baltic Sea. *Marine Ecology Progress Series* 95, pp. 133-139.
- Burska, D., Pryputniewicz, D., Falkowska, L., 2005. Stratification of particulate organic carbon and nitrogen in the Gdańsk Deep (southern Baltic Sea). *Oceanologia* 47, pp. 201-217.
- BACC Author Team, 2008. Assessment of Climate Change for the Baltic Sea Basin. Springer-Verlag, Berlin, pp. 473.
- Doney, S. C., Linsay, K., Moore, J. K., 2003. Global ocean carbon cycle modeling, In: Fasham M. J. R. (Editor), *Ocean Biogeochemistry*. Springer-Verlag, Berlin, Heidelberg, pp. 217-238.
- Dzierzbicka-Głowacka, L., 2006. Modelling the seasonal dynamics of marine plankton in southern Baltic Sea. Part 2. Numerical simulations. *Oceanologia* 48(1), pp. 41-71.
- Dzierzbicka-Głowacka, L., 2005. Modelling the seasonal dynamics of marine plankton in southern Baltic Sea. Part 1. A Coupled Ecosystem Model. *Oceanologia* 47(4), pp. 591-619.
- Dzierzbicka-Głowacka, L., 2000. Mathematical modelling of the biological processes in the upper layer of the sea. *Diss. Monogr.* 13, Institute of Oceanology, PAS, Sopot, 124 pp. Grzybowski, W., Pempkowiak, J., 2003. Preliminary results on low molecular weight organic substances dissolved in the waters of the Gulf of Gdańsk. *Oceanologia* 45 (4), pp. 693-704.
- Kuliński, K., Pempkowiak, J., 2008. Dissolved organic carbon in the southern Baltic Sea: Quantification of factors affecting its distribution. *Estuarine, Coastal and Shelf Science* 78, pp.38-44.
- Renk, H., 2000. Primary production in the southern Baltic. *Sea Fisheries Institute in Gdynia, Stud. Mater* 35 (A), 78 pp.
- Witek, Z., 1993. Structure and function of marine ecosystem in Gdańsk Gulf on the basis of studies performed in 1987. *Scientific Committee on Oceanic Research* 63, pp.1-23.

Dissolved organic phosphorus in the Baltic Sea: Temporal and spatial variations

Monika Nausch, Günther Nausch, D. Setzkorn, B. Sadkowiak, Ä. Welz

Leibniz Institute for Baltic Sea Research, Rostock-Warnemünde, Germany (monika.nausch@io-warnemuende.de)

Phosphorus is an essential nutrient for phytoplankton and bacterial growth. Dissolved inorganic phosphorus (DIP) and dissolved organic phosphorus (DOP) are the sources which can be taken up by these organisms. DIP is the preferred substrate and is often exhausted in natural systems during the growth season. Then DOP becomes the only available phosphorus pool. On the other hand, phytoplankton and heterotrophic bacteria produce DOP either by exudation or release after cell death. Additional sources are release by protozoo- and zooplankton as well as allochthonous input by rivers (see figure).



Sources and sinks of DOP

By searching the ASFA data base, about 6000 papers were found testifying that the function of DIP in biochemical cycling and nutrition is intensively studied. In comparison, only about 400 published papers could be found for DOP and thus the knowledge about the detailed function and mechanisms of transformation of DOP in biogeochemical cycling is scarce. A fundamental step in studying the role of DOP is the knowledge of concentrations and pool sizes. In this sense we have studied temporal and spatial variations of DOP in the Baltic Sea.

Depth profiles demonstrate that that DOP occurs in significant concentrations only in the surface up to 40 m depth. Below a depth of 80 m not any DOP concentrations could be measured.

The seasonality of DOP concentrations has been studied in the years 2000 to 2005 in the eastern Gotland Basin. Mean values of these six years increased from $0.14 \pm 0.07 \mu\text{M}$ in February/March to $0.26 \pm 0.04 \mu\text{M}$ in July and August.

To study the spatial distribution of DOP, samples were taken on two cruises over the entire Baltic Sea, done from 17 June to 17 July 2008, and from 22 February to 11 March 2009. In summer, maximum DOP concentrations of $0.32 \mu\text{M} \pm 0.05 \mu\text{M}$ were measured in the Baltic Proper. The concentration decreased northwards. Lowest concentrations were found at

the northernmost station in the Bothnian Bay. Concentrations became also lower in the more oligotrophic Kattegat and Skagerrak. The distribution pattern in February/March were similar in the Baltic Proper and the Gulfs, but the concentrations were below those of the preceding summer. In contrast, DOP concentrations in the Kattegat and Skagerrak exceeded those in the Baltic Proper because the phytoplankton spring bloom was initiated there.

It was shown manifold, that DOP cannot be taken up by phyto- and bacterioplankton in total (e.g. Benitez-Nelson & Buesseler 1999, Björkman and Karl 2003, Nausch and Nausch 2006). DOP comprises two proportions, one which can be taken up by organisms is called the bioavailable proportion (BAP) and one proportion, the refractory DOP, is persistent for longer times. Only the BAP can support plankton growth in summer when DIP is depleted. In summer 2008, these fractions were determined at 14 stations in the Gulfs of Finland and Bothnia and in the Baltic Proper. In these experiments, BAP is that proportion which is taken up by heterotrophic bacteria after carbon and nitrogen amendment in time course experiments over 6 days. BAP constituted a proportion between 27 % in the Baltic Proper and 37 % in the Gulf of Finland. But due to lower DOP concentrations in the Gulf of Finland the absolute BAP concentrations are lower there than in the central regions. The DIP limited Bothnian Bay has only minor BAP concentrations. Summing up DIP and BAP concentrations, the highest quantity of usable phosphorus was found in the Bornholm Basin decreasing northwards and was scarce in the Bothnian Bay. From Spearman Rank correlations can be deduced that the quantity of BAP is predominantly determined by phytoplankton concentrations (*Chla*) and its nutrition state.

For the Baltic Sea it can be summarized that BAP and DOP concentrations are coupled to the phytoplankton development and their nutrition state. The central Baltic Sea seems to have the best phosphorus conditions in summer 2008 followed by the Gulf of Finland. Along with DIP, DOP and BAP concentrations decrease in the Gulf of Bothnia. Especially in the northernmost parts are no phosphorus reserves available. Allochthonous input was not visible.

References

- Benitez-Nelson CR, KO Buesseler (1999) Variability of inorganic and organic phosphorus turnover rates in the coastal ocean. *Nature* 389: 502-505
- Björkman KM, DM Karl (2003) Bioavailability of dissolved organic phosphorus in the euphotic zone at station ALOHA, North subtropical gyre. *Limnol Oceanogr* 48: 1049-1057
- Nausch M, Nausch G (2006) Bioavailability of dissolved organic phosphorus in the Baltic Sea. *Mar Ecol Prog Ser* 321: 9-17

Factors influencing the acid-base (pH) balance in the Baltic Sea: A sensitivity analysis

Anders Omstedt¹, Moa Edman¹, Leif Anderson² and Hjalmar Laudon³

¹Department of Earth Sciences: Oceanography, University of Gothenburg, Göteborg, Sweden (Moa.Edman@gvc.gu.se)

²Department of Chemistry, University of Gothenburg, Göteborg, Sweden

³Department of Forest and Environment, SLU Umea, Umea, Sweden

1. Abstract

From calculations based on the marine carbon system and box- and numerical modelling, the sensitivity of the Baltic Sea pH is examined. From a transient long-term calculation, it was demonstrated that the surface carbon system is adjusted to the lateral boundary conditions within some decades, similar to salinity. Long-term calculations are therefore dependent on the lateral conditions, and thus changes on land, in the atmosphere and outside the Baltic Sea.

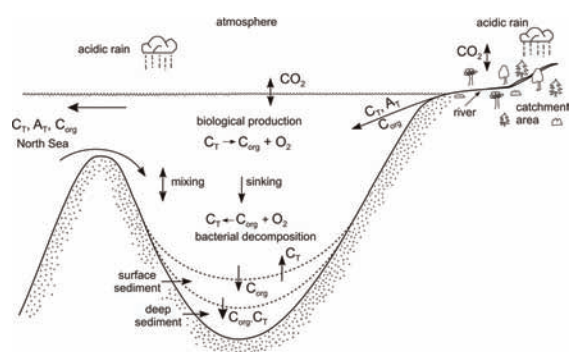


Figure 1. Schematic depiction of the Baltic Sea carbon system

The direct effect on sea water pH from acid precipitation over the Baltic Sea surface area was shown to be small even for significantly increased precipitation rates.

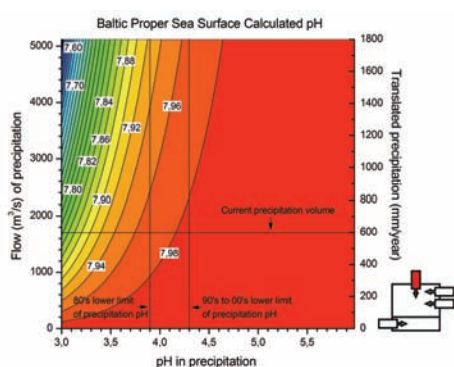


Figure 2. Figure illustrating the Baltic Sea pH sensitivity to changes in precipitation (mm/yr) and A_T ($\mu\text{mol/kg}$)

Indirect effects on land (acid precipitation and land use change) may, however, have stronger influence on the pH balance. The acidification due to river transports of

dissolved organic carbon (DOC) into the marine system seems small. However, the mineralization of DOC may add extra acidification, but this effect is still unknown. Climate change within present estimated range in temperature (some degrees) and salinity (some salinity units) will only marginally change the acid-base (pH) balance. Nor is it likely that a wetter or dryer climate will change the pH balance, due to compensating effects in the marine carbon system. Instead it is direct and indirect effects from fossil fuel burning that may affect the sea water pH and total alkalinity.

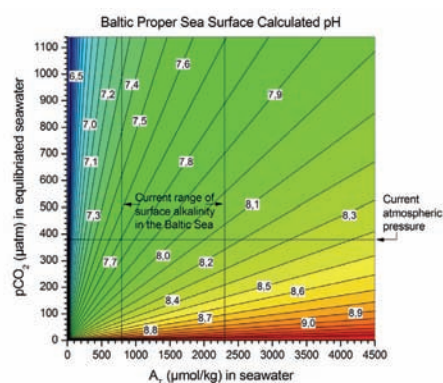


Figure 3. Figure illustrating the Baltic Sea pH sensitivity to changes in CO_2 (μatm) and A_T ($\mu\text{mol/kg}$)

This might cause threats within the Baltic Sea, particularly in the Northern Baltic Sea.

References

- Omstedt, A., Edman, M., Anderson, L.G. and Laudon, H. (2009) Factors influencing the acid-base (pH) balance in the Baltic Sea: A sensitivity analysis. Tellus B, Submitted



Importance of the Szczecin Lagoon for the Odra River mouth area in the light of geochemical studies in the Polish part of the basin

Andrzej Osadczuk, Artur Skowronek, Andrzej Witkowski and Łukasz Maciąg

Institute of Marine Sciences, Faculty of Earth Science, University of Szczecin, Poland (andros@univ.szczecin.pl)

The Szczecin Lagoon is an area of a key importance for the Odra River discharge system. Exchange of water between the Odra and the Baltic Sea happens via a shallow lagoony system which includes three relatively long and narrow straits. The lagoon is strongly affected by anthropogenic impacts from industry, shipping and agriculture. A serious problem in the lagoon is the large nutrient load which in turn results in eutrophication.

The average salinity of the Szczecin Lagoon ranges between 0.6 and 0.9 PSU and changes seasonally; the pattern of change differs between various parts of the lagoon. The sedimentation processes are highly specific, and significantly different from either marine, fluvial, or limnic environments. However, the macroscopic structure of the lagoon's organic-mineral muds as well as their lithological and geochemical properties closely corresponds to lacustrine gyttja. The principal components of the muddy sediments are: quartz pelite, amorphous organic matter (up to 12% C_{org}) and biogenic remains (crushed shells of molluscs, ostracods and diatoms) (Osadczuk 2004).

Chemical analyses reveal that concentrations of heavy metals in lagoony sediments in total do not exceed permissible values. Only mercury and zinc show dangerously high levels in some parts of the lagoon bottom. Our measurements reveal 55 samples with concentrations of Hg higher than 1 mg kg^{-1} , and 6 samples with concentrations of Zn higher than 1000 mg kg^{-1} (out of a total of 606 analyses).

Surface sediments are minimally contaminated with PAH's (Polycyclic Aromatic Hydrocarbons) and PCB's (Polychlorinated Biphenyls), but are significantly contaminated by organic compounds of tin (Sn). All analyses revealed concentrations of tributyltin (TBT) above the threshold value. Positive significant correlations were found between some heavy metals as well some toxic substances, e.g.: As and Co, Fe, Pb, Zn, Sn; Cd and Cr, Co, Cu, Hg, Ni, Pb, Zn, Sn, PAH's, C_{12} - C_{35} ; Hg and Cd, Cr, Co, Cu, Ni, Pb, Zn, Sn, PAH's.

There are significant differences in sedimentary conditions between the south-western part and north-eastern part of the Polish part of the lagoon. However, a relatively low degree of sediment contamination indicates that Szczecin lagoon is rather a transit than retention (sedimentary) basin for pollutants. It corresponds to results reported earlier by Lampe (1999).

This research was completed within the project "Lithogenesis and geochemistry of bottom and nearshore sediments of Szczecin Lagoon" granted by the Polish Ministry of the Environment and sponsored by the National Fund for Environmental Protection and Water Management.

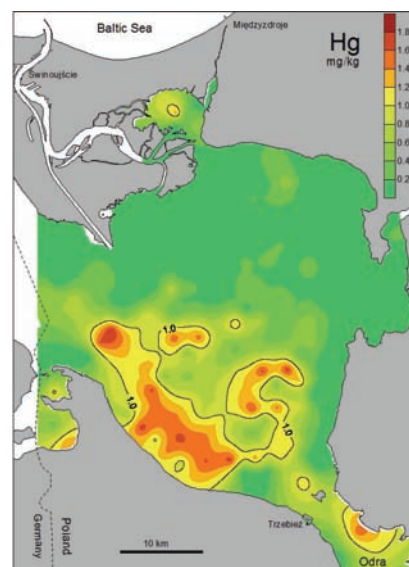


Figure 1. Concentration of mercury in lagoony sediments

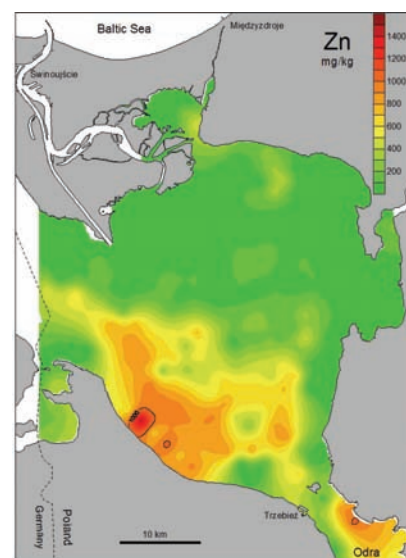


Figure 2. Concentration of zinc in lagoony sediments

References

- Lampe R. (1999), The Odra Estuary as a filter and transformation area, *Acta hydrochim. hydrobiol.*, 27, 5: pp. 292-297.
- Osadczuk A. (2004), Zalew Szczeciński - środowiskowe warunki współczesnej sedymentacji lagunowej. Wydawnictwa Naukowe Uniwersytetu Szczecińskiego, Rozprawy i studia T. (DCXXIII) 549: pp. 156.

Database of published nitrogen concentrations in air and precipitation around the Baltic Sea 1850-1960

Tuija Ruoho-Airola, Maija Parviainen and Virpi Tarvainen

Finnish Meteorological Institute, Air Quality, Helsinki, Finland (tuija.ruoho-airola@fmi.fi)

1. Introduction

The BONUS+ ECOSUPPORT programme (Advanced modeling tool for scenarios of the Baltic Sea ECOsystem to SUPPORT decision making) uses atmospheric nutrient loads to force the biogeochemical models for 1850-2007. The Finnish Meteorological Institute provides the atmospheric load from available published data. Because recent air and precipitation quality data are available at several open databases (e.g. EMEP), we concentrate on older measurement results.

2. Material

A literature search revealed over 40 articles with results of air and precipitation measurements within the influence area of the Baltic Sea between 1850 and 1960. Some of the articles presented a review of a large quantity of older measurements, others published results for a few months of monitoring in a network. Articles about monitoring at individual stations covered often experimental work for some years. A thorough investigation of the early air quality measurements has been published in Eriksson (1952), Miller (1905) and Russel (1919).

In the beginning of the period studied, the monitoring of air and precipitation quality was often performed at agricultural research stations where the personnel were acquainted with strict sampling guidelines and chemical analysis of nutrients in low concentrations. So, in many sites there were methods for air and precipitation analysis available already in the 19th century.



Figure 1. Location of stations with air and/or precipitation quality measurements from 1850 to 1870.

The articles were mostly so old that no electronic version was available. The tables in the articles were scanned, transformed in electronic form and checked carefully for errors in the conversion procedure in order to provide the forcing data needed. Only stations estimated to have influence for the Baltic Sea were included. A quality estimate for the data based on the information given in the article will be performed in 2010.

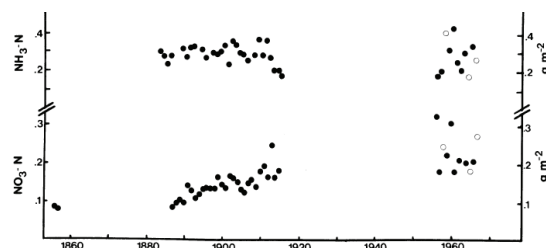


Figure 2. Annual deposition of nitrate and ammonium with precipitation at Rothamsted, UK, by Brimblecombe and Pitman (1980).

3. Location of sampling stations

We present maps showing the location of stations with historical air and/or precipitation data for the nitrogen compounds. Figure 1, as an example, indicates all the sites from where there is data in the database for the earliest period, decades 1850, 1860 and 1870. For some of the stations, the measurements cover years in several decades.

4. Selected analysis of load in different time periods

Repeated monitoring at the same location during different decades enables estimation of the change in the nitrogen load during long time periods. At the Rothamsted station in southern UK, measurements cover the years 1888-1916 and again 1955-66. Brimblecombe and Pitman (1980) analysed carefully the quality of the deposition values. They came to the conclusion that the annual nitrate deposition has increased in that time period from about 1 to 2 g/m², but ammonium deposition has stayed unchanged (Figure 2).

At stations Askov in Denmark and Flahult in Sweden, measurements of the nitrogen compounds in precipitation have been performed in the beginning of the 20th century and again in the 50's. Figure 3 presents annual depositions for nitrate and ammonium at these stations according to Eriksson (1952) and Anonymous (1956-59). In Flahult, the published ammonium load was much lower in the 50's than in 1909, whereas in Askov no clear change in the load can be detected. For nitrate, the level of the load has not changed more than the annual variation in the 50's. After the quality control of the data in the database, the changes in the nitrogen load can be analysed more regionally.

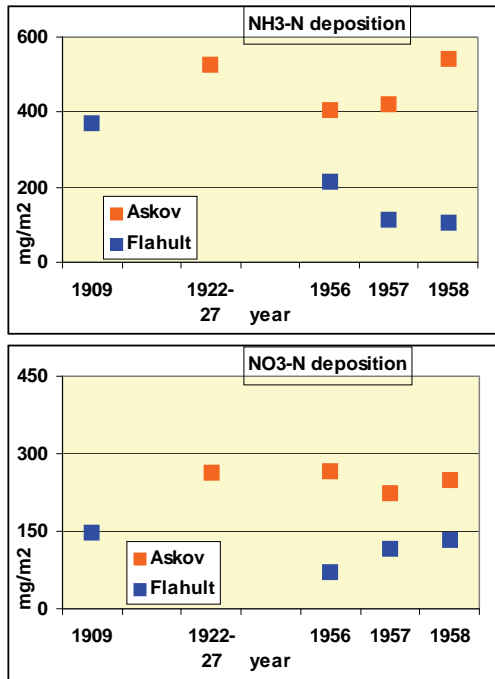


Figure 3. Annual deposition of ammonium (upper panel) and nitrate (lower panel) with precipitation at Askov, Denmark and Flahult, Sweden according to a review of Eriksson (1952) and Anonymous (1956, 1957 and 1958).

References

- Anonymous (1956, 1957, 1958 and 1959). Current Data on the Chemical Composition of Air and Precipitation. Note. Tellus, vol. 8-11.
- Brimblecombe P. and Pitman J. (1980) Long-term deposit at Rothamsted, southern England, Tellus, 32, 3, pp. 261-267.
- Eriksson E. (1952) Composition of Atmospheric Precipitation. I Nitrogen compounds. Tellus, 4, 3, pp. 215-232.
- Miller N.H.J. (1905) The amounts of nitrogen as ammonia and as nitric acid, and of chlorine in the rainwater collected at Rothamsted. J. Agr. Sci. 1, pp. 280-303.
- Russel E.J. and Richards E.H. (1919) The amount and composition of rain falling at Rothamsted, J. Agr. Sci. 9, pp. 309-337.

Do the ratio of pigments and carbon content in main groups of algal classes depend on trophicity? Preliminary results

Mirosława Ostrowska¹, Joanna Stoń-Egiert¹, Maria Łotocka¹ and Roman Majchrowski²

¹Institute of Oceanology, Polish Academy of Science, Sopot, Poland, (ostra@iopan.gda.pl)

²Pomeranian University in Słupsk, Poland

1. Aim

The far-reaching aim of our investigations is to describe how the pigment composition in main taxon groups of phytoplankton in Baltic (that is *Bacillariophyceae*, *Dinophyceae*, *Cryptophyceae*, *Chlorophyceae* and cyanobacteria) depends on trophicity. In this work the relation between content of different groups of phytoplankton species and concentration and composition of chlorophylls and carotenoids in samples of marine water from regions of Southern Baltic with different chlorophyll *a* concentrations were analysed.

2. Materials and method

Our investigations were carried out on experimental data collected in different regions of Southern Baltic during cruises of r/v Oceania from 1999 to 2005 (see Figure 1). The species of the major taxonomic groups were determined using Utermöhl's sedimentation techniques (Willen 1962) and an inverted microscope (Axiovert M35, Carl Zeiss, Germany) fitted with phase contrast and differential interference contrast. Phytoplankton counts were carried out in accordance with the COMBINE programme of HELCOM (1997). The carbon contents in phytoplankton samples were calculated according to Menden-Deuer and Lessard (2000). The pigment concentrations were determined using RP-HPLC methods, commonly used in oceanographic measurements (Stoń and Kosakowska 2002, Stoń-Egiert and Kosakowska 2005). The samples were taken mainly in eutrophic regions (chlorophyll *a* range; 0,42 - 35,3). The range of concentrations of main taxon groups and chosen pigments are given in Table 1.

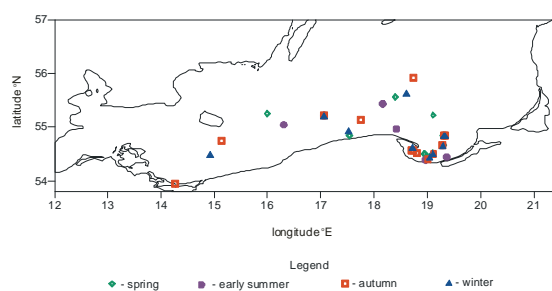


Figure 1. Spatial distribution of measuring stations in 1999-2005 in the southern Baltic.

3. Results and conclusions

The first step was to determine the correlation between concentrations of taxon groups and pigment concentrations in samples of marine water - the most significant are given in correlation matrix - Table 2. As we can see, the taxon groups *Bacillariophyceae*, *Dinophyceae*, *Chlorophyceae*, cyanobacteria show the best correlations with pigments often treated as markers enabling groups of algal classes to be defined (Jeffrey et al. 1997, Wright and Jeffrey 2006).

Table 1. Ranges of biomass contents of phytoplankton classes [$\mu\text{gC dm}^{-3}$] (represented by organic carbon content) and concentrations of selected pigments [$\mu\text{g dm}^{-3}$] noted in samples from Southern Baltic ecosystems (designation: B- biomass, C – concentration).

Parameter	Range of concentrations	Mean
B _{Bacill}	0.000344 – 17.27	0.869
B _{Cyano}	0.0173 – 28.6	2.13
B _{Dino}	0.00369 – 5.83	0.675
B _{Crypto}	0.00658 – 0.0871	0.0159
B _{Chloro}	0.000224 – 1.03	0.133
C _{Chl a}	0.42 – 35.3	2.13
C _{fuco}	0.023 – 7.597	0.824
C _{zeax}	0.00798 – 0.441	0.102
C _{peri}	0.00277 – 7.64	0.830
C _{allox}	0.0384 – 3.32	0.384
C _{lut}	0.0081 – 1.62	0.337

On the other hand, the correlation between the concentration of *Cryptophyceae* and Alloxantin known as their pigment-marker is rather weak. It can be caused by the fact, that analyses were performed for whole water samples, not for individual isolated taxon groups, and by methodological errors

Table 2. The correlation matrix for phytoplankton species group (represented by organic carbon content) [$\mu\text{g C dm}^{-3}$] and chosen pigment concentrations [$\mu\text{g dm}^{-3}$].

		pigment				
		peri	fuco	allox	zeax	lut
groups of algae species	B _{Cyano}	0,016	0,195	0,294	0,500	0,445
	B _{Crypto}	-0,377	0,000	0,044	0,309	0,233
	B _{Dino}	0,729	0,317	0,574	-0,015	0,280
	B _{Bacill}	0,451	0,710	0,449	0,002	0,350
	B _{Chloro}	0,664	0,574	0,560	0,113	0,828

Next, for chosen pigments and species groups, we analysed the relationship between the ratios: pigment concentration to species group and water trophic index. As an indicator of trophicity we assume the sum of different form of chlorophyll *a* concentration according to the classification from Woźniak et al 1992. Figure 2 presents these relationships. The equations described investigated dependence are given below:

$$C_{\text{fuco}}/B_{\text{Bacill}} = 0.327 C_a^{-0.215}$$

$$C_{\text{zeax}}/B_{\text{Cyano}} = 0.179 C_a^{-0.385}$$

$$C_{\text{peri}}/B_{\text{Dino}} = 0.00183 C_a^{0.998}$$

$$C_{\text{allox}}/B_{\text{Crypto}} = 0.107 C_a^{0.711}$$

$$C_{lut}/B_{Chloro} = 0.329 C_a^{-1.04}$$

As we can see, in the case of *Bacillariophyceae* and cyanobacteria, the values of exponents are close to zero, pointing to the weak relationship between trophicity and pigment content, while the values of exponent for *Dinophyceae*, *Chlorophyceae* and *Cryptophyceae* indicate a distinct dependence of investigated ratio on trophicity. These preliminary results encourage us to further investigations.

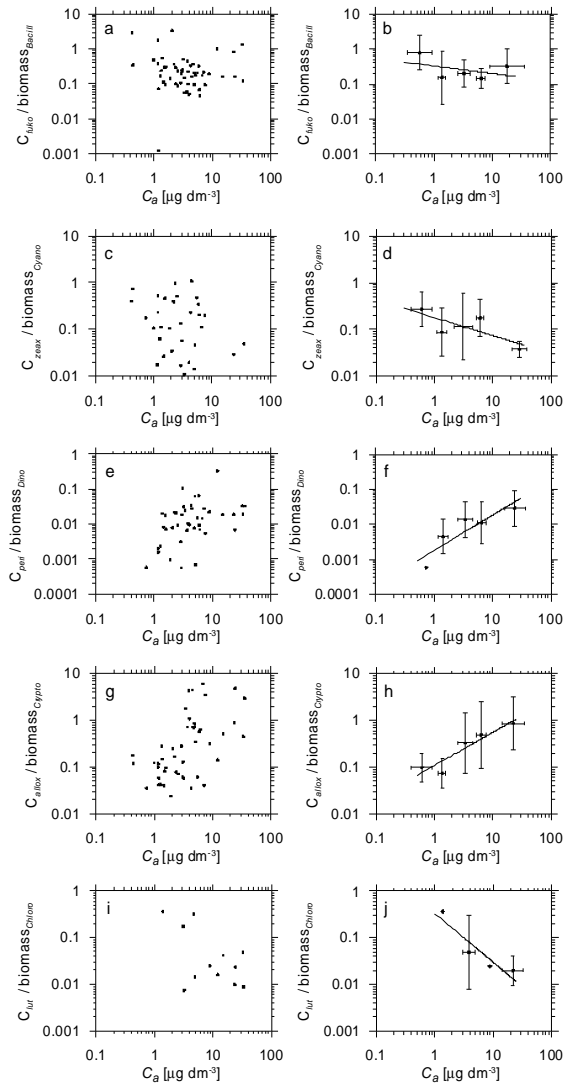


Figure 2. The dependence of ratios of pigment-markers concentration to phytoplankton classes on chlorophyll *a* concentration for five main group of phytoplankton classes: (a,b) - ratio of *Bacillariophyceae* to fucoxanthin; (c,d) - ratio of cyanobacteria to zeaxanthin; (e,f) - ratio of *Dinophyceae* to peridinin; (g,h) - ratio of *Cryptophyceae* to alloxanthin; (i,j) - ratio of *Chlorophyceae* to lutein.

Left column – position of experimental points, right column – mean and standard deviation calculated from experimental data for different trophic types of sea water (i.e. for selected ranges of chlorophyll *a* concentration).

References

- HELCOM, 1997, Manual for Marine Monitoring in the COMBINE programme of HELCOM, Part C, Programme for monitoring of eutrophication and its effects, Annex C-6, Phytoplankton species composition, abundance and biomass, C6-1 – C6-8
- Jeffrey S.W., Mantoura R.F.C., Wright S.W., 1997, Phytoplankton pigments in oceanography: guidelines to modern methods, Unesco Publishing, Paris, pp. 661.
- Menden-Deuer S., Lessard E.J., 2000, Carbon to volume relationships for dinoflagellates, diatoms, and other protist plankton, *Limnol. Oceanogr.*, 45(3), 569-579
- Stoń J., Kosakowska A., 2002, Phytoplankton pigments designation – an application of RP-HPLC in qualitative and quantitative analysis, *J. Appl. Phycol.*, 14, pp. 205-210
- Stoń-Egiert J., Kosakowska A., 2005, RP-HPLC determination of phytoplankton pigments – comparison of calibration results for two columns, *Mar. Bio.*, 147, pp. 251-260
- Willen T., 1962, Studies on the phytoplankton of some lakes connected with or recently isolated from the Baltic, *Oikos* 13, 169-199
- Woźniak B., Dera J., Koblenz-Mishke O. I., 1992, Bio-optical relationships for estimating primary production in the Ocean, *Oceanologia*, 33, 5-38
- Wright S.W., Jeffrey S. W., 2006, Pigment markers for phytoplankton production [in:] *Marine Organic Matter: Biomarkers, Isotopes and DNA*, J.K. Volkman, (ed.), Springer-Verlag, Berlin, 71-104.

Response of Polish rivers (Vistula, Oder) to reduced pressure from point sources and agriculture during the transition period (1988-2008)

Marianna Pastuszak and Krzysztof Pawlikowski

Sea Fisheries Institute, 81-332 Gdynia, ul. Kofłataja 1, Poland (marianna@mir.gdynia.pl)

1. Introduction

Riverine geochemistry and material fluxes have already been much altered on the global scale by agriculture, deforestation, mining, urbanization, industrialization, irrigation, and damming, which have generally appeared in this order (Meybeck 2001).

It is estimated that in the Baltic catchment (Figure 1), over 60% of nitrogen (N) and ca. 50% of phosphorus (P) in the riverine outflow originates from diffuse sources, and in the diffuse outflow of nutrients, agricultural activity plays a key role (HELCOM 2004). The diffuse outflow, as well as point sources, are considered the main sources of nitrogen and phosphorus discharged by the Vistula and Oder River, the two out of seven largest rivers feeding the Baltic Sea (Pastuszak 2009, Pastuszak and Witek 2009, Kowalkowski and Buszewski 2006, Behrendt et al. 2005).

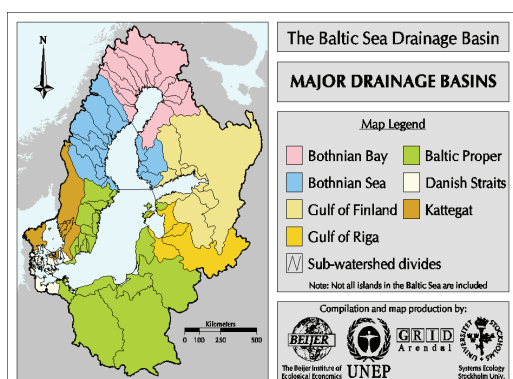


Figure 1. The Baltic Sea drainage basin (source: UNEP/GRID Arendal)

In 2000, the total riverine nitrogen and phosphorus loads entering the Baltic Sea amounted to 706 thousand tonnes and 31.8 thousand tonnes, respectively. The bulk (over 80%) of the N and P load was discharged by monitored rivers, with about 40% of the N load and 50% of the P load originating from the catchment area of the Baltic Proper. Approximately 75% of the riverine nitrogen and 83% of phosphorus were discharged by the region's three rivers: the Vistula, the Oder, and the Nemunas. In 2000, the contribution of Poland to the overall loads of N and P constituted 26% and 37% of total nitrogen and total phosphorus, respectively (HELCOM 2004).

Long-term data sets are available, encompassing various aspects of agricultural activity, and the handling of industrial and municipal waste-water in Poland, as well as a 21 year data set on nutrient concentrations and water flow in the main Polish rivers draining over 50% of the entire Baltic agricultural land and discharging annually ca. 50 km³ of fresh waters into the Baltic Sea (Pastuszak 2009). Thus, it was very tempting for us to evaluate the response of these rivers to huge changes which took place in the Polish economy during the transition period. We believe that knowledge presented here will be useful (i) in the modeling studies carried in the Oder and Vistula basin and such

studies are in progress, and (ii) in the implementation of the river basin management plans within the EU Water Framework Directive, and in selection of adequate measures to achieve good ecological and chemical status by 2015.

2. Results

The transition period in Poland was characterized by a significant drop in the application of mineral fertilizers at the beginning of the 1990s, directly affecting the N and P balance in Polish agriculture (Figure 2, Eriksson et al. 2007, Kopiński 2007), but also by great positive changes in waste water handling. A high N or P surplus in agriculture constitutes a potential threat for the environment.

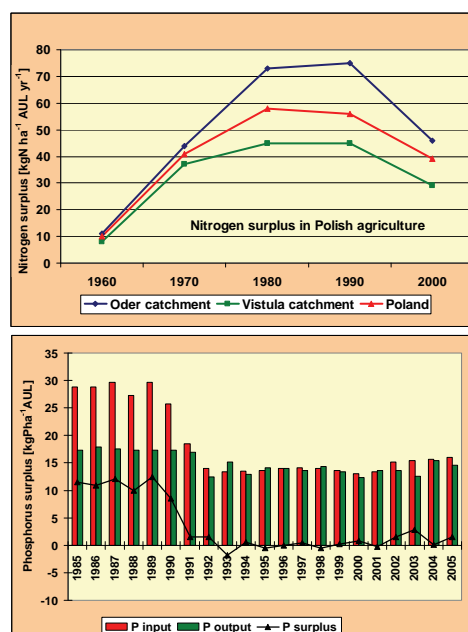


Figure 2. Nitrogen and phosphorus surplus in Polish agriculture in the respective periods of time 1960-2000 and 1995-2005; the "soil surface" method was applied in the calculations and the procedure follows the OECD recommendations (AUL – agriculturally utilized land; source: Eriksson et al. 2007; Kopiński 2007).

The steadily growing number of tertiary treatment waste water plants and increasingly economic water use in the country resulted in: (i) a reduction by half the volume of industrial and municipal waste waters discharged into rivers and soil, (ii) a ten times lower volume of untreated waters that may be a threat to the environment (Figure 3, Pastuszak and Witek 2009).

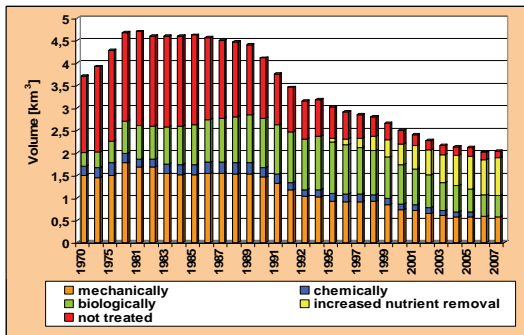


Figure 3. Volume of industrial and municipal waste water (requiring treatment and treated) discharged to the surface waters or ground over the years 1970-2007 (Pastuszak and Witek 2009).

In the period 1992-2006, as many as 29 hot spots situated in Poland became deleted from the HELCOM list (HELCOM 2009). Such dramatic changes must have had an impact on riverine N and P outflow from diffuse as well as point sources. Our studies show that concentrations of total nitrogen (TN) and phosphorus (TP), dissolved inorganic nitrogen (DIN) and phosphorus and (DIP) in the Vistula and Oder Rivers have dropped significantly, with more dramatic changes being seen in the Oder waters. In the period 1988-2008, the average TN concentrations in the Vistula and Oder dropped from 3,1 to 2,2 mg dm⁻³ and from 4,7 to 2,8 mg dm⁻³, respectively; on average, TP in these rivers dropped from 0,22 mg dm⁻³ to 0,17 mg dm⁻³ and from 0,55 to 0,22 mg dm⁻³, respectively. Most pronounced is the decrease of the average DIP concentrations in the Oder waters changing from 0,2 mg dm⁻³ in 1990 to 0,04 mg dm⁻³ in 2008 (Figure 4; Pastuszak and Witek 2009).

For the entire study period, nutrient concentrations in the Vistula were lower than those in the Oder River. This is attributed to: (i) a larger area with wetlands and meadows (retaining N and P, therefore reducing the leaching), and (ii) less intensive agriculture (lower consumption of mineral fertilizers, much lower N-NO₃ loss from the 0-90 cm soil layer to groundwater, smaller sizes of farms oriented at less intensive production resulting in lower concentrations of animals per 100 ha of cultivated soil) in the Vistula basin as compared with the Oder basin (Fotyma et al. 2009). In contrast, the Oder basin is characterized by a much higher contribution of point sources to the emission of N and P (Kowalkowski and Buszewski 2006, Behrendt et al. 2005). In case of both rivers there is a strong correlation between TN and water outflow, pointing to predominating diffuse origins of N in both basins; the lack of such a correlation for P in the Oder basin indicates other P sources than diffuse outflow. Over the last decade, a significant decrease was observed in both rivers for TP, DIP, and a less pronounced decrease for TN loads, discharged to the Baltic Sea (Pastuszak and Witek 2009).

A statistical estimation of the declining trend in nutrient loads carried with the Vistula and Oder waters will be possible after calculating so called flow normalized loads (Hussian et al. 2004; Stålnacke and Grimvall 2001). The outflow of nitrogen is strongly positively correlated with water outflow, calling for further elaboration of the data. The results of these calculations will soon be published in a peer reviewed international journal. It arises from these, so far unpublished data, that nutrient loads in both rivers show statistically a significant decline in N and P loads in the Vistula and Oder River in 1988-2008.

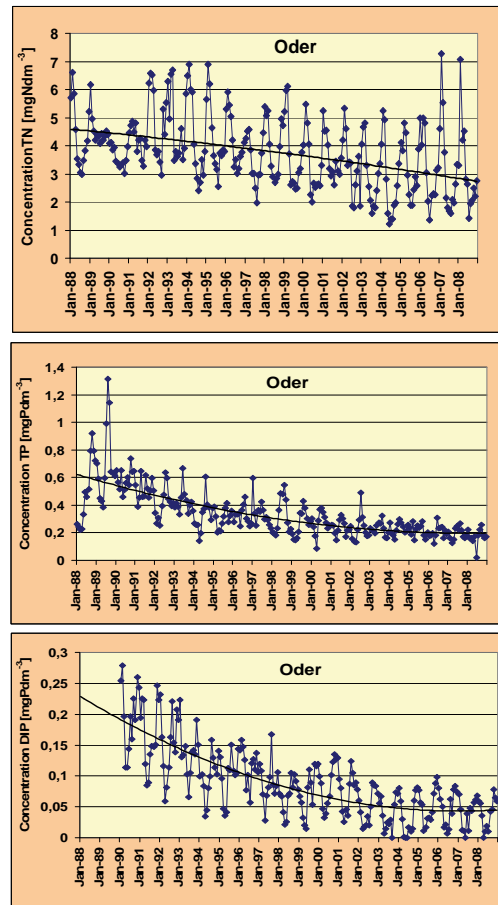


Figure 4. Average monthly concentrations of total nitrogen (TN), total phosphorus (TP), and dissolved inorganic phosphorus (DIP) in the Oder (Krajnik Dolny) over the period 1988-2008 (DIP values in the years 1988-1990 are lacking) (Pastuszak and Witek 2009).

References

- Behrendt H., Opitz D., Korol R., Strońska M., 2005. Changes of the nutrient loads of the Odra River during the last century – their causes and consequences. ICID 21st European Regional Conference, 15-19 May 2005, Frankfurt (Oder) and Słubice – Germany and Poland. 9 pp.
- Eriksson H., Pastuszak M., Löfgren S., Mörth C-M., Humborg C., 2007. Nitrogen budgets of the Polish agriculture 1960-2000 – Implications for riverine nitrogen loads to the Baltic Sea. *Biogeochemistry*, 77: 265-281.
- Fotyma M., Igras J., Kosiński J., 2009. Wykorzystani i straty obszarowe azotu i fosforu z polowej produkcji roślinnej [In:] Igras J., Pastuszak M. (eds.) *Udział polskiego rolnictwa w emisji związków azotu i fosforu do Bałtyku*, pp.105-158.
- HELCOM, 2004. The Fourth Baltic Sea Pollution Load Compilation (PLC-4). *Baltic Marine Environ. Protection Com. Proc. No. 93*.
- HELCOM, 2009. HELCOM JCP pollution Hot Spots as for March 2008. (http://www.helcom.fi/projects/jcp/hotspots/en_GB/hotspots/).
- Hussian M., Grimvall A., Petersen W., 2004. Estimation of the human impact on nutrient loads carried by the Elbe River. *Environmental Monitoring and Assessment* 96:15-33.

- Kopiński J., 2007. Weryfikacja wyników projektu HELCOM nt. Wpływu różnych scenariuszy decyzyjnych na zrzut substancji biogennych do Bałtyku realizowanego przez MARE, IUNG, Puławy, 112 pp.
- Kowalkowski T., Buszewski B., 2006. Emission of nitrogen and phosphorus in Polish rivers: past, present, and future in the Vistula River catchment. *Environmental Engineering Science*, 23(4):615-622.
- Meybeck M., 2001. River Basin under Anthropocene Conditions. [In:] Bodungen B.V. & Turner R.K. (eds.) *Science and Integrated Coastal Management*, Dahlem University Press, pp. 275-294.
- Pastuszek M., 2009. Charakterystyka zlewiska Morza Bałtyckiego [In:] Igras J., Pastuszek M. (eds.) *Udział polskiego rolnictwa w emisji związków azotu i fosforu do Bałtyku*, pp. 14-35.
- Pastuszek, M., Witek Z., 2009. Odpływ wód i substancji biogenicznych Wisłą i Odrą z obszaru Polski [In:] Igras J., Pastuszek M. (eds.) *Udział polskiego rolnictwa w emisji związków azotu i fosforu do Bałtyku*, pp. 268-302.
- Stålnacke P., Grimvall A. 2001. Semiparametric approaches to flow normalization and source apportionment of substance transport in rivers. *Environmetrics* 12: 233-250.

Use of a spatially-irregular simulation model to study nitrogen and phosphorus transformation processes and dynamics of dissolved oxygen in the ecosystem of the Neva Bay, Gulf of Finland

Podgornyj K.A.

I.D. Papanin Institute for the Biology of Inland Waters of the Russian Academy of Sciences (kap@ibiw.yaroslavl.ru)

1. Object of the study

The Neva Bay of the Gulf of Finland is a complex ecosystem, complex for both field ecological studies and for the elaboration of mathematical models. The peculiarity of the Neva Bay is due to a number of causes: (I) the formation of its water mass is significantly influenced by Lake Ladoga, the waters of which flow into the Neva Bay with river Neva's drainage at a speed of 2400-2500 m³/s; (II) the yearly water exchange factor due to river waters inflow is equal to 66, conditioning the water renewal once in 5-6 days on average, and even two times faster in the central transit zone; (III) the Neva Bay is a shallow water body with dominating depths of 3-5 m, intensive wind mixing of water masses, diverse processes of biogeochemical transformation taking place within the water body; (IV) great influence of the Baltic Sea which affects the water's salinity and temperature, water level and structures of biological communities; (V) the Neva Bay is a region with high level of technogenic impact upon the environment; (VI) the Neva Bay ecosystem is influenced by the Saint-Petersburg flood control facilities being established presently. Due to the joint action of all the aforementioned factors the Neva Bay is characterized by an extremely high spatial and temporal variability of water quality. A huge amount of data on the Neva Bay ecosystem condition has been accumulated over more than a century of observations. There is a certain experience in elaboration of mathematical models of different types and purposes, the creation of an integrated system of decision-making support for Saint-Petersburg and Leningrad oblast water resources management.

2. Aims of the study

The aims of the study were to: (I) devise an imitational, spatially irregular model of the Neva Bay ecosystem on the basis of (i) an all-round system analysis of data from observations and (ii) based on literature; (II) study the most important patterns of transformation and cycles of nitrogen, phosphorus compounds as well as dynamics of dissolved oxygen utilizing numerical experiments, to make a quantitative evaluation of processes determining the production potential of the Neva Bay.

3. General description of the model and utilized digital methods

The imitational model of the Neva Bay ecosystem contains the following developed and programmatically realized general blocks: (I) hydrodynamic - to calculate the non-stationary, vertically averaged structure of currents in the water body; (II) hydro-thermodynamic - for calculation of the photoperiod, components of the thermal balance and temperature regime of the water body; (III) hydro-optical - for calculation of optical characteristics of the water column; (IV) block for the description of processes of nitrogen and phosphorus compounds' transformation in the water body and the dynamics of dissolved oxygen; (V) block to

calculate the time of cycle and flow of matter between the selected (aggregated) model parameters of the ecosystem; (VI) block for the evaluation of imitational parameters of the model. All calculations in the model are carried out only on the basis of standard meteorological, hydrological, hydrochemical and hydrobiological information. Block (IV) of the imitational model considers 17 variables of state: concentrations of dissolved fractions of organic nitrogen and phosphorus, inorganic phosphorus, ammonium, nitrite, nitrate nitrogen, nitrogen and phosphorus contained in the detritus, concentration of dissolved oxygen, biomasses of hydrobionts (heterotrophic bacteria, phytoplankton, protists and zooplankton) in nitrogen and phosphorus units (see Figures 1, 2).

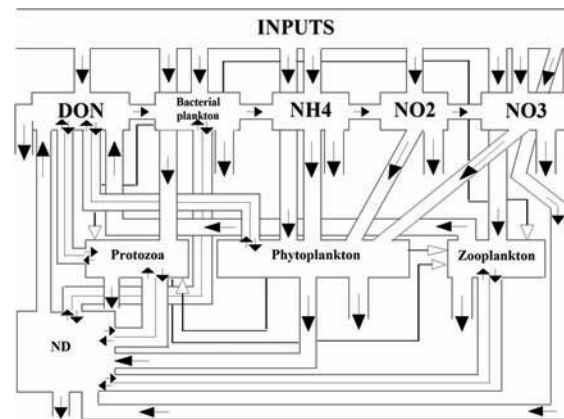


Figure 1. The Nitrogen cycle.

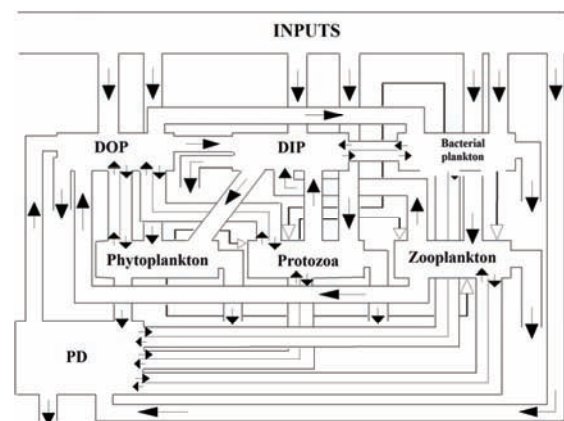


Figure 2. The Phosphorus cycle.

The task of modeling spatially irregular water ecosystem dynamics is divided in two main stages. The model's calculation begins with numerical integration of thermo-hydrodynamic system equations in time step τ . As a result of modeling hydrological complex values of current speed, flows of shortwave solar radiation, photoperiod values averaged by depth and vertically averaged water

temperature are determined. Then, a system of equations of turbulent diffusion and compounds' transformation is integrated for the same time interval. Solving this task allows finding values of biotic ecosystem components' concentrations at the end of the set time increment. Building of computational algorithms is based upon utilization of various schemes of splitting equations on physical processes and spatial coordinates. All algorithms and schemes of numeric integration of equation systems, method of calculating of warm air flows on the surface of the water body at different conditions of stratification of near-water layer of air, variants of calculation of heat flow on the bottom of the water body, algorithm of the procedure of evaluation of parameters of the imitational model are thoroughly discussed (Podgornyj 2000, 2003). Calculations have been performed on a uniform rectangular grid of 500 x 500 m. A time increment of 30 seconds was used for the numeric integration of differential equations in order to provide stability of the calculations. Calculations of current fields, temperature and biotic ecosystem components have started from the moment of clearing of the Neva Bay from ice and continued until October the 31st. Changes of hydro-meteorological situation over the waterbody took place every day of the model time.

4. Main results

Modeling was performed for four observation years - from 1984 to 1987. Results indicate a reasonably good quantitative and qualitative correspondence of model estimates and present data of observations. Teal's criterion was used as an index of the model's performance with its value fluctuating from zero to one; a full agreement of the model results with observed values is indicated by zero. A comparison of temperature fields show that Teal's criterion fluctuates from 0,0307 to 0,2093 with an average value of 0,0781. Values for biotic components fluctuate from 0,2306 to 0,3778 with an average value of 0,2812. In the dissolved organic matter, nitrogen and phosphorus present in detritus constitute 45 - 75%, 10 - 30% in the phytoplankton and 10 - 20% in the composition of heterotrophic bacteria. The role of zooplankton in the Neva Bay is not important. The main fraction of mineral nitrogen is the nitrate nitrogen is 60-70%. Nitrite nitrogen constitutes less than 5%. The ratio of Nmin/DIP fluctuated from 30 to 190, the Norg/Porg ratio from 16 to 40, the Ntot/Ptot ratio from 23 to 49, and their yearly dynamics have quantitative differences from year to year. The variability of the most important ecosystem components were evaluated using the model: DIP: 2,02 - 20,08 ($\mu\text{g/l}$); DOP: 1,30 - 12,25 ($\mu\text{g/l}$); PD: 19,60 - 35,06 ($\mu\text{g/l}$); - 31,96 - 191,97 ($\mu\text{g/l}$); - 4,50 - 18,14 ($\mu\text{g/l}$); - 160,05 - 468,20 ($\mu\text{g/l}$); DON: 237,87 - 943,41 ($\mu\text{g/l}$); ND: 196,04 - 400,12 (mcg/l). These results are in accordance with data of perennial observations. Data of the model and observations show that nitrogen and phosphorus content in the water of the Neva Bay seems not to be a factor limiting the water body bioproductivity. This is indicated by a discrepancy of rather low levels of phytoplankton development at quite high concentrations of biogenic elements. The contribution of the phytoplankton's primary production to the total supply of organic matter is not high. Results of modeling and observational data show that the main reason for the intensive development of heterotrophic processes in the Neva Bay are values of allochthonous organic matter. Influence of the flood control facilities complex is generally low and may be seen only on a few increments of the calculation grid (5-10 increments on average relative wind conditions). However, this problem requires a more detailed study.

References

- Podgornyj K.A. Calculation of parameters of thermohydrodynamic interaction, characteristics of heat balance and water temperature in unstratified waterbodies. - Yaroslavl: YaGTU press, 2000. - 100 p. [In Russian]
- Podgornyj K.A. Mathematical modeling of freshwater ecosystems of unstratified waterbodies (algorithms and numerical methods). - Rybinsk: "Rybinsk press house", 2003. - 328 p. [In Russian]

Ecological and hydrological field studies in southern Karelia within the easternmost part of the Baltic Sea Basin: The Onego/Ladoga lakes system

Tatiana Sazonova¹, Victor Bolondinsky¹ and Vladislava Pridacha¹

¹ Institute of Meteorology, Forest Institute, Karelian Research Center of the Russian Academy of Sciences, Petrozavodsk, Karelian Republic, The Russian Federation (alt86@rambler.ru)

1. Summary

The information about ecophysiological investigations of responses of woody plants (*Pinus sylvestris* L., *Picea abies* L., *Betula pendula* Roth.) to different natural and anthropogenic factors in conditions of the north-western Russia is presented in this report. These investigations have been conducted during more than 40 years in the Forest Institute of the Karelian Research Center of Russian Academia of Science on the territory of the Republic of Karelia in forests of Eastern European taiga (Figure 1).



Figure 1. Southern Karelia, the northeastern part of the Baltic Sea Basin.

2. History and the objectives of our research

Long-term investigations in the northern taiga of Karelia were organized by Dr. L. Kaipainen, who was an initiator of studies of biophysics of woody plants in the Karelian Research Center in Petrozavodsk. Major studies were conducted at the “Gabozero” Research Station located 50 km north of Petrozavodsk in bilberry pine forest (Figure 2). At the Station, we established an automatic system for continuous monitoring of the environmental factors and main physiological processes in woody plants, namely photosynthesis, transpiration, water flux, water potentials, and growth rate. Data from the sensors are recorded on 65 channels multipoint electronic potentiometers at intervals of about 1-6 minutes

3. Results at the Gabozero research station

We assessed patterns of water movement in the soil-plant-atmosphere system and quantified the influence of internal

factors (such as water storage, resistances) on water exchange dynamics. We established a stability of annual

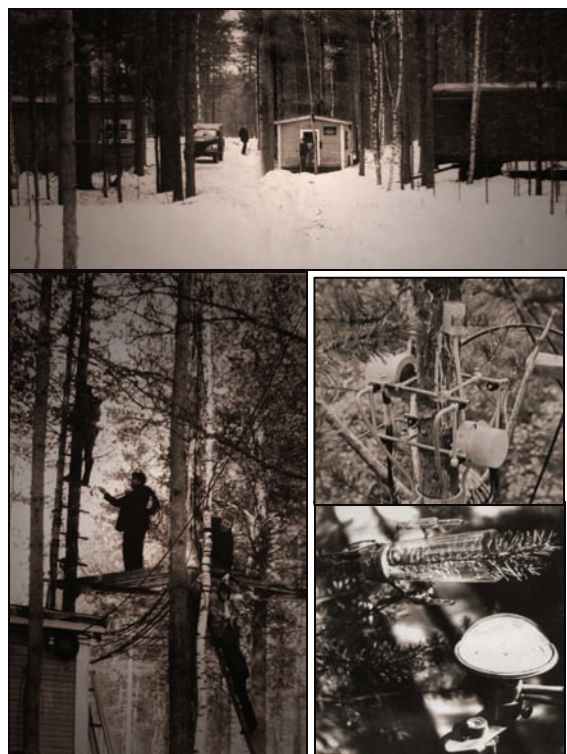


Figure 2. Gabozero Research Station

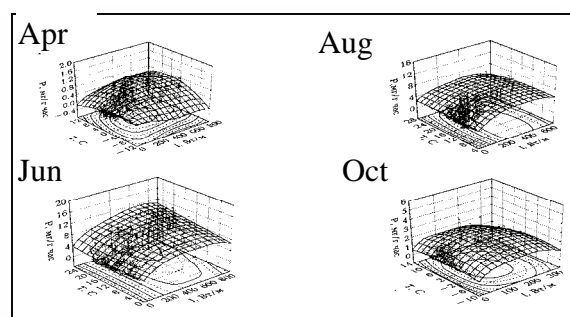


Figure 3. Experimental values of photosynthesis (P) approximated with spline-function of temperature (T) and illumination (I) and contours of transections of these functions for four months during the warm season.

average values of water fluxes in plant stems and gradients of water potentials. Dynamics of daily and seasonal CO₂ exchange in the woody plant shoots were defined and quantified. Thereafter, we developed a model of the potential CO₂ exchange as a function of environmental factors and investigated effects of the main regulatory environmental factors on water regime and

photosynthesis. We found that the high rate of these processes was observed within a large range of the hydro-meteorological factors, suggesting that the species under study have adapted to the wide range of growth conditions. Figure 3 presents an example of our results for photosynthesis in the pine forest.

4. Field studies across the north taiga of Karelia

In addition to the stationary system of measurements, portable equipment was used to perform ecological measurements in different forest types. We found that needle transpiration capacity ($41.7 \text{ mm Mg}^{-1}\text{yr}^{-1}$) and xylem water conductivity ($101 \text{ ton m}^{-2} \text{ yr}^{-1}$) were constant in the forest types of different productivity. On the base of analysis of our own data and data available in literature, it has been found that annual photosynthetic productivity averaged over crown in the middle-aged pine trees ($1.52 \pm 0.13 \text{ gC g}^{-1}\text{yr}^{-1}$) is constant in similar climatic conditions (Karelia, Finland, Sweden). Using the portable system of measurement of gas exchange (Li-Cor), photosynthesis and respiration measurements of coniferous trees exposed to toxic pollutants were conducted in the north of Karelia, (Kostomuksha Mining Plant (“Костомукшский ГОК”) and on Kola Peninsula. Monchegorsk and North Nickel Mining Plants (“Мончегорский комбинат», “Североникель”). Among the results of this research, we estimated photosynthetic sink of CO_2 into pine forests in normal (background) conditions and near large sources of industrial pollution.



Figure 4. In the field

5. Laboratory studies

We assessed the acquisition of efficient and biological (internal) ratio optima for nitrogen, phosphorus, and potassium for *Pinus sylvestris* L., in the vegetative tests (equal to 53:28:19 and 55:8:37, respectively). Comparison of these values with those obtained for *Pinus sylvestris* L. under natural growth conditions showed their affinity with an internal optimum. Our finding indicates that the optimization of mineral nutrition in nature follows the path of stabilization of the internal (biological) optimum. These results provide an experimental confirmation of the idea of a plant organism development strategy, which is not aimed to achieve maximum economic efficiency but to maintain some steady state, favorable to life of the species.

6. Last remarks

On the base of field studies conducted during several decades, the scopes of natural variability of main physiological characteristics of woody plants were revealed in a wide range of environmental conditions of large region of the north-western taiga zone. For these conditions, we determined quantitative values of parameters of CO_2 exchange, water regime, and mineral nutrition of trees, (parameters crucial for stability of woody plants) that will be presented at the Conference.



Figure 5. In the laboratory.

References (mostly in Russian)

- Kaipainen L.K., Bolondinsky V.K., Sazonova T.A., Sofronova G.I. (1995) Water regime and photosynthesis of Scots pine under industrial pollution, *J. Russ. Plant Physiol.* **43**, 451–456.
- Kaipainen L.K., Bolondinsky V.K., Sofronova G.I. (1998) Photosynthesis carbon stock in pine stands under industrial pollution, *Ecology*. 1998. № 2. 83–88.
- Sazonova T.A., Pridacha V.B. (2002) Mineral nutrition optimization of the coniferous plants, *Agrochemistry*. 2002, № 2, 23–30.
- Bolondinsky V.K., Kaipainen L.K. (2003) Photosynthesis dynamics in pine stands, *J. Russ. Plant Physiol.* **50**, 105–114.
- Voronin P.Yu., Kononov P.V., Bolondinsky V.K., Kaipainen L.K. (2004) Chlorophyll index and photosynthesis carbon stock in forests of Northern Eurasia, *J. Russ. Plant Physiol.* **51**, 390–395.
- Sazonova T.A., Pridacha V.B., Terebova E.N., Schreders S.M., Kolosova S.W., Talanova T.Yu. (2005) Morphophysiological response of Scots pine trees to industrial pollution, *Lesovedenie*. 2005, № 3. 11–19.
- Sazonova T.A., Pridacha V.B. (2005) The contents of mineral nutrients in the organs of pine and spruce at different soil conditions, *Lesoved.*, 2005, № 5. 25–31.
- Sazonova T. A., Kolosova S.W. (2005) The effect of environmental factors on the parameters of water metabolism of *Pinus sylvestris*, *Picea abies* (Pinaceae) and *Betula pendula* (Betulaceae), *Botanical J.* 2005, № 8, 1227–1235.
- Sazonova T.A., Pridacha V.B., Kolosova S.V. (2009) The contents of mineral nutrients in xylem sap of *Pinus sylvestris* (Pinaceae), *Rastitelnye resursy*. № 1, 113–121.
- Sazonova T.A., Pridacha V. B. (2009) Effect of industrial pollution on the mineral and water metabolism in pine and spruce. *Transactions of KarRC RAS*. № 3, 75–85.

Phosphate release at the sediment surface during anoxic conditions: Myths, mysteries and facts

Bernd Schneider

Leibniz Institute for Baltic Sea Research, Warnemünde, Germany (bernd.schneider@io-warnemuende.de)

1. Introduction

It is generally believed that the release of phosphate from the sediments increases at anoxic conditions. The excess phosphate may then enhance biological production and thus furthers the expansion of anoxic bottom waters. We have tested this hypothesis by analyzing a 40 years monitoring time-series for the concentrations of O_2 , H_2S and PO_4 and by studying the release of total CO_2 and phosphate during a period of stagnation in the Gotland Sea deep water. The importance of the dissolution of iron-hydroxo-phosphates (Fe-P) for the PO_4 budget is re-evaluated.

2. Time-series data

In order to relate the PO_4 release to the mineralization of organic matter (OM), the apparent oxygen utilization (AOU_{org}) was calculated taking into account the formation of H_2S and nitrification/denitrification. The PO_4 concentrations in the Gotland Sea deep water ($z > 100$ m) are plotted as a function of AOU_{org} in Fig. 1 and indicate the processes that control the PO_4 concentrations. The slight mean increase of the PO_4 concentrations during oxic conditions (green dots) is attributed to the mineralization of OM. A drastic increase of PO_4 occurs at the transition to anoxic conditions (red dots). This indicates the dissolution of Fe-P that were previously deposited at the sediment surface during oxygenation of anoxic waters. However, at H_2S concentrations larger than about $50 \mu\text{mol/L}$ (blue dots), the Fe-P pool is exhausted and the PO_4 release is confined again to the mineralization of OM. The PO_4 accumulation continues then until an inflow of oxygen-rich water occurs which causes again deposition of Fe-P at the sediment surface. The precipitation and dissolution of Fe-P constitutes a closed cycle and may cause a PO_4 accumulation in the deep basins, but has no effect on the overall PO_4 budget and on the productivity of the Baltic Sea

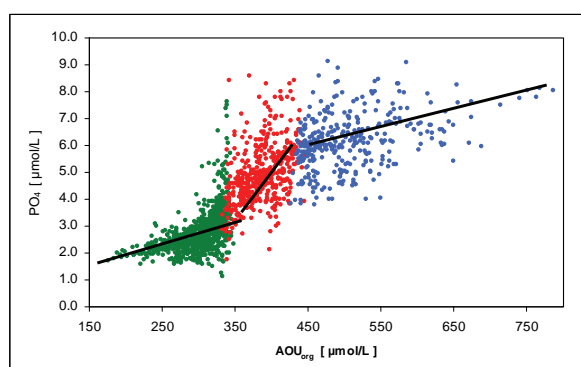


Figure 1. Phosphate concentrations (IOW Monitoring data 1969 – 2009) as a function of the apparent oxygen utilization (AOU_{org}). (Green: oxic, red and blue dots: H_2S concentrations below and above $50 \mu\text{mol/L}$, respectively).

3. Analysis of a stagnation period

The data in Fig. 1 refer to many transitions between oxic and anoxic conditions. Hence, the scatter of the data in the PO_4/AOU_{org} diagram is considerable and impedes the establishment of quantitative relationships. Therefore, we analyzed an individual stagnation period (May 2004 – July 2006) for which also data for total CO_2 concentrations (C_T) were available. C_T is directly related to the OM mineralization and was used to quantify PO_4 transformations that interfere with the mineralization process. Furthermore, vertical mixing coefficients between sub layers ($\Delta z = 20$ m) in the deep water were determined using the temporal changes in the salinity distributions (Schneider et al., 2010). This facilitated the establishment of mass balances and the determination of sinks/sources for PO_4 (Q_{PO_4}) and C_T (Q_{CT}). The accumulated Q_{PO_4} was linearly correlated with the accumulated Q_{CT} during the development of anoxic conditions in the beginning of the stagnation period (Fig. 2). The slope corresponded to a C/P ratio of 41 and was by a factor of 2.5 lower than the Redfield C/P ratio (106) for OM. This clearly indicates PO_4 release by the dissolution of Fe-P during the initial phase of the stagnation. However, at a Q_{CT} (accum.) of $260 \mu\text{mol/kg}$ that corresponds to a H_2S concentration of about $60 \mu\text{mol/L}$, the PO_4 release decreased and the corresponding regression line yielded a C/P ratio of 115 (Fig. 2, red line). This value agrees reasonably with the Redfield C/P ratio. Hence, after the temporary dissolution of Fe-P, the PO_4 release is controlled again by the mineralization of OM.

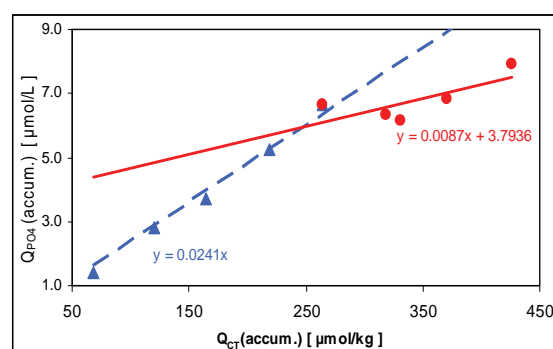


Figure 2. Relationship between the accumulated phosphate release (Q_{PO_4}) and the accumulated total CO_2 production (Q_{CT}) in the bottom water of the Gotland Sea during a period of stagnation. Red circles refer to H_2S concentrations $> 60 \mu\text{mol/L}$.

References

Schneider, B., Nausch, G., Pohl, C., 2010. Mineralization of organic matter and nitrogen transformations in the Gotland Sea deep water. *Mar. Chem.* (in press).

Simulating dissolved organic carbon in the Baltic Sea catchment area

Guy Schurgers¹, Paul Miller¹, Carl-Magnus Mörrth^{2,3}, Teresia Wällstedt³, Alla Yurova⁴ and Benjamin Smith¹

¹ Department of Earth and Ecosystem Science, Lund University, Sweden (guy.schurgers@nateko.lu.se)

² Baltic Nest Institute, Stockholm Resilience Centre, Sweden

³ Department of Geology and Geochemistry, Stockholm University, Sweden

⁴ Hydrometeorological Centre of Russia, Moscow, Russia

1. Introduction

Fluxes of dissolved organic carbon (DOC) from the land surface contribute a significant source of organic carbon to the Baltic Sea carbon balance. DOC is produced from microbial processes in soils, dissolved in soil water, and transported through rivers into the Baltic Sea. Wetlands, in particular those with peat accumulation, are considered the main terrestrial sources of DOC in the Baltic Sea catchment area.

2. Model and experiment setup

A mechanistic algorithm for DOC production, adsorption and desorption in soils (Yurova et al. 2008) is incorporated in the LPJ-GUESS dynamic global vegetation model framework (Smith et al. 2001, Sitch et al. 2003). LPJ-GUESS simulates the carbon balance in vegetation, litter and soil carbon pools, wetland dynamics are accounted for (Wania et al. 2009). The DOC algorithm simulates production of DOC from soil carbon pools as well as sorbed organic carbon in the soil. The fluxes of DOC are applied in the CSIM model (Mörrth et al. 2007) for integration over the watersheds in the Baltic Sea catchment area.

LPJ-GUESS is forced with monthly climate data originating from the RCA regional climate model for the period 1961-2005. Land use is prescribed applying observed land use classes. Concentrations and fluxes of DOC are calculated. The fluxes of DOC are applied in CSIM to simulate river catchment fluxes of DOC into the Baltic Sea.

3. Results

This model setup is applied to assess the spatial and temporal dynamics of DOC fluxes: their transport from the land surface into the rivers, and from the rivers into the Baltic Sea. Local as well as catchment-scale trends in DOC fluxes are analysed for the simulation period (1961-2005) and will be presented. Interannual variability in the DOC flux into the Baltic Sea will be assessed. For selected watersheds, the results will be compared to observations from head water and river water.

References

- Mörrth C-M, Humborg C, Eriksson H, Danielsson Å, Medina MR, Löfgren S, Swaney DP, Rahm L (2007) Modeling riverine nutrient transport to the Baltic Sea: A large-scale approach, *Ambio*, 36, pp. 124-133
- Sitch S, Smith B, Prentice IC, Arneth A, Bondeau A, Cramer W, Kaplan JO, Levis S, Lucht W, Sykes MT, Thonicke K, Venevsky S (2003) Evaluation of ecosystem dynamics, plant geography and terrestrial carbon cycling in the LPJ Dynamic Global Vegetation Model, *Global Change Biology*, 9, pp. 161-185

Smith B, Prentice IC, Sykes MT (2001) Representation of vegetation dynamics in the modelling of terrestrial ecosystems: comparing two contrasting approaches within European climate, *Global Ecology and Biogeography*, 10, pp. 621-637

Wania R, Ross I, Prentice IC (2009) Integrating peatlands and permafrost into a dynamic global vegetation model: 1. Evaluation and sensitivity of physical land surface processes, *Global Biogeochemical Cycles*, 23, GB3014

Yurova A, Sirin A, Buffam I, Bishop K, Laudon H (2008) Modeling the dissolved organic carbon output from a boreal mire using the convection-dispersion equation: Importance of representing sorption, *Water Resources Research*, 44, W07411

Long term changes in phytoplankton pigment characteristics in the southern Baltic region

Joanna Stoń-Egiert

Marine Physics Department, Institute of Oceanology, Polish Academy of Science, Sopot, Poland, (aston@iopan.gda.pl)

1. Aim

The variability in the occurrence and contents of Baltic phytoplankton pigments against the hydrographic background, considering long term changes.

2. Materials and method

The research was focused on southern Baltic Sea ecosystems including the Gulf regions (both Gulf of Gdansk and Pomeranian Bay) and open waters (Figure 1). The analyses were based on empirical material collected during 10 years of exploration of Baltic Sea waters on r/v 'Oceania' and r/v 'Baltica'. During 46 cruises in 1999–2008, over 1200 samples of surface water were taken for measurements of chlorophylls and carotenoids content by use of a chromatographic method (RP-HPLC) (Stoń and Kosakowska 2002, Stoń-Egiert and Kosakowska 2005).

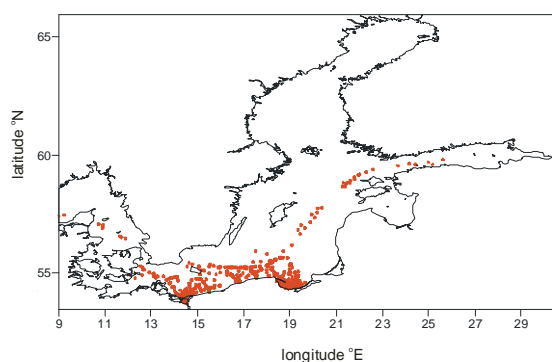


Figure 1. Spatial distribution of measuring stations in 1999–2008.

3. Results and conclusions

Laboratory analysis of the phytoplankton pigments composition in different ecosystems identified three groups of compounds: chlorophylls (chlorophyll *a*, chlorophyllide *a*, divinyl chlorophyll *a*, phaeophytin *a*, chlorophyll *b*, chlorophyll *c1+c2*, chlorophyll *c3*), photosynthetic carotenoids (peridinin, fucoxanthin, α -carotene, 19'hex-fucoxanthin, prasinoxanthin, canthaxanthin, echinenone, 19'but-fucoxanthin) and photoprotecting carotenoids (diadinoxanthin, alloxanthin, zeaxanthin, lutein, neoxanthin, violaxanthin, β -carotene, diatoxanthin, myxoxanthophyll, antheraxanthin).

The recurring trend of pigment content in a year-long cycle was confirmed in successive years of the investigations. It is distinctly shown by the example of mean chlorophyll *a* concentrations (Figure 2a). The fluctuations of pigment concentrations in different ecosystems show that the level of pigment amounts in open water ecosystems are regular and stable in time. However, in Gulf ecosystems, the seasonality of pigment content were distinctly marked. The Gulf waters were more rich in biological matter than open waters, and more dynamic changes in phytoplankton pigment concentration occurred there. The seasonal changes of the phytoplankton biomass are connected with blooms of

individual phytoplankton groups. The biggest pigment diversity occurred in spring and autumn samples. These situations are visible in distributions of mean values of carotenoids which are considered to be the marker of individual phytoplankton classes. As an example of changes of mean values of fucoxanthin concentrations (Figure 2b) we observed the seasonal (spring and autumn) growth of biomass of *Bacillariophyceae* in Baltic phytoceenoses.

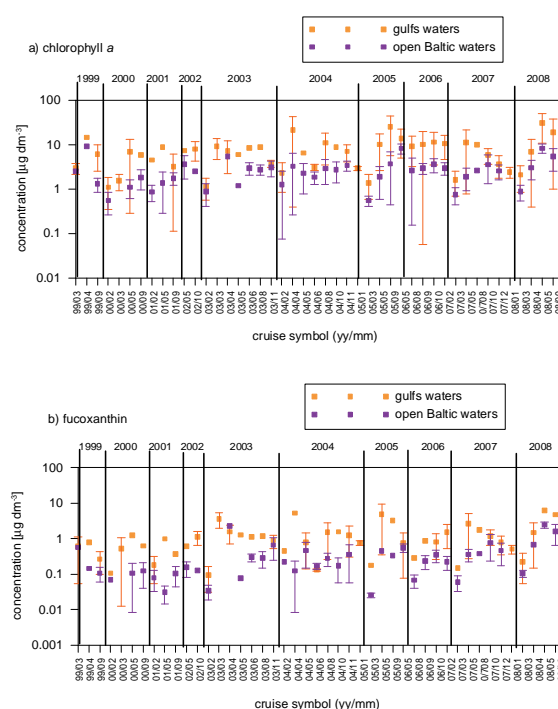


Figure 2. The variability of mean values of a) chlorophyll *a* concentrations and b) fucoxanthin concentrations (presented values – mean and standard deviation) identified in surface layer in gulfs region (Gulf of Gdansk and Pomeranian Bay) and waters of open Baltic in successive measuring years 1999–2008.

The mean photosynthetic carotenoid contents in the Gulf region was approximately 4.3-times higher compared to their contents in the open Baltic Sea (from 0.94-times in June 2006 to 13.9-times in April 2006). In case of photoprotectant carotenoids – their concentrations were about 3.1-times higher in Gulf waters then in samples from the open Baltic Sea (from 0.93-times in November 2003 to 8.62-times in April 2005). The quantitative proportions among mean values of sum of main pigments groups (i.e. chlorophylls *a*, *b*, *c*, photosynthetic and photoprotectant carotenoids) identified in surface samples from both ecosystems are presented in Figure 3. The analysis of their mutual proportion during 10 years of investigations revealed, that chlorophyll *a* content ranged from 45 to 77% of total pigments content in samples, chlorophyll *b* – 0.55 - 17.5%, chlorophylls *c* – 2.9 - 13.4

%, photosynthetic carotenoids PSC – 4.1 - 28% and carotenoids PPC – 2.2 - 28.4%.

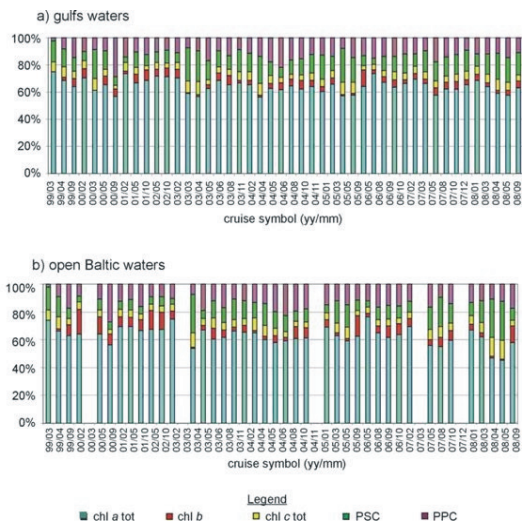


Figure 3. Quantitative proportions among mean of total pigments groups content: chlorophylls *a* (chl *a* tot), chlorophyll *b* (chl *b*), chlorophylls *c* (chl *c* tot), photosynthetic carotenoid (PSC), photoprotectant carotenoids (PPC) in following measuring cruises in a) gulfs region and b) open Baltic region.

References

- Stoń J., Kosakowska A., 2002, Phytoplankton pigments designation – an application of RP-HPLC in qualitative and quantitative analysis, *J. Appl. Phycol.*, 14, pp. 205-210
- Stoń-Egiert J., Kosakowska A., 2005, RP-HPLC determination of phytoplankton pigments – comparison of calibration results for two columns, *Mar. Bio.*, 147, pp. 251-260

Towards a comprehensive biogeochemical model of the Baltic Sea

Letizia Tedesco^{1,2}, Tapani Stipa¹, Antti Westerlund¹ and Alexsi Nummelin¹

¹ Finnish Meteorological Institute, Helsinki, Finland (letizia.tedesco@fmi.fi)

² currently at Finnish Environment Institute, Helsinki, Finland (letizia.tedesco@ymparisto.fi)

1. Introduction

This presentation aims to introduce the novel implementation of the Biogeochemical Flux Model (BFM, Vichi et al. 2007a,b; <http://www.bfm.cmcc.it>) in the Baltic Sea. BFM is a direct descendant of the European Regional Seas Ecosystem Model (ERSEM I and ERSEM II, Baretta et al. 1995, Baretta-Bekker et al. 1997). The BFM is a modular and comprehensive biogeochemical model, largely used and validated in the open ocean environment and in regional seas, such as the Adriatic Sea, Mediterranean Sea, North Sea, subtropical Atlantic Ocean and global ocean, in either climate and operational modes (Ruardij et al. 1997, Allen et al. 1998, Vichi et al. 1998, Zavatarelli et al. 2000, Allen et al. 2001, Obernosterer et al. 2001, Petihakis et al. 2002, Taylor et al. 2002, Vichi et al. 2003a, Vichi et al. 2003b, Vichi et al. 2004,; Raick et al. 2005, Vichi et al. 2007a, Vichi et al. 2007b).

The BFM is a complex ecosystem model and its very modular way of development allows versatile usage for scientific purposes. In fact, its standard configuration, which includes four groups of primary producers (diatoms, flagellates, picophytoplankton and large phytoplankton), one group of aerobic and anaerobic bacteria and two groups of secondary producers (microzooplankton and mesozooplankton) may be simplified, removing groups that are not of interest, or may be made more detailed including new functional groups relevant for the model applications.

In contrast to other simpler models of the Baltic Sea (e.g. Neumann et al. 2000), every living and non-living group is made of one or more constituents (e.g. C, P, N, Si, Chl, etc). The ratio between different constituents is not fixed, but may vary in a given range, allowing for relevant form of acclimation, such as dark periods and nutrient stress.

2. Methods and model implementation in the Baltic Sea

The implementation of BFM in the Baltic Sea is currently undergoing in the framework of the Baltic Sea Forecasting Center of the EU MyOcean project. The physical model is the HIROMB-BOOS model. The General Ocean Turbulence Model (GOTM, <http://www.gotm.net>) is providing a modular coupler for BFM, as well as a potential turbulence closure scheme.

The Baltic Sea presents many peculiarities in comparison to many coastal seas, such as the seasonal presence of sea ice for several months per year, very shallow waters, high stratification of waters, abundant river inputs, and diffuse international ship traffic between several harbours. These features highly require the need of an ecosystem model able to reproduce the complexity of the Baltic Sea ecosystem that is able to include peculiar groups of organisms, such as for instance cyanobacteria that are important relative contributors to the whole biomass and are also of concern for their toxic potential. The newest BFM for the Baltic represents two groups of cyanobacteria. The aim is the identification of areas where the cyanobacteria blooms add to the nitrogen balance of the Baltic Sea.

Another peculiar feature of the Baltic Sea is the vernal dinoflagellates bloom. Spring blooms of dinoflagellates are

very uncommon in other oceans but usually do develop in the Baltic Sea. Cold adapted dinoflagellates play a relevant role since they may compete with diatoms and the food web structure may switch from the classical diatoms-mesozooplankton-fish food web to the microbial loop (dinoflagellates-bacteria-microzooplankton). Cold adapted dinoflagellates are also differently contributors to the carbon export. While diatoms are an important sink for atmospheric CO₂, cold-adapted dinoflagellates are staying in the water column longer time and enhance the production of dissolved organic carbon.

BFM also embeds a benthic (Ruardij and Van Raaphorst 1995) and sea ice (Tedesco et al. under review) components, which are not regularly included in ocean modelling. Considering the shallowness of the Baltic Sea, its pelagic waters are strongly connected to the benthic system. It will thus be a natural choice to study the fate of the biomass after sinking to the seafloor. Besides, the Baltic Sea is partly seasonally ice-covered and its novel sea ice component can allow further studies on the sea ice-ocean coupling dynamics, in particular in the context of sea ice algae seeding phytoplankton bloom that is, so far, not yet proven in the Baltic Sea.

3. Acknowledgements

This work is supported by the EU MyOcean project. LT is very grateful to Dr. Marcello Vichi for the help provided in the process of model implementation for the Baltic Sea.

References

- Allen, J., Blackford, J., Radford, P. (1998) A 1-D vertically resolved modelling study of the ecosystem dynamics of the Middle and Southern Adriatic Sea, *J. Mar. Syst.*, 18, pp. 265–286
- Allen, J., Blackford, J., Holt, J., Proctor, R., Ashworth, M., Siddorn, J. (2001) A highly spatially resolved ecosystem model for the North West European Continental Shelf, *Sarsia*, 86, pp. 423–440
- Baretta, J., Ebenhöh, W., and Ruardij, P. (1995) The European Regional Seas Ecosystem Model, a complex marine ecosystem model, *J. Sea Res.*, 33, pp. 233–246
- Baretta-Bekker, J., Baretta, J., and Ebenhoeh, W. (1997) Microbial dynamics in the marine ecosystem model ERSEM II with decoupled carbon assimilation and nutrient uptake, *J. Sea Res.*, 38, pp. 195–212
- Neumann, T. (2000) Towards a 3-D ecosystem model of the Baltic Sea, *J. Mar. Syst.*, 25, pp. 405–419
- Obernosterer, I., Ruardij, P., Herndl, G. (2001) Spatial and diurnal dynamics of dissolved organic matter (DOM) fluorescence and H₂O₂ and the photochemical oxygen demand of surface water DOM across the subtropical Atlantic Ocean, *Lymnol. Oceanogr.*, 46 (3), pp. 632–643
- Petihakis, G., Triantafyllou, G., Allen, I.J., Hoteit, I., Dounas, C. (2002) Modelling the spatial and temporal variability of the Cretan Sea ecosystem, *J. Mar. Syst.*, 36, pp. 173–196

- Raick, C., Delhez, E.J.M., Soetaert, K., Gregoire, M. (2005) Study of the seasonal cycle of the biogeochemical processes in the Ligurian Sea using a 3D interdisciplinary model, *J. Mar. Syst.*, 55, pp. 177–203
- Ruardij, P., Van Raaphorst, W. (1995) Benthic nutrient regeneration in the ERSEM ecosystem model of the North Sea, *J. Sea Res.*, 33 (3–4), pp. 453–483
- Ruardij, P., Haren, H.V., Ridderinkhof, H. (1997) The impact of thermal stratification on phytoplankton and nutrient dynamics in shelf seas: a model study, *J. Sea Res.*, 38 (3–4), pp. 311–331
- Taylor, A.H., Allen, J.I., Clark, P.A. (2002) Extraction of a weak climatic signal by an ecosystem, *Nature*, 416, pp. 629–632
- Tedesco, L., Vichi, M., Jaapala, J., Stipa, T. (Under Review), A dynamical biologically-active layer for numerical studies of the sea ice ecosystem, *Ocean Modelling*
- Vichi, M. (2002), Predictability studies of coastal marine ecosystem behavior. Ph.D. thesis, University of Oldenburg, Oldenburg, Germany, URL <http://docserver.bis.uni-oldenburg.de/publikationen/dissertation/2002/vicpre02/vicpre02.html>
- Vichi, M., Zavatarelli, M., Pinardi, N. (1998) Seasonal modulation of microbial-mediated carbon fluxes in the Northern Adriatic Sea, *Fisheries Oceanogr.*, 7 (3/4), pp. 182–190
- Vichi, M., May, W., Navarra, A. (2003a) Response of a complex ecosystem model of the northern Adriatic Sea to a regional climate change scenario, *Clim. Res.*, 24, pp. 141–159
- Vichi, M., Oddo, P., Zavatarelli, M., Coluccelli, A., Coppini, G., Celio, M., Fonda Umani, S., Pinardi, N. (2003b) Calibration and validation of a one-dimensional complex marine biogeochemical fluxes model in different areas of the northern Adriatic shelf, *Ann. Geophys.*, 21, pp. 413–436
- Vichi, M., Ruardij, P., Baretta, J.W. (2004) Link or sink: a modeling interpretation of the open Baltic biogeochemistry, *Biogeosciences*, 1, pp. 79–100
- Vichi, M., Pinardi, N., Masina, S., (2007a) A generalized model of pelagic biogeochemistry for the global ocean ecosystem: Part I. Theory, *J. Mar. Syst.*, 64, pp. 89–109
- Vichi, M., Masina, S., Navarra, A. (2007b) A generalized model of pelagic biogeochemistry for the global ocean ecosystem: Part II. Numerical simulations., *J. Mar. Syst.*, 64, pp. 110–134
- Zavatarelli, M., Baretta, J., Baretta-Bekker, J., Pinardi, N. (2000) The dynamics of the Adriatic Sea ecosystem; an idealized model study. *Deep-Sea Res., Part 1, Oceanogr. Res. Pap.*, 47, pp. 937–970

Modeling nutrient balance for the Western Bug catchment under global change and data scarce conditions

Tatyana Terekhanova, Björn Helm, and Jens Tränckner

Institute of Urban Water Management, Technische Universität Dresden, Germany (bjoern.helm@tu-dresden.de)

1. Introduction

In order to achieve an efficient management on river basin scale, it is necessary to differentiate the main emission sources and their spatial distribution along the river. Mass flow balance models are often applied for this purpose. Especially in regions with scarce data the applied balance models rely often on experience from probably similar cases. Validation is rather difficult, since measurements are not available.

For the countries of East-Central Europe the period after the political changes in the late 1980s and early 1990s, had strong impact on economic, demographic and land use conditions. This period serves as reference to show influences of global change on river water quality in the region.

2. Western Bug river basin

With a catchment area of almost 40 000km² Western Bug is the biggest tributary of Vistula river. It is a transboundary river situated in Ukraine, Belarus and Poland.

The river is one of the major sources but also threats of Warsaw's drinking water supply (Niemirycz et al. 1997) and accounts for 15% of the nutrient pollution in the Vistula (Zabokrytska 2006, HELCOM 2005). The discussion about the main sources of pollution is controversial. While TACIS (2001) mentions urban and rural waste water as a main polluter of the river, UNECE (2007) found that 84 % of nitrogen and 68 % of phosphorus pollution are caused by diffuse sources. According to HELCOM (2005), Lviv waste water system is among the 20 biggest single polluters in the Baltic Sea catchment.

Besides this unclear situation about sources of nutrient pollution, heavy metals and pesticides are considered as main sources of contamination in Western Bug (Bodnarchuk 2009).



Figure 1. Location of Western Bug basin

3. Modeling approach

The MONERIS nutrient emissions model (Behrendt et al. 1999) was set up for the upper part of the Western Bug basin. The catchment was divided into 18 sub-basins regarding morphological, topological and water

management criteria. For the period 1980 – 2003, several model configurations including different input data sets were applied. For the best validated model configurations development scenarios are introduced, which include environmental, technical and socio-economic changes in the basin.

4. Data scarcity

The political changes in the Ukraine were accompanied by institutional discontinuities. Within the considered period, the responsible institution for the administration of environmental data changed five times. Moreover, there are several authorities responsible for data acquisition. Consequently one focus was on homogenization and synthesis of multiple input data sources.

Under the difficult present economic situation of the Ukraine a high portion of data sources was available only as historic data, e.g. soil maps and sewer system maps. They were digitized and parameterized.

The historically denser hydrological gauging network was used to generate hydrographs at now unobserved points by multi-regression methods.

Geostatistics and geodata processing were applied to generalize, interpolate and substitute missing information e.g. for the tile drainage system as shown in Figure 1.

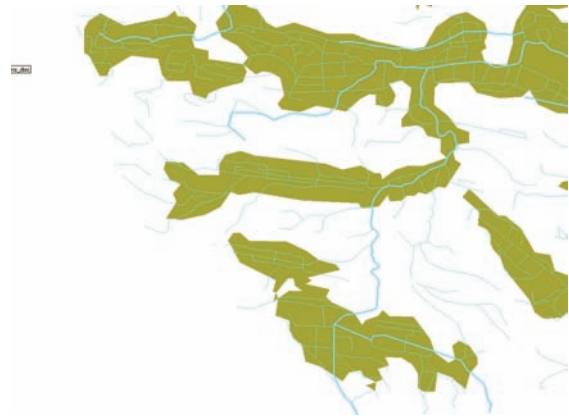


Figure 2. Estimated tile drainage areas (green) from water body density

5. Preliminary results

The model was run for two data sets, which partially differ in “basic” data sources (Ukrainian and remote), but include the same time-series data. The results validation have shown better fit of model with “local data”, especially, for calculated runoff and TP load. But the “remote” results fit better reference TN load (Figure 3). MONERIS quantifies that total nutrients emissions in Western Bug basin for long-term conditions account ca. 4600 tones TN/a and ca. 250 tones TP/a.

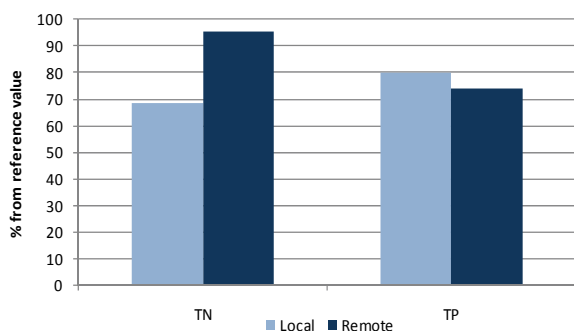


Figure 3. MONERIS calculated long-term TN and TP loads in % of reference value

The main sources of nitrogen are agriculture (59% in total) and other sources (22%). In spite of expectations, the portion of nitrogen delivered from urban settlements is only 10%. Sources partition in this manner for all sub-basins, except Poltava 1 (see below), where the city of Lviv is situated. There the part of input from urban settlements reaches ca. 80%. But due to relatively small weight of subbasins emission in total amount, it does not influence the source partitioning for the entire catchment (Figure 4A).

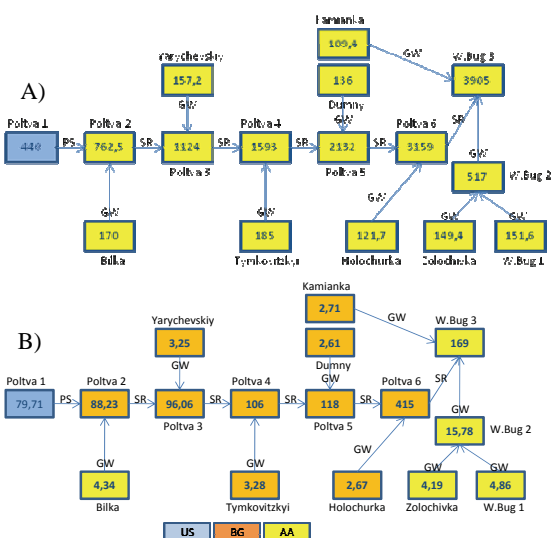


Figure 4. Resulting TN (A) and TP (B) loads in W.Bug basin. Numbers in the boxes are resulting loads at the outlet of the sub-basin; color of boxes correspond to the main sources: US – urban system, BG – background, AA – agricultural areas; the pathways are designated as following PS – point sources, GW – groundwater, SR – surface flow.

The phosphorous emissions are originating mainly from urban settlements (47%), geogenic background (31%) and agriculture (21%). The main delivering sub-basin is Plotva1 where the city of Lviv (44% of total input) is situated. Nevertheless, background emission prevails in other sub-basins (Figure 4B).

6. Conclusions

The evaluation of preliminary modeling results has shown the necessity of further data base improvement. In particular, the extension of validation data is required e.g. data about nutrient loads in sub-basins. As a consequence of the high influence on the MONERIS results, uncertainties of such input data as land cover and soil structure in the basin have to be minimized.

The results of two data sets application, where in “local” set the tile drained areas were not taken into consideration, have shown that “presence of tile drainage” reduces runoff and, consequently, nutrients load in other pathways. Therefore, additional data acquisition is desirable for evaluation of the role of existing tile drainage systems in the basin hydrology, i.e. their catchment areas, specific runoff and nutrients concentrations.

Since the river basin is not a static system, modeling with static models as MONERIS requires extension of the time series, which would include several statuses of the mass exchanges within basin. Moreover, to estimate the part of lost information by application of static model, the revalidation of hot spots with process-based models is desirable.

Based on a readjustment of the representation of relevant processes and input data, scenarios shall be applied that represent the influences of projected global change as well as measures to enhance water quality for present state.

References

- Behrendt, H., et al. (1999) Nährstoffbilanzierung der Flussgebiete Deutschlands. UBA Texte 75/99, Berlin, Germany.
- Bodnarchuk, T (2009) BASELINE ASSESSMENT OF WATER CONTAMINATION IN UKRAINIAN PART OF WESTERN BUG BASIN, 23rd European Regional Conference International Commission on Irrigation and Drainage, Lviv
- Niemirycz G.A. et al. (Edts.) (1997) The Vistula River in Poland, in: Best, International river water quality: pollution and restoration, 2nd International River Quality Symposium, Gdansk
- UNECE (2007) Our Waters: Joining Hands Across Borders – First Assessment of Transboundary Rivers, Lakes and Groundwater, UNECE Report., pp. 84 – 91, ISBN: 9789211169720
- HELCOM (2005) Evaluation of transboundary pollution loads, Helsinki Commission, pp 8 – 14, Helsinki
- Zabokrytska, M.R., Khilchevskiy, V.K., Manchenko, A.P.. (2006) Hydroecological status of Zakhidnyj’ Buh Basin in the territory of the Ukraine. Kiev, Nika Zentr.

Simulation of nutrient transport from different depths during an upwelling event in the Gulf of Finland

Germo Väli¹, Victor Zhurbas^{1,2}, Jaan Laanemets¹, Jüri Elken¹

¹Marine Systems Institute at Tallinn University of Technology, Akadeemia tee 21, 12618, Estonia (germo.vali@phys.sea.ee)

²Shirshov Institute of Oceanology, Nakhimovski Prospekt 36, 117997, Moscow, Russia

1. Introduction

Coastal upwelling events caused by the along-shore westerly (easterly) wind forcing in the Gulf of Finland bring nutrient-rich deeper water to the surface layer near Finnish (Estonian) coastline. Due to difference in the vertical locations of nutriclines in the Gulf of Finland (Laanemets et al. 2004) during summer, the transport of phosphorus during an upwelling event exceeds the transport of nitrates in relation to the Redfield ratio, and therefore, in the nitrate-limited Baltic Sea, upwelling events are one of the main phosphorus sources, together with turbulent mixing (Vahtera et al. 2005), for the formation of the nitrogen fixing cyanobacteria blooms during the nutrient depleted summer period. The total mass of nutrients brought to the upper 10 m layer is dependent on whether the upwelling is on the northern or the southern sides of the Gulf – near the Estonian coastline, the transport is more intense due to greater depths and bottom slopes (Laanemets et al. 2009, Zhurbas et al. 2008).

The objectives of this study are:

a) to track the nutrient transport from different depths to the surface of the Gulf of Finland during a coastal upwelling event on the southern and the northern part of the Gulf, b) using the theory of cross-shelf momentum flux divergence (Lentz and Chapman 2004) to detect the possible locations of on-shore flow within the water column, compensating the wind-driven off-shore Ekman transport in the surface layer and resulting high nutrient transport during an upwelling event.

2. Model setup

We applied the Princeton Ocean Model – POM – which is a primitive equation, σ coordinate, free surface, hydrostatic model with 2.5 moment turbulence closure sub-model embedded (Mellor and Yamada 1982; Blumberg and Mellor 1983). The model domain includes the whole Baltic Sea, closed at the straits. Digital topography was taken from Seifert et al. 2001. We used 41 equally spaced σ layers in the vertical direction. Horizontal resolution was 0.5 nm inside the Gulf of Finland and 2 nm elsewhere. The simulation period was from 20th July 1999 to 29th July 1999. Atmospheric forcing (wind stress and heat flux) was taken from a meteorological data set of the Swedish Meteorological and Hydrological Institute (SMHI), and wind stress was calibrated to fit the wind observations at Kalbadagrund weather station (Finnish Meteorological Institute). The initial thermohaline fields were constructed with the help of a Data Assimilation System coupled with the Baltic Environmental Database (see <http://nest.su.se/das>). Initial nutrient fields were based on field measurements from a Finnish R.V. Aranda in summer 1999, extrapolated uniformly over the Baltic Sea (Zhurbas et al. 2008).

In order to model the transport of nutrients from a certain depth range $[z-\Delta z/2, z+\Delta z/2]$, series of experiments were conducted with the initial nutrient concentration introduced only into one σ -layer closest to a given depth z (i.e.

$-\sigma \cdot H \approx z$), where H is the water depth. To leave the total initial nutrient mass unchanged, the nutrient concentration in z -coordinates, $C(z)$, is related with that of σ -coordinates, $C(\sigma)$, as $C(\sigma) = C(z) \cdot \Delta z / (\Delta \sigma \cdot H)$.

Within the experiments, the amount of horizontally integrated nutrients in the upper 10 m layer was collected as a function of time and initial depth of 2-m thick nutrient layers. The nutrient transport simulation started on 22nd of July 1999 and lasted for 7 days in every model run. The actual wind fields were turned 180 degrees for modeling the upwelling event along the Estonian coast.

3. Results

Maps of time-series of the nutrient mass brought to the upper 10 m layer in the Gulf of Finland from a 1 m thick layer located at different depths during an upwelling event (Figure 1) show that the main source for phosphorus is between 17 to 40 m for upwelling on both sides of the Gulf of Finland – near the Finnish coastline it is slightly shallower.

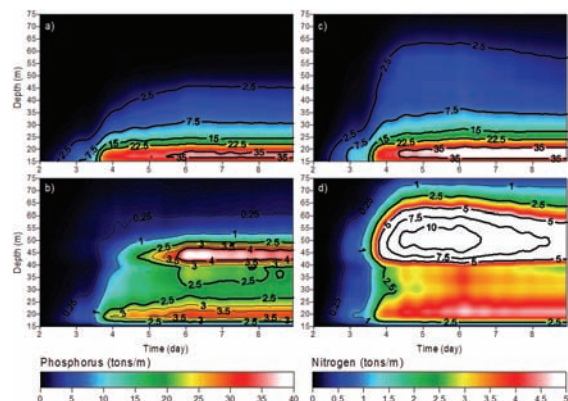


Figure 1. Maps of time-series of total nutrient transport in tons to the upper 10 m layer in the Gulf of Finland obtained from the series of experiments. Time is plotted as day starting on 20th of July 1999 and depth is depth, where nutrients were located as the initial source from which it was brought to the surface layer. On the left hand are the results for upwelling along the Finnish coast and on the right hand side for the upwelling along the Estonian coast.

Transport is the highest from 17 m near the Finnish coastline (Figure 1a) and from 17 to 19 m near the Estonian coastline (Figure 1c) as more than 35 tons/m of phosphorus was brought to the surface layer from the depth range. With increasing depth, the transport of phosphorus is reduced to 2.5 tons/m in 45 m depth for upwelling near the Finnish coastline, and 65 m near the Estonian coastline, respectively. For nitrogen, the behavior is slightly different - the highest transport is from depths of 40 to 65 m near the Estonian coast (Figure 1d) and 43-49 m near the Finnish coast (Figure 1b), but the amount differs more than 2.5 times. Near the Estonian coast, more

than 10 tons/m of nitrogen is brought to the surface layer from depths 45-55 m, while near the Finnish coast, the highest values were more than 4 tons/m from depths 40-45 m. More than a ton/m of nitrogen is brought to the surface layer at depths less than 53 meters near the Finnish coastline but for the Estonian coast it is less than 73 m depth.

Near the Finnish coast, phosphorus is more likely brought to the surface layer from depths below 20 m, as shown on the maps of time-series of the ratio of nutrient transport from a given depth to the cumulative transport to the upper 10 m layer (Figure 2). More than 2.5 % per meter of the phosphorus is brought to the surface from depths less than 25 m on both shores (Figure 2a, Figure 2c). Nitrogen near the Finnish coast is mainly brought to the surface from depths 17-23 m (more than 2.5%/m) and from depths 40-50 m (Figure 2b). Near the Estonian coast, the most intense transport of nitrogen is from depths 45-53 m (more than 3.5%/m) and 43-57 m (more than 2.5%/m) (Figure 2d).

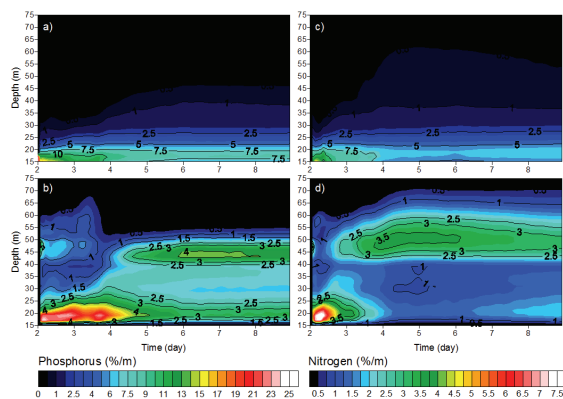


Figure 2. Maps of time-series of ratios (in % per meter) of total nutrient transport to the upper 10 m layer from shown depth to the total sum of nutrient concentration in the upper 10 m layer, obtained from the series of experiments. On the left hand sides, results for the upwelling near the Finnish coast are shown, and on the right hand side near the Estonian coast.

Model results indicate that transport of nutrients depends on the bathymetry of the Gulf of Finland and the vertical structure of the nutrients. The nitrogen concentration has a strong vertical gradient in the depth range from 40-60 m, while the phosphates are distributed more uniformly within the water column. As a result, the transport of phosphorus is greater from near surface depths and the transport of nitrates is greater from depths larger than 40 m, where there is a sudden increase in concentrations.

4. Conclusions

Preliminary results show that the transport of nutrients during the upwelling event in the Gulf of Finland comes from similar depth range on both shores of the Gulf, while the amounts are higher near the Estonian coast due to greater depth and bottom slope. The main source of phosphorus is located just beneath the nutrient depleted upper 10 m layer but for the nitrogen the transport is more efficient from depth range of 40 to 60 m.

References

Blumberg, A. F., and G. L. Mellor (1983), Diagnostic and prognostic numerical calculation studies of the South Atlantic Bight, *J. Geophys. Res.*, 88, pp. 4579-4592

- Laanemets, J., K. Kononen, J. Pavelson, E.-L. Poutanen (2004), Vertical location of seasonal nutriclines in the western Gulf of Finland, *J. Mar. Sys.*, 52, pp. 1-13
- Laanemets, J., V. Zhurbas, J. Elken, E. Vahtera (2009), Dependence of upwelling mediated nutrient transport on wind forcing, bottom topography and stratification in the Gulf of Finland: model experiments, *Boreal Env. Res.*, 14, pp. 213-225
- Lentz, S. J., and D. C. Chapman (2004), The importance of nonlinear cross-shelf momentum flux during wind-driven coastal upwelling, *J. Phys. Oceanogr.*, 34, pp. 2444-2457
- Mellor, G. L., and T. Yamada (1982), Development of a turbulence closure model for geophysical fluid problems, *Rev. Geophys.*, 20, pp. 851-875
- Seifert, T., F. Tauber and B. Kayser (2001), A high resolution spherical grid topography of the Baltic Sea – revised edition. Baltic Sea Science Congress 2001: Past, Present and Future – A Joint Venture. Abstract Volume. Stockholm Marine Research Centre, Stockholm University, p. 298
- Vahtera, E., J. Laanemets, J. Pavelson, M. Huttonen, K. Kononen (2005), Effect of upwelling on the pelagic environment and bloom-forming cyanobacteria in the Western Gulf of Finland, Baltic Sea, *J. Mar. Sys.*, 58, pp. 67-82
- Zhurbas, V., J. Laanemets, E. Vahtera (2008), Modeling of the mesoscale structure of coupled upwelling/downwelling events and the related input of nutrients to the upper mixed layer in the Gulf of Finland, Baltic Sea, *J. Geophys. Res.*, 113, C05004, doi:10.1029/2007JC004280,

A methodological approach for the assessment of the ecological status of urban water bodies (Saint-Petersburg as a case study)

Valery Vuglinsky¹, Tatiana Gronskaya¹ and Natalia Lemeshko¹

¹ State Hydrological Institute, Saint-Petersburg, Russia (vvuglins@vv4218.spb.edu)

1. Water bodies of St. Petersburg

The modern drainage system of St. Petersburg consists of 720 rivers, streams and canals with common length of about 960 km and nearly 2600 lakes, reservoirs, ponds with a common water surface equal to 23 km². One tenth of the city area is occupied by water surface, and Saint-Petersburg is one of most watering cities of the world.

Almost all water bodies are under strong anthropogenic influence increasing with growing urban population and urban area, which is why it is necessary to study the ecological conditions of water bodies of the urban area.

2. The method of assessment of the ecological status of urban water bodies

A new methodological approach for the assessment of the ecological status of urban water bodies has been developed. The suggested approach is based on complex and integral estimates of the trophic state, the water quality and the hydrological regime to the diagnostics of ecological status of urban water ecosystems.

For the assessment of the ecological status of water bodies of St. Petersburg, data on the hydrological regime and ecological conditions (hydrochemical, hydrobiological and sanitary characteristics) for the period 2002-2008 were used. An ecological database for the 128 rivers, canals and streams and 158 lakes, ponds and reservoirs over the urban territory of St. Petersburg have been developed (Vuglinsky et al., 2002).

3. Results

This approach was applied practically to study 286 water bodies. The regularities and peculiarities of the hydrological regime, water quality and other components of the ecological status have been revealed for the above-mentioned water bodies. The study showed that only 9% of the water bodies were clean and 34% were extremely dirty (Fig. 1). Among these water bodies: 56% - eutrophic, 3% - hypertrophic, 36% - methotrophic and only 5% - oligotrophic.

In addition, based on this methodology, a concept of the optimal ecological monitoring for urban water bodies has been developed. The protecting and rehabilitation measures are proposed for urban water bodies for the future.

This methodological approach was used for the development of the "Programme of restoration of urban water bodies during period of 2008-2013" (Vuglinsky et al. 2009).

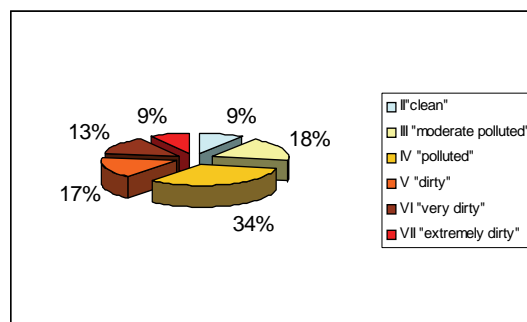


Figure 1. Distribution of water bodies of St. Petersburg according to their ecological rank of pollution.

References

- Vuglinsky V.S., Gronskaya T.P., Varfolomeeva I.V., Litova T.E. (2002) Cadastre of water bodies of urban territories. In book: Water bodies of St. Petersburg. "Saint-Petersburg".
- Vuglinsky V.S., Gronskaya T.P., Lemeshko N.A., Litova T. E. (2009). Results of complex researches of inventory of water bodies of St.Petersburg with assessment of their ecological state, «Izvestiya RGO», Vol.141, No.1, pp. 66-7

Modelling biogeochemical fluxes in the Vistula Lagoon

Mariusz Zalewski¹, Zbigniew Witek² and Magdalena Wielgat-Rychert²

¹ Sea Fisheries Institute in Gdynia, ul. Kołłątaja 1, 81-332 Gdynia, Poland (mariusz.zalewski@mir.gdynia.pl)

² Pomeranian University in Słupsk, ul. Arciszewskiego 22, 76-200 Słupsk, Poland

1. Introduction

The Vistula Lagoon is one of the largest lagoons of the southern coast of the Baltic Sea. It is shallow, brackish and receives high loads of nutrients and organic matter. In consequence, this eutrophied basin is highly productive (Chubarenko and Margoński 2008). The Vistula Lagoon receives and modifies nutrient loads from the drainage basin covering 24000 km² and populated by about one million inhabitants. The degree of modification and retention of nutrient loads in the Vistula Lagoon, before they finally reach the Baltic Sea, has not yet been determined because of insufficient knowledge about the lagoon system functioning, especially with respect to biogeochemical processes.

Most biogeochemical fluxes are difficult to measure directly but can be roughly estimated by a modeling procedure. Our calculations were based on modelling, using the field data collected by various research institutions during the 1998-2000 period used for model calibration. The study was initiated within the MANTRA-East project (Integrated Strategies for the Management of Transboundary Waters on the Eastern European fringe, EU FP5, Contract No. EVK1-CT-2000-00076) and developed further after termination of this project.

2. Model description

To simulate biogeochemical processes taking place in the Vistula Lagoon, a three-dimensional water quality module (Delft3D-WAQ) and its zero-dimensional version (constructed using STELLA software) were used. The model covers cycles of carbon, nitrogen, phosphorus, silicon (only in 3D version) and oxygen in the water column and the sediment. The processes included (Delft Hydraulics, 2001):

- algal growth, respiration, mortality and uptake of nutrients;
- sedimentation and resuspension of algae and particulate matter;
- nitrification and denitrification;
- phosphorus adsorption/desorption on/from inorganic matter;
- mineralization of particulate and dissolved organic matter in water column, and mineralization of organic matter in sediment;
- oxygen exchange with atmosphere;
- inflow, outflow and atmospheric deposition.

The following forcing functions in the biogeochemical model were considered: water temperature, ice cover, irradiance at the water surface, wind speed, and discharge of substances.

3. Modelling results

Area-averaged phytoplankton gross primary production in the Vistula Lagoon in the years 1998-2000 was estimated to 250-350 gC m⁻² yr⁻¹. The results of our calculations allow insights into the factors controlling primary production in the Lagoon. Light availability in the water column was a very important factor governing primary production. Light turned out to be a limiting factor for phytoplankton growth to a greater degree than nutrients. During the vegetation

season, the euphotic zone reached only from 1 to 1.5 m depth.

Light penetration depended strongly on the amounts of suspended matter. Its concentrations ranged usually from 20 to 100 g m⁻³. These are very high values, several times higher than values noted in rivers. Such large amounts of suspended solids result from frequent resuspension of the bottom sediment, which is a typical feature for shallow water bodies exposed to wind induced mixing. Despite the fact that inorganic matter was the most important component of the total suspended matter in terms of mass, it seemed that organic detritus influenced the light conditions in water to a greater extent. High substance-specific extinction coefficient, 40 times higher for detritus than for inorganic matter, was the reason of such a situation. Also, dissolved organic matter (DOM) influenced light extinction in the Vistula Lagoon water significantly.

Nitrogen fixation by cyanobacteria might influence phytoplankton primary production in the Lagoon to a various degree, depending on climate conditions. In the warm summer of 1999, primary production based on fixed nitrogen amounted to 18 gC m⁻² (about 5% of the annual production), but only to about 0.1 gC m⁻² in the cooler year 2000 (about 0.02% of the annual production). According to a rough assessment, in 1999 cyanobacteria may have fixed about 2700 tonnes (about 3.2 gN m⁻² yr⁻¹), while in the year 2000 – about 10 tonnes of nitrogen. As compared to riverine input, nitrogen fixation was not a significant source of nitrogen. In 1999, it constituted presumably about 1/5 of the riverine input.

On the basis of empirical data (Aleksandrov 2005), the water column mineralization rate of organic matter in a model simulation was set to the value that resulted in production/destruction ratio in the pelagial equal to about 1.5; that means that the pelagic community respiration constituted about 70% of the gross primary production. Such model set resulted in substantially higher pelagic mineralization as compared to mineralization in sediment. Mineralization in the pelagic zone constituted 70% of the overall carbon mineralization in the ecosystem and 80% of phosphorus and nitrogen mineralization. Seasonal variability of mineralization fluxes in the pelagic zone was much higher than in the sediment as a result of simultaneous changes of temperature and organic matter content in the water column. In the sediment, the organic matter content did not change significantly, only temperature changes influenced mineralization. In winter, organic matter content in water dropped steeply, and mineralization in sediment dominated over the pelagic process.

During calibration of the nitrification process in the model, attention was paid to proper reconstruction of the nitrate concentration peak during the winter-spring season in the Lagoon and to securing appropriate nitrate flux fuelling denitrification. The resulted model simulations indicated highest nitrification fluxes in summer, with relatively intensive nitrification taking place also in winter. In the model, maximum denitrification fluxes were observed in spring, when high nitrate concentrations in

water were present. In the summer period, when the rates of mineralization of organic matter and nitrification were high, denitrification also reached higher values. The annual denitrification flux was estimated at $7-10 \text{ gN m}^{-2} \text{ yr}^{-1}$.

In a shallow, but vast water body, such as the Vistula Lagoon, sedimentation of suspended matter to the bottom might occur only under calm weather conditions. Even moderate water waving disturbs loose surface layer of the sediment and causes resuspension of particles. According to the model simulation, largest sedimentation fluxes of the total suspended matter were noted at the beginning of ice-cover periods. Spring and summer conditions most often favoured sedimentation over resuspension, however, sedimentation fluxes did not reach values as high as resuspension fluxes. The strongest resuspension events were observed during autumn and ice-free winter periods. In general, resuspension fluxes were higher (though opposite) than sedimentation fluxes. In 2000, resuspension and sedimentation fluxes were almost balanced, while in 1998 and 1999 resuspension prevailed over sedimentation about 1.4 times. Prevalence of resuspension over sedimentation denotes erosion of the Vistula Lagoon bottom. According to model simulations, the erosion rate was about 0.2 mm yr^{-1} .

Sedimentation was the most important input of nutrients to the sediment. On the other hand, between 15 and 20% of the sedimented nitrogen and between 25 and 40% of the sedimented phosphorus were "re-exported" to the water column due to resuspension. However, the most important process of nutrients removal from sediments appeared to be the mineralization of organic matter and subsequent release of N-NH_4 and P-PO_4 to the water column. It seems that ammonium nitrogen released from sediments did not play a significant role as a nitrogen source for phytoplankton uptake, because it was quickly nitrified in the near-bottom layer and further denitrified. In the model, sediment organic nitrogen mineralization flux was similar or even lower than denitrification flux.

Photosynthesis was the main source of oxygen in the Vistula Lagoon. Atmospheric input of oxygen was estimated at about 6 to 10% of the input from photosynthesis. Oxygen consumption in the ecosystem was to a large degree correlated to its photosynthetic release. In a model simulation, total oxygen consumption corresponded to 95% of the gross primary production and revealed the same seasonal changes. The mineralization in the water column, the mineralization in the sediment, and the phytoplankton respiration were responsible for about 50%, 26-28%, and 16-18% of the oxygen consumption, respectively. About 5-6% of the oxygen consumption was due to nitrification.

Differences between oxygen inputs and outputs in the Vistula Lagoon were small, therefore in terms of carbon-oxygen budget the Lagoon can be considered as a balanced system. The nutrient budget indicates that there was no carbon, nitrogen and phosphorus accumulation in the Vistula Lagoon. Nitrogen retention, constituting 35 % of the riverine inflow, was a result of denitrification. However, the negative budget of suspended matter pointed to the erosion of Lagoon's bottom.

References

Aleksandrov S.V., 2005. Pervichnaya produkcja planktona w Kurshskom i Vislinskom zalivach Baltijskogo morja [Plankton primary production in the Kuronian and Vistula lagoons, the Baltic Sea]. In: *Gidrobiologicheskie issledovania v basene Baltijskogo moria, Atlanticheskome i Tikhom okeanach na rubezhe tysacheletij*, Kaliningrad, pp. 8-17.

Chubarenko B.V., Margoński P., 2008. The Vistula Lagoon. [In:] *Ecology of Baltic Coastal Waters*. Schiewer U. (ed.). *Ecological Studies 197*. Springer-Verlag Berlin Heidelberg, pp. 167-196.

Delft Hydraulics, 2001. *User Manual Delft 3D WAQ*. Delft, The Netherlands.

Using multi-year circulation simulations to identify areas of reduced risk for marine transport. Application to the Gulf of Finland

Oleg Andrejev¹, Alexander Sokolov², Tarmo Soomere³, Kai Myrberg¹ and Bert Viikmäe³

¹Finnish Environmental Institute/Marine Research Centre, Helsinki, Finland (Oleg.Andrejev@ymparisto.fi)

²Baltic Nest Institute, Stockholm Resilience Centre, Stockholm University, Sweden

³Institute of Cybernetics at Tallinn University of Technology, Tallinn, Estonia

1. Aims

Intensive shipping in the Gulf of Finland makes the gulf extremely vulnerable to human activity. One of the key problems is that ship-caused pollution frequently affects vulnerable areas far from the accident site. According to the classical definition, the related risks are expressed in terms of the product of the probability of occurrence of a disaster and the cost of consequences of this disaster.

A way to address the consequences by means of a proper choice of the fairway has been proposed in (Soomere and Quak 2007). This method of reduction of consequences of the possible accidents is based, in essence, on the use of current-driven patterns of propagation of adverse impacts. In other words, the potential impact of ship traffic or other anthropogenic activities could be made less dangerous based on detailed knowledge of intrinsic patterns of circulation of the Gulf. In particular, the knowledge of circulation could help us to determine a fairway with minimal risk to hit coast with pollutants in case of an accident. Solutions of this type are especially important for elongated, semi-enclosed basins like the Gulf of Finland.

Recent numerical investigations (Andrejev et al. 2004) show that the mean circulation of the gulf possesses quite high persistency in certain layers situating below the thin surface layer (Figure 1).

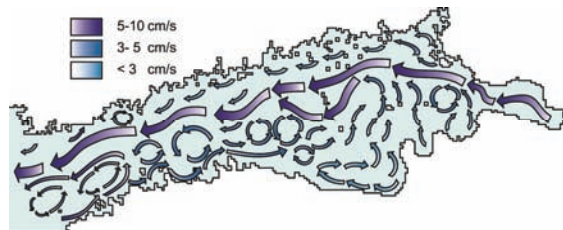


Figure 1. Scheme of mean circulation in upper layers of the Gulf of Finland (Andrejev et al. 2004)

There exist also several flow patterns that become evident over certain time intervals (usually over season but sometimes over several years, Soomere et al. 2010a). Somewhat unexpectedly, such patterns indicate the possibility of rapid flow pathways across the Gulf of Finland (Figure 2). The presence of such patterns in a particular sea region is one of the preconditions for successful identification of the regions that are at high and low risk in terms of current-driven transport of adverse impacts.

The problem of determination of such regions is a classical example of an inverse problem. One of feasible ways of its solution is statistical analysis of a large pool of solutions to an associated direct problem of current-driven transport of adverse impact (Soomere et al. 2010b).

The use of this type of solutions, however, is connected with the need to estimate the persistency and variability of the patterns, and to quantify the confidence and uncertainty related with their practical use. A more consistent way

towards a feasible solution of such a complicated inverse problem is to use several complementary parameters of different physical origin such as water age or the typical time scale it takes for pollutants to hit the coastal zone. To a first approximation, the uncertainties are estimated by means of calculation of the location of the equiprobability line (the probability of propagation of an adverse impact from which to the opposite coasts is equal) by means of different methods (Soomere et al. 2010a).

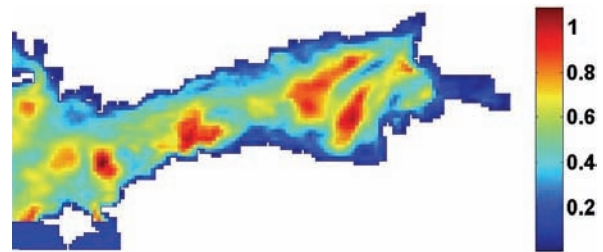


Figure 2. The North-South component of the average net transport in the Gulf of Finland over August–October 1988 based on the analysis of quasi-two-dimensional trajectories of water particles in the surface layer calculated with the use of the TRACMASS trajectory tracing code (Döös 1995) and precomputed current fields from the Rossby Centre (Swedish Hydrological and Meteorological Institute) circulation model (Meier 2001).

Here we introduce and estimate a measure which reflects the overall probability of hitting of any section of the coast by an adverse impact stemming from the open sea. This measure serves as a source of alternative information to find a safe marine fairway in terms of coastal protection. The novel aspect of the proposed research is that we explicitly account for the dispersion properties of water particles.

2. Methods and data

The method used here is based on calculation of trajectories of passive particles moved due to current field in the upper layer. In essence, it follows the ideas described in (Soomere et al. 2010a) but uses a different, high-resolution model for the Gulf of Finland, a different scheme for the on-line calculation of trajectories of water particles during the simulations of the currents, and a different method for inserting and further handling the particles. Moreover, we do not separate the coast of the Gulf of Finland into parts as it used to be in (Soomere et al., 2010).

The current field of the Gulf of Finland was calculated by OAAS baroclinic, hydrodynamic model (Andrejev et al. 2004) for the period of 1987–1991 on the grid with spatial resolution of 1 nautical mile (nm) and constant vertical discretization of 1 m. Initial and open boundary conditions were retrieved from the Rossby Centre (Swedish

Hydrological and Meteorological Institute, SMHI) Baltic Sea circulation model (RCO) results with a spatial resolution of 2 nm and 41 layers with different thickness intervals.

The simulation period was divided into intervals with duration of 10 days. Two particles were released in each grid cell of the uppermost layer at the beginning of each time interval. In order to model dispersion of water particles, random fluctuations were added to the current velocity. Importantly, dispersion parameterized by random fluctuation acts differently to the different particles even if they were released at the same place and time. This makes it possible to consider a variety of particles inserted into the same grid cell but distributed over the cell area and impacted by slightly modified velocities. As a result, particles, even released from the same point, would follow different trajectories. Doing so describes realistically current-driven propagation of pollution in the upper layer and partially also current-induced drift of lost containers, small craft without propulsion, etc.

For each grid cell from which the particles were released a variable was defined with its value depending on the number of particles that reach the coast during 10 days. Its value is set to zero if none of particles came to the coast, 0.5 if one particle did it and 1 if both particles came to the coast. An average of this variable over the whole simulation period produces a measure of potential danger to the coast stemming from particular grid points. The obvious limits of the measure are zero – "no risk" and 1 – "maximal risk".

3. Discussion

The analysis of the two-dimensional distribution of this variable reveals a clear pattern of areas of reduced and increased risk for the coastal area. The areas of reduced risk, propagation of pollution from which to the coast is small, are a good candidate for the location of the optimal fairway for the Gulf navigation. These results to some extent match the outcome of similar studies of Soomere et al. (2010 a,b) but also reveal several new features of the structure of the current-induced transport. The analysis of the similarities and differences provides important information about sensitivity of the entire method with respect to small errors and natural variations in the properties of the currents.

The results are also discussed in the light of potential improvements of the accuracy and spatial and vertical resolution of the current fields. In general, it is desirable to undertake a detailed study of the sensitivity of the outcome with respect to the quality and resolution of the circulation models.

Acknowledgements

The authors thank H.E.M. Meier for providing forcing and boundary conditions for the Gulf of Finland regional circulation model and the RCO circulation modelling results, K. Döös for providing the TRACMASS environment and B. Viikmäe for providing the image for Figure 2. Financial support from the BONUS+ Baltic Way project is gratefully acknowledged.

References

- Andrejev Oleg, Myrberg Kai, Alenius Pekka, and Lundberg Peter (2004) Mean circulation and water exchange in the Gulf of Finland - a study based on three-dimensional modelling, *Boreal Environment Research*, Vol. 9, No. 1, pp. 1–16.
- Döös Kristofer (1995) Inter-ocean exchange of water masses, *Journal of Geophysical Research*, Vol. 100, No. C7, pp. 13499–13514.

Meier H.E. Markus (2001) On the parameterization of mixing in three-dimensional Baltic Sea models, *Journal of Geophysical Research*, Vol. 106, pp. 30,997–31,016.

Soomere Tarmo, Quak Ewald (2007) On the potential of reducing coastal pollution by a proper choice of the fairway, *Journal of Coastal Research*, Special Issue 50, pp. 678–682.

Soomere Tarmo, Delpeche Nicole, Viikmäe Bert, Quak Ewald, Meier H.E. Markus, Döös Kristofer (2010b) Patterns of current-induced transport in the surface layer of the Gulf of Finland, *Boreal Environment Research*, submitted.

Soomere Tarmo, Viikmäe Bert, Delpeche Nicole, and Myrberg Kai (2010a) Towards identification of areas of reduced risk in the Gulf of Finland. *Proceedings of Estonian Academy of Science*, vol. 59, No. 2 (in press).

Frequencies of spring floods in the Belarus part of the Baltic Sea Basin related to the atmospheric circulation

Irina Danilovich and Ryhor Chekan

Hydrometeorological Center of Belarus, 220014, Nezavisimosti Ave, 110, Minsk, Belarus (irina-danilovich@yandex.ru)

1. Introduction

The high spring flooding is the most important and remarkable event in the hydrological cycle in the Republic of Belarus. Nearly each year, floods cause significant destructive damage to the adjoining territories and the cost of recovery from high floods can be enormous. The intensity of spring flooding in the Belarus part of the Baltic Sea Basin is defined by the density of the river network, its morphometric characteristics and hydrometeorological conditions during the season before the floods.

Water resources of the Baltic Sea basin within Belarus are formed in the Zapadnaya Dvina, Neman, and Narev River basins with a mean annual runoff of about 26 cubic kilometers. The annual outflow to the neighboring countries is on average 13.9 cubic kilometers to Latvia via the Zapadnaya Dvina River, 9 cubic kilometers to Lithuania via Neman and Viliya, and 3.1 cubic kilometers to Poland via Zapadny Bug and Narev.

2. Formation of spring floods

Variations in the streamflow over the year strongly depend on climatic conditions. Deviations of climatic elements from average levels caused by, e.g., changes in the atmospheric circulation modify the conditions which determine the streamflow characteristics. A simple indicator characterizing the atmospheric circulation over the north Atlantic is the North Atlantic Oscillation Index (henceforth, NAO). It characterizes the pressure gradient between the Icelandic Low and the Azores High. Its value, especially in winter, determines the intensity of zonal air circulation over the North Atlantic and Europe.

Occurrence of warm and wet winters (in the positive NAO stage) as well as frosty and snowy ones (in the negative NAO stage) in Central Europe crucially affects the discharge of rivers in this region (Hisdal et al. 2004, Wrzesinski, 2004). The main aim of this study was to determine the effect of the North Atlantic circulation on variations in the flow regimes of the rivers within the Republic of Belarus and estimate frequencies of floods. For this purpose, an analysis of the correlations between the NAO index and their monthly, seasonal and annual discharges was made. The stability of the correlations and the significance of differences in the monthly, seasonal and annual discharges under conditions of extreme values of the NAO indices were also studied.

The North Atlantic Oscillation affects the Belarusian Rivers most strongly in winter and spring. In the positive stage of NAO, when winters are milder with frequent thaws, January-to-March discharges are higher and flood events form as early as the end of February and the beginning of March (Danilovich et al., 2007). Furthermore, in the positive NAO stage, due to a smaller snow cover water equivalent, the snowmelt flood waves carry distinctly smaller maximum discharge volumes. They usually occur in April, and in the case of the Neman River, in March.

The situation changes in a negative stage of NAO with more severe winters. The stream alimentation in these winters is limited in the first months of the year, which in turn leads to

lower January-to-March discharges. The snowmelt period starts later (March/April), and the peaks of the meltwater flood waves, while also occurring in April, are much higher. Higher discharges are also observed in May, in the stage of flood-wave recession.

In a year with positive NAO indexes in the cold season (December through March; NAO_{DJFM}) the discharges during spring snowmelt period usually do not reach the average mean values. In a year with negative NAO_{DJFM} indexes the discharges rise above the average and floods are significant. All significant floods observed over the Belarus part of the Baltic Sea Basin have occurred in the years with negative NAO indexes (Table 1).

Table 1. Frequencies of spring floods and NAO indexes.

Years with spring floods and NAO_{DJFM} indexes			
1929	-1.03	1958	-1,02
1931	-0.16	1962	-2,38
1932	-0.50	1963	-3,60
1940	-2,86	1965	-2,88
1941	-2,31	1968	-1,04
1947	-2,71	1970	-1,89
1951	-1,26	1974	1,23(Muhavets)
1953	0,18	1975	1,63
1956	-1,73	1979	-2,25

The outstanding flooding occurred within the Zapadnaya Dvina River Basin in 1878, 1929, 1941, 1951, 1956, the Neman River Basin – 1886, 1931, and the Muhavets River Basin in 1974, 1979. Since the beginning of instrumental observations, the most significant flooding was observed in 1931 on the Zapadnaya Dvina River and in 1958 on the Neman and Shchara rivers. The flooding in 1931 was caused by a special combination of hydrometeorological conditions of the region. In the autumn before flooding a high level of precipitation (about 130-150% of the average) and deep ground freezing were documented. Until the end of winter 1931, the maximum snow water equivalent reached 150-200% of the average. Finally, the snowmelt was influenced by high air temperatures, was quite rapid, and amplified by additional precipitation. The maximal flood stage in 1931 was the highest for the whole observing period.

References

- Danilovich I., Wrzesinski D., Nekrasova L. (2007) Impact of the North Atlantic Oscillation on river runoff in the Belarus part of the Baltic Sea basin. *Nordic Hydrology*. Vol. 38. № 4–5. pp. 413–423.
- Hisdal H. et al. (2004) Has streamflow changed in the Nordic countries? *Materials of XXIII Nordic Hydrological Conference, NHP Report №48*. Tallinn. – pp. 633-643.
- Wrzesinski D. (2004) Flow regimes of rivers of Northern and Central Europe in various circulation periods of the North Atlantic oscillation (NAO). - *Materials of XXIII Nordic Hydrological Conference, NHP Report №48*. Tallinn. – pp. 670-679.

Towards a quantification of areas of high and low risk of pollution in the Gulf of Finland, with the application to ecologically sensitive areas

Nicole C. Delpêche, Tarmo Soomere and Bert Viikmäe

Institute of Cybernetics, Tallinn University of Technology, Tallinn, ESTONIA (nicole.delpêche@gmail.com)

1. Introduction

The Baltic Sea and the coastal areas surrounding it are often regarded as very vulnerable and sensitive areas. There is ever increasing pressure to the nearshore due to a number of different factors, for example, illegal and deliberate accidental discharges of oil, release of hazardous substances from the sea bottom, migration of invasive species and anthropogenic pollution, etc. In recent years increased shipping and industrial activities in the adjacent countries continuously increases the possibility for pollution and accidents to occur.

In this paper we employ the potential of the novel way of mitigation of certain type of current-driven hazards in the context of the Gulf of Finland (GoF). This basin serves as the main marine highway connecting Russia (one of the biggest oil and gas producers, and increasing importer of other products) with the rest of Europe. Within recent years there has been an increase in maritime traffic and oil terminals in the GoF. In the event that an oil accident occurs at sea the time it takes to make decisions, to get to the site and deal with the problem is of vital importance. Also of importance to decision makers is determination of the primary areas that would be affected and need to be protected and also the areas that would be least affected.

Thus many investments and studies have been performed on: (a) implementation of rules, regulations and standards that vessels are to comply with in order to avoid accidents at sea (b) the plan of action that is to be implemented in the event that an oil spill occurs and (c) determining the areas that are at risk for pollution, otherwise ecologically sensitive or should be protected in the Gulf of Finland.

In this paper we address the complementary problem of determining which open sea areas in the GoF serve as the most (or least) probable source of adverse impacts for these sensitive regions. In other words, the aim is to estimate the inverse problem: which areas are of high or low risk (e.g. in terms of pollution) for known sensitive and/or protected areas. The problem will be solved, to a first approximation, by means of determination of pollution trajectories with the use of a Lagrangian trajectory model.

The further analysis of the trajectories allows making clear the most/least common areas from where pollution may travel to in a particular sensitive region. These areas are called areas of high and low risk (in terms of the potential of pollution propagation from these areas to sensitive regions) based on the trajectory model. First we consider the nearshore as a generic example of sensitive region and extend the analysis to actual locations of sensitive and/or protected areas.

2. Methodology

A Lagrangian trajectory code TRACMASS (developed by Prof. K. Döös, University of Stockholm) which uses pre-computed velocity fields calculated by the Rossby Centre global circulation model (Regional Ocean model, RCO) with a resolution of 2×2 nautical miles are the main tools used to simulate the trajectories. These trajectories are calculated based on a linear interpolation of the velocity

field in each point of selected grid cells. The position of these trajectories is then updated every six hours. The user defines the source point where the pollution may have been started (the initial position and depth of the trajectories) and at what time (starting and ending time of propagation). It is also possible to make backwards integration of trajectories, that is, to determine where pollution may have originated given that there is information on where the pollution was sighted. In this study, the trajectories were restricted to the uppermost layer of the RCO model with a thickness of 3 m.

Averaging of the transport patterns of the trajectories determines parameters such as the net transport (the patterns of which illustrate the areas that may have fast and slow moving trajectories), ratio of average net and bulk transport (which illustrates whether the flow is predominantly unidirectional or vortice-dominated). These results are useful addition for background knowledge on the patterns of currents in the Gulf of Finland (Soomere et al. 2010).

The GoF was also divided into 3131 grid cells and simulations are made over numerous time windows with duration of 20 days to determine where the trajectories may travel. A statistical analysis is then made on the end of each trajectory. For instance, once the average trajectories for a given grid cell travel to the coast within the above time period, this cell is assigned to be a part of a high risk area with respect to the nearshore and vice versa. We report now analysis of the results for the years 1987–1991.

3. Results

The data was analysed both seasonally and yearly for the GoF. As expected, the patterns of average net transport reproduced several well-known features of the transport patterns in the GoF, for instance, frequently occurring strong net transport on the northern and southern coast of the gulf (Soomere et al. 2010). The yearly averaged results show that at the entrance of the gulf a strong inflowing surface current frequently occurs on southern side of the Gulf of Finland whilst a similar outflowing current is usually present on the northern side. These results coincide well with previous studies performed on the GoF for example in Andrejev et al. (2004).

The results also showed substantial seasonal variation and high variability of the transport patterns in different years. In some years the method indicates a strong across axis current and coastal currents are present (Figure 1). This feature suggests that potential pollution in the middle of the GoF would rapidly (within a few days) travel to the coast. These seasonal patterns occur frequently but not always every year. Thus there exists some uncertainty for when these patterns may be present. However their existence is of importance especially with identification of path of pollutants and fairway design.

Similar patterns in the ratio of average net and bulk transport allow us to identify the areas of fast moving flow but also the areas where possible mostly local eddy-driven circulation may exist. These results are useful for when

identifying suitable pathways for areas of high and low risk.

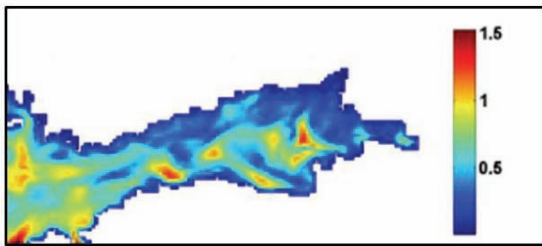


Figure 1. Net Transport across axis component for the spring (March to May) 1988. The color bar represents the number of grid cells (2 nautical miles) traveled per day. Red color indicates areas of intense transport across the axis of the gulf.

Furthermore, the method of Lagrangian trajectories allows systematic depicting of a map of areas of high and low risk for vulnerable areas, for example, to the nearshore. Figure 2 depicts a qualitative map of the level of risk of hitting of any part of the nearshore (not separated into the southern and northern sections) by pollution released in different sea areas. The map is normalized so that the areas with very low risk are clearly distinguishable.

The areas of very low risk are distributed unevenly over the GoF. A chain of areas of low risk in the western part of the gulf is located essentially asymmetrically with respect to the axis of the gulf and is situated close to the Finnish archipelago. There is a small area of low risk located almost exactly at the axis of the gulf in its narrowest part near Tallinn.

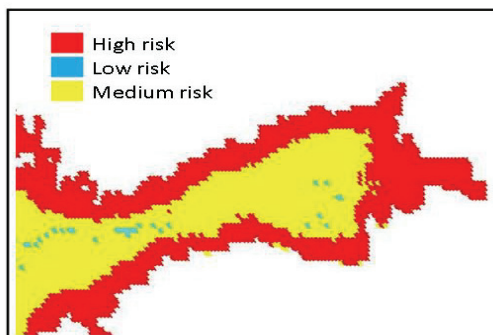


Figure 2. Qualitative distribution of areas of low and high risk for coastal areas for 1988.

Similar maps constructed for different time periods also reveal substantial seasonal variation. One of the areas of major risk to the several sections of the nearshore (not shown here) is located at the entrance of the GoF. Rapid propagation of adverse impacts from this area to the coast has the highest probability during the windy season.

So far the methodology applied has mainly determined the areas of high and low risk with respect to generic impact to the shoreline. Further quantification of the risks is possible by means of definition of different importance levels in terms of, for instance, the minimum distance to a vulnerable section. A more accurate distribution of the risks can be constructed by means of applying the method in use for estimates of the risk for specific ecologically sensitive areas and protected zones. These areas such as Designated Baltic Sea protected areas, important bird areas and UNESCO Biosphere areas (Figure 3) are mostly located along the

coastline but sometimes involve certain wider parts of the nearshore of the Gulf of Finland and its entrance (HELCOM 2008).



Figure 3. Ecologically sensitive areas in the Gulf of Finland according to HELCOM (2008).

The use of realistic location of sensitive areas evidently will change the appearance of the risk maps; for example, accounting for the small islands and shoals north to the NE Estonian coast means that there are virtually no low-risk regions in this sea area. We shall demonstrate several variations of such maps constructed with respect to different sensitive and/or protected areas.

Only few areas were identified as totally low risk areas for 1998 (Figure 2) and a large portion was identified as providing medium-level risk. Such a classification is preliminary and should be refined in the future based on more extensive calculations.

4. Concluding remarks

This study is an early attempt to quantify different open sea areas in terms of current-induced transport of adverse impacts to the existing sensitive and/or nature protection areas in the Gulf of Finland. First, a Lagrangian trajectory model was used to identify areas of high and low risk of pollution to the coastal areas in general. Combining these results with the outcome of ecological studies and locations of protected areas allow building a more detailed map of low-risk areas.

A further step in the analysis and quantifying the risk to marine and coastal environment involves accounting for the degree of sensitivity to different sensitive areas.

References

- Andrejev, O., Myrberg, K., Alenius, P., Lundberg, P.A. (2004). Mean circulation and water exchange in the Gulf of Finland – a study based on three dimensional modeling, *Boreal Environmental Research*, Vol. 9, pp. 1–16.
- Döös K. (1995). Inter-ocean exchange of water masses, *Journal of Geophysical Research*, Vol. 100(C7), pp. 13499–13514.
- HELCOM. (2008). Marine Spatial Planning GIS database, http://maps.helcom.fi/website/MSP_development/viewer.htm
- Soomere, T., Delpêche, N., Viikmäe, B., Quak, E., Meier, H. E. M., and Döös, K. (2010). Patterns of current-induced transport in the surface layer of the Gulf of Finland. *Boreal Environmental Research*, submitted.

Spatio-temporal changes in thunderstorm frequency in Estonia

Sven-Erik Enno

Department of Geography, University of Tartu, Tartu, Estonia (sven-erik.enno@ut.ee)

1. Introduction

Thunderstorms are among the most damaging weather events. They cause lightning, heavy precipitation and flooding, hail and stormy winds. Remarkable economic losses are possible.

The development of national and international lightning detection systems during the last decades has made it possible to study thunder climate by using flash density as the main measure. Many authors have published regional studies about the spatial and temporal distribution of lightning. In Europe, e.g., Tuomi and Mäkelä (2008) in Finland, Sonnadara et al. (2006) in Sweden, Rivas Soriano et al. (2005) on the Iberian Peninsula, Schulz et al. (2005) in Austria and Finke and Hauf (1996) in southern Germany have analysed flash density. In North America, a continental scale lightning detectors network covers most of Canada (Burrows et al. 2002) and the United States with surrounding sea areas (Orville and Huffines 2001, Orville et al. 2002).

However, time series from lightning detection networks are short, so the studies mentioned above cover only 3 to 15 years. Longer thunderstorm climate studies are possible by using visual observations from weather stations. As networks of weather stations were developed at many locations during the 19th century, it is possible to study long-term fluctuations in thunderstorm activity and their relationships with climate changes. Changnon and Changnon (2001) published a climatic analysis of thunderstorm frequency for the US during 1896–1995. They used data from 86 stations all over the country. The annual number of thunder days registered at the stations was used as main measure. Shwehdi (2005) used the annual numbers of thunder days observed at weather stations to study thunderstorm climate in Saudi-Arabia.

Continuous visual thunder observations are available for the entire 20th century at some Estonian weather stations. However, much more data are available for the second half of the 20th century. Many local-scale studies have been written based on visual thunder observations in Estonia. None of these studies have so far been published internationally.

The main goal of this study is to describe the spatial distribution of thunderstorms over Estonia and to analyse long-term fluctuations in thunderstorm activity.

2. Data and method

Annual numbers of thunder days for 23 weather stations were obtained from the Estonian Meteorology and Hydrology Institute (EMHI). A thunder day is defined as a day when thunder was registered at least once. A thunderstorm is registered when the sound of thunder is heard by the observer. Distant night time storms with visible lightning but without audible thunder are not registered as thunderstorm events.

Three different study periods were used in the analysis. Between 1991 and 2003, data from all Estonian stations were available in a computer format. Thus, a short-term thunder day map was compiled for the period 1991–2003. During 1950–2000, data from 11 stations were analysed for inter-annual variability and long-term trends. A long-term

thunder day map was also compiled for the period 1950–2000. For one station in Tartu, south-eastern Estonia, a century-long data series from 1901 to 2000 was used to study possible long-scale fluctuations and trends.

3. Results and discussion

It can be concluded that the main thunder season in Estonia is between May and September, when the 50-year average monthly number of thunder days is larger than one. The peak of thunder activity seems to be in July with a normal number of thunder days 3 to 7 at different stations. In April, one thunder day per two years, in October, one thunder day per three years and in November, one thunder day per 10 years is normal. From December to March, thunder is even a rarer phenomenon. Consequently, more than 75 % of annual thunder days occur in June, July and August. May and September give about one fifth of annual thunder days, April and October give about 5 %. Less than a half per cent of all days with thunder occur between November and March.

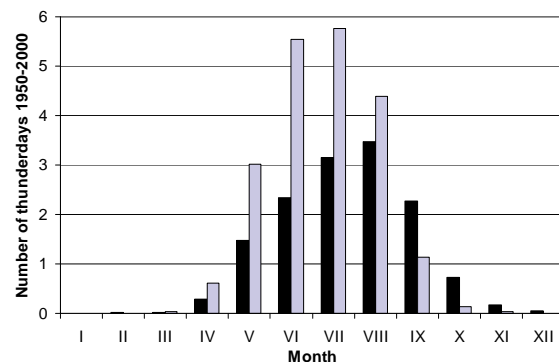


Figure 1. Monthly average numbers of thunder days during 1950–2000 for Võru (gray) and Vilsandi (black).

A significant difference appeared between monthly distributions of thunderstorms at coastal and inland stations (see Figure 1 for the comparison of Võru and Vilsandi stations). The Vilsandi station is located on the western coast of the Island of Saaremaa and is directly affected by the open waters of the Baltic Sea. Võru in south-eastern Estonia is the most continental station. It is 150 km east of the nearest sea (Gulf of Riga) and 300 km east of the open waters of the Baltic Sea. As shown in Figure 1, the sea lowers the overall thunderstorm activity and shifts it towards autumn. Thus, a continental station in Võru shows a clear peak in July and June, whereas the maritime Vilsandi has the highest thunderstorm frequency in August. It is well known that the sea warms up slowly during spring and early summer, but remains relatively warm during autumn when inland cools rapidly. This means that thunder development over the sea is inhibited during spring and early summer, but it is enhanced during autumn. It is also obvious from local studies that the sea strongly affects the diurnal distribution of thunderstorm activity, but this is not further discussed here.

The territorial distribution of thunderstorms was studied for the period 1991–2003 (data from 23 meteorological stations were used) and 1950–2000 (data from 11 stations). It can be concluded from both periods that the annual number of thunderstorm days rises from the west to the east on the Estonian territory. On the western islands, as well as in the western and north-western coastal regions, there are only 12–16 thunder days, in central Estonia there are about 18 and in the eastern part of the country 20–22 days with thunderstorms per year. Less thunder in the coastal regions and on the islands is associated with the influence of the sea. The sea surface is relatively cool during summer afternoons and it does not favour the development of updrafts and local thunderstorms. Hence, thunderstorms in the coastal regions are mostly associated with fronts. In addition to the frontal storms, the inland stations also experience many local thunderstorms, especially during the afternoon hours. The landscape in the eastern part of Estonia features more hills, so the ignition and development of local convection is supported by the relief. That explains why eastern Estonia has the highest annual numbers of thunder days.

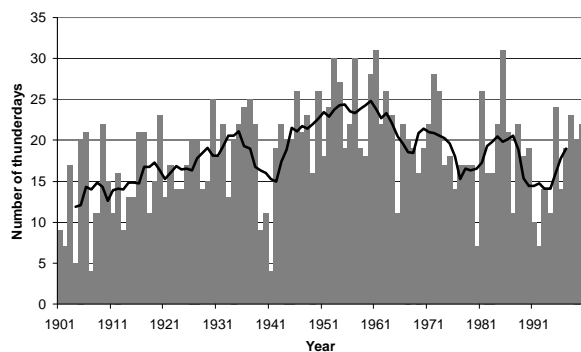


Figure 2. Annual numbers of thunder days in Tartu from 1901 to 2000 and a 7-year moving average.

Long-time trends of the annual numbers of thunder days were studied mainly for period 1950–2000 and data from 11 weather stations were used. In addition, changes during a longer period of 1901–2000 were studied for the Tartu station.

First, it can be concluded that the annual number of thunderstorm days fluctuates remarkably. June, July and August with the largest number of thunderstorms showed the variation coefficients of 0.5–0.8 in the number of days with thunder. The maximum numbers of thunder days per month extended to 14–15. These high rates were observed in June, July and August at some inland stations. Different years showed remarkably different thunderstorm frequencies. Observations at different stations show that at some of them, only 1–10 thunder days per year can be found. On the other hand, the maximum number of thunder days has been as high as 26–42 at the 11 stations studied.

During 1950–2000, four thunder-rich periods appeared, separated by lower activity periods. The thunder-rich periods occurred in the end of the 1950s, in the first half of the 1970s, in the mid-1980s and in the end of the 1990s. The strongest minimum was observed in the beginning of the 1990s. There are only a few statistically significant trends in the monthly numbers of thunder days. By the way, in the annual number of thunder days, statistically significant recession trends were found for some stations. However, fluctuations in the annual numbers of days with thunderstorms seem to be clearer than long-term trends.

The study of the long period 1901–2000 in Tartu (Figure 2) suggests that the 1950s were the most thunder-rich period in the 20th century. As the long-term analyses at other 10 stations begin with the year 1950, it can be the explanation of the reliable recession trends. It is interesting that in Changnon and Changnon (2001), at 86 stations, an average annual thunder day graph for the United States shows a similar mid-century peak as at the Tartu station in Estonia.

This is an ongoing project, so a similar analysis of spatial distribution and long-term trends of thunderstorm activity will be done for Latvia and Lithuania.

4. Acknowledgements

Acknowledgements to the personnel of Estonian Meteorology and Hydrology Institute who helped to obtain the data needed for the study.

References

- Burrows, W.R., King, P., Lewis, P.J., Kochtubajda, B., Snyder, B., Turcotte, V. (2002) Lightning occurrence patterns over Canada and adjacent United States from lightning detection network observations, *Atmosphere-Ocean*, 40, 59-81
- Changnon, S.A., Changnon, D. (2001) Long-term fluctuations in thunderstorm activity in the United States, *Climatic Change*, 50, 489-503
- Finke, U., Hauf, T. (1996) The characteristics of lightning occurrence in southern Germany, *Contributions to atmospheric physics*, 69, 361-374
- Orville, R. E., Huffines, G. R. (2001) Cloud-to-ground lightning in the United States: NLDN results in the first decade, 1989–98, *Monthly Weather Review*, 129, 1179-1193
- Orville, R.E., Huffines, G.R., Burrows, W.R., Holle, R.L., Cummins, K.L. (2002) The North American Lightning Detection Network (NALDN)-First results: 1998-2000, *Monthly Weather Review*, 130, 2098-2109
- Rivas Soriano, L., De Pablo, F., Tomas, C. (2000) Ten-year study of cloud-to-ground lightning activity in the Iberian Peninsula, *Journal of Atmospheric and Solar-Terrestrial Physics*, 67, 1632-1639
- Schulz, W., Cummins, K., Diendorfer, G., Dorninger, M. (2005) Cloud-to-ground lightning in Austria: A 10-year study using data from a lightning location system, *J. Geophys. Res.*, 110, D09101
- Shwehdi, M.H. (2005) Thunderstorm distribution and frequency in Saudi Arabia, *Journal of Geophysics and Engineering*, 2, 252-267
- Sonnadara, U., Cooray, V., Götschl, T. (2006) Characteristics of cloud-to-ground lightning flashes over Sweden, *Physica Scripta*, 74, 541-548
- Tuomi, T.J., Mäkelä, A. (2008) Thunderstorm climate of Finland 1998-2007, *Geophysica*, 44, 67-80

Integrated Water Resource Management for the Western Bug catchment as a multi-scale - multi-objective approach

Björn Helm, Tatyana Terekhanova and Frank Blumensaat

Institute of Urban Water Management, Technische Universität Dresden, Germany (bjoern.helm@tu-dresden.de)

1. Introduction

The concept of Integrated Water Resource Management (IWRM) is a powerful framework for the multi-objective evaluation of human water use and its social, economic and environmental consequences. It is thus one pillar for sustainable development under changing global boundary conditions (UNESCO, 2009).

In order to capture entities of mass and energy fluxes, IWRM should apply to river basins (Grambow 2007). For mesoscale basins, water and matter fluxes are determined by processes of different spatial and temporal scales. Regarding the plurality of aspects involved, a single model approach necessarily fails to equally describe the multitude of processes and to represent them with the adequate exactness.

2. Western Bug river basin

With a catchment area of almost 40 000km², Western Bug is the biggest tributary of the Vistula river. It is a transboundary river situated in Ukraine, Belarus and Poland. The river is one of the major sources of pollution and threats of Warsaw's drinking water supply (Niemirycz et al. 1997) and accounts for 15% of the pollution in the Vistula (Zabokrytska 2006, HELCOM 2005). TACIS (2001) mentions urban and rural waste water as a main polluter of the river. In contrast, UNECE (2007) found that 84 % of nitrogen and 68% of phosphorus pollution are caused by diffuse sources. According to HELCOM (2005), the Lviv wastewater system is among the 20 biggest single polluters in the Baltic Sea catchment.

Besides this unclear situation about sources of nutrient pollution, heavy metals and pesticides are considered as main sources of contamination in Western Bug (Bodnarchuk 2009).

3. Bottom up – top down approach

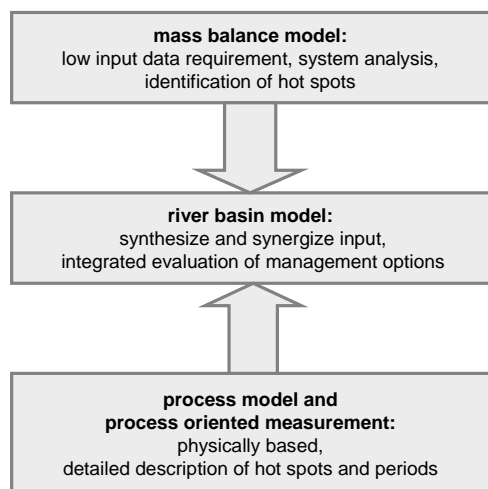


Figure 1. Schematic model approach towards integrated river basin modeling

For the representation of river basins, three fundamental model types can be distinguished. Mass balance models operate on lumped aggregation units, e.g. subcatchments or raster cells, they describe annual or monthly input-output relations with more or less integration of physical boundary information. Mass balance models require relatively few input data, they give a consistent evaluation for the entire basin and serve thus for system analysis and identification of “hot regions” rather than hot spots. Process models describe physically based individual aspects of the water management – river basin system. They have a high spatial and temporal resolution and require detailed input data e.g. in form of process oriented measurements.

Both model approaches vary in resolution, itemization and predictive scope. Their results thus need to be synthesized in a river basin model. These models operate on an intermediate resolution. They have the capability to integrate the consistency of the mass balance approach and the validity of (in case various) process models.

4. Implementation

The approach is realized as a case study within the International Water Alliance (IWAS) project for the pilot region Western Bug basin. It shows the overall approach for the area.

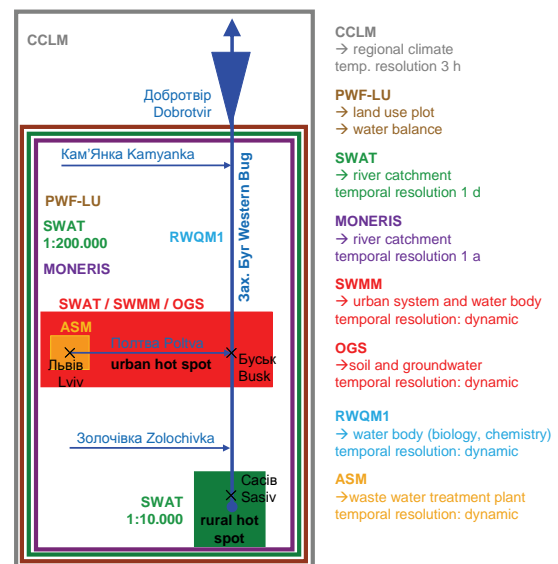


Figure 2. Model system for Western Bug basin

First steps for the implementation of the bottom up – top down approach were undertaken for the urban hot spot Lviv waste water system – Poltva river as receiving water body. As described above, this subsystem is identified as major polluter for Western Bug river.

Mass balance modeling was set up with MONERIS tool (Behrendt 1999). The catchment was divided into 11

subbasins regarding morphological, topological and water management criteria.

For the process analysis, a three months high resolution (5 minutes) measurement campaign in the waste water system and two weeks of medium resolution river water sampling (1h) were conducted. The measured time series serve for an enhanced system analysis and the setup of a SWMM (Huber 1995) model. The model serves to evaluate the performance of Lviv waste water system, comprising sewer system, sewer overflow and waste water treatment plant.

5. Preliminary results

According to first results of mass balance modeling, major sources for nitrogen are agriculture and other sources (e.g. atmospheric deposition), and urban sources and background (geogenic, erosion) for phosphorus.

High resolution measurements in the waste water system show that Lviv waste water treatment plant is highly charged and that sewer overflow is frequent (Figure 3).

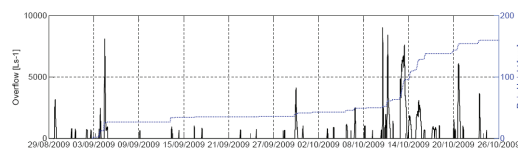


Figure 3. Sewer overflow discharge and corresponding rain height

Figure 4 shows a comparison of measurements in the river body and corresponding resulting loads from the MONERIS model. Measured reference represents an autumn dry weather period. While the resulting load from the Lviv wastewater system (WWTP) is underestimated by the model, loads in the lower rural subbasins are overestimated.

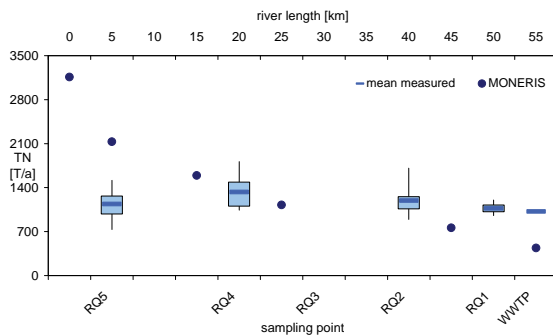


Figure 4. Process based measurement (as boxplot with 25 and 75 percentile) vs. preliminary MONERIS model results

6. Perspective

The development of the process model for the wastewater system and water body is in an advanced state. Results will support the validation of the balance model. Through the elaboration it became clear that the urban system is not represented in a satisfying way by MONERIS. Tests are conducted in order to evaluate sensitivities and limitations of the implemented approach.

An integration of the results of process and balance models in a river basin model is envisaged. The evaluation of the modeling results within a multi-objective framework allows for a synergetic retention of acquired knowledge.

References

- Behrendt, H., et al. (1999) Nährstoffbilanzierung der Flussgebiete Deutschlands. UBA Texte 75/99, Berlin, Germany.
- Bodnarchuk, T (2009) Baseline assessment of water contamination in Ukrainian part of Western Buh basin, 23rd European Regional Conference International Commission on Irrigation and Drainage, Lviv
- Grambow, M. (2007). Wassermanagement, Vieweg+Teubner.
- Huber W.C. (1995), EPA Storm Water Management Model-SWMM. In: V.P. Singh, Editor, Computer Models of Watershed Hydrology, Water Resources Publications, Highlands Ranch, CO, pp. 783–808.
- Niemirydz (1997) The Vistula River in Poland, in: Best, G.A. et al. (Eds.) International river water quality: pollution and restoration, 2nd International River Quality Symposium, Gdansk
- UNECE (2007) Our Waters: Joining Hands Across Borders – First Assessment of Transboundary Rivers, Lakes and Groundwater, UNECE Report., pp. 84 – 91, ISBN: 9789211169720
- UNESCO (2009) IWRM Guidelines at River Basin Level, p.1, Tokio
- HELCOM (2005) Evaluation of transboundary pollution loads, Helsinki Commission, pp 8 – 14, Helsinki
- Zabokrytska, M. R., Khilchevskiy, V.K., Manchenko, A.P. (2006). Hydroecological status of Zakhidnyj' Buh Basin in the territory of the Ukraine. Kiev, Nika Zentr.

Extreme storm surge events in the Pomeranian Bay and their impact on water levels in the Lower Odra River

Halina Kowalewska-Kalkowska

Institute of Marine Sciences, University of Szczecin, Poland (halkalk@univ.szczecin.pl)

1. Introduction

Storm surges in the Pomeranian Bay (southern Baltic Sea) represent a particular threat for the low-lying coastal areas of the Szczecin Lagoon and the downstream Odra reach. These rapid, non-periodic, short-term sea level fluctuations are associated with passages of low-pressure systems over the Baltic Sea and result from the combined effects of persistent strong onshore winds and changes in atmospheric pressure at the sea surface. When they overlap with already high sea levels in the Baltic Sea, the resulting sea level may be very high, reaching extreme values in some cases (Sztobryn et al. 2005, Wiśniewski and Kowalewska-Kalkowska 2007).

The most dangerous storm surges in the Odra mouth occur during the passages of deep and intensive low pressure systems near the coast of the southern Baltic Sea, with an extensive system of winds from the northern sector. Under such circumstances, when the sea level in the Bay is higher than that in the Lagoon, the Bay's brackish water enters the Lagoon and raises the water level both there and in the Lower Odra channels (Kowalewska-Kalkowska and Wiśniewski 2009). Such surges pose a threat for the Odra mouth as they are capable of flooding coastal areas, polders, and areas adjacent to rivers, causing many problems to inhabitants of the West Pomerania, like on 15 October 2009, when the wind-driven water backflow in the Odra mouth caused a flooding event not only at the coasts of the Szczecin Lagoon but also in Szczecin. As a result of the heavy storm surge in the Pomeranian Bay coasts (0.69 m above the alarm level in Świnoujście) and strong (11 Bft) northerly winds, the water level in the Szczecin Lagoon reached 0.64 m above the alarm level (Trzebież). In the Lower Odra channels, the alarm levels were exceeded by 0.55 m in Szczecin (the West Odra) and by 0.85 m in Podjuchy (the East Odra). The effect of the storm surge was observed also at other gauges of the Lower Odra channels.

The study deals with the magnitude, extent, and duration of storm surges within the whole Odra mouth caused by extreme storm surge events in the southern Baltic Sea over the recent years.

2. Wind-driven backflow in the Odra mouth

The stormy autumn-winter season of 2006/2007 resulted in a significant number of storm surges at the Pomeranian Bay coasts. In early November 2006, one of the heaviest storm surges over the recent years occurred, resulting from the passage of deep and intensive low-pressure system over the Baltic Sea. At the southern Pomeranian Bay coasts, the sea level reached 1.45 m above MSL (0.65 m above the alarm level) on 1 November. The Szczecin Lagoon water level fluctuations followed, with a time lag, the sea level changes. In Trzebież, the maximum water level, observed 2 days after the sea level maximum, reached 0.70 m above MSL (0.10 m above the alarm level). As a result of the 3-day-long prevalence of winds from the northern sector, the warning levels were exceeded for more than three days, the alarm levels being exceeded for more than one day. The water level rise was also recorded by the gauges located in the Lower Odra channels, resulting in exceeding the warning levels in the West Odra and alarm levels in the East Odra.

During the storm surge discussed, the slope of free surface of water between the Pomeranian Bay and the Szczecin Lagoon remained reversed for more than one day, and was as high as 1.1 m on 1 November.

As a result of the passage of a series of intensive low-pressure systems over the Baltic Sea and initial high sea levels in the Baltic Sea in January and February 2007, as many as 10 storm surge events were recorded at the coasts of the Pomeranian Bay. During 6 of them the level of 1.0 m above MSL, as recorded in Świnoujście, was exceeded. The highest sea level of 1.40 m above MSL (0.60 m above the alarm level) was observed on 19 January 2007. During the night of 24 January, the level of 1.0 m above MSL was exceeded for 12 hours. During the period discussed, raised water levels were observed both in the Szczecin Lagoon and in the Lower Odra channels. In the Szczecin Lagoon, the warning levels were exceeded for more than 23 days, the alarm levels being exceeded for more than 12 days. In Trzebież, the highest water level of 0.97 m above MSL (0.37 m above the alarm level) was observed on 25 January 2007. The same day, in Szczecin the water level rise up to 1.05 m above MSL (0.25 m above the alarm level) was observed. The levels exceeding 1.0 m above MSL were remaining for a half a day. The alarm levels were recorded for more than 3 days, while the warning levels were observed for more than 16 days. Gauges located at the East Odra recorded the alarm levels for 23 days and the warning levels for almost one month continuously.

As reported by Buchholz (1990), the resulting wind-driven water backflow in the Odra River may penetrate as high up the river as to Gozdowice (160 km south from the sea). In contrast, effect of the instantaneous Odra discharge on water levels in the river's mouth area is of less importance because, even during Odra flood events, the water level increases by only a few centimetres as the flood wave enters the Szczecin Lagoon. Such a situation is aptly exemplified by the biggest Odra flood event in summer 1997. While in Gozdowice the alarm levels were being exceeded for 37 days and the water level rose up to 2.49 m above the alarm level, the recorded levels in Szczecin were remaining below the warning states.

References

- Buchholz W. (1990) Materiały do Monografii Dolnej Odry, Warunki hydrologiczno-hydrodynamiczne, Prace IBW, 22, Wyd. IBW PAN, Gdańsk
- Kowalewska-Kalkowska H., Wiśniewski B. (2009) Storm surges in the Odra mouth area in the 1997-2006, *Boreal Env. Res.*, 14, pp. 183-192
- Sztobryn M., Stigge H.-J., Wielbińska D., Weidig B., Stanisławczyk I., Kańska A., Krzysztofik K., Kowalska B., Letkiewicz B., Mykita M. (2005) Storm surges in the Southern Baltic (Western and Central parts), Report No. 39, Bundesamt für Seeschifffahrt und Hydrographie, Rostock, Hamburg
- Wiśniewski B., Kowalewska-Kalkowska H. (2007) Water level fluctuations in the Odra River mouth area in relation to passages of deep low-pressure systems, *Oceanol. Hydrobiol. Stud.*, 36, 1, pp. 69-82

Drought analysis of the Mediterranean region using the z-score

Aleksandra Kržič¹ and Ivana Tošić²

¹SEE-VCCC, Republic Hydrometeorological Service of Serbia, Belgrade, Serbia (alexandra.k255@gmail.com)

²Institute of Meteorology, Faculty of Physics, Belgrade, Serbia

1. Introduction

Transformations can be useful when someone is interested in working simultaneously with batches of data that are related, but not strictly comparable. In situations of this sort, a reexpression of the data in terms of standardized anomalies can be very helpful. The idea behind the standardized anomaly is to try to remove the influences of location and spread from a batch of data. The physical units of the original data cancel, so standardized anomalies are always dimensionless quantities (Wilks 2006). Z-scores are commonly used for the identification of various drought characteristics, such as duration, magnitude, and intensity at different standard truncation levels.

2. Data and methodology

In this work the z-score is obtained from the results of the EBU-POM model. The EBU-POM is a two-way coupled regional climate model, with Eta/NCEP limited area model as its atmospheric part and Princeton Ocean Model as its ocean part (Djurdjević and Rajković 2008). Concentrations of the greenhouse gasses were changed following the A2 scenario. Atmospheric model horizontal resolution was 0.25° and ocean model horizontal resolution was 0.2° .

The z-score for precipitation is simply the standardization of a given time series. Here the z-score is used for determining drought properties, drought duration, magnitude and intensity for the reference period (1961-1990) and the future period (2071-2100) at different truncation levels (0, -1, -1.5, -2). The summation of deficits over a particular period is referred to as the drought magnitude, while drought intensity is the ratio of drought magnitude to its duration. The relationships between drought duration and magnitude are provided in the form of scatter diagrams with the best straight-line fits.

3. Preliminary results

Magnitude-duration curves with correlation coefficient at truncation level 0 for four Mediterranean cities and for two periods of time are presented in Figure 1. It can be observed that increase in the drought duration results in increased drought magnitude. Correlation coefficients are near 1 for both periods of time and all four cities.

Figure 2 presents difference in maximal drought duration of the future (2071-2100) and the reference period (1961-1990) at truncation level 0 (upper panel) and -1.5 (lower panel). In most parts of the Mediterranean we can expect longer duration of drought periods at truncation level 0, but something shorter at truncation level -1.5. The increase in drought duration at truncation level -1.5 can be observed in the Alpine region, the Pyrenees, western Balkan and Alexandria region.

4. Conclusions

The EBU-POM model was used for the future projections of drought in Mediterranean region according to the A2 scenario. It can be expected longer duration of drought periods in most parts of the Mediterranean, especially in western Mediterranean.

References

- Djurdjević, V., Rajković, B. (2008) Verification of a coupled atmosphere-ocean model using satellite observations over the Adriatic Sea. *Annales Geophysicae*, 26, 1935–1954
- Wilks, D.S. (2006) *Statistical methods in the atmospheric sciences*. Academic press, second edition

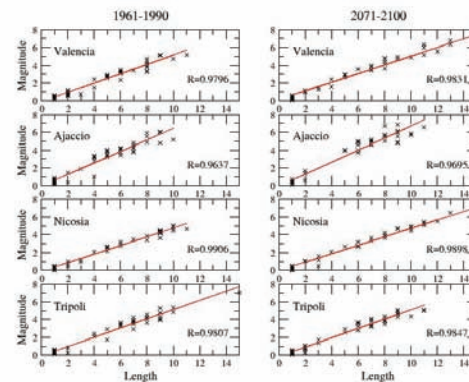


Figure 1. Magnitude–duration curves at truncation level 0 for: Valencia, Ajaccio, Nicosia and Tripoli.

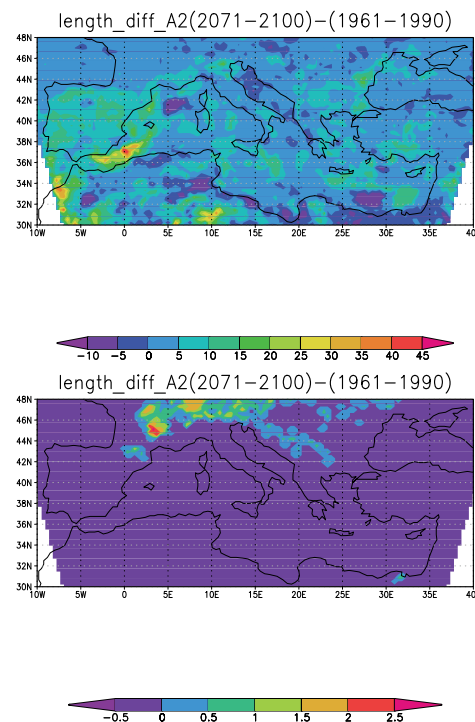


Figure 2. Difference in maximal drought duration of the future (2071-2100) and the reference period (1961-1990) at truncation level 0 (upper panel) and -1.5 (lower panel).

Drought analysis of the Mediterranean region according to the A2 scenario using the Standard Precipitation Index

Aleksandra Kržič¹, Ivana Tošić², Borivoj Rajković² and Vladimir Djurdjević²

¹SEE-VCCC, Republic Hydrometeorological Service of Serbia, Belgrade, Serbia (alexandra.k255@gmail.com)

²Institute of Meteorology, Faculty of Physics, Belgrade, Serbia

1. Introduction

One of the several drought indices is the Standard Precipitation Index (SPI), developed by McKee et al. (1993). The SPI was designed to quantify the precipitation deficit for multiple time scales. These time scales reflect the impact of drought on the availability of the various types of water resources. It is widely used because it allows a reliable and relatively easy comparison between different locations and climates.

The SPI can be computed for any time period from 1 to 72 months, but users can choose the time scale most appropriate for their particular application to compute the SPI. For example, agricultural users may be interested in shorter time periods, such as the SPI for 3 or 6 months, while hydrologists or water managers might be more interested in SPI values for 12 or 24 months (Edwards and McKee 1997).

2. Data and methodology

In this study, the relative SPI time series with the 12-month time scale (SPI12) for gridded data obtained from the EBU-POM model were analyzed. The EBU-POM is a two-way coupled regional climate model, with the Eta/NCEP limited area model as its atmospheric part and Princeton Ocean Model as its ocean part (Djurdjević and Rajković 2008). In our runs, concentrations of the greenhouse gases were changed following the A2 scenario. Atmospheric model horizontal resolution was 0.25° and ocean model horizontal resolution was 0.2°.

Computing the SPI begins with building a frequency distribution from annual precipitation data at a location for a specified time period. A gamma probability density function is fitted to the precipitation data during the period 1961-1990 (calibration period), and the cumulative distribution of precipitation is determined. An equiprobability transformation is then made from the cumulative distribution to the standard normal distribution with a mean of zero and variance of one for the period 2071-2100. This transformed probability is the SPI value, which varies between +2.0 and -2.0 (Table 1), with extremes outside this range occurring 5% of the time (Edwards and McKee 1997). The index is negative for drought and positive for non-drought conditions.

Table 1. Classification scale for SPI values

SPI values	Category
2.00 and above	Extremely wet
1.50 to 1.99	Very wet
1.00 to 1.49	Moderately wet
-0.99 to 0.99	Normal
-1.00 to -1.49	Moderately dry
-1.50 to -1.99	Severely dry
-2.00 and less	Extremely dry

3. Preliminary results

Mean august SPI12 values over the Mediterranean region are represented in Figure 1. Moderately dry climate is expected over greater part of the Mediterranean, while severely dry climate is expected in southern Greece. Absolute frequencies of SPI12 are calculated for four Mediterranean cities (Figure 2) for three drought categories and one cumulative (SPI12<-1). The highest frequency of extremely dry conditions (SPI12<-2) is expected to occur in Valencia, while moderately dry conditions will prevail in Ajaccio, Nicosia and Tripoli.

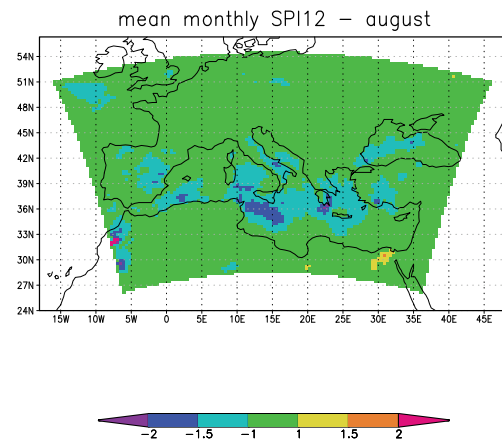


Figure 1. Mean august SPI12 values for the Mediterranean region during the period 2071-2100.

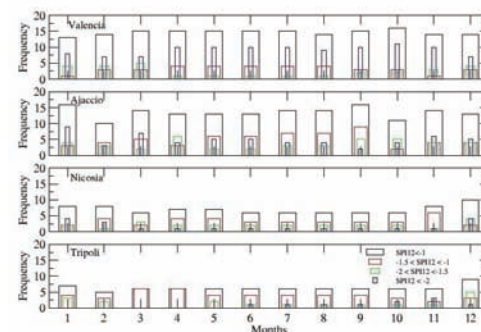


Figure 2. Absolute frequencies of SPI12 for: Valencia, Ajaccio, Nicosia and Tripoli.

4. Conclusions

We have presented a high spatial resolution, multi-temporal climatology for the 21st century. The climatology is based on the annual SPIs calculated on a 0.2° grid across the Mediterranean region for the future period 2071-2100. The droughts are expected over greater part of Mediterranean, as found by other authors (Quadrelli et al. 2001, Pashiardis and Michaelides 2008).

References

- Djurdjevic, V., B. Rajkovic (2008) Verification of a coupled atmosphere-ocean model using satellite observations over the Adriatic Sea. *Annales Geophysicae*, 26, 1935–1954
- Edwards, D. C., T. B. McKee (1997) Characteristics of 20th century drought in the United States at multiple time scales. *Climatology Rep. 97-2*, Department of Atmospheric Science, Colorado State University, Fort Collins, CO, 155 pp
- McKee, T. B., N. J. Doesken, J. Kleist (1993) The relationship of drought frequency and duration to time scales. Preprints, Eighth Conf. on Applied Climatology, Anaheim, CA, Amer. Meteor. Soc., 179–184
- Pashiardis, S., S. Michaelides (2008) Implementation of the Standardized Precipitation Index (SPI) and the Reconnaissance Drought Index (RDI) for regional drought assessment: A case study for Cyprus. *European Water 23/24*: 57-65
- Quadrelli, R., M. Lazzeri, C. Cacciamani, S. Tibaldi (2001) Observed winter Alpine precipitation variability and links with large-scale circulation patterns. *Climate Research*, 17, 275-284

Identifying high risk areas of pollution in the western Baltic Sea

Andreas Lehmann, Hans-Harald Hinrichsen and Klaus Getzlaff

Leibniz Institute of Marine Sciences at University of Kiel, Germany (alehmann@ifm-geomar.de)

1. Introduction

One of the main aims of the BONUS+ Project "BalticWay" is to identify areas that are at high and low risk of coastal pollution in the Baltic Sea. About 76 ports handle more than 1 million t of cargo per year in the Baltic Sea including the Kattegat. The busiest port is St. Petersburg, Russia with more than 14,500 ship operations per year. The number of ship operations (passages, excluding ferry traffic) is estimated at 150,000 per year, and it is assumed that shipping activities will considerably increase in the near future. The Baltic's narrow straits and shallow waters, many of them covered by ice for prolonged periods in winter, make navigation very challenging, and increase the risk of shipping accidents. The main environmental effects of shipping and other activities at sea include air pollution, illegal deliberate and accidental discharges of oil, hazardous substances and other wasters and the unintentional introduction of invasive alien organisms via ship ballast water or hulls. Shipping also adds to the problem of eutrophication of the Baltic Sea with its nutrient inputs from sewage discharges and nitrogen oxides (NO_x) emissions.

The already environmentally sensitive Baltic Sea and its coastal areas are susceptible at high risk for pollution and unintended introduction of invasive species, as for example the jelly fish *Mnemiopsis leidyi* which was firstly observed in the Baltic Sea in October 2006.

2. Methods and concepts

On the basis of 3-dimensional numerical model simulations (BSIOM, Lehmann et al. 2002) of the whole Baltic Sea including Skagerrak and Kattegat we used a Lagrangian particle tracking model (Hinrichsen et al. 1997) to identify high risk areas of pollution for the western Baltic Sea. Circulation and drift track models are operated subsequently. The advantage of an offline subsequent processing of the drift track model is that drifters can be released freely within the 3-d model fields and drift tracking can be forward or backward.

BSIOM has been forced by realistic atmospheric conditions for the period 1997-2008, taken from the Swedish Meteorological and Hydrological Institute (SMHI Norrköping, Sweden) meteorological database (Lars Meuller, pers. comm.) which covers the whole Baltic drainage basin on a regular grid of 1° x 1° with a temporal increment of 3 hours, thus providing realistic three-dimensional current fields for the whole Baltic Sea. Along official ship routes in the western Baltic Sea in a distance of 2 km, drifters have been launched every fifth day of a year. In total 46,800 drifters have been released in one year. Typical drift duration was 10 days. High risk areas of pollution have been identified for those areas where high numbers of drifters reached the coast. Calculated risk areas are a function of the distance from the point of release to the coast, the atmospheric forcing and underlying current fields which are topographically steered.

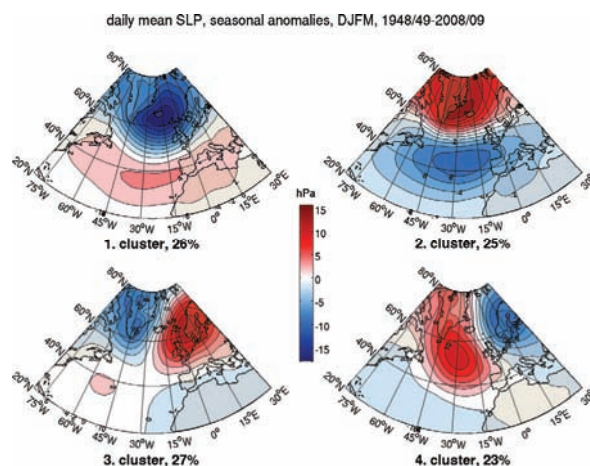


Figure 1. Winter climate regimes derived from cluster analysis of daily mean SLP from NCEP/NCAR re-analysis data for the period 1948-2008.

3. Atmospheric variability

The climate of the Baltic area, and thus the current system in the Baltic Sea, is controlled by large pressure systems that govern the air flow over the continent: The Icelandic Low, the Azores High and the winter high/summer low over Russia. The NAO is a circulation factor strongly influencing the climate of Europe, and its influence is strongest during the winter months (Hurrell and van Loon 1997). From cluster analysis applied over the Atlantic domain we can identify four winter climate regimes in daily SLP (Figure 1). Two of them correspond to the negative and positive phases of the NAO, while the third and fourth regimes display strong anticyclonic ridges over Scandinavia/eastern Europe (the "Blocking" regime) and off western Europe (the "AtlRidge" regime; Figure 1). Approximately, the four winter regimes occur with about the same frequency (20-30%) of all winter days. However, over certain periods the contributions might be different with shifts especially between the NAO-pattern.

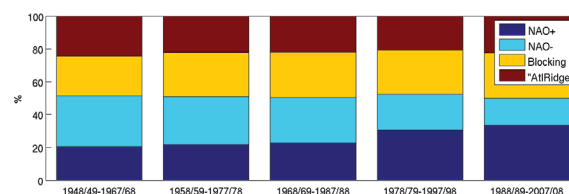


Figure 2. Occurrence of climate winter regimes in different 20-year periods P1: 1948-1968, P2: 1958-1978, P3: 1968-1988, P4: 1978-1998, P5: 1988-2008

The contribution in percentage in each winter (DJFM) season that represents a given regime relative to the 20-year periods (P1-P5) are collected in Figure 2. For the periods P1-P3 NAO⁻ dominated NAO⁺ conditions, since P4, the fraction of NAO⁺ increased at the expense of NAO⁻ conditions.

4. Results

Different atmospheric climate regimes force different circulation regimes in the Baltic Sea (Lehmann et al. 2002), and thus the resulting drift pattern will depend on the prevailing forcing conditions. Furthermore, atmospheric variability even over a monthly period is high which in turn causes high variability of the corresponding current patterns. In Figure 3 the endpoints of drift tracks after 5 and 10 days, red and yellow dots, respectively, are displayed for the winter 2006. The winter 2006 can be characterized as a NAO⁻ winter. Drifters remained relatively close to the positions where they have been released (along black lines). In contrast the winter 2007 was a NAO⁺ winter with strong westerly winds and indeed the drift patterns show much higher dispersion.

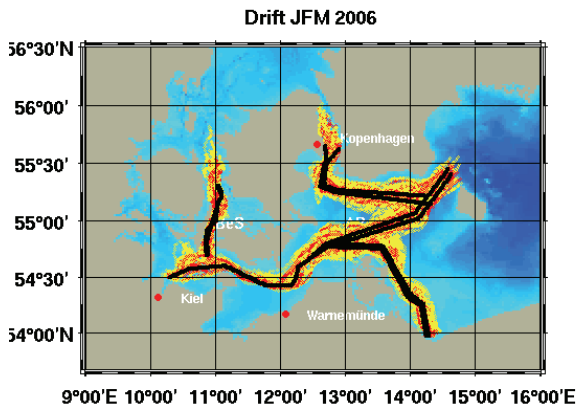


Figure 3 Endpoints of drift tracks after 5 (red dots) and 10 days (yellow dots) for winter (DJF) 2006. Drifters have been released in a distance of 2 km along the ship routes (black lines)

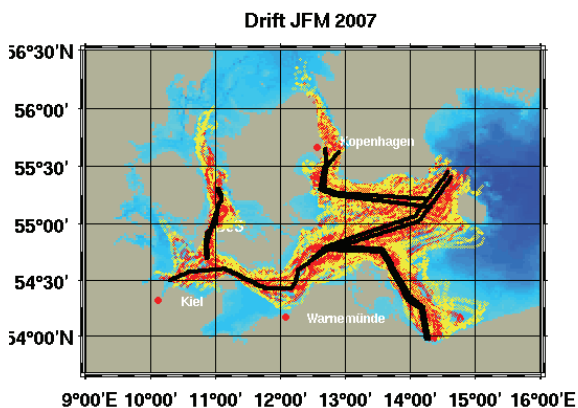


Figure 4 Endpoints of drift tracks after 5 (red dots) and 10 days (yellow dots) for winter (DJF) 2007. Drifters have been released in a distance of 2 km along the ship routes (black lines)

The identification of high risk areas of pollution depends on the specific currents the drifters are exposed to. During calm atmospheric conditions wind drift is small and the dispersion is forced by the residual circulation only, and drifters remain relatively close to the positions where they have been released. Strong wind causes fast drift and increases the risk that pollution will hit the coast. To account for the different atmospheric forcing conditions the probability of drifters hitting the coast if launched along the official ship routes has been calculated for 2007 (Figure 5). Generally, ship routes close to the coast such as the narrow Danish Straits are areas of increased risk. More offshore the prevailing atmospheric conditions determine risky parts along the ship routes.

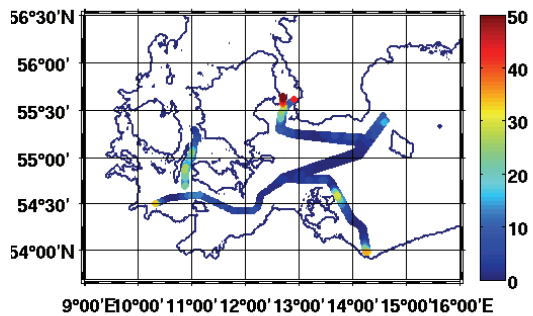


Figure 5. Probability [%] of drifters hitting the coast if released along official ship routes for 2007

References

- Hurrell JW, van Loon H (1997) Decadal variations in climate associated with the North Atlantic oscillation. *Clim. Change*, 36:301-326.
- Hinrichsen H-H, Lehmann A, St John M, Brüggel B (1997) Modeling the cod larvae drift in the Bornholm Basin in summer 1994. *Continental Shelf Res. Vol. 17, No. 14*, 1765-1784.
- Lehmann A, Hinrichsen H-H, Krauss W (2002) Effects of remote and local atmospheric forcing on circulation and upwelling in the Baltic Sea. *Tellus* 54A:299-316.

Circulation of groundwater below a rippled sea bed

Stanisław R. Massel

Institute of Oceanology of the Polish Academy of Sciences, Sopot, Poland (smas@iopan.gda.pl)

1. Introduction

Permeable sands are most common in the coastal environment and relict sands cover approximately 70% of the continental shelves. In shallow waters, high nutrient concentrations boost phytoplankton growth to generate about 30% of the total oceanic primary production in a zone covering less than 10% of the world's ocean area (Huettel & Rusch, 2000).

The velocity of flow as well as the amount of water circulating within the permeable beach body is important for the biological status of the organisms inhabiting the beach sand. Although the biodiversity and biomass of organisms within the beach body are low, recent findings have shown that marine sands transfer energy very effectively (Węśławski et al., 2000). Despite the fact that solar radiation penetrates only the upper 5 mm of sand, sandy coastlines contain primary producers, mainly diatoms and green-blue algae which are able to convert solar radiation into organic carbon with an efficiency reading 67 gC/m² per year.

A number of physical processes contribute to the dynamic nature of the chemical and biological composition of sandy bottom. Storms induce resuspension and redistribution of sediments at a frequency of weeks to months. Moreover currents and waves transport sediments at a time scale of the order of hours to days (Shum, 1993).

In particular, wave-induced oscillations, bottom currents and tidal flows generate circulation of pore water which is a significant transport mechanism of solutes and suspended particular matter. Most of the existing solutions are dedicated to the case of the horizontal bottom. In particular, Massel et al. (2004, 2005) used the Biot theory for the multiphase flow and developed of the close form an analytical solution for wave- induced flow with various air content in the sand skeleton.

However, sea bottom is rarely flat and bottom ripples have significant effects on the pattern of pore water flow. Laboratory experiments on the flow over sandy sediment with simulated biogenic surface structures showed an increase of interfacial fluid exchange up to 7-fold (Huettel et al., 1996). This conclusion was confirmed also by the Shum (1992) numerical model.

In this paper, simple mathematical models are presented for pore water circulation below rippled sea bottom. In contrast to the Shum's solution, the paper is focused on the pattern of the circulation cells of the pore water. Two cases of induced flow are considered. First, the circulation induced by bottom current with constant velocity is examined using the conformal mapping technique. Secondly, the circulation of pore water in the beach body induced due to waves and set-up mechanism is discussed.

2. Mathematical models

In the first model, it was assumed that the single ripple is located on the horizontal bottom. Ripple is in the form of segment of circle of radius r and height of ripple is equal

b . In the water column, at the sea bottom, water current has a velocity u_0 . Pore water circulation in the porous media was obtained through the conformal mapping in such a way that this area becomes the lower half plane. Water pressure p_0 on now horizontal interface surface become a boundary condition for water circulation within sandy bottom. The pressure distribution of pore water can be found from the Poisson integral (Massel, 2010):

$$p(x, y) = \frac{1}{\pi} \int_{-\infty}^{\infty} p_0(t) \frac{y dt}{(t-x)^2 + y^2}$$

According to the Darcy law, components of pore water velocity are proportional to the corresponding gradients of the pore water pressure.

In Fig. 1 an example of the stream function pattern below the ripple is shown. Two circulation cells are clearly seen. Therefore along the central plane, under the ripple, vertical velocity is directed upwards, while outside of the bottom form these velocities are negative.

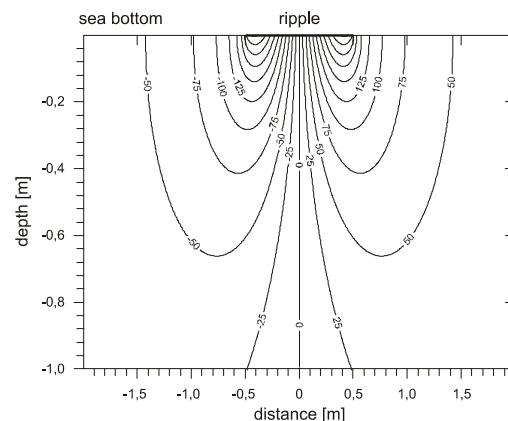


Figure 1. Stream lines pattern below a single ripple

Velocity in the porous layer is of the order of some centimeters per hour, under the assumption that the filtration coefficient is $K_f = 10^{-4}$ m/s.

In the real natural situation, the sea bottom is usually covered by a sequence of ripples induced by surface waves. In the model a system of N sinusoidal ripples with amplitudes b and length λ is assumed. In front of the ripples system, incoming waves, with some wave height H and period T , as well as reflected waves with height $K_R H$ (K_R is the reflection coefficient) are observed. Behind the ripples, only outgoing waves with height $K_T H$ exist (K_T is the transmission coefficient). For the area with ripples, so called refraction-diffraction equation was solved.

In Fig. 2 an example of a stream function field in the porous media is given. Under the sinusoidal ripples system, the sequence of the circulation cells is shown.

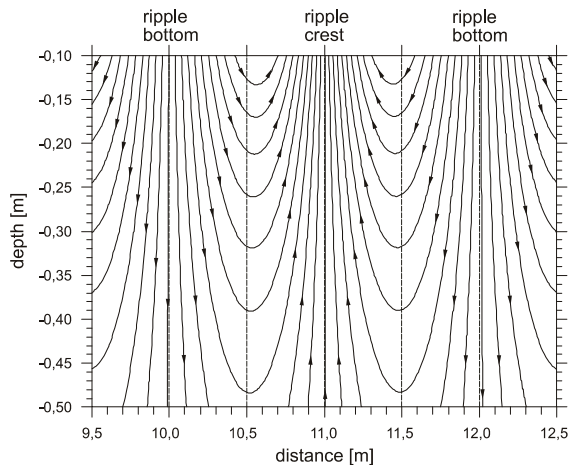


Figure 2. Stream function under ripple crests and bottom

Porous layer, nutrient and pollutants transport is determined by the advection and diffusion, and modeled by the advection-diffusion equation for concentration c :

$$\frac{\partial c}{\partial t} + \frac{\partial(cu)}{\partial x} + \frac{\partial(cv)}{\partial y} + \frac{\partial(cw)}{\partial z} = D\nabla^2 c,$$

in which u , v and w are the water velocity components, resulting from the mathematical modes described above. Because of very small pore water velocity, the diffusion coefficient D was used. According to Shum (1993), for the porous media, the coefficient $D \approx 10^{-9} + 10^{-7} \text{ m}^2/\text{s}$.

In very shallow water depth, the radiation stress mechanism produces some denivelation of the mean water level. Due to this denivelation, some extra stationary pressure is created which induces also the circulation of the pore water in permeable media. Results of the modelling indicate that under waves action, close waterline a vertical "barrier" was formed with vertical velocity flow only (Massel, 2001). This barrier separates sea water from the inland water flowing to the sea.

In summary, it is pointed out that the mathematical models discussed above help to put some insight into the role of the sea bottom form for the uptake of particulate organic matter into permeable shelf sediments. It should be noted that the geometrical form of the bottom ripples are not crucial for the mathematical models showed above and the given methodology can be extended to arbitrary shapes of sea ripples.

References

- Huettel, M., Ziebis, W., Forster, S. (1996) Flow-induced uptake of particulate matter in permeable sediments, *Limnol. Oceanogr.*, 41, 309-322.
- Huettel, M., Rusch, A. (2000) Transport and degradation of phytoplankton in permeable sediment, *Limnol. Oceanogr.*, 45, 534-549.
- Massel, S.R. (2001) Circulation of groundwater due to wave set-up on a permeable beach. *Oceanologia*, 43, 279-290.

- Massel, S.R., Przyborska, A., Przyborski, M. (2004) Attenuation of wave-induced groundwater pressure in shallow water. Part 1. *Oceanologia*, 46, 383-404.
- Massel, S.R., Przyborska, A., Przyborski, M. (2004) Attenuation of wave-induced groundwater pressure in shallow water. Part 2. Theory, *Oceanologia*, 47, 291-323.
- Massel, S.R. (2010) *Hydrodynamic Processes in Marine Ecosystems*. Gdańsk Univ. Press, Gdańsk, 502pp (in press in Polish)
- Shum, K.T. (1993) The effects of wave-induced pore water circulation on the transport of reactive solutes below a rippled sediment bed. *Jour.Geoph. Res.*, 98, 10,289-10,301.
- Węśławski, J.M., Urban-Malinga, B., Kotwicki, L., Opaliński, K., Szymelfenig, M., Dutkowski, M. (2000) Sandy coastlines – are there conflicts between recreation and natural values? *Oceanol. Studies*, 29, 5-18.

Tsunami waves in coastal zones due to an asteroid impact

Stanisław R. Massel

Institute of Oceanology of the Polish Academy of Sciences, Sopot, Poland (smas@iopan.gda.pl)

1. Introduction

Usually tsunami waves are related to the earthquakes, slope failure or underwater volcano eruptions. However, possible impact of asteroids in the ocean may also produce giant sea waves. The use of methods of marine geology provides many other evidences of oceanic impacts of asteroids. The geographical distribution of the known historical asteroid impacts into the sea, given by Kharif and Pelinovsky (2005), showed eight very large asteroids entries in the region of Australia, South America, Mexico, North America and Europe. In particular, some historical, as well as hypothetical, tsunami events in the North Sea were discussed recently by Bork et al. (2007).

It should be noted that the asteroids are still impacting into the earth atmosphere and ocean surface. During one year about one million asteroids with total weight of about 1000 tons are impacting on the Earth surface. Moreover, observations during 22 months provided by geostationary satellites showed 25 asteroids of radius $0.75\text{m} < r < 1.19\text{m}$ impacted on the Earth (Ward & Asphaug, 2002).

Quite recently information on two asteroid events have been published. In particular, in the article "The rock that fell to Earth" (*Nature*, 2009), the well documented event of the asteroid impact in Sudan was described. Totally of 280 fragments, weighing of 60 kilograms, were found. On January 20, 2009, the Polish and German newspapers, (*Dziennik Bałtycki* – „Meteoryt uderzył w Bałtyk jak grom z jasnego nieba” (in Polish), and *Ostseezeitung* – „Meteorit vermutlich in Ostsee gestürzt” (in German) reported the asteroid which exploded over the Southern Baltic.

In the present paper, the modelling of tsunami propagation from source point in deep water to the coastline is discussed, with special attention given to the waves transformation over shoaling water depth and to the energy dissipation due to wave breaking.

2. Tsunami propagating on constant water depth

The spherical asteroid of radius r_a is falling vertically on water surface with speed V_a . We assume that asteroid excavates a radially symmetric parabolic cavity (Ward and Asphaug, 2000):

$$\zeta_0(r) = \begin{cases} -d_c \left[1 - \left(\frac{r}{r_c} \right)^2 \right] & \text{for } r \leq r_d \\ 0 & \text{for } r > r_d \end{cases}$$

in which d_c is the cavity depth, r_c is the inner radii and r_d is the outer radii of crater. All of the water within cavity is deposited into a bordering lip of the crater and contributes totally to the tsunami.

The solution in the polar coordinate system of the initial value problem for tsunami propagation on the constant water depth takes the form of the Bessel-Fourier integral.

In Figure 1 the example of surface elevation $\zeta(t, r)$ due to impact of asteroid of the radius $r_a = 2.5\text{m}$ at the distance of $r_1 = 1000\text{m}$, from the impact centre, is shown. The water depth was assumed be constant and equal to $h = 100\text{m}$. The first disturbance arrives at the observation point after about 50 sec and the highest positive amplitude reaches the value of about 8.2m, while the highest negative amplitude is of the same order of magnitude.

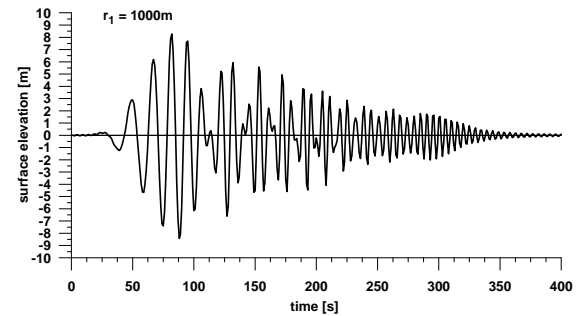


Figure 1. Surface oscillation at distance $r_1 = 1000\text{m}$ from impact

3. Tsunami propagating on slowly varying water depth and wave run-up on coast

Waves generated by the asteroid impact, which may be sometimes very high in the deep ocean, are particularly dangerous for coasts surrounding the ocean basin. This is due to both the changing of water depth and the rising of the tsunami waves amplitude before final breaking. The simplest approach for wave propagation over slowly varying topography is based on the concept of energy balance between two separated wave rays. It is assumed that these rays are straight lines.

Therefore, the energy flux is changed along the wave ray according to the following formula (Massel 1989):

$$\frac{d(EC_g)}{dr} = -(D_f + D_{br})$$

in which $E = \frac{1}{4} \rho g A^2(r, \omega)$, A is the amplitude of wave component and $C_g(r, \omega)$ is the group velocity at distance r , and ω is the wave frequency. At the right hand side of the above equation, the terms D_f and D_{br} describe energy losses due to bottom friction and wave breaking, respectively.

For our purpose we use the wave breaking parameterization based on exact solution for energy dissipation in a bore (Massel (1989, 2007), and for later calculation, it is useful to represent the surface elevation $\zeta(t, r)$ in a simple form using the Hilbert Transform. Therefore the surface elevation $\zeta(t, r)$ becomes:

$$\zeta(t, r) = A(t, r) \cos[\theta(t, r)]$$

in which:

$$A(t, r) = \sqrt{\zeta^2(t, r) + \xi^2(t, r)}$$

and:

$$\theta(t, r) = \text{arctg} \left(\frac{\xi(t, r)}{\zeta(t, r)} \right)$$

where function $\xi(t, r)$ is the Hilbert Transform of the known time series $\zeta(t, r)$, i.e.:

$$\xi(t, r) = H[\zeta(t, r)]$$

It should be noted that the differentiation of the function $\theta(t, r)$ provides the so called instantaneous frequency ω as follows:

$$\omega(t, r) = \frac{d\theta(t, r)}{dt}$$

To illustrate the influence of wave breaking on the wave transformation over the slope, let us consider the wave motion due to the impact of an asteroid of radius $r_a = 2.5\text{m}$. We assume that the slope of the bottom is equal $1/20$. For example, Figure 2 shows the surface elevation at water depth $h_2 = 5\text{m}$ with and without breaking. It should be noted that higher amplitudes are reduced while the smaller ones at the end of wave packet remain unchanged as they are smaller than the limiting ones.

Now the wave surface close to shoreline is treated as the initial one for the determination of wave run-up on the beach. As tsunami waves contain a lot of frequencies, the solution is obtained through the superposition of the elementary solutions of the type given for example by Voltzinger et. al. (1989):

$$\zeta(t, r) \approx \int_{-\infty}^{\infty} A(\omega) J_0 \left[\sqrt{\frac{4\omega^2 |r|}{g\beta}} \right] \exp(i\omega t)$$

in which β is the bottom close shoreline, $A(\omega)$.

In the paper, examples of solution for various bathymetries and various initial wave parameters are given.

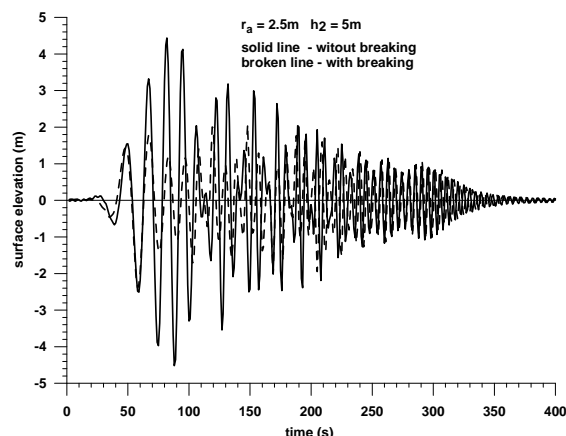


Figure 2. Surface oscillation close to waterline at water depth $h = 5\text{m}$

References

- Bork, I., Dick, S., Kleine, E., Müller-Navarra, S. (2007) Tsunami - a study regarding the North Sea coast. BSH, Nr. 41/2007, Hamburg, 77pp.
- Kharif, Ch., Pelinovsky E.N. (2005) Asteroid impact tsunami. C. R. Physique, 6: 361-366.
- Massel, S.R. (1989) Hydrodynamics of Coastal Zones. Elsevier Science Publ., Amsterdam, 336pp.
- Massel, S.R. (2007) Ocean Wave Breaking and Marine Aerosol Fluxes. Springer, New York, 323pp.
- Massel, S.R. (2010) Hydrodynamic Processes in Marine Ecosystems. Gdańsk Univ. Press, Gdańsk, 502pp (in press in Polish)
- Voltzinger, N.E., Klevanny, K.A., Pelinovsky, E.N. (1989) Long-wave Dynamics of the Coastal Zone. Gidrometeoizdat, Leningrad, 271pp (in Russian).
- Ward, S.N., Asphaug, E. (2002) Impact tsunami - Eltanin. Deep-Sea Res., 49, 1073-1079.
- Ward, S.N., Asphaug, E. (2000) Asteroid impact tsunami: a~probabilistic hazard assessment. Icarus, 145.

Baltic inflows – Extreme oceanographic events

Jan Piechura and Robert Osinski

Institute of Oceanology, Polish Academy of Sciences, Sopot, Poland (piechura@iopan.gda.pl)

Based on high resolution measurements done by the Institute of Oceanology PAS in Sopot, the processes of water inflow pathways and transport in the Southern Baltic Sea are described.

High-resolution numerical modelling is used to investigate these phenomena as well. The last major inflow from 2003 is investigated in detail. The dynamics of salty water in Slupsk Furrow is shown in both measurements and simulations. The processes of overflowing sills e.g. at Slupsk Sill are of pulsation character. The amount of salty water entering particular deep areas is estimated. The results show that inflows are unusual events and cause extreme water property changes.

Temporal variability of extreme precipitation in Estonia 1961-2008

Kalev Päädam and Piia Post

Institute of Physics, University of Tartu, Tartu, Estonia (kalevai@gmail.com)

1. Introduction

One of the biggest problems of climate change is the possible change in the precipitation regime. No single answer has been found so far, but the general agreement is that warmer winters bring more cyclonal weather and precipitation. This has been observed already in Estonia (Jaagus 2006). The yearly amount of precipitation has also increased in the second half of the 20th century. Warm season precipitation is characterized by a large temporal variability which is why detecting long-term changes is impossible.

Research in Estonia so far has tended to focus on precipitation extremes using fixed thresholds, rather than using percentiles of daily precipitation sums (Mätlik and Post 2008, Tammets 2007). This study uses percentiles to analyse if extreme precipitation has increased, if trends are statistically significant and if there are different trends for summer and winter.

2. Data and methods

This study is based on the dataset of daily precipitation from the Estonian Meteorological and Hydrological Institute (EMHI). The dataset covers 40 stations and the period from 1961 to 2008 and was chosen because of its homogeneity.

To quantify extreme precipitation in stations, we use values of 0.95 and 0.99 percentiles of daily precipitation distributions. Percentiles were found separately for cold and warm seasons. The cold season is defined as November to April and the warm season as May to October. After finding percentiles of daily precipitation for every station, the number of days with the value above or equal to the percentile was counted. These days were called extreme precipitation events. The time series of annual values of extreme precipitation events were investigated for stations, for different regions in Estonia and also for the whole country. We found linear trends in the time series to estimate the tendency of changes. An estimation of statistical significance of the trends was performed by using the Mann-Kendall test.

3. Preliminary results

The 0.99 percentiles of daily precipitation distributions for Estonian stations vary between 18.9 – 25.3 mm in the warm season and 9.9 - 15.8 mm in the cold season, the 0.95 ones are 9.3 – 13.1 mm and 5.2 – 8.8 mm, respectively.

There are tendencies in both directions in extreme precipitation temporal changes, if time series of stations are looked at separately, while grouping the stations in regions and summing up the events over the whole country gives more stable trends. Looking at averages over all stations' data there is a 2.2% increase of extreme precipitation events (events over 0.99 percentile) for summer on significance levels of 99%. For winter, the increase is 4.3% on a significance level of 95%. The total number of extreme precipitation events has increased too as can be seen from Figure 1.

Regionalization shows that during the warm season the increase of extreme precipitation originates from inland stations, but for the cold season, differences are small between regions.

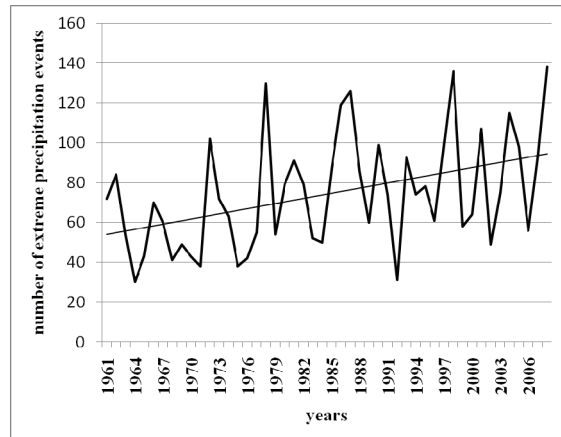


Figure 1. The number of extreme precipitation events (over 0.99 percentile) in Estonia during the warm season has significantly increased ($\alpha = 0.01$).

4. Conclusions

Results show that extreme precipitation events are becoming more common. This study aimed to investigate whether global warming has affected the overall amount of extreme precipitation in Estonia. Although the results show a clear upward trend, the 48-year period is too short to decide whether the changes are of anthropogenic origin or the result of normal climate variability.

References

- Jaagus, J. (2006). Climatic changes in Estonia during the second half of the 20th century in relationship with changes in large-scale atmospheric circulation. *Theoretical and Applied Climatology*, Vol 83, No 1, pp. 77-88
- Mätlik, O and Post, P. (2008). Synoptic weather types that have caused heavy precipitation in Estonia in the period 1961-2005. *Estonian Journal of Engineering*, Vol 14, No 3, pp. 195 - 208
- Tammets, T. (2007). Distribution of extreme wet and dry days in Estonia in last 50 years. *Proceedings of Estonian Academy of Science. Engineering*, Vol 13, No 3, pp. 252-257

Recent dynamics and prediction of heavy precipitation events in Lithuania

Egidijus Rimkus, Justas Kažys, Arūnas Bukantis

Department of Hydrology and Climatology, Vilnius University, Lithuania (egidijus.rimkus@gf.vu.lt)

1. Introduction

Under changing climate conditions, special attention must be paid to extreme weather changes. Alterations of average temperature or the amount of precipitation usually are not so important compared to a possible increase of number and intensity of extreme events. Regional differences are also more noticeable as weather extremes can be significantly strengthened by local factors.

An analysis of heavy precipitation events in Lithuania is presented in this work. Research was divided into two parts: 1. a spatial distribution and dynamics of heavy precipitation events in Lithuania during the observation period (1961-2008), and 2. climate predictions for the 21st century, according to outputs of CCLM.

2. Data and methods

Daily data from 17 meteorological stations were used for the analysis of heavy precipitation events in Lithuania, covering the period from 1961 to 2008. Annual and seasonal heavy precipitation values and the recurrence of extreme daily and 3-day precipitation events were analyzed. The spatial distribution of heavy precipitation events in Lithuania was determined; the trends of such precipitation events were identified. A Mann-Kendal test was used for statistical significance evaluation of observed trends. Also, daily and 3-day annual maxima probabilities were calculated, using the Generalized Extreme Value (GEV) distribution. 10, 30 and 100 years return periods were analyzed. Some results show that the GEV distribution fits the extreme precipitation data well (Wang and Zhang 2008; Hanel and Buishand 2009). Finally, atmospheric circulation processes during heavy precipitation events were described, using the adapted Hess and Brezowski macrocirculation form classification (Hess and Brezowsky 1952). Three main circulation forms were distinguished: zonal, meridional and mixed. Predictions of changes of the number of heavy precipitation events in Lithuania are also presented in this study. Output data of the regional climate model CCLM (COSMO – Climate Limited-area Model) for the period 1971–2100 were used. Predictions were based on A1B and B1 emission scenarios.

3. Variability of heavy precipitation events during observation period

Despite of the relatively small area and quite negligible differences in altitude, there are significant differences in spatial distribution of heavy precipitation events in Lithuania. The mean annual number of cases when the daily precipitation amount exceeds 10 mm, fluctuates from 12.4 to 21.9 and from 5.3 to 10.5, while 3-day precipitation exceeded 20 mm (Figure 1). Most precipitation events during observation period were observed in the Zemaiciai highlands and the coastal lowlands.

The probability of maximum precipitation for a 10 year return period appears to be related to the spatial distribution: the highest values can be expected in the western part (55–60 mm daily and 75–85 mm in 3-days),

and the smallest in the central Lithuanian plain (45–50 mm and 60–70 mm, respectively).

The seasonal distribution of heavy precipitation events differs between Lithuanian regions. In the western part, most heavy precipitation events were observed during late summer and autumn, due to the impact of the warm Baltic Sea, whereas in other parts of Lithuania, such events were more common only for the summer months.

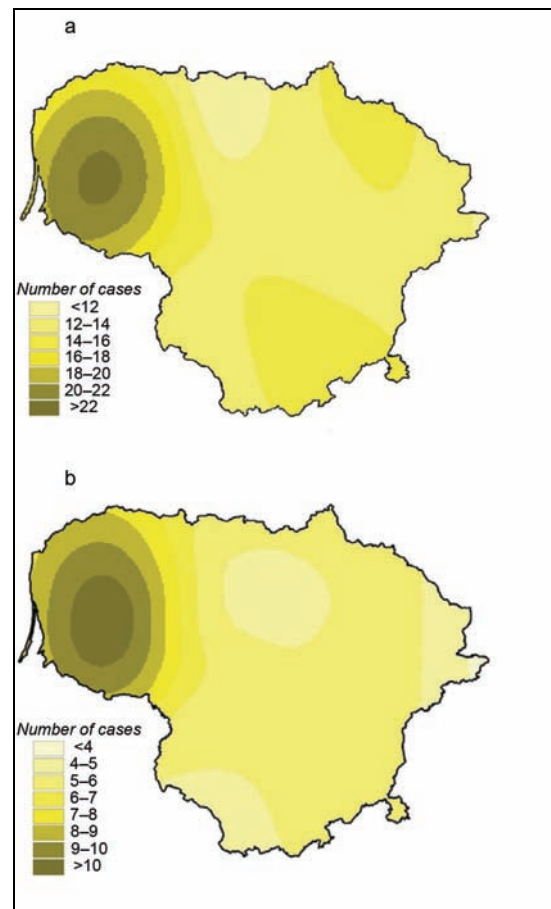


Figure 1. Mean number of cases when daily precipitation amount exceeds 10 mm (a) and 3-days precipitation amount exceeds 20 mm (b) in Lithuania in 1961–2008.

The number of heavy precipitation events, its percentage in total precipitation sums and annual daily and 3-days maxima noticeably increased during the 1961–2008 period. The highest statistically significant positive trends were noted for heavy precipitation cases (daily >10mm) and changes in annual maxima (3-days period). Also, positive trends of mean annual maxima of heavy precipitation were calculated for all meteorological stations by splitting the 1961-2008 year period in two parts. The period from the mid 80's to the end of the 90's was very rich in heavy precipitation events.

More than one third of heavy precipitation events were observed during the zonal atmospheric circulation mode. The presence of the central part of a cyclone over

Lithuania is the most common synoptic situation during heavy precipitation events. Under such conditions, the record high of daily precipitation was observed in Telšiai (103,8 mm).

4. Predicted changes of heavy precipitation events in 21st century

According to CCLM outputs, the annual precipitation over Lithuania in the 21st century will increase up to 22% (Figure 2). Winter precipitation will increase more rapidly due to advection of more frequent warm and moist air masses. Almost no changes are expected in summer. Largest changes will be in the Žemaičiai highlands and the coastal lowlands.

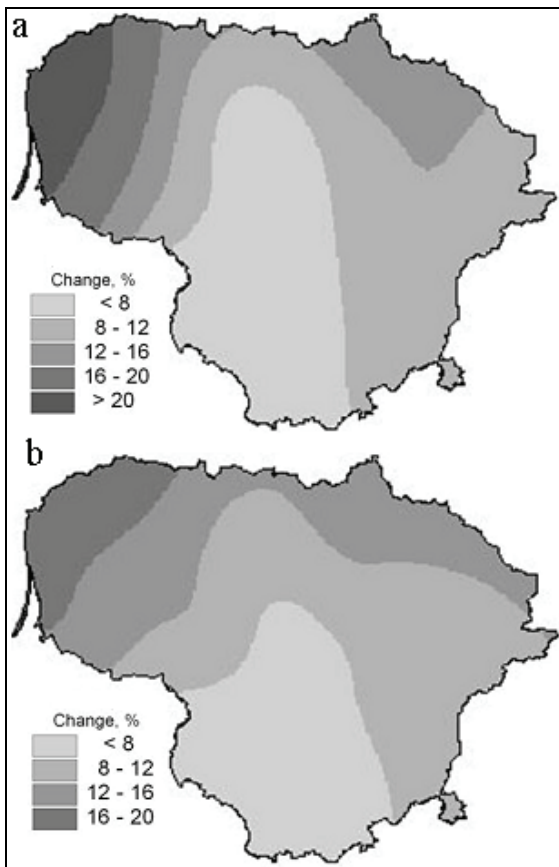


Figure 2. Annual precipitation changes between the period 1971-2000, and the projected period 2071-2100, according the CCLM model output, based on the A1B (a) and B1 (b) emission scenarios.

The number of days with precipitation will rise (up to 5% until the end of 21st century). Significant changes will be observed especially in spring (up to 10%). Heavy precipitation will also increase in Lithuania. The number of one day heavy precipitation cases will mostly change in the Žemaičiai highlands and the coastal lowlands (>30%). Larger changes in almost the entire territory are predicted under the A1B emission scenario, and only in the northern part, changes will be greater according to the B1 emission scenario. In the western part, changes will be most significant in autumn, and in east Lithuania in winter.

During the first thirty year period of the 21st century, the number of 3-days heavy precipitation events will also

increase significantly. Both scenarios predict large positive changes in the most eastern as well as western parts of Lithuania. In autumn, the increase will be most significant, while in summer, it will probably stay the same during the observation period.

The daily and 3-days precipitation amount probability for 10-year and a 100-year return period will increase in the western part of Lithuania according to the A1B scenario. On the other hand, the model based on the B1 scenario predicts a decrease of probability of precipitation amount in this area for both analyzed return periods. Other parts of Lithuania will experience similar, but less significant changes compared to the observation period of 1971-2000.

Acknowledgements

This work was performed within the BSR Interreg IVB Project „Climate Change: Impacts, Costs and Adaptation in the Baltic Sea Region (BaltCICA)“

References

- Hanel, M., Buishand, T. A. (2009). A non-stationary index-flood model for precipitation extremes in transient RCM runs, Geophysical Research Abstracts, 11, EGU2009-4346
- Wang, J., Zhang, X. (2008). Downscaling and projection of winter extreme daily precipitation over North America, *Journal of Climate*, 21, 5, pp. 923–937
- Hess, P., Brezowsky, H. (1952). Katalog der Grosswetterlagen Europas, Bibliothek des Deutschen Wetterdienstes in der US-Zone, 33

Submarine groundwater discharge to the Gulf of Gdańsk.

B.Szymczycha, L.Kotwicki and J.Pempkowiak

Institute of Oceanology, Polish Academy of Sciences, Sopot, Poland (beat.sz@iopan.gda.pl)

1. Introduction

Submarine groundwater discharge (SGD) is one of the water pathways connecting land and ocean in the global water cycle. Moreover it has been recently recognized as important process influencing the coastal zone. In comparison with well known and typically large point sources of surface water inputs (e.g., rivers and streams), which are gauged and well analysed, estimations of groundwater inputs are much more difficult due to a lack of simple methods to gauge these fluxes. Groundwater in many areas has become contaminated and therefore is a source of nutrients, trace metals, organic compounds and radionuclides. Hence it is important for the marine geochemical cycles of elements and may cause an environmental deterioration of coastal zones. SGD to the coastal area usually occurs as a slow diffuse flow but can be found as large point sources in certain areas. Groundwater flows are typically temporally and spatially variable, complicating efforts to characterize site-specific flow regimes.

2. Submarine groundwater discharge to the Gulf of Gdańsk.

Recently, the SGD in the Gulf of Gdańsk was investigated. Water samples were collected by bathometers, seepage meter and piezometers during several sampling campaigns, and then analysed. Nutrients (Table 1), dissolved inorganic carbon (DIC), dissolved organic carbon (DOC) (Figure 1) and trace metals were measured in collected samples. The concentrations of some chemical compounds correlate well with salinity and pH. These results will be discussed in terms of biogeochemical element transformations and consequences for the element fluxes into the water column. Further SGD studies are essential for a better understanding of coastal areas of the Gulf of Gdańsk and processes taking place there, including toxic substances discharge.

Table 1. Characteristics of concentrations of some chemical compounds in water samples from the Hel Peninsula.

Chemical compounds	The lowest and highest concentrations
NH_4^+	1,12-19[umol/l]
NO_3^-	0,12-0,8[umol/l]
NO_2^-	0,09-0,5 [umol/l]
SiO_2	7,6-43[umol/l]
PO_4^{3-}	0,01-18,8[umol/l]

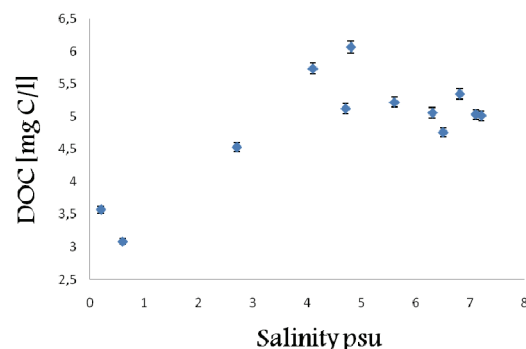


Figure 1. Relationships between salinity and DOC in water samples collected at the groundwater impacted and non-impacted sites in the Hel Peninsula.

References

- Barwell, V.K., Lee, D.R., (1981) Determination of horizontal-to-vertical hydraulic conductivity ratios from seepage measurements on lake beds, *Water Resour Re*, 17, pp. 565–70.
- Burnett, W.C., et al., (2006) Quantifying submarine groundwater discharge in the coastal zone via multiple methods, *Sci. Total Environ*. 367, pp. 498–543.
- Mulligan, A.E., Charettem, M.A., (2009). Groundwater Flow to the Coastal Ocean, *Encyclopedia Ocean Sciences*, pp. 3842-3851.
- Krest, J.M., Moor, W.S., Rama, J., (1999) 226Ra and 228Ra in the mixing zone of the Mississippi and Atchafalaya Rivers: indicators of groundwater input., *Mar. Chem*. 64, pp. 129–152.
- Krest, J.M., Moore, W.S., Gardner, L.R., (2000) Marsh nutrient export supplied by groundwater discharge: evidence from radium measurements, *Glob Biogeochem Cycles*, 14, pp. 167–76.
- Szymczycha, B., Kotwicki, L., Pempkowiak, J., (2010) Submarine Groundwater Discharge (SGD) to the Baktic Sea, Annual Set The Environment Protection, submitted.
- Vogler, S., Szymczycha, B., Gentz, T., Dellwig O., Kotwicki, L., Schlüter M., Böttcher, M.E., (2010) The impact of submarine groundwater discharge (SGD) on a coastal ecosystem of the southern Baltic Sea: Results from the AMBER project, Conference Abstract: BONUS ANNUAL CONFERENCE 2010

Utilizing lagrangian trajectories for reducing environmental risks

Bert Viikmäe¹, Tarmo Soomere,¹ Nicole Delpeche,¹ H.E. Markus Meier^{2,3} and Kristofer Döös³

¹ Institute of Cybernetics at Tallinn University of Technology, Tallinn, Estonia (bert@ioc.ee)

² Swedish Meteorological and Hydrological Institute, Norrköping, Sweden

³ Department of Meteorology, University of Stockholm, Sweden

1. Background

The Gulf of Finland is an elongated sub-basin of the Baltic Sea with a length of about 400 km, width between 48 and 125 km and a mean depth of 37 m. One of the largest threats to this region (which is designated as a Particularly Sensitive Sea Area by the International Maritime Organization in July 2005) is oil transportation that has seen an increasing trend over the last 15 years in the Gulf of Finland and is forecasted to exceed 200 million tons by year 2010.

The drift of oil spills, lost containers, etc. is influenced by wind stress, waves, and currents. The properties of transport by wind and waves are quite well known, but the field of currents is created under the influence of several local and remote forcing factors, which makes a prediction quite challenging. It is even more complicated in strongly stratified sea areas such as the Gulf of Finland where the drift frequently is steered by multi-layered dynamics.

The surface currents in the Gulf of Finland are highly variable both seasonally and annually. Recent analyses have demonstrated the existence of semi-persistent patterns of currents in the Gulf and in some other parts of the Baltic Sea (Andrejev et al. 2004a, Soomere et al. 2010b, and references therein). These patterns are superimposed by rapid pathways of the current-driven transport (Soomere et al. 2010a).

This combination of complexity of circulation and persistence of certain transport patterns serves as a precondition for a technology that uses the marine dynamics for reducing the risk of coastal pollution. The key idea is a systematic increase of time during which an adverse impact (for example, an oil spill) reaches a vulnerable area after an accident has happened (Soomere and Quak 2007). In other words, the goal is to minimize the risk of coastal pollution in terms of maximizing the time it takes to hit the coast by smart placing of human activities. The coastal areas usually have the largest ecological value, thus in this study we consider the nearshore as the most valuable area, which should be protected from pollution.

While the probability of coastal pollution for ocean coasts can be reduced by optimizing ship routes, the problem for narrow bays, like the Gulf of Finland, is how to minimize the probability of hitting either of the opposite coasts. The first order solution to this problem is the equiprobability line, the probability of propagation of pollution from which to either of the coasts is equal. For wider sea areas, there may be an area, propagation of pollution from which to either of the coasts is unlikely – area of reduced risk. The safe fairway would either follow the equiprobability line or cross an area of reduced risk. The idea, therefore, is to produce an operational drift model to forecast drift after an accident has already occurred, but rather to identify areas, which are statistically safer to travel to.

2. Method

The problem is addressed by statistical analysis of the results of the Lagrangian trajectory model TRACMASS (Döös 1995, de Vries and Döös, 2001) that uses pre-computed Eulerian velocities calculated by the Rossby Centre Global Circulation model (Regional Ocean Model, RCO, Meier

2001). The RCO model has a horizontal resolution of 2×2 nautical miles and uses 41 vertical levels in z -coordinates. The thickness of the uppermost layer is 3 m. The model is forced by wind data on the 10 m level, air temperature and specific humidity on the 2 m level, precipitation, cloudiness and sea level pressure fields, and accounts for river inflow and water exchange through the Danish Straits. This data set is calculated from the ERA-40 re-analysis using a regional atmosphere model with a horizontal resolution of 25 km. As the atmospheric model tends to underestimate extreme wind speeds, the wind is adjusted using simulated gustiness.

The trajectories are calculated based on a linear interpolation of the velocity field in each point of grid cells. The position of the trajectories is updated every six hours. The user of the model specifies the source point(s) where the pollution may have started. Trajectories of particles are then simulated (usually for a few weeks in the Gulf of Finland conditions) and results saved for further analysis. The simulations for the same initial positions of particles are restarted from another time instant. The process is repeated over a chosen time period. For this particular study, the particles are restricted to stay in the uppermost layer. Although the resulting dynamics of trajectories is not exactly Lagrangian, doing so apparently is adequate for modelling of transport of lost containers and oil spills by the dynamics of the upper layer.

The entire water mass is expected to be renewed in 3–5 years in the Gulf of Finland. In the years 1987–1992 no major inflows of saline water occurred and also no exceptional changes of stratification (Andrejev et al. 2004b). Thus, the period of 1987–1991 was used in our simulations.

Two methods are used for numerical estimation of the equiprobability line and areas of reduced risk (Soomere et al. 2010b). The direct method is based on point-wise analysis of the trajectories for each of $N = 3131$ grid cells in the gulf with the time lag of 10 days. Four particles ($N_i = 4, 1 \leq i \leq N$) are placed in each grid cell. If three or all four particles reach nearshore, the cell is assumed the value of $c = \pm 1$ depending on whether the southern or northern coast was hit. If no more than two tracers reached a coast within the time period, the cell is assumed the value $c = 0$. Another method, involving a certain local smoothing, consists of dividing the gulf into clusters of 3×3 cells and placing one particle in each cell. By tracing nine trajectories in each cluster (one from each cell) it is established whether or not the majority of the trajectories end up at one of the coasts. The basic idea is the same as above; only the values of $N_i = 9, 1 \leq i \leq N$ and the initial positions of the tracer with respect to the centres of the grid cells are different.

3. Results

A number of simulations were performed to estimate the typical time during which the particles reached the shore. The number of particles entering nearshore showed high

variability: their count varied from 0 up to about 60 percent. The smallest number of hits to the coast occurred during the calm season (April – July) and the highest during the windy season. In average, about 30% of particles released near the axis of the gulf hit the coast within the first 10 days.

The typical time for a hit in calm and windy seasons also varied. In May 1987, a few hits to the coast took place already during the first day, while in July the first hit occurred on the seventh day. In May no more than 19 percent of particles were simultaneously nearshore and almost no hits starting from the eighth day, but in July this percentage was 44. Simulation results showed that the typical time of the first hit to the coast was three days in 1987. The typical time of highest amount on particles simultaneously residing in the nearshore was 11 days.

Hitting the northern and the southern coastal areas showed also extreme variability. In the simulation started on 01.10.1987, almost all hits were to the northern coast and in a simulation started on 12.12.1987 the majority of particles reached the southern coast. In both cases 58% of particles reached the shore during 20 days.

The maps of the resulting probabilities (Figure 1) reveal the presence of two different regions in the Gulf. In the western part there is a well-defined probability gradient across the gulf whereas in the east there is a large area of low risk (probability values of relevant grid cells are less than 0.1) with respect to coastal pollution. Propagation of pollution from this area (that can be interpreted as an area of reduced risk) to coastal areas can be considered unlikely.

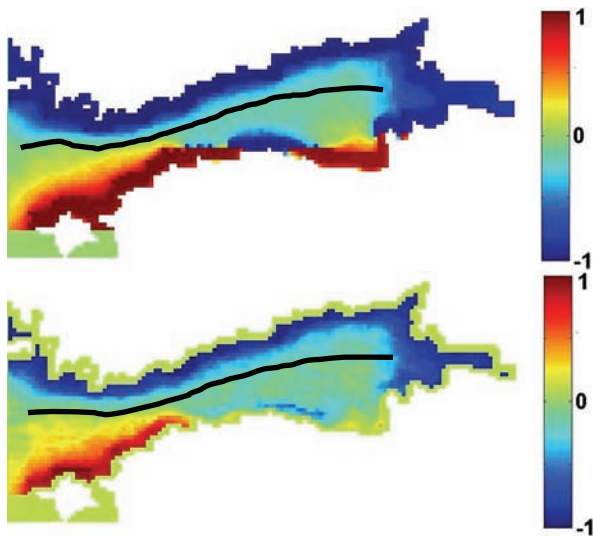


Figure 1. Probabilities of hitting the shore for the years 1987–1991 with the direct (upper panel) and the smoothing method (lower panel). The red and blue colours indicate high probabilities of hitting the southern and northern coasts, respectively (Soomere et al. 2010).

Both methods show substantial seasonal and also certain inter-annual variability, which is the largest in the entrance of the Gulf in the area affected by the dynamics of the Baltic Sea. The probability maps from both methods are qualitatively similar. The distance between estimates of the line differ is maximally 6–7 km. The difference serves as an implicit measure of uncertainty related with this sort of solution.

We also demonstrate the maps of impact times for adverse impacts stemming from different sea areas. These maps basically show the time it takes for a tracer to hit the coast. The impact times showed large seasonal variability.

4. Conclusions

The main aim of this research was to find a first-order solution to an inverse problem: not to avoid something from happening, but to find areas where an accident would least likely affect the coastal areas. The results revealed that a well-defined equiprobability line exists in some parts of the Gulf of Finland. Typically, it is substantially shifted from the axis of the Gulf.

The relatively small difference in the location of the lines obtained by two methods indicates a reasonable level of uncertainty connected with this type of solution. The risk of hitting the southern coast is considerably larger in the western part of the gulf whereas in the eastern part there is an area of low risk with respect to coastal pollution. The simulation results showed substantial seasonal variability (especially in the western part of the Gulf) and also some inter-annual variability.

In conclusion, using a trajectory model accompanied by pre-computed velocity fields and performing several statistical analyses, serves as a reasonable method to find areas of high and low risk of coastal pollution, thus minimizing the consequences of an accident.

Acknowledgements

This study was performed in the framework of the BONUS+ project BalticWay (financed by the BONUS EEIG), which attempts to identify the regions in the Baltic Sea that are associated with increased risk compared to other sea areas and to propose ways to reduce the risk of them being polluted by placing activities in other areas that may be less affected.

References

- Andrejev, O., Myrberg, K., Alenius, P., and Lundberg, P. A. 2004a. Mean circulation and water exchange in the Gulf of Finland - a study based on three-dimensional modelling. *Boreal Env. Res.* 9(1), 1–16.
- Andrejev, O., Myrberg, K., and Lundberg P. A. 2004b. Age and renewal time of water masses in a semi-enclosed basin – Application to the Gulf of Finland. *Tellus* 56A, 548–558.
- Döös, K. 1995. Inter-ocean exchange of water masses. *J. Geophys. Res.* 100(C7), 13499–13514.
- Meier, H.E.M. 2001. On the parameterization of mixing in three-dimensional Baltic Sea models, *J. Geophys. Res.* 106, 30,997–31,016.
- Soomere, T. and Quak, E. 2007. On the potential of reducing coastal pollution by a proper choice of the fairway. *J. Coast. Res., Special Issue* 50, 678–682.
- Soomere, T., Delpeche, N., Viikmäe, B., Quak, E., Meier, H. E. M., and Döös, K. 2010a. Patterns of current-induced transport in the surface layer of the Gulf of Finland. *Boreal Env. Res.*, submitted.
- Soomere, T., Viikmäe, B., Delpeche, N., and Myrberg K. 2010b. Towards identification of areas of reduced risk in the Gulf of Finland. *Proc. Estonian Acad. Sci.* 59(2), in press.
- Vries P. de and Döös K. 2001. Calculating Lagrangian trajectories using time-dependent velocity fields. *Journal of Atmospheric and Oceanic Technology* 18(6), 1092–1101.

Changes of mean and peak river runoff in Belarus during the 20th century

Alexander Volchek¹, Jrii Stefanenko¹, Sergey Parfomuk¹, Vladimir Luksha¹, Anastasiya Volchek¹, Oksana Natarova² and Tatiana Shelest³

¹ Brest State Technical University, Brest, Republic of Belarus (volchak@tut.by)

² Institute for Nature Use, Minsk, Republic of Belarus

³ Brest State University, Brest, Republic of Belarus

1. Changes of mean river runoff

The purpose of this research is the estimation of changes of mean and extreme river runoff in Belarus during the 20th century for the Neman River, the West Dvina River and the Bug River. Long-term monthly mean and peak observations of runoff are used as input. The data were received from the Republican Meteorological Center of the Ministry of Natural Resources and Environmental Protection of the Republic of Belarus.

A comparative analysis of hydrographs of the Neman River runoff was executed using the following indices: percent of variation in the runoff for separate periods and seasons; date of passing of the peak of the spring high water; amount of high waters in one year.

On average for the period 1961 to 2005, runoff of the Neman River in spring accounts for 41% of the annual runoff. During the summer-autumn season, 37 % of the total annual runoff is observed and 22% is observed during the winter season. The November runoff is higher than in October, except for years with exceptionally high runoff. The greatest water flow in the winter season occurs in January.

Comparative analysis of the water regime of the Neman River for the period of observations during 1961 to 2005 has shown that there were systematic changes. These include a significant decrease of the peak flow during the spring freshet and a moderate increase of the flow in summer-autumn and especially in winter seasons. These changes are connected to appropriate climatic variations observed in the same period. Frequent prolonged winter thaws have increased the infiltration of snowmelt water into the soil, and consequently lead to increase of minimum (winter) flow, reduction of the stream flow during the spring high water period, and the earlier passage of the peak flow.

An increase of minimum stream flow in the summer-autumn period was caused (in addition to, climatic factors) by human impact in the form of wide-scale melioration projects. Though the scale of these projects in the Neman River Basin are much less than to those implemented in Polesye, nevertheless, they cannot be ignored. In the last years, the number of freshet periods for very high -flow years has increased up to 4, for the high-flow years this number increased from 2 to 3 per year to 3 to 4 per year, and did not change for other years. Similar runoff variations were observed on other rivers of the Baltic Sea Basin in the Republic of Belarus. So the runoff variations in the West Dvina River Basin are characterized by increase in winter and decrease in the summer-autumn season. Observations of the runoff variations in the Vilia region show a runoff decrease in the spring and summer-autumn seasons and an increase in the winter time. However in the small watersheds where large anthropogenic impact has occurred (offloading, pumping and/or the discharging the ground waters etc.), natural runoff was significantly disturbed and its tendencies deviate from observed over the large river basins.

For correct runoff quantification it is necessary to partition it into anthropogenic and natural components using expression:

$$M_{est.} = M_{izm.} \pm \Delta M_{aper.} \pm \Delta M_{k.lim.} \pm \Delta M_{antr.}, \quad (1)$$

where $M_{est.}$ – total runoff, which would be observed without global climate and local anthropogenic disturbances; $M_{izm.}$ – the measured amount of the runoff at given period; $\Delta M_{aper.}$ – the “natural” runoff fluctuations of the runoff caused by climate variations; $\Delta M_{k.lim.}$ – the runoff changes caused by global warming; $\Delta M_{antr.}$ – the runoff changes caused by local anthropogenic impact.

The size of $\Delta M_{aper.}$ is usually estimated as an anomaly from the average runoff amount during for the study period (i.e., as an anomaly from its long-term normal value). The size of $\Delta M_{k.lim.}$ can be estimated using regression analysis (if the element $\Delta M_{antr.}$ is absent), or with the help of regional «precipitations – temperature – runoff» models.

Usually, the natural runoff fluctuations ($\Delta M_{aper.}$) are spatially asynchronous, while the runoff changes caused by global climate change ($\Delta M_{k.lim.}$) have a more coherent systematic character for the large areas. This allows us to separate the contribution of these two factors to the river runoff.

The element $\Delta M_{antr.}$ shows cumulative influence on the runoff by human activity. Its estimation may be associated with big errors due to the absence of mass measurements.

The need to use of formula (1) emerged from analyses of initial hydrometeorological data observed by various methods. When we discovered statistically significant deviations in the runoff time series that lead to a significant influence of the last term of (1), our procedure was amended to include additional statistical methods. Specifically:

- to reveal changes in the flow tendencies, we used integrated difference curves;
 - systematic changes in hydrological time series were estimated using linear and quadratic trend analyses;
 - to test our hypotheses about differences in statistical parameters, Student and Fisher criteria were used.
- After all hypotheses about influence on the runoff of warming climate were tested, the impact of large-scale land use was assessed.

The analysis of hydrographs in West Dvina River Basin provided estimates of the time series homogeneity and revealed the rivers where anthropogenic influence were substantial and are visually appreciable (e.g., due to the change of the basin area, redistribution of the runoff, etc.). Thereafter, statistical analyses provided estimates of the impact of hydraulic engineering, land use, and climatic warming. The analysis of the intra-seasonal changes in the West Dvina River runoff showed an increase in annual

river runoff in the river basin during the 1981 - 2005 period compared to the 1960-1980 period by 23.6% (at the Polotsk hydrological station) to 27.2 % (at the Vitebsk hydrological station).

The minimal runoff increased in the summer-autumn on average by 23 % and in winter by 52%. We should repeat that the winter runoff increase can be associated with prolonged winter thaw periods in the last years and an intensive snowmelt that recharged subsurface water reservoirs. This development also caused a depletion of the water available for the maximal runoff in the spring high water season by approximately 11.5 %.

2. Changes of peak river runoff

The longest period of instrumental observations for peak runoff is available on the Neman River at station Grodno (since 1878). For other rivers the period of supervision is much shorter. Expansion of the hydrological network had begun in the 1920–1930's, and then continued, especially in the second half of the 20th century.

The greatest peak flows on the Neman River were reported in 1885, 1903, 1920–1930, 1950, 1962 and 1985. The rivers in the Bug River Basin have a shorter period of river gauge observations. Therefore, we can report here only peak flow during the last 50 years. In this period, the greatest peak flows were reported in the second half of 1970's years (1974, 1975, 1979 and 1980).

Thus, on the rivers of the Neman River and the Bug River Basins (within the Belarus territory), the greatest peak flows were reported during the 1970's of the century. Since the middle of 1980's, the size of the maximum peak flow in the rivers of these basins has significantly decreased.

To reveal the changes in maximum peak flow, quantitative estimates were made. To avoid errors related to recurrence and spatially inhomogeneous nature of formation of the peak flow, we assessed for all rivers the same period (1966 – 2005). This period was divided into 2 intervals: 1966–1985 and 1986–2005. For each of the 20-year-long periods, we defined average values of the maximum peak runoff. If the observation period at a particular river was less than 15 years at least in one of these intervals, the river was not included in our assessment. This procedure left us with 25 runoff time series for which we estimated the change in the maximum peak flow. The estimates are presented in the form of factors of the runoff:

$$k_i = (Q_{av2} - Q_{av1})/Q_0, \quad (2)$$

where Q_{av1} and Q_{av2} are the mean values of the maximum peak flow during 1966–1985 and 1986–2005 respectively and Q_0 is an average value of the maximum peak runoff for the entire 1966–2005 period. Factors k_i were mapped using the coordinates of the river basin centers (Figure 1). This figure shows a spatial structure of change of maximum peak flow at the rivers in the Neman River and the Bug River Basins in the 1986–2005 period compared to the 1966–1985 period. Positive factors (that are absent in this figure) would indicate an increase in the mean sizes of the maximum peak runoff during the last 20 years, while the negative k_i -values show its reduction.

Figure 1 shows a significant reduction of maximum peak runoff in 1986–2005 in comparison with the 1966–1985 period over the rivers of the western part of Belarus. The values of changes vary. The largest reduction of the maximum peak runoff is reported for the Bug River Basin where the decreases average 60–70 % or more. A smaller peak flow reduction is found at the rivers of the Neman River Basin (30–40 %).

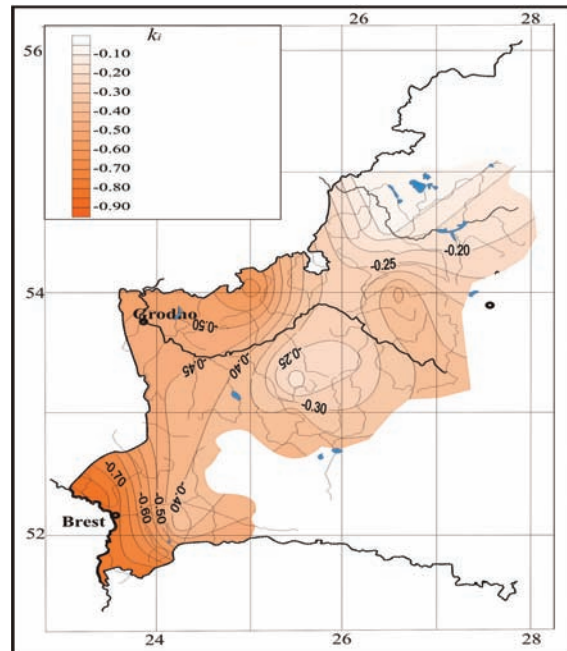


Figure 1. The spatial structure of change of the maximum peak runoff during 1986–2005 as compared to the previous 20 years.

The average long-term value of the maximum peak flow over the entire Belorussian territory is equal to 30–35 $l/(s \cdot km^2)$. The size of the maximum peak runoff in the Neman River Basin is equal to 25–30 $l/(s \cdot km^2)$, and its smallest changes were documented at the left-bank tributaries. The average long-term values of the maximum peak flow in the Bug River Basin are close to country averages [25–35 $l/(s \cdot km^2)$].

3. Conclusion

Analyses of the river gauge data during the period of instrumental observations, revealed different runoff changes across the Republic of Belarus as well as within different hydrological seasons. The latest changes in the Belorussian rivers' runoff to the Baltic Sea show a decrease in the peak of spring high water, an increase of minimum summer-autumn and winter water discharges, and also some increase in the autumn and winter mean flow. There was a large change in the maximum peak runoff at the rivers of the western part of Belarus during the last decades of the 20th century. The causes of changes have mostly a climatic origin but in some watersheds the role of regional human impact was found to be also quite considerable.

References

- Dzisko. Blakitnaya kniga Belarusi: Encycl. / Belarus. Minsk, 1994. 415 p.
- Hydrological resources of the USSR. Vol. 5: Byelorussia and upper Dnepr. 1966. pp. 92 – 141.

Droughts in Poland: Recent variability and future predictions

Joanna Wibig

Department of Meteorology and Climatology, University of Lodz, Lodz, Poland (zameteo@uni.lodz.pl)

1. Introduction

Drought is a slowly building up natural hazard. It stems from a lack of precipitation but is triggered also by higher than normal temperatures. Since the 1950s, precipitation in Poland reveals a slightly increasing tendency in annual totals and a decreasing trend in the ratio of summer to winter precipitation amounts (Kozuchowski 2004). The number of days with precipitation is increasing (Wibig 2008). Any changes in heavy precipitation events are not observed (Wibig 2008), but the analysis of dryness using Ped's index showed an increasing tendency in Lodz in Poland for the period 1904-2000 (Podstawczyńska 2008). The current paper concentrates on droughts in Poland in the period 1951-2006 and projections for 2021-2050.

2. Data and methods

The term "drought" expresses a deficiency of fresh water resources from the climatological mean. The disastrous effect of drought is a consequence of a deficit in precipitation but also of soil moisture at the onset of dry period. Moreover, any realistic definition of drought should be site specific. In this paper three drought indices were used: effective drought index (EDI), standardized precipitation index (SPI) and Ped's Index (P).

The EDI is computed from daily precipitation totals. The first step is the calculation of effective precipitation EP , which is the weighted sum of daily precipitation totals on i days before the day of interest:

$$EP_i = \sum_{n=1}^i \left[\left(\sum_{m=1}^n P_m \right) / n \right],$$

where P_m is the precipitation m days before. Then EDI is calculated as:

$$EDI = \min(0, EP_i - \overline{EP}_i) / STEP_i,$$

where \overline{EP}_i and $STEP_i$ are mean and standard deviation of EP_i respectively (Byun and Wilhite, 1999).

The SPI is calculated by fitting the gamma distribution $G(x)$ for all $x > 0$, where x is daily precipitation total. Since this distribution is undefined for $=0$, the cumulative probability $H(x)$ is used:

$$H(x) = q + (1 - q)G(x)$$

where q is a probability of daily precipitation equal 0. This distribution is then transformed into the standard normal distribution using after Lloyd-Hughes and Saunders (2002) the approximate conversion provided by Abramowitz and Stegun (1965):

$$SPI = - \left(t - \frac{c_0 + c_1 t + c_2 t^2}{1 + d_1 t + d_2 t^2 + d_3 t^3} \right)$$

for $0 < H(x) \leq 0.5$

$$SPI = + \left(t - \frac{c_0 + c_1 t + c_2 t^2}{1 + d_1 t + d_2 t^2 + d_3 t^3} \right)$$

for $0.5 < H(x) < 1$, where

$$t = \sqrt{\ln \left[\frac{1}{(H(x))^2} \right]} \quad \text{for } 0 < H(x) \leq 0.5$$

$$t = \sqrt{\ln \left[\frac{1}{(1 - H(x))^2} \right]} \quad \text{for } 0.5 < H(x) < 1$$

and

$$c_0=2.515517, c_1=0.802853, c_2=0.010328, \\ d_1=1.432788, d_2=0.189269, d_3=0.001308.$$

The Ped's index P is defined by:

$$P_i = \frac{T_i - \bar{T}}{\sigma_T} - \frac{R_i - \bar{R}}{\sigma_R},$$

where \bar{T} and \bar{R} are long term mean and σ_T and σ_R are standard deviations of temperature and precipitation respectively (Ped, 1975).

The Mann Kendall (MK) test was used for trend detection (Mann, 1945; Kendall, 1975). The MK test statistics S is defined by :

$$S = \sum_{i=1}^{n-1} \sum_{j=i+1}^n \text{sgn}(x_j - x_i)$$

where

$$\text{sgn}(x_j - x_i) = \begin{cases} +1, & x_j > x_i \\ 0, & x_j = x_i \\ -1, & x_j < x_i \end{cases}$$

and n is the sample size. The statistics S is approximately normally distributed with mean $E(S) = 0$ and variance

$$\text{Var}(S) = \frac{n(n-1)(2n+5) - \sum_{i=1}^n t_i i(i-1)(2i+5)}{18}$$

where t_i is a number of ties of extent i .

The null hypothesis of no trend should be rejected at 5% (10%) significance level if $|Z| > 1.96$ (1.67), where statistics Z is defined as:

$$Z = \begin{cases} \frac{S-1}{\sqrt{\text{Var}(S)}}, & S > 0 \\ 0, & S = 0 \\ \frac{S+1}{\sqrt{\text{Var}(S)}}, & S < 0 \end{cases}.$$

All indices were calculated for all calendar months, seasons and for the whole year for 20 stations in Poland in the period 1951-2006 on the basis of daily precipitation totals and daily mean temperatures.

The effect of global warming on drought patterns over Poland was also analysed by a multi-model ensemble method based on daily precipitation and temperature data of Regional Climate Model simulations under SRES A1B

scenario. The projected precipitation climatology is expressed as a change in all used indices.

3. Selected results

To describe the present climatology of droughts, means of monthly, seasonal and annual values of the EDI were computed. An example for Kalisz is presented in Figure 1. Then the trend MK test was used. Only at two observation points at Sniezka (western Poland, mountainous station at 1603 m a.s.l.) and Slubice (also western Poland), a decreasing trend (more droughts) was significant during large parts of the year.

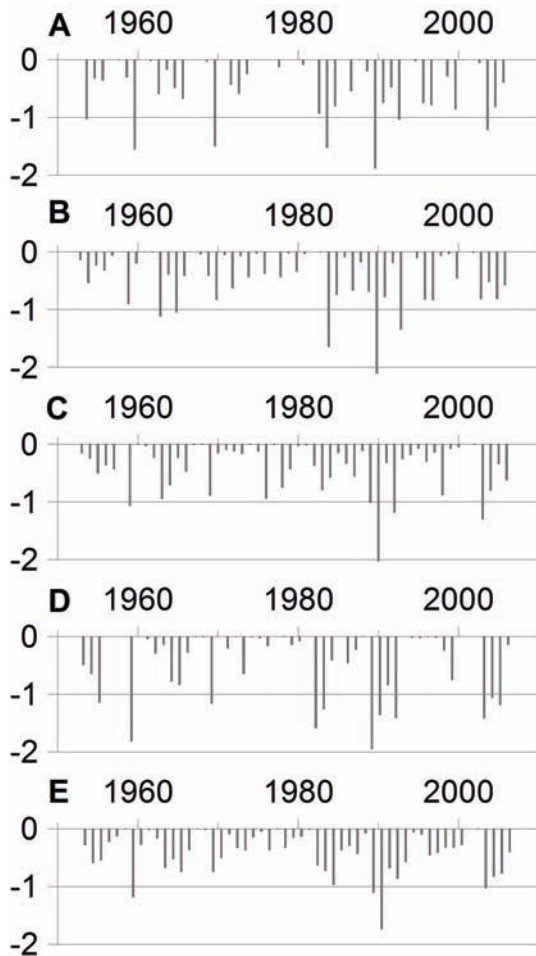


Figure 1. Long-term variability of seasonal mean of EDI index in Kalisz (A - winter, B - spring, C - summer, D - autumn, E - year).

The selected indices differ considerably. The EDI index describes only drought cases and the intensity of events because it presents a cumulate sum of deficit of precipitation according to mean value. The positive values are cut, so the periods with above normal precipitation are not considered. The SPI index presents standardized monthly or seasonal precipitation. Positive values indicate periods of surplus of precipitation, negative indicate on drought. Ped's index is a difference between standardised monthly or seasonal temperature and standardised monthly or seasonal precipitation. It is the only index taking into account also temperature. In Figure 2, the comparison of spring values of all indices for Lodz is presented. There is a significant correlation between the EDI and SPI, whereas Ped's index is not correlated with other two.

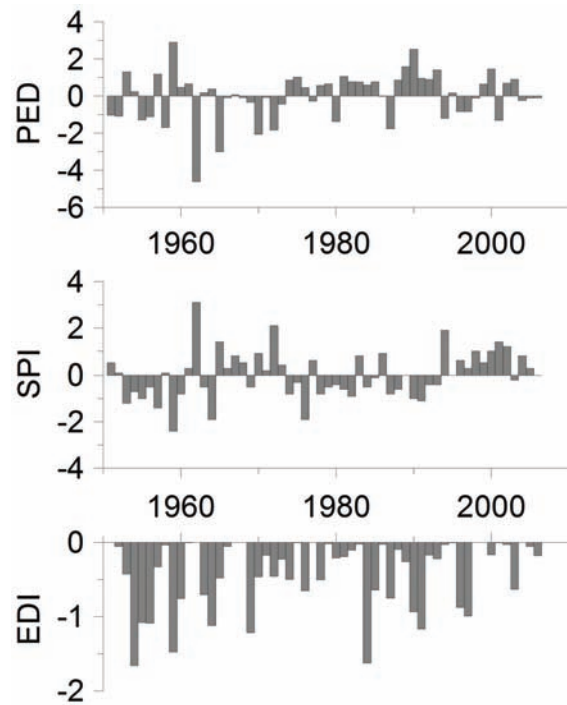


Figure 2. Comparison of long-term courses of spring values of three indices for Lodz.

4. Acknowledgements

This research was supported by the Polish Ministry of Science and Higher Education under the grant 0533/B/P01/2009/36. The author wishes to thank the IMWM for kindly providing the data.

References

- Abramowitz M, Stegun A (eds), 1965, *Handbook of Mathematical Formulas, Graphs and Mathematical Tables*, Dover Publications, Inc.: New York.
- Byun HR, Wilhite DA (1999) Objective quantification of drought severity and duration. *J Clim*, 12, pp. 2747–2756
- Kendall MG (1975) *Rank correlation methods*. Griffin, London, UK
- Kożuchowski K, Zmienność opadów atmosferycznych w Polsce w XX i XXI wieku. [in:] K. Kożuchowski ed. *Skala, uwarunkowania i perspektywy współczesnych zmian klimatycznych w Polsce*, Łódź, 2004, Wyd. „Biblioteka”, pp. 46-57, 2004.
- Lloyd-Hughes B, Saunders MA, 2002, A drought climatology for Europe, *Int. J. Climatol.* 22, pp. 1571-1592.
- Mann HB (1945) Nonparametric tests against trend. *Econometrica*, 13, pp. 245–259
- Ped DA (1975) On indicators of droughts and wet conditions (in Russian). *Proc USSR Hydrometeor Centre*, 156, pp. 19–39.
- Podstawczyńska A., Okresy suche i wilgotne w Łodzi w XX wiek, *Acta Universitatis Lodzianensis, Folia Geographica Physica*, 8: pp. 9-25., 2008.
- Wibig J., Variability of weather extremes in Poland in the period 1951-2006. [in:] *Cambio climatico regional y sus impactos* (ed. J. Sigro Rodriguez, M. Brunet India, E. Aguilar Anfrons), Publicaciones de la Asociacion Espanola de Climatologia, ser. A 6: pp. 469-479., 2008.

Physical characteristics of extreme storm surges and falls on the Polish coast

Bernard Wiśniewski¹ and Tomasz Wolski²

¹ Faculty of Navigation, Maritime University of Szczecin, Szczecin, Poland (natal@univ.szczecin.pl)

² Faculty of Geosciences, University of Szczecin, , Szczecin, Poland

1. The causes of extreme storm surges and falls along the Polish coast

Three causes can be distinguished in explaining the physical features of extreme storm surges and falls along the Polish coast:

- the state of filling the southern Baltic immediately preceding a storm, i.e. the level existing before the sea surface level begins to oscillate,
- action of wind fields,
- deformation of the sea surface due atmospheric pressure lows rapidly moving across the southern and central Baltic Sea. The latter are mesoscale lows characterized by a large atmospheric pressure drop creating the so called pressure-induced wave and generating surges and falls throughout the entire Baltic Sea.

Attention is drawn to this last factor occurring during disastrous storms, as it is generally neglected in the literature on the subject.

2. Physical characteristics of extreme storm surges and falls

The deformation of the sea level is simultaneously created by the wind and the characteristics of the field of the pressure. Effects of the influence of the wind and so called pressure-induced wave can be concerted - both factors bank up the water stage at sea-coasts or lower it. Both factors can be also discordant – i.e. one of the factors raises the water stage, the second lowers it (Figure 1). An additional difficulty is the fact that local conditions of the coast and the hypsography at the bottom near the shore and in the ports have a large influence on the oscillating sea-level.

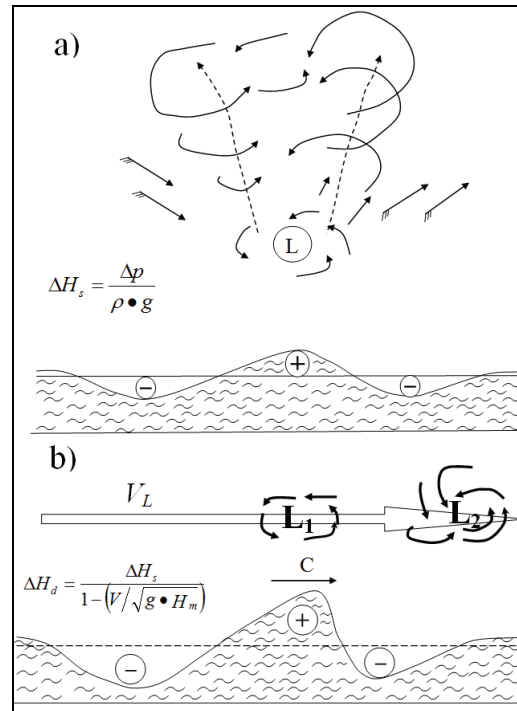


Figure 1. Diagram of sea surface deformation caused by a low pressure system

References

- Lisowski K, (1961) Nieokresowe wahania poziomu Bałtyku pod wpływem czynników anemobarycznych Archiwum Hydrotechniki, Vol. 8, No. 1, pp. 17-42
- Wielbińska Z., (1964) Wpływ cyrkulacji atmosfery na poziom morza. Prace PIHM, Vol.2, Warszawa
- Wiśniewski B., (1997) Zmienność zapasu wody pod stępką statku w czasie wezbrań sztormowych, Inżynieria Morska i Geotechnika, Vol. 5., pp. 325-327
- Wiśniewski B., Holec M., (1983) Zarys Oceanografii, cz. 2, Dynamika Morza, Wyd. Wyższa Szkoła Marynarki Wojennej, Gdynia
- Wiśniewski B., Wolski T., (2008) Ekstremalne poziomy morza na polskim wybrzeżu, Zintegrowane Zarządzenie Obszarami Przybrzeżnymi w Polsce, Vol. 3, pp. 85-100

Hydrological modeling of the lake flow using “Hydrograph” model

Sergey Zhuravlev¹, Yuri Vinogradov²

¹ Saint-Petersburg State University, chair of hydrology, Saint-Petersburg, Russia (hydromod@gmail.com)

² State Hydrological Institute, Saint-Petersburg, Russia (vinograd1950@mail.ru)

1. Introduction

The distributed hydrological “Hydrograph” model developed at the State Hydrological Institute was applied to the lakes of different sizes in the Lake Ladoga Basin. The method of modeling of lake outflow is proposed. The algorithm of calculating of lake outflow regulation was integrated into the model “Hydrograph”. The method was validated at a number of lakes within the Russian part of the Baltic drainage.

2. Study Area

The largest lake within the Russian part of the Baltic drainage is Lake Ladoga. Its basin comprises an area of 276000 km². The main singularity of the Lake Ladoga Basin is the high percentage of lake water surface area relative to the entire basin (12%). The effect of lake outflow regulation depends on lake area and volume (fig. 1, fig. 2).

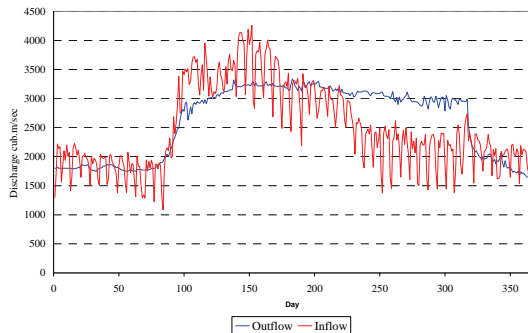


Figure 1. Lake Ladoga (surface area 17700 km²) inflow and outflow

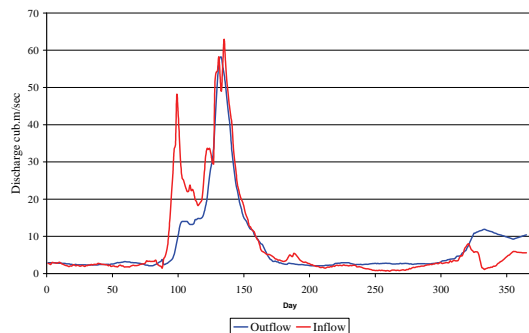


Figure 2. Lake Korobozha (surface area 6.4 km²) inflow and outflow

Several lakes of different surface area (from 6.4 to 17700 km²) and watershed area (from 95 to 276000 km²) within the Russian part of Baltic drainage basin were selected for validation of the method.

3. Methods

The present study uses the distributed “Hydrograph” model for the simulation of lake outflow. The following parameters

need to be known: The inflow into the lake, the surface area and the stage/discharge curve in the outlet in order to simulate the lake level and outflow. The inflow into the lake is simulated by the “Hydrograph” model. The stage/discharge curve in the outlet is approximated with the power function:

$$H = aQ_{out}^n + H_0$$

H is lake level, Q_{out} is lake outflow, a, n are empirical coefficients and H_0 is the level of the inactive storage capacity.

The basic equation of the method is a mass balance equation of the lake:

$$H_1 = H_0 - E_1 + \Delta H_1 - H_{Q1}$$

$$H_i = H_{i-1} - E_i + \Delta H_i - H_{Qi}$$

H_0 is the initial lake level, E is evaporation, ΔH is level change and H_{Qi} is outflow.

Lake outflow at any moment in time is estimated by a mass balance equation and the stage/discharge curve:

The objective functions such as Nash-Sutcliffe efficiency were applied for definition of convergence of modeled and measured lake outflow and level.

4. Results

Modeling results for 19 years (1971-1989) indicate tolerable possibilities of the “Hydrograph” model for studying the processes of lake outflow. It has been established that it is necessary to take into account lake outflow regulation in order to apply hydrological modeling within the Russian part of Baltic drainage basin.

References

- Vinogradov Yu.B, (1988) Mathematical Modeling of runoff formation processes (in Russian), 234 pp
- R. Bourdillon et al., (2010) Modification of the Lake Flow Algorithm of the Distributed Hydrological Model HYDROTEL When Modelling Lakes with Multiple Outlets, Journal of hydrological Engineering

A northern European perspective on adaptation to climate change

Sten Bergström

Swedish Meteorological and Hydrological Institute, Norrköping, Sweden (sten.bergstrom@smhi.se)

1. Introduction

Northern Europe is not the part of the world that is identified to be the most vulnerable to climate change, but there are some obvious concerns and needs for adaptation. Impacts on flooding, water resources and on the hydropower system have been discussed for a long time and numerous studies have been carried out. A summary of the Nordic co-operation on climate change and renewable energy resources, can be found in Fenger (2007). The need for adaptation has also been discussed on a governmental level, for example in Sweden by the Commission on Climate and Vulnerability (SOU 2007).

A more recent concern is the growing awareness that sea level rise may become a threat also in Northern Europe, in spite of the fact that a part of the area is the subject to land uplift since the last glaciation. Most big cities are located by the sea, often at a river mouth, and the exploitation pressure on the shore-lines is strong. The recent assessment by the Dutch Deltacommittee (Deltacommissie 2008) has, among others, delivered a more worrying message than IPCC did in 2007 (IPCC 2007).

2. Water resources

It is not easy to predict how global warming will affect the flood risks in the Nordic climate, where the most extreme floods are generated by a combination of snowmelt and rainfall. What is most evident is that a warmer climate will result in shorter and less stable winters, with smaller spring floods and more frequent and less predictable floods in winter. At the same time, climate scenarios indicate that there is a risk of an increase in the most extreme rainfalls. But a higher temperature is also expected to cause increased evaporation. The total picture is therefore a complex one. In regions in the north, with long winters and a lot of snow, a decrease in the problems in conjunction with spring floods may be expected unless there is an appreciable rise in winter precipitation. In the south, where rain floods dominate, flooding problems may increase unless the increase in evaporation is sufficient to counterbalance the rise in precipitation.

Studies of the impacts of climate change on water resources in the Nordic area are normally based on the combined use of different emissions scenarios, output from several global climate models and regional climate models and a hydrological runoff model. Several combinations of modelling components are used, to explore uncertainties in the estimates. This is the strategy chosen within the Nordic Climate and Energy Systems-project (CES).

It is a complex process to go from a climate model to an off-line hydrological simulation without losing statistical information about how temperatures, precipitation and evapotranspiration are changing in the new climate. Therefore efforts have also been spent on the interface between models.

At present most of the work relies upon regional climate scenarios from the European ENSEMBLES project, providing a large international co-ordinated ensemble of regional climate scenarios (about 22 in total), which facilitates uncertainty analyses and other statistical processing.

But the use of ensembles of models also leads to ensembles of results, to be digested and understood by the decision makers.

3. Dam safety in a changing climate

For the hydropower industry, a new situation has arisen. Large investments are presently made to upgrade dams to comply with the current safety requirements. But now it is also realised that the hazards of global warming cannot be ignored. A similar interest has also been shown by the Swedish mining industry, which has joined the hydropower industry in studies on climate and dam safety. However, existing regional climate scenarios continue to vary over a wide range, especially in the case of extreme precipitation within areas as small as a catchment area. In other words, precisely what is of the greatest interest from a dam safety point of view. It is also recognized that new climate calculations likely will appear as science advances. A new attitude must be developed by the dam owners to deal with this moving target. A new dimension has arrived in dam safety philosophy and work.

4. Big cities where rivers meet the sea

Coastal cities are normally located where rivers meet the sea, like Rotterdam, London, Hamburg, Saint Petersburg, Riga and Stockholm. This makes them particularly vulnerable to climate change. Areal planning is driven by a strong desire to exploit the shore-lines at the same time as sea-level rise is a growing concern. The picture is complex as exemplified by the planned restoration of the outlet of Lake Mälaren in Stockholm, the Slussen area. It shows that adaptation to climate change requires a broad perspective and a new way of thinking. The safety of the fresh water reservoir for two million people is at stake, as well as flood protection for Stockholm and several inland cities located by the lake. You may think that the rate of uplift of land after the last glaciation will save Stockholm, but recent research tells a different story. The accelerated sea level rise is reflected in the very long record of sea levels from Stockholm in Fig. 1. It shows that the long term trend caused by land uplift now is broken.

There is certainly a lot of focus on future sea levels these days. Everyone seems to want a good estimate of the global levels in 2100. But that is not the end of sea level rise, rather the beginning. Any serious city planner should at least consider what comes after 2100 as well. This is crucial for all long term coastal zone development. And it is difficult to find a more suitable candidate for international scientific co-operation.

For city planners there are more aspects to consider. Storm drainage is already a problem today. The systems for management of spillwater are sometimes very old and their load is growing with the expansion of the urban areas. Unfortunately the message from most climate modeling studies is that extreme precipitation will gradually increase with increased temperatures.

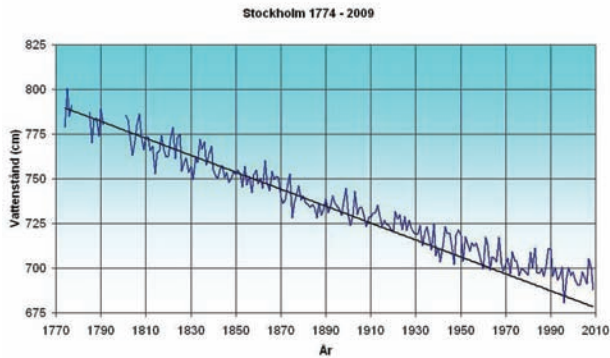


Figure 1. The record of annual mean sea levels in Stockholm since 1774 shows that land is still rising faster than the sea but that the net effect is shrinking. From SMHI (2009).

Still more complex is the situation in the Lake Vänern – River Göta älv system including the city of Gothenburg (Fig. 2). Here we are facing new risks for rising sea levels in an area already at risk today. Along the geologically unstable River Göta älv flood risks may increase at the same time as we need better possibilities to release water from the flood prone lake Vänern. This lake is the largest in the European union and the third largest in Europe.

A critical situation in 2000-2001 confirmed that the situation is unacceptable all the way from the sea to the inland city of Karlstad. Unfortunately most available regional climate simulations indicate aggravation of the problems with a warmer climate. Flood risks will increase and Sea level rise will exceed the uplift of land. And new developments are planned along the shore-lines.



Figure 2. The Lake Vänern – River Göta älv system on the Swedish west coast is an example of a complex adaptation situation.

5. The decision maker s perspective

Understanding climate change and its impacts is a challenge for decision makers. It requires societal overview and a new way of thinking, as we can no longer rely fully on past observations. It is also a challenge for the scientists. They have to explain the uncertainties in climate modelling and why the target is moving, and also why the user cannot expect one single and lasting answer. Communication

between the user and the scientist has thus become crucial. The Swedish power and mining industries have recognized this. The ongoing research on impacts of climate change on design floods for dams is therefore carefully monitored by a committee with representatives from the dam safety authority, the power industry, the mining industry and SMHI. The task is to analyze new results and to recommend how climate change shall be accounted for in future design studies. This will have strong impact on future design of dams but also on physical planning along the shorelines in Sweden, as the same flood criteria are used for flood risk mapping.

The prospect of a changing climate and the ensuing uncertainty related to planning necessitates a new strategy. It is more than ever before important to add extra margins in the design. This may not be so expensive compared to the costs of doing this afterwards, when a project is completed. Another key concept is flexibility. It is likely that future findings on climate change will force us to review and reconsider some of our basis for design from time to time. Flexibility means that a project is designed so that it can be modified technically in the future if this is found necessary.

But the most important aspect is that of societal development. Even though we are concerned about a changing climate we have to realize that society is changing faster than climate. The consequences of imprudent planning without proper respect for climate variability will only be aggravated by a changing climate.

6. Acknowledgements

The Swedish research on climate change and design floods is financed by the Swedish dam safety authority (Svenska Kraftnät) and the power industry via Elforsk. The Nordic co-operation, within the CES-project, is financed by Nordic Energy Research.

References

- Deltacommissie (2008) Working together with water - A living land builds for its future Findings of the Deltacommissie 2008.
- Fenger (ed. 2007) Impacts of Climate Change on Renewable Energy Sources – their Role in the Nordic Energy System. Nord 2007:003. Nordic Council of Ministers, Copenhagen.
- IPCC (2007) Climate Change 2007: The Physical Science Basis. Contribution of Working Group I to the Fourth Assessment Report of the Intergovernmental Panel on Climate Change [Solomon, S., D. Qin, M. Manning, Z. Chen, M. Marquis, K.B. Averyt, M. Tignor and H.L. Miller (eds.)]. Cambridge University Press, Cambridge, United Kingdom and New York, NY, USA, 996 pp.
- SMHI (2009) Havsvattenstånd vid svenska kusten (In Swedish, "Sea Levels at the Swedish Coast"). SMHI Faktabladd nr 41, July 2009.
- SOU (2007) Sweden facing climate change – threats and opportunities. Final report from the Swedish Commission on Climate and Vulnerability. Swedish Governmental Official Reports SOU 2007:60, Stockholm.

The perceptions of Baltic region climate scientists pertaining to climate change in the Baltic region: Results of the survey SurBACC 2010

Dennis Bray

Institute for Coastal Research, GKSS, Geesthacht, Germany (dennis.bray@gkss.de)

1. Purpose of the survey

Recently, a report titled “Assessment of Climate Change for the Baltic Sea Basin” (BACC Author Team, 2008) was published. A survey of BACC (SURBACC) was endorsed by BALTEX administration. The survey questionnaire was designed to assess scientist’s perceptions of the broader state of the climate sciences as they pertain to the Baltic region, to allow comment on and to evaluate compilation process, content and knowledge gaps in the BACC report, as well as to identify future research priorities.

2. Preliminary results

At the time of writing, data are still being collected. Therefore, only preliminary results can be offered at this time. To date, 108 responses have been received.

3. Is global warming occurring?

The data in Table 1 seem to suggest that there is little disagreement among Baltic region climate scientists that climate change is underway.

Table 1. Is climate change, whether natural or anthropogenic, occurring now?

	number	percent
not at all	1	.9
2	0	0
3	2	1.9
4	5	4.6
5	16	14.8
6	20	18.5
very much	61	56.5
don’t know	3	2.8
total	108	100

missing cases = 12

The data in Table 2, however, seem to suggest there is some doubt over the attribution of anthropogenic causes.

Table 2. Most of the recent or near future climate change is, or will be, a result of anthropogenic causes.

	number	percent
not at all	4	3.7
2	10	9.3
3	7	6.5
4	26	24.3
5	18	16.8
6	17	15.9
very much	22	20.6
don’t know	3	2.8
total	107	100

missing cases 13

4. The Baltic region

Questions were also designed specifically for the Baltic region. The results to two such questions are presented in Tables 3 and 4.

Table 3. How much do you think that through the process of downscaling and regional modeling it is now possible to determine patterns of climate change for the Baltic Sea region?

	number	percent
not at all	1	1
2	4	4
3	15	5.2
4	21	21.2
5	32	32.3
6	14	14.1
very much	4	4
don’t know	8	8.1
total	99	100

missing cases = 21

Table 4. How much do you think that through the process of downscaling and regional modeling it is now possible to determine patterns of sea level change for the Baltic Sea region?

	number	percent
not at all	2	2
2	7	7.1
3	27	27.6
4	13	13.3
5	20	20.4
6	13	13.3
very much	2	2.0
don’t know	4	4.3
total	98	100

missing cases = 22

While a considerable knowledge is indicated in the above data, there is also the suggestion that there is room for improvement. By making such assessments, it is possible to assign research priorities.

4. The BACC report

The BACC Report was an attempt to synthesize the knowledge of climate change pertaining to the Baltic Sea region. One purpose of the survey was to assess the satisfaction of the scientific community with report. The following two tables are an sample of the sentiments of the Baltic climate science community.

Table 5. How well do you feel your area of expertise is represented in the BACC Report? (asked only of those claiming to be aware of the report)

	number	percent
not at all	1	1.5
2	4	6
3	11	16.4
4	6	9
5	11	16.4
6	19	28.4
very much	7	10.4
don't know	7	11.9
total	67	100

Missing cases = 53

Table 6. Do you think a second BACC Report on climate and climate change in the Baltic Sea region sometime in the future would be a good idea? (asked only of those claiming to be aware of the report)

	number	percent
not at all	1	1.5
2	2	3.1
3	0	0
4	3	4.6
5	4	6.2
6	21	32.3
very much	30	46.2
don't know	4	6.2
total	65	100

Missing cases = 55

5. Conclusion

Such a survey is a systematic means of gathering information designed to elicit information directly from the scientific community. At the pragmatic level it provides insights for the Baltic science community that may serve to identify knowledge gaps and research opportunities, or at the very least, generate topics for further discussion.

Meteorologically possible potato yields for Estonia, derived from climate change scenarios

Triin Saue^{1,2} and Jüri Kadaja¹

¹ Estonian Research Institute of Agriculture, Estonia (triin.saue@eria.ee)

² Department of Geography, University of Tartu, Estonia

1. Introduction

The changing of the climate system is now hardly disputed (IPCC 2007). This century will likely see a rise in average global surface temperature, while the changes in precipitation are regionally different. In most climate change scenarios, the lengthening of the vegetation period and its earlier beginning can be expected for the higher latitudes, including the Baltic Sea area. The resulting responses of plant species and agricultural crops are however diverse. As the relationship between climate, crop growth and yield is complicated, it cannot be described in terms of simple and average relationships.

Potato is one of the most important agricultural crops in Estonia. For this species, the temperature rise is expected to decrease the overall yields, since potato is best adapted to temperate climates (Haverkort 1990). On the other side, in Estonia, yields may go up because of the lengthening of the growing season. Due to its high water sensitivity, potato is also very sensitive to changes in the precipitation regime, and the need for irrigation is expected to become evident in most areas. In Estonia, excess water may also cause significant yield losses (Saue and Kadaja 2009).

The main objective of this work is to generate future values of meteorologically possible potato crop yields to estimate the influence of climate change on agrometeorological resources for potato growth in Estonia.

2. Material and methods

Meteorologically possible yields of potato were computed for the years 2050 and 2100, using the production process model POMOD (Sepp and Tooming 1991, Kadaja and Tooming 2004). Meteorologically possible yield (MPY) is the maximum yield conceivable under existing radiation and meteorological conditions and it expresses agrometeorological resources, while its long-time mean value characterizes the agroclimatic resources. By using this tool we can transform the complex meteorological conditions into their yield equivalent and thus assess the agrometeorological resources of different periods. In the present work we use the meteorological conditions projected into the future to assess possible changes in crop growing conditions.

For model simulations, future weather data were required. To achieve temperature and precipitation data for the years 2050 and 2100, climate change scenarios for Estonia were generated using a simple coupled gas-cycle/climate model MAGICC which has been one of the primary models used by IPCC since 1990; the 5.3 version of the software used in our work is consistent with the IPCC Fourth Assessment Report, Working Group 1 (IPCC 2007).

Greenhouse gas emission scenarios are derived from different assumptions about human activities, policies, and technological applications. Four alternative emission scenarios were used in our study to generate climate change scenarios for Estonia: A1B, a scenario of a more

integrated world with rapid economic growth and spread of new and efficient technologies with a balanced emphasis on all energy sources; A2, a scenario of very heterogeneous world with an emphasis on family values and local traditions; B1, a scenario of a world of “dematerialization” and introduction of clean technologies; and B2, a scenario of a world with an emphasis on local solutions to economic and environmental sustainability. Later, we only discuss the results of A2 (predicting the highest increase in temperature) and B1 (the smallest increase in temperature) scenarios. The climate change scenarios were created using SCENGEN, a simple software tool that enables to use the results from the MAGICC and GCM experiments. In this work we used mean monthly air temperature and precipitation data averaged over 20 GCM experiments available in SCENGEN. The period 1961-1990 was used as the baseline to calculate current climatology. The data are displayed in a grid resolution of 2.5° latitude/longitude, thus the Estonian territory is covered by three grid boxes, with medium coordinates 58.8°N/21.3°E, 58.8°N/23.8°E and 58.8°N/26.3°E. We have chosen one meteorological station to describe each of those boxes: Kuressaare, Tallinn and Tartu, accordingly. To obtain future daily weather data for the present study, historical daily weather data in those three stations during the period 1965-2009 were changed on the basis of mean monthly weather changes for year 2050 and 2100 in all climate change scenarios. This means that the variability in these future climates was almost identical to that of the historical climate. As the variability of climate in the future may alter (Mearns 2000), it is important to assess the impacts of both mean climate changes and changes in climate variability. However, analyses within the CLIVARA project (Barrow et al. 2000) with and without changes in climatic variability have shown that the scenario with changes in climatic variability generally did not result in different changes in mean yields and coefficient of variation for potato.

3. Results

3.1. Climate change

Results of the four emission scenarios, each containing 20 GCM experiments used in SCENGEN, provide a wide variety of possible climate change scenarios. We will discuss the results by two scenarios, achieved by using the average of all models. All scenarios project the increase in annual mean temperature, the highest warming is supposed to take place during the cold part of the year (Figure 1). During the period from April to September, the increase of air temperature will be lower. Average annual precipitation is also predicted to increase (Figure 2), however, changes in the annual range of monthly precipitation vary between models and scenarios and are less certain than changes in temperature. On average, the highest change in precipitation is predicted for January and November. Of the summer season, June

shows the highest increase. For August and September a small increase or a slight decrease is predicted. All the projected climatic tendencies have already been noted during the last century (Jaagus 1996, 2006), indicating evident climate warming in Estonia. In previous analogous works (Jaagus 1996, Kont et al. 2003), temperature rise has been predicted to even higher; however, a moderate warming is more realistic.

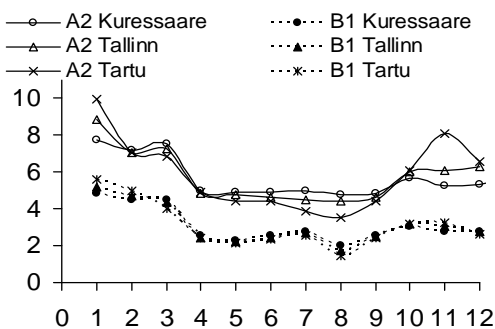


Figure 1. Changes in monthly mean air temperature (°C) in Tartu, Tallinn and Kuressaare for the year 2100 calculated as a mean of 20 GCM experiments for A2 and B1 emission scenarios.

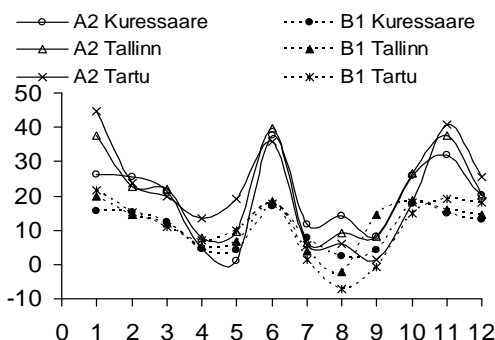


Figure 2. Percentage changes in monthly mean precipitation in Tartu, Tallinn and Kuressaare for the year 2100 calculated as a mean of 20 GCM experiments for A2 and B1 emission scenarios.

3.2. Potato yields

For the late variety 'Anti', the long-term mean MPY values, calculated using historical climate data and describing the climatic resources for plant growth during given period, are 60.0 t ha⁻¹ in Tartu, 55.4 in Tallinn and 51.1 in Kuressaare. For the early variety 'Maret' the values are 44.4, 45.4 and 39.5, respectively. Those numbers are achieved by optimizing the planting time.

For the early variety, all scenarios predict yield losses in all given localities (Figure 3). Stronger scenarios cause higher losses, up to 37 % in Tartu and 33% in Kuressaare and Tallinn by the year 2100. For the late variety, rise in yields is predicted for the year 2050. A lower temperature increase through milder scenarios is more favorable for potatoes – the B1 scenario predicts 3% yield rise in Tartu, 4% in Kuressaare and 13 % in Tallinn, while for the A2 scenario, the rise is less than 0.5 % in Tartu and Kuressaare, 11 % in Tallinn. Tallinn seems to be the most scoring station also for the year 2100. Here, the negative effect of change on yields only appears for the most warming scenario in A2, while the least warming in B1 causes a 9% yield rise. In Tartu and Kuressaare, all

scenarios predict yield losses up to 20 % for 2100, as compared to the present climate.

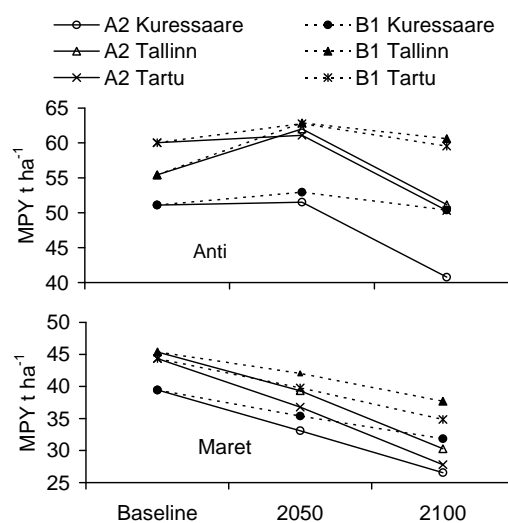


Figure 3. Mean values of the meteorologically possible yield (MPY) of late potato variety 'Anti' and early potato variety 'Maret' for baseline (1965-2009), years 2050 and 2100.

References

- Barrow EM, Hulme M, Semenov MA, Brooks RJ (2000), Climate change scenarios, in: Downing TE, Harrison PA, Butterfield RE, Lonsdale KG (eds), Climate change, climatic variability and agriculture in Europe: an integrated assessment. Research report no. 21, Environmental Change Institute, University of Oxford, pp. 11–27
- Haverkort AJ (1990) Ecology of potato cropping systems in relation to latitude and altitude, *Agricultural systems*, 32., 3., pp. 251-272
- IPCC (2007) Climate change 2007: The physical science basis: Contribution of Working Group I to the Fourth Assessment Report of the Intergovernmental Panel on Climate Change, Cambridge University Press.
- Jaagus J (1996) Climatic trends in Estonia during the period of instrumental observations and climate change scenarios, in: Punning J-M (ed.), Estonia in the System of Global Climate Change, 4., Institute of Ecology Publication, Tallinn, pp., 35-48
- Jaagus J (2006) Climatic changes in Estonia during the second half of the 20th century in relationship with changes in large-scale atmospheric circulation, *Theor. Appl. Climatol.*, 83., pp. 77-88
- Kadaja J, Tooming H (2004) Potato production model based on principle of maximum plant productivity, *Agric. For. Meteorology*, 127., 1-2., pp. 17-33
- Kont A, Jaagus J, Aunap R (2003). Climate change scenarios and the effect of sea-level rise for Estonia. *Global and Planetary Change*, 36(1-2), 1 - 15.
- Mearns LO (2000) Climatic change and variability, In: Reddy KR, Hodges HF (eds) Climate change and global crop productivity, CABI Publishing, Wallingford, pp. 7–35
- Saue T, Kadaja J (2009) Modelling crop yield response to precipitation redistribution on slopes, *Biologia*, 64., 3., pp. 502-506
- Sepp J, Tooming H (1991) Productivity resources of potato, *Gidrometeoizdat, Leningrad* [in Russian with English abstract]

Connections between the atmospheric circulation type and the modelled potato crop yield in Estonia

Mait Sepp¹ and Triin Saue^{1,2}

¹ Department of Geography, University of Tartu, Estonia (mait.sepp@ut.ee)

² Estonian Research Institute of Agriculture, Saku, Estonia

1. Introduction

Living nature and climate are closely connected. Several parameters of living nature (e.g. growth of trees, crop yield, migration of birds and insects) are directly or indirectly dependent on weather conditions. Often, these parameters are not only depending on one meteorological element, but on a combination of many weather conditions. In that case, the correlation with the traditional meteorological parameters (air temperature, precipitation) is quite moderate. The atmospheric circulation types can also be regarded as integrated variables of different meteorological parameters. One can decide by the position of low and high pressure areas and the concurrent air flow, whether the given circulation type brings about a sunny, warm and rainless, or a relatively cool and rainy weather at the observed location. The purpose of this analysis is to study the influence of general atmospheric circulation on the potato crop yield in Estonia. Our aim is to find out how the spring, summer, and yearly circulation conditions affect the yields of early and late potato varieties in three different locations in Estonia that represent somewhat diverse climatic conditions. Although Estonia is a relatively small country, the weather may largely differ in the coastal areas, the Baltic Sea islands and inland Estonia.

2. Data and methods

The applied atmospheric circulation data included the circulation type frequencies of all the 73 classifications from the COST 733 catalogue 1.2 (Huth et al. 2008), consisting of spring (MAM), summer (JJA) and the annual sums in the Baltic Sea region (domain 05 by COST 733). Classifications presented in the catalogue are generated using SLP data obtained from ERA40. Accordingly, the analysed period is 1957-2002.

The potato data included the time series of meteorologically possible yield (MPY), calculated using the potato production process model POMOD (Sepp and Tooming 1991, Kadaja and Tooming 2004). MPY, the maximum yield that certain plant species and varieties are able to produce under the given meteorological conditions, enables us to estimate the agro-meteorological resources of different years and locations. Its long-term average describes the agro-climatic resources. The input data for POMOD are the daily meteorological data (air temperature, precipitation, solar radiation), the value of the initial water storage in the soil (or the date when the soil moisture fell below the field capacity), the date for a stable temperature rise over 8°C, the dates for the first and last night frosts (≤ -2 °C), and the date of the stable temperature fall under 7°C. The different locations are described by their geographic coordinates and the hydrological parameters of the soil (wilting point, field capacity and maximum water capacity). The applied characteristic parameters for potato varieties are the parameters of photosynthesis and respiration, as well as the growth functions. For this study, the list of data was derived from using the characteristic data system of three Estonian meteorological stations (Tallinn, Tartu, Kuressaare) and the

biological parameters of two potato varieties (early Maret, late Anti) (Saue and Kadaja, 2009). Of the three meteorological stations used, Tartu is located in the mainland and has a relatively continental climate; Kuressaare is located in the West-Estonian archipelago and clearly represents the maritime climate; Tallinn lies on the Estonian northern coast and there is also maritime climate, but not as clearly expressed as in Kuressaare.

To discover the connections between MPY and the general atmospheric circulation, the correlation analysis was applied. In order to test the liability of the linear correlation, the Student t-test was used, where the value of statistic liability was set to $p < 0.01$.

The results of the correlation analysis are evaluated in two aspects. Firstly, we studied which classifications describe the potato crop yield distribution better. To achieve that, all the circulation types that had statistically relevant connections were added. Here, one must bear in mind that one circulation type may give a statistically significant correlation in both spring and summer seasons, as well as in different potato varieties. Such concurrences were not taken into account in adding the circulation types. To decrease the effect of the different number of circulation types in the classifications, the result sum was divided by the number of circulation types in the classification.

Secondly, it was studied which circulation types give positive and which give negative correlations. To achieve that, the MSLP map of each statistically liable correlation type in the COST 733 catalogue was examined. According to the position of low and high pressure areas, we decided which weather conditions in Estonia are concurrent with each type.

Table 1 The number of circulation types with statistically significant correlation and dominating pressure areas on the MSLP type map. Abbreviations: Tr – Tartu, TI – Tallinn, Ku – Kuressaare, M – early potato type Maret, A – late potato type Anti, Y – year, Sp – spring, Su – summer, n – negative correlation, p – positive correlation, L – low, H – high, N/S – the general direction of air masses that flow into Estonia depending on the position of pressure areas. ? – situations where the dominating pressure area or the direction of air masses cannot be determined.

	TrM	TIM	KuM	TrA	TIA	KuA
Y/n	12/L	9/L	17/H	28/H	11/N	92/H
Y/p	1/L?	3/L	28/H-L	1/L?	8/L	58/L
Sp/n	17/L	17/L	11/L	15/L	2/S?	-
Sp/p	5/H	1/H?	2/L?	-	1/S?	2/Sn?
Su/n	10/L	15/H	84/H	10/L	2/?	130/H
Su/p	4/?	11/L	69/L	3/L	2/?	108/L

3. Results and discussion

The correlation analysis of potato crop yield and circulation types shows quite symptomatically that, as a rule, there are more circulation types that give negative connections. Therefore, those types that bring about a decrease in the potato crop yield are more clearly represented (Table 1).

The studied geographical locations and seasons appear to be clearly different. The summer season and the location of Kuressaare stand out with respect to the number of statistically relevant circulation types. There are somewhat more connections in the case of the late variety Anti in Kuressaare (Table 1). In the case of other potato time series, there are up to ten times less types that give connections. Similar results apply to the yearly sums. In the spring, there are surprisingly few types that give strong connections. It seems that the spring circulation connections do not affect the meteorologically possible potato yields. In the inland station, early potato variety seems to be more sensitive to the spring conditions, while in Kuressaare potatoes are practically not affected by the spring conditions. Why don't the spring circulation types influence the crop yield? Probably because the given crop yield calculations are made from the date when the temperature rises and stays over 8°C. Even though night frost often postpones that date, the earliest planting date is 1 May. Therefore, the thus calculated potato yield is not affected by the weather conditions of March and April, but only by the initial water supply in the soil. The large correlation between the annual sums and calculated potato yields is also fairly surprising. One may assume that the correlation lies in the fact that those circulation types that bring about harder winter conditions are also responsible for the drought in the summer.

Analyzing which circulation types give positive or negative correlations with the yields, we can generalize that such types form relatively similar groups. That means that, for example, a negative correlation is given by similar circulation types from different classifications. Typically, the negative correlation derives from circulation types that are totally opposite to the circulation conditions that give positive correlation and vice versa. Depending on the geographical location and season, the positive correlation is given by types that bring about a dominant low pressure area in the MSLP map of the domain. Usually, we can distinguish 2-3 (or up to 5) similar circulation patterns in similar low pressure area classes that still have a different dominant low pressure area positions. Often, such low pressure area types give a strong correlation where the whole domain is covered by the low pressure area and its centre lies either in the centre of the domain or the low pressure area covers the northern part of the domain and its centre lies either in the north-west or north-east from Estonia. The similar characteristic of all these combinations is the fact that there is a westerly flow above Estonia, and there is a rainy and a cooler weather than is typical for the summer.

Opposite to the low pressure area is a situation where the high pressure area is dominant in the domain. In that case there are also 2-3 contrasting circulation patterns that give strong correlations with the potato yields. One typical pattern describes a situation where the high pressure area covers the whole domain and its centre lies above the Baltic Sea. In the case of other high pressure area situations, the anti-cyclone covers the northern part of the domain and depending on the position of the centre of the pressure area, the eastern or north-eastern winds are dominant in Estonia. In the context of the summer weather, such types bring about sunny weather and temperatures that are warm above

the average, which could mean a lack of water that is needed for potato growth in habitats that often suffer from drought, like Kuressaare.

4. Conclusions

- a) Those types that affect the crop yield negatively clearly stand out from the circulation types.
- b) Circulation tends to effect less the potato yield of Kuressaare which represents a maritime climate. The circulation affects more the yield of early potato types.
- c) The spring circulation conditions have little effect on the potato yield; only the early potato types are affected to an extent – there is a clear negative effect of low pressure areas on the potato crop yield of the early types – the more cyclones, the cooler the weather, and the lower the soil temperature.
- d) In terms of the summer circulation conditions, we can see a regional difference – the coastal locations (Tallinn, Kuressaare) are rather more negatively affected by the high pressure areas (higher temperatures, drought), while Tartu is negatively affected by the low pressure areas. Thus, the coastal areas are directly influenced by the summer droughts, but the potato yield in inland Estonia is more limited by excessive humidity.
- e) The effect of circulation conditions on potato crop yield of the whole year is similar to the effect of the summer circulation conditions. Tallinn is an exception, because there the effect of the annual sum is similar to the effect of the low pressure area on Tartu. In connection with the annual sum, the possible effect of winter on the crop yield is still undetermined. However, because the effect of spring on the crop yield is lower than expected, there is no reason to presume that the effect of the preceding winter would be significant.

References

- Huth, R., Beck, C., Philipp, A., Demuzere, M., Ustrnul, Z., Cahynová, M., Kyselý, J. and Tveito, O. E. (2008), *Classifications of Atmospheric Circulation Patterns. Recent Advances and Applications. Annals of the New York Academy of Sciences*, 1146, pp105-152
- Kadaja J, Tooming H (2004) Potato production model based on principle of maximum plant productivity, *Agric. For. Meteorology*, 127., 1-2., pp. 17-33
- Saue, T.; Kadaja, J. (2009). Simulated crop yield - an indicator of climate variability. *Boreal Environment Research*, 14(1), 132 - 142.
- Sepp J, Tooming H (1991) Productivity resources of potato, *Gidrometeoizdat, Leningrad* [in Russian with English abstract]

Climate services – concepts and examples

Hans von Storch and Insa Meinke

Institute of Coastal Research, GKSS and CLiSAP KlimaCampus, Hamburg (hvonstorch@web.de)

The concept of anthropogenic climate change has two implications – one is decadal predictability (conditional upon the prediction of the anthropogenic drivers) and the possibility of a partial steering of future climate (by steering the drivers). The latter leads to mitigation policies, the former to adaptation policies.

Both types of policies need a scientific underpinning – for mitigation: knowledge about climate sensitivity against the different drivers– and for adaptation: knowledge about the regional and local manifestation of future climate change and variability. In both cases, a dialog between science and stakeholders, including the public and policymakers, is needed.

An important element of such climate service is the recognition that scientific knowledge is not per se accepted as superior in the public arena. Instead, culturally constructed knowledge claims compete with scientifically constructed knowledge claims. Even if it may appear plausible that science is a better advisor of political and economic decisions, it is often other understanding of complex phenomena, which dominate the decision processes. To help making scientific arguments to "win" this competition, science must understand the competing knowledge claims, and must examine the utility of scientific knowledge in dealing with problems related to climate policy.

In the Institute of Coastal Research of GKSS Research Centre, we have established the regional "Norddeutsches Klimabüro", which acts as a knowledge broker between regional climate science (at GKSS in Geesthacht and CLiSAP in Hamburg) and regional and local stakeholders. The task of this "Büro" is to provide scientific knowledge for stakeholders and to link the scientific questioning to problems encountered by stakeholders. Its toolbox comprises regular personal exchanges, a consistent and homogeneous data set "CoastDat" about ongoing and possible future climate, climate change and climate impact, and the collection and assessment of knowledge about regional and local climate and impact issues.

References

- Meinke, I., and H. von Storch, (2008): The North German Climate Office – an interface between science and practice, Proc. 8. Katatrophenvorsorge, 15./16.10.2007, Karlsruhe University
- von Storch, H., 2009: Climate Research and Policy Advice: Scientific and Cultural Constructions of Knowledge. *Env. Science Pol.* 12, 741-747
<http://dx.doi.org/10.1016/j.envsci.2009.04.008>
- von Storch, H. and I. Meinke, (2008): Regional climate offices and regional assessment reports needed. *Nature geosciences* 1 (2), 78, doi:10.1038/ngeo111

Warm season degree-days in south-western Belarus and their dynamics

Alexander Volchek, Oleg Meshik and Vladimir Luksha

Brest State Technical University, Brest, Republic of Belarus, Volchak@tut.by, mop@bstu.by, vvluksha@gmail.com

1. Introduction

During the last decade the question of the influence of natural and anthropogenic factors on climatic changes is widely discussed. There is a consensus among the international Earth Science community that most of the ongoing “global warming” (an increase of global surface air temperature to unprecedented values for the period of instrumental observations) has occurred due to anthropogenic emissions of greenhouse gases (Intergovernmental Panel on Climate Change, IPCC, 2007). The IPCC Report projects for the middle of the 21st century an increase of approximately 2.5°C for the annual surface air temperature of the Northern Hemisphere and for the northern extratropical land areas where Belarus resides, higher temperature changes are expected. For Belarus, such changes are rather significant and will have a serious impact on the economy. In particular, the temperature increases will lead to a longer duration of the vegetation period. The nation is located in an area of sufficient moisture supply (droughts are quite rare here) and the projected temperature rise (if the moisture supply (precipitation) remains the same), will allow higher production and harvest of agricultural crops. The temperature rise will inevitably cause structural changes in the hydrological cycle. First it will cause an increase in total evaporation. Associated with it changes in precipitation are also possible. Predicted climatic changes in surface energy and water budget in Belarus imply a necessity to account for these changes in planning of agriculture, water supply, melioration, and other human activities.

2. Climatology and changes in the seasonal cycle: Surface air temperature

Surface air temperature is one of the basic climate characteristics. In the warm season, it is mostly defined by the surface radiation balance while during the cold period of the year, advection heat sources (i.e., atmospheric circulation) significantly contributes to its climatological pattern. We shall describe the seasonal cycle using the average monthly surface air temperature. Maximum monthly surface air temperatures over Belarus are registered in July (63 % of years), and minimum - in January (53 % of years). In certain years the warmest months are observed in June (17 % of years) and in August (20 % of years), and the lowest - in February (32 % of years) and December (13 % of years).

For numerous engineering applications, average long-term values of surface air temperature and its derivatives (normals) are used. However, in different reference sources for these normals, the temperature values vary because different averaging periods were used in these sources.

The normals are supposed to be calculated for the “reference” period that is sufficient for an estimation of the parameters of its probabilistic distribution. It is anticipated that these parameters should remain “stable” outside of the given period for sufficiently long time. In the changing climatic conditions, this stability for any pre-selected period cannot be stipulated in advance. It is a function of the time allocation and duration of the reference period and the presence of autocorrelation in the time series. It is difficult

enough to pick the climatological time series in Belarus that have statistical homogeneity. Durations of the time series are usually over 50 years. Presence of considerable missing data, changes in observational practice, replacement of the instruments, etc. may not allow receiving statistically homogeneous time series. Therefore, for analyses of these time series, we used metadata (data about the data) in addition to statistical methods. Metadata allow us to account for artificial (non-climatic) changes in our time series prior to any statistical analyses. To design various engineering objects with limited life time we use “normals”. Their estimates start with temporal averaging of initial data. The majority of engineering objects will last for at least 20-30 years and it is necessary to consider in their design expected changes in climate. When using long time series for engineering design, it is possible to deform the actual situation because the trends, which manifested themselves mostly during the last decades, are smoothed out after the temporal averaging over the entire reference period and cannot serve as a good guide for the future climate conditions. Therefore, we calculated climatic normals for engineering assessments, using only the last 30 years (1975 - 2004). This approach allows us to account (to some extent) for the ongoing climatic changes. To estimate the latest temperature changes over the nation, we used of the data archives of the Belorussian Republican Hydrometeorological Centre. For our research we selected the 60-year-long time series of surface air temperatures from 1945 to 2004 and averaged them over six consecutive decades. The time series were partitioned into two 30-year parts: from 1945 to 1974 - before the construction of major melioration systems in the nation and their consequent impact on environment (the land reclamation peak was in the 1972 through 1974 period) and from 1975 to 2004, which is a period of stable functioning of the constructed hydro-melioration systems.

Table 1. Average long-term values of air temperatures and their difference in the investigated territory, °C

City	Period	1	2	3	4	5	6	7	8
Brest	1975-2004	-2.7	-2.1	1.9	8.2	14.1	16.8	18.6	18.1
	1945-1974	-4.7	-3.6	0.0	7.7	13.5	17.1	18.5	17.6
	difference	2.0	1.5	1.9	0.4	0.6	-0.2	0.1	0.5
Pruzhanjy	1975-2004	-3.6	-3.2	0.9	7.4	13.3	16.2	17.5	17.3
	1945-1974	-5.9	-4.7	-0.6	6.9	12.8	16.6	17.9	16.9
	difference	2.3	1.5	1.5	0.4	0.5	-0.4	-0.4	0.4
Pinsk	1975-2004	-3.7	-3.2	1.2	8.0	14.1	16.8	18.4	17.7
	1945-1974	-6.3	-4.8	-0.8	7.0	13.3	17.0	18.1	17.0
	difference	2.6	1.6	2.0	1.0	0.8	-0.2	0.3	0.7
Ivacevichi	1975-2004	-3.8	-3.3	1.0	7.5	13.7	16.6	18.1	17.2
	1945-1974	-6.1	-4.8	-0.8	7.0	13.1	16.8	18.0	17.0
	difference	2.3	1.5	1.8	0.5	0.6	-0.3	0.1	0.2
Gancevichi	1975-2004	-4.2	-3.8	0.6	7.3	13.4	16.3	17.9	17.0
	1945-1974	-6.6	-5.1	-1.1	6.8	12.8	16.5	17.7	16.5
	difference	2.4	1.3	1.7	0.6	0.6	-0.2	0.2	0.4
Baranovichi	1975-2004	-4.4	-4.0	0.3	7.1	13.2	16.1	17.4	17.0
	1945-1974	-6.6	-5.4	-1.5	6.5	12.8	16.5	17.8	16.9
	difference	2.2	1.4	1.8	0.6	0.4	-0.4	-0.4	0.2

City	Period	9	10	11	12	Year	Σ_{4-10}	$\Sigma_{>10^{\circ}\text{C}}$
Brest	1975-2004	13.1	8.1	2.5	-1.5	7.9	97.0	2595
	1945-1974	13.2	7.5	2.6	-1.6	7.3	95.0	2530
	difference	-0.1	0.7	-0.1	0.0	0.6	2.0	65.3
Pruzhaný	1975-2004	12.4	7.3	1.7	-2.3	7.1	91.4	2412
	1945-1974	12.6	6.8	1.9	-2.2	6.6	90.5	2382
	difference	-0.2	0.5	-0.1	-0.1	0.5	0.9	30.2
Pinsk	1975-2004	12.7	7.4	1.7	-2.5	7.4	95.1	2532
	1945-1974	12.5	7.3	1.9	-2.6	6.6	92.1	2436
	difference	0.2	0.1	-0.2	0.1	0.7	2.9	96.3
Ivacevichi	1975-2004	12.4	7.3	1.6	-2.4	7.1	92.7	2455
	1945-1974	12.5	6.6	1.7	-2.3	6.5	91.0	2398
	difference	-0.1	0.6	-0.1	-0.1	0.6	1.7	57.3
Gancevichi	1975-2004	12.0	6.9	1.4	-3.0	6.8	90.8	2394
	1945-1974	11.9	6.3	1.5	-2.7	6.2	88.4	2314
	difference	0.2	0.6	-0.1	-0.3	0.6	2.4	80.0
Baranovichi	1975-2004	12.0	6.8	1.1	-3.0	6.6	89.7	2355
	1945-1974	12.4	6.5	1.2	-2.9	6.2	89.4	2346
	difference	-0.3	0.4	-0.1	-0.1	0.5	0.3	9.2

To estimate the dynamics of temperature changes over the southwestern part of Belarus, we calculated the differences of average long-term values of temperatures of air for 1975-2004 and for 1945-1974 (Table 1).

The warming over the entire southwestern Belarus in the first half of year (January - May), and the January warming were so considerable, that January ceases to be the coldest month in the year. The increase of the surface air temperature in March is connected with frequent low-snow cold seasons in 1975 – 2004, and thus with a decrease of the heat expenditures on snowmelt. As a result, most of radiation and advection spring heat influxes began contributing to the air heating. Certainly, this tendency should lead to socio-economic decisions. Growth of winter and spring temperatures leads to an increase of duration of the vegetation period for agricultural crops. For the southwest part of Belarus, this provides and (as we hope) will provide in the future more favorable temperature conditions for intensification of agricultural production. As a whole, growth of the sums of temperatures of air for the warm period (April - October) takes place also. A special importance for agriculture production is represented by an increase in the degree-days with the surface air temperature above 10°C (Figure 1).

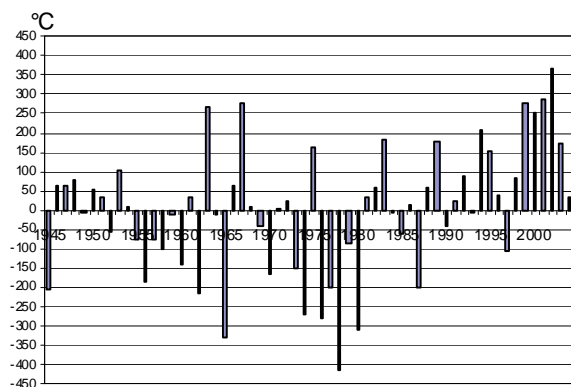


Figure 1. Deviation of the sums of air temperatures $>10^{\circ}\text{C}$ from long-term average for 1945 - 2004 in Brest

The same situation (as in Brest) is observed at other stations of the southwestern part of Belarus. The largest gain in degree-days for the last thirty years is observed in Pinsk

96.3°C (3.8 %). Taking into account that for last thirty years, the degree-days with $T > 10^{\circ}\text{C}$ increase in a direction from north to east and southwest, there was a displacement of the borders of the agro-climatic zones in Belarus by approximately 40-50 km in this direction.

3. Conclusions

In the recent past, the southwest part of Belarus had an insufficient amount of warm season degree-days for high-productive crops. In the last decades, the regional temperatures in the warm season have increased and agriculture fields began receiving additional surface heat. This provides an opportunity for intensification of agricultural production (the use of new highly productive kinds of agricultural crops). Climate of Belarus became less continental and the annual amplitudes of surface air temperature in the region have decreased.

References:

Intergovernmental Panel on Climate Change (IPCC), 2007: *Climate Change 2007: The Physical Science Basis*. Contribution of Working Group I to the Fourth Assessment Report of the Intergovernmental Panel on Climate Change, S. Solomon, D. Qin, M. Manning, Z. Chen, M. Marquis, K.B.M. Tignor and H.L. Miller, Eds., Cambridge University Press, Cambridge, United Kingdom and New York, NY, 996 pp.

“Ecohydrological dams” for compensation of climate change and reduction of fluxes nutrients and pollutants from the river basins in to Baltic Sea

Maciej Zalewski^{1,2}

¹ European Regional Centre for Ecohydrology u/a UNESCO, International Institute of Polish Academy of Sciences, Lodz, Poland (mzal@biol.uni.lodz.pl)

² Department of Applied Ecology, University of Lodz, Poland

1. Ecohydrology

Until the end of the 20th century, water management was dominated by a mechanistic approach focused on the elimination of threats such as floods and droughts, and provision of water to societal needs. The biological structure of ecosystems around 1900 was mostly used as indicator of ecological status (Kolkwitz and Marsson 1908). Declining water quality at the global scale and increasing progress in the predictive potential of ecology and limnology provided the background for the development of integrative sustainability science, i.e. Ecohydrology (EH). The basic question of EH is: What is the hierarchy of factors regulating the dynamics of hydrological–biological interactions? And further, how should it be used to solve environmental and societal problems with reference to Integrated Water Resources Management (IWRM) and in the frame of such policies as e.g. the EU Water Framework Directive (WFD 2000)?

Aquatic ecosystems are complex entities studied in a multidisciplinary approach by considering the hierarchy of various regulatory environmental factors. However, their regulation needs society as an additional reference point, combining natural science with an integrative transdisciplinary science and management.

2. The role of reservoirs for the reduction of droughts and nutrient pollution of the Baltic Sea

In the face of global change considered as climate stochasticity, increase and population growth as far as standard of living improvement, the traditional view on role of dams in basin scale ecological processes shaping (e.g. Power et al. 1996) has to be reconsidered.

The good example is provided by the climatic scenarios of HELCOM in the southern Baltic Sea catchment where annual precipitation is 600 mm and 70% of the area is agricultural land. According to predictions, summer river flow may decrease even to 50%, whereas in winter may increase up to 70% (HELCOM Thematic Assessment 2007). If such drastic changes will appear, extreme floods and droughts, especially in agriculture and urbanized catchments, will be a severe threat for sustainable development. As a consequence, the land cover in catchments is modified by man (following the First Principle of Ecohydrology). The quantification of the water budget in forested and deforested parts of the catchment has to be done towards a restitution of land cover and buffering strips at critical points of landscape (Zalewski et al. 2003). New dams have to be constructed with the enhanced resilience for eutrophication and with bypass systems for maintaining migration and restoration of reophilic fish (Zalewski and Welcomme 2001), minimizing negative effects of impoundments on ecological processes and biodiversity and increase river basin resilience (Figure 1).

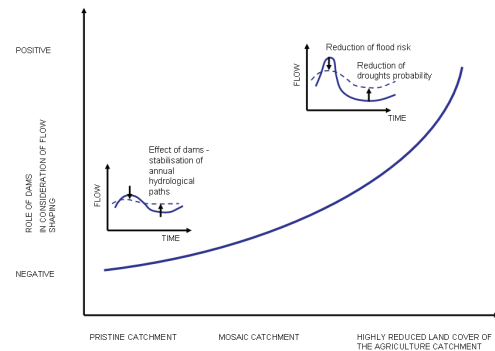


Figure 1. Positive role of dams in consideration of ecological flow shaping in highly modified landscapes in the face of global climate changes.

3. The new design of environment friendly “eco-hydrological dams”

The most negative form of impact by traditionally constructed dams on river ecosystem is the disruption of continuity. The consequences are a decline of biodiversity and fisheries, especially of migratory fish populations. Also, the disturbance of the nutrients composition results in an increasing probability of toxic algal blooms. Additionally, the decline in mineral and organic matter transfer to the costal zone reduces deposition and fertilization, which in turn modifies habitats and trophic status, and as a consequence negatively affects costal fisheries at costal zones habitats.

The prototype of an environment friendly dam is projected Nieszawa dam on the Vistula River, where migration of fish and aquatic organisms will be guaranteed not only by traditional fish ladder but additionally by a bypass channel (Figure 2), which will transfer permanently 2% low Vistula of the flow which makes approximately 8m³ which is half of the average flow of the largest left tributary of Vistula. The loss of less than 2% of flow transferred by the bypass does not significantly reduce hydroenergy gain.

The structure and plant composition of the “vegetation refuge” at the banks and construction of an island containing the gradient of aquatic and terrestrial habitats has been based on long term research and observations on central Poland large reservoirs (Sulejow and Jeziorsko).

The second important challenge is the reduction of the transfer pollutants: POP, dioxins, heavy metals, from land to the Baltic Sea and thus prevention of its bioaccumulation in fish. Most of these pollutants bind with organic matter. The shaping of the reservoir hydrodynamics towards the creation of sedimentation zones near banks allows for a periodical transfer of concentrated organic matter in sedimentary zones from the bottom of the reservoir to bioenergy plantations where

nutrients stimulate production of bioenergy, and pollutants are fixed in wood and burned.

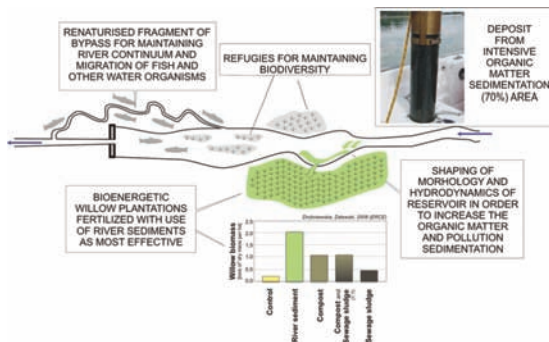


Figure 2. Example of “environment friendly” dam solutions.

4. The “ecohydrological dam” for sustainability of the Vistula River and reduction of the impact on the Baltic Sea - An ecohdrological perspective

The basin scale positive effect of the “ecohydrological dam” on sustainability of the Vistula River basin, Baltic Sea and society can be summarized as follows:

- Production of hydroenergy and reduction emission of CO₂
- Adaptation to the global climate change by providing the water for agriculture, rising groundwater level in neighborhood landscape, restitution declining wetlands.
- Reduction of eutrophication and toxic algal blooms in Baltic Sea by trapping and converting nutrients in to bioenergy.
- Reduction of POP, dioxins and heavy metals load to the Baltic Sea and reduction bioaccumulation in fish.
- Increased potential to maintain environmental flow in Vistula River and good ecological status of the floodplain in case long term drought.

5. Ecohydrology and environmental science

EH provides three new aspects to environmental sciences and their implementation: (1) The use of ecosystem properties as new management tools complementary and harmonized with hydro-technical solutions; (2) The necessity to enhance the ecosystem’s carrying capacity towards UN Millennium Development Goals by using the interplay between hydrology and biota. The analysis of dynamic oscillations of the ecosystem, productivity and succession reflected by nutrients/pollutants absorbing capacity vs. human impacts should be the key for process regulation; (3) The use of “dual regulation” to improve water resources, biodiversity and ecosystem services for society (expressed as carrying capacity).

6. Ecohydrology for the implementation of the Water Framework Directive and reversing Baltic Sea degradation – Methodology of the scientific perspective

Ecohydrology (EH) is defined as sub-discipline of hydrology that focuses on ecological processes occurring within the hydrological cycle and strives to utilize such processes for enhancing environmental sustainability. The first step in defining the role of EH for the implementation of the Water Framework Directive (WFD) should be the analysis of the the pattern of the scientific methodologies which stimulate the recent progress in environmental sciences. Such progress has been directly translated in to “good ecological status “of inland and costal waters. From an evolutionary perspective the paradigms in environmental

sciences during the last decades, three stages are distinguished: INFORMATION – structure states, relationships; KNOWLEDGE – by integration of different scientific disciplines the synergies between information is highlighting the patterns and processes, (e.g. Ecohydrology). The third most advanced stage of science WISDOM - ability to use the information and knowledge to develop innovative solutions of the environmental problems with the consideration of the society priorities. The conceptual framework for transition from the first to the second and third stage is provided by the three principles of Ecohydrology. They cover the three aspects, respectively. Hydrological – information on abiotic structure of the river basin dynamics, hydrological processes and spatial temporal specific of anthropogenic impacts. Ecological – the potential for basin resilience enhancement and Ecotechnological – use information and knowledge for development new ecological biotechnologies and system solutions.

The conclusion from the above analysis is, that to accelerate cost efficient implementation of the Water Framework Directive, more efforts have to be done towards a transition from research, in which we are collecting information, to the area of science in which interdisciplinary efforts deepening our knowledge of the processes, regulatory mechanisms within the ecosystems and further progress from knowledge to wisdom has to be done by broader involvement of integrative environmental scientists in large scale projects not only on environment restoration but also in to any development of European infrastructure.

BALTEX become good example of the approach which covers in a balanced way all three components information, knowledge and wisdom.

References

- Kolkwitz R. and Marsson M. (1908) Oekologie der pflanzlichen Saprobien. Ber. dtsh. bot. Ges., No. 26, pp. 505–519
- Power ME., Dietrich WE., Finlay JC. (1996), Dams and Downstream Aquatic Biodiversity: Potential Food Web Consequences of Hydrologic and Geomorphic Change. Environmental Management, Vol. 20 No. 6, pp. 887-895
- Zalewski M. and Welcomme R. (2001), Restoration of sustainability of physically depredated fish habitats – The Model of Intermediate Restoration. Ecohydrology & Hydrobiology Vol.1 No. 3, pp. 279-282
- Zalewski M., Santiago-Fandino V., Neate J. (2003), Energy, water, plant interactions: “Green Feedback” as a mechanism for environmental management and control through the application of phytotechnology and Ecohydrology, Hydrological Processes, Vol. 17, pp. 2753-2767

Design practice for urban drainage, incorporating climate change impacts

Qianqian Zhou¹, Karsten Arnbjerg-Nielsen¹, Peter Steen Mikkelsen¹, Kirsten Halsnæs² and Susanne Balslev Nielsen³

¹ DTU Environment, Copenhagen, Denmark (qiaz@env.dtu.dk)

² Risø DTU, Copenhagen, Denmark

³ DTU Management, Copenhagen, Denmark

1. Introduction

A rapid increase in frequency and intensity of precipitation extremes has been observed in Northern Europe, most likely due to climate change. Several studies have indicated that there is increased damage and associated costs of urban drainage, owing to climate change. In order to maintain the acceptable risk level of flooding, there is a need to revisit the established design practices and develop a framework incorporating possible climate change impacts into the actual design of urban drainage. This framework will have substantial consequences on the overall cost of urban drainage in terms of investments and/or damage.

This paper represents initial results of a study that aims at identifying new principles for assessment of urban drainage adaptation measures for high return periods. It is of high interest to understand the regional impacts of ongoing climate change and develop practical guidelines that integrate socio-economic analysis, city planning and risk analysis tools.

2. Flood risk framework

Flood risk analysis consists of an analysis of hazards and vulnerabilities (Figure 1). Hazard analysis focuses on the characterization of the frequency and magnitude of floods. Vulnerability analysis puts a high emphasis on providing tools to establish damage cost functions for monetary goods and non-monetary goods, such as recreational value and disamenity averting value.

Climate change will influence the hazards by changing the precipitation patterns. There will be increased probability of flooding due to the climate change. Vulnerabilities will be inspected over time, but primarily caused by the drivers that are not associated with the climate change.

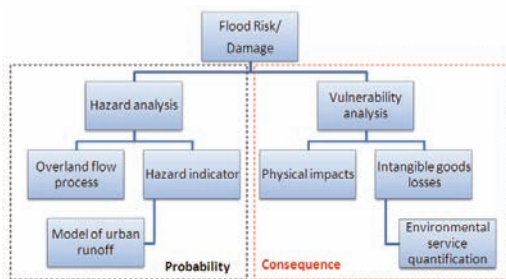


Figure 1: Urban flood risk framework

3. Flood risk framework applied for urban drainage

Urban flood risk is defined in relation to the flood return periods (Figure 2). Daily rain is mainly perceived as nuisance, which requires routine maintenance and control of pollution. Design rain provides minimum service standards for the drainage design. Heavy rain indicates the events with extreme rainfall intensities. The targeted design envelope of urban drainage is a combination of

different probabilities of these three rainfall events (Figure 2). Events that used to be inside the envelope will become unacceptable due to the increase in probability. Damage will occur more frequently to physical assets and natural systems. The increase in rainfall design intensities will therefore lead to a significant increase in the flood risk (Arnbjerg-Nielsen and Fleischer 2009).

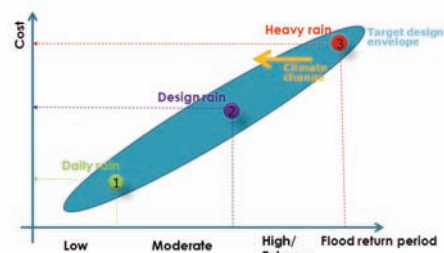


Figure 2: Three stages of urban flood risk

The incorporation of climate change impacts into the targeted design envelope has been a big challenge for urban drainage designers. Two strategies are discussed.

- **Business as usual:** There is no need to take measures if the society is persuaded to accept the increased flood risk. Furthermore, decision makers could 'wait' for the time being in order to collect more information if there are high uncertainties and irreversibilities to implement adaptation measures.
- **Planned adaptation:** Adaptation could be adopted on hazards and/or vulnerabilities. Hazard adaptation aims to counteract the increased probability, and it could be mainly achieved by physical measures and enhanced resilient strategies. Vulnerability adaptation relies on lessening the exposure of vulnerable receptors from flood hazards by landuse change, social activities etc.

4. Economic tools

Economic tools (Cost Benefit Analysis, CBA) will be applied complementary to achieve suitable adaptation measures at a minimum cost. CBA concerns the optimization of economic resource allocation; in principle, a CBA values all benefits and costs of different adaptation scenarios and chooses the one with greater benefits than costs.

5. Results

Hazard analysis is performed by carrying out a conceptual model in Mike Urban to obtain a better understanding of overland land flow process linking to catchment characteristic (Figure 3). The conceptual catchment consists of 1D sewer network and 2D surface model. The detailed setup of model parameters is shown in Table 1.

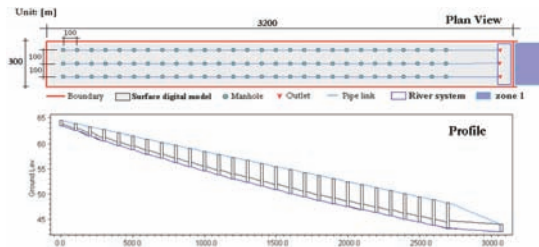


Figure 3: Setup of conceptual model. It has been designed to be a regular Danish catchment with flat and small subareas. The sewer is designed for return period $T=2$ years storm event.

Table 1: Basic parameter setup of conceptual model

Parameter	Definition	Value	Unit
Impervious degree	Degree of paved areas of subcatchment	40	%
Connection ratio	Degree of paved areas that are connected to the sewer	100	%
Friction	Roughness of overland flow	32	M
Slope	Slope of subcatchment	6	‰
Sewage capacity	Design rainfall intensity for the sewer network	2	yr
Catchment size	Area of subcatchment	1	ha

Assessing the relative importance of the contribution of individual catchment characteristics to the overall hazards is conducted with first order analysis (Lei 1996 and Yen 1989). The model output is expressed as a nonlinear function of the catchment variables:

$$Y = f(X_1, X_2, \dots, X_n)$$

The dependent variable Y implies any detrimental effects, such as simulated water depth. X_i describes the catchment characteristics, such as impervious degree, slope etc. The variance of Y is formulated as a summary of the variation propagation from all parameters:

$$V(Y)^2 \approx \sum_{i=1}^n \left(\frac{\partial Y}{\partial X_i} \right)^2 V(X_i)^2$$

The first-order partial deviation of Y with respect to X_i indicates the relative sensitivity assessment of X_i . Thus, the sensitivity of each variable is defined as:

$$S_{X_i} = \frac{\left(\frac{\partial Y}{\partial X_i} \right)^2 \cdot V(X_i)^2}{V(Y)^2}$$

The reasonable associated variations of input parameters are shown in Table 2, which were mainly obtained from the studies documented by Arnbjerg-Nielsen and Harremoes 1996 and Huber et al. 1988.

Current city planning starts to reflect its significant influence on urban flood risk management. However, there is a lacking of thorough understanding of the synergy between these two fields. An effective city planning often fails to be formulated. A model simulation showed that a large decrease in flood hazards could be achieved by proper city planning.

6. Conclusions

Two main conclusions are discussed below:

- The imperviousness, connection ratio and slope have been found to be significant in the overland flow process. The existing sewage capacity and roughness condition of overland flow are found not important for extreme events.
- Negative effects of urbanization have been observed. Furthermore, it is shown that proper city planning will lead to a considerable decrease in urban flood

risk. A significant principle of managing the risk in respect of spatial planning is to avoid constructing building perpendicular to sewers' direction.

Table 2: Associated reasonable variations of parameters

Parameter	Variation descriptions
Impervious degree	Catchment imperviousness varies between 20%-80%, the typical range is around 30%-60%.
Connection ratio	The reasonable variation of connection ratio is about 70%-100%.
Friction	Roughness of overland flow varies between $2-80 \text{ m}^{1/3}\text{s}^{-1}$. It is of a high probability to have values between $5-65 \text{ m}^{1/3}\text{s}^{-1}$.
Slope	Denmark is rather flat; a slope range of 1-10 ‰ has been taken into account.
Sewage capacity	The recommended service standard of urban drainage is $T=2$ and/or 5yr for storm water system

Table 3: Assessment of relative importance of variations of catchment characteristics (X_i). The detrimental effect Y refers to the simulated maximum water depth of overland flow.

	Mean	Standard deviation	Coefficient of variation	Relative importance
Connection ratio	0.85	0.15	0.18	35%
Impervious degree	0.4	0.15	0.38	30%
Friction	32	27	0.84	3%
Slope	6	3	0.5	30%
Sewage	2	-	-	1%

7. Further work

The principles of new adaptation measures are still being developed. The achieved outputs from the conceptual model will be further tested with a case study. More effort will be made to establish a suitable damage function that transfers the observed hazards to actual damage costs.

References

- Arnbjerg-Nielsen, K., Fleischer, H.S. (2009): Feasible adaptation strategies for increased risk of flooding in cities due to climate change. Water Science and Technology
- Arnbjerg-Nielsen, K. and Harremoes, P. (1996): The importance of inherent uncertainties in state-of-the-art urban storm drainage modeling for ungauged small catchments. Journal of Hydrology
- Huber, W.C., R.E. Dickinson(1988). Storm Water Management Model, version 4: User's Manual, Environmental Research Laboratory, Athens, Georgia.
- Lei J.H. (1996). Uncertainty analysis of Urban Rainfall-Runoff Modelling. Ph.D. Norwegian University of Science and Technology, Trondheim, Norway
- Yen, B.C. (1989), Risk Analysis and Management of Natural and Man-Made Hazards. Engineering approaches to risk and Reliability Analysis. ASCE, New York.

International BALTEX Secretariat Publication Series

ISSN 1681-6471

- No. 1:** Minutes of First Meeting of the BALTEX Science Steering Group held at GKSS Research Centre in Geesthacht, Germany, 16-17 May, 1994. August 1994.
- No. 2:** Baltic Sea Experiment BALTEX – Initial Implementation Plan, 84 pages. March 1995.
- No. 3:** First Study Conference on BALTEX, Visby, Sweden, August 28 – September 1, 1995. Conference Proceedings. Editor: A. Omstedt, SMHI Norrköping, Sweden, 190 pages. August 1995.
- No. 4:** Minutes of Second Meeting of the BALTEX Science Steering Group held at Finnish Institute of Marine Research in Helsinki, Finland, 25-27 January, 1995. October 1995.
- No. 5:** Minutes of Third Meeting of the BALTEX Science Steering Group held at Strand Hotel in Visby, Sweden, September 2, 1995. March 1996.
- No. 6:** BALTEX Radar Research – A Plan for Future Action, 46 pages. October 1996.
- No. 7:** Minutes of Fourth Meeting of the BALTEX Science Steering Group held at Institute of Oceanology PAS in Sopot, Poland, 3-5 June, 1996. February 1997.
- No. 8:** *Hydrological, Oceanic and Atmospheric Experience from BALTEX*. Extended Abstracts of the XXII EGS Assembly, Vienna, Austria, 21-25 April, 1997. Editors: M. Alestalo and H.-J. Isemer, 172 pages. August 1997.
- No. 9:** The Main BALTEX Experiment 1999-2001 – *BRIDGE*. Strategic Plan, 78 pages. October 1997.
- No. 10:** Minutes of Fifth Meeting of the BALTEX Science Steering Group held at Latvian Hydro-meteorological Agency in Riga, Latvia, 14-16 April, 1997. January 1998.
- No. 11:** Second Study Conference on BALTEX, Juliusruh, Island of Rügen, Germany, 25-29 May 1998. Conference Proceedings. Editors: E. Raschke and H.-J. Isemer, 251 pages. May 1998.
- No. 12:** Minutes of 7th Meeting of the BALTEX Science Steering Group held at Hotel Aquamaris in Juliusruh, Island of Rügen, Germany, 26 May 1998. November 1998.
- No. 13:** Minutes of 6th Meeting of the BALTEX Science Steering Group held at Danish Meteorological Institute in Copenhagen, Denmark, 2-4 March 1998. January 1999.
- No. 14:** BALTEX – BASIS Data Report 1998. Editor: Jouko Launiainen, 96 pages. March 1999.
- No. 15:** Minutes of 8th Meeting of the Science Steering Group held at Stockholm University in Stockholm, Sweden, 8-10 December 1998. May 1999
- No. 16:** Minutes of 9th Meeting of the BALTEX Science Steering Group held at Finnish Meteorological Institute in Helsinki, Finland, 19-20 May 1999. July 1999.

- No. 17:** Parameterization of surface fluxes, atmospheric planetary boundary layer and ocean mixed layer turbulence for BRIDGE – What can we learn from field experiments? Editor: Nils Gustafsson. April 2000.
- No. 18:** Minutes of 10th Meeting of the BALTEX Science Steering Group held in Warsaw, Poland, 7-9 February 2000. April 2000.
- No. 19:** BALTEX-BASIS: Final Report, Editors: Jouko Launiainen and Timo Vihma. May 2001.
- No. 20:** Third Study Conference on BALTEX, Mariehamn, Island of Åland, Finland, 2-6 July 2001, Conference Proceedings. Editor: Jens Meywerk, 264 pages. July 2001.
- No. 21:** Minutes of 11th Meeting of the BALTEX Science Steering Group held at Max-Planck-Institute for Meteorology in Hamburg, Germany, 13-14 November 2000. July 2001.
- No. 22:** Minutes of 12th Meeting of the BALTEX Science Steering Group held at Royal Netherlands Meteorological Institute (KNMI), De Bilt, The Netherlands, 12-14 November 2001. April 2002.
- No. 23:** Minutes of 13th Meeting of the BALTEX Science Steering Group held at Estonian Business School (EBS), Centre for Baltic Studies, Tallinn, Estonia, 17-19 June 2002. September 2002.
- No. 24:** The eight BALTIMOS Field Experiments 1998-2001. Field Reports and Examples of Measurements. Editors: Burghard Brümmer, Gerd Müller, David Schröder, Amélie Kirchgäßner, Jouko Launiainen, Timo Vihma. 138 pages. April 2003,.
- No. 25:** Minutes of 14th Meeting of the BALTEX Science Steering Group held at Lund University, Department of Physical Geography and Ecosystems Analysis, Lund, Sweden, 18 - 20 November 2002. May 2003.
- No. 26:** CLIWA-NET: BALTEX BRIDGE Cloud Liquid Water Network. Final Report. Editors: Susanne Crewell, Clemens Simmer, Arnout Feijt, Erik van Meijgaard, 53 pages. July 2003.
- No. 27:** Minutes of 15th Meeting of the BALTEX Science Steering Group held at Risø National Laboratory, Wind Energy Department, Roskilde, Denmark, 8 - 10 September 2003. January 2004.
- No. 28:** Science Plan for BALTEX Phase II 2003 – 2012. February 2004, 43 pages.
- No. 29:** Fourth Study Conference on BALTEX, Gudhjem, Bornholm, Denmark, 24 - 28 May 2004, Conference Proceedings. Editor: Hans-Jörg Isemer, 189 pages. May 2004.
- No. 30:** Minutes of 16th Meeting of the BALTEX Science Steering Group held at Gudhjem Bibliotek, Gudhjem, Bornholm, Denmark, 23 May 2004. October 2004.
- No. 31:** BALTEX Phase I 1993-2002 – State of the Art Report. Editors: Daniela Jacob and Anders Omstedt, 181 pages, October 2005.
- No. 32:** Minutes of 17th Meeting of the BALTEX Science Steering Group held at Poznan, Poland, 24 – 26 November 2004. November 2005.
- No. 33:** Minutes of 18th Meeting of the BALTEX Science Steering Group held at Meteorological Observatory Lindenberg – Richard Aßmann Observatory, Germany, 18 – 20 October 2005. February 2006.

- No. 34:** BALTEX Phase II 2003 – 2012 Science Framework and Implementation Strategy, 95 pages. April 2006.
- No. 35:** BALTEX Assessment of Climate Change for the Baltic Sea Basin. Summary. Editors: The BACC lead author group, 26 pages. June 2006.
- No. 36:** Minutes of 19th Meeting of the BALTEX Science Steering Group held at Ågrenska Villan of Göteborg University Sweden, 23 – 24 May 2006. October 2006.
- No. 37:** Minutes of 20th Meeting of the BALTEX Science Steering Group held at St. Petersburg, Russia, 6 – 7 December 2006. March 2007.
- No. 38:** Fifth Study Conference on BALTEX, Kuressaare, Saaremaa, Estonia, 4 - 8 June 2007. Conference Proceedings. Editor: Hans-Jörg Isemer, 209 pages. May 2007.
- No. 39:** Minutes of 21st Meeting of the BALTEX Science Steering Group held at Kuressaare, Saaremaa, Estonia, 3 June 2007. September 2007.
- No. 40:** Minutes of 22nd Meeting of the BALTEX Science Steering Group held at SMHI, Norrköping, Sweden, 23-25 January 2008. May 2008.
- No. 41:** 2nd International Lund RCM Workshop: 21st Challenges in Regional-scale Climate Modelling. Lund University, 4-8 May 2009. Workshop Proceedings. Editors: Burkhardt Rockel, Lars Bärring and Marcus Reckermann. 292 pages, April 2009.
- No. 42:** International Conference on Climate Change – The environmental and socio-economic response in the southern Baltic region. University of Szczecin, 25-28 May 2009. Conference Proceedings. Editors: Andrzej Witkowski, Jan Harff and Hans-Jörg Isemer. 140 pages, May 2009.
- No. 43:** Minutes of 23rd Meeting of the BALTEX Science Steering Group held at Finnish Meteorological Institute, Helsinki, Finland, 12 - 14 January 2009. July 2009.
- No. 44:** BALTEX Phase II 2003 – 2012 Revised Objectives. A Summary Amendment to the BALTEX Phase II Science Framework and Implementation Plan. 23 pages. November 2009.
- No. 45:** Minutes of 24th Meeting of the BALTEX Science Steering Group held at the University of Riga, Riga, Latvia, 16 - 18 November 2009. March 2010.
- No. 46:** Sixth Study Conference on BALTEX. Conference Proceedings. Międzyzdroje, Island of Wolin, Poland, 14-18 June 2010. Editor: Marcus Reckermann and Hans-Jörg Isemer, 181 pages. May 2010.

Copies are available upon request from the International BALTEX Secretariat.